

Methods in
Molecular Biology 1478

Springer Protocols



Christian Dahmann *Editor*

Drosophila

Methods and Protocols

Second Edition

EXTRAS ONLINE

 Humana Press

METHODS IN MOLECULAR BIOLOGY

Series Editor

John M. Walker

School of Life and Medical Sciences

University of Hertfordshire

Hatfield, Hertfordshire, AL10 9AB, UK

For further volumes:
<http://www.springer.com/series/7651>

Drosophila

Methods and Protocols

Second Edition

Edited by

Christian Dahmann

Institute of Genetics, Technische Universität Dresden, Dresden, Germany

 **Humana Press**

Editor

Christian Dahmann
Institute of Genetics
Technische Universität Dresden
Dresden, Germany

ISSN 1064-3745

ISSN 1940-6029 (electronic)

Methods in Molecular Biology

ISBN 978-1-4939-6369-0

ISBN 978-1-4939-6371-3 (eBook)

DOI 10.1007/978-1-4939-6371-3

Library of Congress Control Number: 2016948818

© Springer Science+Business Media New York 2016

This work is subject to copyright. All rights are reserved by the Publisher, whether the whole or part of the material is concerned, specifically the rights of translation, reprinting, reuse of illustrations, recitation, broadcasting, reproduction on microfilms or in any other physical way, and transmission or information storage and retrieval, electronic adaptation, computer software, or by similar or dissimilar methodology now known or hereafter developed.

The use of general descriptive names, registered names, trademarks, service marks, etc. in this publication does not imply, even in the absence of a specific statement, that such names are exempt from the relevant protective laws and regulations and therefore free for general use.

The publisher, the authors and the editors are safe to assume that the advice and information in this book are believed to be true and accurate at the date of publication. Neither the publisher nor the authors or the editors give a warranty, express or implied, with respect to the material contained herein or for any errors or omissions that may have been made.

Printed on acid-free paper

This Humana Press imprint is published by Springer Nature

The registered company is Springer Science+Business Media LLC New York

Preface

The fruit fly *Drosophila melanogaster* is one of the most powerful genetically tractable model organisms. Work using *Drosophila* has made many valuable contributions to our understanding of animal development, behavior, and physiology and of human disease. Inspiring work and new research avenues often depend on the development of novel techniques. The use of transposons to generate transgenic flies and the adaptation of yeast systems to express genes or make mosaic animals are to name but a few of the techniques that led to breakthroughs in *Drosophila* research. Descriptions of these and other important methods were included in the first edition of *Drosophila: Methods and Protocols* published in 2008. Since then, the thriving fly researcher community continued to refine and invent techniques. The current second edition of this book in part tries to reflect this effort and covers some of these more recent methods. The book starts with a description of FlyBase, a database of genes and genomes, followed by the presentation of systems for versatile gene expression in the fly. Chapters detailing methods of gene knockdown and editing, including CRISPR-Cas9, and protein knockdown then follow. Live imaging has become an important aspect of studying *Drosophila* and so the next chapters are devoted to methods detailing live imaging of different tissues and organs followed by chapters describing how to quantify image data and how to probe tissue mechanics by laser ablation. The next two chapters provide methods for analyzing transcription followed by protocols to study growth, metabolism, aging, and behavior in *Drosophila*. The book closes with chapters on electrophysiological recordings and methods to establish cell lines.

I thank all the authors for their expert contribution to this volume and hope that this book will be a valuable source of hands-on protocols and reviews for molecular, cell, and developmental biologist using *Drosophila* as model system in their work.

Dresden, Germany

Christian Dahmann

Contents

1	Using FlyBase, a Database of <i>Drosophila</i> Genes and Genomes	1
	<i>Steven J. Marygold, Madeline A. Crosby, Joshua L. Goodman, and The FlyBase Consortium</i>	
2	The GAL4 System: A Versatile System for the Manipulation and Analysis of Gene Expression	33
	<i>Elizabeth E. Caygill and Andrea H. Brand</i>	
3	The Q-System: A Versatile Expression System for <i>Drosophila</i>	53
	<i>Olena Riabinina and Christopher J. Potter</i>	
4	Analysis of MicroRNA Function in <i>Drosophila</i>	79
	<i>Geetanjali Chawla, Arthur Luhur, and Nicholas Sokol</i>	
5	Methods for High-Throughput RNAi Screening in <i>Drosophila</i> Cells	95
	<i>Maximilian Billmann and Michael Boutros</i>	
6	A Guide to Genome-Wide In Vivo RNAi Applications in <i>Drosophila</i>	117
	<i>Aynur Kaya-Çopur and Frank Schnorrer</i>	
7	Creating Heritable Mutations in <i>Drosophila</i> with CRISPR-Cas9	145
	<i>Fillip Port and Simon L. Bullock</i>	
8	Performing Chromophore-Assisted Laser Inactivation in <i>Drosophila</i> Embryos Using GFP	161
	<i>Anne Pélissier-Monier, Bénédicte Sanson, and Bruno Monier</i>	
9	deGradFP: A System to Knockdown GFP-Tagged Proteins	177
	<i>Emmanuel Caussinus and Markus Affolter</i>	
10	Sample Preparation and Mounting of <i>Drosophila</i> Embryos for Multiview Light Sheet Microscopy	189
	<i>Christopher Schmied and Pavel Tomancak</i>	
11	Cultivation and Live Imaging of <i>Drosophila</i> Imaginal Discs	203
	<i>Simon Restrepo, Jeremiah J. Zartman, and Konrad Basler</i>	
12	Cultivation and Live Imaging of <i>Drosophila</i> Ovaries	215
	<i>Maureen Cetera, Lindsay Lewellyn, and Sally Horne-Badovinac</i>	
13	Segmentation and Quantitative Analysis of Epithelial Tissues	227
	<i>Benoit Aigouy, Daiki Umetsu, and Suzanne Eaton</i>	
14	Laser Ablation to Probe the Epithelial Mechanics in <i>Drosophila</i>	241
	<i>Pruthvi C. Shivakumar and Pierre-Francois Lenne</i>	
15	Rapid Ovary Mass-Isolation (ROMi) to Obtain Large Quantities of <i>Drosophila</i> Egg Chambers for Fluorescent In Situ Hybridization	253
	<i>Helena Jambor, Pavel Mejstrik, and Pavel Tomancak</i>	
16	Chromatin Immunoprecipitation for Analyzing Transcription Factor Binding and Histone Modifications in <i>Drosophila</i>	263
	<i>Yad Ghavi-Helm, Bingqing Zhao, and Eileen E.M. Furlong</i>	

17	Protocols to Study Growth and Metabolism in <i>Drosophila</i>	279
	<i>Katrin Strassburger and Aurelio A. Teleman</i>	
18	Protocols to Study Aging in <i>Drosophila</i>	291
	<i>Matthew D.W. Piper and Linda Partridge</i>	
19	Protocols to Study Behavior in <i>Drosophila</i>	303
	<i>Wendi S. Neckameyer and Parag Bhatt</i>	
20	Electrophysiological Recordings from Lobula Plate Tangential Cells in <i>Drosophila</i>	321
	<i>Alex S. Mauss and Alexander Borst</i>	
21	Methods to Establish <i>Drosophila</i> Cell Lines	333
	<i>Alain Debuc, Timothy L. Megraw, and Antoine Guichet</i>	
	<i>Index</i>	353

Contributors

MARKUS AFFOLTER • *Growth & Development, Biozentrum, University of Basel, Basel, Switzerland*

BENOIT AIGOY • *IBDM—Institut de Biologie du Développement de Marseille, Marseille, France*

GIULIA ANTONAZZO • *The FlyBase Consortium, Department of Physiology, Development and Neuroscience, University of Cambridge, Cambridge, UK*

HELEN ATTRILL • *The FlyBase Consortium, Department of Physiology, Development and Neuroscience, University of Cambridge, Cambridge, UK*

PHILLIP BAKER • *The FlyBase Consortium, Department of Biology, University of New Mexico, Albuquerque, NM, USA*

KONRAD BASLER • *Institute of Molecular Life Sciences, University of Zurich, Zurich, Switzerland*

PARAG BHATT • *Department of Pharmacological and Physiological Science, St Louis University School of Medicine, St. Louis, MO, USA*

MAXIMILIAN BILLMANN • *Division of Signaling and Functional Genomics, German Cancer Research Center (DKFZ), Heidelberg University, Heidelberg, Germany*

ALEXANDER BORST • *Max-Planck-Institute of Neurobiology, Martinsried, Germany*

MICHAEL BOUTROS • *Division of Signaling and Functional Genomics, German Cancer Research Center (DKFZ), Heidelberg University, Heidelberg, Germany*

ANDREA H. BRAND • *The Gurdon Institute and Department of Physiology, Development and Neuroscience, University of Cambridge, Cambridge, UK*

KRIS BROLL • *The FlyBase Consortium, Biological Laboratories, Harvard University, Cambridge, MA, USA*

NICHOLAS BROWN • *The FlyBase Consortium, Department of Physiology, Development and Neuroscience, University of Cambridge, Cambridge, UK*

SIMON L. BULLOCK • *Division of Cell Biology, MRC Laboratory of Molecular Biology, Cambridge, UK*

EMMANUEL CAUSSINUS • *Institute of Molecular Life Sciences, University of Zurich, Zurich, Switzerland*

ELIZABETH E. CAYGILL • *The Gurdon Institute and Department of Physiology, Development and Neuroscience, University of Cambridge, Cambridge, UK*

MAUREEN CETERA • *Department of Molecular Genetics and Cell Biology, The University of Chicago, Chicago, IL, USA; Committee on Development, Regeneration and Stem Cell Biology, The University of Chicago, Chicago, IL, USA*

GEETANJALI CHAWLA • *Department of Biology, Indiana University, Bloomington, IN, USA*

MARTA COSTA • *The FlyBase Consortium, Department of Physiology, Development and Neuroscience, University of Cambridge, Cambridge, UK*

RICHARD CRIPPS • *The FlyBase Consortium, Department of Biology, University of New Mexico, Albuquerque, NM, USA*

MADELINE A. CROSBY • *The Biological Laboratories, Harvard University, Cambridge, MA, USA*

CHRISTIAN DAHMANN • *Institute of Genetics, Technische Universität Dresden, Dresden, Germany*

ALAIN DEBEC • *Institut Jacques Monod, UMP 7592—CNRS, Université Paris Diderot, Paris, France; Department of Biomedical Sciences, College of Medicine, Florida State University, Tallahassee, FL, USA*

SUZANNE EATON • *Max Planck Institute of Molecular Cell Biology and Genetics, Dresden, Germany*

DAVID EMMERT • *The FlyBase Consortium, Biological Laboratories, Harvard University, Cambridge, MA, USA*

CASSANDRA EXTRAVOUR • *The FlyBase Consortium, Biological Laboratories, Harvard University, Cambridge, MA, USA*

KATHLEEN FALLS • *The FlyBase Consortium, Biological Laboratories, Harvard University, Cambridge, MA, USA*

EILEEN E.M. FURLONG • *European Molecular Biology Laboratory, Genome Biology Unit, Heidelberg, Germany*

SUSAN RUSSO GELBART • *The FlyBase Consortium, Biological Laboratories, Harvard University, Cambridge, MA, USA*

WILLIAM GELBART • *The FlyBase Consortium, Biological Laboratories, Harvard University, Cambridge, MA, USA*

YAD GHAVI-HELM • *European Molecular Biology Laboratory, Genome Biology Unit, Heidelberg, Germany*

JOSHUA L. GOODMAN • *Department of Biology, Indiana University, Bloomington, IN, USA*

SIAN GRAMATES • *The FlyBase Consortium, Biological Laboratories, Harvard University, Cambridge, MA, USA*

GARY GRUMBLING • *The FlyBase Consortium, Department of Biology, Indiana University, Bloomington, IN, USA*

ANTOINE GUICHET • *Institut Jacques Monod, UMP 7592—CNRS, Université Paris Diderot, Paris, France*

SALLY HORNE-BADOVINAC • *Department of Molecular Genetics and Cell Biology, The University of Chicago, Chicago, IL, USA; Committee on Development, Regeneration and Stem Cell Biology, The University of Chicago, Chicago, IL, USA*

HELENA JAMBOR • *Max Planck Institute of Molecular Cell Biology and Genetics, Dresden, Germany*

THOMAS KAUFMAN • *The FlyBase Consortium, Department of Biology, Indiana University, Bloomington, IN, USA*

AYNUR KAYA-ÇOPUR • *Max Planck Institute of Biochemistry, Martinsried, Germany*

PIERRE-FRANCOIS LENNE • *Aix-Marseille Université, CNRS, IBDM, Marseille, France; UMR7288, CNRS, Aix-Marseille Université, Marseille, France*

LINDSAY LEWELLYN • *Department of Biological Sciences, Butler University, Indianapolis, IN, USA*

ARTHUR LUHUR • *Department of Biology, Indiana University, Bloomington, IN, USA*

STEVEN J. MARYGOLD • *Department of Genetics, University of Cambridge, Cambridge, UK*

BEVERLEY MATTHEWS • *The FlyBase Consortium, Biological Laboratories, Harvard University, Cambridge, MA, USA*

ALEX S. MAUSS • *Max-Planck-Institute of Neurobiology, Martinsried, Germany*

TIMOTHY L. MEGRAW • *Department of Biomedical Sciences, College of Medicine, Florida State University, Tallahassee, FL, USA*

PAVEL MEJSTRIK • *Max Planck Institute of Molecular Cell Biology and Genetics, Dresden, Germany*

GILLIAM MILLBURN • *The FlyBase Consortium, Department of Physiology, Development and Neuroscience, University of Cambridge, Cambridge, UK*

BRUNO MONIER • *Université Toulouse III-Paul Sabatier, Toulouse, France; Laboratoire de Biologie Cellulaire et Moléculaire du Contrôle de la Prolifération, CNRS, UMR5088, Toulouse, France*

WENDI S. NECKAMEYER • *Department of Pharmacological and Physiological Science, St Louis University School of Medicine, St. Louis, MO, USA*

LINDA PARTRIDGE • *Institute of Healthy Ageing and Department Genetics, Evolution and Environment, University College London, London, UK; Max Planck Institute for Biology of Ageing, Köln, Germany*

ANNE PÉLISSIER-MONIER • *Université Toulouse III-Paul Sabatier, Toulouse, France; Centre de Biologie du Développement, CNRS, UMR5547, Toulouse, France*

NORBERT PERRIMON • *The FlyBase Consortium, Biological Laboratories, Harvard University, Cambridge, MA, USA*

MATTHEW D.W. PIPER • *Institute of Healthy Ageing and Department Genetics, Evolution and Environment, University College London, London, UK; School of Biological Sciences, Monash University, Clayton, Victoria, Australia*

LAURA PONTING • *The FlyBase Consortium, Department of Physiology, Development and Neuroscience, University of Cambridge, Cambridge, UK*

FILLIP PORT • *Division of Cell Biology, MRC Laboratory of Molecular Biology, Cambridge, UK; Division of Signaling and Functional Genomics, German Cancer Research Center (DKFZ), Heidelberg, Germany*

CHRISTOPHER J. POTTER • *The Solomon H. Snyder Department of Neuroscience, The Center for Sensory Biology, Johns Hopkins University School of Medicine, Baltimore, MD, USA*

SIMON RESTREPO • *Institute of Molecular Life Sciences, University of Zurich, Zurich, Switzerland*

ALIX REY • *The FlyBase Consortium, Department of Physiology, Development and Neuroscience, University of Cambridge, Cambridge, UK*

OLENA RIABININA • *The Solomon H. Snyder Department of Neuroscience, The Center for Sensory Biology, Johns Hopkins University School of Medicine, Baltimore, MD, USA*

BÉNÉDICTE SANSON • *Department of Physiology, Development and Neuroscience, University of Cambridge, Cambridge, UK*

GILBERTO DOS SANTOS • *The FlyBase Consortium, Biological Laboratories, Harvard University, Cambridge, MA, USA*

CHRISTOPHER SCHMIED • *Max Planck Institute of Molecular Cell Biology and Genetics, Dresden, Germany*

FRANK SCHNORRER • *Max Planck Institute of Biochemistry, Martinsried, Germany*

ANDREW SCHROEDER • *The FlyBase Consortium, Biological Laboratories, Harvard University, Cambridge, MA, USA*

PRUTHVI C. SHIVAKUMAR • *Institut de Biologie du Développement de Marseille, IBDM UMR7288, CNRS, Aix-Marseille Université, Marseille, France*

NICHOLAS SOKOL • *Department of Biology, Indiana University, Bloomington, IN, USA*

NICOLE STAUDT • *The FlyBase Consortium, Department of Physiology, Development and Neuroscience, University of Cambridge, Cambridge, UK*

RAYMUND STEFANCSIK • *The FlyBase Consortium, Department of Physiology, Development and Neuroscience, University of Cambridge, Cambridge, UK*

KATRIN STRASSBURGER • *German Cancer Research Center (DKFZ), Heidelberg, Germany*
VICTOR STRELETS • *The FlyBase Consortium, Department of Biology, Indiana University, Bloomington, IN, USA*
CHRISTOPHER TABONE • *The FlyBase Consortium, Biological Laboratories, Harvard University, Cambridge, MA, USA*
AURELIO A. TELEMAN • *German Cancer Research Center (DKFZ), Heidelberg, Germany*
JIM THURMOND • *The FlyBase Consortium, Department of Biology, Indiana University, Bloomington, IN, USA*
PAVEL TOMANAK • *Max Planck Institute of Molecular Cell Biology and Genetics, Dresden, Germany*
DAIKI UMETSU • *Graduate School of Life Sciences, Tohoku University, Sendai, Japan*
JOSE-MARIA URBANO • *The FlyBase Consortium, Department of Physiology, Development and Neuroscience, University of Cambridge, Cambridge, UK*
MAGGIE WERNER-WASHBURN • *The FlyBase Consortium, Department of Biology, University of New Mexico, Albuquerque, NM, USA*
JEREMIAH J. ZARTMAN • *Department of Chemical and Biomolecular Engineering, University of Notre Dame, Notre Dame, IN, USA*
BINGQING ZHAO • *European Molecular Biology Laboratory, Genome Biology Unit, Heidelberg, Germany*
PINGLEI ZHOU • *The FlyBase Consortium, Biological Laboratories, Harvard University, Cambridge, MA, USA*
MARK ZYTKOVICZ • *The FlyBase Consortium, Biological Laboratories, Harvard University, Cambridge, MA, USA*

Chapter 1

Using FlyBase, a Database of *Drosophila* Genes and Genomes

Steven J. Marygold, Madeline A. Crosby, Joshua L. Goodman, and The FlyBase Consortium*

Abstract

For nearly 25 years, FlyBase (flybase.org) has provided a freely available online database of biological information about *Drosophila* species, focusing on the model organism *D. melanogaster*. The need for a centralized, integrated view of *Drosophila* research has never been greater as advances in genomic, proteomic, and high-throughput technologies add to the quantity and diversity of available data and resources.

FlyBase has taken several approaches to respond to these changes in the research landscape. Novel report pages have been generated for new reagent types and physical interaction data; *Drosophila* models of human disease are now represented and showcased in dedicated Human Disease Model Reports; other integrated reports have been established that bring together related genes, datasets, or reagents; Gene Reports have been revised to improve access to new data types and to highlight functional data; links to external sites have been organized and expanded; and new tools have been developed to display and interrogate all these data, including improved batch processing and bulk file availability. In addition, several new community initiatives have served to enhance interactions between researchers and FlyBase, resulting in direct user contributions and improved feedback.

This chapter provides an overview of the data content, organization, and available tools within FlyBase, focusing on recent improvements. We hope it serves as a guide for our diverse user base, enabling efficient and effective exploration of the database and thereby accelerating research discoveries.

Key words FlyBase, *Drosophila*, Database, Genetics, Genomics, Translational research

1 Introduction

Since its inception in 1992, FlyBase has provided an online repository of biological data about *Drosophila* species, focusing on the model organism *D. melanogaster*. Data in FlyBase are either curated manually from the primary research literature or are incorporated computationally from various sources, with the two input streams being integrated into a series of ‘report’ pages and other portals on

*The members of the FlyBase Consortium are listed in the Acknowledgements.

the website. Many links to related data and resources at external databases are also incorporated. As a result, FlyBase serves as a nexus for all *Drosophila*-related information.

While the core purpose of FlyBase has not changed significantly over the years, we have had to continually review our data integration and presentation strategies to reflect the changing nature of *Drosophila* research. For example, when FlyBase was founded, the genomic sequence of *D. melanogaster* (or any other metazoan) was not yet known, and DNA microarray and RNA-Seq technologies did not yet exist. Since then, the volume of relevant data has increased massively as whole-genome and high-throughput studies have become increasingly common, and the number of new datasets and novel resource collections has expanded. Furthermore, the FlyBase user base has diversified as more researchers from other disciplines take advantage of the *Drosophila* system to conduct their experiments—particularly those interested in modeling human diseases.

Much of the information in FlyBase is partitioned into 20 different data classes, each with an associated report on the website (Table 1). Traditional reports, such as those for genes, alleles, or references, have been supplemented with several new ones in recent years to reflect the different reagents being used and new data types being produced. New or improved tools have also been developed in order to effectively search and analyze these novel data. A list of all current FlyBase tools, along with a brief description of their functionalities, is provided in Table 2 and specific use cases will be presented in context below.

Table 1
Data classes and reports in FlyBase

Data class/report	Number of records ^a		Factor change	Comment
	FB2007_01	FB2015_04		
<i>Genetic/genomic data</i>				
Genes (sequenced)	58,101 (27,377)	246,273 (192,537)	4.2 (7.0)	Large increase owing to incorporation of non- <i>D. melanogaster</i> genomes
Transcripts	39,018	293,576	7.5	Large increase owing to incorporation of non- <i>D. melanogaster</i> genomes
Polypeptides	34,302	256,047	7.5	Large increase owing to incorporation of non- <i>D. melanogaster</i> genomes
Alleles	108,697	226,157	2.1	
Aberrations	32,412	22,608	0.70	Decrease owing to removal of ‘potential’ DrosDel deletions

(continued)

Table 1
(continued)

Data class/report	Number of records ^a		Factor change	Comment
	FB2007_01	FB2015_04		
Balancers	540	608	1.1	
Recombinant constructs	24,693	111,788	4.5	Large increase owing to incorporation of several genome-wide construct collections
Insertions	72,782	174,464	2.4	
Natural transposons	1189	1472	1.2	
Sequence features	n/a	184,028	n/a	New in FB2009_05
Physical interactions	n/a	16,075	n/a	New in FB2011_01
<i>Integrated data</i>				
Large dataset metadata	n/a	709	n/a	New in FB2009_05
Gene groups	n/a	278	n/a	New in FB2015_02
Human disease models	n/a	44	n/a	New in FB2015_04
<i>Reagents</i>				
Stocks	85,022	140,101	1.6	
Strains	n/a	284	n/a	New in FB2015_01
Cell lines	n/a	188	n/a	New in FB2009_06
Clones	304,240	723,550	2.4	
<i>Other</i>				
References (papers)	184,744 (78,122)	212,340 (94,736)	1.1 (1.2)	
Images	870	1258	1.4	

^aThe number of records at the time of writing (FB2015_04, September 2015) is compared to that of the previous review [1] (FB2007_01, August 2007)

An overview of the FlyBase database was last presented in 2008 [1]. The main purpose of the current chapter is to provide a primer on how users can best use FlyBase today, with an emphasis on new and updated features. Inevitably, some areas are only mentioned briefly: the reader is referred to documentation on the FlyBase website and cited publications for more details.

Table 2
Tools in FlyBase

Tool name	Function/usage
<i>Query tools and portals</i>	
QuickSearch	Simplified searches on various data classes
QueryBuilder	Advanced search on a field-by-field level for most data classes
Vocabularies	Search or browse all controlled vocabularies used to annotate records
CytoSearch	Search for genetic objects mapped via cytology-based data
RNA-Seq Profile	Find genes with specific patterns of expression across modENCODE developmental stage, tissue, treatment, or cell line RNA-Seq data
Interactions Browser	Explore genetic and physical interactions via static images
ImageBrowse	Browse through <i>Drosophila</i> images by organ system, life-cycle, tagma, or germ layer
<i>Genomic/Map tools</i>	
BLAST	NCBI BLAST for finding nucleotide and protein sequences in <i>Drosophila</i> and dozens of related species
GBrowse	Graphical or tabular representation of the 12 sequenced <i>Drosophila</i> genomes
CytoSearch	Search for genetic objects mapped via sequence-based data
Feature Mapper	Search for sequence-mapped features that overlap a specific region or gene
RNA-Seq By Region	Evaluate the expression levels of exons, introns and/or intergenic regions from modENCODE developmental and tissue RNA-Seq data
Coordinates Converter	Convert coordinates between different genome releases (e.g. <i>D. melanogaster</i> R5 to R6)
<i>Retrieve/convert tools</i>	
Batch Download	Bulk download of individual report fields, FASTA or XML files in a variety of formats
Coordinates Converter	(See Coordinates Converter above)
Upload/Convert IDs	Update lists of old IDs, convert lists (e.g. genes to alleles), or upload IDs into a hit list

2 The Homepage

The main purpose of the homepage is to provide an indication of, and intuitive access to, all available data and tools in FlyBase (Fig. 1). In addition, the homepage highlights new features within FlyBase and advertises topical issues of interest to the fly community.

Fig. 1 The FlyBase homepage

2.1 Overview

The ‘Navigation Bar’ (NavBar) along the top of this (and every FlyBase) page incorporates drop-down menus containing links to key pages. For example, the ‘Tools’ menu lists all FlyBase tools, grouped by usage, and includes a ‘Tools Overview’ page to help users with search strategies. ‘Downloads’ contains links to all bulk data files that are available to download (see Subheading 10.2), also with an overview page describing them. The ‘Links’ menu has direct links to major external sites, such as the Berkeley *Drosophila* Genome Project (BDGP) and modENCODE, along with a comprehensive list of ~250 network and ~75 reagent resources of interest to *Drosophila* researchers. A new ‘Community’ menu has been added to group features that facilitate interactions between researchers and FlyBase, such as Fast-Track Your Paper (FTYP) and the FlyBase Community Advisory Group (FCAG) (see Subheading 11).

The ‘About’ menu collates general information about the FlyBase database and consortium, and includes links to FlyBase release notes and to a listing of FlyBase-authored publications. The ubiquitous NavBar also features the ‘Jump to Gene’ box (see Subheading 2.3).

Immediately below the NavBar on the homepage are prominent pictographs providing direct links to the most popular tools. Direct links to important community features are shown on the left-hand side of the homepage, including FTYP and the ‘FlyBase Newsletter’. Beneath these are links to general ‘News’ items and upcoming ‘Meetings’ and ‘Courses’. New or improved features within FlyBase are usually accompanied by an extended ‘Commentary’—an abbreviated teaser section is shown on the homepage, and all recent teasers cycle in order that several concurrent improvements can be brought to the attention of users. A link is also provided to view all current and previous Commentaries.

The FlyBase website is updated with new data (and often new features) about 6 times per year (see the ‘Release Schedule’ link under the ‘About’ menu of the NavBar). The header and footer of the homepage, and indeed every FlyBase page, state the version number and date of release of the FlyBase instance currently being viewed (Fig. 1). For example, ‘FB2015_04’ indicates the 4th release of 2015 and was used for compiling the data and screenshots in this chapter. It is important that users take note of this release number when using FlyBase data to direct experiments, and quote it when referring to FlyBase data in publications. Summary statistics for the current release and a record of general changes to FlyBase in each release are provided as ‘Release Notes’ and ‘New in this release’ pages, respectively, accessible via the NavBar ‘About’ menu. If needed, previous FlyBase releases (and accompanying ‘Release Notes’) are available via the ‘Archives’ menu of the NavBar.

2.2 QuickSearch

QuickSearch, located at the heart of the homepage, is the primary search tool on FlyBase and can be used to access all data types (Fig. 1). It has been significantly improved in recent years to make it as intuitive and flexible as possible [2]. The ‘Simple’ tab provides a Google™-type functionality in that any text can be entered and a search is performed across the entire database for possible matches. Using the ‘Data Class’ tab restricts the search to the specified class and, optionally, just to symbols, names and IDs (rather than ‘All text’).

Other QuickSearch tabs offer dedicated search options for particular data classes or associated data. The ‘References’ tab allows field-specific searching of the comprehensive set of *Drosophila*-specific publications in the FlyBase bibliography [3]. Similarly, the ‘Human Disease’ and ‘Gene Groups’ tabs facilitate searching of these particular classes of integrated data (see Subheading 9). Rather than searching by data class, the remaining QuickSearch tabs allow searching for entities that share Expression, Phenotype, Protein Domain, or Gene Ontology (GO) annotations.

If a query in QuickSearch, or any other FlyBase tool, results in multiple possible matches, then a tabular ‘hit list’ is produced [4]. The hit list serves as a core list-management tool in FlyBase and can be manipulated in several ways. The entire list, or a selected subset, can be: sorted by the entries in any of the columns; analyzed or refined by criteria appropriate to the given data; converted to a related data class (e.g., alleles converted to genes); downloaded as a list; or exported to other FlyBase tools for further refinements or to download specified data.

2.3 Jump to Gene

‘Jump to Gene’ is a navigation tool located in the NavBar and is thus available from all FlyBase pages. It is useful for quickly moving between Gene Reports where the current FlyBase gene symbol or ID (FBgn number) is known. (Greek characters must be spelled out, e.g., ‘ α -Est1’ as ‘alpha-Est1’.) In fact, ‘Jump to Gene’ also accepts current FlyBase IDs for all data classes, thus providing a direct route to other reports of interest. Note that input not recognized as a valid symbol or ID is treated as a gene synonym and a best match to a gene will be attempted. As the best match may not be to the intended gene, ‘Jump to Gene’ should not be used as a query tool—the ‘Simple’ or ‘Data Class’ tabs of QuickSearch should be used when the current FlyBase symbol or ID is not known for certain or when conducting a search.

3 The Gene Report

The Gene Report is the best place to start for users interested in a particular gene [2] (Fig. 2). In addition to listing gene-centric data (e.g., genomic location, expression data, orthologs), this report also summarizes data more fully described in separate reports (e.g., mutant alleles, phenotypes of those alleles, protein interaction data) and provides many links both within FlyBase and to external sites where additional information or details can be found. As such, Gene Reports act as hubs from which to explore all that is known about *Drosophila* genes.

The upper ‘always open’ part of the Gene Report has recently been reorganized to emphasize functional information, including a new section labeled ‘Families, Domains and Molecular Function’ (Fig. 2). This section highlights membership of the gene to any FlyBase ‘gene groups’ (see Subheading 9.2) or UniProt protein families, any predicted UniProt or InterPro domains/motifs, and summarized molecular function data based on FlyBase GO annotations. At the top of the report, the ‘General Information’ section includes gene identifiers (FlyBase ID, symbol, name, and CG number), the ‘Feature type’ (e.g., ‘protein coding gene’, ‘miRNA gene’, or ‘pseudogene’), and the ‘Gene Model Status’, which helps to distinguish genes currently localized to the sequenced genome

FB2015_04, released September 3, 2015

FlyBase

Gene *Dmel\zip*

Home Tools Downloads Links Community Species About Help Archives Jump to Gene Go

FlyGene Wiki Help Open All Close All

General Information

Symbol	<i>Dmel\zip</i>	Species	<i>D. melanogaster</i>
Name	zipper	Annotation symbol	CG15792
Feature type	protein_coding_gene	FlyBase ID	FBgn0265434
Gene Model Status	Current	Stock availability	17 publicly available
Also Known As	Myoll, Myo, Myo II, MHC, Myo-II, nmMHC, E(br), Mhc-c		

Genomic Location

Cytogenetic map	60E11-60E12	Sequence location	2R:24,990,570..25,011,965 [-]
-----------------	-------------	-------------------	-------------------------------

Genomic Maps

GBrowse

Decorated FASTA

Get genome region

Gene region

Get FastA

Families, Domains and Molecular Function

Gene Group Membership (FlyBase)	MYOSINS
Protein Family (UniProt, Sequence Similarities)	Belongs to the TRAFAC class myosin-kinesin ATPase superfamily. Myosin family. (ECO:0000305). (Q99323)
Protein Domains/Motifs	<p>UniProt (Sequence Similarities) Contains 1 IQ domain. (ECO:0000255 PROSITE-ProRule:PRU00116). (Q99323) ; Contains 1 myosin motor domain. (ECO:0000305). (Q99323)</p> <p>InterPro IQ motif, EF-hand binding site; Myosin head, motor domain; Myosin tail; Myosin, N-terminal, SH3-like; Myosin-like IQ motif-containing domain; P-loop containing nucleoside triphosphate hydrolase</p>
Molecular Function (see GO section for details)	<p>Experimental Evidence myosin light chain binding</p> <p>Predictions/Assertions ATP binding; ATPase activity, coupled; motor activity</p>

Gene Ontology (GO): (47 terms)

- Molecular Function (4 terms)
- Biological Process (31 terms)
- Cellular Component (12 terms)
- Summaries
- Recent Updates
- Interactions and Pathways
- Expression Data
- Alleles and Phenotypes
 - Summary of Allele Phenotypes
 - Phenotypic Description from the Red Book (Lindsley and Zimm 1992)
 - Classical Alleles (30)
 - Alleles Carried on Transgenic Constructs (22)
 - Deletions and Duplications
 - Transgenic Constructs and Insertions
- Orthologs
- Human Disease Model Data
- Gene Model and Products
- Genomic Location and Detailed Mapping Data
- Stocks and Reagents
 - Stocks Listed in FlyBase (17)
 - Genomic Clones (1)
 - cDNA Clones (157)
 - RNAi and Array Information
 - Antibody Information
 - Other Information
 - External Crossreferences and Linkouts
 - Synonyms and Secondary IDs (69)
 - References (460)

Fig. 2 The Gene Report, using *zipper* as an example. The ‘Alleles and Phenotypes’ and ‘Stocks and Reagents’ sections have been opened to show the first tier of subsections

from those whose gene model is incomplete/withdrawn or genes defined only by mutations. Below this is a section summarizing ‘Genomic Location’ information. It gives the cytogenetic position and sequence coordinates of the gene, alongside a graphical snapshot of its genomic location and convenient options to download FASTA files associated with the gene model.

The remaining data are organized into separate sections that are closed by default and can be opened by clicking on their title bars (Fig. 2). Several of these have been updated in recent years. For example, the ‘Gene Ontology (GO)’ section that displays the full set of GO annotations [5] now clearly distinguishes terms based on experimental evidence from those based on predictions/assertions. The ‘Summaries’ section that follows has also been revised and now contains additional entries including a description of the FlyBase gene group to which the gene belongs and a functional summary imported from UniProt. Further down the page, the ‘Orthologs’ section now contains three discrete subsections. The first, labeled ‘OrthoDB Orthologs’, displays the orthologs of the given gene as computed by OrthoDB [6], arranged into taxonomic groups. The second subsection, ‘Human Orthologs’ specifically highlights the orthologous human gene(s) (again inferred by OrthoDB). Here, links are provided to the corresponding Ensembl [7], HUGO Gene Nomenclature Committee (HGNC [8]) and Online Mendelian Inheritance in Man® (OMIM® [9]) gene and phenotype (disease) reports. Finally, the ‘External Data’ subsection features link-outs to species-specific orthologs determined by the integrative ortholog prediction tool, DIOPT [10]. Note that link-outs such as these appear in several sections of the Gene Report and are consolidated in the ‘External Cross-references and Linkouts’ section toward the bottom of the report, facilitating navigation between databases.

Several other Gene Report sections have seen more significant updates, including expression data, physical interactions, and models of human disease. These are described separately below.

Querying genes and gene-related data: Gene Reports themselves are best found via the ‘Jump to Gene’ box on the NavBar or via the ‘Simple’ or the ‘Data Class (genes)’ tabs of QuickSearch. GO and Protein Domain annotations can be searched via their dedicated QuickSearch tabs. Strategies for searching for data in other sections or fields of the Gene Report are detailed below, or may be addressed using QueryBuilder [11] or the ‘Simple’ tab of QuickSearch.

4 Alleles and Phenotypes

The generation and study of mutants have been central to *Drosophila* research ever since its very beginnings [12] and remain a major component of FlyBase today. These data are summarized on the relevant Gene Report in the ‘Alleles and Phenotypes’ section

(Fig. 2), and are described in full in separate Allele Reports (not shown). FlyBase makes extensive use of controlled vocabularies (CVs or ‘ontologies’) in recording allelic and phenotypic data [13, 14]. These are collections of related terms (e.g., ‘allele class’, ‘phenotypic class’, ‘fly anatomy’) arranged into parent–child hierarchies. They allow a single, defined term to be used across all FlyBase annotations, which in turn allows users to search with that term (or any of its synonyms) to retrieve all records annotated with it or its children. CV terms and associated annotations can be queried using the Vocabularies tool [11] (formerly TermLink), accessible via the pictograph on the homepage or the Tools menu of the NavBar.

4.1 Classical Alleles, Transgenic Constructs, and Insertions

Classical alleles are defined as mutations that affect a gene at its endogenous locus. They are presented in Allele Reports and also appear in the ‘Classical Alleles’ subsection on the Gene Report (Fig. 2). They traditionally include point mutations, insertional mutations and intragenic deletions, though more recent additions include lesions induced by various recombination-mediated techniques and site-specific cleavage events. Where known, mutations are annotated with an ‘origin of mutation’ term (e.g., ‘ethyl methanesulfonate’ or ‘CRISPR/Cas9’), an ‘allele class’ term (e.g., ‘amorphic allele’) and details of their molecular lesion. If the mutation is caused by an insertion of a transposable element, then both an Allele Report and an Insertion Report are created to completely describe the lesion, with a prominent link forged between them.

The molecular details and uses of transgenic constructs appear in dedicated Recombinant Construct Reports. In addition, an associated Allele Report is created in such cases in order to properly and fully capture phenotypic data. That is, the Alleles data class in FlyBase comprises both ‘classical alleles’ and ‘alleles carried on transgenic constructs’, as indicated within the ‘Alleles and Phenotypes’ section of the Gene Report (Fig. 2). The allele ‘origin of mutation’ CV has been expanded to accommodate this convention and so includes terms such as ‘in vitro construct—RNAi’. The relationship between constructs and their associated alleles is clearly indicated and reciprocally linked in their respective report pages. Similarly, any specific insertions of a transgenic construct are captured in Insertion Reports and are reciprocally linked to their corresponding Recombinant Construct Report.

Recombinant Construct or Insertion Reports, as appropriate, are also made for reporters (e.g., lacZ or GFP) or binary drivers (e.g., GAL4). Again, an associated Allele Report is made in all these cases so that phenotypic (and expression) data dependent on their use can be stored and presented in a consistent manner across the database. Note that FlyBase uses a species prefix to distinguish genes originating from ‘foreign’ (non-*D. melanogaster*) species, and so these examples appear as alleles of ‘*Eco*\lacZ’, ‘*Arv*\GFP’, and ‘*Scer*\GAL4’ on the website.

Transgenic techniques and resources are constantly expanding [15]. FlyBase responds to the former by devising suitable curation strategies and/or revising CVs as appropriate. One response to the latter is the creation of the Large Dataset Metadata Report that collates the metadata and membership of large-scale collections of constructs, insertions, etc. (see Subheading 9.1). The report page of each member contains basic descriptive information about the collection, together with a link to the respective metadata report.

Querying alleles, constructs, and insertions: Specific alleles, transgenic constructs or insertions are best searched via the ‘Data Class’ tab of QuickSearch. As mentioned, the Vocabularies tool is useful to find instances of particular allele classes or mutagenic techniques, which can then be refined further using other FlyBase tools. CytoSearch, FeatureMapper, or GBrowse (see Subheading 7) are the preferred methods if you are looking for reagents that are mapped to specific genomic regions.

4.2 Phenotypes

Phenotypic data are attached to alleles or allele combinations using terms from the ‘phenotypic class’ and ‘fly anatomy’ CVs. The phenotype CV comprises ~190 terms that are commonly used to describe *Drosophila* phenotypes, such as ‘lethal’, ‘sterile’, ‘homeotic’ or ‘Minute’ [13]. The anatomy CV is much larger, comprising >8800 terms that can be used to comprehensively describe *Drosophila* anatomy [14]. Both types of CV term can be refined through the use of ‘qualifier’ terms that restrict the meaning of the term to a specific developmental stage, sex or other experimental/genetic condition—these appear after a ‘pipe’ symbol on the website, for example ‘small body | larval stage’. Any additional genotypic components that are necessary for the given phenotype, such as alleles *in trans* or GAL4 drivers, are included in the phenotype annotation and appear with the prefix ‘with’ on the website. CV-based phenotypic annotations are often supplemented with free text clarifications or extra details. All phenotypic statements in FlyBase are curated from the published literature.

CV-based phenotype annotations are shown with their associated allele in a table on the Gene Report in the ‘Summary of Allele Phenotypes’ subsection (Fig. 2). Clicking on an individual allele takes you to the corresponding Allele Report that additionally contains any free text description of the phenotype together with the source reference(s).

Querying phenotypes: The dedicated ‘Phenotype’ tab in QuickSearch facilitates searching of alleles by phenotypic class and/or anatomy terms, with an option to refine the search through the use of qualifiers. The Vocabularies tool offers a browsable view of the same data, while QueryBuilder can be used to compose more complex combinatorial queries.

4.3 Disease Model Annotations

Drosophila alleles or allele combinations that generate phenotypes stated to be models of human disease are additionally annotated

using appropriate terms from the Disease Ontology [16, 17]. As for regular phenotypes, disease model annotations may be associated with either classical alleles (of fly genes orthologous to human ‘disease genes’) or with transgenic alleles (where disease-causing forms of human genes, or their *Drosophila* orthologs, are expressed via transgenic constructs). The criterion for disease annotation in FlyBase is that the phenotype must recapitulate some aspect of the disease pathology, though this can range from anatomical defects or behavioral abnormalities to cellular or molecular changes. Additional alleles may be described as modifying a disease model, either ‘ameliorating’ or ‘exacerbating’ it, if genetic interactions are observed. This information is presented in tabulated form in both the Gene Report and Allele Report in the section titled ‘Human Disease Model Data’ as well as in the new Human Disease Model Report (*see* Subheading 9.3).

Querying disease model annotations: The ‘Human Disease’ tab of QuickSearch and the Vocabularies tool can both be used to find a Disease Ontology term and view records annotated with it.

5 Expression Data

Separate Gene Expression Reports have been retired from FlyBase in favor of integrating these data into the Gene Report in a dedicated ‘Expression Data’ section (Fig. 2). Expression data may derive from either ‘low-’ or ‘high-throughput’ studies.

5.1 Low-Throughput Expression Data

Traditional expression assays, such as *in situ* hybridization or immunolocalization to embryos or tissues, and stage- or tissue-specific Northern blots, are presented in the first three subsections of the ‘Expression Data’ section: ‘Transcript Expression’, ‘Polypeptide Expression’, and ‘Expression Deduced from Reporters’. These are data from the published literature, captured in a highly controlled format using the FlyBase anatomy and developmental stage CVs. For nuanced aspects of an expression pattern additional free-text descriptions are provided. Embryonic transcript expression data include data from the BDGP [18], which comprises *in situ* hybridizations using cDNA probes for over 7000 genes, plus descriptions conforming to the FlyBase anatomy CV. The actual *in situ* images can be viewed by following the ‘BDGP expression data’ link in the subsection ‘External Data and Images’ (*see* Subheading 5.3).

Querying low-throughput expression data: The use of hierarchical CVs allows expression data captured at a very detailed level to be queried using more general terms. The QuickSearch ‘Expression’ tab provides a dedicated interface for this type of query. It also allows combinatorial queries, typically to specify both stage and tissue. The initial hit list returned by this query is of endogenous genes for which the expression pattern is observed; reporter constructs or insertions can be retrieved by selecting one of the alternative result options at the top of the initial hit list.

5.2 High-Throughput Expression Data

Within the ‘Expression Data’ section of the Gene Report, the ‘High-Throughput Expression Data’ subsection includes expression plots of high-throughput mRNA RNA-Seq data from modENCODE [19] and mRNA microarray data from FlyAtlas [20]. FlyBase has produced quantitative views of these data in different stages, tissues, and cell culture types presented as bar graphs (Fig. 3). For the RNA-Seq data, RPKM counts [21] (reads per kilobase per million reads) have been calculated, averaged over the exonic extents of the gene. A further subsection, ‘Expression Clusters’, provides links to datasets consisting of genes possessing similar mRNA RNA-Seq expression dynamics, as determined by modENCODE [19, 22].

Querying high-throughput expression data: Several new FlyBase tools that use the calculated RPKM data have been developed. The

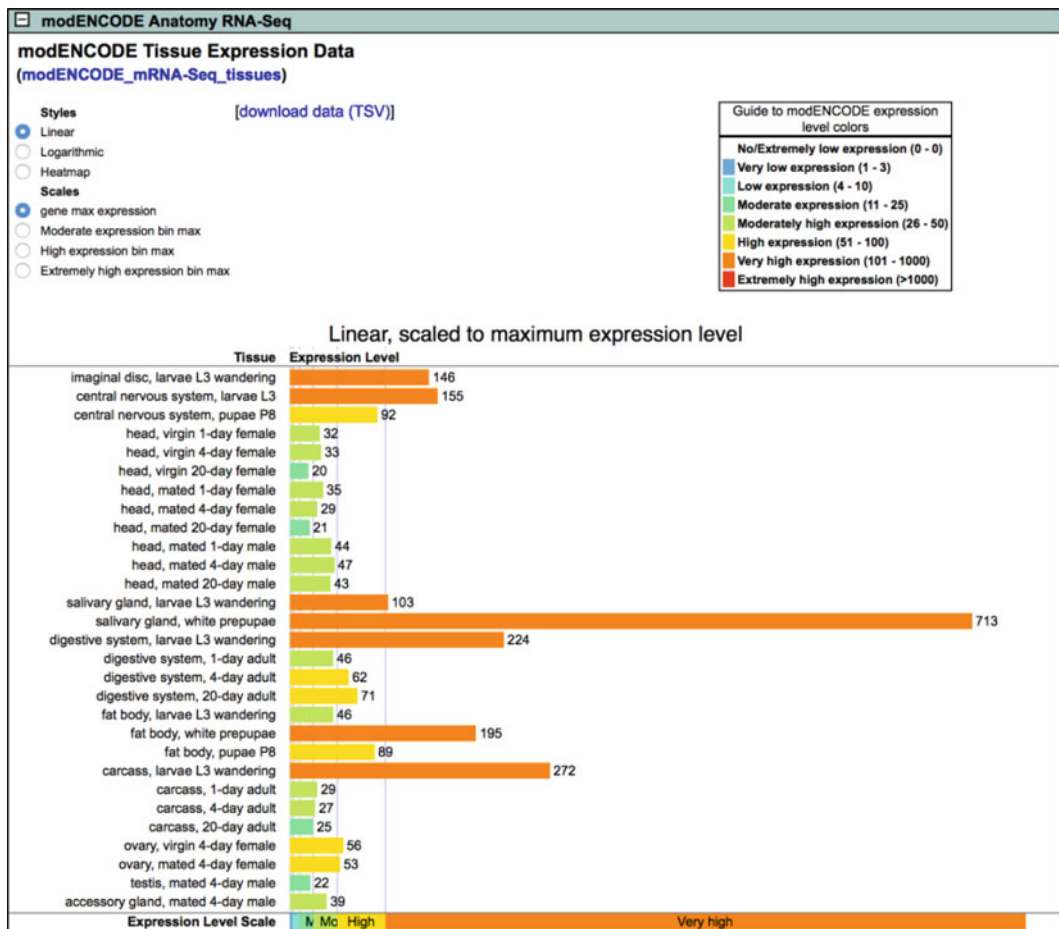


Fig. 3 High-throughput expression data. Bar graph of modENCODE RNA-seq tissue expression data for the *zipper* gene, as shown within the ‘Expression Data’ section of the Gene Report. In this example, the view is configured to be linear and scaled to the gene’s maximum expression level

versatile ‘RNA-Seq Profile’ tool allows retrieval of genes with user-defined RNA-Seq expression patterns and levels (values are binned); this tool can be accessed from a pictograph on the homepage, from the Tools menu of the NavBar, or from the QuickSearch ‘Expression’ tab. A section of the QuickSearch ‘Expression’ tab also provides options to ‘Search for similarly expressed genes’, using the modENCODE RNA-Seq datasets. The ‘RNA-Seq by Region’ tool returns the average RPKM over a specified genomic region and also offers the option of a gene-specific query that returns an exon-by-exon RPKM count; this tool can be accessed from the Tools menu or from the ‘High-Throughput Expression Data’ subsection of the Gene Report.

5.3 External Link-Outs

The final ‘Expression Data’ subsection on the Gene Report is ‘External Data and Images’, with gene-specific links to other databases that include expression data for *Drosophila*. There are links to the original BDGP *in situ* data, as well as FlyExpress [23] analyses that use the BDGP data and allow a ‘Find Similar Patterns’ option. The FlyAtlas link provides the underlying microarray data used for the bar graphs described above. For the FlyExpress and SliceSeq [24] databases, sample images are shown.

6 Interactions

Both genetic and physical interaction data are presented in FlyBase. The former are primarily recorded in Allele Reports, while the latter are given in dedicated Physical Interaction Reports; both are summarized in the ‘Interactions and Pathways’ section of the relevant Gene Report page. Both types of interaction can be viewed either as a graphical ‘network diagram’ provided by esyN [25] or within the FlyBase Interactions Browser tool that includes additional viewing and configuration options [4]. The ‘External Data’ subsection of the ‘Interactions and Pathways’ part of the Gene Report provides link-outs to relevant pages at third-party interaction databases, including BioGRID [26], DROID [27], and InterologFinder [28].

6.1 Genetic Interactions

Genetic interaction data are recorded at the allele level using phenotypic class and anatomy CV terms (and optional qualifiers), similar to phenotype annotations but with the addition of terms such as ‘enhanced by’ or ‘suppressor of’ to indicate the nature of the interaction, together with the interacting allele. (Negative results, e.g., ‘not enhanced by’, are also captured.) In addition to enhancer/suppressor-type interactions, synthetic phenotypes that are present in a mutant combination but absent in single mutant conditions are also captured. All these interaction statements appear in the ‘Interactions’ section of the Allele Report, alongside free text clarifications where necessary. All genetic interaction statements in FlyBase are curated from the published literature.

The allele-level genetic interaction statements are used to compute a gene-level summary of these data, and this appears as a table within the ‘Summary of Genetic Interactions’ subsection in the Gene Report. This table shows the interacting genes, the nature of the interaction (limited to enhancer/suppressor-type interactions), and the reference(s) supporting the interaction. These gene-level interactions are used to power the esyN network diagram.

Querying genetic interactions: Both allele-level and gene-level genetic interaction data can be queried directly via the Interactions Browser tool. More specific and/or combinatorial searches may be conducted using QueryBuilder.

6.2 Physical Interactions

The Physical Interaction Report displays pairwise physical interaction data for gene products, either protein–protein or RNA–protein. Each report includes the experimental assays used (e.g., co-immunoprecipitation, peptide mass fingerprinting), the role of each protein in an assay (e.g., bait or prey; whether a tagged or endogenous protein was used), the esyN network diagram, and a link to the Interactions Browser tool. With the goal of producing a set of high-confidence pairwise interactions, our current focus is on smaller-scale physical interaction data curated from the literature, which usually include multiple types of support for a described interaction. High-throughput interaction datasets are curated only when the authors take care to filter out false positives—criteria for curation may include: multiple negative control purifications, accounting for protein abundance in assessing the likelihood that a purified factor is a contaminant, a calculation of the confidence level, and an explicit cut-off to separate high confidence and lower confidence interactions. Examples are the DPiM dataset [29], the Hippo Pathway Interactome [30], and the ECIA extracellular interactome [31].

Within the ‘Summary of Physical Interactions’ subsection of the Gene Report, all pairwise physical interactions involving that gene product are presented in tabulated form, with assays used, attributed publications, and links to the corresponding Physical Interaction Report.

Querying physical interactions: The ‘Simple’ or the ‘Data Class (physical interactions)’ tabs of QuickSearch can be used to find interactions involving a given gene or to search for assay terms present in the Physical Interaction Report.

7 Genomic Data

Genomic data in FlyBase comprise gene model annotations (i.e., the exon–intron structure and transcription and translation start/termination sites of genes) and any other sequence-based features that can be mapped to specific genomic coordinates, whether endogenous (e.g., regulatory regions, origins of replication) or describing a lesion/reagent (e.g., insertion sites, RNAi amplicons). All these data

are viewable through the FlyBase implementation of GBrowse [32] (Fig. 4). Many are also associated with discrete Sequence Feature Reports and are searchable through the FeatureMapper tool [11] (Fig. 5). Note that FlyBase currently uses release 6 of the sequenced *D. melanogaster* genome [33]—the Coordinates Converter tool, accessible from the Tools menu of the NavBar, can be used to convert data from release 3, 4, or 5 coordinates [32].

7.1 Gene Model Annotations in FlyBase

For *D. melanogaster*, FlyBase has produced manually annotated gene models for over a decade [34]. Since 2010, RNA-Seq data [19, 35] and new transcription start site data [33, 36] have supported many major changes in the gene model annotations for this species. This prompted a comprehensive review of all existing gene models and the annotation of several thousand new genes, primarily long non-coding RNA genes [34]. Transcript and protein data are tabulated in the ‘Gene Model and Products’ section of the Gene Report (Fig. 2), with links therein to more detailed reports. *D. melanogaster* gene models continue to be updated regularly based on new high-throughput and literature-based data. An updated gene model set is submitted to GenBank approximately once a year and serves as the NCBI RefSeq set for this species.

For eight of the other sequenced *Drosophila* species (*D. ananassae*, *D. erecta*, *D. pseudoobscura pseudoobscura*, *D. simulans*, *D. yakuba*, *D. mojavensis*, *D. virilis*, and *D. willistoni*), the long-standing CAF1-generated gene model annotations [37] have been replaced recently by sets generated by NCBI as part of their GNOMON annotation pipeline [38]. Gene model annotations for three other species (*D. grimshawi*, *D. persimilis*, and *D. sechellia*) have not been updated owing to poor genome assembly quality or to lack of RNA-Seq data, which provides the primary basis for robust annotation by the GNOMON pipeline.

Querying gene model data: Gene models can be searched directly in GBrowse (Subheading 7.2) or via the CytoSearch or FeatureMapper tools (both accessible via the Tools menu of the NavBar). The FlyBase BLAST tool allows sequence-based queries against annotated transcripts or proteins from the 12 *Drosophila* species mentioned above. For *D. melanogaster*, Sequence Ontology terms and controlled comments have been used extensively to describe gene models and transcripts [34, 39]. These enable queries for exceptional cases, such as all genes with dicistronic transcripts or all transcripts annotated with non-canonical translation

Fig. 4 (continued) (C) Mousing over an individual RNA-Seq junction produces a pop-up that provides read counts; relative read counts of the two selected junctions indicate that the small alternative exon is not present in the majority of *stmA* transcripts. (D) Mousing over a Transgenic Insertion Site produces a pop-up with additional information, including whether there is a publicly available stock. For other genomic reagents, such as the Point Mutations and RNAi amplicons shown, availability of stocks can be determined by clicking through to the full reports

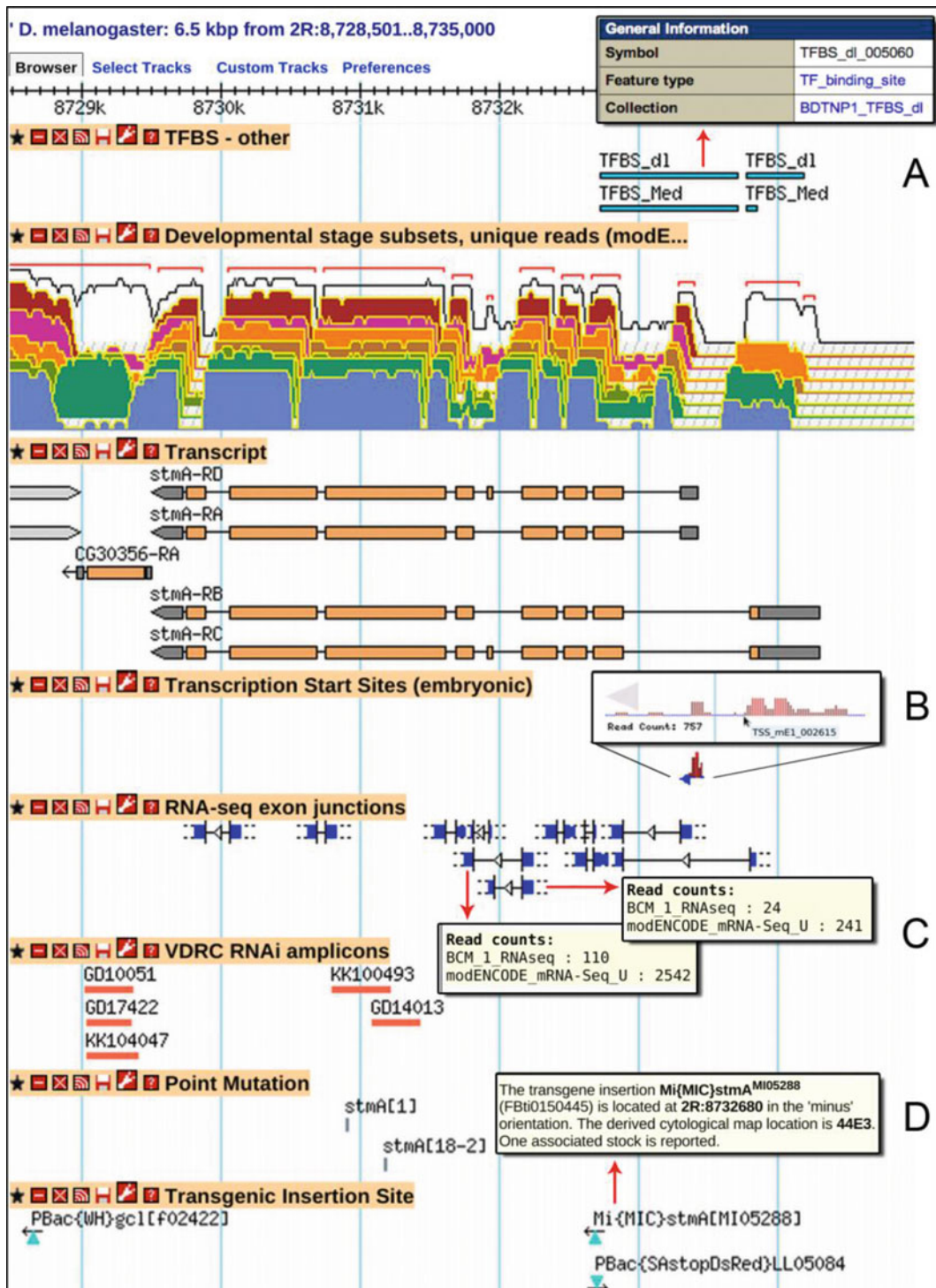


Fig. 4 GBrowse. This view of sequence features and genomic data in the region of the *stmA* gene has been customized by: (1) using the 'Select Tracks' option at the upper left to turn several default tracks off and new data tracks on; and (2) using track-specific options accessed from the wrench/spanner icon in the title bar to select a subset of the RNA-Seq dataset shown; and (3) dragging tracks to preferred positions vertically. (A) Clicking on most objects in GBrowse links to the full FlyBase report for that feature, as shown here for a transcription factor binding site (TFBS) sequence feature. (B) By zooming in, the details of a defined Transcription Start Site (TSS) can be seen, including a bar graph of TSS distribution within the defined region and the total number of reads.

Mapping Options

Reference Landmark(s) or Region(s)
Enter ID, Symbol, annotation ID or Sequence Region:
2R:8728501..8735000

Set region type to map
Sequence of the Landmark
 Include overlapping (not fully enclosed within query region) features

Species: D. melanogaster

Map Features:

<input type="checkbox"/> Gene Models	<input type="checkbox"/> Noncoding Features	<input type="checkbox"/> Mapped Mutations
<input type="checkbox"/> Genes	<input type="checkbox"/> Regulatory Regions	<input checked="" type="checkbox"/> Transgene insertion sites
<input checked="" type="checkbox"/> mRNA (transcript)	<input type="checkbox"/> Insulator class I	<input checked="" type="checkbox"/> Point Mutation
<input type="checkbox"/> exon	<input type="checkbox"/> Insulator class II	<input type="checkbox"/> Sequence Variant
<input type="checkbox"/> five_prime_UTR	<input type="checkbox"/> Protein binding site	<input type="checkbox"/> Uncharacterized Change in Seq.
<input type="checkbox"/> three_prime_UTR	<input type="checkbox"/> Enhancers	<input type="checkbox"/> Aberration Junction
<input type="checkbox"/> tRNA	<input type="checkbox"/> Silencers	<input type="checkbox"/> Complex Substitution
<input type="checkbox"/> miRNA	<input type="checkbox"/> TFBS - HOT spot analysis	<input type="checkbox"/> Indels
<input type="checkbox"/> snRNA	<input type="checkbox"/> TFBS - zinc finger domain	<input type="checkbox"/> Rescue Fragment
<input type="checkbox"/> snoRNA	<input type="checkbox"/> TFBS - homeodomain	<input type="checkbox"/> RNAI Reagents and Data
<input type="checkbox"/> CDS (polypeptide)	<input type="checkbox"/> TFBS - helix-loop-helix domain	<input type="checkbox"/> DGRC-1 amplicons
<input type="checkbox"/> Natural TE	<input type="checkbox"/> TFBS - BTB/POZ domain	<input type="checkbox"/> DGRC-2 oligos
<input type="checkbox"/> Aligned Evidence	<input checked="" type="checkbox"/> TFBS - other	<input type="checkbox"/> DRSC RNAi amplicons
<input type="checkbox"/> cDNA	<input type="checkbox"/> Origin of replication	<input checked="" type="checkbox"/> VDRC RNAi amplicons
<input type="checkbox"/> ESTs	<input type="checkbox"/> RNA Editing Sites	<input type="checkbox"/> TRIP RNAi amplicons
<input checked="" type="checkbox"/> RNA-seq Exon Junctions	<input type="checkbox"/> Putative Brain Enhancers	<input type="checkbox"/> BKNA RNAi amplicons
<input type="checkbox"/> Peptide Atlas peptides	<input type="checkbox"/> VDRC Vienna Tiles GAL4 lines	<input type="checkbox"/> HFA RNAi amplicons
<input type="checkbox"/> Microarray Features		
<input type="checkbox"/> Affymetrix v1		
<input type="checkbox"/> Affymetrix v2		

Check all **Uncheck all**

Group output features by type GFF lines output

Submit Query

2R:8728501..8735000



mRNA (transcript)				to HitList
2R:8724258..8728999	-->	mRNA		gcl-RB
2R:8724258..8728999	-->	mRNA		gcl-RA
2R:8728964..8729501	<->	mRNA		CG30356-RA
2R:8729502..8734304	<->	mRNA		stmA-RB
2R:8729502..8734304	<->	mRNA		stmA-RC
2R:8729502..8733436	<->	mRNA		stmA-RD
2R:8729502..8733436	<->	mRNA		stmA-RA
RNA-seq Exon Junctions				to HitList
2R:8729812..8730133	<->	exon_junction		Dmel:r6:2R:8729879:8730064:-
2R:8730622..8730819	<->	exon_junction		Dmel:r6:2R:8730688:8730749:-
TFBS - other				to HitList
2R:8732722..8733712	-->	TF_binding_site		TFBS_Med_002594
2R:8733774..8733845	-->	TF_binding_site		TFBS_Med_002595
2R:8732722..8733712	-->	TF_binding_site		TFBS_dl_005060
2R:8733774..8734183	-->	TF_binding_site		TFBS_dl_005061
Transgene insertion sites				to HitList
2R:8733055..8733055	-->	transposable_element_insertion_site		PBac(WH)stmA[f03887]
2R:8733630..8733630	-->	transposable_element_insertion_site		PBac(RB)stmA[e00058]
Point Mutations				to HitList
2R:8730896..8730896	<->	point_mutation		stmA[1]
2R:8731170..8731170	<->	point_mutation		stmA[18-2]
VDRC RNAi amplicons				to HitList
2R:8729022..8729354	<->	RNAi_reagent		dsRNA-GD10051
2R:8729037..8729346	<->	RNAi_reagent		dsRNA-GD17422

Fig. 5 FeatureMapper. (1) Query interface. In this example, a single sequence range has been entered and several mapped features have been selected (corresponding to the GBrowse view shown in Fig. 4). The default output is to group features by type in HTML format. (2) Mapping results. The sequence coordinates, strand and

start sites, using QueryBuilder or the ‘Simple’ tab of QuickSearch. ‘Transcripts’ and ‘Polypeptides’ are data class options in QuickSearch and QueryBuilder, thus allowing class-specific and field-specific queries of gene products, respectively.

7.2 GBrowse

GBrowse, a genome annotation viewer that is part of the Generic Model Organism Database (GMOD) tool suite [40], is used by FlyBase to show gene models and supporting data, such as cDNAs, ESTs, RNA-Seq data, transcription start sites, gene predictions, and aligned proteins [32] (Fig. 4). In addition, this versatile tool allows representation of many other types of sequenced-based data and reagents—essentially anything that maps to the genome can be represented on GBrowse. By using the ‘Select Tracks’ option, the user can choose to view mapped genetic variants such as mutational lesions, transgenic insertions, aberration extents, and aberration breakpoints; regions carried on transgenic constructs such as rescue fragments and RNAi reagents; microarray oligonucleotides and RNAi amplicons; or high-throughput mapping of transcription-factor binding sites, insulator elements, and RNA-editing sites. When zoomed in to a range of 100–200 bp, the tracks indicating forward/reverse translation and ‘DNA/GC content’ switch to the nucleotide or protein sequence. The current version of this tool is GBrowse2 [41], which allows rapid customization options: for example, a selected track can be moved by simply dragging the track title bar vertically, and tracks can be closed, opened, or removed using the icons in the track title bar. Moreover, navigation within a genomic region has been facilitated by limited smooth-track panning (side-to-side sliding) and by a function that allows the user to lasso a smaller region and zoom in.

RNA-Seq expression data [19, 42] are particularly informative when viewed in GBrowse. In 2010, FlyBase debuted a new topographical presentation of these data for GBrowse that allows visual assessment of many RNA-Seq tracks at once (Fig. 4). By clicking on the wrench/spanner icon in the track title, the presentation can be changed from *log2* to linear, and from tilted to vertical; specific tracks corresponding to different tissues and/or development stages can be shown or hidden. RNA-Seq exon junction data [19, 35], presented in a separate track on GBrowse, are extremely useful for judging alternative splicing and isoform-specific expression.

GBrowse supports a number of download options, accessible from the drop-down menu on the upper right of the page, including a FASTA file of the sequence shown and an HTML table view or a GFF file of all the mapped genes and features selected. The sequence of a lassoed genomic region can also be viewed and downloaded.

Fig. 5 (continued) symbol of each sequence feature are presented in a table. Links to hit lists are shown for each group to enable further analyses or downloads. (Note that only a subset of hits of each type is shown in this example.)

GBrowse can be accessed from one of the pictograph buttons at the top of the homepage or via the Tools menu on the NavBar. In addition, there is a link to the appropriate genomic region in GBrowse on the reports for every localized gene and mapped sequence feature. A genomic BLAST hit obtained using the FlyBase BLAST tool also includes a link to the relevant region in GBrowse.

7.3 Sequence Features and Other Genomic Data Tracks

‘Sequence features’ are defined as regions of DNA/RNA that can be mapped to the genome sequence and to which a discrete function can usually be ascribed. They include endogenous regions such as enhancers, insulators, transcription factor binding sites, transcription start sites and origins of replication, as well as experimental reagents that map to the genome, such as RNAi reagents and putative enhancer element constructs. Sequence features appear within discrete tracks on GBrowse and are associated with dedicated report pages. (Note that certain GBrowse tracks, including point mutations, transgenic insertions, and aberration extents, are not classed as ‘sequence features’ and are instead associated with specific Allele, Insertion, or Aberration Reports.) Most sequence features currently in FlyBase were generated in response to the modENCODE project [22] and similar large-scale experiments [43, 44].

The Sequence Feature Report is flexible, in order to accommodate many different types of genome-associated data. The typical report includes a link to the Large Dataset Metadata Report (see Subheading 9.1) to which it belongs, the sequence itself and its genomic location, a genome snapshot showing the alignment of that feature alongside other sequence features included within that region, and links to any relevant external websites/databases. Clicking on the ‘GBrowse’ link near the top of the page goes to a full genome view of the respective region in GBrowse.

Querying sequence features and other genomic data tracks: Limited querying can be performed within GBrowse itself by specifying a ‘Landmark or Region’ and selecting particular tracks for display. A better approach is to use FeatureMapper (Fig. 5), which provides an intuitive interface for retrieval of specified genome features in one or more genomic regions, with results presented in a convenient table that includes an option to export to a hit list where possible. The CytoSearch tool allows retrieval of genes, aberrations, and transgenic insertions mapped to the genomic sequence. Sequence features are also included as a specific option in the ‘Data Class’ tab of QuickSearch.

8 Reagents

There are several ways to find reagents associated with a specific gene or genomic region. The ‘Stocks and Reagents’ section of the Gene Report is a good place to start. Here, subsections list publicly

available fly stocks, genomic and cDNA clones, cell-based RNAi reagents and antibodies described in the published literature (Fig. 2). Other reagents are best found by searching a genomic region of interest using GBrowse, FeatureMapper, or CytoSearch. For example, the Janelia/GMR [45] and VDRC [44] putative enhancer collections are not associated with specific genes, while some classes of transgenic insertions are not listed in the Gene Report. Moreover, a visual representation of the location of a sequence-based reagent relative to the gene of interest is often informative when planning experiments.

8.1 Stocks

Stock Reports display the stock list genotype and the source collection, together with the stock number hyperlinked to the specific record at the appropriate stock center to facilitate ordering. There are links to Stock Reports from other appropriate reports (primarily alleles, aberrations, transgenic constructs, and insertions) throughout FlyBase. The Bloomington *Drosophila* Stock Center is the most widely represented source, though many others are included—a complete list can be found in the ‘Links’ menu on the NavBar.

Querying stocks: Stocks can be searched specifically by selecting ‘stocks’ in the ‘Data Class’ tab of QuickSearch.

8.2 Strains

FlyBase Strain Reports contain data about wild type strains such as ‘Oregon-R’, significant mutant strains such as ‘iso-1’ (the *D. melanogaster* strain sequenced by the BDGP [33]), as well as the 200 or so inbred lines generated by the *Drosophila* Genetics Reference Panel [46]. The reports include information on the origin and history of the strain alongside any known genetic or phenotypic components (e.g., the ‘iso-1’ strain harbors several mutations). Where relevant, links are also provided to Large Dataset Metadata Reports (Subheading 9.1) that describe strain collections, and to Stock Reports to facilitate ordering. (Note that stocks are instances of strains in theory, but they are effectively distinct in time and place and may have characteristics that differ from the strains from which they descended.)

Querying strains: Strains can be searched using the QuickSearch ‘Simple’ tab.

8.3 Cell Lines

Cell Line Reports display data obtained from the *Drosophila* Genomics Resource Center (DGRC) on cell lines, such as ‘Kc167’ or ‘S2R+’. The reports include the source and development stage of each line, its sex and karyotype (where known), and any parental or descendant lines. A link back to the DGRC is also provided for additional data and ordering information.

Querying cell lines: Cell lines can be searched specifically by selecting ‘cell lines’ in the ‘Data Class’ tab of QuickSearch.

8.4 cDNAs

cDNAs are shown in GBrowse and appear in the ‘Stocks and Reagents’ section of the Gene Report of the aligned gene(s). Links from GBrowse go to the GenBank report; links from the Gene

Report go to the FlyBase Clone Report. The Clone Report includes the sequence, links to GenBank, and fields for ‘Known Problems’ and ‘FlyBase assessment’. Examples of known problems are clones that are chimeric or that contain genomic DNA or transposon sequences. The FlyBase assessment field displays a note if the clone has been replaced, for example “Caution: This cDNA clone replaced by FI01005”. There is also a link to the DGRC where clones are available from that resource.

Querying cDNAs: cDNA clones can be searched specifically by selecting ‘clones’ in the ‘Data Class’ tab of QuickSearch. FeatureMapper should be used to find cDNAs associated with a specific gene or genomic region.

9 Integrated Reports

As the amount of *Drosophila* data and resources increase in FlyBase, it has become both necessary and useful to organize and integrate related data into discrete sets or collections. This has multiple benefits, including the ability to associate metadata across a range of related entities, and to present related data to users in new ways that aid comprehension. To date, FlyBase has developed three types of such integrated reports.

9.1 Large Dataset Metadata

Large Dataset Metadata Reports, previously named Library/Collection Reports, provide information on large datasets and reagent collections that apply to the set as a whole. Examples of datasets are the protein interaction network defined by the *Drosophila* Protein interaction Mapping (DPiM) project [29], the set of RAMPAGE transcription start sites [36], and datasets generated by the modENCODE project [22]. Examples of collections are the set of dsRNA amplicons used for RNAi-knockdown assays in cell culture by the *Drosophila* RNAi Screening Center [49], the set of defined X-chromosome duplications made by the Bloomington Stock Center [50], and several large construct and insertion collections. Metadata describing cDNA libraries are also captured in this format. The Large Dataset Metadata Report includes the type of dataset or collection, a brief description of the set, a summary of the experimental details, and a link to download all the associated features. Links to external data repositories and reagent sources are provided where relevant. The ‘Description’ field of the dataset report is propagated to each member report; reciprocal links are provided.

Querying large dataset metadata: The ‘Simple’ or the ‘Data Class (large dataset metadata)’ tabs of QuickSearch can be used to find datasets and collections of interest.

9.2 Gene Groups

Gene Group Reports have been introduced to allow easy access to, and analysis of, related sets of *D. melanogaster* genes and their associated data [47]. Examples of gene groups include members of a gene family (Actins, Wnts, etc.), subunits of a protein complex (proteasome, ribosome, etc.), or other functional groupings (protein kinases, Ubiquitin E3 ligases, etc.). All gene groups in FlyBase are based on published literature and the basis for the membership of each group is clearly attributed. The main feature of these reports is a ‘Members’ table that lists the genes comprising the group, arranged into a series of subgroups where appropriate. Buttons are provided to facilitate the downloading of associated data (phenotypes, expression data, protein interactions, etc.) using Batch Download (Subheading 10.2), or to further refine or analyze the gene set by exporting it to a standard hit list. Also shown are links to equivalent gene groups for other organisms, including nematodes (WormBase [48]) and humans (HGNC [8]). To aid navigation, the ‘Families, Domains and Molecular Function’ section of the Gene Report contains a link to any associated gene group(s) (Fig. 2).

Querying gene groups: Gene groups can be retrieved by entering the symbol/name of a group or any member gene in the ‘Gene Groups’ tab of QuickSearch. This tab also includes a link to a browsable list of all current gene groups in FlyBase.

9.3 Human Disease Models

Human Disease Model Reports provide a less specialized entry point into FlyBase for researchers interested in *Drosophila* models of human disease [17]. Data from numerous outside sources, including OMIM, and from recent reviews are presented in a general ‘Disease Summary’ section, followed by information on orthology between a human gene implicated in the disease and the related *Drosophila* gene(s). For many diseases, multiple causative genes have been implicated; OMIM describes these as different disease subtypes and groups them into ‘phenotypic series’. In the Human Disease Model Report, such a phenotypic series of subtypes is presented in a table titled ‘Related Diseases’, which includes links to other relevant Human Disease Model Reports and provides a quick view of which disease subtypes have been modeled in flies.

The major portion of the disease report is devoted to ‘Experimental Findings’ in *Drosophila*, focusing on disease-related implications and results. Descriptions of specific experiments are meant to be generally accessible, with links to Allele Reports with more detailed information. Results may include data using both fly genes and human genes introduced into flies. The ‘Experimental Findings’ section initiates with a FlyBase-authored summary that presents a concise review, including phenotypes, interactions, and suitability of the model for drug assays; in addition, new findings and emerging mechanistic themes are highlighted. At the end of this section, a link to the FlyBase Disease Wiki is provided; comments

and contributions from users are encouraged, especially those with expertise in the specific disease model. The last sections of the report draw relevant data from other sections of FlyBase, including physical interaction data for the orthologous *Drosophila* gene(s), a table of genetic reagents and stocks useful for investigations of human disease, and a table of Disease Ontology-based annotations of alleles used for that disease model (see Subheading 4.3).

There are links to relevant Human Disease Model Reports in the ‘Human Disease Model Data’ section of Gene Reports (Fig. 2). Note that many such links are found in FlyBase Gene Reports for human genes (e.g., *Hsap\SNCA* and *Hsap\TARDBP*).

Querying Human Disease Model Reports: These reports can be found by using the ‘Human Disease’ or ‘Simple’ tabs of QuickSearch, or by searching the Disease Ontology within the Vocabularies tool.

10 Bulk Data Analysis and Downloads

Users increasingly want to be able to process data in bulk. They may have generated a hit list of genes (or any other data class) within FlyBase, or have a list of IDs from elsewhere to upload, and wish to analyze/refine this list or obtain associated data. Alternatively, users may wish to directly obtain bulk data files corresponding to a particular data type for processing off-line.

10.1 Uploading and Analyzing Data

A list of IDs (e.g., gene symbols or CG numbers, allele or insertion symbols, FlyBase identifiers) can be pasted or uploaded into the Upload/Convert IDs tool (Fig. 6; accessed via the Tools menu on the NavBar). This tool will then validate the list, updating any obsolete IDs to the current version where possible, and generate a ‘Conversion report’ clearly indicating if any of the submitted IDs failed verification. The user can choose to correct these cases, or ignore them before proceeding to convert the list into a standard FlyBase hit list (see Subheading 2.2). This list can then be further analyzed/refined before being exported or downloaded as required.

10.2 Downloading Data

Batch Download is a powerful tool for generating customized output files in various formats for most data types in FlyBase [11]. Users may arrive at Batch Download via a hit list (as described above), by navigating to it from the Tools menu of the NavBar, or by clicking on its pictograph on the homepage. If the first, then the input list will be pre-filled (Fig. 6); otherwise the user can paste in or upload a list of symbols or IDs directly. Depending on the

Fig. 6 (continued) (first column, red box). The ‘HitList Conversion Tools’ button (orange box) is then clicked and ‘Export to Batch Download’ is selected (not shown). (4) The Batch Download interface shows the search box pre-populated with the four final gene IDs. In this example, transcript sequences in FASTA format have been selected for download with the results being sent to a ‘File’

Upload/Convert IDs

Validate Only (Update to Current IDs)

Validate and Convert into: Genes

Enter IDs or Symbols:
FBgn0011706
skl
abc
FBgn0010852
FBgn0064894
FBgn0038233
CG1274

or Upload File of IDs:
Browse... No file selected.

Go Reset

You may enter FlyBase IDs or Symbols, including Annotation Symbols and Clone Names.

IDs: Submitted: 7 Validated/Updated: 6 Unknown: 1 Final Converted: 6

Export converted IDs to: [FlyBase HitList](#) file, uniq IDs only file, conversion table

Conversion report

Submitted ID	Current ID	Converted ID	Related record
CG1274	FBgn0040308	FBgn0040308	Jafrac2
FBgn0010852	FBgn003997	FBgn0003997	hid
FBgn0038233	FBgn0038233	FBgn0038233	HtrA2
abc - unknown ID			
FBgn0011706	FBgn0011706	FBgn0011706	rpr
skl	FBgn0036786	FBgn0036786	skl
FBgn0064894	FBgn0015946	FBgn0015946	grim

6 matches Convert to Genes

Results Analysis/Refinement HitList Conversion Tools

#	Symbol	Name	Annotation ID	Cytology	Alleles #	Stocks #	Clones #
1	grim	grim	CG4345	75C4-75C4	61	10	35
2	hid	head involution defective	CG5123	75C1-75C1	81	133	33
3	HtrA2	HTRA2-related serine protease	CG8464	88C3-88C3	32	6	1
4	Jafrac2	Thioredoxin peroxidase 2	CG1274	63A3-63A3	12	5	25
5	rpr	reaper	CG4319	75C6-75C6	93	16	8
6	skl	sickle	CG13701	75C6-75C6	17	5	15

Batch Download

Output Format FASTA Sequence Database Format Field Data

Output Options Transcripts Chado XML As HTML table

Send results to: File Enter IDs, Symbols or Sequence Coordinates:
FBgn0015946
FBgn0036786
FBgn0003997
FBgn0011706

or Upload File of IDs: Browse... No file selected.

Allow synonyms Get FASTA Reset

You may enter FlyBase IDs, Symbols, Annotation Symbols, Clone Names or PubMed IDs.

Fig. 6 Batch upload and download. (1) The Upload/Convert IDs tool is used to type/paste in a mixture of gene identifiers. (2) The resulting validation report shows that six of the seven entries were validated/updated. Note that in two cases a secondary FBgn ID was entered and updated successfully. The 'FlyBase HitList' button (orange box) is then clicked to export the IDs. (3) The resulting hit list shows the six validated genes in a table with columns appropriate to the gene data class. At this stage, two of the genes have been de-selected

nature of the input and the desired outcome, the output format can then be specified as ‘FASTA Sequence’ (with the option to further specify introns, UTRs, CDS, etc.), ‘Database Format’ (XML), or as ‘Field Data’ (with output options of an HTML table, a tab-separated value (tsv) file, or in the same format as the pre-computed files described below). If the ‘Field Data’ option is selected, the user can then specify any combination of data fields (appropriate to the given data class) from a page styled in the same format as a standard FlyBase report page.

Bulk files of FlyBase data can be downloaded using our FTP site (<ftp://ftp.flybase.org/releases/>) or the ‘Downloads’ menu of the NavBar on the website (see the ‘Overview’ page under the Downloads menu for more details). ‘Precomputed files’ contain particular slices of FlyBase data that users or collaborators have requested over the years or are otherwise difficult to obtain in bulk (Table 3). Notable recent additions include *D. melanogaster* unique protein isoforms, RPKM gene expression values, gene groups, and physical

Table 3
Precomputed bulk data files available from FlyBase

File name	Brief description
<i>Genetic/genomic data</i>	
gene_map_table_*	Localization information for <i>Drosophila</i> genes
gene_orthologs_*	Dmel genes and orthologs in sequenced <i>Drosophila</i> species
gene_association.fb	Gene Ontology terms assigned to Dmel genes
gene_summaries_*	Automated gene summaries as shown on Gene Reports
gene_rpkm_report_*	Dmel gene expression values based on RNA-Seq
dmel_unique_protein_isoforms_*	Dmel genes and their unique protein isoforms
allele_phenotypic_data_*	CV phenotypic data associated with alleles
allele_human_disease_model_data_*	Disease model data associated with alleles
gene_genetic_interactions_*	Summary of Dmel gene-level genetic interactions
allele_genetic_interactions_*	Allele-level genetic interactions with CV terms
physical_interactions_*	Dmel gene pairs whose products physically interact
insertion_mapping_*	Localization information for Dmel insertions
<i>Integrated data</i>	
dataset_metadata_*	All dataset/collections and all associated features
gene_group_data_*	All gene groups, relationships and members

(continued)

Table 3
(continued)

File name	Brief description
<i>Reagents</i>	
genomic_clone_data_*	Genomic clone IDs, names, and accession numbers
cDNA_clone_data_*	cDNA/EST IDs, names, library, and accession numbers
<i>Other data files</i>	
fbrf_pmrid_pmcid_doi_fb_*	All IDs for references in FlyBase that have a PMID
species.ab	Data on all species in FlyBase, including abbreviations
<i>Correspondence tables</i>	
fb_synonym_fb_*	Symbols, names and synonyms for most features in FlyBase
fbgn_NAseq_Uniprot_*	FlyBase gene IDs ↔ nucleotide and protein accessions
fbgn_annotation_ID_*	Current and secondary FBgn and annotation IDs for genes
fbgn_fbtr_fbpp_*	FlyBase gene IDs ↔ FlyBase transcript and polypeptide IDs
fbal_to_fbgn_*	FlyBase allele IDs ↔ FlyBase gene IDs
cyto-genetic-seq	Dmel cytogenetic map ↔ genetic map ↔ genomic coord.
<i>Ontology files</i>	
fly_anatomy	Fly anatomy ontology (FBbt)
fly_development	Fly developmental stage ontology (FBdv)
flybase_controlled_vocabulary	FlyBase miscellaneous ontology (FBcv)
flybase_stock_vocabulary	FlyBase stock ontology (FBsv)
go-basic	Gene ontology (GO)
image	FlyBase image ontology (FBbi)
so	Sequence ontology (SO)
doid	Human disease ontology (DO)

Note that only a subset of the available files is shown here

*Represents the release number, for example 'fb_2015_04'; 'Dmel' = *D. melanogaster*

interactions. Also included are several useful correspondence tables and the ontology files used in FlyBase (Table 3). In addition, Chado XML (database format) files are provided for all FlyBase data classes and comprehensive sets of FASTA, GFF, and GTF files are available for the 12 originally sequenced and annotated *Drosophila* species (see Subheading 7.1). The FASTA files comprise many different cuts of genomic data, including annotation categories such as small RNA

classes and pseudogenes, components of gene model annotations such as exons, introns, UTRs and predicted translations, as well as other genome features such as transposons and intergenic sequences. As described above, Batch Download can also be used to obtain specified subsets of data in precomputed file, Chado XML or FASTA format by selecting the appropriate output options.

Most bulk files are regenerated for every release of FlyBase. Those corresponding to the current or previous (archived) versions of FlyBase are found under the appropriate submenus/subfolders on the web/FTP site. The release version used for a particular file is indicated in the file name and in the header lines of the file itself.

11 The FlyBase Community

FlyBase engages with our user community through multiple approaches. The primary method for users to get in touch with FlyBase about any matter remains our ‘Contact FlyBase’ page, accessible via the ‘Help’ menu on the NavBar or the link in the footer of any FlyBase page. All other community resources are grouped under the ‘Community’ menu of the NavBar and/or are found on the homepage.

If a user wants to specifically alert us to a *Drosophila* publication or data therein to be added to FlyBase, then the ‘Fast Track Your Paper’ (FTYP) tool should be used [51]. This tool allows the user to indicate the key genes studied and flag data types present in a paper. The resulting gene-to-publication links are submitted directly to the FlyBase database while the data type information is used to prioritize the paper for more detailed curation. We actively solicit FTYP submissions using our ‘EmailAuthor’ pipeline, whereby the corresponding author of a *Drosophila* publication is automatically sent an email that includes a link to a personalized FTYP form [51]. Approximately 50% of authors respond to this request, thereby reducing by half the amount of manual triaging to be done by FlyBase curators.

Our recently launched ‘FlyBase Community Advisory Group’ (FCAG) is a worldwide group of over 500 volunteers (lab heads, postdocs, students, technicians) who use FlyBase for a range of purposes. We contact this group up to six times per year with a survey on a variety of subjects to get feedback about how data collection, presentation, and searching on FlyBase can be improved. By consulting this relatively large, diverse group of researchers, we hope to implement changes to FlyBase that are helpful for the greatest number of people.

Users may also help improve FlyBase by contributing to the Human Disease Wiki (described in Subheading 9.3) or the FlyGene Wiki. There is a link to the latter at the top and within the ‘Summaries’ section of each Gene Report. This is pre-seeded with

the automatically generated FlyBase summary and users are encouraged to modify or add to this text to build up a more complete and readable summary of each gene's main features and functions.

The FlyBase Forum is a Google™ Group that provides an alternative, more open platform for users to interact both with FlyBase and with each other. The forum has two areas: one for general questions and discussions about FlyBase and *Drosophila* protocols, etc., and the other for relevant job postings.

Users are made aware of new or changed features in FlyBase through any of several means. First, there are the 'News' and 'Commentary' sections of the FlyBase homepage (Fig. 1). Second, users can sign up to receive an occasional Newsletter via email by clicking the link on the homepage. The Newsletter contains release announcements, significant website updates, and other important *Drosophila* community news. Third, to obtain more frequent updates, users can follow FlyBase on Twitter™ by clicking on the icon in the footer of any FlyBase page. Fourth, users can choose to subscribe to any FlyBase record (a specific gene, transgenic construct, reference, etc.) and receive automatic updates through a feed reader by clicking the icon in the 'Recent Updates' section of any report page. Finally, users have the opportunity to see and hear about FlyBase updates in person at the Annual *Drosophila* Research Conference in the USA and the biennial European *Drosophila* Research Conference, where FlyBase representatives give presentations and are available to answer questions. Previous conference presentations and pamphlets can be obtained via the 'FlyBase Guides' link under the 'Help' menu in the NavBar.

Acknowledgements

FlyBase is funded by the National Human Genome Research Institute at the U.S. National Institutes of Health (#U41HG000739, PI W.M. Gelbart) and the U.K. Medical Research Council (#G1000968, PI N.H. Brown). Support is also provided by the Indiana Genomics Initiative and the National Science Foundation through XSEDE resources provided by Indiana University. At the time of writing, the FlyBase Consortium included William Gelbart, Norbert Perrimon, Cassandra Extavour, Kris Broll, Madeline Crosby, Gilberto dos Santos, David Emmert, Sian Gramates, Kathleen Falls, Beverley Matthews, Susan Russo Gelbart, Andrew Schroeder, Christopher Tabone, Pinglei Zhou, Mark Zytkovicz; Nicholas Brown, Giulia Antonazzo, Helen Attrill, Marta Costa, Steven Marygold, Gillian Millburn, Laura Ponting, Alix Rey, Nicole Staudt, Raymund Stefancsik, Jose-Maria Urbano; Thomas Kaufman, Josh Goodman, Gary Grumblig, Victor Strelets, Jim Thurmond; Richard Cripps, Maggie Werner-Washburne, Phillip Baker.

Dedication

We wish to mark the passing of our colleague and one of FlyBase's founders, Dr. William Gelbart, who continued in his role of PI until his death. Bill's leadership, enthusiasm, insight and humor will be greatly missed.

References

1. Drysdale R, FlyBase Consortium (2008) FlyBase: a database for the *Drosophila* research community. *Methods Mol Biol* 420:45–59
2. McQuilton P, St Pierre SE, Thurmond J et al (2012) FlyBase 101—the basics of navigating FlyBase. *Nucleic Acids Res* 40:D706–D714
3. Marygold SJ, Leyland PC, Seal RL et al (2013) FlyBase: improvements to the bibliography. *Nucleic Acids Res* 41:D751–D757
4. Wilson RJ, Goodman JL, Strelets VB et al (2008) FlyBase: integration and improvements to query tools. *Nucleic Acids Res* 36:D588–D593
5. Tweedie S, Ashburner M, Falls K et al (2009) FlyBase: enhancing *Drosophila* Gene Ontology annotations. *Nucleic Acids Res* 37:D555–D559
6. Kriventseva EV, Tegenfeldt F, Petty TJ et al (2015) OrthoDB v8: update of the hierarchical catalog of orthologs and the underlying free software. *Nucleic Acids Res* 43:D250–D256
7. Cunningham F, Amode MR, Barrell D et al (2015) Ensembl 2015. *Nucleic Acids Res* 43:D662–D669
8. Gray KA, Yates B, Seal RL et al (2015) Genenames.org: the HGNC resources in 2015. *Nucleic Acids Res* 43:D1079–D1085
9. OMIM®: Online Mendelian Inheritance in Man®. <http://omim.org>
10. Hu Y, Flockhart I, Vinayagam A et al (2011) An integrative approach to ortholog prediction for disease-focused and other functional studies. *BMC Bioinformatics* 12:357
11. St Pierre SE, Ponting L, Stefancsik R et al (2014) FlyBase 102—advanced approaches to interrogating FlyBase. *Nucleic Acids Res* 42:D780–D788
12. Morgan TH (1910) Sex limited inheritance in *Drosophila*. *Science* 32:120–122
13. Osumi-Sutherland D, Marygold SJ, Millburn GH et al (2013) The *Drosophila* phenotype ontology. *J Biomed Semantics* 4:30
14. Costa M, Reeve S, Grumblung G et al (2013) The *Drosophila* anatomy ontology. *J Biomed Semantics* 4:32
15. Mohr SE, Hu Y, Kim K et al (2014) Resources for functional genomics studies in *Drosophila melanogaster*. *Genetics* 197:1–18
16. Kibbe WA, Arze C, Felix V et al (2015) Disease Ontology 2015 update: an expanded and updated database of human diseases for linking biomedical knowledge through disease data. *Nucleic Acids Res* 43:D1071–D1078
17. Millburn GH, Crosby MA, Gramates LS et al (2016) FlyBase portals to disease model research in *Drosophila*. *Dis Model Mech* 9:245–252
18. Tomancak P, Beaton A, Weiszmann R et al (2002) Systematic determination of patterns of gene expression during *Drosophila* embryogenesis. *Genome Biol* 3, RESEARCH0088
19. Graveley BR, Brooks AN, Carlson JW et al (2011) The developmental transcriptome of *Drosophila melanogaster*. *Nature* 471:473–479
20. Robinson SW, Herzyk P, Dow JA et al (2013) FlyAtlas: database of gene expression in the tissues of *Drosophila melanogaster*. *Nucleic Acids Res* 41:D744–D750
21. Mortazavi A, Williams BA, McCue K et al (2008) Mapping and quantifying mammalian transcriptomes by RNA-Seq. *Nat Methods* 5:621–628
22. modENCODE Consortium, Roy S, Ernst J et al (2010) Identification of functional elements and regulatory circuits by *Drosophila* modENCODE. *Science* 330:1787–1797
23. Kumar S, Konikoff C, Van Emden B et al (2011) FlyExpress: visual mining of spatio-temporal patterns for genes and publications in *Drosophila* embryogenesis. *Bioinformatics* 27:3319–3320
24. Combs PA, Eisen MB (2013) Sequencing mRNA from cryo-sliced *Drosophila* embryos to determine genome-wide spatial patterns of gene expression. *PLoS One* 8:e71820
25. Bean DM, Heimbach J, Ficorella L et al (2014) esyN: network building, sharing and publishing. *PLoS One* 9, e106035
26. Chatr-Aryamontri A, Breitkreutz BJ, Oughtred R et al (2015) The BioGRID interaction database: 2015 update. *Nucleic Acids Res* 43:D470–D478
27. Murali T, Pacifico S, Yu J et al (2011) Droid 2011: a comprehensive, integrated resource for protein, transcription factor, RNA and gene

interactions for *Drosophila*. Nucleic Acids Res 39:D736–D743

28. Wiles AM, Doderer M, Ruan J et al (2010) Building and analyzing protein interactome networks by cross-species comparisons. BMC Syst Biol 4:36

29. Guruharsha KG, Rual JF, Zhai B et al (2011) A protein complex network of *Drosophila melanogaster*. Cell 147:690–703

30. Kwon Y, Vinayagam A, Sun X et al (2013) The Hippo signaling pathway interactome. Science 342:737–740

31. Ozkan E, Carrillo RA, Eastman CL et al (2013) An extracellular interactome of immunoglobulin and LRR proteins reveals receptor-ligand networks. Cell 154:228–239

32. dos Santos G, Schroeder AJ, Goodman JL et al (2015) FlyBase: introduction of the *Drosophila melanogaster* Release 6 reference genome assembly and large-scale migration of genome annotations. Nucleic Acids Res 43:D690–D697

33. Hoskins RA, Carlson JW, Wan KH et al (2015) The Release 6 reference sequence of the *Drosophila melanogaster* genome. Genome Res 25:445–458

34. Matthews BB, Dos Santos G, Crosby MA et al (2015) Gene model annotations for *Drosophila melanogaster*: impact of high-throughput data. G3 (Bethesda) 5:1721–1736

35. Daines B, Wang H, Wang L et al (2011) The *Drosophila melanogaster* transcriptome by paired-end RNA sequencing. Genome Res 21:315–324

36. Batut P, Dobin A, Plessy C et al (2013) High-fidelity promoter profiling reveals widespread alternative promoter usage and transposon-driven developmental gene expression. Genome Res 23:169–180

37. Drosophila 12 Genomes Consortium, Clark AG, Eisen MB et al (2007) Evolution of genes and genomes on the *Drosophila* phylogeny. Nature 450:203–218

38. The NCBI Eukaryotic Genome Annotation Pipeline. http://www.ncbi.nlm.nih.gov/genome/annotation_euk/process/

39. Crosby MA, Gramates LS, Dos Santos G et al (2015) Gene model annotations for *Drosophila melanogaster*: the rule-benders. G3 (Bethesda) 5:1737–1749

40. GMOD: the Generic Model Organism Database project. http://gmod.org/wiki/Main_Page

41. Stein LD (2013) Using GBrowse 2.0 to visualize and share next-generation sequence data. Brief Bioinform 14:162–171

42. Berger C, Harzer H, Burkard TR et al (2012) FACS purification and transcriptome analysis of *Drosophila* neural stem cells reveals a role for Klumpfuss in self-renewal. Cell Rep 2:407–418

43. Pfeiffer BD, Jenett A, Hammonds AS et al (2008) Tools for neuroanatomy and neurogenetics in *Drosophila*. Proc Natl Acad Sci U S A 105:9715–9720

44. Kvon EZ, Kazmar T, Stampfel G et al (2014) Genome-scale functional characterization of *Drosophila* developmental enhancers in vivo. Nature 512:91–95

45. Jenett A, Rubin GM, Ngo TT et al (2012) A GAL4-driver line resource for *Drosophila* neurobiology. Cell Rep 2:991–1001

46. Mackay TF, Richards S, Stone EA et al (2012) The *Drosophila melanogaster* Genetic Reference Panel. Nature 482:173–178

47. Attrill HL, Falls K, Goodman JL et al (2016) FlyBase: establishing a Gene Group resource for *Drosophila melanogaster*. Nucleic Acids Res 44:D786–D792 doi:[10.1093/nar/gkv1046](https://doi.org/10.1093/nar/gkv1046)

48. Harris TW, Baran J, Bieri T et al (2014) WormBase 2014: new views of curated biology. Nucleic Acids Res 42:D789–D793

49. Flockhart IT, Booker M, Hu Y et al (2012) FlyRNAi.org—the database of the *Drosophila* RNAi screening center: 2012 update. Nucleic Acids Res 40:D715–D719

50. Cook RK, Deal ME, Deal JA et al (2010) A new resource for characterizing X-linked genes in *Drosophila melanogaster*: systematic coverage and subdivision of the X chromosome with nested, Y-linked duplications. Genetics 186:1095–1109

51. Bunt SM, Grumblng GB, Field HI et al (2012) Directly e-mailing authors of newly published papers encourages community curation. Database (Oxford) 2012:bas024

Chapter 2

The GAL4 System: A Versatile System for the Manipulation and Analysis of Gene Expression

Elizabeth E. Caygill and Andrea H. Brand

Abstract

Since its introduction in 1993, the GAL4 system has become an essential part of the *Drosophila* geneticist's toolkit. Widely used to drive gene expression in a multitude of cell- and tissue-specific patterns, the system has been adapted and extended to form the basis of many modern tools for the manipulation of gene expression in *Drosophila* and other model organisms.

Key words *Drosophila*, UAS, GAL4, Bipartite system, GAL80, Split GAL4, Clonal analysis, Gene expression profiling

1 Introduction

The GAL4 system [1] was developed by Andrea Brand and Norbert Perrimon in the Department of Genetics at Harvard Medical School in a collaboration that brought together Andrea's background in yeast genetics and molecular biology and Norbert's expertise in *Drosophila* genetics. Prior to joining the Perrimon lab, Andrea was a Post Doctoral Fellow in Mark Ptashne's lab in the Department of Biochemistry at Harvard University. At the time the Ptashne lab were studying the yeast transcriptional activator GAL4, and found that GAL4 could activate transcription in organisms other than yeast [2–5]. Andrea was inspired by a seminar given by Walter Gehring who, while visiting the Ptashne lab in 1986, presented his lab's as yet unpublished work on enhancer trapping in *Drosophila* [6]. Gehring described how random integration into the *Drosophila* genome of a P-element containing an enhancerless *lacZ* gene was able to generate multiple lines that expressed β-galactosidase in cell type- and tissue-specific patterns. Andrea theorized that substituting GAL4 for *lacZ* would provide the ability to drive UAS-dependent gene expression in any cell- or tissue-specific pattern in vivo. Encouraged by Norbert, Andrea moved to the Perrimon lab in early 1988 to put theory into practice.

Prior to the development of the GAL4 system [1], ectopic gene expression in *Drosophila* could be achieved in a global transient pulse by cloning a coding sequence downstream of a heat shock promoter [7], or in a tissue-specific manner using a defined promoter fragment [3–5]. Heat shock promoters provided inducible but ubiquitous expression. Tissue-specific promoters allowed expression to be restricted to smaller subsets of cells but were limited to the number of defined regulatory regions. Both required creation of a different transgenic line for each experimental manipulation. The GAL4 system introduced a bipartite approach that allowed the generation of independent transgenic lines containing a target gene and its transcriptional activator [1]. A simple cross of these two lines results in expression of the target gene in a pattern dictated by the expression of GAL4. In the absence of GAL4 the target gene is essentially silent, allowing for the tissue-specific gene manipulations that would be lethal when less restricted. The ease of hopping a GAL4-containing P-element to capture the expression pattern of new uncharacterized enhancers resulted in large numbers of GAL4 lines being quickly generated. A panoply of fly lines expressing GAL4 in distinct spatial and temporal patterns are now available for researchers to use. Every driver line can be used to drive expression of an unlimited number of target genes allowing for large-scale misexpression [8, 9] and knock-down [10, 11] screens. Conversely, each GAL4-responsive target gene can be crossed to any number of different GAL4 lines to investigate gene function in different tissues or at different times during development, or to label cells using GAL4-responsive cell markers for cell type-specific identification or lineage tracing.

2 Key Features of the GAL4 System

In yeast, GAL4 regulates the galactose metabolism. Transcriptional activation of galactose utilization genes occurs when GAL4 binds to the upstream activation sequence (UAS) containing varying numbers of a 17-mer repeat [12, 13]. GAL4 binds to DNA as a dimer through a Zn(2)-Cys(6) zinc finger [14, 15]. The N-terminal region mediates both dimerization [16] and DNA binding [17, 18] and contains a nuclear localization signal [19], while an acidic C-terminal domain controls transcriptional activation [20]. GAL4 directly interacts with the Tral component of the SAGA complex, recruiting Mediator and the general transcriptional machinery to initiate transcription [21, 22]. This ability to activate transcription is retained when GAL4 is expressed in other species including plants [2], human cell lines [3, 4], zebrafish [23], and *Drosophila* [5].

The GAL4 system is bipartite. A transgenic driver line expressing GAL4 in a characterized pattern is crossed to a second transgenic line carrying a UAS-dependent transgene (Fig. 1). The

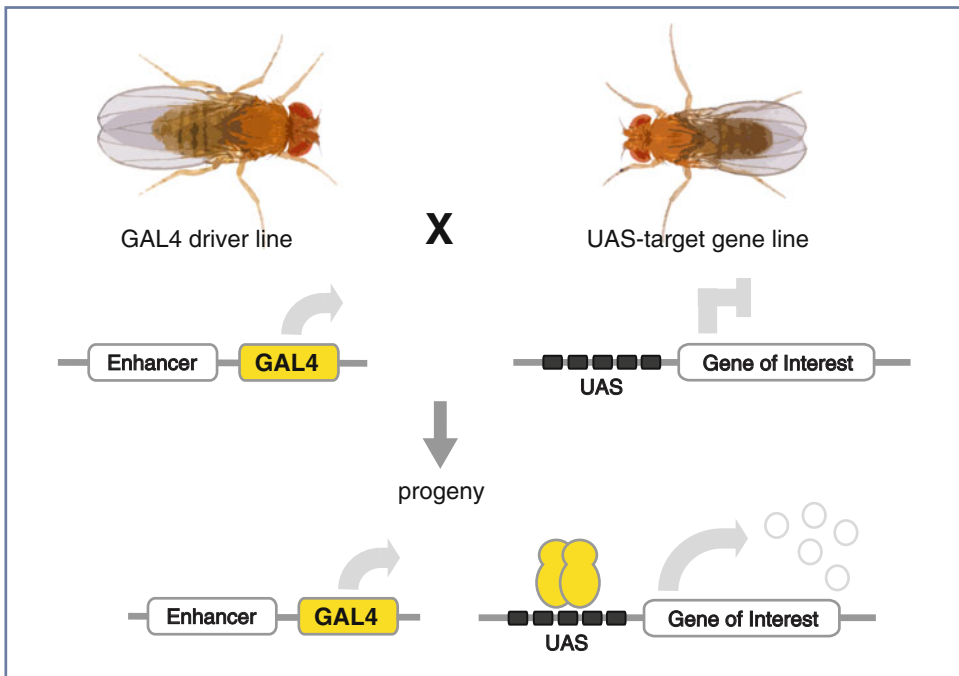


Fig. 1 The Basic GAL4 System. GAL4 driver and UAS-target gene fly lines are generated and maintained as separate stocks. In the absence of GAL4 there is no expression of the target gene. Crossing a fly expressing GAL4 to a fly carrying a UAS-target genes results in targeted gene expression in the progeny of the cross

progeny of the cross express the transgene wherever GAL4 is expressed. Driver lines can be generated by two main methods: the cloning of characterized regulatory regions, or the random integration of GAL4 into the genome to trap unknown enhancers. The specific and efficient expression of GAL4 from a known enhancer was first demonstrated by the cloning of the Rh2 regulatory region into the pGaTB vector upstream of GAL4 and an hsp70 transcriptional terminator [1]. The resulting Rh2-GAL4 was able to drive specific expression of a GAL4-responsive marker in the expected pattern in the photoreceptor cells of the ocelli. To generate novel patterns of GAL4 expression, GAL4 was used to create an enhancer detection vector, pGawB. The pGawB vector, adapted from the lacZ-based enhancer detection technique [6], contains GAL4 fused to the weak P-transposase promoter. Random P-element-based integration of GAL4 results in a pattern of GAL4 expression that is dictated by the transcriptional activity of the site of integration. Mobilization of the vector by the introduction of the constitutively active P-transposase gene $\Delta 2-3$ generated hundreds of independent transgenic lines all expressing GAL4 in different patterns [1].

Since the publication of the GAL4 system, thousands of GAL4 driver lines have been generated and characterized both from the cloning of known enhancers [1] and from large- and small-scale enhancer trap screens [24–26]. Two recent projects, The Janelia

Farm Flylight Project [27–31] and the Vienna Tile (VT) library [38], have generated large numbers of new lines expressing GAL4 under the control of defined DNA elements. Both projects cloned genomic fragments into a vector containing GAL4, a *Drosophila* synthetic core promoter [27] of TATA, Initiator (Inr) [32], Motif Ten Element (MTE) [33], and Downstream promoter element (DPE) [34] sequence motifs, and an attB site to allow for site-specific genomic attP/attB integration using phi-C31 integrase [35] providing reproducibility and control over the effect of integration site on construct expression [36]. The VT library at the Vienna Drosophila Resource Center (VDRC) contains over 8000 GAL4 lines expressing GAL4 under the control of ~2 kb genomic DNA fragments. The lines have been characterized for expression in the brain (<http://brainbase.imp.ac.at/bbweb>, unpublished) and throughout embryogenesis [44]. The Janelia Farm Flylight project created 7000 driver lines using overlapping intergenic 3 kb fragments surrounding selected candidate genes. The lines were characterized for expression in embryonic [29], larval [31], and adult CNS [28], and larval imaginal disks [30]; many are available from the Bloomington Drosophila Stock Center at Indiana University.

GAL4-responsive target gene lines are created by cloning the gene of interest downstream of a UAS. The original pUAST contains a tandem array of five optimized GAL4 binding sites, the hsp70 basal promoter, and an SV40 transcriptional terminator [1]. This vector has been modified by the addition of an attB site downstream of the SV40 terminator to allow site-specific genomic integration [37]. The addition of a 67 bp intron from *Drosophila* Myosin heavy chain (Mhc IVS16) in the 5'UTR and increasing the number of UAS sites have both been shown to increase the level of GAL4-dependent target gene expression [38]. It is worth noting, however, that increasing the strength of reporter expression too much can lead to toxicity [38]. Expression in the female germline requires a modified vector, UASp, with an alternative P transposase minimal promoter and first intron and K10 3'UTR sequences [39]. Many *Drosophila* genes have corresponding UAS lines available. The Zurich ORFeome Project provides publically available fly lines via the FlyORF website for the expression of a large collection of ORFs and miRNAs [37, 40, 41].

3 Refining Expression

Experimental design may demand expression in a more limited time window or with greater tissue specificity than a GAL4 line of choice alone can provide. The basic bipartite system can be modified in a number of ways to refine expression, producing more specific spatial and temporal patterns.

3.1 *GAL80*

The activity of GAL4 can be repressed by physical interaction with the yeast GAL80 protein [42]. A dimer of GAL80 binds to the C-terminal ends of the GAL4 dimer so that, while it can still bind to a UAS sequence, it can no longer activate transcription [43]. This interaction of GAL4 and GAL80 can be taken advantage of to refine the expression pattern of GAL4-dependent transgenes.

Spatial refinement can be achieved by combining distinct GAL4 and GAL80 expression patterns. Where the expression patterns overlap, the activity of GAL4 and thus the expression of the GAL4-responsive transgene will be inhibited. Lines expressing GAL80 in different patterns can be produced in the same way as GAL4 lines, either by enhancer trapping [44] or by cloning of known enhancer elements. Temporal specificity can be achieved using a temperature-sensitive allele of GAL80 [1, 45]. The Temporal And Regional Gene Expression Targeting (TARGET) system [46] takes advantage of a variant of GAL80 that while ubiquitously expressed under control of the tubulin 1 α promoter is only active at permissive temperatures. Thought to be the result of a single glycine to arginine substitution at amino acid 203 of GAL80, GAL80^{ts} is unable to bind GAL4 at restrictive temperatures above 29 °C but retains its repressive function at the permissive temperature of 18 °C [47] (Fig. 2a). Controlling the activity of GAL80^{ts} through temperature shifts provides temporal control of GAL4-dependent transgene expression. Limiting expression to defined temporal windows can help to define critical periods for the effects of misexpression or rescue experiments. Temperature-sensitive alleles of GAL4 itself have been generated and tested in *Drosophila* [48], however the ease of combining tubGAL80^{ts} with already established GAL4 drivers cause the TARGET system to be more commonly used.

3.2 *Ligand-Inducible GAL4*

Temporal activity of GAL4-induced expression can also be regulated using hormone-inducible variants of GAL4, GAL4-ER [49] and GeneSwitch GAL4 [50]. GAL4-ER is a fusion of GAL4 and the ligand-binding domain of the human estrogen receptor that is activated by estradiol [49]. The GeneSwitch system (Fig. 2b) uses a fusion of the DNA binding domain of GAL4, the ligand-binding domain of the human progesterone receptor, and a part of the activation domain of the human NF-kappa-B subunit p65 [50–52]. GeneSwitch responds to the presence of the synthetic steroid mifepristone (RU-486). The steroid ligands can be delivered in food or by larval bathing. While the on- and off-kinetics of transgene response are slower than seen with tubGAL80^{ts}, the systems are highly dose-responsive allowing the level of transgene expression to be tightly controlled. They also avoid any adverse effects of the elevated temperatures required by TARGET. Geneswitch GAL4 enhancer trapping [51] has been used to generate over 3000 lines that show nervous system expression [53]. Tools for ligand inducible manipulations in other tissues are limited by the choice of GAL4 drivers available.

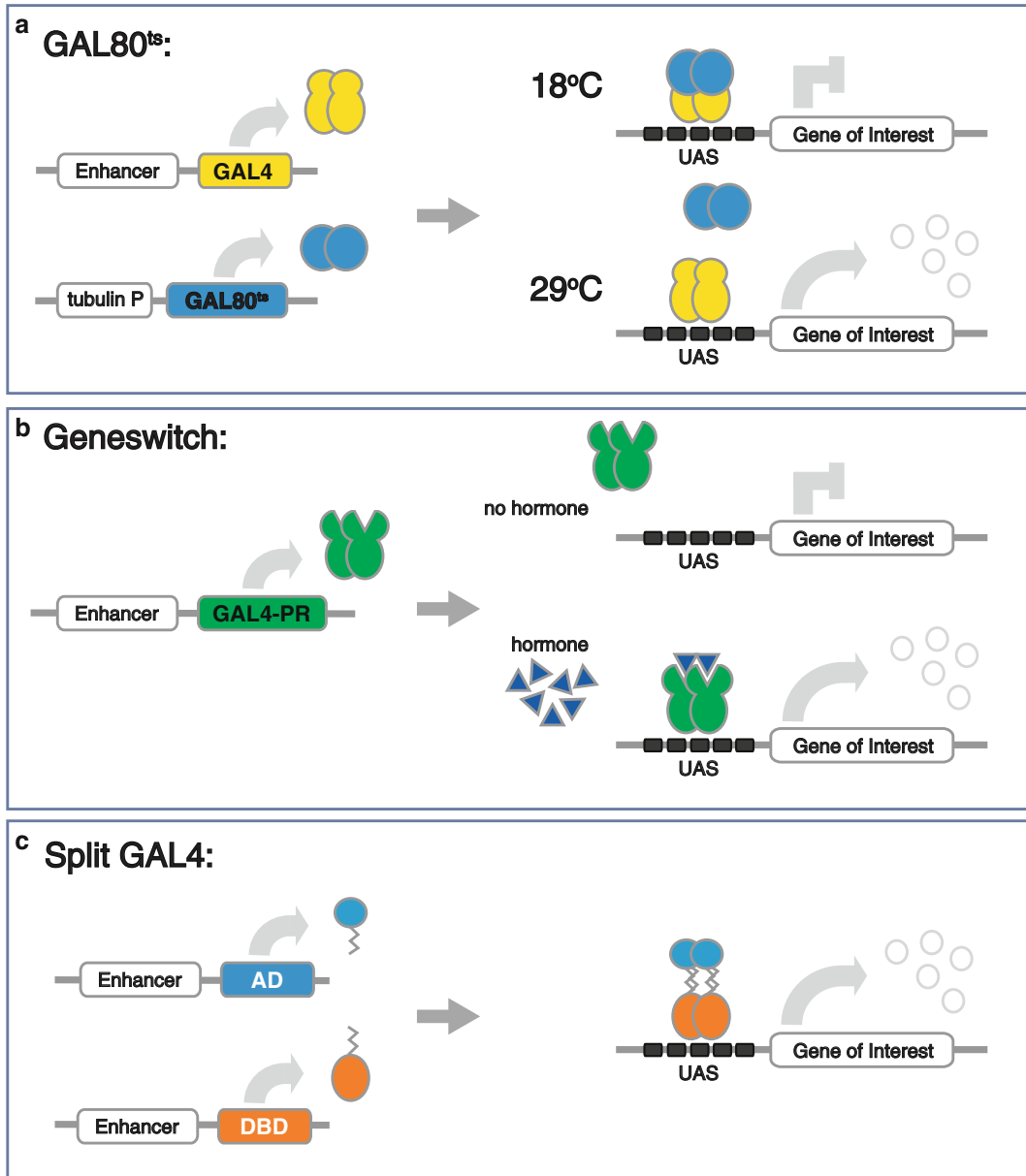


Fig. 2 Modifications to the basic GAL4 system. The GAL4 system can be modified in a number of ways to modulate GAL4 expression both spatially and temporally. (a) The presence of a ubiquitously expressed temperature-sensitive allele of GAL80 (tubGAL80^{ts}) will result in inhibition of GAL4 activity at the permissive temperature of 18 °C. At the restrictive temperature of 29 °C GAL80^{ts} cannot bind GAL4, therefore GAL4 activity is not inhibited and GAL4-dependent transgenes will be expressed. (b) The GeneSwitch system provides an example of ligand-inducible GAL4. Fusion of the GAL4 DNA binding domain to the ligand binding domain of the progesterone receptor results in GAL4 activity only in the presence of the drug RU486. (c) The activation domain and the DNA binding domain of GAL4 can be expressed separately from Split GAL4 hemi-drivers. Where their expression domains overlap dimerization reconstitutes an active GAL4

3.3 Split GAL4

A high degree of spatial refinement of GAL4-mediated gene expression can be achieved utilizing Split GAL4 (Fig. 2c) [54]. The system takes advantage of the modular nature of the GAL4 protein [17, 20] to create a combinatorial system. The DNA binding domain and transcriptional activation domains of GAL4 are separated and fused independently to heterodimerizing synthetic leucine zippers via a polyglycine spacer. The expression of each fusion protein is driven by different enhancer elements, creating “hemi-drivers”. In cells where both hemi-drivers are expressed, transcription of GAL4-dependent target genes is activated [54]. The splitting of GAL4 results in lower levels of expression than can be obtained with full-length GAL4 [54]. This has been compensated for by the use of alternative activation domain hemi-drivers. Both the activation domains from the Herpes Simplex Virus 1 transcription factor VP16, and the human NF-kappa-B subunit p65 drive more strongly than the GAL4 DNA binding domain [38, 54]. However, this increase in strength can result in a broadened expression domain, and switching the activation domain sacrifices the possibility of use in conjunction with GAL80 and GAL80^{ts}, as the GAL80 interaction domain is no longer present. Split GAL4 lines can refine expression patterns to very small numbers of cells, allowing for example, the manipulation of small groups of neurons in behavioral studies. A large collection of Split GAL4 p65AD hemi-driver lines have been created focusing on neuronal expression patterns [28, 55].

4 Clonal Analysis

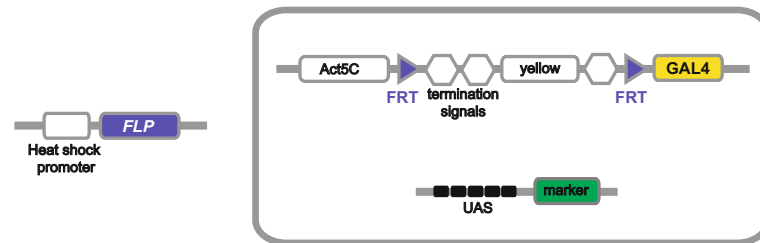
Another set of tools that GAL4 has revolutionized are those used to make and analyze the effect of gene expression in clones. Labeling a cell and its progeny allows the examination of cell lineages, while manipulation of gene expression within a clone can be used to answer questions of autonomy and non-autonomy. Both approaches require the generation of marked clones of cells.

4.1 FLP-Out GAL4

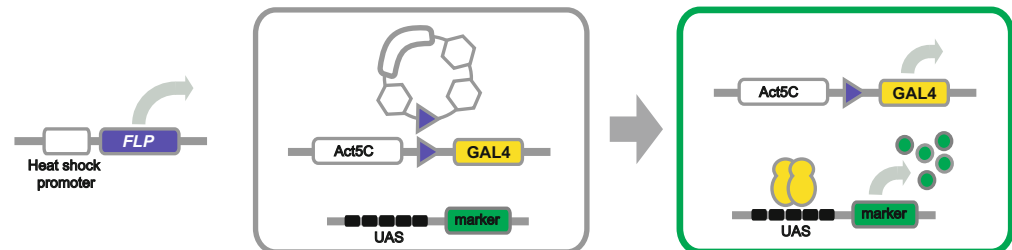
The *Saccharomyces cerevisiae* enzyme FLP is a recombinase that recognizes 34 bp FLP recombination target sequences (FRTs) and catalyses site-specific recombination between them [56], activity that is maintained when expressed in *Drosophila* [57]. This activity forms the basis of FLP-out technology where recombinase can be used to remove FRT-flanked transcription termination signals separating a CDS and a promoter [58]. The FLP/FRT system and the GAL4 system were combined in constructs in which the Actin5C promoter is separated from GAL4 by a FLP-out cassette containing two transcription termination signals and a 7.7 kb DNA fragment containing the *yellow* gene and its regulatory elements (Fig. 3a) [59]. To generate clones of cells expressing GAL4, flies

A. FLP-out GAL4

Initial State:

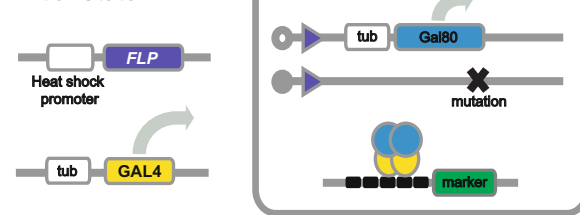


Heat Shock (37°C):



B. MARCM

Initial State:



Heat Shock (37°C):

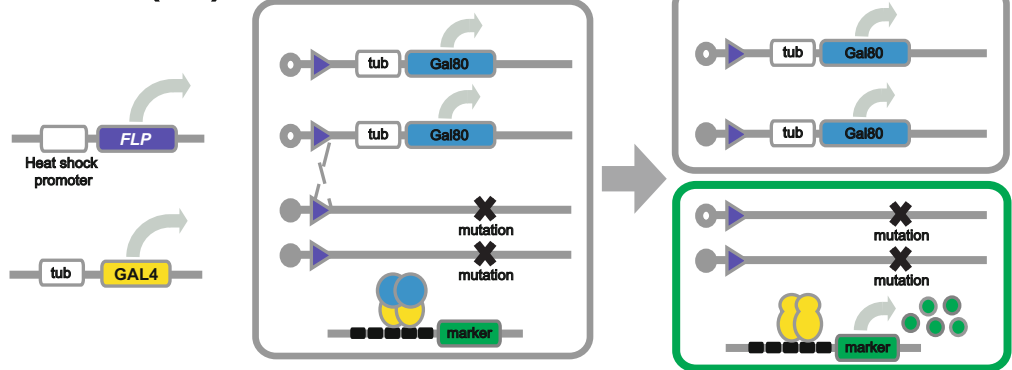


Fig. 3 Clonal analysis. (a) Expression of UAS constructs in clones can be achieved using FLP-out GAL4. Heat shock at 37 °C induces expression of a heat shock-inducible FLP recombinase. The recombinase acts on the FLP-out cassette catalyzing recombination between direct FRT repeats. Recombination removes the yellow marker and the transcription termination signals, allowing the expression of GAL4 under control of the Actin promoter. (b) Positively marked mutant clones can be made using MARCM. Heat shock at 37 °C induces expression of FLP recombinase that catalyzes recombination between FRTs on homologous chromosomes carrying either the mutation of interest or a tubGAL80 construct. Segregation of the GAL80 from the mutation into different daughter cells relieves repression of a GAL4 inducible marker in the mutant cells, labeling the mutant clone

carrying the cassette are crossed to flies expressing the FLP recombinase under control of the *hsp70* heat shock promoter [57]. Heat shocking staged progeny of the cross at 37 °C provides a temporally controlled pulse of recombinase expression. Recombination between the FRTs removes the transcription termination signals and the *yellow* gene and allows expression of GAL4. The timing and duration of the heat shock dictates the number of cells in which the recombination event occurs. The event is stably inherited; creating a clone of cells that expresses GAL4 and GAL4-dependent UAS transgenes. The combination of *hsp70* driven FLP and the FLP-out cassette will result in random clone induction across all tissues of the heat-shocked animal. To restrict clones to a specific tissue a GAL4 driver line can be used to drive expression of UAS-FLP in combination with *tubGAL80^{ts}* to restrict the timing of clone induction [60, 61].

Changes to the basic Actin GAL4 FLP-out cassette can modify the system to suit different purposes. A new method, CoinFLP [62], adds a second choice of FRT to generate mosaic tissues with reproducible ratios of GAL4-expressing and non-expressing cells, allowing the effect of GAL4-dependent gene expression or knock-down on the contribution to the mosaic tissue to be assessed. The system uses a tissue-specific enhancer to drive FLP recombinase in the presence of an Actin5C GAL4 FLP-out cassette that contains two different pairs of FRTs: canonical FRTs and FRT3. Recombination between either pair of FRTs is mutually exclusive and the choice between the two events will occur randomly. Recombination between the classical FRTs results in excision of a transcriptional stop cassette allowing expression of GAL4. When FRT3 recombination occurs the excision event removes one of the canonical FRT sites, the stop cassette remains, and no GAL4 is produced.

4.2 MARCM

The FLP/FRT system can also be used to generate loss-of-function clones. In heterozygous mutant tissue, mitotic recombination between FRTs on homologous chromosome arms can generate clones of cells homozygous for mutations that lie distal to the FRT [63]. Mosaic Analysis with a Repressible Cell Marker (MARCM) [64] (Fig. 3b) takes advantage of the ability of GAL80 to repress GAL4 activity to produce positively labeled clones. Both GAL4 and GAL80 are expressed ubiquitously from the tubulin 1 α promoter. The *tubGAL80* transgene is placed distal to an FRT in trans to the mutation. Recombination results in two populations of daughter cells, one that is wildtype and inherits two copies of *tubGAL80* and one that is homozygous mutant and loses the *tubGAL80*. Loss of GAL80 relieves repression of GAL4 and allows expression of a marker in the mutant clone. Originally created to visualize neuronal projections using membrane-bound fluorescent markers, MARCM is now widely used in all tissue types to positively label mutant clones.

While MARCM allows the identification of one of the two daughter cells and its progeny generated by a mitotic recombination event, two techniques, twin-spot MARCM [65] and twin-spot generator [66], build on MARCM to allow the visualization of both daughter cells and their progeny. Twin-spot MARCM uses a CD8-GFP and a CD2-RFP that before recombination are both silenced by specific miRNAs. Recombination results in segregation of the reporters and their repressors into different daughter cells allowing for each reporter to be expressed in one for the two daughter cells. Twin-Spot Generator (TSG) is based on the Mosaic Analysis with Double Markers (MADM) system used in mice [67]. Two reciprocal chimeric sequences of EGFP and mRFP1 do not produce functional fluorescent proteins until recombination occurs at an FRT site containing intron that separates each half of the chimera. TSG does not rely on the loss of a repressor for marker expression, an advantage when visualization of the clone soon after induction is necessary.

5 Repressing Genes Using GAL4/UAS

GAL4-driven UAS constructs can be used not only to express genes of interest, but also to knock-down or knock-out gene function [1, 68]. Following discoveries that RNAi [69] and CRISPR/Cas9 [70, 71] technologies are functional in *Drosophila* [72–74], UAS transgenes have been developed to reduce or remove gene expression in a tissue-specific manner. This important advance has allowed for high-throughput screening of tissue-specific gene knock-down [10, 11].

5.1 UAS-IR and UAS-shmiR

RNAi-based gene knock-down can be achieved by expressing inverted repeat (IR) sequences complementary to the gene of interest that will be processed by the cellular machinery to produce functional siRNAs (Fig. 4a). This approach has been taken by the Vienna Drosophila Resource Center (VDRC), where two generations of lines are available that target 91% of *Drosophila* protein coding genes. The randomly inserted P-element based GD library [75] and the phiC31-based KK library (Keleman et al., unpublished), both express target gene complementary IRs ranging between 109 and 415 bp long. A second collection, the Transgenic RNAi project (TRiP), focuses on *Drosophila* orthologs of human disease-associated genes. TRiP UAS-IR constructs contain inverted repeats separated by the *white* intron [76] to increase processing efficiency. In an effort to limit off-target effects by reducing the diversity of siRNAs produced, a second TRiP targeting approach was designed based on the structure of microRNAs (miRNAs) [77, 78] (Fig. 4b). A 21 nt targeting sequence complementary to the gene of interest is cloned into the pre-*miR-1* sequence.

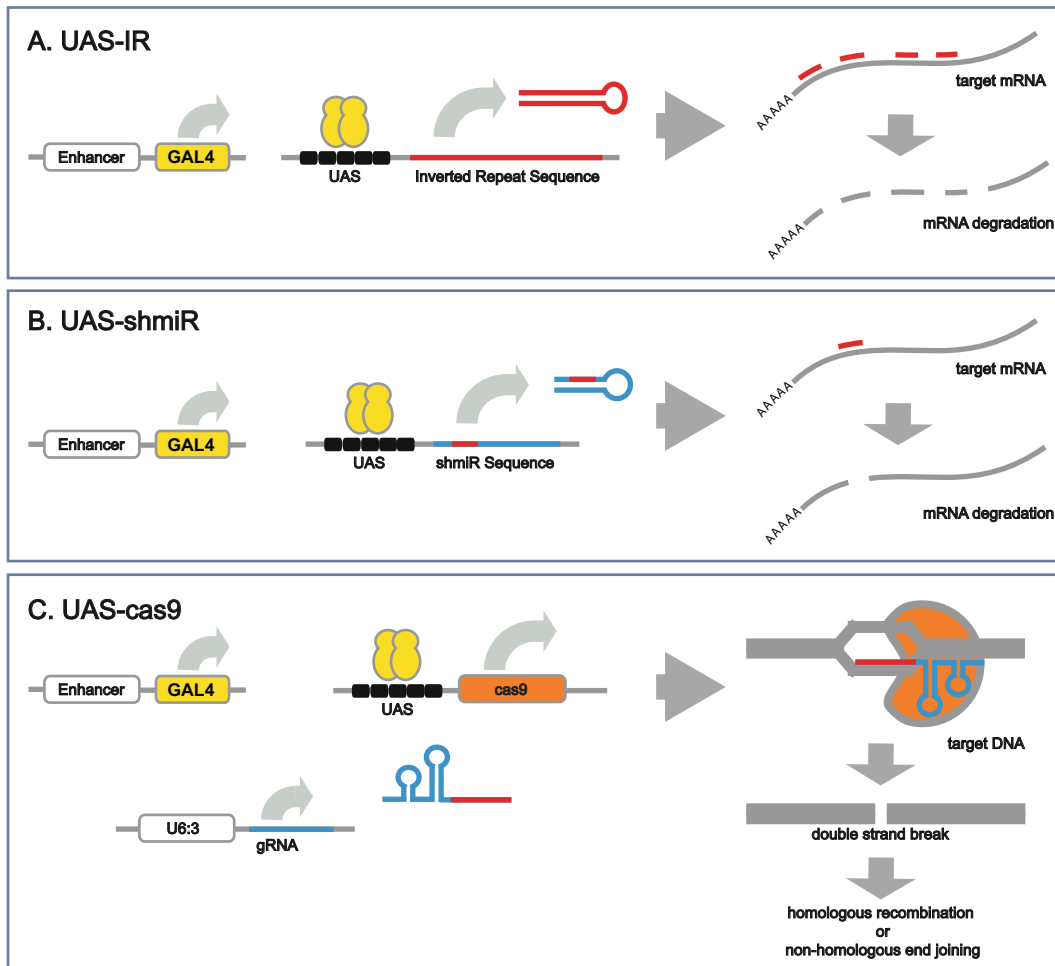


Fig. 4 Repressing genes using the GAL4 system. (a) RNAi-based gene knockdown can be achieved by expressing inverted repeats complementary to the gene of interest. These repeats will fold into a long double-stranded RNA that will be processed to produce multiple siRNAs against the target gene. (b) More specific knockdown can be achieved using UAS-shmiR constructs. A single targeting siRNA is cloned into the miR-1 backbone. Processing by cellular machinery produces only that siRNA. (c) Tissue-specific gene knock-outs can be achieved using a GAL4-dependent version of Cas9 and the CRISPR/Cas9 gene targeting. A ubiquitously expressed chimeric gRNA targeting the gene of interest is expressed in conjunction with UAS-cas9 resulting in biallelic gene targeting where Cas9 is driven

Processing of these artificial miRNAs, called short hairpin/miRNAs (shmiRs), produces only the cloned targeting sequence, increasing the specificity of target gene knock-down.

5.2 UAS-cas9/ CRISPR

Targeted genome editing has advanced greatly with the introduction of the Clustered Regularly Interspaced Short Palindromic Repeats (CRISPR)/CRISPR-associated (Cas) system from the bacterial adaptive immune response [79] which provides a fast and efficient method for generating gene knock-outs in a number of organisms including *Drosophila* [70, 71, 73, 74]. Combining the

CRISPR/*cas9* system with the GAL4 system can result in cell type-specific gene targeting [80, 81] (Fig. 4c). Guide RNAs (gRNAs) targeting the gene of interest are expressed ubiquitously using a U6:3 promoter. Expression of the RNA-guided endonuclease Cas9 is driven in response to GAL4 from a UAS-*cas9* construct. Crossing flies carrying these two constructs results in biallelic gene targeting [80, 81] creating tissue-specific gene knock-out with the spatial and temporal control afforded by the GAL4 system. Increased specificity by reduction of potential off-target effects could be achieved using a UAS-*cas9*^{D10A} nickase. A D10A mutation in the RuvCI domain removes the ability of Cas9 to cleave the strand non-complementary to the guide RNA [82]. However, expression with two gRNAs targeting opposite DNA strands flanking the target site can still produce site-specific double-strand breaks [83, 84].

6 Cell Type-Specific Gene Expression Profiling with GAL4

Many interesting questions regarding gene expression and its control of cell fate and cell function require profiling the expression patterns of specific cell types. The newly developed Targeted DamID technique provides a way to use the cell-type specificity of GAL4 driver lines to profile gene expression *in vivo* without the need for cell isolation [85].

6.1 Targeted DamID

DNA adenine methyl-transferase identification (DamID) [86, 87] maps the binding of proteins to DNA or chromatin. Expression of a fusion protein of the *Escherichia coli* DNA adenine methyl-transferase (Dam) to a protein of interest results in methylation of the associated genomic DNA that can be isolated by methylation-sensitive restriction enzyme digest and subsequent amplification. The toxicity of expressing high levels of Dam has previously prevented it from being combined with the GAL4 system [85]. Targeted DamID uses ribosome re-initiation to create GAL4-inducible Dam constructs. Eukaryotic ribosomes are able to reinitiate translation of a secondary ORF in bicistronic messages at a low frequency that depends on the size of the primary ORF [88]. GAL4-inducible Dam constructs express Dam fusion proteins as a secondary ORF following a fluorescent marker allowing Dam fusion proteins to be expressed using a GAL4 driver, introducing both cell type specificity and temporal control to the system. Targeted DamID can be used to map the interactions of any DNA- or chromatin-associated protein in a cell type-specific manner, *in vivo*, without the need for cell isolation, crosslinking, or antibodies. The presence of RNA polymerase II (PolII) across a gene body is indicative of transcription of that gene. A Dam-PolII fusion can therefore be used to map the occupancy of PolII, providing a

method of profiling gene expression in any subset of cells that have a corresponding GAL4 driver (Fig. 5). This technique has been successfully used to determine the transcriptional profiles of neural stem cells populations in the *Drosophila* larval brain [85].

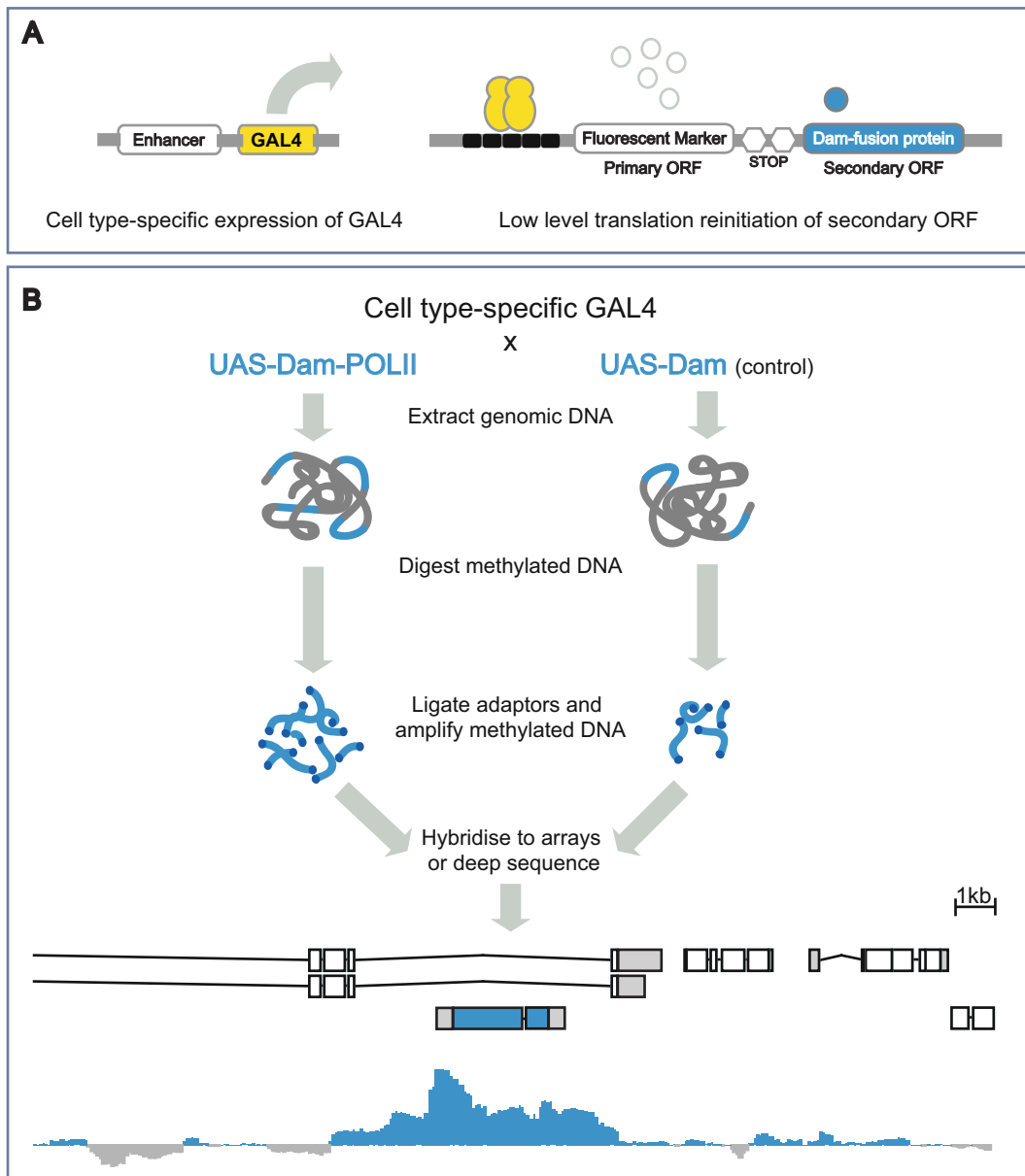


Fig. 5 Transcriptional profiling using Targeted DamID. (a) Targeted DamID allows the GAL4-dependent expression of Dam fusion proteins using bicistronic constructs. The fusion protein is a secondary ORF and is translated at very low levels after rare ribosome reinitiation. (b) Cell type-specific transcriptional profiling can be achieved using a GAL4 driver to express a Dam-PolII fusion protein

7 Further GAL4-Based Tools

The GAL4 system has formed the basis of a variety of innovative techniques designed to address specific questions in *Drosophila* research.

7.1 Fly-FUCCI

Many experiments require an analysis of the phases of the cell cycle. Fluorescent Ubiquitination-based Cell Cycle Indicator (FUCCI) was created to visualize the cell cycle phases in mammalian systems [89] and zebrafish [90]. Recently, a *Drosophila*-specific FUCCI system (Fly-FUCCI) has been developed [91]. The system relies on GAL4-dependent expression of a pair of fluorescent markers, EGFP and mRFP1, or CFP and Venus, tagged with different cell cycle-dependent degradation signals. G2, M, and G1 phases are marked by fluorophores tagged with the dE2F1 PIP-box that mediates degradation by the S phase ubiquitin ligase CRL4^{Cdt2}. Similarly, S, G2, and M phases are marked by fluorophores tagged with the D-box of Cyclin B that mediates degradation by APC/C. Expression of these constructs with a GAL4 driver allows live visualization of the cell cycle dynamics of the tissue of interest.

7.2 dBrainbow/ Flybow

The labeling of single or small groups of cells or lineages via clonal analysis has provided critical anatomical information about neuronal projection patterns. To individually label and investigate the architecture of multiple neurons in relation to one another, researchers have turned to Brainbow technology [92], reviewed recently here [93]. This technology has been adapted for the fly in two iterations, dBrainbow [94] and Flybow [95]. Both use GAL4-dependent expression of constructs containing multiple fluorophores separated by loxP sites in the case of dBrainbow, or the FRT variant mFRT71 in the case of Flybow. Heat shock-induced expression of either Cre recombinase or a modified FLP recombinase catalyzes stochastic recombination events that result in the expression of a single fluorophore or a combination of fluorophores in each cell. The choice is stably inherited by the progeny of that cell, allowing lineages to be mapped. The fluorescent markers used in dBrainbow are cytoplasmic, while Flybow uses membrane tagged markers, giving it the advantage for studying fine neuronal architecture.

7.3 G-TRACE

Often the ability to draw accurate conclusions from an experiment utilizing a GAL4 driver relies on accurately knowing where and when the driver is expressed. This is made possible with the GAL4 Technique for Real-time And Clonal Expression (G-TRACE) [96]. G-TRACE allows visualization of both real-time and historical expression from a GAL4 driver line. Real-time expression is reported via the GAL4-dependent expression of the fluorescent marker UAS-RFP. Historical expression is revealed by the activity of FLP recombinase, expressed in a GAL4-dependent manner. The recombinase recognizes FRT sequences flanking a transcriptional

termination signal that separates a Ubiquitin-p63E promoter fragment from EGFP. Removal of the termination signal allows EGFP expression, and once initiated the expression is independent of GAL4. G-TRACE can provide important information about the expression driven by a GAL4 driver line that can be crucial to the interpretation of experimental results.

7.4 InSITE

The ability to swap the effector molecule driven in a given expression pattern, for example converting a GAL4 driver line into one that expresses GAL80 or a Split GAL4 hemi-driver, can be of great use when designing experiments. The Integrase Swappable In vivo Targeting Element (InSITE) system [97] uses a combination of Cre and FLP recombinase and Φ C31 integrase to perform recombinase-mediated cassette exchange (RMCE), swapping the GAL4 in InSITE enhancer trap and promoter fusion lines for any desired effector molecule or reporter gene. The swap requires the presence of attP and loxP sites flanking the element to be replaced and attB, loxP, and flanking FRTs in the donor element limiting its compatibility with many existing GAL4 lines. However, once compatible lines are created recombination can be stimulated by microinjection of the donor elements or a simple genetic cross. Transgenic lines carrying the donor cassettes are available from the Bloomington Stock Center.

8 The Future of GAL4

The GAL4 system has become the workhorse of *Drosophila* genetics and molecular biology. The number of characterized GAL4 driver lines continues to grow providing an ever-increasing number of specific patterns of expression. The ability to label cells, express or knock-down genes of interest, make targeted mutations, and analyze genome-wide protein-DNA interactions allows researchers to ask highly specific questions *in vivo*. The success of the GAL4 system has inspired the generation of other binary expression systems, for example LexA/lexAop [98] and the Q system [99], that can be used independently or in combination with GAL4/UAS gene expression.

The value of the GAL4 system to *Drosophila* researchers has encouraged the transfer of the system to a variety of organisms ranging from plants to *Xenopus* [104, 105]. Enhancer trap screens have generated numerous GAL4 lines in *Arabidopsis* (J. Haseloff, unpublished), rice [100], zebrafish [101, 102], and mosquito [103].

Acknowledgements

We thank Janina Ander, Seth Cheetham, Jelle van den Ameele, and Owen Marshall for comments on the manuscript. This work was funded by a Wellcome Trust Senior Investigator Award

(103792/Z/14/Z) and BBSRC Project Grant (BB/L007800/1) to A.H.B. A.H.B. acknowledges core funding to the Gurdon Institute from the Wellcome Trust (092096) and CRUK (C6946/A14492).

References

1. Brand AH, Perrimon N (1993) Targeted gene expression as a means of altering cell fates and generating dominant phenotypes. *Development* 118:401–415
2. Ma J, Przibilla E, Hu J et al (1988) Yeast activators stimulate plant gene expression. *Nature* 334:631–633. doi:[10.1038/334631a0](https://doi.org/10.1038/334631a0)
3. Webster N, Jin JR, Green S et al (1988) The yeast UASG is a transcriptional enhancer in human HeLa cells in the presence of the GAL4 trans-activator. *Cell* 52:169–178
4. Kakidani H, Ptashne M (1988) GAL4 activates gene expression in mammalian cells. *Cell* 52:161–167
5. Fischer JA, Giniger E, Maniatis T, Ptashne M (1988) GAL4 activates transcription in *Drosophila*. *Nature* 332:853–856. doi:[10.1038/332853a0](https://doi.org/10.1038/332853a0)
6. O’Kane CJ, Gehring WJ (1987) Detection *in situ* of genomic regulatory elements in *Drosophila*. *Proc Natl Acad Sci U S A* 84:9123–9127
7. Struhl G (1985) Near-reciprocal phenotypes caused by inactivation or indiscriminate expression of the *Drosophila* segmentation gene ftz. *Nature* 318:677–680
8. Rørth P (1996) A modular misexpression screen in *Drosophila* detecting tissue-specific phenotypes. *Proc Natl Acad Sci U S A* 93:12418–12422
9. Bellen HJ, Levis RW, Liao G et al (2004) The BDGP gene disruption project: single transposon insertions associated with 40% of *Drosophila* genes. *Genetics* 167:761–781. doi:[10.1534/genetics.104.026427](https://doi.org/10.1534/genetics.104.026427)
10. Mummery-Widmer JL, Yamazaki M, Stoeger T et al (2009) Genome-wide analysis of Notch signalling in *Drosophila* by transgenic RNAi. *Nature* 458:987–992. doi:[10.1038/nature07936](https://doi.org/10.1038/nature07936)
11. Saini N, Reichert H (2012) Neural stem cells in *Drosophila*: molecular genetic mechanisms underlying normal neural proliferation and abnormal brain tumor formation. *Stem Cells Int* 2012:486169. doi:[10.1155/2012/486169](https://doi.org/10.1155/2012/486169)
12. Guarante L, Yocom RR, Gifford P (1982) A GAL10-CYC1 hybrid yeast promoter identifies the GAL4 regulatory region as an upstream site. *Proc Natl Acad Sci U S A* 79:7410–7414
13. Giniger E, Varnum SM, Ptashne M (1985) Specific DNA binding of GAL4, a positive regulatory protein of yeast. *Cell* 40:767–774
14. Baleja JD, Marmorstein R, Harrison SC, Wagner G (1992) Solution structure of the DNA-binding domain of Cd2-GAL4 from *S. cerevisiae*. *Nature* 356:450–453. doi:[10.1038/356450a0](https://doi.org/10.1038/356450a0)
15. Marmorstein R, Carey M, Ptashne M, Harrison SC (1992) DNA recognition by GAL4: structure of a protein-DNA complex. *Nature* 356:408–414. doi:[10.1038/356408a0](https://doi.org/10.1038/356408a0)
16. Kakidani H, Leatherwood J, Mostashari F, Ptashne M (1989) An amino-terminal fragment of GAL4 binds DNA as a dimer. *J Mol Biol* 209:423–432
17. Keegan L, Gill G, Ptashne M (1986) Separation of DNA binding from the transcription-activating function of a eukaryotic regulatory protein. *Science* 231:699–704
18. Johnston M (1987) Genetic evidence that zinc is an essential co-factor in the DNA binding domain of GAL4 protein. *Nature* 328:353–355. doi:[10.1038/328353a0](https://doi.org/10.1038/328353a0)
19. Silver PA, Keegan LP, Ptashne M (1984) Amino terminus of the yeast GAL4 gene product is sufficient for nuclear localization. *Proc Natl Acad Sci U S A* 81:5951–5955. doi:[10.1073/pnas.104.04.012](https://doi.org/10.1073/pnas.104.04.012)
20. Ma J, Ptashne M (1987) Deletion analysis of GAL4 defines two transcriptional activating segments. *Cell* 48:847–853
21. Bhaumik SR, Raha T, Aiello DP, Green MR (2004) *In vivo* target of a transcriptional activator revealed by fluorescence resonance energy transfer. *Genes Dev* 18:333–343. doi:[10.1101/gad.114840](https://doi.org/10.1101/gad.114840)
22. Lin L, Chamberlain L, Zhu LJ, Green MR (2012) Analysis of Gal4-directed transcription activation using Tra1 mutants selectively defective for interaction with Gal4. *Proc Natl Acad Sci U S A* 109:1997–2002. doi:[10.1073/pnas.1116340109](https://doi.org/10.1073/pnas.1116340109)
23. Scheer N, Campos-Ortega JA (1999) Use of the Gal4-UAS technique for targeted gene expression in the zebrafish. *Mech Dev* 80:153–158
24. Yang MY, Armstrong JD, Vilinsky I et al (1995) Subdivision of the *Drosophila* mushroom bodies by enhancer-trap expression patterns. *Neuron* 15:45–54

25. Manseau L, Baradaran A, Brower D et al (1997) GAL4 enhancer traps expressed in the embryo, larval brain, imaginal discs, and ovary of *Drosophila*. *Dev Dyn* 209:310–322. doi:[10.1002/\(SICI\)1097-0177\(199707\)209:3<310::AID-AJA6>3.0.CO;2-L](https://doi.org/10.1002/(SICI)1097-0177(199707)209:3<310::AID-AJA6>3.0.CO;2-L)

26. Hayashi S, Ito K, Sado Y et al (2002) GETDB, a database compiling expression patterns and molecular locations of a collection of Gal4 enhancer traps. *Genesis* 34:58–61. doi:[10.1002/gene.10137](https://doi.org/10.1002/gene.10137)

27. Pfeiffer BD, Jenett A, Hammonds AS et al (2008) Tools for neuroanatomy and neurogenetics in *Drosophila*. *Proc Natl Acad Sci U S A* 105:9715–9720. doi:[10.1073/pnas.0803697105](https://doi.org/10.1073/pnas.0803697105)

28. Jenett A, Rubin GM, Ngo T-TB et al (2012) A GAL4-driver line resource for *Drosophila* neurobiology. *Cell Rep* 2:991–1001. doi:[10.1016/j.celrep.2012.09.011](https://doi.org/10.1016/j.celrep.2012.09.011)

29. Manning L, Heckscher ES, Purice MD et al (2012) A resource for manipulating gene expression and analyzing cis-regulatory modules in the *Drosophila* CNS. *Cell Rep* 2:1002–1013. doi:[10.1016/j.celrep.2012.09.009](https://doi.org/10.1016/j.celrep.2012.09.009)

30. Jory A, Estella C, Giorgianni MW et al (2012) A survey of 6,300 genomic fragments for cis-regulatory activity in the imaginal discs of *Drosophila melanogaster*. *Cell Rep* 2:1014–1024. doi:[10.1016/j.celrep.2012.09.010](https://doi.org/10.1016/j.celrep.2012.09.010)

31. Li H-H, Kroll JR, Lennox SM et al (2014) A GAL4 driver resource for developmental and behavioral studies on the larval CNS of *Drosophila*. *Cell Rep*. doi:[10.1016/j.celrep.2014.06.065](https://doi.org/10.1016/j.celrep.2014.06.065)

32. Smale ST, Baltimore D (1989) The “initiator” as a transcription control element. *Cell* 57:103–113

33. Lim CY, Santoso B, Boulay T et al (2004) The MTE, a new core promoter element for transcription by RNA polymerase II. *Genes Dev* 18:1606–1617. doi:[10.1101/gad.1193404](https://doi.org/10.1101/gad.1193404)

34. Burke TW, Kadonaga JT (1996) *Drosophila* TFIID binds to a conserved downstream basal promoter element that is present in many TATA-box-deficient promoters. *Genes Dev* 10:711–724

35. Groth AC, Fish M, Nusse R, Calos MP (2004) Construction of transgenic *Drosophila* by using the site-specific integrase from phage phiC31. *Genetics* 166:1775–1782

36. Markstein M, Pitsouli C, Villalta C et al (2008) Exploiting position effects and the gypsy retrovirus insulator to engineer precisely expressed transgenes. *Nat Genet* 40:476–483. doi:[10.1038/ng.101](https://doi.org/10.1038/ng.101)

37. Bischof J, Bischof J, Maeda RK et al (2007) An optimized transgenesis system for *Drosophila* using germ-line-specific phiC31 integrases. *Proc Natl Acad Sci U S A* 104:3312–3317. doi:[10.1073/pnas.0611511104](https://doi.org/10.1073/pnas.0611511104)

38. Pfeiffer BD, Ngo T-TB, Hibbard KL et al (2010) Refinement of tools for targeted gene expression in *Drosophila*. *Genetics* 186:735–755. doi:[10.1534/genetics.110.119917](https://doi.org/10.1534/genetics.110.119917)

39. Rørth P (1998) Gal4 in the *Drosophila* female germline. *Mech Dev* 78:113–118

40. Bischof J, Björklund M, Furger E et al (2013) A versatile platform for creating a comprehensive UAS-ORFeome library in *Drosophila*. *Development* 140:2434–2442. doi:[10.1242/dev.088757](https://doi.org/10.1242/dev.088757)

41. Bischof J, Sheils EM, Björklund M, Basler K (2014) Generation of a transgenic ORFeome library in *Drosophila*. *Nat Protoc* 9:1607–1620. doi:[10.1038/nprot.2014.105](https://doi.org/10.1038/nprot.2014.105)

42. Nogi Y, Shimada H, Matsuzaki Y et al (1984) Regulation of expression of the galactose gene cluster in *Saccharomyces cerevisiae*. II. The isolation and dosage effect of the regulatory gene GAL80. *Mol Gen Genet* 195:29–34

43. Ma J, Ptashne M (1987) The carboxy-terminal 30 amino acids of GAL4 are recognized by GAL80. *Cell* 50:137–142

44. Suster ML, Seugnet L, Bate M, Sokolowski MB (2004) Refining GAL4-driven transgene expression in *Drosophila* with a GAL80 enhancer-trap. *Genesis* 39:240–245. doi:[10.1002/gene.20051](https://doi.org/10.1002/gene.20051)

45. Matsumoto K, Toh-e A, Oshima Y (1978) Genetic control of galactokinase synthesis in *Saccharomyces cerevisiae*: evidence for constitutive expression of the positive regulatory gene gal4. *J Bacteriol* 134:446–457

46. McGuire SE, Le PT, Osborn AJ et al (2003) Spatiotemporal rescue of memory dysfunction in *Drosophila*. *Science* 302:1765–1768. doi:[10.1126/science.1089035](https://doi.org/10.1126/science.1089035)

47. McGuire SE, Mao Z, Davis RL (2004) Spatiotemporal gene expression targeting with the TARGET and gene-switch systems in *Drosophila*. *Sci STKE* 2004:pl6. doi:[10.1126/stke.2202004pl6](https://doi.org/10.1126/stke.2202004pl6)

48. Mondal K, Dastidar AG, Singh G et al (2007) Design and isolation of temperature-sensitive mutants of Gal4 in yeast and *Drosophila*. *J Mol Biol* 370:939–950. doi:[10.1016/j.jmb.2007.05.035](https://doi.org/10.1016/j.jmb.2007.05.035)

49. Han DD, Stein D, Stevens LM (2000) Investigating the function of follicular subpopulations during *Drosophila* oogenesis through hormone-dependent enhancer-targeted cell ablation. *Development* 127:573–583

50. Osterwalder T, Yoon KS, White BH, Keshishian H (2001) A conditional tissue-specific transgene expression system using inducible GAL4. *Proc Natl Acad Sci U S A* 98:12596–12601. doi:[10.1073/pnas.221303298](https://doi.org/10.1073/pnas.221303298)
51. Roman G, Endo K, Zong L, Davis RL (2001) P[Switch], a system for spatial and temporal control of gene expression in *Drosophila melanogaster*. *Proc Natl Acad Sci U S A* 98:12602–12607. doi:[10.1073/pnas.221303998](https://doi.org/10.1073/pnas.221303998)
52. Burcin MM, Schiedner G, Kochanek S et al (1999) Adenovirus-mediated regulable target gene expression in vivo. *Proc Natl Acad Sci U S A* 96:355–360. doi:[10.1073/pnas.96.2.355](https://doi.org/10.1073/pnas.96.2.355)
53. Nicholson L, Singh GK, Osterwalder T et al (2008) Spatial and temporal control of gene expression in *Drosophila* using the inducible GeneSwitch GAL4 system. I. Screen for larval nervous system drivers. *Genetics* 178:215–234. doi:[10.1534/genetics.107.081968](https://doi.org/10.1534/genetics.107.081968)
54. Luan H, Peabody NC, Vinson CR, White BH (2006) Refined spatial manipulation of neuronal function by combinatorial restriction of transgene expression. *Neuron* 52:425–436. doi:[10.1016/j.neuron.2006.08.028](https://doi.org/10.1016/j.neuron.2006.08.028)
55. Aso Y, Hattori D, Yu Y et al (2014) The neuronal architecture of the mushroom body provides a logic for associative learning. *Elife*. doi:[10.7554/elife.04577](https://doi.org/10.7554/elife.04577)
56. Andrews BJ, Proteau GA, Beatty LG, Sadowski PD (1985) The FLP recombinase of the 2 micron circle DNA of yeast: interaction with its target sequences. *Cell* 40: 795–803
57. Golic KG, Lindquist S (1989) The FLP recombinase of yeast catalyzes site-specific recombination in the *Drosophila* genome. *Cell* 59:499–509
58. Struhl G, Basler K (1993) Organizing activity of wingless protein in *Drosophila*. *Cell* 72(4):527–540
59. Ito K, Awano W, Suzuki K et al (1997) The *Drosophila* mushroom body is a quadruple structure of clonal units each of which contains a virtually identical set of neurones and glial cells. *Development* 124:761–771
60. Basler K, Struhl G (1994) Compartment boundaries and the control of *Drosophila* limb pattern by hedgehog protein. *Nature* 368:208–214. doi:[10.1038/368208a0](https://doi.org/10.1038/368208a0)
61. Jiang H, Patel PH, Kohlmaier A et al (2009) Cytokine/Jak/Stat signaling mediates regeneration and homeostasis in the *Drosophila* midgut. *Cell* 137:1343–1355. doi:[10.1016/j.cell.2009.05.014](https://doi.org/10.1016/j.cell.2009.05.014)
62. Bosch JA, Tran NH, Hariharan IK (2015) CoinFLP: a system for efficient mosaic screening and for visualizing clonal boundaries in *Drosophila*. *Development* 142:597–606. doi:[10.1242/dev.114603](https://doi.org/10.1242/dev.114603)
63. Xu T, Rubin GM (1993) Analysis of genetic mosaics in developing and adult *Drosophila* tissues. *Development* 117:1223–1237
64. Lee T, Luo L (1999) Mosaic analysis with a repressible cell marker for studies of gene function in neuronal morphogenesis. *Neuron* 22:451–461
65. Yu H-H, Chen C-H, Shi L et al (2009) Twin-spot MARCM to reveal the developmental origin and identity of neurons. *Nat Neurosci* 12:947–953. doi:[10.1038/nn.2345](https://doi.org/10.1038/nn.2345)
66. Griffin R, Sustar A, Bonvin M et al (2009) The twin spot generator for differential *Drosophila* lineage analysis. *Nat Methods* 6:600–602. doi:[10.1038/nmeth.1349](https://doi.org/10.1038/nmeth.1349)
67. Zong H, Espinosa JS, Su HH et al (2005) Mosaic analysis with double markers in mice. *Cell* 121:479–492. doi:[10.1016/j.cell.2005.02.012](https://doi.org/10.1016/j.cell.2005.02.012)
68. Brand AH, Manoukian AS, Perrimon N (1994) Ectopic expression in *Drosophila*. *Methods Cell Biol* 44:635–654
69. Fire A, Xu S, Montgomery MK et al (1998) Potent and specific genetic interference by double-stranded RNA in *Caenorhabditis elegans*. *Nature* 391:806–811. doi:[10.1038/35888](https://doi.org/10.1038/35888)
70. Cong L, Ran FA, Cox D et al (2013) Multiplex genome engineering using CRISPR/Cas systems. *Science* 339:819–823. doi:[10.1126/science.1231143](https://doi.org/10.1126/science.1231143)
71. Mali P, Yang L, Esvelt KM et al (2013) RNA-guided human genome engineering via Cas9. *Science* 339:823–826. doi:[10.1126/science.1232033](https://doi.org/10.1126/science.1232033)
72. Kennerdell JR, Carthew RW (1998) Use of dsRNA-mediated genetic interference to demonstrate that frizzled and frizzled 2 act in the wingless pathway. *Cell* 95:1017–1026
73. Gratz SJ, Wildonger J, Harrison MM, O'Connor-Giles KM (2013) CRISPR/Cas9-mediated genome engineering and the promise of designer flies on demand. *Fly (Austin)* 7(4):249–255
74. Bassett AR, Tibbit C, Ponting CP, Liu J-L (2013) Highly efficient targeted mutagenesis of *Drosophila* with the CRISPR/Cas9 system. *Cell Rep* 4:220–228. doi:[10.1016/j.celrep.2013.06.020](https://doi.org/10.1016/j.celrep.2013.06.020)
75. Dietzl G, Chen D, Schnorrer F et al (2007) A genome-wide transgenic RNAi library for con-

ditional gene inactivation in *Drosophila*. *Nature* 448:151–156. doi:[10.1038/nature05954](https://doi.org/10.1038/nature05954)

76. Ni J-Q, Liu L-P, Binari R et al (2009) A *Drosophila* resource of transgenic RNAi lines for neurogenetics. *Genetics* 182:1089–1100. doi:[10.1534/genetics.109.103630](https://doi.org/10.1534/genetics.109.103630)

77. Haley B, Hendrix D, Trang V, Levine M (2008) A simplified miRNA-based gene silencing method for *Drosophila melanogaster*. *Dev Biol* 321:482–490. doi:[10.1016/j.ydbio.2008.06.015](https://doi.org/10.1016/j.ydbio.2008.06.015)

78. Ni J-Q, Zhou R, Czech B et al (2011) A genome-scale shRNA resource for transgenic RNAi in *Drosophila*. *Nat Methods* 8:405–407. doi:[10.1038/nmeth.1592](https://doi.org/10.1038/nmeth.1592)

79. Wiedenheft B, Sternberg SH, Doudna JA (2012) RNA-guided genetic silencing systems in bacteria and archaea. *Nature* 482:331–338. doi:[10.1038/nature10886](https://doi.org/10.1038/nature10886)

80. Port F, Chen H-M, Lee T, Bullock SL (2014) Optimized CRISPR/Cas tools for efficient germline and somatic genome engineering in *Drosophila*. *Proc Natl Acad Sci U S A* 111:E2967–E2976. doi:[10.1073/pnas.1405500111](https://doi.org/10.1073/pnas.1405500111)

81. Xue Z, Wu M, Wen K et al (2014) CRISPR/Cas9 mediates efficient conditional mutagenesis in *Drosophila*. *G3 (Bethesda)* 4(11):2167–2173. doi:[10.1534/g3.114.014159](https://doi.org/10.1534/g3.114.014159)

82. Jinek M, Chylinski K, Fonfara I et al (2012) A programmable dual-RNA-guided DNA endonuclease in adaptive bacterial immunity. *Science* 337:816–821. doi:[10.1126/science.1225829](https://doi.org/10.1126/science.1225829)

83. Ran FA, Hsu PD, Lin CY, Gootenberg JS (2013) Double nicking by RNA-guided CRISPR Cas9 for enhanced genome editing specificity. *Cell* 154(6):1380–1389

84. Ren X, Yang Z, Mao D et al (2014) Performance of the Cas9 nickase system in *Drosophila melanogaster*. *G3 (Bethesda)* 4:1955–1962. doi:[10.1534/g3.114.013821](https://doi.org/10.1534/g3.114.013821)

85. Southall TD, Gold KS, Egger B et al (2013) Cell-type-specific profiling of gene expression and chromatin binding without cell isolation: assaying RNA Pol II occupancy in neural stem cells. *Dev Cell* 26:101–112. doi:[10.1016/j.devcel.2013.05.020](https://doi.org/10.1016/j.devcel.2013.05.020)

86. van Steensel B, Henikoff S (2000) Identification of in vivo DNA targets of chromatin proteins using tethered dam methyltransferase. *Nat Biotechnol* 18:424–428. doi:[10.1038/74487](https://doi.org/10.1038/74487)

87. van Steensel B, Delrow J, Henikoff S (2001) Chromatin profiling using targeted DNA adenine methyltransferase. *Nat Genet* 27:304–308. doi:[10.1038/85871](https://doi.org/10.1038/85871)

88. Zielke N, Edgar BA (2015) FUCCI sensors: powerful new tools for analysis of cell proliferation. *Wiley Interdiscip Rev Dev Biol*. doi:[10.1002/wdev.189](https://doi.org/10.1002/wdev.189)

89. Sakaue-Sawano A, Kurokawa H, Morimura T et al (2008) Visualizing spatiotemporal dynamics of multicellular cell-cycle progression. *Cell* 132:487–498. doi:[10.1016/j.cell.2007.12.033](https://doi.org/10.1016/j.cell.2007.12.033)

90. Sugiyama M, Sakaue-Sawano A, Iimura T et al (2009) Illuminating cell-cycle progression in the developing zebrafish embryo. *Proc Natl Acad Sci U S A* 106:20812–20817. doi:[10.1073/pnas.0906464106](https://doi.org/10.1073/pnas.0906464106)

91. Zielke N, Korzelius J, van Straaten M et al (2014) Fly-FUCCI: a versatile tool for studying cell proliferation in complex tissues. *Cell Rep*. doi:[10.1016/j.celrep.2014.03.020](https://doi.org/10.1016/j.celrep.2014.03.020)

92. Livet J, Weissman TA, Kang H et al (2007) Transgenic strategies for combinatorial expression of fluorescent proteins in the nervous system. *Nature* 450:56–62. doi:[10.1038/nature06293](https://doi.org/10.1038/nature06293)

93. Richier B, Salecker I (2014) Versatile genetic paintbrushes: Brainbow technologies. *Wiley Interdiscip Rev Dev Biol*. doi:[10.1002/wdev.166](https://doi.org/10.1002/wdev.166)

94. Hampel S, Chung P, McKellar CE et al (2011) *Drosophila* Brainbow: a recombinase-based fluorescence labeling technique to subdivide neural expression patterns. *Nat Methods* 8:253–259. doi:[10.1038/nmeth.1566](https://doi.org/10.1038/nmeth.1566)

95. Hadjieconomou D, Rotkopf S, Alexandre C et al (2011) Flybow: genetic multicolor cell labeling for neural circuit analysis in *Drosophila melanogaster*. *Nat Methods* 8:260–266. doi:[10.1038/nmeth.1567](https://doi.org/10.1038/nmeth.1567)

96. Evans CJ, Olson JM, Ngo KT et al (2009) G-TRACE: rapid Gal4-based cell lineage analysis in *Drosophila*. *Nat Methods* 6:603–605. doi:[10.1038/nmeth.1356](https://doi.org/10.1038/nmeth.1356)

97. Gohl DM, Silies MA, Gao XJ et al (2011) A versatile in vivo system for directed dissection of gene expression patterns. *Nat Methods* 8:231–237. doi:[10.1038/nmeth.1561](https://doi.org/10.1038/nmeth.1561)

98. Lai S-L, Lee T (2006) Genetic mosaic with dual binary transcriptional systems in *Drosophila*. *Nat Neurosci* 9:703–709. doi:[10.1038/nn1681](https://doi.org/10.1038/nn1681)

99. Potter CJ, Tasic B, Russler EV et al (2010) The Q system: a repressible binary system for transgene expression, lineage tracing, and mosaic analysis. *Cell* 141:536–548. doi:[10.1016/j.cell.2010.02.025](https://doi.org/10.1016/j.cell.2010.02.025)

100. Johnson AAT, Hibberd JM, Gay C et al (2005) Spatial control of transgene expression in rice (*Oryza sativa* L.) using the GAL4

enhancer trapping system. *Plant J* 41:779–789. doi:[10.1111/j.1365-313X.2005.02339.x](https://doi.org/10.1111/j.1365-313X.2005.02339.x)

101. Kawakami K, Abe G, Asada T et al (2010) zTrap: zebrafish gene trap and enhancer trap database. *BMC Dev Biol* 10:105. doi:[10.1186/1471-213X-10-105](https://doi.org/10.1186/1471-213X-10-105)

102. Otsuna H, Hutcheson DA, Duncan RN et al (2015) High-resolution analysis of central nervous system expression patterns in zebrafish Gal4 enhancer-trap lines. *Dev Dyn* 244:785–796. doi:[10.1002/dvdy.24260](https://doi.org/10.1002/dvdy.24260)

103. O’Brochta DA, Pilitt KL, Harrell RA et al (2012) Gal4-based enhancer-trapping in the malaria mosquito *Anopheles stephensi*. *G3 (Bethesda)* 2:1305–1315. doi:[10.1534/g3.112.003582](https://doi.org/10.1534/g3.112.003582)

104. Chae J, Zimmerman LB, Grainger RM (2002) Inducible control of tissue-specific transgene expression in *Xenopus tropicalis* transgenic lines. *Mech Dev* 117:235–241

105. Hartley KO, Nutt SL, Amaya E (2002) Targeted gene expression in transgenic *Xenopus* using the binary Gal4-UAS system. *Proc Natl Acad Sci U S A* 99:1377–1382. doi:[10.1073/pnas.022646899](https://doi.org/10.1073/pnas.022646899)

Chapter 3

The Q-System: A Versatile Expression System for *Drosophila*

Olena Riabinina and Christopher J. Potter

Abstract

Binary expression systems are flexible and versatile genetic tools in *Drosophila*. The Q-system is a recently developed repressible binary expression system that offers new possibilities for transgene expression and genetic manipulations. In this review chapter, we focus on current state-of-the-art Q-system tools and reagents. We also discuss *in vivo* applications of the Q-system, together with GAL4/UAS and LexA/LexAop systems, for simultaneous expression of multiple effectors, intersectional labeling, and clonal analysis.

Key words Binary expression system, Q-system, QF, QF2, QF2^w, LexAQF, GAL4QF, QUAS, QS, Quinic acid, Chimeric transactivators, Intersectional expression, Mitotic recombination, MARCM, Mosaic analysis, *Neurospora crassa*

1 Introduction

Spatial and temporal control of transgene expression is essential for studies of gene and cell function. Expression of GFP and other reporters uncover the anatomy of cellular circuits and the activity of cells [1–3]; gene knockdown by RNAi or gene overexpression emphasizes gene function [4, 5]; expression of neurotoxins, or expression of light- or temperature-sensitive channels, alters cell function by inhibiting synaptic transmission [6], or by hyperpolarizing or depolarizing the cell [7–9]; expression of cellular toxins or apoptotic genes [10, 11] eliminates defined cells to reveal their role in a circuit or complex tissue. Binary expression systems, such as GAL4/UAS [12], LexA/LexAop [13], tTA/TRE [14], and the Q-system [15], are designed to direct efficient transgene expression that can be fine-tuned to suit various experimental needs (reviewed in ref. [16]).

The Q-system is a binary expression system that offers an easy and flexible means to manipulate cell and circuit function [15, 17]. The Q-system consists of two core components, a “driver” and a “reporter”, and two additional components, a “repressor” and a drug that counteracts the repressor (Fig. 1). The driver components of

Binary expression systems

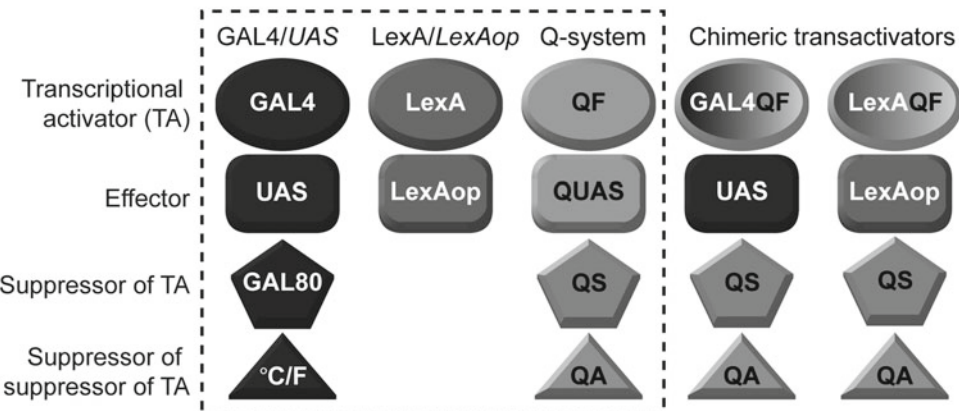


Fig. 1 Binary expression systems. The GAL4/UAS and the Q-system consist of a transcriptional activator (TA, ovals), an effector (rectangles), a suppressor (pentagons), and a suppressor of the suppressor (triangles). The LexA/LexAop system consists only of a TA and an effector. The three systems function independently of each other, but reporter and suppressor activities can be swapped by using Chimeric transactivators (two right columns). GAL4QF binds to the UAS effector sequence (of the GAL4/UAS system), and is suppressed by the QS suppressor (of the Q-system). Similarly, LexAQF binds to the LexAop effector sequence (of the LexA/LexAop system), and is suppressed by QS

the Q-system are transgenes that carry enhancer and promoter sequences specific to the cells of interest upstream of a transcription factor, QF. The reporter components are transgenes that carry the QF binding sequence, QUAS, upstream of genes coding for fluorescent proteins, toxins, ion channels, or other effectors. The repressor components are transgenes that carry the QS gene, placed downstream of UAS or another enhancer. Normally the “driver” and the “reporter” transgenes are kept in different fly stocks and are brought together by genetic crosses in variable combinations as determined by the purpose of a particular experiment.

The design of the Q-system is similar to GAL4/UAS [12] and LexA/LexAop [13] systems (Fig. 1), and because the three systems do not cross-react, they can be used simultaneously for sophisticated genetic manipulations. The need for the Q-system came from two major limitations of the GAL4/UAS and LexA/LexAop systems. First, the transactivator LexA does not have its own repressor [13], thus it is not possible to repress GAL4 and LexA independently. Second, GAL80, the repressor of GAL4, cannot control temporal expression of transgenes independently of the ambient temperature [18, 19]. The Q-system offers a useful alternative to the GAL4/UAS system in experiments where the activity of repressor needs to be switched on or off at a certain point in time, but changes in ambient temperature need to be avoided, e.g., due to the strong behavioral preference *Drosophila* have toward temperatures around 24 °C [20].

GAL4/UAS and the Q systems can also be utilized to drive different reporters in overlapping subsets of cells, when independent temporal control of the reporters is required.

The Q-system also enables sophisticated intersectional and double-MARCM (Mosaic Analysis with a Repressible Cell Marker) experiments to be performed [15, 21–23]. It is often required to express transgenes in a small number of cells that have similar function, e.g., olfactory projection neurons that target a single glomerulus. There are several thousand existing *GAL4* lines, but the use of them is often hampered by the fact that, in addition to the cells of interest (projection neurons from the previous example), *GAL4* is also expressed in many other cells (e.g., other types of neurons, often with unknown function). Therefore, *UAS-geneX* effectors will alter the function of both cells in and outside of the target tissue. Intersectional approaches between *GAL4/UAS* and Q systems can “clean up” a line by restricting expression of reporters to a subset of cells where both *GAL4* and QF are expressed [15, 17]. Conventional MARCM allows the expression of a reporter in one of the two cells that are produced by a mitotic cell division [21, 23]. Coupled MARCM utilizes *GAL4/UAS* and Q systems [15, 17] together, and allows the expression of two different reporters and/or effectors in the two clusters of cells that originated from one mitotic cell division. This feature is very useful in the studies of cell proliferation, cell fate, and other developmental processes (see also refs. [24–26]).

The applications of the Q-system reach beyond *Drosophila* genetics. Currently (June 2016), the Q-system has been successfully used in cultured mammalian cells [15], *C. elegans* [27] and zebrafish [28], and is under development in plants (*Arabidopsis*) and mosquitoes (*Anopheles gambiae*) (Riabinina et al, *in review*).

2 *Neurospora qa* Gene Cluster

The Q-system is based on the *qa* gene cluster of the bread fungus *Neurospora crassa* (Fig. 2a) [15, 29]. The genes of the *qa* cluster control the metabolism of quinic acid, which allows *Neurospora* to use quinic acid as an alternative carbon source in conditions of low glucose [29]. The *qa* cluster contains seven genes, two of which are regulatory (the transcriptional activator *qa-1F* and its repressor *qa-1S*), and five are enzymatic or structural. The QA-1F protein binds to a specific DNA sequence (5'-**GGR TAA RYR TTT ATC C-3'**, where R is A/G, Y is C/T) present in several copies upstream of the *qa* genes, initiating their transcription [30, 31]. In conditions of low quinic acid, the interaction between QA-1S and QA-1F proteins prevents QA-1F from binding transcriptional machinery required for activating the expression of the *qa* genes [32]. In conditions of high quinic acid, the quinic acid binds to QA-1S which disrupts its binding to QA-1F. QA-1F can now

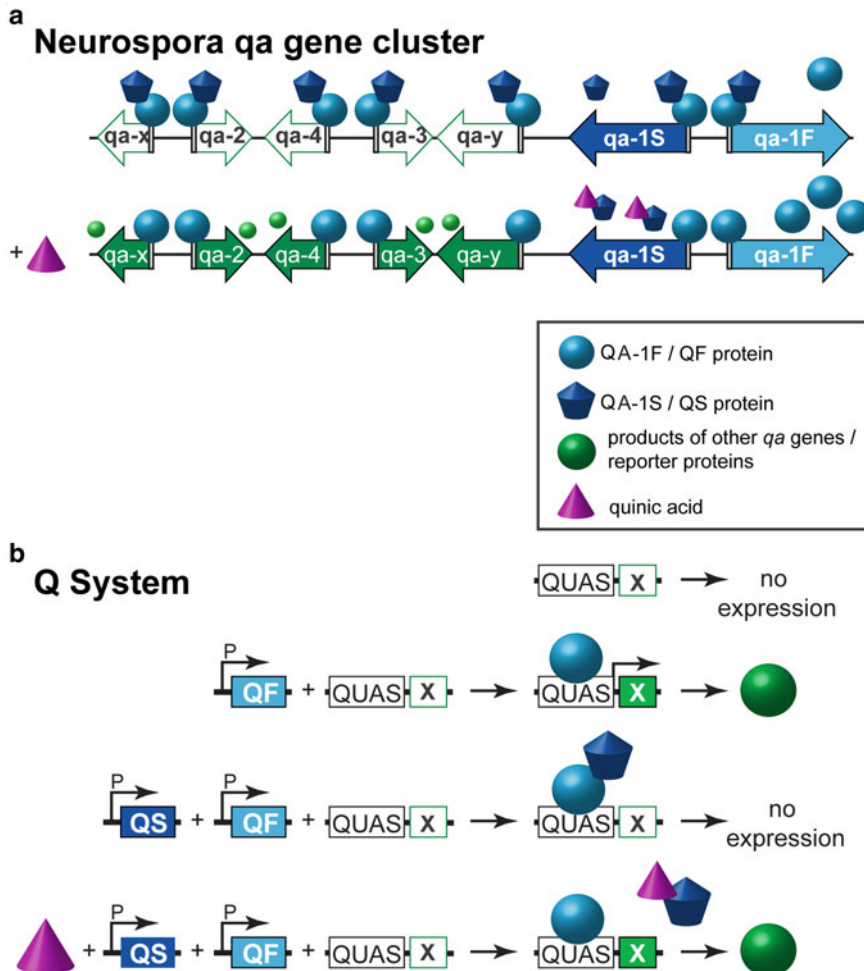


Fig. 2 Activation and repression of transcription in the *Neurospora qa* gene cluster and in the Q-system. (a) *Neurospora qa* gene cluster. Top row: The *qa* gene cluster consists of five structural and enzymatic genes (white and green arrows) and two regulatory genes (blue arrows). The transactivator QA-1F (light blue rectangle) binds to a 16bp sequence (white rectangle) upstream of the seven genes. The repressor QA-1S (dark blue cupcake) binds to QA-1F in conditions of low quinic acid. Bottom row: In conditions of high quinic acid (QA, purple cone), QA binds to QA-1S and prevents the interaction between QA-1F and QA-1S. QA-1F can now drive transcription of the genes involved in quinic acid catabolism (green arrows and green spheres), the QA-1S repressor, and also self-amplify. (b) The Q-system. First row: No expression of a reporter protein X is observed when only a QUAS-X construct is present in the genome. Second row: The expression of X is observed (green sphere) when a promoter-QF (P-QF) and a QUAS-X transgene are present in the genome. Third row: When QF and QS are expressed in the same cell (e.g., by the same promoter P), QS will suppress QF, and no reporter will be expressed. Fourth row: Feeding flies with quinic acid (QA) relieves QS-induced suppression, and the reporter X is expressed

associate with the transcriptional machinery and activate transcription. Similarly to GAL4, QA-1F has been predicted to have a modular structure [31, 33–39], consisting of a Zn₂/Cys₆ zinc finger DNA binding domain (DBD), a middle domain (MD), and an acidic activation domain (AD) that binds QA-1S or molecular

factors that initiate transcription. In contrast to GAL4 and QF, LexA consists of a DBD only, and thus needs to be paired with an activation domain (the commonly used ones are VP16 [21], p65 [40], GAL4 AD [21]) to initiate transcription. As such, LexA also does not have a specific independent suppressor.

3 Components of the Q-System

Regulatory genes *qa-1F* and *qa-1S*, together with the *qa-1F* binding sequence, were cloned out of *Neurospora*, and adapted for use in *Drosophila* as the Q-system [15]. For simplicity, QA-1F, QA-1S, and the *qa-1F* binding site were renamed to QF, QS, and QUAS, respectively. The components of the Q-system are analogous to those of GAL4/UAS and LexA/LexAop systems (Fig. 1): QF, GAL4, and LexA are transcription factors (TF) that can drive expression of transgenes by binding to their specific activation sequences (QF binds to QUAS, GAL4 binds to UAS, and LexA binds to LexAop). QS and GAL80 are repressors of TFs that bind to the activation domain of QF or GAL4 respectively and prevent initiation of transcription. The activity of the repressor can be silenced by a non-toxic drug, quinic acid, in the case of QS, or by temperature, in the case of a temperature-sensitive variant of GAL80 (Fig. 2b).

In the original version of the Q-system [15], the transactivator QF appeared to be toxic when broadly expressed. The cause of this toxicity was unknown. In addition, QF enhancer-trap lines were often mis-expressed in the trachea, presumably because a part of the QF DNA sequence acted as a cryptic tracheal enhancer in *Drosophila*. To remove the cryptic enhancer, second-generation versions of QF, named QF2 and QF2^w, were re-codonized by manually choosing codons predicted to have average expression strength in *Drosophila* [41]. To find and eliminate the region of QF most responsible for general toxicity, the structural domains of QF (DBD, MD, and AD) were paired with those of GAL4 or LexA. Expression of these chimeric transactivators in vivo under the control of the strong neuronal promoter *synaptobrevin* indicated that the QF MD was the major source of lethal toxicity. In addition, the QF MD turned out to be dispensable for QF function. Therefore, the QF MD was removed from QF to yield QF2 (Fig. 3). Thus, in contrast to the original QF, QF2 has the QF DBD fused directly to QF AD. The resulting transactivator retains high-activity levels and is repressible by QS, similarly to the original QF [41].

An alternative QF2 has also been generated: QF2^w. There is only a slight difference between the coding sequences of QF2 and QF2^w: the last two amino acids (glutamic acid and glutamine) on the C-terminus of QF2 were replaced by four lysines in QF2^w (Fig. 3). This mutation changed the charge on the C-terminus from negative (E-Q) to positive (K⁺ K⁺ K⁺ K⁺), making QF2^w a

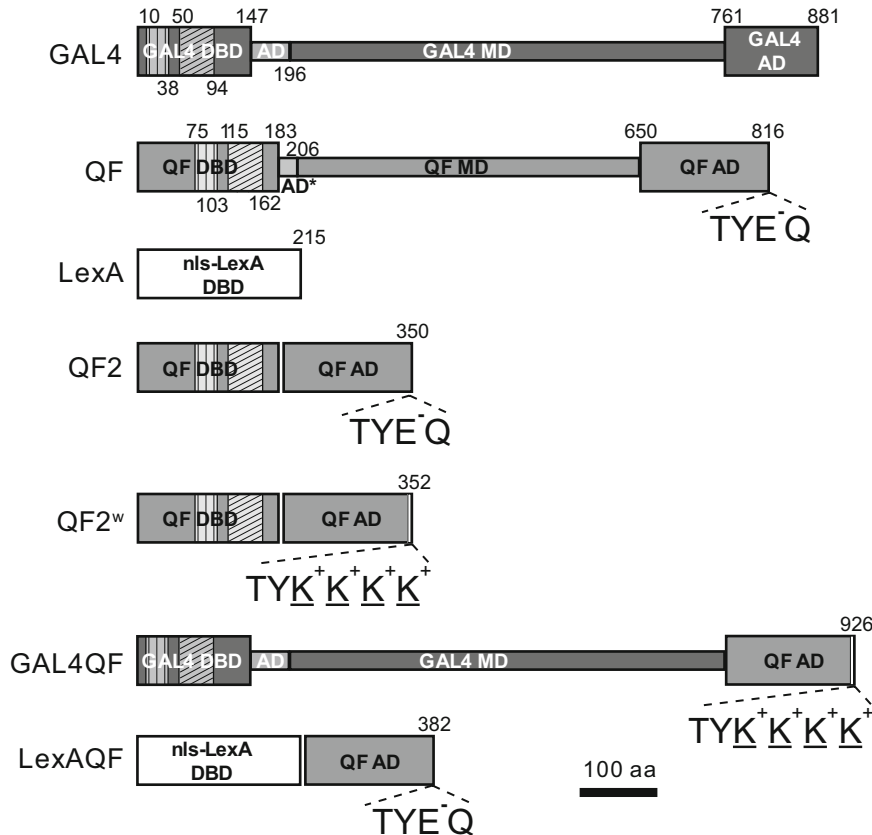


Fig. 3 Transactivator schematics. Schematic representations of GAL4, original QF, LexA, QF2, QF2^w, GAL4QF, and LexAQF. The transactivators consist of modular regions: DNA binding domain (DBD), middle domain (MD), and activation domain (AD). Vertical hatching indicates Zn₂/Cys₆ zinc finger motifs, diagonal hatching mark dimerization domains. Numbers above and below schemes indicate amino acid position. Constructs are drawn to scale. C-terminal amino acids are indicated for transactivators with the QF AD to highlight differences between the ADs of QF/QF2/LexAQF and QF2^w/GAL4QF

weaker transcriptional activator than QF2 (see also ref. 42), but also better repressible by QS. QF2 thus may be a preferred choice when very high transcriptional activity is required. We note, however, that having QF2 expressed ubiquitously or very widely may still compromise the health of fly stocks. A solution could be to have a *tubulinP-QS* transgene in the same stock (e.g., Bloomington Stock #51957), or to use the weaker QF2^w transactivator for wide expression patterns. The fact that QS alleviates effects of QF2 indicates that the activation domain of QF2 may be sequestering non-specific targets or the transcriptional machinery of a cell. This phenomenon is not unique to the QF2 activation domain, as it has been similarly observed that high levels of GAL4, driven by a strong promoter, compromise the health of a cell [43].

Expression levels of reporters, driven with QF2 and QF2^w, can be fine-tuned in many ways. The expression levels can be dramatically increased by using 10, 15, 20, or 40 QUAS repeats for effector

lines instead of the usual 5 [40, 44]; by including regulatory elements such as IVS, Syn21, and WPRE into effector constructs [45]; by creating multimeric reporter proteins [44]; by using site-directed φC31 integrase to place QF and QUAS transgenes into more highly expressing attP sites [40, 46]; or by using stronger terminator sequences such as *SV40* or *p10* instead of *hsp70* in QF and QUAS constructs [45]. No clear temperature dependence of QF2/2^w efficiency has been observed [41].

The Q-system can be used simultaneously with the *GAL4/UAS* system. To fully benefit from the availability of two repressible binary systems, they must function completely independently of each other. It has been verified in the adult brain and in the larval imaginal disks that QF fails to activate transcription downstream of *UAS*, and *GAL4* fails to act on *QUAS* [15]. The cross-repression between the two systems is also absent: *GAL80* does not reduce the activity levels of QF, and QS does not affect *GAL4*. Expression of *GAL4* and QF2/QF2^w simultaneously in the same cell does not lead to toxicity or downregulation of expression [41]. This mutual independence allows, among many other applications, to extend the classical MARCM analysis of mitotic clones with Coupled MARCM and Double MARCM (see below).

4 Temporal Control of Expression by Quinic Acid

All currently existing versions of transactivators with the QF AD (original QF, QF2, QF2^w, *GAL4QF*, and *LexAQF* (see below)) are well repressed by QS, with the repression of QF2 by QS possibly more efficient at higher temperatures [41]. The QS-induced repression may be removed by feeding the larvae or adult flies food containing quinic acid (QA). QA is a naturally occurring non-toxic drug with anti-oxidative properties. It can be dissolved in water to concentrations of up to 6% by weight, and added to the standard solidified fly medium by making holes in the food and pipetting the QA solution into them (0.3 ml of solution per 10 ml of food). This method works well for larva, but may lead to insufficient QA consumption in adult flies. QA consumption may be increased by keeping flies in vials with 1% agarose gel, complemented with 1% sucrose and 6% QA [41]. To provide flies with a source of protein, the gel may be supplemented with fresh yeast paste made from dry yeast and 3% QA solution, neutralized to pH 7 by NaOH. The effectiveness of QA to suppress QS does not appear to be altered when the QA solution is neutralized. Adding into the vial a small piece of tissue paper, moistened with the same neutralized QA solution, can provide extra moisture if necessary.

The effect of QA depends on the amount of QA in the food, and on the duration of exposure to QA. Larvae are particularly amenable to QA treatment [41]. In the case of adult flies, raised on normal fly medium and transferred after eclosion to a QA-containing

vial, the maximum effect of QA was reached after about 3 days of exposure, although an increase in reporter expression may be seen *in vivo* already after 6 h [15].

The effect of QA can be seen only in cells that have absorbed QA from the environment or from fly hemolymph after the fly has fed on QA. For instance in the adult brain, olfactory and gustatory receptor neurons, neurons in the optic lobes and PI neurons appear to be most accessible to QA [41]. Other brain areas, however, are less affected by QA, presumably due to the glial “blood–brain barrier” [47] that prevents diffusion of QA into these cells.

5 Chimeric Transactivators

Chimeric transactivators GAL4QF and LexAQF were initially generated in an attempt to uncover the source of QF toxicity. GAL4QF was generated by fusing the GAL4 DBD and the GAL4 MD with the weakened QF AD (Fig. 3). LexAQF was generated by fusing the LexA DBD with the original QF AD (Fig. 3). Both transactivators drive strong expression *in vivo* of reporters placed under the control of *UAS* (for GAL4QF) or *LexAop* (for LexAQF), when examined in larval and adult neurons, larval imaginal disks and larval body wall muscles [41]. Both chimeric TAs are also suppressible by QS [41]. This feature is particularly useful for LexAQF as it allows for the suppression of *LexAop* reporter expression independently of GAL4/GAL80. This will allow for the use of LexAQF in MARCM experiments simultaneously with GAL4. GAL4QF also allows for the suppression of *UAS* reporter expression independently from GAL80. This may be used together with GAL4 in experiments where temporal control of expression by temperature-sensitive GAL80^{ts} is desirable only for some cells of an expression pattern. In addition, the QS-induced repression of GAL4QF and LexAQF can be relieved by QA in much the same way as with QF, QF2, and QF2^w [41].

6 Intersectional Expression with the Q-System

GAL4/*UAS* and Q systems are independent repressible binary expression systems, that, together with LexA/*LexAop*, chimeric transactivators and FLP/FRT [48] or other recombinases [49], enable the ability to achieve a variety of expression patterns. These modified expression patterns may be viewed as logic gates (Table 1). In the simplest possible case, the same effector or two different effectors may be expressed in cells that are covered by a GAL4 and a QF driver lines (Fig. 4). This approach has been used in a number of studies [50–60], e.g., to express different Ca²⁺ reporters in olfactory projection neurons and Kenyon cells of the Mushroom body

Table 1
Available Q-system reagents

Stock number	Q-transgene	Purpose/function	Reference
Driver lines with original QF			
36347	jav-QF	Expresses QF in chordotonal organs in the pattern of the <i>jav</i> (inactive) gene	[74]
36346, 36349	nompC-QF	Expresses QF in chordotonal organs <i>vchA</i> , <i>vchB</i> , <i>lch5</i> and <i>lch1</i> , the class III sensory neurons <i>vdaD</i> , <i>v'pda</i> , <i>ldaB</i> , <i>ddAA</i> and <i>ddAF</i> and the <i>dmd1</i> sensory neurons in the pattern of the <i>nompC</i> gene.	[74]
36357	Synj-QF	Expresses QF in the nervous system, imaginal disks, gut and salivary glands in the pattern of the <i>synj</i> (Synaptojanin) gene.	[74]
36365	Tbh-QF	Expresses QF in the larval nerve cord in the pattern of the Tyramine beta-hydroxylase gene, targets octopaminergic neurons.	[75]
52244, 52245	Tdc2-QF	Expresses QF under control of <i>Tdc2</i> (Tyrosine decarboxylase 2) regulatory sequences, targets tyraminergic neurons.	[76]
52250, 52251, 57359, 57362	Trh-QF	Expresses QF under control of <i>Trh</i> (Tryptophan hydroxylase) regulatory sequences.	[76]
36345, 36348	TrpA1-QF	Expresses QF in class IV larval sensory neurons in the pattern of the <i>TrpA1</i> gene.	[74]
36370	Trp1-QF	Expresses QF in Bolwig's organ and eye imaginal disks in the pattern of the <i>trp</i> gene.	[74]
30014, 30015, 30037, 30038, GH146-QF 30039		Expresses QF in subsets of projection neurons.	[15]
41573	Mz19-QF	Expresses QF in olfactory projection neurons.	[51]
30016, 30043, 30042, 30019, EnhancerTrap-QF 30018		Enhancer trap lines generated by random insertion at various genomic loci	[15]
30017, 30020	SwappableEnhancer Trap-QF	Enhancer trap lines generated by random insertion at various genomic loci. These lines allow replacement of QF with another gene.	[15]
57361, 57363, 57364	Ddc-FRT-stop-FRT-QF	Expresses QF in the pattern of the <i>Ddc</i> (Dopa decarboxylase) gene upon FLP-mediated removal of a transcriptional stop cassette.	Contributed by Tom Hart and Matt Scott

(continued)

Table 1
(continued)

Stock number	Q-transgene	Purpose/function	Reference
57358, 57365	Trh-FRT-stop-FRT-QF	Expresses QF in the pattern of the Trh (Tryptophan hydroxylase) gene upon FLP-mediated removal of a transcriptional stop cassette.	Contributed by Tom Hart and Matt Scott
	InSITE-QF	Enhancer-trap lines from InSITE collection	[64]
	IR76b-QF	Expresses QF in a subset of neurons in the pattern of chemosensory receptor IR76b	[77]
	Or67d-QF	Expresses QF in a subset of neurons in the pattern of olfactory receptor OR67d	[59]
Driver lines with QF2			
51957, 51958	α Tubulin-QF2	Expresses QF2 ubiquitously under the control of α Tubulin84B	[41]
51955, 51956, 51959	nsyb-QF2	Expresses QF2 pan-neuronally under the control of n-syb.	[41]
60320	Chat-QF2	Trojan-MiMIC line that expresses QF2 in the pattern of cholinacetyl transferase, targets cholinergic neurons.	[66]
60315	vGlut-QF2	Trojan-MiMIC line that expresses QF2 in the pattern of vesicular glutamate transporter, targets glutamatergic neurons	[66]
60323	Gad1-QF2	Trojan-MiMIC line that expresses QF2 in the pattern of glutamic acid decarboxylase 1, targets GABAergic neurons	[66]
Driver lines with QF2 ^{w(tek)}			
51961	Actin5C-QF2 ^w	Expresses QF2 ^w under the control of the Act5C promoter.	[41]
51962, 51963	α Tubulin-QF2 ^w	Expresses QF2 ^w ubiquitously under the control of α Tubulin84B	[41]
51960, 51964, 51965	nsyb-QF2 ^w	Expresses QF2 ^w pan-neuronally under the control of n-syb.	[41]
59283	pGMR-QF2 ^w	Expresses QF2 ^w under the control of the GMR promoter in the eye-antennal imaginal disk.	[41]
Driver lines with GAL4QF			
51945, 51946, 51947	nsyb-GAL4QF	Expresses the GAL4 DNA-binding domain fused to the QF2 ^w activation domain pan-neuronally under the control of n-syb.	[41]

59284, 59285	Actin5C-GAL4QF	Expresses GAL4QF under the control of the Act5C promoter.	[41]
Driver lines with LexAQF			
51953, 51954	nsyb-LexAQF	Expresses the LexA DNA-binding domain fused to the QF activation domain pan-neuronally under the control of n-syb.	[41]
62567, 62568	Actin5C-LexAQF ^w	Expresses LexAQF ^w under the control of the Act5C promoter.	[41]
60319	Chat-LexAQF	Trojan-MiMIC line that expresses LexAQF in the pattern of cholinacetyl transferase, [66] targets cholinergic neurons.	
60314	vGlu-LexAQF	Trojan-MiMIC line that expresses LexAQF in the pattern of vesicular glutamate transporter, targets glutamatergic neurons	[66]
60324	Gad1-LexAQF	Trojan-MiMIC line that expresses LexAQF in the pattern of glutamic acid decarboxylase 1, targets GABAergic neurons	[66]
Available by request from C. Potter, JHU		Expresses LexAQF ubiquitously under the control of α Tubulin84B upon FLP-mediated removal of transcriptional stop cassette	
QUAS reporter lines			
52259, 52260	10xQUAS-ChR2. T159C-HA	A variant of Channelrhodopsin, excitatory blue light-activated sodium channel, tagged with HA.	[76]
58401, 58402	QUAS-FRT-stop-FRT- ChR2.TR-mCherry	A variant of Channelrhodopsin, excitatory blue light-activated sodium channel tagged with mCherry, that will be expressed upon excision of FRT-stop-FRT cassette.	[59]
58400	QUAS-ChR2. TR-mCherry	A variant of Channelrhodopsin, excitatory blue light-activated sodium channel, tagged with mCherry.	[59]
36356, 36367	QUAS-CHE1A.YFP	A variant of Channelrhodopsin, excitatory blue light-activated sodium channel, tagged with YFP.	[74]
55106, 55107, 55108, 55109, QUAS-X::CycB 55110, 55115, 55116, 55120	Cyclin B, tagged with RFP or Venus YFP, to mark cells in S, G2, and M phases of cell cycle. Reagent of the Fly-FUCCI system.	Cyclin B, tagged with RFP or Venus YFP, to mark cells in S, G2, and M phases of cell cycle. Reagent of the Fly-FUCCI system.	[78]
55106, 55107, 55108, 55109, QUAS-X::E2F1 55115, 55116, 55119, 55120	E2F1, tagged with CFP or GFP, to mark cells in S, G2, and M phases of cell cycle. Reagent of the Fly-FUCCI system.	E2F1, tagged with CFP or GFP, to mark cells in S, G2, and M phases of cell cycle. Reagent of the Fly-FUCCI system.	[78]

(continued)

Table 1
(continued)

Stock number	Q-transgene	Purpose/function	Reference
30008, 30126, 30127	QUAS-FLP	FLP recombinase	[15]
52226, 52227	QUAS-R-GECO	RGECO calcium reporter	[58]
30001, 30002, 30003	QUAS-mCD8:GFP	Membrane-bound GFP	[15]
52263, 52264	10xQUAS-6XGFP	Cytoplasmic hexameric GFP for extra-strong labeling.	[44]
36351	QUAS-nSyb: mCherry-HA	Cherry- and HA-tagged n-syb protein for labeling presynaptic terminals	[74]
36358	QUAS-nSyb:GFP-myc	GFP- and myc-tagged n-syb protein for labeling presynaptic terminals	[74]
30134, 30135, 30136	QUAS-FRT-stop-FRT- mCD8:GFP	GFP, fused to membrane tag CD8, expressed upon FLP-mediated removal of transcription stop	[15]
36355, 36366	QUAS-eNpHR	Halorhodopsin, inhibitory yellow light-activated chloride channel.	[74]
30006, 30007	QUAS-nuclacZ	LacZ (beta-galactosidase) for labeling nuclei.	[15]
36352, 36353, 36363, 36364	QUAS-Rab3	Synaptic vesicle membrane-associated protein Rab3, tagged with GFP or mCherry.	[74, 76]
52255	10xQUAS-2xHA-Rab3	Synaptic vesicle membrane-associated protein Rab3, tagged with HA.	[74, 76]
52269, 52270	10xQUAS-6XmCherry	Cytoplasmic hexameric red fluorescent protein mCherry for extra-strong labeling.	[44]
30004, 30005, 30037, 30043, 30118	QUAS-mtdTomato- 3xHA	Membrane-bound red fluorescent protein tdTomato.	[15]
30128	QUAS-FRT-stop-FRT- shibire ^{1s}	Temperature-sensitive shibire protein, expressed upon FLP-mediated recombination that removes the transcriptional stop cassette.	[15]
30010, 30011, 30012, 30013	QUAS-shibire ^{1s}	Temperature-sensitive shibire protein. Inhibits synaptic transmission at 29 °C and above.	[15]
41565, 41566	QUAS-Ten-a	Presynaptic teneurin	[51]
41571, 41572	QUAS-Ten-m	Postsynaptic teneurin	[51]
61658, 61811	QUAS-p65AD::CaM	p65 activation domain, fused to Calmodulin. Component of activity-dependent labeling system TRIC.	[61]

61659, 61660	QUAS-FRT-stop-FRT- p65 activation domain, fused to Calmodulin. Expressed upon FLP-mediated recombination that removes the transcriptional stop cassette. Component of activity-dependent labeling system TRIC.	[61]
52230	QUAS-ChIEF- tdTomato	A variant of Channelrhodopsin, excitatory blue light-activated sodium channel, tagged with tdTomato.
30009	QUAS-dm	Diminutive (<i>Drosophila</i> myc).
51948, 51949, 51950	QUAS-GAL80	GAL80, repressor of GAL4
52231	QUAS-GCaMP3	GCaMP3 calcium reporter for live imaging
	QUAS-spH	Synapto-pHluorin, a pH-sensitive mutant of GFP that allows to monitor synaptic vesicle release.
	QUAS-Brp-Short- mStraw	Bruchpilar-Short protein, fused to mStrawberry, to label sites of presynaptic neurotransmitter release.
	QUAS-GFP11	A GRASP version of GFP for labeling synaptic connections.
QS repressor lines		
30021, 30022, 30024, 52112	α Tubulin-QS	Expresses QS, the repressor of TA's with QF AD, under the control of α Tubulin84B promoter
30033	UAS-QS	Expresses QS, the repressor of TA's with QF AD, under the control of UAS
		[15]

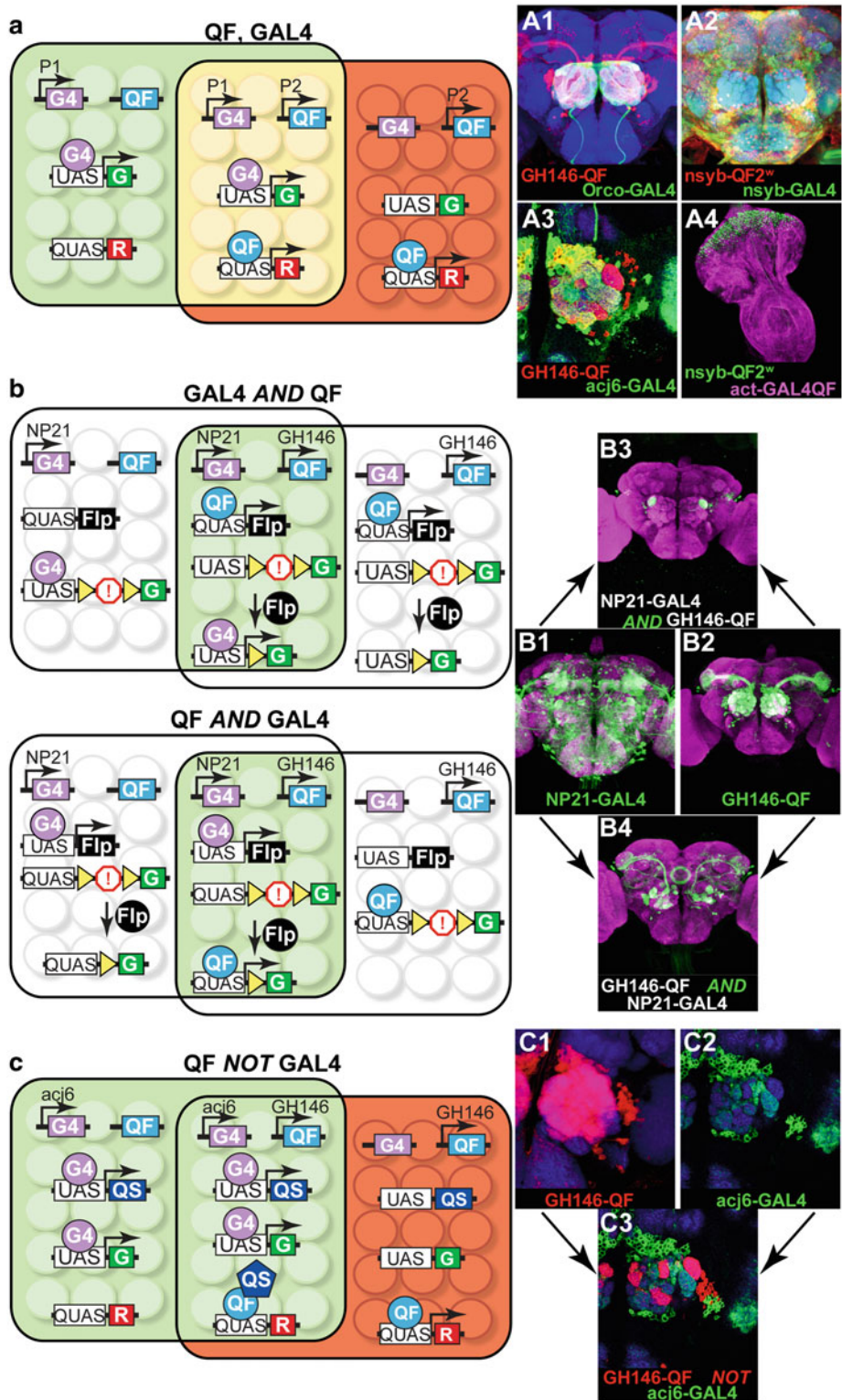


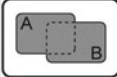
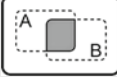
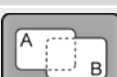
Fig. 4 Intersectional labeling. **(a)** Simultaneous expression of two different reporters in overlapping subsets of cells with the GAL4/UAS and the Q-system. In the schematics on the *left*, the genotype of the fly is: *P1-GAL4, P2-QF, UAS-GFP, QUAS-RFP*. Enhancers P1 (green area) and P2 (red area) are active in partially overlapping subsets of cells (yellow area). **A1:** Expression in olfactory receptor neurons (green) and olfactory projection neurons (red) with *GH146-QF, QUAS-mtdt-3xHA, Orco-GAL4, UAS-mCD8-GFP*. **A2:** Pan-neuronal co-expression

[58], to express Channelrhodopsin in olfactory receptor neurons but a Ca^{2+} reporter in projection neurons [59, 61], or to label one subpopulation of projection neurons with GFP and another one with RFP to visualize their overlap [60].

A practical application of the Q-system is to use it to narrow down expression patterns from many currently available GAL4 expression lines, such as the Janelia GAL4 enhancer collection [62], the MiMIC collection [63], or the InSITE collection [64]. It may be useful to express an effector only in the cells that belong to the overlapping expression patterns of two selected enhancer lines, e.g., a Janelia-GAL4 line and an InSITE-QF line. Alternatively, neurons of a GAL4 line may be selectively targeted based on their overlap (or lack of overlap) with the expression patterns of a neurotransmitter or other gene of interest, e.g., by utilizing such reagents as *TβH-QF* (octopaminergic neurons), *Cha-QF2* (cholinergic neurons), *GADI-QF2* (GABAergic neurons), or *nompC-QF* (mechanosensory neurons) (Table 2). Limiting expression may be achieved in a variety of ways, conceptualized by AND, NOT, and XOR logic operations (Fig. 4, Table 2) [15, 65]. For many operations, an *FRT-transcriptional stop-FRT* cassette is essential. FLPase, when expressed in a cell, will permanently remove the transcriptional stop cassette from the cell and all its progeny. The optimal strategy depends on the availability of driver, reporter and repressor lines, and also on the possible off-target labeling that may arise at early developmental stages. For example, the two approaches to the AND intersection

Fig. 4 (continued) of nuclear β -galactosidase (red) and membrane-bound GFP (green). Genotype: *nsyb-QF2w*, *QUAS-nucLacZ*, *nsyb-GAL4*, *UAS-mCD8-GFP*. A3: Antennal lobe innervation of two partially overlapping projection neuron populations. Genotype: *GH146-QF*, *QUAS-mtdt-3xHA*, *acj6-GAL4*, *UAS-mCD8-GFP*. Antennae were removed to eliminate *Acj6*+ olfactory neuron innervations in the antennal lobe. A4: Ubiquitous (purple) and neuronal (green) expression in the eye-antennal imaginal disk of a third instar larva. Genotype: *nsyb-QF2w*, *QUAS-mCD8-GFP*, *actin-GAL4QF*, *UAS-mtdt-3xHA*. Brain regions (blue) depict anti-nc82 staining in A1–A3. Schematic and image in (a) and A3 reprinted with permission from [15]. (b) Limiting expression to cells that express both transactivators. Two possible ways to achieve a GAL4 AND QF intersection are diagrammed. Genotype of top schematic and B3: *NP21-GAL4*, *GH146-QF*, *QUAS-FLP*, *UAS-FRT-stop-FRT-GFP*. Genotype of bottom schematic and B4: *NP21-GAL4*, *GH146-QF*, *UAS-FLP*, *QUAS-FRT-stop-FRT-GFP*. B1: Expression pattern of *NP21-GAL4* line, as visualized by the *UAS-mCD8-GFP* reporter (green). B2: Expression pattern of *GH146-QF* lines as visualized by the *QUAS-mCD8-GFP* reporter (green). B3 and B4: Expression patterns of the AND intersections. The difference between B3 and B4 arises due to the developmental timing of FLPase expression. See main text for details. Purple color depicts anti-nc82 staining. Schematic and images in (b) reprinted with permission from ref. 15. (c) Using one transactivator to limit the expression pattern of the other transactivator: QF NOT GAL4 intersectional example. Genotype of the flies: *acj6-GAL4*, *GH146-QF*, *UAS-QS*, *UAS-GFP*, *QUAS-RFP* (schematic and C3). The *acj6-GAL4* line drives the GFP reporter and the QS repressor, which silences QF in those cells where GAL4 and QF expression patterns overlap. QF is active in the cells where GAL4 is not expressed, resulting in the RFP labeling. C1: Expression pattern of *GH146-QF*, visualized with *QUAS-mtdt-3xHA* (red). C2: Expression pattern of *acj6-GAL4*, visualized with *UAS-mCD8-GFP* (green). C3: Expression pattern of QF NOT GAL4 intersection. The final expression pattern in red is limited to where QF, but not GAL4, is expressed. Blue color depicts anti-nc82 staining. Schematic and images in (c) reprinted with permission from ref. 15

Table 2
Intersectional expression

Logic operation	Description	Transgenes required ^a “QF” stands for QF, QF2, or QF2 ^w . “R” stands for Reporter. “>” stands for FRT site.
A OR B		<ol style="list-style-type: none"> 1. A-GAL4, B-QF, UAS-R, QUAS-R 2. A-GAL4, B-GAL4QF, UAS-R 3. A-GAL4, B-LexAQF, UAS-R, LexAop-R 4. A-QF, B-GAL4QF, UAS-R, QUAS-R 5. A-QF, B-LexAQF, QUAS-R, LexAop-R 6. A-GAL4QF, B-LexAQF, UAS-R, LexAop-R
B NOT A		<ol style="list-style-type: none"> 1. A-GAL4, B-QF, UAS-QS, QUAS-R 2. A-QF, B-GAL4, QUAS-GAL80, UAS-R 3. A-GAL4, B-LexAQF, UAS-QS, LexAop-R 4. A-LexAQF, B-GAL4, LexAop-GAL80, UAS-R
A AND B		<ol style="list-style-type: none"> 1. A-GAL4, B-QF, UAS-FLP, QUAS>stop>R 2. A-GAL4, B-QF, QUAS-FLP, UAS>stop>R 3. A-GAL4, B-LexAQF, UAS-FLP, LexAop>stop>R 4. A-GAL4, B-LexAQF, LexAop-FLP, UAS>stop>R 5. A-LexAQF, B-QF, QUAS-FLP, LexAop>stop>R 6. A-LexAQF, B-QF, LexAop-FLP, QUAS>stop>R 7. A-GAL4QF, B-QF, UAS-FLP, QUAS>stop>R 8. A-GAL4QF, B-QF, QUAS-FLP, UAS>stop>R 9. tub>GAL80>, A-GAL4, UAS-R, B-FLP
NOT A		<ol style="list-style-type: none"> 1. A-GAL4, tub-QF, UAS-QS, QUAS-R 2. A-QF, tub-GAL4, QUAS-GAL80, UAS-R 3. A-GAL4, act-LexAQF, UAS-QS, LexAop-R
A→B		<ol style="list-style-type: none"> 1. A-GAL4, B-QF, tub>QF>, UAS-FLP, QUAS-R 2. A-QF, B-GAL4, tub>GAL4>, QUAS-FLP, UAS-R 3. A-GAL4, B-LexAQF, tub>LexAQF>, UAS-FLP, LexAop-R 4. A-QF, B-LexAQF, tub>LexAQF>, QUAS-FLP, LexAop-R 5. A-GAL4QF, B-LexAQF, tub>LexAQF>, UAS-FLP, LexAop-R
A XOR B		<ol style="list-style-type: none"> 1. A-GAL4, UAS-R, A-QS, B-QF, QUAS-R, B-GAL80 2. A-GAL4, UAS-R, A-QS, B-GAL4QF, B-GAL80 3. A-GAL4, UAS-R, A-QS, B-LexAQF, LexAop-R, B-GAL80
A NOR B		<ol style="list-style-type: none"> 1. A-GAL4, B-QF, tub>R>, UAS-FLP, QUAS-FLP 2. tub-GAL4, UAS-R, A-QF, QUAS-GAL80, B-LexAQF, LexAop-GAL80 3. tub-GAL4, UAS-R, A-GAL80, B-GAL80
A NAND B		<ol style="list-style-type: none"> 1. tub>R>GAL4, UAS-R, A-QF, QUAS-FLP, B-LexAQF, LexAop-GAL80 2. tub>R>GAL4, UAS-R, A-FLP, B-GAL80 3. tub-GAL4, UAS-R, A-QF, QUAS-FLP, B-LexAQF, LexAop>stop>GAL80
A XNOR B		<ol style="list-style-type: none"> 1. A-FLP, B-QF, tubP>GAL4>, QUAS>GAL80>GAL4, UAS-R

^aThis list is not exhaustive; alternative genetic combinations are possible

could give rise to different final readouts. These differences are based on two parameters: (1) which line (GAL4 or QF) drives FLPase expression; this can potentially label all cells that developmentally expressed the chosen transcription factor up to the timepoint of investigation; (2) which line (GAL4 or QF) drives final reporter expression; this potentially labels only those cells normally labeled at the chosen timepoint. For instance, the two ways to achieve the AND intersection between *NP21-GAL4* and *GH146-QF* lines are shown in Fig. 4. *NP21-GAL4* drives expression in many cells in the adult brain, including some of the olfactory projection neurons. *GH146-QF* drives expression only in the olfactory projection neurons in the adult. In the first case, *NP21-GAL4* drives *UAS-FLPase* expression, while *GH146-QF* drives GFP expression from *QUAS-FRT-transcriptional stop-FRT-GFP* constructs that have excised their *FRT-transcriptional stop-FRT* cassette. The resulting expression pattern includes a subset of olfactory projection neurons targeting 5 glomeruli, normally labeled by *GH146-QF* in the adult fly, and also cells of the ellipsoid body, which are not normally labeled by *GH146-QF* in the adult. The labeled projection neurons are ones where *NP21-GAL4* had been expressed at some point during development (which led to the removal of the *FRT-transcriptional stop-FRT*) and now visualized by *GH146-QF* activity. It is also possible that labeling is visible in the adult in cells where GFP had been produced at an earlier developmental stage, i.e., in the pupa, but is not produced in the adult. This perdurance of GFP is presumably the reason for the labeling in the ellipsoid body neurons. In the other possible AND intersectional approach, *GH146-QF* drives *QUAS-FLPase* expression, while *NP21-GAL4* drives GFP expression from *UAS-FRT-transcriptional stop-FRT-GFP* constructs that have excised their *FRT-transcriptional stop-FRT* cassette. This genotype results in labeling of only olfactory projection neurons that target only one glomerulus since these are the only neurons that express *NP21-GAL4* at the adult stage. Thus, the final readout from an AND intersection strongly depends on which line (GAL4 or QF) is used to report developmental versus final expression patterns. It is often informative to perform both approaches. In general, it is often advantageous to choose the line (GAL4 or QF) that expresses most strongly in the tissue of interest at the timepoint of interest for the final readout (visualized by the *FRT-stop-FRT* reporter).

Table 1 lists Q-system reagents that have been published or otherwise publicized, and will be good starting places for intersectional approaches. For example, InSITE [64], MiMIC [63], and Trojan-MiMIC [66] collections are useful tools for recapitulating interesting expression pattern with various driver constructs.

7 Mosaic Analyses with the Q-System

Genetic mosaics allow for the study of gene function in a small subpopulation of cells, to label one or a few cells out of a full expression pattern, or to investigate cells born at defined developmental timepoints. The *GAL4/UAS* system has been extensively used for these purposes [21, 23–25, 67–71]. The Q-system, used together with *GAL4/UAS*, allows for even more advanced mosaic labeling and gene manipulation. We discuss here two approaches for mosaic analyses: FLP-mediated removal of an *FRT-transcriptional stop-FRT* cassette [72, 73], and Mosaic Analysis with Repressible Cell Marker (MARCM) [15, 21].

The simplest form of mosaic analysis requires three transgenic components: (1) a driver line (e.g., *GH146-QF*) which drives expression of a reporter; (2) the reporter transgene (e.g., *QUAS-FRT-stop-FRT-mtdT*) where the transcriptional stop cassette (*FRT-stop-FRT*) can be removed by the FLP recombinase; and (3) a ubiquitous heatshock promoter driving FLPase expression (*hsFLP*). The FLP recombinase will be expressed when the flies are placed at temperatures above 29 °C. Longer heat shock times, or higher temperatures up to 38 °C, can induce more FLPase expression. This is a useful way to regulate the extent of the *FRT-stop-FRT* excision. FLP-mediated excision may occur during or shortly after the heatshock treatment, resulting in labeling in a random subset of cells where the driver line is expressing. By adjusting the duration of the heatshock and the strength of the *hsFLP* line, it is possible to label anywhere from only a few cells to most cells out of the driver line expression pattern [48]. In contrast to *UAS-FLP/QUAS-FLP* discussed above, the effects of *hsFLP* are much more random because the FLPase is expressed only during the heatshock treatment. This results in low amount of FLPase in a cell and thus low probability of successful DNA targeting. This method is particularly useful to study cell and circuit anatomy, and also to drive expression of effectors (e.g., TrpA1, Channelrhodopsin, halorhodopsin, toxins, etc.) with the purpose of examining behavioral phenotypes of individual flies and relating them to the affected cells [73].

The Q FLP-out method, described above, may be used together with the analogous *GAL4* FLP-out method, to independently label cells from two different expression patterns.

Temporally refined mosaic analysis is possible using the MARCM technique [21]. This technique induces mosaic labeling based on birthdates of the labeled cells. Here the transgene expression (e.g., driven by *GH146-QF*) is suppressed throughout the animal (e.g., by ubiquitous QS from *tubulinP-QS*), but may be relieved in cells that, due to *hsFLP*-mediated recombination of homologous chromosomes during mitotic cell division, have lost the *tubP-QS* repressor-coding gene (Fig. 5). By experimentally

selecting the developmental stage of the animals to be heatshocked, it is possible to reproducibly label specific cells of interest born at particular developmental times. In the example shown in Fig. 5a, two of the homologous chromosomes carry the *FRT* sequence at the same genomic position, with one of the chromosomes carrying the ubiquitous repressor transgene *tubP-QS* distal to the *FRT* sequence. Ubiquitous expression of QS prevents QF activity in all cells. The same animal also carries *PI-QF* (e.g., *GH146-QF*), *QUAS-GFP*, and *hsFLP* transgenes that can be located elsewhere in the genome apart from the chromosome arms distal to the *FRT* sites. Upon 37 °C heatshock, the FLP recombinase will be expressed, and can cause mitotic recombination at the *FRT* sites in a random subset of cells born at or shortly after the heatshock treatment. Only one of the cells produced from the cell division will be positively labeled by the marker (e.g., GFP). All progeny (if any) of the labeled cell will also be labeled, resulting in clones of labeled cells (Fig. 5A1–A4). If mitotic recombination had not occurred, the two daughter cells would remain unlabeled.

GAL4-MARCM [21] may be used simultaneously with Q-MARCM [15] or LexAQP-MARCM [41]. The two MARCM events will drive two different reporters (e.g., *UAS-GFP* and *QUAS-RFP*) and, depending on the genomic arrangement of transgenes, can be either independent of each other (independent double MARCM for mosaic labeling of overlapping or non-overlapping subsets of cells), or they can be coupled to label both progenies of a single cell division (coupled MARCM). Independent double MARCM might be utilized to simultaneously label (and manipulate) cells not marked by the same GAL4 reporter (e.g., glia labeled by GAL4 and neurons labeled by QF; or two different neuronal populations that innervate a common target). Independent double MARCM could also be used to label cells born at the same developmental timepoint but which are not marked by the same GAL4 line. In addition, independent and coupled MARCM enables clones of labeled cells to be generated that also carry homozygous mutant alleles of genes of interest. By examining morphology, number and distribution of the labeled cells it is possible to study the effects of gene mutations on development or anatomy. Coupled MARCM also allows to examine the fate of two progenies born in one cell division, which can be used for mapping cell lineages and division patterns [15]. Figure 5b provides the schematics of independent double MARCM labeling for partially overlapping GAL4 and QF driver lines, driving GFP and RFP, respectively. The repressor transgenes GAL80 and QS can be located on different arms of two homologous chromosomes (as shown on Fig. 5b) or on non-homologous chromosomes. The driver and reporter transgenes must be located on chromosome arms non-homologous to those with repressor transgenes. Upon FLP-mediated recombination, some GAL4-expressing cells may

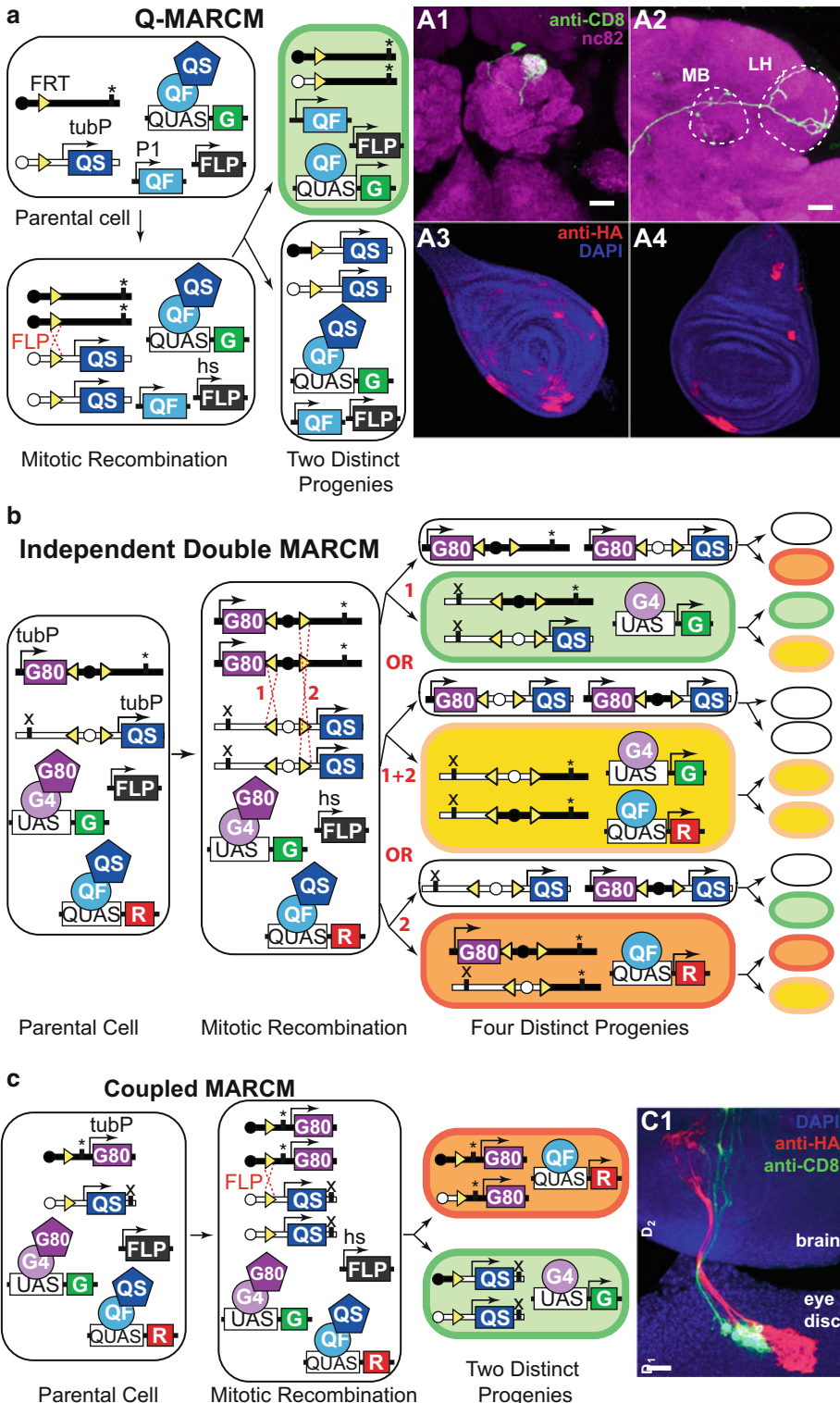


Fig. 5 MARCM analysis. **(a)** Q-MARCM. The genotype of the parental cell is: *hsFLP*, *FRT* site (homozygous) recombined with *tubulin-QS* (heterozygous), *P1-QF*, *QUAS-GFP*. “**” marks the location of a recessive mutation that may be studied in the labeled cells. Upon FLPase-mediated mitotic recombination, one of the two postmitotic cells will lose the *tubulin-QS* transgene and start expressing GFP (top). The other postmitotic cell will remain unlabeled (bottom). **A1** and **A2**: Q-MARCM labeling of a single olfactory projection neuron, visualized in

lose the *GAL80* transgene and express GFP (case 1). If a heatshock is repeated at a later stage, another FLP-mediated recombination may occur, leading to the loss of the QS repressor and expression of both GFP and RFP, thus labeling the cells yellow. Simultaneous RFP and GFP expression is possible only in the cells that belong to the expression patterns of both the GAL4 and the QF drivers. Interestingly, progeny of the unlabeled twin, produced after the first heatshock, may produce RFP-labeled cells upon a second heatshock, provided that both GAL4 and QF drivers are active in these cells. Subsequent heatshocks will not change the expression profile of the cells that already underwent two FLP-mediated recombinations during mitotic cell divisions, but may affect the cells that underwent zero or one FLP-recombination prior to the heatshock. Another possible option (case 2) is that upon the first heatshock a cell will lose both *GAL80* and *QS* repressor genes, thus being labeled yellow. Subsequent heatshocks will not alter the expression profile of this cell's or its twin's progeny. The last option (case 3) is analogous to case 1, but results in the loss of the QS repressor in QF-expressing cells. The outcome of independent double MARCM will be labeling that includes red, green, and yellow cells, with yellow being dominant when the expression patterns of the GAL4 and QF lines are identical. Some of the cells that underwent FLPase-mediated recombination will remain unlabeled. Independent double MARCM thus allows for the investigation of cells born at two distinct timepoints. However, due to the random nature of FLPase-mediated recombination, the number of cells that undergo two FLP recombination events may be low.

To label both progeny from a single cell division, Q-MARCM and GAL4-MARCM can be coupled by placing repressor transgenes

Fig. 5 (continued) the antennal lobe (A1), the mushroom body (MB, A2), and the lateral horn (LH, A2). Genotype: *hsFLP*, *UAS-mCD8-GFP* (X); *GH146-QF*#53, 82BFRT, *tub-QS*/82BFRT (III). A3 and A4: Q-MARCM labeled clones in the leg (A3) and wing (A4) imaginal disks of a third instar larva. Genotype: *hsFLP1*, *QUAS-mtdT-3xHA* (X); *ET40-QF* (II); 82BFRT, *tubP-QS*/82BFRT (III). Schematic and brain images reprinted with permission from ref. 15. **(b)** Independent double MARCM. The genotype of the parental cell is: *hsFLP* (also present in all progeny cells), *P1-QF*, *P2-GAL4*, *UAS-GFP*, *QUAS-RFP*, *FRT* site (homozygous) recombined with *tubulin-GAL80* (heterozygous), a different *FRT* site (homozygous) recombined with *tubulin-QS* (heterozygous). “**” and “x” mark independent recessive mutations that may be studied in postmitotic cells. There are three possible outcomes of a heatshock-induced mitotic recombination at the *FRT* sites (1 or 2 or 1 + 2). The progenitors for each event are schematized with each generating a labeled and an unlabeled cell. Upon a second heatshock, mitotic recombination may happen again, altering the expression profiles of the progeny. See main text for details. Schematic modified with permission from ref. 15. **(c)** Coupled MARCM. The genotype of the parental cell is: *hsFLP* (also present in all progeny cells), *P1-GAL4*, *P1-QF*, *UAS-GFP*, *QUAS-RFP*, *FRT* site (homozygous) recombined with *tubulin-GAL80* (heterozygous) or with *tubulin-QS* (heterozygous). “**” and “x” mark independent recessive mutations that may be studied in postmitotic cells. FLP-mediated recombination during mitosis at the *FRT* site followed by chromosome segregation result in all progeny being labeled either with GFP or with RFP. C1: Coupled MARCM clones in the eye-antennal imaginal disk send processes that innervate the brain of a third-instar larva. Genotype: *hsFLP1*, *QUAS-mtdT-3xHA*, *UAS-mCD8-GFP* (X); *ET40-QF* (II); 82BFRT *tubP-QS/tubP-GAL4* 82BFRT *tubP-GAL80* (III). Schematic and image reprinted with permission from ref. 15

on homologous chromosome arms (Fig. 5c). This way, after a FLPase-mediated homologous recombination event, one twin will lose the GAL80 repressor but retain QS, while the other will retain GAL80 but lose QS. The first twin will start expressing GAL4-driven GFP, and the second twin will start expressing QF-driven RFP. Subsequent heatshocks will not alter the labeling pattern.

MARCM analysis is not limited to the labeling of cells, but also allows mosaic expression of effector transgenes (e.g., RNAi, toxin, Channelrhodopsin, etc.). It can also be used to generate positively labeled homozygous mutant cells if a mutant gene allele is located on the same homologous FRT chromosome arm as the FRT repressor transgenes [21]. Wildtype and mutant cells will be labeled by different markers, and their morphology and number may be easily examined [15, 21]. In addition, Q-MARCM and GAL4-MARCM can be utilized alongside standard GAL4 and Q-system-mediated transgenic expression. For example, Q-MARCM could be used to label single neurons, while GAL4 utilized to express RNAi in varying target tissues. This could reveal how genetic disruption of one tissue population affects the neuronal targeting of a different population.

8 Future Directions

The Q-system represents a versatile set of genetic tools that can be used in situations in which a single binary expression system has proven to be experimentally insufficient. Many QF, QUAS, and QS fly stocks are already publicly available from the Bloomington Drosophila Stock Center (<http://flystocks.bio.indiana.edu/Browse/Qsystem/Qintro.htm>). Table 1 summarizes all currently published or available Q-system lines. With the recent development of QF2, QF2^w, GAL4QF, and LexAQF, we expect many more transgenic lines to be generated in the near future by our and other labs. As additional creative uses for the Q-system are introduced, the utility of the Q-system will extend beyond what is described here.

A number of useful modifications could be developed in the future for the *Drosophila* Q-system: split-QF for additional intersectional expression control; QF2/QF2^w enhancer trap lines or QF2 expression collections to increase the number of available Q-system expression patterns; improved methods to deliver QA across the glia to the neurons to increase QA effects on central brain neurons; the development of QS variants with altered affinities for QA; and the development of temperature-sensitive QF or QS variants for temporal control of Q-system activity.

A genetic technique allowing *GAL4* lines to be easily converted to *QF2* lines was reported. This work includes many new useful *QF2* driver lines. Lin C-C, Potter CJ (2016) Editing transgenic DNA components by inducible gene replacement in *Drosophila melanogaster*. *Genetics* In press.

Acknowledgements

We thank Chun-Chieh Lin, Qili Liu, Sha Liu, Darya Task and Olga Markova for their helpful comments on the manuscript.

References

1. Ramaekers A, Quan X-J, Hassan BA (2012) Genetically encoded markers for drosophila neuroanatomy. In: The making and un-making of neuronal circuits in *Drosophila*. Humana Press, Totowa, NJ, pp 49–59
2. Silbering AF, Bell R, Galizia CG, Benton R (2012) Calcium imaging of odor-evoked responses in the *Drosophila* antennal lobe. *J Vis Exp*:e2976
3. Simpson JH (2009) Mapping and manipulating neural circuits in the fly brain, Advances in genetics. Academic, New York, pp 79–143
4. Dietzl G, Chen D, Schnorrer F, Su K-C, Barinova Y, Fellner M, Gasser B, Kinsey K, Oppel S, Scheiblauer S et al (2007) A genome-wide transgenic RNAi library for conditional gene inactivation in *Drosophila*. *Nature* 448:151–156
5. Duffy JB (2002) GAL4 system in *Drosophila*: a fly geneticist's Swiss army knife. *Genesis* 34:1–15
6. Sweeney ST, Broadie K, Keane J, Niemann H, O'Kane CJ (1995) Targeted expression of tetanus toxin light chain in *Drosophila* specifically eliminates synaptic transmission and causes behavioral defects. *Neuron* 14:341–351
7. Hamada FN, Rosenzweig M, Kang K, Pulver SR, Ghezzi A, Jegla TJ, Garrity PA (2008) An internal thermal sensor controlling temperature preference in *Drosophila*. *Nature* 454:217–220
8. Lima SQ, Miesenböck G (2005) Remote control of behavior through genetically targeted photostimulation of neurons. *Cell* 121:141–152
9. Paradis S, Sweeney ST, Davis GW (2001) Homeostatic control of presynaptic release is triggered by postsynaptic membrane depolarization. *Neuron* 30:737–749
10. Hay BA, Wassarman DA, Rubin GM (1995) *Drosophila* homologs of baculovirus inhibitor of apoptosis proteins function to block cell death. *Cell* 83:1253–1262
11. Grether ME, Abrams JM, Agapite J, White K, Steller H (1995) The head involution defective gene of *Drosophila melanogaster* functions in programmed cell death. *Genes Dev* 9:1694–1708
12. Brand AH, Perrimon N (1993) Targeted gene expression as a means of altering cell fates and generating dominant phenotypes. *Development* 118:401–415
13. Lai S-L, Lee T (2006) Genetic mosaic with dual binary transcriptional systems in *Drosophila*. *Nat Neurosci* 9:703–709
14. Bello B, Resendez-Perez D, Gehring WJ (1998) Spatial and temporal targeting of gene expression in *Drosophila* by means of a tetracycline-dependent transactivator system. *Development* 125:2193–2202
15. Potter CJ, Tasic B, Russler EV, Liang L, Luo L (2010) The Q system: a repressible binary system for transgene expression, lineage tracing, and mosaic analysis. *Cell* 141:536–548
16. Venken KJT, Simpson JH, Bellen HJ (2011) Genetic manipulation of genes and cells in the nervous system of the fruit fly. *Neuron* 72:202–230
17. Potter CJ, Luo L (2011) Using the Q system in *Drosophila melanogaster*. *Nat Protoc* 6:1105–1120
18. McGuire SE, Le PT, Osborn AJ, Matsumoto K, Davis RL (2003) Spatiotemporal rescue of memory dysfunction in *Drosophila*. *Science* (New York, NY) 302:1765–1768
19. Lue NF, Chasman DI, Buchman AR, Kornberg RD (1987) Interaction of GAL4 and GAL80 gene regulatory proteins in vitro. *Mol Cell Biol* 7:3446–3451
20. Sayeed O, Benzer S (1996) Behavioral genetics of thermosensation and hygrosensation in *Drosophila*. *Proc Natl Acad Sci* 93:6079–6084
21. Lee T, Luo L (1999) Mosaic analysis with a repressible cell marker for studies of gene function in neuronal morphogenesis. *Neuron* 22:451–461
22. Luo L, Lee T, Nardine T, Null B, Reuter J (1999) Using the MARCM system to positively mark mosaic clones in *Drosophila*. *Dros Inf Serv* 82:102–105
23. Lee T, Luo L (2001) Mosaic analysis with a repressible cell marker (MARCM) for *Drosophila* neural development. *Trends Neurosci* 24:251–254
24. del Valle Rodriguez A, Didiano D, Desplan C (2012) Power tools for gene expression and clonal analysis in *Drosophila*. *Nat Methods* 9:47–55
25. Griffin R, Binari R, Perrimon N (2014) Genetic odyssey to generate marked clones in *Drosophila* mosaics. *Proc Natl Acad Sci* 111:4756–4763

26. St Johnston D (2002) The art and design of genetic screens: *Drosophila melanogaster*. *Nat Rev Genet* 3:176–188
27. Wei X, Potter CJ, Luo L, Shen K (2012) Controlling gene expression with the Q repressible binary expression system in *Caenorhabditis elegans*. *Nat Methods* 9:391–395
28. Subedi A, Macurak M, Gee ST, Monge E, Goll MG, Potter CJ, Parsons MJ, Halpern ME (2013) Adoption of the Q transcriptional regulatory system for zebrafish transgenesis. *Methods* (San Diego, Calif) 66(3):433–440
29. Giles NH, Geever RF, Asch DK, Avalos J, Case ME (1991) The Wilhelmine E. Key 1989 invitational lecture. Organization and regulation of the qa (quinic acid) genes in *Neurospora crassa* and other fungi. *J Hered* 82:1–7
30. Patel VB, Schweizer M, Dykstra CC, Kushner SR, Giles NH (1981) Genetic organization and transcriptional regulation in the qa gene cluster of *Neurospora crassa*. *Proc Natl Acad Sci* 78:5783–5787
31. Baum JA, Geever R, Giles NH (1987) Expression of qa-1F activator protein: identification of upstream binding sites in the qa gene cluster and localization of the DNA-binding domain. *Mol Cell Biol* 7:1256–1266
32. Huiet L, Giles NH (1986) The qa repressor gene of *Neurospora crassa*: wild-type and mutant nucleotide sequences. *Proc Natl Acad Sci* 83:3381–3385
33. Tsuji G, Kenmochi Y, Takano Y, Sweigard J, Farrall L, Furusawa I, Horino O, Kubo Y (2000) Novel fungal transcriptional activators, Cmr1p of *Colletotrichum lagenarium* and Pig1p of *Magnaporthe grisea*, contain Cys2His2 zinc finger and Zn(II)2Cys6 binuclear cluster DNA-binding motifs and regulate transcription of melanin biosynthesis genes in a developmentally specific manner. *Mol Microbiol* 38:940–954
34. Zhang L, Bermingham-McDonogh O, Turcotte B, Guarente L (1993) Antibody-promoted dimerization bypasses the regulation of DNA binding by the heme domain of the yeast transcriptional activator HAP1. *Proc Natl Acad Sci* 90:2851–2855
35. Hidalgo P, Ansari AZ, Schmidt P, Hare B, Simkovich N, Farrell S, Shin EJ, Ptashne M, Wagner G (2001) Recruitment of the transcriptional machinery through GAL11P: structure and interactions of the GAL4 dimerization domain. *Genes Dev* 15:1007–1020
36. Walters KJ, Dayie KT, Reece RJ, Ptashne M, Wagner G (1997) Structure and mobility of the PUT3 dimer. *Nat Struct Mol Biol* 4:744–750
37. Kraulis PJ, Raine ARC, Gadhavi PL, Laue ED (1992) Structure of the DNA-binding domain of zinc GAL4. *Nature* 356:448–450
38. Marmorstein R, Carey M, Ptashne M, Harrison SC (1992) DNA recognition by GAL4: structure of a protein-DNA complex. *Nature* 356:408–414
39. Ma J, Ptashne M (1987) Deletion analysis of GAL4 defines two transcriptional activating segments. *Cell* 48:847–853
40. Pfeiffer BD, Ngo T-TB, Hibbard KL, Murphy C, Jenett A, Truman JW, Rubin GM (2010) Refinement of tools for targeted gene expression in *Drosophila*. *Genetics* 186:735–755
41. Riabinina O, Luginbuhl D, Marr E, Liu S, Wu MN, Luo L, Potter CJ (2015) Improved and expanded Q-system reagents for genetic manipulations. *Nat Methods* 12:219–222
42. Gill G, Ptashne M (1987) Mutants of GAL4 protein altered in an activation function. *Cell* 51:121–126
43. Kramer JM, Staveley BE (2003) GAL4 causes developmental defects and apoptosis when expressed in the developing eye of *Drosophila melanogaster*. *Genet Mol Res* 2:43–47
44. Shearin HK, Macdonald IS, Spector LP, Stowers RS (2014) Hexameric GFP and mCherry reporters for the *Drosophila* GAL4, Q, and LexA transcription systems. *Genetics* 196:951–960
45. Pfeiffer BD, Truman JW, Rubin GM (2012) Using translational enhancers to increase transgene expression in *Drosophila*. *Proc Natl Acad Sci U S A* 109:6626–6631
46. Markstein M, Pitsouli C, Villalta C, Celniker SE, Perrimon N (2008) Exploiting position effects and the gypsy retrovirus insulator to engineer precisely expressed transgenes. *Nat Genet* 40:476–483
47. Edwards TN, Meinertzhagen IA (2010) The functional organisation of glia in the adult brain of *Drosophila* and other insects. *Prog Neurobiol* 90:471–497
48. Golic KG, Lindquist S (1989) The FLP recombinase of yeast catalyzes site-specific recombination in the *drosophila* genome. *Cell* 59: 499–509
49. Bischof J, Basler K (2008) Recombinases and their use in gene activation, gene inactivation, and transgenesis. In: *Drosophila*. Humana Press, Totowa, NJ, pp 175–195
50. Pitman JL, Huettneroth W, Burke CJ, Krashes MJ, Lai S-L, Lee T, Waddell S (2011) A pair of inhibitory neurons are required to sustain labile memory in the *Drosophila* mushroom body. *Curr Biol* 21:855–861

51. Hong W, Mosca TJ, Luo L (2012) Teneurins instruct synaptic partner matching in an olfactory map. *Nature* 484:201–207

52. Mosca TJ, Luo L (2014) Synaptic organization of the *Drosophila* antennal lobe and its regulation by the Teneurins. *eLife* 3:e03726

53. Prieto-Godino LL, Diegelmann S, Bate M (2012) Embryonic origin of olfactory circuitry in *Drosophila*: contact and activity-mediated interactions pattern connectivity in the antennal lobe. *PLoS Biol* 10:e1001400

54. Wang K, Gong J, Wang Q, Li H, Cheng Q, Liu Y, Zeng S, Wang Z (2014) Parallel pathways convey olfactory information with opposite polarities in *Drosophila*. *Proc Natl Acad Sci* 111:3164–3169

55. Herrera SC, Martín R, Morata G (2013) Tissue homeostasis in the wing disc of *Drosophila melanogaster*: immediate response to massive damage during development. *PLoS Genet* 9:e1003446

56. Silies M, Gohl DM, Fisher YE, Freifeld L, Clark DA, Clandinin TR (2013) Modular use of peripheral input channels tunes motion-detecting circuitry. *Neuron* 79:111–127

57. Parnas M, Lin AC, Huetteroth W, Miesenböck G (2013) Odor discrimination in *Drosophila*: from neural population codes to behavior. *Neuron* 79:932–944

58. Li H, Li Y, Lei Z, Wang K, Guo A (2013) Transformation of odor selectivity from projection neurons to single mushroom body neurons mapped with dual-color calcium imaging. *Proc Natl Acad Sci* 110:12084–12089

59. Liang L, Li Y, Potter CJ, Yizhar O, Deisseroth K, Tsien RW, Luo L (2013) GABAergic projection neurons route selective olfactory inputs to specific higher-order neurons. *Neuron* 79:917–931

60. Strutz A, Soelter J, Baschwitz A, Farhan A, Grabe V, Rybak J, Knaden M, Schmuken M, Hansson BS, Sachse S (2014) Decoding odor quality and intensity in the *Drosophila* brain. *eLife* 3:e04147

61. Gao XJ, Riabinina O, Li J, Potter CJ, Clandinin TR, Luo L (2015) A transcriptional reporter of intracellular Ca^{2+} in *Drosophila*. *Nat Neurosci* 18:917–925

62. Pfeiffer BD, Jenett A, Hammonds AS, Ngo T-TB, Misra S, Murphy C, Scully A, Carlson JW, Wan KH, Laverty TR et al (2008) Tools for neuroanatomy and neurogenetics in *Drosophila*. *Proc Natl Acad Sci U S A* 105:9715–9720

63. Venken KJT, Schulze KL, Haelterman NA, Pan H, He Y, Evans-Holm M, Carlson JW, Levis RW, Spradling AC, Hoskins RA et al (2011) MiMIC: a highly versatile transposon insertion resource for engineering *Drosophila melanogaster* genes. *Nat Methods* 8:737–743

64. Gohl DM, Silies MA, Gao XJ, Bhalerao S, Luongo FJ, Lin C-C, Potter CJ, Clandinin TR (2011) A versatile *in vivo* system for directed dissection of gene expression patterns. *Nat Methods* 8:231–237

65. Pérez-Garijo A, Fuchs Y, Steller H (2013) Apoptotic cells can induce non-autonomous apoptosis through the TNF pathway. *eLife* 2:01004

66. Diao F, Ironfield H, Diao F, Luan H, Shropshire W, Ewer J, Marr E, Potter CJ, Landgraf M, White BH (2015) Plug-and-play genetic access to *Drosophila* cell types using exchangeable exon cassettes. *Cell Rep* 10:1410–1421

67. Griffin R, Sustar A, Bonvin M, Binari R, del Valle Rodriguez A, Hohl AM, Bateman JR, Villalta C, Heffern E, Grunwald D et al (2009) The twin spot generator for differential *Drosophila* lineage analysis. *Nat Methods* 6:600–602

68. Yu H-H, Chen C-H, Shi L, Huang Y, Lee T (2009) Twin-spot MARCM to reveal the developmental origin and identity of neurons. *Nat Neurosci* 12:947–953

69. Evans CJ, Olson JM, Ngo KT, Kim E, Lee NE, Kuoy E, Patananan AN, Sitz D, Tran P, Do M-T et al (2009) G-TRACE: rapid Gal4-based cell lineage analysis in *Drosophila*. *Nat Methods* 6:603–605

70. Hadjieconomou D, Rotkopf S, Alexandre C, Bell DM, Dickson BJ, Salecker I (2011) Flybow: genetic multicolor cell labeling for neural circuit analysis in *Drosophila melanogaster*. *Nat Methods* 8:260–266

71. Hampel S, Chung P, McKellar CE, Hall D, Looger LL, Simpson JH (2011) *Drosophila* Brainbow: a recombinase-based fluorescence labeling technique to subdivide neural expression patterns. *Nat Methods* 8:253–259

72. Kosman D, Small S (1997) Concentration-dependent patterning by an ectopic expression domain of the *Drosophila* gap gene knirps. *Development* 124:1343–1354

73. Stockinger P, Kvitsiani D, Rotkopf S, Tirián L, Dickson BJ (2005) Neural circuitry that governs *Drosophila* male courtship behavior. *Cell* 121:795–807

74. Petersen LK, Stowers RS (2011) A gateway MultiSite recombination cloning toolkit. *PLoS One* 6:e24531

75. Stowers RS (2011) An efficient method for recombineering GAL4 and QF drivers. *Fly* 5:371–378

76. Shearin HK, Dvarishkis AR, Kozeluh CD, Stowers RS (2013) Expansion of the gateway multisite recombination cloning toolkit. *PLoS One* 8:e77724
77. Zhang YV, Ni J, Montell C (2013) The molecular basis for attractive salt-taste coding in *Drosophila*. *Science* 340:1334–1338
78. Zielke N, Korzelius J, van Straaten M, Bender K, Schuhknecht GFP, Dutta D, Xiang J, Edgar BA (2014) Fly-FUCCI: a versatile tool for studying cell proliferation in complex tissues. *Cell Rep* 7:588–598
79. Cavanaugh DJ, Geratowski JD, Wooltorton JRA, Spaethling JM, Hector CE, Zheng X, Johnson EC, Eberwine JH, Sehgal A (2014) Identification of a circadian output circuit for rest:activity rhythms in *Drosophila*. *Cell* 157:689–701

Chapter 4

Analysis of MicroRNA Function in *Drosophila*

Geetanjali Chawla, Arthur Luhur, and Nicholas Sokol

Abstract

MicroRNAs are short noncoding, ~22-nucleotide RNAs that regulate protein abundance. The growth in our understanding of this class of RNAs has been rapid since their discovery just over a decade ago. We now appreciate that miRNAs are deeply embedded within the genetic networks that control basic features of metazoan cells including their identity, metabolism, and reproduction. The *Drosophila melanogaster* model system has made and will continue to make important contributions to this analysis. Intended as an introductory overview, here we review the current methods and resources available for functional analysis of fly miRNAs for those interested in performing this type of analysis.

Key words *Drosophila melanogaster*, microRNA, miRNA

1 Introduction

This chapter reviews molecular and genetic methods and resources for the analysis of microRNA (miRNA) function in the *Drosophila melanogaster* (*D. melanogaster*) model system. Biochemical analysis of the fly system has also provided critical insights into the upstream pathways that control miRNA production. We start with a brief summary of fly miRNA biogenesis, but see two excellent recent reviews [1, 2] and their references for more detailed descriptions of this aspect of fly miRNAs.

Mature miRNAs are ~22 nucleotides (nts) long but are derived from slightly longer, ~70-nt RNAs that fold into hairpin structures known as pre-miRNAs. These pre-miRNAs are transcribed within even longer primary transcripts, or pri-miRNAs, that can be hundreds or thousands of base-pairs long. Pri-miRNAs are cleaved by a ribonuclease complex containing two proteins, Drossha and Pahsa, to release pre-miRNAs, which are exported from the nucleus and subsequently cut by a second ribonuclease Dicer. This cleavage releases two different short RNAs coming from either the 5' or 3' arm of the hairpin. Current naming conventions distinguish these related miRNAs with -5p or -3p suffixes, respectively, [3] and usually one of these predominates while the other is degraded. Once

released, the active miRNA incorporates into a protein complex that includes Argonaute1 (Ago1) and directs this silencing complex to partially complementary sequences of target mRNAs, usually to quench their translation or promote their degradation. Below, we summarize methods to identify miRNAs as well as characterize their expression patterns, targets, and *in vivo* functions.

2 Identification

The previous version of this chapter described early efforts to identify 78 *D. melanogaster* miRNAs via molecular cloning and sequencing of small RNAs as well as *in silico* predictions [4]. Since that chapter was published in 2008, the construction and deeper sequencing of numerous small RNA libraries as well as the detailed characterization of 12 genomes of related *Drosophila* species [5] has identified many additional miRNAs. The current tally of fly miRNA hairpins is 256 [3] and these include both canonical miRNAs as well as mirtrons, which are derived from spliced introns and follow a slightly altered biogenesis pathway [5–11]. The rate at which new miRNAs are discovered has decreased in recent years, suggesting that the total number of fly miRNAs has reached its upper limit [11]. This section summarizes recent miRNA identification efforts as well as some resulting insights into miRNA biogenesis and modifications. Please *see* ref. [1] and [2] for more detailed discussion of miRNA biogenesis in flies and other models.

Groups associated with the Model Organism Encyclopedia of DNA Elements (modENCODE) project have assembled a comprehensive catalog of the small RNA contingent of the fly transcriptome. Collectively, the analysis of roughly 1.5 billion sequencing reads identified 146 new miRNAs [6, 7, 10–13]. These reads were obtained from RNA libraries generated from various developmental stages, tissues, mutants, cell lines, and protein immunoprecipitates (IP). For example, IP of Ago1 from total tissue extract enriches the isolation of miRNAs engaged in silencing since Ago1 is a critical component of the miRNA effector complex. Identified miRNAs originated from both sense and anti-sense transcription units, intergenic regions, introns, intron–exon junctions as well as occasionally from the untranslated and coding regions of genes [7]. In addition to cataloguing processed small RNAs, Graveley et al. also annotated a set of 23 primary miRNA transcripts using deep sequencing and cap analysis of gene expression (CAGE). The magnitude of these deep sequencing efforts has provided a detailed picture of the small RNA landscape, capturing not only abundantly produced mature miRNAs but also byproducts generated during miRNA processing. As outlined below, analysis of these byproducts has revealed unanticipated aspects of miRNA production.

2.1 *Mirtrons*

Mirtrons were identified as hairpins whose 5' and 3' ends coincide with intron termini [9]. These hairpins are released by splicing, bypassing the usual miRNA processing by Drosha and Pasha. Initial analysis of approximately one million reads identified 14 mirtrons and subsequent analysis of 17 additional million reads identified 5 more [6, 9]. A computational machine learning approach using the original 14 mirtrons as a training set yielded 51 additional mirtron candidates, and six of these were found in modENCODE small RNA data sets [8]. The total number of fly mirtrons is currently estimated to be ~30 [8].

2.2 *IsomiRs and miRNA Modifications*

Mature miRNAs can have multiple isoforms, termed isomiRs, due to heterogeneities that arise at both 5' and 3' termini [7, 10, 14]. Sequence heterogeneity at the 5' end is likely due to alternative processing by Drosha and/or Dicer [7]. A prominent example is miR-210: two versions of miR-210—one with one additional 5' nucleotide—are equally represented in RNA libraries [10]. Modifications at the 3' end are due to untemplated additions, including uridylation and adenylation, as well as trimming [1, 2]. The exonuclease Nibbler, for example, is responsible for 3' trimming of miR-34 mature sequence, resulting in multiple miR-34 isoforms [14, 15]. The consequences of these modifications are not known, but likely impact either miRNA stability and/or miRNA–target interactions.

In addition, miRNA sequences can be edited post-transcriptionally by the Adenosine Deaminase acting on RNA (ADAR) enzyme. Editing events can change miRNA seed sequences, affect processing by Drosha/Pasha/Dicer, and even alter Ago-sorting preference [7]. Deep sequencing analysis of processed miRNAs identified three mature miRNAs, miR-100, miR-971, and miR-33*, that frequently contained A to G nucleotide changes. Subsequent analysis of miR-100 and its co-transcribed neighbors, let-7 and miR-125, identified additional editing events in the hairpins of all three miRNAs and found that some of these editing events control the differential expression of the three mature miRNAs *in vitro* and *in vivo* [16].

2.3 *Additional miRNA Hairpin Products*

Additional products of miRNA hairpins are functional including loop sequences. For example, miR-34 and miR-317 hairpin loop sequences were recovered in IPs of the miRNA effector Ago1 [17]. These loop sequences were generated during miRNA biogenesis and, consistent with their association with Ago1, were functional and repressed the expression of reporter transgenes containing complementary sequences. The *in vivo* function of these hairpin RNAs as well as the byproducts of other miRNA hairpins remains to be determined.

3 Spatiotemporal Detection

Knowledge of the expression of miRNAs is crucial for understanding the functional roles of miRNAs. This section outlines methods that have been utilized for detecting the spatiotemporal expression patterns of fly miRNAs.

3.1 Transcriptional Reporters

The expression pattern of primary miRNA transcripts can be determined by generating transgenic lines containing promoter/enhancer fragments fused to reporters such as GFP or LacZ. Such an approach has been utilized to determine *in vivo* expression of miR-1 [18–20], miR-124 [21], miR-278 [22], miR-309/3/286/4/5/6-1/6-2/6-3 [18], and the *let-7-Complex* (*let-7-C*) locus [23]. Designing transcriptional reporters requires prior knowledge of the transcription start site that can be mapped using 5'RACE. This helps preclude open reading frames present in the 5'UTR of primary miRNA transcripts in the reporter and its subsequent degradation by nonsense-mediated decay.

3.2 Sensors

“MiRNA sensors” are ubiquitously expressed transgene reporters (GFP or luciferase) that contain one or more perfectly complementary miRNA binding sites in the 3'UTR. The miRNA sensors function like a target for miRNA-mediated destruction via the RNA interference machinery, and hence their expression is reduced in regions of high miRNA activity. This technique has been successfully used to report functional read-outs of miRNAs as well as in genetic screens for functional characterization of the miRNA biogenesis pathway [16, 24–31]. One limitation of this technique is reporter protein perdurance, which could mask the activity of dynamically expressed miRNAs. More recently, cleavable sensor oligonucleotides have been described that report miRNA expression in live mammalian cells [32]. Use of these activatable sensors will allow researchers to report dynamics of miRNA-mediated regulation in diverse contexts such as cell fate determination.

3.3 *In Situ* Hybridization

In situ hybridization (ISH) is an invaluable method to directly visualize mRNAs at a cellular resolution in whole organisms and tissues as well as tissue sections. This hybridization-based technique has been utilized to study the expression pattern of both primary as well as processed miRNAs in specific cell types. The most popular ISH techniques involve the use of alkaline phosphatase or fluorophore-conjugated probes and fluorescent tyramide signal amplification (TSA)-based procedures [33]. Primary miRNA transcripts have been detected with antisense probes corresponding to the genomic DNA surrounding the miRNA hairpin precursor. This approach was successfully used to monitor the dynamic expression of pri-miRNAs involved in patterning of

D. melanogaster embryos [34–36]. Since processing of a primary miRNA transcript is a regulated event, the temporal and spatial expression of the parental primary transcripts may or may not coincide with the expression of the miRNA that it generates [37]. Thus, several advances have been made to facilitate ISH detection of mature miRNAs. Labeled locked nucleic acid (LNA) probes and either a colorimetric or fluorescent method for probe detection have been successfully used to detect miRNA expression in *D. melanogaster*, including let-7, miR-1, miR-7, miR-10, miR-34, miR-252, miR-956, and miR-980 [19, 38–43]. LNA probes are a class of RNA analogs in which the 2' oxygen and the 4' carbon positions in the ribose ring are connected or “locked” to create increased stability relative to DNA or RNA when they are base-paired with complementary DNA or RNA. The development of LNA probes has circumvented the limitations associated with detection of mature miRNAs that have a lower hybridization potential owing to their short length. More recently, immunofluorescence coupled to in situ hybridization (IF-ISH) protocols for dual detection of protein and miRNA have been described for *D. melanogaster* tissues [33]. These will likely allow simultaneous detection of miRNAs in specific cell types (for e.g. stem cells) that can be marked and visualized with antibodies in specific tissues.

3.4 Northern Blot Analysis

Northern blot analysis has been used extensively for the detection of mature and precursor miRNAs in diverse tissues and cell lines [22, 23]. The technique involves running total RNA on a denaturing polyacrylamide gel followed by its transfer to a nitrocellulose membrane. The RNA is fixed onto the membrane by UV crosslinking and incubated with antisense radiolabeled or fluorescent probes. Though Northern analysis does not require any special equipment and also provides high-quality confirmation, the low level of sensitivity, large amounts of RNA required as well as the time-consuming protocols have resulted in improvisation of the traditional protocol [44]. For instance, the use of LNA-modified northern probes that exhibit higher thermal stability and show improved hybridization properties has increased the sensitivity of the Northern blotting technique and allowed more specific detection of miRNAs [45, 46].

3.5 Quantitative Real-Time PCR

Quantitative real-time PCR (qRT-PCR) is the most widely used method to detect and quantify miRNA levels. This technique relies on reverse transcription of the miRNA followed by qPCR with real-time monitoring. Some of the limitations of miRNA reverse transcription are (1) the short length of the miRNA, (2) the presence of the mature miRNA sequence in the precursor and primary miRNA transcript, and (3) the lack of common sequence features like poly (A) tails.

Two main methods have been developed to reverse transcribe miRNAs: universal and miRNA-specific reverse transcription. In the

first approach, the 3' end of all miRNAs are elongated with a poly(A) tail using an *E. coli* poly(A) polymerase (miRCURY, Exiqon). This is followed by reverse transcription with an oligo(dT) primer containing a universal primer-binding sequence. PCR amplification is enabled by a miRNA-specific forward primer and a reverse primer that anneals to the 3' portion of the miRNA as well as the poly(A) tail with SYBR green dye as the detector. The second approach utilizes a stem-loop primer for reverse transcription (Taqman, Life Technologies) (Fig. 1a, d) and has been useful for detection of *D. melanogaster* miRNAs [16, 47, 48]. The stem-loop sequence in the primer reduces annealing to the primary and precursor miRNA, thereby increasing specificity of the assay. This assay method is not affected by genomic DNA contamination and is able to discriminate between miRNAs that differ by just one nucleotide.

Another advantage of this approach is that it can be easily scaled up for high-throughput analysis. For example, commercially available customizable plates and microfluidic cards can be designed to assay entire sets of miRNAs (Fig. 1a, d). Some of the advantages of this assay system include high sensitivity and a wide dynamic range. qRT-PCR is the only method that can provide absolute miRNA quantitation and is accomplished by generating standard curves from synthetic oligonucleotides of known concentration [49].

3.6 miRNA Microarrays

Microarray technology is a high-throughput approach to monitor expression of several miRNAs in a single experiment. This technique involves purification of small RNAs from cells and tissues followed by fluorescent labeling of the enriched small RNA fraction (Fig. 1b, d). The labeled RNA is hybridized to arrays that are spotted with the appropriate high-affinity probes specific to mature RNAs. Microarray scanners are used to detect the spot intensity of the double-stranded fragments. Either constitutively expressed miRNAs or U6 snRNA or tRNA is used for data normalization. Although microarray analysis may require optimization to determine the best hybridization condition, it allows the simultaneous comparison of expression levels of several miRNAs in a single experiment at a low cost. The expression profiles obtained from the microarray analysis need further validation by other quantitative techniques like Northern analysis or real-time PCR. This approach has been utilized to determine age-modulated expression of miRNAs in adult fly brains [50], whole animals [51], and during embryogenesis in flies overexpressing dMyc [52].

3.7 Deep Sequencing

In the past couple years, next-generation sequencing technology (NGS) has allowed high-throughput detection of small RNAs with a high degree of reliability [53]. NGS technology allows sequencing of large numbers of DNA fragments in parallel, producing millions of short reads in a single run of an automated sequencer [54, 55]. The most widely adopted NGS platform that has been

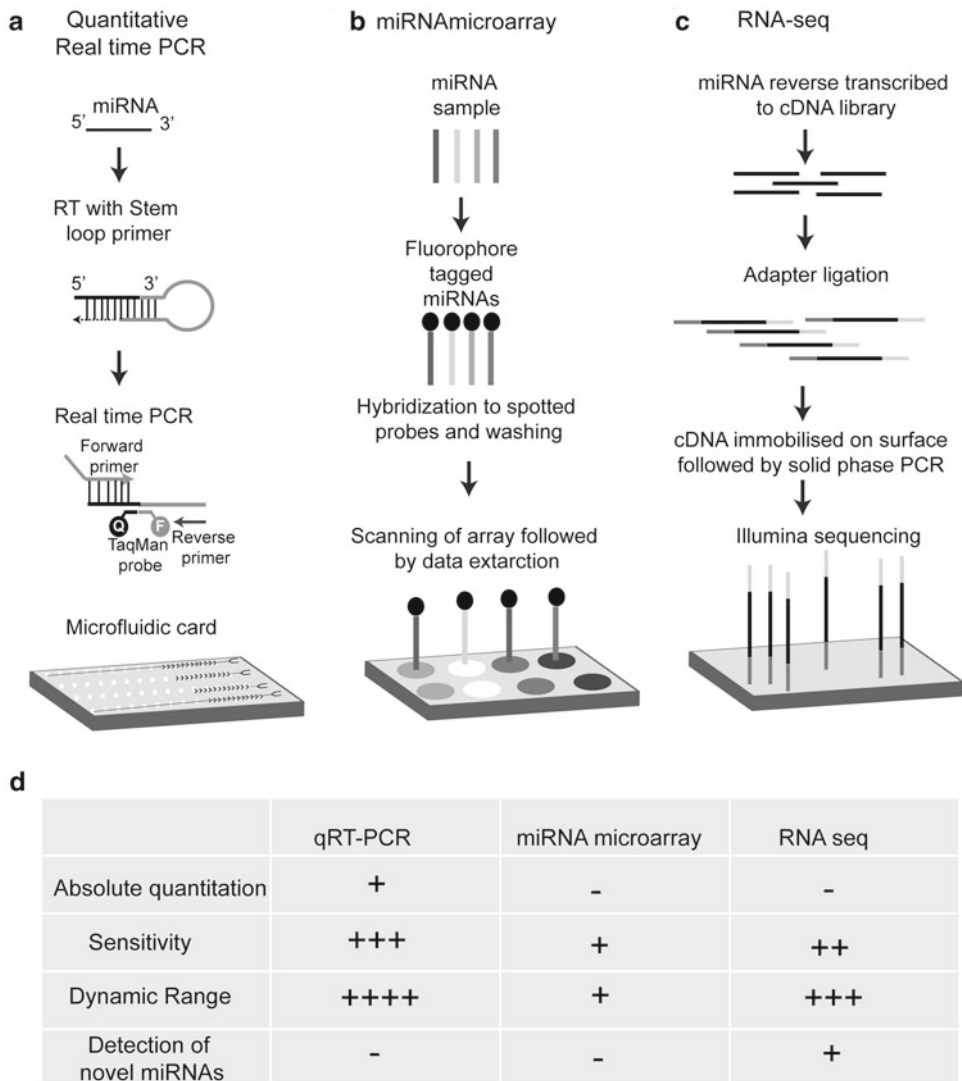


Fig. 1 Methods for profiling miRNAs. (a) TaqMan quantitative real-time PCR (qRT-PCR). The miRNA in the RNA sample is reverse transcribed with a stem-loop primer that base-pairs to the 3' end of the miRNA. The resulting cDNA is amplified in the presence of a miRNA-specific forward and reverse primer in presence of a miRNA-specific Taqman probe. The Taqman probe has a fluorescent reporter linked to its 5' end and a nonfluorescent quencher at the 3' end of the probe. During PCR, the Taqman probe anneals specifically to the sequence between forward and primer sites. As the DNA polymerase proceeds along the template, it cleaves the Taqman probe that is hybridized to the template. This cleavage separates the fluorescent reporter from the quencher dye, resulting in an increase in fluorescence of the reporter. Taqman miRNA assays are available in an array format and can be used for high-throughput analysis of miRNAs. (b) MiRNA microarrays. miRNAs in an RNA sample are fluorescently labeled and hybridized to DNA-based capture probes (with LNA-modified bases) spotted on arrays. The microarrays are washed and scanned to detect fluorescence intensity. (c) RNA-seq. A cDNA library is generated by reverse transcription of miRNAs in the sample RNA. The cDNAs in the library are ligated to adapter molecules that allow the library to be affixed to a solid phase. The Illumina/Solexa technology utilizes a “bridged amplification” that occurs on the surface of the flow cell. After amplification, the flow cell is exposed to reagents required for sequencing. (d) Table comparing different available methods for miRNA profiling

successfully used in the *D. melanogaster* model is the Illumina/Solexa technology [7, 11, 56] (Fig. 1c, d). One of the advantages of using RNA sequencing (RNA-seq) over microarray profiling is that it allows discovery of novel miRNAs. Other advantages include the extremely high level of sensitivity and resolution that allows detection of miRNAs that are very similar to one another, including isomiRs that differ by a single base. However, the analysis of data obtained from NGS platforms requires substantial computational support and it cannot provide an absolute quantitative view of these transcripts. For a given sample analyzed by RNA-seq, miRNA quantitation is expressed as a number relative to the total number of sequence reads for the sample, thus comparisons between samples with high variance in miRNA expression are not reliable owing to the difference in the number of reads. Furthermore, the number of reads obtained for any miRNA may not necessarily correlate with its actual abundance owing to the biases introduced during sample preparation and sequencing.

4 Targets

MiRNAs carry out their biological functions by regulating the expression of target mRNAs. Estimates suggest that an individual miRNA can regulate hundreds of targets and the fly has been a premier system for ascertaining which of its targets is biologically relevant. This section summarizes methods for identifying and verifying miRNA targets.

4.1 Bioinformatic Strategies

A first step in identifying miRNA targets is the use of target prediction algorithms. The most common of these include TargetScan, Pictar, and miRanda [57]. These programs search curated sets of 3'UTR sequences for likely miRNA-binding sites based on various criteria including sequence complementarity, duplex free energy, and conservation [43, 57–62]. A frequently imposed guideline requires the presence of six contiguous base-pairs in the target that are complementary to the 5' end, or “seed” region, of the miRNA [57]. Recently, Chi et al. proposed an additional guideline for target recognition that permits the presence of a “nucleation bulge” in the seed region [63, 64]. This interaction requires only five consecutive base-pairings at the position 2–6 of the miRNA to form a sufficiently stable duplex. Incorporation of this guideline into future algorithms will likely improve predictions.

One current limitation of these commonly used algorithms is that they are not updated frequently with new 3'UTRs. They therefore rely on outdated 3'UTR information and are missing more recently identified alternative 3'UTR, isoform-specific 3'UTR, or extended 3'UTR sequences [65]. Direct integration of revised annotations into the target prediction tools should address

this problem. In addition, manually curated 3'UTR sequences can be searched for predicted miRNA binding sites using the RNAhybrid program [66].

In addition, the high rates of false discovery of target prediction algorithms have emphasized the need for direct methods to identify mRNA targets [64]. One such method used in flies is the identification of mRNAs present in Ago1 complexes purified from cell lines and embryos, since these IPs should be enriched for miRNA targets [67, 68]. Analogous methods have been used in other model systems [64, 69–71] which include a crosslinking step between protein and mRNA that facilitates the identification of miRNA-bound mRNA regions. More widespread use of these approaches in flies could identify *in vivo* miRNA targets and lead to considerably more accurate and powerful miRNA target prediction tools.

4.2 Strategies for Validating miRNA Targets

Targets identified from the approaches described above must be verified *in vivo*. A common and rapid method to determine whether a miRNA binding site is functional involves using cell culture-based reporter assay, in which the 3'UTR of the target gene of interest is placed downstream of a reporter gene. Reporters bearing mutated miRNA binding sites are used as negative control. MiRNAs are transfected, and the expression of the reporters was analyzed. Transgenic animals harboring such reporters are used to analyze predicted target 3'UTRs *in vivo*, and such verified reporters can also be used as the miRNA sensors described in Subheading 3.3.

The current gold standard to validate predicted miRNA targets relies on genetic manipulations. The genetic loss or gain of a miRNA should have a predictive effect on the expression of responsive mRNA targets, leading to their elevation or reduction respectively. Available resources to manipulate miRNA levels are described in Subheading 5 below. Furthermore, the functional relevance of individual miRNA–target relationships can be assessed with genetic interaction assays. Based on the assumption that miRNA phenotypes are a consequence of target overexpression, these assays usually test whether particular phenotypes are suppressed by the reduction of target expression due to heterozygosity or RNAi-mediated knock down. This approach has identified a number of functional miRNA/mRNA interactions, including between *miR-8* and its targets *atrophin* [59], *U-shaped* [58], and components of the Toll pathway [72], *miR-9a* and its multiple targets *dystroglycan* [73], *senseless* [74], and *dLMO* [75], *miR-14* and *sugarbabe* [61], *miR-124* and its targets *anachronism* [21] and *transformer* [76], *miR-184* and *saxophone* [77], *miR-263a/b* and *head involution defective* [78], *miR-278* and *expanded* [22], *miR-279* and its targets *unpaired* [60] and *nerfin-1* [79], the *miR-310/313* cluster and *khc-73* [80] as well as the *wingless* pathway [81], and between the *miR-100/let-7/miR-125* cluster and *chronologically inappropriate morphogenesis* [62] as well as a second target *abrupt* [82].

A very recently described approach employs genome editing to evaluate the functional and physiological relevance of particular miRNA–target relationships. The clustered regularly interspaced short palindromic repeat (CRISPR)/Cas9 system allows manipulation of sequences within endogenous genetic loci [83]. Using this system, Bassett et al. deleted predicted binding sites of the *bantam* miRNA within 3'UTR sequences of its previously established target, *enabled* [84]. Contrary to expectations, these manipulations did not lead to elevated Enabled expression in vivo or to known wing boundary phenotypes associated with elevated Enabled. While these results suggest that *bantam* may not regulate *enabled* during wing formation, it remains possible that the edited *enabled* 3'UTR retains cryptic or non-canonical *bantam* binding sites. Nevertheless, this approach will likely become a widely used assay to evaluate the physiological relevance of specific miRNA–target interactions, since it bypasses the potential pleiotropic effects resulting from miRNA knockout or overexpression.

5 In Vivo Functions

As with any other genes, the in vivo function of miRNAs is determined by analyzing the consequences of their overexpression and depletion in animals and cell lines. A series of recently described reagent collections greatly facilitate this type of analysis, and are summarized here.

5.1 Conditional Expression of microRNAs

Three groups have independently prepared collections of transgenic strains for the conditional expression of most fly miRNAs [24, 85, 86]. These three overlapping collections are based on the UAS/Gal4 system and contain individual or clusters of miRNAs under UAS control. The specifics of each collection vary, and are summarized in Table 1. Key differences between the collections include the design of transformation plasmid, the method of transgenesis, the location of the resulting transgenes, and number of individual miRNAs represented. Many miRNAs are included in all three collections, allowing the opportunity to easily verify results using independently generated but presumably equivalent reagents.

To date, these collections of UAS-miRNA transgenes have been used to screen for miRNAs whose elevated or ectopic expression lead to wing phenotypes and embryonic lethality [24, 85]. These types of analyses can be extended to additional tissues and developmental stages as well as to the cellular and molecular levels in order to verify predicted targets. Conditional expression of a genome-wide miRNA library has also been applied to cell culture in order to systematically identify miRNAs that regulate specific 3'UTRs [87]. This approach identified a set of miRNAs that regulate components

of the *hedgehog* signaling pathway that were subsequently verified in intact animals, and can be used to identify miRNAs that regulate additional 3'UTRs of particular interest as well.

5.2 Genetic Depletion of microRNAs

MiRNA function has been inferred from the phenotypic analysis of mutants in core miRNA processing components as well as individual miRNAs or miRNA clusters. Genetic analysis of core components has usually focused on *dicer*, *drosha*, *pasha*, and *argonaute*, but is confounded by observations that these loci have nonoverlapping, miRNA-independent functions and consequently distinct phenotypes [26, 88]. Therefore, a clearer picture of the roles of miRNAs in particular biological processes can be obtained from individual mutants, although the creation of such mutants has historically been laborious and time-consuming. To date, mutations in 16 miRNA loci have been reported using homologous recombination and P-element excision, including *miR-1*, *miR-7*, *miR-8*, *miR-9a*, *miR-9c*, *miR-11*, *miR-12/-283/-304*, *miR-34*, *miR-92b*, *miR-100/let-7/miR-125*, *miR-124*, *miR-263a/-263b*, *miR-278*, *miR-279/-996*, *miR-309/-3/-286/-4/-5/-6-1/-6-2/-6-3*, *miR-310/-311/-312/-313*, *miR-969*, *miR-989*, *bantam*, and *iab-4/-8* [19–22, 27, 39, 50, 59, 74, 77–80, 82, 89–98]. This collection of mutants disrupts a total of 33 miRNAs due to miRNA clustering, and rescuing transgenes are available to probe some of the individual members of such clusters.

Table 1
UAS-miRNA Libraries for conditional expression

No. of miRNAs	Insertion location	Plasmid	No. of UAS sites	Promoter/5'UTR ORF	3'UTR	miRNA flanking sequence ^a	Ref.
64	Various attP sites ^b	pUAST.attB-SLIC	5	HSP70	none	SV40 ~200bp	[86]
14	Various attP sites ^b	pUASP.attB-SLIC	14	P-transposase	none	K10 ~200bp	[86]
33	P-element insertions	pUAST-dsRed	5	HSP70	DsRed	SV40 ~200bp	[86]
180	attP ZH-86F8	pW20	10	HSP70	none	SV40 miR-1 base	[24]
149	P-element insertions	pUAST-dsRed	5	HSP70	DsRed	SV40 ~400bp	[85]
107	attP2, 68A4	pWalium10-LUC	10	HSP70	Luciferase	SV40 ~400bp	[85]

^aIndicates amount of endogenous surrounding sequence included for each miRNA. Roughly 150 bp of miR-1 flanking sequence was included for all UAS-miRNA transgenes from ref. 24

^bVarious attP sites include M(attP)ZH-86FB, P(CaryP)attP2-68A4, P(CaryP)attP16, and PBAC(attP-3B)VK00037

The set of available miRNA mutants will expand considerably due to a large-scale effort by Stephen Cohen's lab that has generated 77 new mutants by targeted homologous recombination (Stephen Cohen, personal communication). Together with previously reported mutants, the collection encompasses 95 mutant loci deleting 130 miRNAs that collectively account for the overwhelming majority (>99%) of all *D. melanogaster* miRNA sequence reads. This resource will allow individual researchers to comprehensively evaluate the role of miRNAs in most developmental processes using standard techniques including mosaic analysis of cells and tissues of interest. Potential redundancy can be addressed via the combination of multiple mutants. Techniques will need to be developed to genetically deplete miRNAs in post-mitotic cells in order to examine their roles in differentiated cells, including during tissue remodeling and aging.

5.3 microRNA Sponges

miRNA sponges complement miRNA mutants for the analysis of loss-of-function phenotypes. Sponges are transgenically encoded transcripts that contain nucleotide repeats that are complementary to a particular miRNA. Conditional expression of these transcripts likely sequesters the targeted miRNA, interfering with its normal function. Sponges have been generated to 11 miRNAs to date, including miR-2b, -2c, -6, -7, -8, -9a, 13a, -13b, 92b, and -276 [85, 92, 96, 99]. Current sponge design includes 20 tandem repeats located within the 3'UTR of dsRed, which is used to monitor sponge expression, under UAS control. Case studies found that sponges for miR-7, -8, and 9a elicited similar though milder phenotypes as previously characterized genetic mutants [99]. Thus, current efforts to generate a comprehensive transgenic sponge library will facilitate functional analysis, allowing the use of specific Gal4 drivers to simultaneously knock down multiple miRNAs in specific populations of dividing or differentiated cells and tissues. However, since sponge transcript levels must be saturating, analysis is best performed with multiple insertions of the same sponge and in a background with reduced miRNA gene dosage. Even then, this approach may not effectively sequester the most abundant miRNAs, like miR-1. Furthermore, to eliminate concerns about false-positive and false-negative phenotypes, results with sponges will need to be confirmed with genetic mutants.

5.4 Other Antisense Techniques

In addition to transgenic sponges, other antisense technologies have been employed to disrupt fly miRNA function. For example, sequence-specific antisense oligonucleotides that block the function of individual miRNAs can be easily transfected into cultured cells in order to characterize cellular and molecular phenotypes [100]. An analogous approach has also been pioneered in intact adults that injected with cholesterol-modified antisense oligonucleotides to investigate the role of let-7 in post-mitotic neurons

[101]. Key issues of working with such “antagomirs” include their effective and specific delivery as well as the occurrence of false-positive phenotypes due to off-target effects. The latter is of particular concern, given that embryonic phenotypes reported in an early study on antagomirs have not been shared by subsequently generated genetic mutants [102]. Thus, caution is merited when using antagomirs and any phenotypes identified from antisense injection should be verified in cells or tissues genetically depleted of the targeted miRNA.

6 Final Thoughts

The *D. melanogaster* model system provides an ever-increasing repertoire of resources and methods available to study miRNAs. With a manageable number of miRNA genes and mutations available in many of them, the role of miRNAs in complex biological processes can be comprehensively analyzed at molecular and cellular resolution. Thus, the fly model will likely continue to serve as a powerful tool to explore the biological roles of these fascinating molecules.

References

1. Amere SL, Zamore PD (2013) Diversifying microRNA sequence and function. *Nat Rev Mol Cell Biol* 14(8):475–488
2. Ha M, Kim VN (2014) Regulation of microRNA biogenesis. *Nat Rev Mol Cell Biol* 15(8):509–524
3. Kozomara A, Griffiths-Jones S (2014) miRBase: annotating high confidence microRNAs using deep sequencing data. *Nucleic Acids Res* 42(Database issue):D68–D73
4. Sokol NS (2008) An overview of the identification, detection, and functional analysis of *Drosophila* microRNAs. *Methods Mol Biol* 420:319–334
5. Stark A et al (2007) Systematic discovery and characterization of fly microRNAs using 12 *Drosophila* genomes. *Genome Res* 17(12):1865–1879
6. Berezikov E et al (2010) Evolutionary flux of canonical microRNAs and mirtrons in *Drosophila*. *Nat Genet* 42(1):6–9, author reply 9–10
7. Berezikov E et al (2011) Deep annotation of *Drosophila melanogaster* microRNAs yields insights into their processing, modification, and emergence. *Genome Res* 21(2):203–215
8. Chung WJ et al (2011) Computational and experimental identification of mirtrons in *Drosophila melanogaster* and *Caenorhabditis elegans*. *Genome Res* 21(2):286–300
9. Ruby JG, Jan CH, Bartel DP (2007) Intronic microRNA precursors that bypass Drosha processing. *Nature* 448(7149):83–86
10. Ruby JG et al (2007) Evolution, biogenesis, expression, and target predictions of a substantially expanded set of *Drosophila* microRNAs. *Genome Res* 17(12):1850–1864
11. Wen J et al (2014) Diversity of miRNAs, siRNAs, and piRNAs across 25 *Drosophila* cell lines. *Genome Res* 24(7):1236–1250
12. Lau NC et al (2009) Abundant primary piRNAs, endo-siRNAs, and microRNAs in a *Drosophila* ovary cell line. *Genome Res* 19(10):1776–1785
13. Graveley BR et al (2011) The developmental transcriptome of *Drosophila melanogaster*. *Nature* 471(7339):473–479
14. Liu N et al (2011) The exoribonuclease Nibbler controls 3' end processing of microRNAs in *Drosophila*. *Curr Biol* 21(22):1888–1893
15. Han BW et al (2011) The 3'-to-5' exoribonuclease Nibbler shapes the 3' ends of microRNAs bound to *Drosophila* Argonaute1. *Curr Biol* 21(22):1878–1887

16. Chawla G, Sokol NS (2014) ADAR mediates differential expression of polycistronic microRNAs. *Nucleic Acids Res* 42(8):5245–5255
17. Okamura K et al (2013) Functional small RNAs are generated from select miRNA hairpin loops in flies and mammals. *Genes Dev* 27(7):778–792
18. Biemar F et al (2005) Spatial regulation of microRNA gene expression in the *Drosophila* embryo. *Proc Natl Acad Sci U S A* 102(44):15907–15911
19. Sokol NS, Ambros V (2005) Mesodermally expressed *Drosophila* microRNA-1 is regulated by Twist and is required in muscles during larval growth. *Genes Dev* 19(19):2343–2354
20. Kwon C et al (2005) MicroRNA1 influences cardiac differentiation in *Drosophila* and regulates Notch signaling. *Proc Natl Acad Sci U S A* 102(52):18986–18991
21. Weng R, Cohen SM (2012) *Drosophila* miR-124 regulates neuroblast proliferation through its target anachronism. *Development* 139(8):1427–1434
22. Teleman AA, Maitra S, Cohen SM (2006) *Drosophila* lacking microRNA miR-278 are defective in energy homeostasis. *Genes Dev* 20(4):417–422
23. Chawla G, Sokol NS (2012) Hormonal activation of let-7-C microRNAs via EcR is required for adult *Drosophila melanogaster* morphology and function. *Development* 139(10):1788–1797
24. Schertel C et al (2012) Functional characterization of *Drosophila* microRNAs by a novel *in vivo* library. *Genetics* 192(4):1543–1552
25. Pressman S et al (2012) A systematic genetic screen to dissect the MicroRNA pathway in *Drosophila*. *G3 (Bethesda)* 2(4):437–448
26. Luhur A et al (2014) Drosha-independent DGCR8/Pasha pathway regulates neuronal morphogenesis. *Proc Natl Acad Sci U S A* 111(4):1421–1426
27. Brennecke J et al (2003) bantam encodes a developmentally regulated microRNA that controls cell proliferation and regulates the proapoptotic gene hid in *Drosophila*. *Cell* 113(1):25–36
28. Lai EC, Tam B, Rubin GM (2005) Pervasive regulation of *Drosophila* Notch target genes by GY-box-, Brd-box-, and K-box-class microRNAs. *Genes Dev* 19(9):1067–1080
29. Stark A et al (2003) Identification of *Drosophila* MicroRNA targets. *PLoS Biol* 1(3):E60
30. Forstemann K et al (2005) Normal microRNA maturation and germ-line stem cell maintenance requires Loquacious, a double-stranded RNA-binding domain protein. *PLoS Biol* 3(7):e236
31. Brennecke J et al (2005) Principles of microRNA-target recognition. *PLoS Biol* 3(3):e85
32. Yoo B et al (2014) Detection of miRNA expression in intact cells using activatable sensor oligonucleotides. *Chem Biol* 21(2):199–204
33. Toledoano H et al (2012) Dual fluorescence detection of protein and RNA in *Drosophila* tissues. *Nat Protoc* 7(10):1808–1817
34. Aboobaker AA et al (2005) *Drosophila* microRNAs exhibit diverse spatial expression patterns during embryonic development. *Proc Natl Acad Sci U S A* 102(50):18017–18022
35. Kosman D et al (2004) Multiplex detection of RNA expression in *Drosophila* embryos. *Science* 305(5685):846
36. Stark A et al (2008) A single Hox locus in *Drosophila* produces functional microRNAs from opposite DNA strands. *Genes Dev* 22(1):8–13
37. Thomson JM et al (2006) Extensive post-transcriptional regulation of microRNAs and its implications for cancer. *Genes Dev* 20(16):2202–2207
38. Soni K et al (2013) miR-34 is maternally inherited in *Drosophila melanogaster* and *Danio rerio*. *Nucleic Acids Res* 41(8):4470–4480
39. Li X, Carthew RW (2005) A microRNA mediates EGF receptor signaling and promotes photoreceptor differentiation in the *Drosophila* eye. *Cell* 123(7):1267–1277
40. Kucherenko MM et al (2012) Steroid-induced microRNA let-7 acts as a spatio-temporal code for neuronal cell fate in the developing *Drosophila* brain. *EMBO J* 31(24):4511–4523
41. Lemons D, Pare A, McGinnis W (2012) Three *Drosophila* Hox complex microRNAs do not have major effects on expression of evolutionarily conserved Hox gene targets during embryogenesis. *PLoS One* 7(2):e31365
42. Marrone AK et al (2012) Dg-Dys-Syn1 signaling in *Drosophila* regulates the microRNA profile. *BMC Cell Biol* 13:26
43. Toledoano H et al (2012) The let-7-Imp axis regulates ageing of the *Drosophila* testis stem-cell niche. *Nature* 485(7400):605–610

44. Laneve P, Giangrande A (2014) Enhanced northern blot detection of small RNA species in *Drosophila melanogaster*. *J Vis Exp* doi:[10.3791/51814](https://doi.org/10.3791/51814)

45. Okamura K et al (2007) The mirtron pathway generates microRNA-class regulatory RNAs in *Drosophila*. *Cell* 130(1):89–100

46. Varallyay E, Burgyan J, Havelda Z (2007) Detection of microRNAs by Northern blot analyses using LNA probes. *Methods* 43(2):140–145

47. Yang Y et al (2009) The bantam microRNA is associated with *drosophila* fragile X mental retardation protein and regulates the fate of germline stem cells. *PLoS Genet* 5(4):e1000444

48. Varghese J, Cohen SM (2007) microRNA miR-14 acts to modulate a positive auto-regulatory loop controlling steroid hormone signaling in *Drosophila*. *Genes Dev* 21(18):2277–2282

49. Chen C et al (2005) Real-time quantification of microRNAs by stem-loop RT-PCR. *Nucleic Acids Res* 33(20):e179

50. Liu N et al (2012) The microRNA miR-34 modulates ageing and neurodegeneration in *Drosophila*. *Nature* 482(7386):519–523

51. Esslinger SM et al (2013) *Drosophila* miR-277 controls branched-chain amino acid catabolism and affects lifespan. *RNA Biol* 10(6):1042–1056

52. Daneshvar K et al (2013) MicroRNA miR-308 regulates dMyc through a negative feedback loop in *Drosophila*. *Biol Open* 2(1):1–9

53. Friedlander MR et al (2008) Discovering microRNAs from deep sequencing data using miRDeep. *Nat Biotechnol* 26(4):407–415

54. Pritchard CC, Cheng HH, Tewari M (2012) MicroRNA profiling: approaches and considerations. *Nat Rev Genet* 13(5):358–369

55. Ozsolak F, Milos PM (2011) RNA sequencing: advances, challenges and opportunities. *Nat Rev Genet* 12(2):87–98

56. Bentley DR et al (2008) Accurate whole human genome sequencing using reversible terminator chemistry. *Nature* 456(7218):53–59

57. Bartel DP (2009) MicroRNAs: target recognition and regulatory functions. *Cell* 136(2):215–233

58. Hyun S et al (2009) Conserved MicroRNA miR-8/miR-200 and its target USH/FOG2 control growth by regulating PI3K. *Cell* 139(6):1096–1108

59. Karres JS et al (2007) The conserved microRNA miR-8 tunes atrophin levels to prevent neurodegeneration in *Drosophila*. *Cell* 131(1):136–145

60. Luo W, Sehgal A (2012) Regulation of circadian behavioral output via a MicroRNA-JAK/STAT circuit. *Cell* 148(4):765–779

61. Varghese J, Lim SF, Cohen SM (2010) *Drosophila* miR-14 regulates insulin production and metabolism through its target, sugarbabe. *Genes Dev* 24(24):2748–2753

62. Wu YC et al (2012) Let-7-complex microRNAs regulate the temporal identity of *Drosophila* mushroom body neurons via chimmo. *Dev Cell* 23(1):202–209

63. Chi SW, Hannon GJ, Darnell RB (2012) An alternative mode of microRNA target recognition. *Nat Struct Mol Biol* 19(3):321–327

64. Chi SW et al (2009) Argonaute HITS-CLIP decodes microRNA-mRNA interaction maps. *Nature* 460(7254):479–486

65. Smibert P et al (2012) Global patterns of tissue-specific alternative polyadenylation in *Drosophila*. *Cell Rep* 1(3):277–289

66. Rehmsmeier M et al (2004) Fast and effective prediction of microRNA/target duplexes. *RNA* 10(10):1507–1517

67. Easow G, Teleman AA, Cohen SM (2007) Isolation of microRNA targets by miRNP immunopurification. *RNA* 13(8):1198–1204

68. Kadener S et al (2009) A role for microRNAs in the *Drosophila* circadian clock. *Genes Dev* 23(18):2179–2191

69. Hafner M et al (2010) Transcriptome-wide identification of RNA-binding protein and microRNA target sites by PAR-CLIP. *Cell* 141(1):129–141

70. Zisoulis DG et al (2010) Comprehensive discovery of endogenous Argonaute binding sites in *Caenorhabditis elegans*. *Nat Struct Mol Biol* 17(2):173–179

71. Helwak A et al (2013) Mapping the human miRNA interactome by CLASH reveals frequent noncanonical binding. *Cell* 153(3):654–665

72. Lee GJ, Hyun S (2014) Multiple targets of the microRNA miR-8 contribute to immune homeostasis in *Drosophila*. *Dev Comp Immunol* 45(2):245–251

73. Yatsenko AS, Shcherbata HR (2014) *Drosophila* miR-9a targets the ECM receptor Dystroglycan to canalize myotendinous junction formation. *Dev Cell* 28(3):335–348

74. Li Y et al (2006) MicroRNA-9a ensures the precise specification of sensory organ precursors in *Drosophila*. *Genes Dev* 20(20):2793–2805

75. Bejarano F, Smibert P, Lai EC (2010) miR-9a prevents apoptosis during wing development by repressing Drosophila LIM-only. *Dev Biol* 338(1):63–73

76. Weng R et al (2013) miR-124 controls male reproductive success in *Drosophila*. *Elife* 2:e00640

77. Iovino N, Pane A, Gaul U (2009) miR-184 has multiple roles in *Drosophila* female germ-line development. *Dev Cell* 17(1):123–133

78. Hilgers V, Bushati N, Cohen SM (2010) *Drosophila* microRNAs 263a/b confer robustness during development by protecting nascent sense organs from apoptosis. *PLoS Biol* 8(6):e1000396

79. Cayirlioglu P et al (2008) Hybrid neurons in a microRNA mutant are putative evolutionary intermediates in insect CO₂ sensory systems. *Science* 319(5867):1256–1260

80. Tsurudome K et al (2010) The *Drosophila* miR-310 cluster negatively regulates synaptic strength at the neuromuscular junction. *Neuron* 68(5):879–893

81. Pancratov R et al (2013) The miR-310/13 cluster antagonizes beta-catenin function in the regulation of germ and somatic cell differentiation in the *Drosophila* testis. *Development* 140(14):2904–2916

82. Caygill EE, Johnston LA (2008) Temporal regulation of metamorphic processes in *Drosophila* by the let-7 and miR-125 heterochronic microRNAs. *Curr Biol* 18(13):943–950

83. Bassett AR et al (2014) Understanding functional miRNA-target interactions in vivo by site-specific genome engineering. *Nat Commun* 5:4640

84. Becam I et al (2011) Notch-mediated repression of bantam miRNA contributes to boundary formation in the *Drosophila* wing. *Development* 138(17):3781–3789

85. Bejarano F et al (2012) A genome-wide transgenic resource for conditional expression of *Drosophila* microRNAs. *Development* 139(15):2821–2831

86. Szuplewski S et al (2012) MicroRNA transgene overexpression complements deficiency-based modifier screens in *Drosophila*. *Genetics* 190(2):617–626

87. Kim K, Vinayagam A, Perrimon N (2014) A rapid genome-wide microRNA screen identifies miR-14 as a modulator of Hedgehog signaling. *Cell Rep* 7(6):2066–2077

88. Yang JS, Lai EC (2011) Alternative miRNA biogenesis pathways and the interpretation of core miRNA pathway mutants. *Mol Cell* 43(6):892–903

89. Sokol NS et al (2008) *Drosophila* let-7 microRNA is required for remodeling of the neuromusculature during metamorphosis. *Genes Dev* 22(12):1591–1596

90. Bender W (2008) MicroRNAs in the *Drosophila* bithorax complex. *Genes Dev* 22(1):14–19

91. Bushati N et al (2008) Temporal reciprocity of miRNAs and their targets during the maternal-to-zygotic transition in *Drosophila*. *Curr Biol* 18(7):501–506

92. Chen Z et al (2012) miR-92b regulates Mef2 levels through a negative-feedback circuit during *Drosophila* muscle development. *Development* 139(19):3543–3552

93. Fraggi-Grelin F, Lavenant-Staccini L, Therond P (2008) Control of antagonistic components of the hedgehog signaling pathway by microRNAs in *Drosophila*. *Genetics* 179(1):429–439

94. Kugler JM et al (2013) Maternal loss of miRNAs leads to increased variance in primordial germ cell numbers in *Drosophila melanogaster*. *G3 (Bethesda)* 3(9):1573–1576

95. Kugler JM et al (2013) miR-989 is required for border cell migration in the *Drosophila* ovary. *PLoS One* 8(7):e67075

96. Li W et al (2013) MicroRNA-276a functions in ellipsoid body and mushroom body neurons for naive and conditioned olfactory avoidance in *Drosophila*. *J Neurosci* 33(13):5821–5833

97. Sun K et al (2012) Neurophysiological defects and neuronal gene deregulation in *Drosophila* mir-124 mutants. *PLoS Genet* 8(2):e1002515

98. Xu P et al (2003) The *Drosophila* microRNA Mir-14 suppresses cell death and is required for normal fat metabolism. *Curr Biol* 13(9):790–795

99. Loya CM et al (2009) Transgenic microRNA inhibition with spatiotemporal specificity in intact organisms. *Nat Methods* 6(12):897–903

100. Horwich MD, Zamore PD (2008) Design and delivery of antisense oligonucleotides to block microRNA function in cultured *Drosophila* and human cells. *Nat Protoc* 3(10):1537–1549

101. Gehrke S et al (2010) Pathogenic LRRK2 negatively regulates microRNA-mediated translational repression. *Nature* 466(7306):637–641

102. Leaman D et al (2005) Antisense-mediated depletion reveals essential and specific functions of microRNAs in *Drosophila* development. *Cell* 121(7):1097–1108

Chapter 5

Methods for High-Throughput RNAi Screening in *Drosophila* Cells

Maximilian Billmann and Michael Boutros

Abstract

RNA interference (RNAi) is a potent tool for perturbation of gene function in model organisms and human cells. In *Drosophila*, efficient RNAi enables screening approaches for components of cellular processes in vivo and in vitro. In cultured cells, measuring the effect of depleting gene products on a genome-wide scale can systematically associate gene function with diverse processes, such as cell growth and proliferation, signaling and trafficking. Here, we describe methods for RNAi experiments in cultured *Drosophila* cells with a focus on genome-wide loss-of-function screening. We illustrate the design of long double-stranded RNAs and provide protocols for their production by in vitro transcription and delivery in cell-based assays. Furthermore, we provide methods to fine-tune signaling reporters and high-content microscopy assays for genome-wide screening. Finally, we describe essential steps of high-throughput data analysis and how the experimental set-up can improve data normalization using a genome-wide RNAi screen for Wnt pathway activity data as an example.

Key words *Drosophila* cells, RNAi, Double-stranded RNA, Phenotypic readouts, Cell-based assays, High-throughput screening, Data analysis

1 Introduction

RNA interference (RNAi) is a conserved mechanism for post-transcriptional gene silencing. Endogenously transcribed long double-stranded (ds) RNAs are cleaved by the RNase III Drosha into ~70 nucleotide(nt)-long pre-miRNA hairpins [1]. Upon export to the cytoplasm, they are further processed by the RNase III Dicer into 21–22 nt dsRNA fragments and subsequently unwound by helicases [2, 3]. Single-stranded siRNAs associate with Argonaute proteins to form the RNA-induced silencing complex (RISC), which recognize target mRNA by base-pairing and leads to cleavage or translational silencing, depending on the degree of homology [4].

Exploiting this mechanism, exogenously produced RNAi constructs can be transiently transfected or expressed from vectors to silence gene expression [5]. In invertebrate model organisms such as

Caenorhabditis elegans and *Drosophila melanogaster*, RNAi can efficiently be induced by long dsRNAs [6, 7]. Cultured *Drosophila* cells take up long dsRNA molecules (100–800 base-pairs) under starving conditions via receptor-mediated endocytosis and enable fast and efficient loss-of-function experiments [7, 8]. Knockdown efficiency depends not only on the sequence of the dsRNA but also on the targeted mRNA [9]. Moreover, the large number of different siRNAs originating from a long dsRNA mediates high knockdown efficiency of the intended RNA. At the same time, homology of a siRNA with unintended targets can cause off-target effects [10–12]. Therefore, design of dsRNA sequences requires the optimization of knockdown efficiency of the intended gene while minimizing unintended sequence similarity.

The ease of RNAi in *Drosophila* cells has enabled genome-scale functional screening for genes involved in a variety of biological processes. Such screens have used genome-wide RNAi libraries or gene subsets focusing on defined functional groups [13–15]. With the first RNAi screens performed in 2003, RNAi reagent design and the coverage of the used libraries were improved and optimized in the following years [9, 13, 16–18]. Since then, screens have investigated diverse cellular phenotypes using homogenous cell-based assays for viability or the activity of a specific reporter, or single cell-based assays such as microscopy or FACS [13–15, 17].

Homogenous assays quantify phenotypes across the whole cell population in a single well. While homogenous assays measuring, e.g. ATP levels are a fast and simple means to monitor cell fitness, reporter gene assays can measure biological processes such as DNA repair or signaling pathways. To quantify signaling pathway activity, the expression of a detectable reporter gene, such as the firefly luciferase, is regulated by pathway-specific promotor elements. Alternatively, fluorescence-based reporters allow for analyzing cell populations at the single cell level, but often lack the dynamic range of luciferase-based assays. In contrast to homogenous assays, automated microscopy enables the analysis of a cell population including its heterogeneity and single cell phenotypes. Microscopy allows for single-cell phenotyping for morphological alterations and quantification within a single experiment.

Drosophila cell-based assays have been a powerful system for the discovery of functional elements because of several reasons: biological processes are highly conserved and many of human genes have homologs in *Drosophila* [5, 19, 20]. Moreover, the genome is well annotated; yet, it lacks a redundancy often found in mammalian genomes allowing more direct tracing of the genotype to phenotype relation [20].

Interpretation of high-throughput data crucially depends on accounting for technical and biological biases of the experiment. For instance, parameters, such as number of seeded cells, which change over the course of a high-throughput experiment, have to be normalized. Moreover, cell number variation might additionally affect other

features of the data, such as the activity of a signaling cascade. Normalized data require scoring of phenotypes to assess the statistical strength of the results and hit prioritization. The different steps of data normalization and analysis are available in R/Bioconductor software packages using command line or web interfaces [21].

In this chapter, which is an update and extension of a previously published method [22] we provide protocols for RNAi experiments in cultured *Drosophila* cells. We describe the generation of dsRNA, including primer design for the polymerase chain reaction (PCR) on *Drosophila* DNA, one- and two-step PCR amplification of the template, the in vitro transcription and dsRNA purification for small-scale and high-throughput experiments. We explain RNAi experiments with a focus on formats used for current technologies such as RNA sequencing or high-throughput RNAi screening. Finally, based on data from a genome-wide RNAi screen for Wnt regulators, we discuss high-throughput data analysis and highlight how the individual steps depend on the experimental set-up.

2 Materials

2.1 Cell Culture

1. Schneider's *Drosophila* Medium with l-Glutamine supplemented with 10% fetal bovine serum (FBS), 5000 U/ml penicillin, and 5000 µg/ml streptomycin (see Note 1).
2. Express Five SFM Drosophila Medium supplemented with 10× GlutaMAX, 5000 U/ml penicillin, and 5000 µg/ml streptomycin.
3. Phosphate-buffered saline (PBS), pH 7.4.
4. Solution of trypsin (0.25%) and 1 mM ethylenediamine tetraacetic acid (EDTA).
5. Cell scraper (TPP or similar).
6. Trypan Blue.

2.2 Polymerase Chain Reaction

1. 10× PCR buffer: 500 mM KCl, 100 mM Tris–HCl (pH 8.3) and 15 mM MgCl₂. Aliquot and store at -20 °C. Alternatively, use commercially available PCR buffers.
2. Primers (if required, with fused tags or T7-promotor sequences).
3. dNTPs, 10 mM stocks.
4. cDNA or genomic DNA as template.
5. HotStarTaq DNA Polymerase.

2.3 In Vitro Transcription

1. MEGAscript T7 Transcription Kit.
2. T7 RiboMAX Express RNAi System.
3. DNaseI, RNase-free.

2.4 Purification of dsRNA

2.4.1 Small-Scale Purification

2.4.2 High-Throughput Purification (96-Well Format)

1. RNeasy Kit, NucAway Spin Columns.
2. Ethanol, absolute.

1. MultiScreenHTS filter plates with Durapore PVDF membrane (1.2 μ m filter).
2. Bio-Gel P-30 Gel, fine polyacrylamide beads for size exclusion chromatography, 2500–40,000 MW fractionation range.
3. 96-well collection plates.
4. Thermowell Sealing Tape, aluminum.

2.5 RNA Quality Control

1. 2 \times RNA gel-loading buffer: 95% (v/v) deionized formamide, 0.025% (w/v) bromophenol blue, 0.025% (w/v) xylene cyanol, 5 mM EDTA, pH 8.0, 0.025% (w/v) sodium dodecyl sulfate.
2. Agarose gel: E-Gel Precast Agarose Gel, 2% agarose or self-made 2% agarose gel (TAE-buffer) with SYBR Safe.

2.6 RNAi Experiments

2.6.1 RNAi by Bathing (Starvation)

1. Schneider's *Drosophila* Medium with l-Glutamine supplemented with 5000 U/ml penicillin, and 5000 μ g/ml streptomycin.

2. Nuclease-free H₂O.
3. Multidrop dispenser, type 836.

2.6.2 RNAi by Bathing (Serum-Free Growth Condition)

1. Schneider S2 cells (D.Mel-2; Invitrogen).
2. Express Five SFM Drosophila Medium supplemented with 10 \times GlutaMAXTM, and 5000 U/ml penicillin, and 5000 μ g/ml streptomycin.
3. Dimethyldioctadecyl-ammonium bromide (DDAB) transfection reagent, used to increase dsRNA up-take efficiency in S2 cells that grow in serum-free conditions [23].

2.6.3 Liposomal Transfection

2.7 Plasmid Transfection

2.8 Assay Read-out

1. Effectene Transfection Reagent.

1. FuGENE HD Transfection Reagent, Effectene Transfection Reagent.

1. Cell Fitness by Quantification of ATP level
CellTiterGlo Luminescent Cell Viability Assay

2. Signaling Reporter Activity

Dual-Luciferase Reporter Assay System or similar, or home-made kits.

3 Methods

3.1 Design of dsRNAs

1. DsRNAs are transcribed from DNA templates amplified by PCR from cDNA (e.g. expressed sequence tags), first-strand reverse transcription cDNA, or genomic (g)DNA.
2. DsRNAs preferentially target exonic regions, but dsRNA sequences targeting several exons interspersed by small introns also work efficiently (in the latter case, use cDNA rather than gDNA). To enable a rescue of the RNAi phenotype, the dsRNA should target the 3' or 5' untranslated regions to allow expression of an exogenously delivered wildtype gene without the untranslated region.
3. We generally aim to generate dsRNA between 80 and 250 bp in length. While longer dsRNA probes have been efficient for silencing, smaller products often yield less efficient knockdowns.
4. To reduce the probability that the dsRNA targets unintended transcripts, target sequences with homology to other genes are excluded. Therefore, we test dsRNAs for 19-mer homology to unintended genes [10]. Moreover, regions, which encode for highly conserved domains, or those harboring low sequence complexity, such as ubiquitous CAN tri-nucleotide repeats should not be targeted [10].
5. We recommend confirming the primary sequence of a gene of interest, by searching various sequence sources (Publications, National Center for Biotechnology Information and Berkeley Drosophila Genome Project genomic and expressed sequence tags).
6. We recommend the E-RNAi online tool for automated design of optimized long dsRNAs [24]. E-RNAi facilitates target sequence identification, *in silico* dicing of the selected sequence into all possible siRNAs and testing those sequences for potential off-target effects and knockdown efficiency. Finally, E-RNAi provides primer sequences for PCR amplification of the in vitro transcription template from genomic or cDNA using a build-in implementation of the primer3 software [25]. The E-RNAi online tool is accessible at www.e-rnai.org.
7. Alternatively, dsRNA and corresponding primer sequences can be taken from published RNAi libraries targeting different gene regions. The GenomeRNAi database has collected a large collection of dsRNA target regions and associated phenotypes [26].

3.2 Generation of In Vitro Transcription Templates (Amplicons) by PCR

3.2.1 One-Step Generation of Amplicons

To generate DNA templates for the production of dsRNAs by in vitro transcription, a PCR is performed on cDNA or genomic DNA using gene-specific primers, which are fused to T7-promotor sites. The PCR product is subsequently used by the T7 RNA polymerase as a template to synthesize dsRNA. During the design of gene-specific primer using the “E-RNAi” webservice enables direct addition of T7 or SP6 promotor sites (Table 1). For the amplification scheme also *see* Fig. 1a.

1. Perform a standard 100- μ l PCR reaction: use 200 nM of each gene-specific T7-tagged primer, 200 ng DNA as template, 50 μ M of each dNTP, and 2.5 U HotStarTaq DNA polymerase. We have successfully used Taq DNA Polymerase GeneChoice Taq, TaqPlus, and Herculase to amplify PCR products in sufficient quantity for high-yield in vitro transcription reactions.
2. Perform the PCR using a thermal cycler: initial denaturation at 95 °C for 15 min, 30 cycles of denaturation at 94 °C for 30 s,

Table 1

T7-primers used to generate dsRNA by PCR and in vitro transcription

Targeted gene	Forward/ reverse	Tag	Primer sequence
th/ Diap1	For	T7	taatacgactcaataggTCGAATCTCGGGCCGTATAG
th/ Diap1	Rev	T7	taatacgactcaataggCTTTGTTGCTGCTGCT
EGFP	For	T7	taatacgactcaataggACCCTCGTGACCACCTGACCTAC
EGFP	Rev	T7	taatacgactcaataggGGACCATGTGATCGCGCTCTCGT
FLuc	For	T7	taatacgactcaataggGGAAAGAACGCCAAAAAC
FLuc	Rev	T7	taatacgactcaataggGCTCTGGCACAAAATCG
Axn	For	T7	taatacgactcaataggGACCCGGACAGTCCAGTGAT
Axn	Rev	T7	taatacgactcaataggACCAAGGCCACACTCACGATT
Apc	For	T7	taatacgactcaataggTTTTTAGGAACCGAACACGC
Apc	Rev	T7	taatacgactcaataggGGGAGCTTCCTCTGACTG
dsh	For	T7	taatacgactcaataggGTGACCGAGCGGCTAACACAC
dsh	Rev	T7	taatacgactcaataggGGCGTTGATATTGCTCCATT
evi (wls)	For	T7	taatacgactcaataggGTTCAAGGGTGGTCCCATT
evi (wls)	Rev	T7	taatacgactcaataggCTGGGCAGAGTCCTCTGGAT

For forward, Rev reverse

T7 promoter sequences are given in non-capital letters

annealing at 57 °C for 60 s, and elongation at 72 °C for 30 s. Perform the final elongation at 72 °C for 2 min. Cool down to 10 °C. The annealing temperature and elongation time can vary depending on the template length and the Taq polymerase used.

3. Validate the expected size of the PCR product on a 2% E-Gel Agarose Gel.

3.2.2 Two-Step Generation of Amplicons

High-throughput generation of dsRNAs for genome-scale libraries can be done in a 96-well format and with two-step PCR amplification. The latter allows further amplification and prevents potential cross-contamination of PCR product between adjacent wells by performing two consecutive PCRs. The first PCR amplifies the DNA sequence of interest while adding primer binding sites for the second PCR that are distinct from those in the direct neighboring wells. Specifically, while the forward primer has the same tag in all wells, the reverse primer is fused to one of four distinct tags. The second PCR uses fitting primers, and only further amplifies matching template/primer sets. Since the second PCR product serves as template for the in vitro transcription, T7 promotor sites are fused to the second PCR primers. For the amplification scheme also see Fig. 1b.

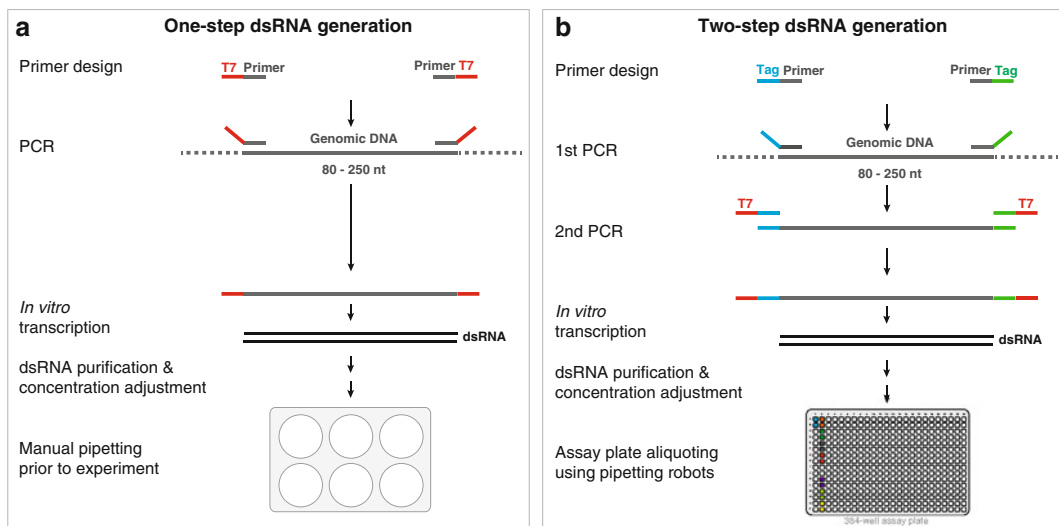


Fig. 1 Generation of dsRNAs for low- and high-throughput experiments. (a) One-step PCR amplification of the in vitro transcription DNA template from genomic DNA and subsequent generation of the dsRNA by in vitro transcription. T7 promotor sequences (red) are directly fused to the forward and reverse primer. The PCR product serves as template for in vitro transcription of dsRNA using a T7 polymerase. (b) Two-step PCR amplification with subsequent in vitro transcription for high-throughput generation of dsRNAs. Different tag sequence combinations (blue, green) are fused to different primer pairs for the first PCR amplification step on genomic DNA. This allows for a second PCR amplification step only if the primer pair of the second PCR matches the sequence tags, attached in the first PCR. Thus, the second PCR assures highly specific amplification of the product of interest in a 96-well plate synthesis format. Upon purification and concentration adjustment, the dsRNAs are transferred into 384-well master and, subsequently, assay plates

1. The first PCR on genomic DNA is performed in a 70 μ l reaction: use 100 ng genomic DNA, 1 \times PCR buffer, 50 μ M of each dNTP, 1.75 U HotStarTaq DNA polymerase, and 200 nM of each (for/rev) gene-specific primer merged to the tag-adaptor sequences (other Taq polymerases have also been successfully used).
2. Perform the PCR using a thermal cycler: initial denaturation at 95 °C for 15 min, 30 cycles of denaturation at 94 °C for 30 s, annealing at 57 °C for 60 s, and elongation at 72 °C for 30 s. Perform the final elongation at 72 °C for 2 min. Cool down to 10 °C.
3. The second PCR is performed in a 100 μ l PCR reaction: use 3 μ l of the first PCR product as template, 1 \times PCR-buffer, 200 nM of each T7-tag-primer, 50 μ M of each dNTP, and 1.5 U HotStarTaq DNA polymerase.
4. Perform the PCR using a thermal cycler: initial denaturation at 95 °C for 15 min, 30 cycles of denaturation at 94 °C for 30 s, annealing at 57 °C for 60 s, and elongation at 72 °C for 30 s. Perform the final elongation at 72 °C for 2 min. Cool down to 10 °C.
5. Validate the expected size of the PCR product on a 2 % E-Gel Agarose Gel.

3.3 *In Vitro Transcription of dsRNA*

The product of the (second) PCR is used as in vitro transcription template. Typically, we do not adjust the concentration of the template; instead, use a defined volume of the (second) PCR product. The normalization of the concentration is done later for the purified dsRNA. Prior purification of PCR product is not required.

1. Perform in vitro transcription reaction in a volume of 50 μ l and use 10 μ l of the (second) PCR product as template. For the reaction we have successfully used different high-yield in vitro transcription kits, such as the MEGAscript T7 Transcription Kit (Invitrogen by Life Technologies), T7 RiboMAX Express RNAi System (Promega), and home-made kits. Follow the manufacturer's protocol to perform the T7 (or SP6) in vitro transcription reaction.
2. Incubate the reaction at 37 °C for 4–24 h. This can be done in a thermal cycler or similar or—for large-scale approaches—in a humid incubator. Since transcription and the annealing of the resulting ssRNAs to become a dsRNA occur simultaneously, no annealing step is required. The yield of the reaction depends on the individual sequences, and can be increased by longer (towards 24 h) incubation. Alternatively, the reaction volume needs to be up-scaled.
3. (Optional, not recommended for high-throughput dsRNA generation) Following incubation, degrade the DNA template by adding 1 U DNaseI to the reaction, and incubate at room temperature for 30 min.

3.4 Purification of dsRNAs

3.4.1 Column Purification (Suitable for Low-Throughput)

3.4.2 Bead-Based Purification in 96-Well Plates (Suitable for High-Throughput)

- Purify dsRNAs using Qiagen's RNeasy columns (or similar) and follow the RNA cleanup protocol. Up to 100 µg of RNA longer than 200 bp can be bound to the column, purified, and eluted. To maximize recovery, elute twice.

For larger synthesis reactions (>100 µg), divide the sample and purify in two or more columns to prevent column overloading.

For large-scale purification of RNA in vitro transcriptions, polyacrylamide bead-based gel filtration is a suitable method.

- Hydrate Bio-Gel P-30 polyacrylamide beads for at least 12 h. 10 g of dry resin are hydrated in 400 ml sterile RNase/DNase-free H₂O. After washing (removal of floating debris), approximately 200 ml hydrated beads are obtained, which is sufficient for 3 96-well filter plates.
- Add 300 µl of Bio-Gel P-30 into the 96-well MultiScreenHTS plates and centrifuge at 1000 ×*g* for 2 min. Repeat this step with 200 µl Bio-Gel P-30.
- Carefully add in vitro transcription reaction on top of the Bio-Gel P-30 bead column and centrifuge at 500 ×*g* for 4 min. The flow-through contains the dsRNA.

3.5 Determination of dsRNA Quality and Concentration

The purified dsRNA requires testing for integrity and correct size.

- Mix 5–10 µl of a 1:20 dilution of the in vitro transcription reaction with 2× RNA gel-loading buffer and heat to 65 °C for 5 min to reduce secondary structures of the RNA. Run on a 2% E-Gel Agarose Gel to confirm the correct size of the transcript.
- To determine the yield, measure the optical density (OD) of a 1:3 dilution at 260 nm (OD₂₆₀) and an extinction coefficient of 45 using the NanoDrop 2000 or 8000 Spectrophotometer. The standard yield of 50 µl reaction is 80–200 µg.
- Cover plates (original, concentration adjusted, or ready-to-use assay plates) with Thermowell aluminum sealing tape and store them at –20 or –80 °C.

3.6 Preparing Assay Plates for High-Throughput RNAi

Genome-wide RNAi library sets comprise a large number of assay plates and thus require controls that enable plate-to-plate normalization and link the data to library annotation. We have designed the HD2 dsRNA library to induce a four-well barcode using viability controls with plate-specific location and orientation. For optimal plate-to-plate and batch-to-batch normalization, 18 wells are reserved to spot assay-specific biological and technical control dsRNAs (Fig. 2a). Technical control dsRNAs target firefly or *Renilla* luciferase, GFP or a gene whose depletion would be detrimental. For instance, in a dual channel assay that uses quantification of

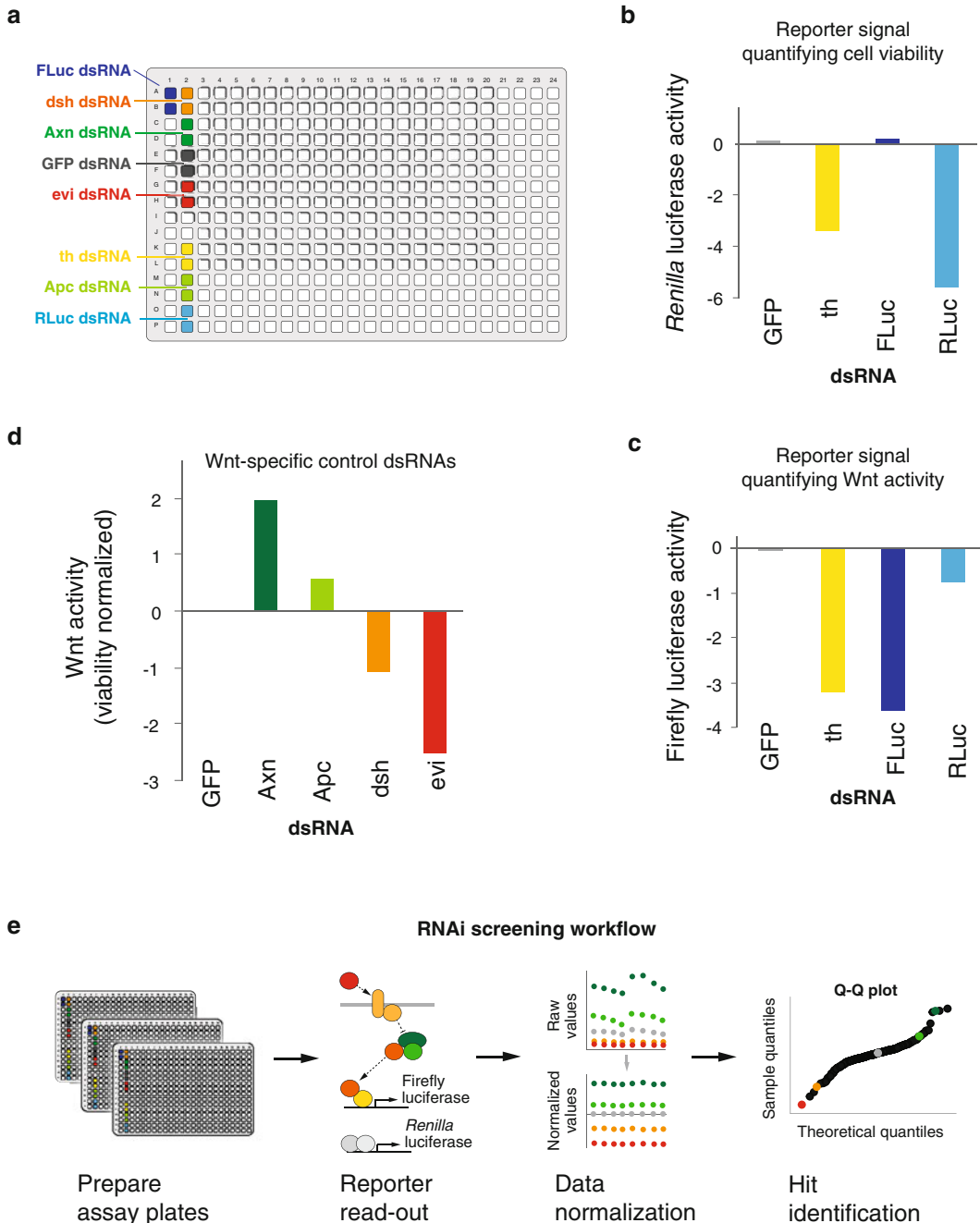


Fig. 2 Assay plate set-up, control selection, and workflow of a genome-wide RNAi screen using a dual-channel reporter system. **(a)** 384-well assay plate set-up of the genome-wide RNAi libraries HD2 and HD3. Wells containing sample or control dsRNA are marked *white* and with different colors, respectively. **(b and c)** Technical control dsRNAs represent the non-targeting control (GFP) or monitor efficient RNAi induction using a dsRNA targeting the Death-associated inhibitor of apoptosis 1 (Daip1/th), which depletes the firefly **(b)** and Renilla **(c)** luciferase activity. dsRNAs targeting the luciferases allow monitoring successful reporter expression, and quantification of the signal of interest, which is particularly crucial for transient plasmid transfection protocols. log2-transformed and median-normalized mean firefly **(b)** and Renilla **(c)** luciferase RLU as measured in a

firefly and *Renilla* luciferase expression, the respective dsRNA targeting the luciferases verify successful plasmid transfection and RNAi induction, while GFP RNAi can be used as non-targeting control (Fig. 2b, c). The biological control dsRNAs target known regulators of the process of interest and illustrate whether a given experiment can address this process. Figure 2d illustrates an optimal biological control panel consisting of inhibitors and positive regulators with intermediate and strong phenotypes.

When aliquoting the library into assay plates, each well should contain 5 μ l of a 0.05 μ g/ μ l dsRNA solution for a final amount of approx. 0.25 μ g dsRNA per well. Assay plates are sealed and stored at -20°C .

3.7 RNAi Experiments in *Drosophila* Cells: General Considerations

RNAi experiments in cultured *Drosophila* cells depend, apart from the RNAi reagent itself, on factors such as the selected cell line or cell handling throughout expansion. The diversity of *Drosophila* cell lines or the phenotypic occurrence (cell size, cell shape, patterns within the population) guides the selection depending on the scientific question. Cherbas and colleagues have transcriptionally characterized 25 *Drosophila* cell lines, and compared their status regarding various cell communication routes [27]. Growth behavior or the ability to take up dsRNAs determines the assay set-up and is particularly important for high-throughput screening. For instance, cells derived from the imaginal disks require transfection protocols, which are more challenging regarding both handling and costs. In contrast, cells derived from embryonic tissues autonomously take up dsRNAs.

Drosophila cells should be maintained at a constant growth rate throughout passaging and expansion for high-throughput experiments. Cells can be kept in disposable plastic cell culture flasks or, during expansion for high-throughput experiments, in large spinner bottles in a cell culture incubator at 25°C without CO_2 . Loosely adherent cells can be detached from the plastic by applying lateral sheer forces or pipetting the media over the cell layer. More adherent cell types can be detached with a plastic scraper. Cells are split when approaching confluence. Depending on the cell line and its growth rate, a certain amount of cells (a

Fig.2 (continued) genome-wide RNAi screen. (d) Biological control dsRNAs that increase (Axn, Apc) or decrease (dsh, evi/wls) the Wnt pathway-specific reporter signal. The specific reporter signal (firefly luciferase activity) is normalized to the viability signal (*Renilla* luciferase activity). Different amplitudes of the specific signal in the biological control wells enable advanced plate and batch effect normalization. (e) Workflow of a genome-wide RNAi screen in *Drosophila* cells using a dual channel reporter assay including data normalization (see Fig. 4) and hit identification

third to 1 in 15 of the flask) is transferred to a new flask containing fresh culture medium.

Cell cultures that are confluent on the day of transfection or show an abnormal shape should be avoided. Both confluent and “stressed” cells show a lower ability to take up dsRNA and lower transfection efficiency.

3.7.1 Small-Scale RNAi (6-Well) by Bathing (Table 2)

1. In 6-well tissue culture plates 15 µg dsRNA/well are added before cell seeding.
2. Growth medium is removed from the culture flask, cells are carefully washed with serum-free medium and subsequently detached in serum-free medium.
3. Stain a small sample of cell solution (50 µl) for viability with Trypan Blue and count in a Neubauer Hemocytometer.
4. Adjust cells in serum-free medium to $0.5\text{--}3 \times 10^6$ cells/ml.
5. Seed 1.5 ml of the cell suspension into each well containing the dsRNA. Alternatively, cells can be seeded first and dsRNAs added in a second step.
6. Incubate cells with the dsRNA at room temperature for 30–60 min (bathing procedure).
7. Add 1.5 ml cell culture medium, containing 10% FBS, to each well.
8. Depending on the assay, the cells are incubated for 2–5 days and subsequently processed (see Note 2).

3.7.2 Small-Scale RNAi (6-Well) Using Liposomal Transfection

1. For transfection of dsRNA or DNA in cells we recommend using liposomal transfection reagents (Effectene or similar) according to the manufacturer’s protocol.
2. To introduce a DNA reporter system, cells can be batch-transfected with the reporter plasmids before dsRNA treatment. Alternatively, the reporter can be transfected together with or after the dsRNA treatment. This depends on the assay and has to be optimized individually.

3.7.3 High-Throughput RNAi (384-Well Plates) By Bathing

High-throughput experiments comprise a large number of cell culture plates and should be separated into batches. The number of plates per batch depends on several factors, such as the time to process a given number of plates, the duration cells can be starved without reducing their fitness, or the sedimentation of cells in suspension. Moreover, the experimental environment (cell culture hood) often limits to number of plates that can be handled at the same time. We have found that up to 50 plates per batch work well for several cell lines.

1. Spin plates at $500 \times g$ for 1 min and clean the surface and the bottom with 70% ethanol before removing the aluminum seals (see Note 3).
2. Growth medium is removed from the culture flask and cells are briefly washed with and subsequently detached in serum-free medium (see Note 4).
3. Stain a small sample of cell solution (50 μ l) for viability with Trypan Blue and count in a Neubauer Hemocytometer.
4. Adjust cell in serum-free medium to $2.5-10 \times 10^5$ cells/ml.
5. Seed 20 μ l of the cell suspension into each well of a 384-well assay plate using a liquid dispensing device, such as a MultiDrop dispenser (see Note 5).
6. Stack plates (plate bottom had been cleaned with 70% ethanol!) and briefly centrifuge at $250 \times g$ for 10 s (see Note 6).
7. Incubate at room temperature for 45–60 min (bathing procedure).
8. Add 25 μ l of serum-containing cell culture medium to each well (see Note 7).
9. Seal plates with aluminum seals to prevent evaporation.
10. Depending on the assay, plates are incubated 3–5 days at 25 °C (see Note 2).

3.7.4 High-Throughput RNAi (384-Well) at Serum-Free Growth Conditions

DsRNA delivery using *Drosophila* cell lines adapted to grow at serum-free conditions further simplifies the bathing delivery approach. In a one-step approach, cells are seeded on the dsRNA without a starvation process and the requirement of subsequent addition of serum-containing medium.

1. Cells are detached, suspended, and counted. Those steps can be done without changing the growth medium prior detaching.
2. Cells are adjusted to $2.5-10 \times 10^5$ cells/ml. To increase dsRNA up-take efficiency, 0.1–0.15 μ l of 0.4 mg/ml DDAB are suspended in the cell suspension.
3. Seed 30 μ l of the cell suspension into each well of the 384-well assay plate.
4. Plates are sealed and briefly centrifuged at $250 \times g$ for 10 s (see Note 6).
5. Depending on the assay, plates are incubated 3–5 days at 25 °C (see Note 2).

3.8 Phenotypic Readouts

3.8.1 Homogenous Luminescence Cell Viability Assays

Homogenous luminescence cell viability assays are a fast and simple means to quantify cell viability and indirectly cell proliferation or death. Commercially available reagents, such as CellTiterGlo (Promega) measure the absolute level of ATP in the well by converting it into a directly proportional luminescent signal, and can be adapted to a high-throughput format.

Table 2**Summary of RNAi protocol in 6- and 384-well plates**

1.1	384-well, 6-well starvation	384-well, serum-free condition
Serum-free medium containing cells [mL]	1.5	0.02
dsRNA [µg]	15	0.25
Serum-containing medium [mL]	1.5	0.025

1. RNAi treatments are performed as described in Subheading 3.7.3 or 3.7.4 in white 384-well LIA plates (Greiner).
2. The assay plates are incubated for 3–5 days, depending on the cell line.
3. On the day of the readout, the assay plates are centrifuged at $300 \times g$ for 1 min and the supernatant is carefully removed using a 24-multichannelwand.
4. Cells are lysed and treated according to the manufacturer's instruction. For CellTiterGlo viability measurements, cells are incubated for 15 min with the reagent before luminescence readouts (Mithras LB940 or similar, Berthold Technologies).

3.8.2 Homogenous Fluorescence Reporter Assays

Homogenous reporter assays measure luciferase activity in a cell population. To normalize the specific signal, such as the activity of a firefly luciferase expressed under a specific promotorm, for general effects such as viability effects or transfection efficacy, a second reporter expressing the Renilla luciferase behind constitutive (e.g. actin) promotorm elements can be used. We recommend transient plasmid transfection for several reasons. First, stably transfected cell lines often must be kept under selective pressure. Moreover, this provides comparability of the same read-out in different cell lines, and scalability of the reporter signal. The latter can be crucial since some treatments in certain cell lines can drive the reporter signal to exceed the detection limit. Furthermore, signaling pathway activity is typically monitored upon induction, for instance by ligand overexpression. Not surprisingly, gene depletion phenotypes change depending on the ligand levels. In conclusion, the optimization of an individual screening assay depends on the selected cell line and how the pathway(s) of interest is adjusted.

Below, we describe a typical genome-wide RNAi screen using dual-channel reporter readout (see Fig. 2e). The specific reporter expresses a firefly luciferase in response to active Wnt signaling and

the *Renilla* luciferase as generic reporter along with a third plasmid constitutively expressing the Wg signaling ligand.

RNAi treatments are performed as described in Subheading 3.7.3 or 3.7.4 in white 384-well LIA plates (Greiner). The plasmid transfection is done 16–32 h past RNAi treatment.

1. Per 384-well, 1.5 ng of the specific and 3 ng of the generic reporter plasmid, and 2 ng of a pAc-wg plasmid are mixed in a total volume of 5 μ l serum-free medium.
2. 0.1 μ l of the transfection reagent FuGENE HD is mixed in a total volume of 5 μ l serum-free medium (see Note 8).
3. Both mixes are merged, incubated at RT for 25–50 min and 10 μ l are added into each well using a multi-dispensing device.
4. Plates are sealed and centrifuged at 250 $\times g$ for 10 s.
5. In total, the assay plates are incubated for 4 days (see Note 2).
6. On the day of the readout, the assay plates are centrifuged at 300 $\times g$ for 1 min and the supernatant is carefully removed using a 24-multichannelwand.
7. Cell lysis and the dual channel readout are performed using commercial Dual-Luciferase Reporter Assay System or homemade reagents. Commonly, cells are incubated for 15 min with lysis buffer. The reagents containing luciferase substrates are added and read out at a multimode microplate reader.

3.8.3 High-Throughput Microscopy

High-throughput microscopy allows for screening for morphological alterations and quantification of multiple phenotypic features at the single cell level. Requirements for high-throughput microscopy are specific and scalable staining protocols, and computational automated segmentation pipelines. How well those requirements are met depends on characteristics of the cell line, such as non-overlapping, uniquely distributed and adhesive growth.

Overall, microscopy-based RNAi screening approaches follow the protocols described in Subheading 3.7.3 or 3.7.4, but with some steps being more crucial.

1. RNAi treatments are performed as described in Subheading 3.7.3 or 3.7.4 in black clear bottom 384-well plates. Since, at the time of the readout, cells must not have reached confluence (at which *Drosophila* cells typically start growing in multiple layers and detach from the well bottom), yet, manifestation of the RNAi phenotype requires several days, as few cells as possible should be seeded.
2. The assay plates are incubated for 3–5 days, depending on the assay. Daily monitor cell growth and confluence for the biological and technical controls by eye. This also allows adapting the time point for fixing the cells (cells should not have reached confluence).

3. Take off growth medium but leave 20 μ l per well to prevent taking off loosely adherent cells (20 μ l rest volume can remain in each well throughout all subsequent steps).
4. Add 40 μ l of the fixation and permeabilization reagent (6% PFA, 0.15% TritonX-100 in PBS) and incubate for 30 min at RT.
5. Wash cells with PBS and proceed with blocking and staining protocols (these require individual adaptation).
6. Analysis of the acquired images can be performed using the software package “EBImage” based on “Bioconductor/R” (<http://www.bioconductor.org/>) or the CellProfiler software (<http://www.cellprofiler.org/>).

3.9 Data Analysis

Analysis of high-throughput data determines its interpretation. To enable optimal data normalization and hit prioritization, technical and biological controls need to be included in the experimental set-up as described in Subheading 3.6. Examination of the technical controls shows the quality of the experiment and whether it can be used for further analysis. Spatial effects within a 384-well plate and plate-to-plate effects should be accounted for. High-throughput experiments such as genome-wide RNAi screens are conducted in several batches and thus require batch-to-batch normalization. For advanced analysis, global tendencies in the data, such as nonlinear relations between signaling activity and viability data can be considered. Finally, the normalized data are scored to identify candidate genes.

The essential steps of high-throughput analysis have been implemented as an R-based software package “cellHTS2”, which is available through “Bioconductor”, a free platform for statistical data analysis (<http://www.bioconductor.org/>) [21]. cellHTS2 is also available as web-based application utility (web-cellhts2.dkfz.de) [28].

In this paragraph, we outline the typical data analysis steps and how this is done in “R” using functions implemented in cellHTS2 (Fig. 3). While the cellHTS2 vignette provides a detailed description of raw data import, annotation and normalization, we summarize the individual steps and illustrate how normalization affects the data and how the experimental set-up supports distinct normalization procedures (Figs. 2 and 4).

1. Import raw data files into a cellHTS object x (Fig. 3). The cellHTS object contains the raw data and allows attaching the configuration and annotation of the experiment. Moreover, the object contains information about the state (annotation, normalization, etc.) of the analysis, which can be accessed using the function state(x).
2. The cellHTS object also contains information about whether one or two channels were measured. Figure 4a, b illustrates

Data analysis workflow	cellHTS2 function for respective analysis step
Load package ↓	> library(cellHTS2)
Import raw data files ↓	> x = readPlateList("Platelist.txt", name = experimentName, + path = dataPath)
Configure data ↓	> x = configure(x, descripFile = "Description.txt", + confFile = "Plateconf.txt", + logFile = "Screenlog.txt")
Normalize data(1) ↓	> xn = normalizePlates(x, scale = "multiplicative", + log = TRUE, method = "median")
Score phenotypes ↓	> xsc = scoreReplicates(xn, sign = "+", method = "zscore") > xsc = summarizeReplicates(xsc, summary = "mean")
Annotate data ↓	> xsc = annotate(xsc, geneIDFile = "GeneIDs.txt", + path = dataPath)
Save scored data ↓	> save(xsc, file = paste(experimentName, ".rda", sep = ""))
Write report of analysis	> out = writeReport(raw = x, normalized = xn, scored = xsc) > browseURL(out)

Fig. 3 Data analysis workflow using cellHTS2. See *Box* for details. (1) Effects of individual normalization parameters on screening data illustrated in Fig. 4

the impact of normalizing a Wnt signaling-specific reporter against the viability effect of the dsRNA treatment.

3. Configure data. This attaches information, for example, on the location of controls on the assay plate (for control selection *see* Fig. 2) or to flag contaminated wells (*see* Note 9). Transform data. To score phenotypes, typically a *z*-score is computed, which assumes normal distributed data. To avoid a violation of this assumption, log₂ transformation of the viability-normalized data is recommended (*compare* Fig. 4b/b' and c/c').
4. Examine technical controls: positive technical controls provide qualitative rather than quantitative information about whether RNAi and plasmid expression worked (Fig. 2b, c).
5. Examine biological controls: While negative, non-targeting controls should approximately match the median of the data, positive biological controls display plate-to-plate and batch-to-batch differences and can be monitored to define the optimal normalization procedure for the data (*see* Note 10) (Figs. 2d and 4). When using the writeReport() function the *z'* factor illustrates how well non-targeting controls can be distinguished from control dsRNAs that are known to generate a phenotype.

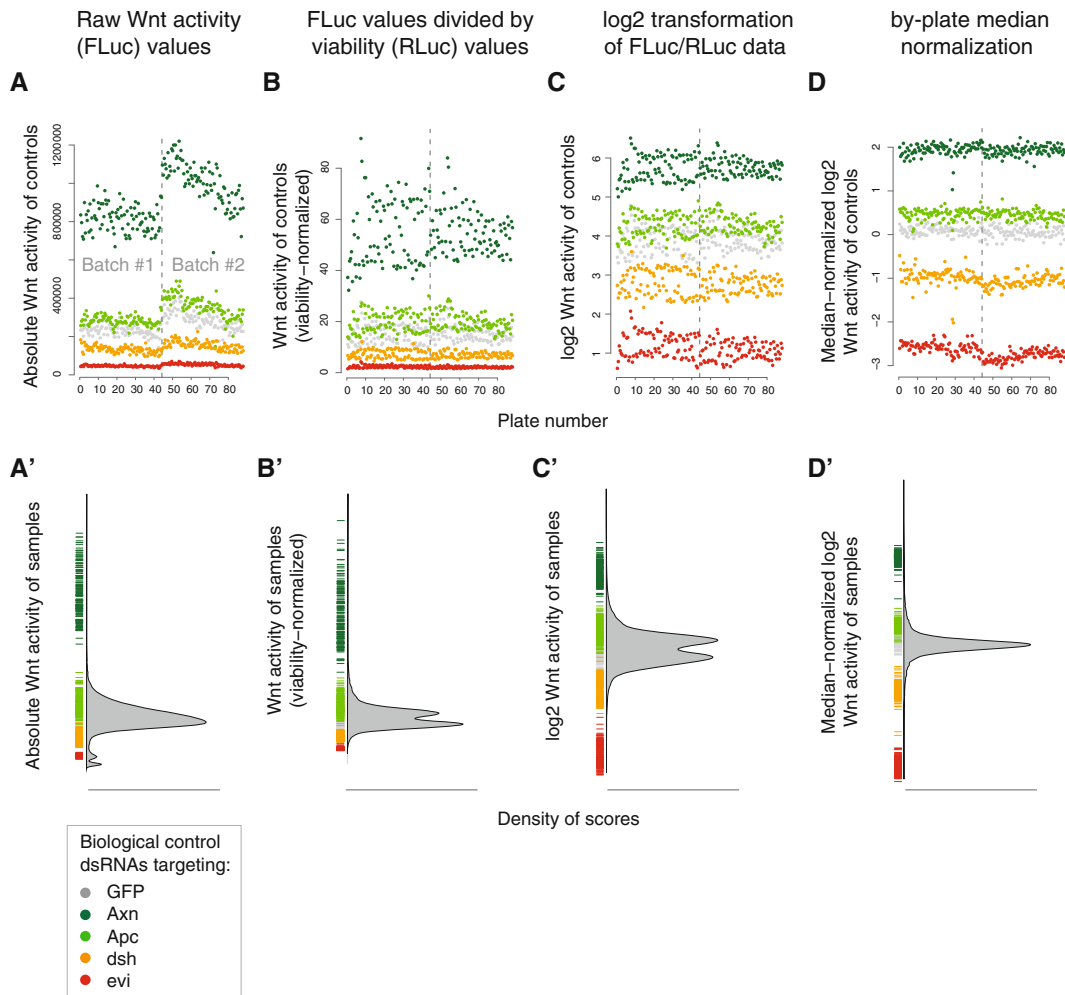


Fig. 4 Data quality assessment and normalization of genome-wide RNAi screening data. **(a and a')** Sample per-plate and overall sample distribution of RLU quantifying firefly luciferase activity in one replicate of a genome-wide RNAi screen. Screening was done in two batches, 44 384-well assay plates each and a plate set-up as illustrated in Fig. 2a. The distribution of the measured values upon knockdown of the biological controls within and between the batches is shown in (a). **(a')** Illustrates the right skewed distribution of the 29,328 sample values, and the match of the biological controls (color-coded) to the distribution. **(b and b')** Using cellHTS2 with dual-channel read-out data, the cellHTS object x (see Fig. 3) contains viability-normalized Wnt signaling activity values, which can be normalized by setting parameters in the function normalizePlates(). **(b)** Illustrates how dividing the Wnt-specific firefly activity values by the cell viability-specific Renilla luciferase values in each well accounts for most of the gradient within and between the batches. **(c and c')** Setting the parameter log = TRUE log2-transforms the viability-normalized Wnt activity values, and generates an approximately symmetric distribution of the data around their mean. **(d and d')** The parameter method = "... " enables to apply various normalization procedures to the data. Setting the parameter method = "median" normalizes the data of each 384-well assay plate to the plate median. Control dsRNAs now have similar values within and between the screening batches (d), and the sample values are approximately normally distributed around their mean (d')

6. Normalize for spatial plate effects. Typical plate effects are gradients over the 384-well plate or row or column-wise patterns. Those effects can be removed by using the median polishing approach using the function `normalizePlates()` with the setting `method = "Bscore"`, which iteratively subtracts the median values from each row and column (see Note 11).
7. Plate-to-plate effects and batch effects can be normalized for, using the plate median (Figs. 3 and 4c, d). However, since focused sets often have a plate-wise bias in the samples, the median of all controls on a plate or of the non-targeting controls using `normalizePlates(..., method = "negatives")` can be more stable.
8. Plate-to-plate effects can affect the variance of the data, even after, e.g. median normalization. This can be estimated from different amplitudes of biological controls. Here, a variance-stabilization setting `normalizePlates(..., varianceAdjust = "byPlate")` might improve the plate-to-plate comparability.
9. Annotate data. This attaches information about the content of the “sample” wells (Figs. 2a and 3).
10. To score the normalized data, *z*-score normalization can be performed for each plate (see Fig. 4); however, this is not recommended for focused sets.

4 Notes

1. Testing serum batches before use in *Drosophila* cell culture experiments is crucial, as some *Drosophila* cell lines are more sensitive to changes in sera than many mammalian cell lines. We recommend careful testing of new batches of sera using growth curves and monitoring cell morphology. Reportedly, batches of Schneider’s medium (Invitrogen) can impair dsRNA uptake-competence.
2. The optimal duration of an RNAi experiment can vary depending on the cell line used, the biological question, and the read-out system. The RNAi effect occurs depending on the growth rate of the cells and the respective protein half-life. However, unpublished data showed that the RNAi phenotypes of several hundred genes in *Drosophila* S2 and S2R+ cells peak between 72 and 120 h past dsRNA treatment, with large variation between different genes. Thus the optimal time point for the phenotypic quantification should be a compromise. A special case needs to be considered if “indirect” phenotypes are measured, such as the RNAi-mediated effect on the infection of *Drosophila* cells by a parasite: the functional depletion of the entry machinery peaks between day 3 and 4 (at which the para-

site should be added), but the infection rate is typically measured at a later time point (for instance 4 days past infection), at which the RNAi effect on the mRNA has largely been withdrawn.

3. Prepared assay plates contain the dsRNA and are stored at -20°C . Centrifugation locates the dsRNA solution and possible condense water droplets at the well bottom. For this reason and for ideal cell growth, the assay plates must be brought to RT before starting the experimental steps.
4. If cells are clumpy raise the EDTA content of the trypsin/EDTA solution and of the washing buffers to 5 mM. This helps separating the cells for homogenous distribution after cell seeding for subsequent microscopy.
5. We recommend using an automated dispensing system for seeding the cells and distributing media in 384-well plates. To minimize sheer stress during seeding with this device, the dispersion speed should be set to “low”.
6. Short centrifugation of the assay plates at $250 \times g$ after cell seeding, supports quick sedimentation and thus more equal distribution of the cells. This is of particular importance for microscopic readouts but also improves homogenous transfection efficacy within a well. If dsRNA delivery requires starvation, plates should be centrifuged before adding the serum-containing medium, and can be stacked without sealing. For this approach, it is crucial that the plate bottom has cleaned properly with ethanol in advance.
7. Cells are kept in serum-free medium throughout the preparation of the cell suspension. Depending on the cell line, the overall duration in serum-free medium should not exceed 90 min. This is of particular importance for large-scale approaches.
8. The amount of the transfection reagent per well requires cell line-dependent optimization. This optimization is usually done independently of the plasmid amount. At optimal transfection reagent concentrations, plasmid amounts can be altered to generate optimal dynamic ranged for the readout or pathway induction states (signaling ligand levels).
9. In high-throughput screening, contaminated wells are not always easy to spot. If, for instance, a *Renilla* luciferase reporter was used for monitoring viability effects, this signal can be used to estimate contaminations using the two technical replicates: build the ratio between each replicate values. If the ratio is much larger than 1 or much smaller than 1, the smaller value was measured in a contaminated well, since values can only significantly decrease.
10. The dynamic range of the biological controls typically varies slightly between batches. There are two possible reasons with

different consequences for the experiment: (1) The variation is caused by changes in cell growth, RNAi or Plasmid transfection efficacy. This can be normalized for. (2) Assuming we monitor pathway activity, the variation is caused by an altered pathway stimulation by, e.g. different ligand expression levels. This causes phenotypic changes of some candidate knock-downs, which cannot be inferred from the biological controls—this effect cannot be normalized for.

11. Median polishing causes problems if too many hits and/or controls with a strong phenotype had been spotted to the same row or column of a 384-well plate. This can become an issue in focused screens or if all controls are spotted into the same row or column.

Acknowledgments

The authors would like to thank Claudia Blass, Bernd Fischer, and Thilo Miersch for critical comments on the manuscript. M. Bi. is supported by a fellowship of the Helmholtz International Graduate School for Cancer Research.

References

1. Lee Y et al (2003) The nuclear RNase III Drosophila initiates microRNA processing. *Nature* 425:1–5
2. Ketting RF et al (2001) Dicer functions in RNA interference and in synthesis of small RNA involved in developmental timing in *C. elegans*. *Genes Dev* 15:2654–2659
3. Zamore P, Tuschl T, Sharp P, Bartel D (2000) RNAi: double-stranded RNA directs the ATP-dependent cleavage of mRNA at 21 to 23 nucleotide intervals. *Cell* 101:25–33
4. Hammond S, Bernstein E, Beach D, Hannon G (2000) An RNA-directed nuclease mediates post-transcriptional gene silencing in *Drosophila* cells. *Nature* 527:524–527
5. St Johnston D (2002) The art and design of genetic screens: *Drosophila melanogaster*. *Nat Rev Genet* 3:176–188
6. Fire A (1998) Potent and specific genetic interference by double-stranded RNA in *Caenorhabditis elegans*. *Nature* 391:806–811
7. Clemens JC et al (2000) Use of double-stranded RNA interference in *Drosophila* cell lines to dissect signal transduction pathways. *Proc Natl Acad Sci U S A* 97:6499–6503
8. Ulvila J et al (2006) Double-stranded RNA is internalized by scavenger receptor-mediated endocytosis in *Drosophila S2* cells. *J Biol Chem* 281:14370–14375
9. Horn T, Sandmann T, Boutros M (2010) Design and evaluation of genome-wide libraries for RNA interference screens. *Genome Biol* 11:R61
10. Kulkarni MM et al (2006) Evidence of off-target effects associated with long dsRNAs in *Drosophila melanogaster* cell-based assays. *Nat Methods* 3:833–838
11. Ma Y, Creanga A, Lum L, Beachy P a (2006) Prevalence of off-target effects in *Drosophila* RNA interference screens. *Nature* 443:359–363
12. Echeverri CJ et al (2006) Minimizing the risk of reporting false positives in large-scale RNAi screens. *Nat Methods* 3:777–779
13. Kiger AA, Baum B, Jones S, Jones MR, Coulson A, Echeverri A, Perrimon N (2003) A functional genomic analysis of cell morphology using RNA interference. *J Biol* 2(4):27
14. Boutros M et al (2004) Genome-wide RNAi analysis of growth and viability in *Drosophila* cells. *Science* 303:832–835
15. Bartscherer K, Pelte N, Ingelfinger D, Boutros M (2006) Secretion of Wnt ligands requires Evi, a conserved transmembrane protein. *Cell* 125:523–533
16. Kuttenkeuler D, Boutros M (2004) Genome-wide RNAi as a route to gene function in

Drosophila. *Brief Funct Genomic Proteomic* 3:168–176

17. Lum L et al (2003) Identification of Hedgehog pathway components by RNAi in Drosophila cultured cells. *Science* 299:2039–2045

18. Ramadan N, Flockhart I, Booker M, Perrimon N, Mathey-Prevot B (2007) Design and implementation of high-throughput RNAi screens in cultured Drosophila cells. *Nat Protoc* 2:2245–2264

19. Friedman R, Hughes AL (2001) Pattern and timing of gene duplication in animal genomes. *Genome Res* 11:1842–1847

20. Bier E (2005) Drosophila, the golden bug, emerges as a tool for human genetics. *Nat Rev Genet* 6:9–23

21. Boutros M, Brás L, Huber W (2006) Analysis of cell-based RNAi screens. *Genome Biol* 7(7):R66

22. Steinbrink S, Boutros M (2008) In Dahmann C (ed) *Methods Mol Biol*, pp 139–53. http://link.springer.com/10.1007/978-1-59745-583-1_8

23. Han K (1996) An efficient DDAB-mediated transfection of Drosophila S2 cells. *Nucleic Acids Res* 24:4362–4363

24. Horn T, Boutros M (2010) E-RNAi: a web application for the multi-species design of RNAi reagents--2010 update. *Nucleic Acids Res* 38:W332–W339

25. Rozen S, Skaletsky H (2000) Primer3 on the WWW for General Users and for Biologist Programmers. *Methods Mol Biol* 132:365–386

26. Schmidt EE et al (2013) GenomeRNAi: a database for cell-based and in vivo RNAi phenotypes, 2013 update. *Nucleic Acids Res* 41:D1021–D1026

27. Cherbas L et al (2011) The transcriptional diversity of 25 Drosophila cell lines. *Genome Res* 21:301–314

28. Pelz O, Gilsdorf M, Boutros M (2010) web cellHTS2: a web-application for the analysis of high-throughput screening data. *BMC Bioinformatics*. <http://www.biomedcentral.com/1471-2105/11/185/>

Chapter 6

A Guide to Genome-Wide *In Vivo* RNAi Applications in *Drosophila*

Aynur Kaya-Çopur and Frank Schnorrer

Abstract

RNAi technologies enable the testing of gene function in a cell-type- and stage-specific manner in *Drosophila*. The development of genome-wide RNAi libraries has allowed expansion of this approach to the genome scale and supports identification of most genes required for a given process in a cell type of choice. However, a large-scale RNAi approach also harbors many potential pitfalls that can complicate interpretation of the results. Here, we summarize published screens and provide a guide on how to optimally plan and perform a large-scale, *in vivo* RNAi screen. We highlight the importance of assay design and give suggestions on how to optimize the assay conditions by testing positive and negative control genes. These genes are used to estimate false-negative and false-positive rates of the screen data. We discuss the planning and logistics of a large-scale screen in detail and suggest bioinformatics platforms to identify and select gene groups of interest for secondary assays. Finally, we review various options to confirm RNAi knock-down specificity and thus identify high confidence genes for more detailed case-by-case studies in the future.

Key words *Drosophila*, RNAi, GAL4-UAS, High-throughput screens, Genetic screens, Off-target effects, *In vivo*, Dicer-2, False-positive, False-negative, False-discovery, VDRC, NIG-FLY, TRiP

1 Introduction

Traditional forward genetic screens in *Drosophila* have applied chemical or transposon-based genome mutagenesis to identify new components of a particular process of interest. Both mutagenesis strategies have been immensely successful and have identified a majority of the plethora of gene functions we know to date [1, 2]. However, both strategies also harbor severe drawbacks. The molecular identification of chemically induced mutants is often very labor-intensive [3], and transposon-based mutagenesis cannot provide a loss-of-function allele for each gene, despite recent progress [4]. Additionally, both strategies do not easily allow gene inactivation in a defined set of cells or at a defined stage of development,

as the induction of mutant clones by *Flip/FRT*-mediated mitotic recombination is limited to dividing cells and always results in a mosaic tissue of wild-type and mutant cells or nuclei [5].

RNA interference (RNAi) technology can in principle solve all of these issues. Since the discovery of double-stranded RNA (dsRNA)-mediated mRNA degradation and gene silencing in *Caenorhabditis elegans* [6, 7], RNAi has been widely applied to test gene function in cell culture systems or *in vivo* using various model organisms [8–12]. Whereas RNAi in *C. elegans* is systemic and simply applied to the entire organism by feeding bacteria expressing dsRNAs [13], RNAi in *Drosophila* is cell autonomous [14]. Thus, the binary GAL4-UAS system [15] can be adapted to express dsRNAs designed against a target gene by simply cloning an inverted repeat downstream of UAS (upstream activation sequence) and generating transgenic animals. This enables tissue- and stage-specific knock-down of a target gene [16]. The expansion of this strategy led to the development of genome-wide RNAi libraries [17, 18], making *Drosophila* the organism of choice for systematic tissue and stage-specific RNAi screens.

Genome-wide RNAi screens have a number of advantages as compared to classical forward screens. First, the researcher knows which gene is currently being tested for a particular function. Second, as hairpins exist for almost all genes, the researcher can mark a gene as tested, which cannot be done with a random mutagenesis approach. Third, by identifying an appropriate GAL4 driver line, gene knock-down can be controlled temporally and spatially and thus, for example, be restricted to pupal or adult stages or to a subset of neurons in the complex brain of an adult fly. Together, these advantages enable RNAi technologies to identify most of the important genes required for a particular process.

RNAi applications can also harbor serious disadvantages. Despite significant progress in reducing the generation of off-target effects by unwanted knock-down of unintended genes [19], off-target effects still remain a significant problem. Additionally, insufficient knock-down by an ineffective RNAi line or a weak GAL4 line may mask gene function in the studied process. Both problems are particularly significant for genome-wide screens, which require a high-throughput assay and are designed to discover novel and often unexpected roles for genes.

In this article, we discuss strategies to design and execute large-scale RNAi screens in an efficient and reliable way. We stress the importance of “quality control” to estimate both the false-discovery and the false-negative rates of the assay before starting the high-throughput screen. We further provide practical tips for the logistics of a large screen, namely using a primary high-throughput assay followed by more sophisticated secondary assays and finally independent verification of the discovered gene functions with additional experiments. Together, this should guide the experimenter to

perform a successful systematic loss-of-function screen—a potential goldmine to discover novel gene functions and generate starting points for future projects.

2 Transgenic RNAi Libraries

Genome-wide RNAi screens have been made possible by the generation of large publicly available RNAi libraries (Table 1). This effort was pioneered by Barry Dickson who generated the VDRC

Table 1
Publicly available RNAi libraries

RNAi library	VDRC		NIG-FLY		TRiP	
Release	GD	KK	Single release		VALIUM1 VALIUM10	VALIUM20 VALIUM21 VALIUM22
Coverage of protein coding genes	89 % 78.7 %		45 % 67.7 %		70 % 3.8 % (V1) 12.8 % (V10)	51.8 % (V20) 0.7 % (V21) 10.7 % (V22)
Number of lines	16,763	9822	11,910		2474	8980
Number of lines per covered gene	1.53	1.04	1.87		1.25 (V1) 1.01 (V10)	1.02 (V20) 1 (V21) 1.03 (V22)
Library features	Long hairpins, high coverage, widely used (see Note 3 for problem with KK library)		Long hairpins, inexpensive, only 200 lines per month, some lines not balanced		Long hairpins Gypsy insulators improve expression (see Note 5 for use of <i>vermillion</i> +)	Short hairpins, germline
Insertion site	Random	{attP} VIE-260 at 40D3 and/or 30B3	Random		{attP}40 at 25C6 or {attP}2 at 68A4	
Marker	<i>white</i> +		<i>white</i> +		<i>vermillion</i> +	
Source	VDRC, Vienna, Austria		NIG-FLY, Mishima, Japan		Bloomington Stock Center, Indiana University, US	
Cost (100/1000 lines)	1745/3320 €		10,000/100,000 ¥ (74/740 €)		750/3900 \$ (664/3450 €)	

For each library, the genome coverage as percentage of protein coding genes (Flybase release R6.03), the number of lines, the number of lines per covered gene, the insertion site, the genetic marker, the ordering source and the estimated cost (February 2015), as well as additional library features are listed.

library in Vienna [17] and was complemented with a collection generated by the NIG-FLY consortium in Japan led by Ryu Ueda. More recently, a team headed by Norbert Perrimon at Harvard Medical School generated the TRiP library that as of 2015 is still being expanded [18].

2.1 VDRC Library (<http://stockcenter.vdrc.at>)

Currently, the RNAi library distributed by the Vienna *Drosophila* Resource Centre (VDRC) has the highest coverage of the genome with 26,585 *Drosophila* transgenic RNAi lines targeting 89% of the protein coding genes with at least one line (see Note 1 for information on the stocks and Note 2 for recent pruning of the libraries). The VDRC collection consists of two releases, the GD (Georg Dietzl) and KK (Krystyna Keleman) libraries.

For the GD library, long inverted repeats (average hairpin length of 323 bp) were cloned into a UAS vector (UAS-IR, marked with *white*+) and transgenes were created by random P-element insertion [17]. The GD library currently consists of 16,763 lines, which covers 78.7% of protein coding genes (1.53 lines per covered gene, Table 1, see Note 2). Since the insertion site of each GD line is random, the levels of hairpin expression can vary. Therefore, it may cause false-negative results in certain tissues but not others (see also Subheading 7.2). Furthermore, some lines are lethal, potentially because of transgene insertion in an essential gene. This may influence the studied phenotype. More important are potential “EP (enhancer-promoter)-effects”, in which the UAS when crossed to a GAL4 line can cause an unwanted overexpression of neighboring genes, potentially leading to a false-positive result (see Subheading 7.1.2). Despite these potential caveats, the GD library was used extensively and in many cases successfully for a number of large-scale screens [20–27] (Table 2).

The second Vienna RNAi library “release” is the KK library [28]. Its major modifications are an updated target design to reduce off-target effects by for example avoiding CAN repeats [29, 30] and cloning of the inverted repeat into an attB vector (marked with *white*+) that allowed site-specific Φ C31-mediated transgenesis [31] into attP-VIE-260B on 2L at 40D3 (see Note 3 for a problem in some stocks). This largely eliminates the problem of expression level variation and mis-expression artifacts. The KK library currently consists of 9822 lines and covers 67.7% of the protein coding genes (1.04 lines per covered gene). It has been successfully used to validate large-scale screen data obtained by the GD library [21, 27]. It was also used efficiently as the primary screen source in recent genome-wide screens [32, 33], including one in the germline [34] (Table 2).

2.2 NIG-FLY Library (<http://www.shigen.nig.ac.jp/fly/nigfly/>)

The National Institute of Genetics (NIG) in Japan has built an RNAi library currently consisting of 11,910 lines, targeting 6313 genes and thus covering 45% of protein coding genes (1.9 lines per covered gene) (Ryu Ueda, personal communication). Similar to the VDRC GD library, the NIG-FLY RNAi constructs contain long

Table 2
Examples of published large-scale RNAi screens

Study	Studied process	RNAi library used in primary screen	GAL4-driver
Yapici et al. (2008)	Post-mating switch	Genome-wide, VDRC	<i>elav</i> -GAL4
Cronin et al. (2009)	Intestinal pathogenic bacterial infection	Genome-wide, VDRC	<i>Hsp70</i> -GAL4; <i>Tub</i> -GAL80-ts
Mummery-Widmer et al. (2009)	Notch signaling, SOP development	Genome-wide, VDRC	<i>pnr</i> -GAL4
Avet-Rochex et al. (2010)	Larval blood cell homeostasis	Large-scale, NIG-FLY	<i>srp</i> -GAL4, <i>cg</i> -GAL4, <i>hmlΔ</i> -GAL4
Lesch et al. (2010)	Wound closure	Selected set of genes, NIG-FLY and VDRC	<i>e22c</i> -GAL4 or <i>A58</i> -GAL4; (UAS- <i>Dcr-2</i>)
Neely et al. (2010a)	Adult heart function	Conserved genes, VDRC	<i>tinCΔ4</i> -GAL4
Neely et al. (2010b)	Heat nociception	Genome-wide, VDRC	<i>elav</i> -GAL4; UAS- <i>Dcr-2</i>
Pospisilik et al. (2010)	Adiposity regulation	Genome-wide, VDRC	<i>Hsp70</i> -GAL4; <i>Tub</i> -GAL80-ts
Schnorrer et al. (2010)	Muscle morphogenesis	Genome-wide, VDRC	<i>Mef2</i> -GAL4
Yamamoto-Hino et al. (2010)	Neural-specific glycosylation	Genome-wide, NIG-FLY	<i>GMR</i> -GAL4
Neumüller et al. (2011)	Neuroblast self-renewal	Genome-wide, VDRC	UAS- <i>Dcr-2</i> ; <i>insc</i> -GAL4
Czech et al. (2013)	piRNA-mediated transposon silencing	Ovarian-expressed genes, VDRC	UAS- <i>Dcr-2</i> ; <i>nos</i> -GAL4
Handler et al. (2013)	Somatic piRNA pathway	Ovarian somatic cell expressed, VDRC	<i>traffic jam</i> -GAL4
Berns et al. (2014)	Development of follicular epithelium	Genome-wide, VDRC	<i>escargot</i> -GAL4; <i>GRI</i> -GAL4
Yan et al. (2014)	Germline stem cell self-renewal	Germline-enriched genes, TRiP library	MTD-GAL4 or UAS- <i>Dcr-2</i> ; <i>nos</i> -GAL4
Reim et al. (2014)	Wing growth and margin formation	Genome-wide, VDRC	<i>c765</i> -GAL4

Authors of the in vivo RNAi screens applied various experimental assays using different RNAi libraries and GAL4-drivers to identify new components in different processes.

inverted repeats (about 500 bp) in a UAS vector (UAS-IR, marked with *white*+) and were inserted into the genome by random P-element integration (see Note 4). Therefore, this library is also subject to position effects (see Subheading 7.1.2). Currently, there is no formal publication of the NIG-FLY library, however it was also used multiple times for primary RNAi screens [35–37], sometimes in combination with the other available libraries [38, 39] (Table 2).

2.3 TRiP Library (<http://www.flrynai.org/TRiP-HOME.html>)

The most recent RNAi library has been generated by the *Drosophila* Transgenic RNAi Project (TRiP) at Harvard Medical School. This library is still expanding in 2015 and stocks are deposited at the Bloomington Stock Center at Indiana University. Currently, the TRiP library covers about 70% of the protein coding genes with 11,454 RNAi lines (Table 1) (Liz Perkins, personal communication). Similar to the VDRC KK library, TRiP lines were made by Φ C31-targeted integration, using attP40 or attP2 sites located on second or third chromosome, respectively [40].

The TRiP constructs were generated with a series of different vectors referred to as the “VALIUM series” (Vermilion-AttB-LoxP-Intron-UAS-MCS). All vectors use *vermilion* as a selectable marker with the rationale that proper gene dosage of *white* has advantages for behavioral studies (see Note 5 for using *vermilion* as a marker). The first generation of VALIUM vectors, VALIUM1 and VALIUM10, contain long double-stranded hairpin sequences (between 400 and 600 bp long hairpins). The hairpin in VALIUM10 is flanked with gypsy insulator sequences leading to increased knock-down efficiency [40, 41].

The second generation of VALIUM vectors, VALIUM20, 21, and 22, contain short hairpin constructs, with 21 bp matching the target mRNA. The design adapted a modified microRNA miR-1 scaffold to mediate efficient knock-down. VALIUM20 mediates efficient knock-down in the soma and weaker knock-down in the germline, whereas VALIUM21 and 22 contain a UASp promoter optimized for knock-down in the germline [18] (see Note 6 for future lines).

2.4 Ordering, Cost, and Transport

Transgenic hairpin lines from all libraries can be ordered online from the three above-mentioned stock centers. As a large-scale screen requires access to many lines, a significant amount of costs can be involved. These costs are frequently changing; a current estimate (February 2015) is given in Table 1.

VDRC promises to fill orders of 100 or more lines within 6 weeks. For a large screen, VDRC offers a purchase order of a given number of stocks per week. NIG-FLY ships ordered stocks once a week with the restriction of delivering 200 lines per month per lab, which limits large-scale screens. TRiP stocks are delivered from Bloomington Stock Center, which also ships at least once per week and has no limit for ordering, and a subset of lines are also available from NIG-FLY. Shipping with a courier generally works quickly and reliably, however has a higher cost than standard post.

In choosing a source for the large screen the lab should not only calculate ordering costs but also the handling and shipping costs. The latter may include customs and veterinarian fees, e.g. for shipment of stocks into the European Union. One shipment each week may thus significantly contribute to the costs and influence the library choice for the large-scale primary screen.

3 Published Large-Scale RNAi Screens in *Drosophila*

The public availability of the RNAi libraries has enabled scientists to functionally investigate a biological question at the systems level, by testing the function of most genes in an unbiased manner. Various large-scale RNAi screens have been done in a number of *Drosophila* tissues at various developmental stages, some of which are listed in Table 2. A more detailed summary of the screens can be found elsewhere [42]. The variety of assay conditions included designs to identify new players in Notch [20] and Wingless signaling [43], as well as in immune susceptibility [26] or adipose cell fate [25]. Tissue-specific RNAi enabled the identification of neuronal genes regulating neuroblast self-renewal [27], egg laying behavior [22] or nociception [23], or discovery of mesodermal genes regulating heart [24] or muscle morphogenesis and function [21]. Recently, large-scale screens have been performed to identify regulators of the piRNA pathway in somatic support cells [33] or in the germline [34] or genes regulating germline stem cell self-renewal [44]. Together, this demonstrates the immense flexibility and the enormous potential of the RNAi libraries for gene function discovery.

Theoretically, the *Drosophila* genome could be functionally annotated with enough screens assaying various conditions. However, the reality is more complicated as RNAi can also create various pitfalls. Unfortunately, the quality assessment of the published large-scale RNAi data varies in stringency, thus some data can be misleading. Here, we give some suggestions on how to plan and perform a large-scale screen and how to critically and quantitatively assess the quality of the obtained data. In our opinion, this is critical to judge the value of functional RNAi data.

4 Establishing a Robust Screening Scheme for a Genome-Wide Screen

Performing a large-scale or even genome-wide RNAi screen is a challenging task that requires serious commitment and time investment. The most critical part of a large-scale screen is a well-designed assay, which allows both high-throughput and high reproducibility to give confidence in the observed phenotype. If both prerequisites are not fulfilled, a large-scale screen is likely to fail. Thus, prior to starting a large-scale screen, we recommend performing a pilot screen to optimize the screening assay, the phenotypic categories,

data storage, as well as assay reproducibility. This pilot screen should also include positive and negative controls to estimate the false-positive and -negative rates of the experimental approach. In the following, we use neuronal and muscle tissues as examples to discuss the principles of establishing a robust screening scheme.

4.1 Positive and Negative Control Genes

For most biological processes studied, including neuronal and muscle development or function, a number of essential genes are already known. Ideally these “positive control genes” should be identified as “positive” in the RNAi screening assay, otherwise the identification of “new genes” is in strong doubt. If no specific genes that function in a particular cell type are known, general “house keeping” genes required for transcription, translation, or energy metabolism in all cell types can be chosen as positive control genes. Efficient knock-down of these genes should kill or strongly compromise the function of the studied cells.

Similarly, it is essential to compile a list of “negative control genes” which have no (reported) function in the tested cell type or assay. Identifying these genes is less trivial; however, Flybase provides a rich data source for known null alleles that, for example, are viable and fertile. Thus, these genes can neither be essential for development nor for function of neurons or muscles.

Ideally, a list with at least 50 positive and 50 negative control genes should be compiled and all available hairpin lines for these genes should be ordered from the library chosen for the large-scale screen. The results from the functional test of these lines in a pilot study can be used to calculate the false-negative and the false-discovery rates. Calculation of the false-negative rate is simple: if 45 out of 50 positive control genes score positive in the screening assay, the false-negative rate is estimated to be 10% (5/50) (Fig. 1). Estimation of the false-discovery rate is more complicated, as it depends on the total percentage of hits in the screen. For example, if from 50 negative control genes 1 scores positive (false-positive rate: 2%) and the total hit rate is 10% (10% of all screened genes scored positive in the assay), then the false-discovery rate is estimated with 20%. However, if the total hit rate is only 1%, then the false-discovery rate can be up to 100%, demonstrating the importance of determining these numbers. In the practical example of the muscle morphogenesis and function screen, both the false-negative and the false-discovery rates were calculated to about 5% using the applied screening conditions [21] (Fig. 1).

4.2 GAL4 Driver

The choice of the GAL4 driver line is very critical for the efficiency of the RNAi knock-down and thus for the success of the screen. A general recommendation is to test the positive control genes with a GAL4 line that is as strong as possible and whose expression starts well before the time point of the phenotypic assay. Consequently, there is sufficient time for loading the cell with the hairpin and knocking down the mRNA (and therefore the protein).

$$\text{false negative rate} = \frac{\text{number of positive control genes scored as negative}}{\text{number of all positive control genes tested}}$$

$$\text{false positive rate} = \frac{\text{number of negative control genes scored as positive}}{\text{number of all negative control genes tested}}$$

$$\text{total hit rate} = \frac{\text{number of all genes scored as positive}}{\text{number of all genes tested}}$$

$$\text{false discovery rate} = \frac{\text{false positive rate}}{\text{total hit rate}}$$

Fig. 1 A guide to calculate false-negative, false-positive, total hit and false-discovery rates of large-scale screen data

The strong *Actin5C*- or *Tubulin*-GAL4 drivers are useful if systemic gene function in many cell types will be investigated. However, one should be aware that *Actin5C*- or *Tubulin*-GAL4 are not always strongly expressed in all cells at all developmental stages. For strong tissue-specific knock-down, it is recommended to use strong tissue-specific drivers like *Mef2*-GAL4 in all muscles or *elav*-GAL4 in all neurons. If only a very specific cell population is of interest, for example a subtype of cells within a tissue, it might be worth using one of the many thousands of GAL4 lines available from DGRC in Kyoto (NP lines), Janelia Farm (deposited largely to Bloomington), or VDRC (Vienna tiles) [45–48] (see Notes 8 and 9 for links to websites). These specific GAL4 lines might even be stronger than the general *Actin5C*- or *Tubulin*-GAL4 lines in a particular cell type.

If pupal or adult stages are of interest, *Hsp70*-Gal4 can be used with repeated heat shocks to ensure efficient knock-down. Alternatively, a combination of a GAL4 driver with *Tub*-GAL80-ts followed by a temperature-shift protocol is useful (TARGET) [25, 49]. We recommend shifting at least 1–2 days before the gene function will be investigated. Alternatively, driver lines that are active at particular developmental stages can be useful. Examples from muscle biology are 1151-GAL4 that is only expressed in adult muscle progenitors or *Act88F*-GAL4, which is largely restricted to the developing and mature flight muscle fibers [50, 51].

4.3 Enhancing Knock-Down Efficiency: Dicer-2, Temperature, and Sex

The identification of a strong GAL4 line alone might not suffice to achieve strong gene knock-down. Overexpression of Dicer-2 (Dcr-2) increases the efficiency of gene knock-down when long dsRNAs are used (VDRC, NIG-FLY, and first generation of TRiP libraries) [17].

Dcr-2 cleaves long dsRNAs into short siRNAs facilitating the degradation of target mRNAs [52]. Ideally one combines the GAL4 driver with UAS-*Dcr-2* in the same stock by recombination or double balancing to make the experimental RNAi crosses easier. UAS-*Dcr-2* is available on all chromosomes from Bloomington Stock Center and VDRC. This appears particularly important in neurons, in which RNAi without overexpression of Dcr-2 has only limited efficiency [17]. However, one should be aware that Dcr-2 overexpression also increases the off-target risk. Thus, we recommend to particularly control for specificity when UAS-*Dcr-2* is used.

It is well documented that GAL4 activity varies with temperature, being more active at higher temperature. Thus, higher temperature increases knock-down efficiency [40, 41, 53]. A simple option is to grow the RNAi cross at a constant high temperature, ranging from 25 to 29 °C [21, 24]. However, if gene function at a late developmental time point should be tested, constant high temperature may often result in earlier lethality, depending on the strength of the GAL4 line used. To avoid such early developmental lethality, RNAi crosses can be set-up at a lower temperature and then shifted to a higher temperature at larval, pupal, or adult stages [20]. In the case of heat shock inducible *Hsp70*-GAL4, shifting to 37 °C for several 1 h time windows is used to induce knock-down [25, 26].

Interestingly, it has been observed that RNAi generally works better in males [17, 21, 40]. It is not entirely clear if this effect is due to higher GAL4 activity or higher efficiency of the RNAi machinery in males. Practically, it means that the control of sex is important for the experiment (also in larvae) and that males might be the better choice for RNAi knock-down assays.

4.4 A Practical Developmental Stage for Screening

The process studied by RNAi-mediated knock-down influences the required developmental stage at which the screening assay can be done: embryos, larvae, pupae, young, or aged adults. Generally, RNAi-mediated knock-down during embryonic stages appears to be inefficient, as few embryonic lethal hits have been found in large screens, such as the muscle screen [21]. This might in part be due to maternal deposition of mRNA or protein, but the main cause seems to be the inefficiency of long dsRNAs mediating knock-down in the embryo. Recently, the use of maternal GAL4s and short hairpins made some progress to efficiently knock-down genes in the embryo [18, 54]. However, the successful application of this method in a large screen is yet to be done.

As a rule of thumb, it is advantageous to choose a stage for the RNAi assay at which the cells have had enough time to eliminate the protein effectively. Thus, expression of the hairpin should ideally start several days before the assay. This can relatively easily be implemented when assaying tissue homeostasis or aging, as the knock-down is applied continuously and the phenotype can be scored in aged adults. Using aged adults may also be advantageous when

assaying the function of neural circuits, as gene knock-down in neurons appears less effective.

As discussed above, an early developmental lethality can be circumvented by the TARGET technology using *Tub*-GAL80-ts [49, 55]. This enables testing for gene function at later developmental stages, even if no GAL4 line with an appropriate temporal expression pattern is available. However, one should be aware that not all assays may tolerate the 30 or 31 °C required to fully inactivate the GAL80-ts, which needs to be applied well in advance (usually at least 1–2 days) before the assay.

4.5 Design of the RNAi Crosses

For practical reasons, we recommend to cross virgin females carrying the GAL4 driver (optionally carrying UAS-*Dcr-2*) to males harboring the UAS-RNAi transgene. Using a Y, heat-shock *hid* virginizer chromosome in the GAL4 driver line will make large-scale collection of virgin females easier [56]. If the phenotypic scoring requires microscopy, it is practical to include a fluorescently tagged fusion protein in the selected virgins. As discussed above, it is often advisable to use F1 male progeny when scoring for the knock-down phenotype. Thus, the use of X-chromosomal hairpin insertions, which can be found at VDRC and NIG-FLY, is less straightforward.

4.6 Screening Assay and Scoring

A phenotypic assay for a large or genome-wide screen should fulfill a number of criteria that are a prerequisite for the success of the screen. The assay should be simple enough to allow phenotypic scoring at high-throughput. The assignment of phenotypic categories should be clearly defined and unambiguous. Binary terms such as “lethal” vs. “viable” or “volant” vs. “flightless” are the easiest to score [20, 21]. Alternatively, quantitative scoring on a defined scale, such as triglyceride levels normalized to protein levels, can be used [25]. All phenotypic categories should use a “term” from a controlled vocabulary. Moreover, for each category, the strength of the phenotype should also be scored, either by assigning it to sub-categories, such as the developmental stage of lethality (embryonal, larval, pupal, pharate, adult) or ideally using a quantitative measure, such as flight ability measured in a graded tube or transposon activity determined by quantitative PCR or reporter activity [21, 33, 34]. A quantitative measure allows assignment of a “cut-off” value above which a phenotype is considered real and the gene will be followed up.

Importantly, the phenotypic assay must be highly robust and reproducible to minimize experimental error and thus reduce the required number of repetitions. If an assay is reliable, a positively scored line above the defined “cut-off” needs only to be re-tested once. Wild type always needs to score as wild type and a mutant positive control should always score as positive in the assay and not only in 9 out of 10 times. Otherwise, 10% of the positive controls are not found because of the noise in the phenotypic assay and not because of ineffective hairpins or variability in the RNAi-mediated

knock-down. A reliable assay with controlled vocabulary becomes even more essential when multiple people collaborate in the project. We recommend optimizing the screening conditions (assay, GAL4-line, temperature, cut-off) with the best-defined positive control genes to make sure the screen works reliably and the phenotype is always spotted. The next step is to move to the pilot screen.

4.7 Pilot Screen

A pilot screen should fine-tune the experimental conditions and the phenotypic scoring to optimize the assay for reproducibility. Importantly, it will also result in a measure of false-positive and false-negative rates. These numbers are important to decide if it is worth performing a large-scale screen or not.

As recommended under Subheading 4.1, RNAi lines for at least 50 positive control and 50 negative control genes should be used in the pilot screen, mixed with at least 100 random lines. All lines should be scored blindly in the assay developed above. If a phenotype is scored above the “cut-off”, the line is retested again blindly, by funneling it into the screening pipeline again. From these results, a false-negative rate and a false-positive rate are calculated (see Subheading 4.1 and Fig. 1). Depending on the outcome, the screening conditions can be adjusted to enable stronger knock-down (stronger GAL4, higher temperature, UAS-*Dcr-2*) or lower off-target risks (lower temperature, no UAS-*Dcr-2*). These results should also be used to adjust the “cut-off”. Finally, a value needs to be defined for when a line is scored as “positive in the screen”, usually above or below an average of the quantitative phenotype of the first test and the re-test. At this stage, the experimenter can make an informed decision whether it is worth moving to the large-scale screen or to further improve the experimental conditions (Fig. 2).

5 Large-Scale Screening

5.1 Planning and Infrastructure

A large-scale or genome-wide RNAi screen requires screening of 10,000–20,000 RNAi lines. Ideally, such a screen is performed in less than 1 year. A possible time schedule for a large-scale screen and the following secondary assays is suggested in Fig. 2. Typically, at least 250 (or even better 500) lines are screened every week with the optimized assay from the pilot screen. The workload during the large-scale screen is very high; thus, the assay can no longer be easily adapted. This again highlights the importance of assay development, which should be completed before the high-throughput screen starts.

Planning of the large screen should not only consider the work required for setting up the crosses and performing the screening assays, but also account for the required infrastructure. Sufficient incubator space to store all the RNAi stocks at least until the end of the re-test is recommended, such that a positive line can be kept in the lab and does not need to be re-ordered for the secondary

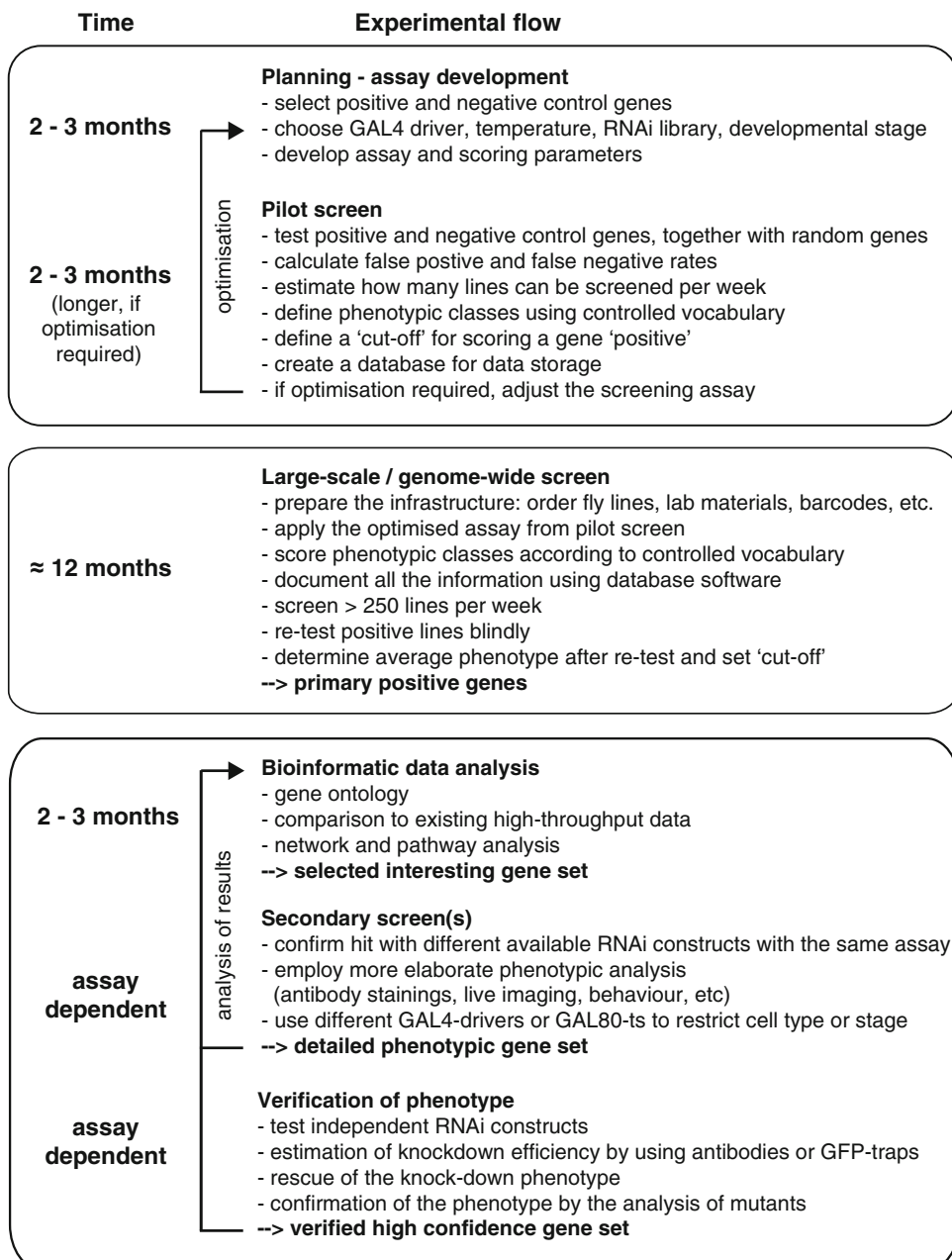


Fig. 2 Experimental flow how to plan and perform a large-scale in vivo RNAi screen

assays. Depending on the assay, incubators set to the chosen assaying temperature and enough microscope time needs to be available. To avoid mistakes in labeling of stocks and RNAi crosses, we strongly advise use of barcodes for every vial and cross and creation of a database that tracks every cross and stores all the phenotypic data (see Fig. 3 for an example database interface).

a Database layout of primary muscle screen

target_gene	CG6464	barcode	1141050602000000	s19	,996666667
GeneName	salm	construct_ID	1525	nr_ON_targets	1
		transformant_ID	3029	nr_OFF_targets	1
Lethality assay					
lethality_m	0	lethality_stage_r	8	assay_1	Katharina
lethality_f	0	lethality_stage_l	8	date_1	30.08.2006
	1	embryonal			
	2	early larval			
	3	late larval			
	4	prepupal			
females?	4	early pupal		assay_2	Frank
zone_1	5	paralyse		date_2	05.09.2006
zone_2	6	sluggis			
zone_3	7	slow			
zone_4	8	adult			
zone_5	9	hyperactiv	undefined		
water	10	uncoordinated	0		
bounce	0	held_out_wings	5		
		erected_wings	0	observation	

b Database summary layout of primary muscle screen

Fig. 3 Database to document the muscle-specific RNAi screen. **(a)** Screenshot from a “primary screen” layout assaying lethality and flight ability. The barcode is used as a unique identifier for each entry. The transformant ID (*blue box*) identifies the hairpin line and is linked to the hairpin’s construct ID and target gene. Date and experimenter name are entered automatically. Lethality penetrance (0–10 = 100 %) and lethality stage are chosen from drop-down menus (*red boxes*). **(b)** “Summary layout” to display all tests done for a given RNAi line and the calculated phenotypic average (*green boxes*)

5.2 Documentation and Statistics

A suitable database for the screen should contain information on all hairpin lines that will be screened as well as their target genes (Fig. 3). It should track all the received stocks and the ones that have been crossed to the GAL4 line with a time stamp. The phenotypic scoring interface should enable entry of the phenotypic category and the strength of the phenotype using a controlled vocabulary, ideally from a drop-down menu to avoid mistakes. It should also allow entry of phenotypic images if they are acquired during the assay. Additionally, the date of the assay and the name of the screener should be tracked. This allows assignment of potential problems to particular screening weeks when the data are analyzed at a later stage of the screen. Each week the database should also automatically generate a table containing all lines that have passed the phenotypic “cut-off” and are scored “positive”. These lines should be re-entered into the screen during the next weeks for blind re-testing. We recommend database programs such as Filemaker or Microsoft Access as suitable data management software, and emphasize that a simple Microsoft Excel sheet is not sufficient (Fig. 3).

As a large screen will last about 1 year, it is important to continuously track the entered screen data to spot potential problems. If suddenly too many or too few positives are scored, action can be taken to spot and solve the potential problem before the damage becomes too large.

At the end of the large screen, when all RNAi lines have been screened once and the positive ones have been re-tested at least once, the quantitative phenotypic data need to be averaged for each line. A final “cut-off” is set that determines if a line scores “positive” in the overall assay and in which of the phenotypic categories. Together, this defines the primary positive genes from the screen, which depending on the assay and phenotypic category can be few or a few hundred genes. These genes are the basis for the bioinformatic analysis discussed in Subheading 9, which can be very helpful in selecting genes or gene groups depending on various enrichment criteria for the secondary assays.

6 Secondary Screens

The secondary screens can have multiple purposes and often apply multiple assays. The first secondary assay should attempt to confirm the phenotypic specificity of the RNAi construct by simply testing other available hairpin constructs for the particular gene, in case only a single hairpin construct scored positive in the primary screen. This should be done in the same assay as performed for the primary screen. Ideally, this is done for all hits from the primary screen and results in a gene list that has been confirmed with at least two independent hairpin constructs. Unfortunately, it frequently happens that not all phenotypes scored for different constructs of the same gene are identical. This can have multiple causes, which will be discussed in Subheadings 7 and 8.

Depending on how many genes were selected from the primary (confirmed) hits, either bioinformatically or because of a particularly interesting phenotypic class, more elaborate secondary assays can be applied. It is often useful to perform a detailed phenotypic assay, possibly using antibody stainings at different developing stages or live imaging, to gain better insight into the cause and origin of the observed phenotypes. Also, sophisticated behavioral analysis may be executed at this stage. Sometimes it might be practical to use different, more restricted GAL4 driver lines or combine GAL4 lines with GAL80 lines to assign the function of the gene to a particular developmental stage or cell type [20, 26, 27, 32]. Ideally, the secondary assays identify a few confirmed genes that are key regulators of the process of interest, which can then be used for case-by-case studies to mechanistically investigate their role in the given process [22, 57].

7 Possible Problems with RNAi

In the ideal scenario, RNAi would eliminate gene function completely and specifically in the targeted cell type in a defined time period. However, unfortunately, this scenario is not always the case. This causes several important problems, including the identification of false-positive hits as well as false negatives. The experimenter needs to be aware of these problems and can apply several strategies to solve or at least minimize them.

7.1 False-Positive Hits

7.1.1 Off-Target Effects

Off-target effects are a serious problem common to all RNAi approaches [58–60]. One can distinguish two types of off-target effects. In the first type, genes that are very similar are knocked-down in addition to the intended “on”-target. In particular long hairpins, which are processed to many siRNAs, will also knock-down highly homologous genes. One example is the actin gene family members, which cannot be specifically targeted with long dsRNA constructs [21]. Generally, these types of off-targets are not a major problem, as they can easily be identified.

The second type of off-targets cannot be easily predicted and thus are a serious concern. Any gene with ≥ 19 -nucleotide perfect match to a region in the dsRNA is a potential off-target [61, 62]. These are easily found by a simple BLAST search. VDRC constructs have a specificity score, the s19 value, ranging from 0 to 1, with 1 indicating no off-target. However, an s19 score of 1 is no guarantee against knock-down of unknown off-targets, which potentially contain only some homology to the seed sequence of one of the produced siRNAs [63]. These off-targets are very difficult to predict. In practical terms, the experimenter can never be sure if the observed phenotype is not caused by unintended knock-down of an unknown off-target gene.

This problem has also not been solved with the introduction of the short hairpin constructs from the TRiP library. They produce only a single miRNA-like scaffold with a 21mer homology to the intended target. However, this single miRNA-like RNA is produced in large amounts, which may also cause a serious problem in case a homology to the seed sequence exists elsewhere in the genome. In human cells it is well established that the esiRNA (endoribonuclease-prepared siRNAs) technology using multiple siRNA results in less severe off-target effects than a single siRNA as the off-targets become diluted [64].

Overexpression of exogenous small RNAs can also cause sequence-independent off-target effects. Since these RNAs utilize the endogenous miRNA pathway components, an excess of exogenous hairpins can saturate some components of this pathway and thus perturb the endogenous small RNA metabolism [65, 66]. These drawbacks demonstrate that an RNAi-induced phenotype ALWAYS needs to be confirmed by a second independent RNAi construct or by rescuing the knock-down phenotype (see Subheading 8), if classical mutants cannot be used.

7.1.2 Insertion Position Effects

The GD library and large parts of the NIG-FLY library have been generated by a random P-element insertion strategy and thus are subject to position effects. The insertion can disrupt the host locus, for example inactivating the host gene, and thus potentially modify the observed phenotype. More problematic are potential “EP-effects” resulting from the overexpression of a gene next to the UAS insertion site in cases where the SV40 termination is not entirely effective. This can have serious consequences, such as promoting strong overgrowth when inserted next to a growth regulator (BJ. Thompson, personal communication).

7.2 False Negatives

RNAi-induced phenotypes can be close to a genetic null phenotype. More often, a hypomorphic or no phenotype is observed after attempted gene knock-down, despite a function for the given gene in the tested cell type. The most common reason is that the hairpin is inefficient in knocking down the target RNA or the protein of the respective gene has a long half-life and thus perdures to fulfill its function despite a reduction of the mRNA. Under Subheading 4.2, we discuss several approaches on how to generally increase the knock-down efficiency.

In particular, the expression level of the randomly inserted RNAi constructs can be variable due to their genomic location. However, even the well-chosen attP sites for the KK and TRiP libraries may not express equally well in all investigated cell types. The insertion of gypsy insulators on both sides of the transgene in the TRiP constructs attempts to reduce these position effects [67].

7.3 Genetic Redundancy

Similar to classical mutants, RNAi also does not solve the problem of genetic redundancy. Genes that share functions can compensate for the loss of the RNAi target and mask its function. However, RNAi does offer one possible solution. Multiple hairpins against genes from the same family or involved in the same process can be combined to overcome genetic redundancy.

8 Verification of the Knock-Down Phenotype

Positive hits from the primary or secondary screen are often only based on the phenotype identified with one RNAi construct. As discussed in Subheading 7.1, these phenotypes need an independent verification before they can be classified as a confirmed “true hit”. Below we recommend several possibilities. At least one of them should be used before a detailed functional study of the respective gene is initiated.

8.1 Independent RNAi Constructs

A widely used approach to confirm the specificity of an RNAi-induced phenotype uses one or more independent RNAi constructs, which target the same gene at non-overlapping regions. The rational is that it is very unlikely to find the same off-target effect when using an entirely different hairpin construct. The different available libraries are a good source for these additional constructs. If no additional constructs are available for the particular gene, these can be generated with a simple cloning step using the available vectors of the respective libraries.

However, it often happens that phenotypes vary when comparing different RNAi constructs. This is likely caused by differences in knock-down efficiencies, which may complicate the interpretation of the results. Is the stronger phenotype then indeed caused by stronger gene knock-down? In such cases, overexpression of Dcr-2 may help to enhance the knock-down efficiency of the suspected “weak” line.

8.2 Estimation of Knock-Down Efficiency

If phenotypic variation between different RNAi constructs is observed, it is advisable to determine the knock-down efficiency by measuring protein levels. A reduction in protein levels that correlates with the phenotypic strength is a good argument for knock-down specificity. We believe that testing protein levels is a better measure than testing mRNA levels, as for some genes we were unable to detect protein, despite only a mild reduction in the respective mRNA levels [21].

8.2.1 Antibody Detection of Protein Levels

If an antibody against the target protein is available, immunohistochemistry gives a good estimation for the knock-down efficiency. Ideally, the protein levels in the cells of interest that express the

GAL4 line are compared to a different control cell/tissue in the same animal. Western blots are more quantitative; however, they can only be used to determine knock-down efficiency if the gene is knocked-down in all cells with a global GAL4 driver or gene expression is restricted to the cell type that expresses the GAL4. If the tissue of interest is large enough, it can also be dissected and loaded for Western blotting.

8.2.2 Gene Traps

By inserting a fluorescent tag (often GFP) or epitope into the intron of genes by using splice acceptor and donor sites, so called “gene traps” are created. There are currently several gene-trap collections available [68–72] (see Note 7 for links to the websites). A GFP trap can also be created easily using the continuously growing MiMIC collection created by the Bellen lab [73]. As these GFP fusions are under endogenous control, they can provide an informative measure of the protein knock-down efficiency. A potential caveat is that not all of these internal GFP fusion proteins are fully functional and thus some lines are not homozygous viable.

The GFP traps can also be used as a flexible tool to provide specificity control. Well characterized hairpins targeting GFP can be used to knock-down the fusion protein, which should result in the same phenotype (if the GFP trap is homozygous) as induced by a gene-specific hairpin [74, 75]. Neumüller and colleagues created several GFP RNAi lines, optimized either for somatic tissue or germline knock-down [74]. One drawback of this approach is that only the GFP-tagged isoforms will be knocked-down. Thus, the location of the GFP trap insertion within a complex gene is critical.

8.3 Rescue of the Knock-Down Phenotype

Rescue of the RNAi-induced knock-down phenotype provides very strong evidence for phenotypic specificity. One simple way to rescue is to overexpress a cDNA of the targeted gene using GAL4-UAS. Although this cDNA can still be targeted by the hairpin, the large amount of cDNA expressed may still rescue the phenotype [76, 77] (AK-Ç, personal observation). The cDNA can also be engineered using silent mutations to an RNAi-resistant cDNA [78]. This is particularly simple if short hairpins are used. A limitation of this approach is that the over-expression of a particular protein may result in a phenotype, and thus must be carefully controlled.

A more elegant strategy uses genomic clones from a related *Drosophila* species that is close enough to maintain function, but diverse enough on the nucleotide level to provide RNAi resistance to the *D. melanogaster* hairpin [79, 80]. Genomic fosmid clones from *Drosophila pseudoobscura* were generated at large scale [81], and for three of four cases a partial rescue of the RNAi induced phenotype in *D. melanogaster* was found. The rescues were likely only partial because the chosen clones are not entirely resistant

against the *D. melanogaster* hairpins [80]. A large collection of these fosmid clones is available; however, transgenic lines for them need to be generated [81].

8.4 Confirmation by Mutants

The ultimate confirmation of an RNAi-induced phenotype can be achieved by the analysis of a genetic mutant. As discussed above, this is often difficult when a gene plays multiple roles in various tissues at different developmental stages. However, a number of recent genome-engineering approaches allowed generation of custom-made alleles that enable efficient cell-type-specific deletion of the gene. This was done by flanking a gene with two FRT elements in *cis* using the available FRT-bearing transposon collections [82, 83] or by inserting a conditional cassette into the gene using CRISPR-mediated genome engineering [84]. CRISPR-based technologies may also harbor the potential to produce tissue-specific mutant phenotypes by expression of the single chimeric guide RNA (sgRNA) in the cell type of interest [85].

9 Data Analysis and Data Presentation

A large-scale in vivo RNAi screen can be very rewarding, resulting in hundreds of putative positive genes. Statistical and bioinformatics analysis of this gene list enables the identification of signaling pathways or gene networks that are significantly enriched amongst the hits. This can simplify the often-difficult choice of which gene or gene groups to focus on for a more detailed analysis. It also allows the investigator to group genes with similar phenotypes and related molecular, cellular, or biological functions. Depending on the complexity of the secondary assay(s), a data analysis step will likely already be necessary after the primary screen. Below are some suggestions of approaches we found useful for data analysis (*see Note 10* for links to websites):

1. **Gene ontology (GO, <http://geneontology.org>)** analysis to identify the enrichment of biological processes, molecular functions, or cellular components amongst the positive genes. It is important to keep in mind that the GO annotation of the fly genome is still somewhat limited, thus GO analysis can bias toward known genes and pathways. We recommend using **GO-elite** [86] for GO-term enrichment. The researcher can employ the latest GO-annotations from Flybase or provide his/her own annotation. As a consequence, GO-elite can be used to look for enrichment of many features, including pathways. GO-elite runs as a stand-alone application and is available for all operating systems.
2. **GORilla** (<http://cbl-gorilla.cs.technion.ac.il> [87]); the **Gene Ontology enRICHment anaLysis and visuaLizAtion** tool is particularly useful to display the enrichment in a hierarchical tree

view, reducing the complexity to a manageable size. GOrilla also exports data to text files for additional analysis and to REViGO for further visualization approaches [88].

3. **DAVID** (<http://david.abcc.ncifcrf.gov> [89]); the Database for Annotation, Visualization and Integrated Discovery can also be useful to identify enriched GO-terms and discover enriched gene groups. Beyond GO, DAVID moreover makes use of biological pathways, literature, protein domains, protein interactions, expression or general annotation for enrichment analysis and can therefore be viewed as a much more versatile enrichment analysis tool. It can also be used to visualize the identified genes on the pathway maps of enriched KEGG pathways. The researcher can however not use his/her own annotation files for enrichment analysis in DAVID.
4. **OMIM** (<http://www.omim.org>); the Online Mendelian Inheritance in Man database, allows identification of fly genes that have homologs to human genes that are associated with genetic disorders. To find the human orthologs the HomoloGENE database is valuable [90].
5. **FlyRNAi** (<http://www.flyrnai.org>); it can be insightful to compare the gene hit list to a database containing hits of many cell-based RNAi screens. This website also contains the **COMPLEAT**, protein **COMPLEx** Enrichment Analysis Tool [91], to analyze the gene list with a focus on protein complexes (<http://www.flyrnai.org/compleat>).
6. **GenomeRNAi** (<http://www.genomernai.org>) is an alternative database that is collecting phenotypic information from published human cell-based and *Drosophila* RNAi screens [92]. This can identify frequent hits, which might be treated with care, as they may not result in specific phenotypes.
7. **Network and pathway analysis** is commonly used to integrate and analyze –omics data of various types. This often leads to a more systematic view of screening data. Integrating –omics data with protein interaction or gene regulatory data moreover helps in selecting genes or gene groups for follow-up studies. **Cytoscape** (<http://www.cytoscape.org>, [93]) is currently the most widely used tool to analyze network and pathway data. Cytoscape 2 and the newer Cytoscape 3 versions both provide in principle the same analysis methods, albeit by using sometimes-different plug-ins. Interaction networks of various kinds (protein–protein, genetic, transcription factor–gene interactions) can be best generated using the **DroID** [94] plug-in in Cytoscape 2. Either the entire interactome, or a more specific, gene-list focused network, can be created with this plug-in. Cytoscape 3 provides a built-in function to upload any interaction data from public databases using the **PSICQUIC** service [95]. The interaction networks are in

this case limited to physical (protein–protein or small molecule–protein) interactions. Networks can in a next step be analyzed for clusters (for instance **MCODE** [96], **ClusterViz** [97]), annotated with and enriched for Gene Ontology terms or pathways (using for example **BINGO** [98] or **ClueGO** [99]). Cytoscape also offers several built-in features for network visualization.

Finally, web-based database and analysis tools like **STRING** [100] can be used for generating and analyzing small interaction networks using a limited number of genes. STRING for instance provides some basic network clustering methods and also allows enrichment analysis of various features (GO, pathways, tissues, or diseases).

10 Notes

1. The fly stocks from the libraries might be infested with mites. Quarantine these stocks by flipping them 3 times on 3 consecutive days.
2. VDRC libraries: In November 2013, a large number of stocks were removed from the collection due to redundancy (multiple insertions of the same hairpin construct) and due to genome annotation changes (constructs that did not map to a gene anymore after the annotation update). Therefore, some lines that were available before may no longer exist.
3. VDRC-KK library: The host strain used for the generation of the VDRC-KK library was recently reported to have an additional, initially un-annotated attP insertion site at 30B3. The initially annotated site at 40D3 can result in nonspecific wing phenotypes, possibly by overexpression of the neighboring gene *tio*, when crossed to a GAL4 line. A suggested solution is to “clean” the chromosome by recombination [101].
4. Fly stocks from the NIG-FLY library may contain white-eyed flies due to balancing problems. Check the eye color when you receive the flies and if necessary, re-balance the stock.
5. The most commonly used marker for transgenic RNAi constructs is a mini-*white*⁺ gene. For detection of the *white*⁺ insertion, the stocks were constructed in a *white* mutant background, usually *white*[1118]. Thus, all VDRC and NIG-FLY stocks contain a *white*[1118] allele on the X-chromosome. As the transgenic mini-white may not entirely rescue all the functions of the endogenous *white* gene, these lines must be backcrossed into a wild-type *white*⁺ background if vision is an important element in the assay. The TRiP library avoided this potential problem by marking the constructs with a *vermillion*⁺ marker. All TRiP stocks have the genotype *y*[1] *sc*[1] *v*[1]; attP2 or

y[1] sc[1] v[1]; attP40 with the *vermillion*+ transgene inserted in attP2 or attP40. The disadvantage of this design is that the RNAi transgene can only be followed in a *vermillion* mutant background, thus crossing a TRiP RNAi line to a *white* mutant stock may result in various eye colors.

6. New TRiP lines: a gene can be nominated at <http://www.flyrnai.org/TRiP-ACC-OVR.html> for priority production, in case no TRiP line exists for that gene.
7. GFP trap lines: https://kyotofly.kit.jp/cgi-bin/stocks/data_search.cgi; <http://www.flyprot.org>
8. Images of enhancer lines: <http://flyview.uni-muenster.de>
<http://flweb.janelia.org/cgi-bin/flew.cgi>
<http://stockcenter.vdrc.at/control/vtlibrary>
9. Links to the RNAi libraries and GAL4 collections:
 VDRC: <http://stockcenter.vdrc.at/control/main>
 NIG-FLY: <http://www.shigen.nig.ac.jp/fly/nigfly>
 TRiP: <http://www.flyrnai.org/TRiP-HOME.html>
 NP-lines: <https://kyotofly.kit.jp/cgi-bin/stocks/index.cgi>
 Janelia: http://flystocks.bio.indiana.edu/Browse/gal4/gal4_Janelia.php
10. Links to bioinformatic tools:
 GO: <http://geneontology.org>
 GORILLA: <http://cbl-gorilla.cs.technion.ac.il>
 DAVID: <http://david.abcc.ncifcrf.gov>
 OMIM: <http://www.omim.org>
 FlyRNAi: <http://www.flyrnai.org>
 COMPLEAT: <http://www.flyrnai.org/compleat>
 GenomeRNAi: <http://www.genomernai.org>
 Cytoscape: <http://www.cytoscape.org>

Acknowledgements

We thank Reinhard Fässler for generous support, Bianca Habermann for help with the bioinformatics section, and Maria Spletter and the entire Schnorrer lab for informative suggestions on this manuscript. Our laboratory is supported by the Max Planck Society, Humboldt Foundation and EMBO postdoctoral fellowships (A.K.-C.), the EMBO Young Investigator Program (F.S.) and the European Research Council under the European Union's Seventh Framework Programme (FP/2007-2013)/ERC Grant 310939.

References

1. Nüsslein-Volhard C, Wieschaus E (1980) Mutations affecting segment number and polarity in *Drosophila*. *Nature* 287:795–801
2. St Johnston D (2002) The art and design of genetic screens: *Drosophila melanogaster*. *Nat Rev Genet* 3:176–188
3. Chen D, Ahlford A, Schnorrer F et al (2008) High-resolution, high-throughput SNP mapping in *Drosophila melanogaster*. *Nat Methods* 5:323–329
4. Bellen HJ, Levis RW, He Y et al (2011) The *Drosophila* gene disruption project: progress using transposons with distinctive site specificities. *Genetics* 188:731–743
5. Lee T, Luo L (2001) Mosaic analysis with a repressible cell marker (MARCM) for *Drosophila* neural development. *Trends Neurosci* 24:251–254
6. Fire A, Xu S, Montgomery MK et al (1998) Potent and specific genetic interference by double-stranded RNA in *Caenorhabditis elegans*. *Nature* 391:806–811
7. Montgomery MK, Xu S, Fire A (1998) RNA as a target of double-stranded RNA-mediated genetic interference in *Caenorhabditis elegans*. *Proc Natl Acad Sci U S A* 95:15502–15507
8. Mohr S, Bakal C, Perrimon N (2010) Genomic screening with RNAi: results and challenges. *Annu Rev Biochem* 79:37–64
9. Sin O, Michels H, Nollen EAA (2014) Genetic screens in *Caenorhabditis elegans* models for neurodegenerative diseases. *Biochim Biophys Acta* 1842:1951–1959
10. Perrimon N, Ni J-Q, Perkins L (2010) In vivo RNAi: today and tomorrow. *Cold Spring Harb Perspect Biol* 2:a003640
11. Boutros M, Ahringer J (2008) The art and design of genetic screens: RNA interference. *Nat Rev Genet* 9:554–566
12. Ding L, Poser I, Paszkowski-Rogacz M, Buchholz F (2012) From RNAi screens to molecular function in embryonic stem cells. *Stem Cell Rev* 8:32–42
13. Timmons L, Fire A (1998) Specific interference by ingested dsRNA. *Nature* 395:854
14. Roignant J-Y, Carré C, Mugat B et al (2003) Absence of transitive and systemic pathways allows cell-specific and isoform-specific RNAi in *Drosophila*. *RNA* 9:299–308
15. Elliott DA, Brand AH (2008) The GAL4 system : a versatile system for the expression of genes. *Methods Mol Biol* 420:79–95
16. Kennerdell JR, Carthew RW (2000) Heritable gene silencing in *Drosophila* using double-stranded RNA. *Nat Biotechnol* 18:896–898
17. Dietzl G, Chen D, Schnorrer F et al (2007) A genome-wide transgenic RNAi library for conditional gene inactivation in *Drosophila*. *Nature* 448:151–156
18. Ni J-Q, Zhou R, Czech B et al (2011) A genome-scale shRNA resource for transgenic RNAi in *Drosophila*. *Nat Methods* 8:405–407
19. Mohr SE, Smith JA, Shamu CE, Neumüller RA, Perrimon N (2014) RNAi screening comes of age: improved techniques and complementary approaches. *Nat Rev Mol Cell Biol* 15:591–600
20. Mummery-Widmer JL, Yamazaki M, Stoeger T et al (2009) Genome-wide analysis of Notch signalling in *Drosophila* by transgenic RNAi. *Nature* 458:987–992
21. Schnorrer F, Schönbauer C, Langer CC et al (2010) Systematic genetic analysis of muscle morphogenesis and function in *Drosophila*. *Nature* 464:287–291
22. Yapiçi N, Kim Y-J, Ribeiro C, Dickson BJ (2008) A receptor that mediates the post-mating switch in *Drosophila* reproductive behaviour. *Nature* 451:33–37
23. Neely GG, Hess A, Costigan M et al (2010) A genome-wide *Drosophila* screen for heat nociception identifies $\alpha 2\delta 3$ as an evolutionarily conserved pain gene. *Cell* 143:628–638
24. Neely GG, Kuba K, Cammarato A et al (2010) A global in vivo *Drosophila* RNAi screen identifies NOT3 as a conserved regulator of heart function. *Cell* 141:142–153
25. Pospisilik JA, Schramek D, Schnidar H et al (2010) *Drosophila* genome-wide obesity screen reveals hedgehog as a determinant of brown versus white adipose cell fate. *Cell* 140:148–160
26. Cronin SJF, Nehme NT, Limmer S et al (2009) Genome-wide RNAi screen identifies genes involved in intestinal pathogenic bacterial infection. *Science* 325:340–343
27. Neumüller RA, Richter C, Fischer A et al (2011) Genome-wide analysis of self-renewal in *Drosophila* neural stem cells by transgenic RNAi. *Cell Stem Cell* 8:580–593
28. Keleman K, Micheler T, VDRC project members (2009) RNAi-phiC31 construct and insertion data submitted by the Vienna *Drosophila* RNAi Center. Personal communication to Flybase

29. Gilsdorf M, Horn T, Arziman Z et al (2010) GenomeRNAi: a database for cell-based RNAi phenotypes. 2009 update. *Nucleic Acids Res* 38:D448–D452
30. Horn T, Sandmann T, Boutros M (2010) Design and evaluation of genome-wide libraries for RNA interference screens. *Genome Biol* 11:R61
31. Bischof J, Maeda R, Hediger M, Karch F, Basler K (2007) An optimized transgenesis system for *Drosophila* using germ-line-specific φ C31 integrases. *Proc Natl Acad Sci* 104:3312
32. Berns N, Woichansky I, Friedrichsen S, Kraft N, Riechmann V (2014) A genome-scale in vivo RNAi analysis of epithelial development in *Drosophila* identifies new proliferation domains outside of the stem cell niche. *J Cell Sci* 127:2736–2748
33. Handler D, Meixner K, Pizka M et al (2013) The genetic makeup of the *Drosophila* piRNA pathway. *Mol Cell* 50:762–777
34. Czech B, Preall JB, McGinn J, Hannon GJ (2013) A transcriptome-wide RNAi screen in the *Drosophila* ovary reveals factors of the germline piRNA pathway. *Mol Cell* 50:749–761
35. Osman D, Gobert V, Ponthan F et al (2009) A *Drosophila* model identifies calpains as modulators of the human leukemogenic fusion protein AML1-ETO. *Proc Natl Acad Sci* 106:12043–12048
36. Yamamoto-Hino M, Kanie Y, Awano W et al (2010) Identification of genes required for neural-specific glycosylation using functional genomics. *PLoS Genet* 6:e1001254
37. Avet-Rochex A, Boyer K, Polesello C et al (2010) An in vivo RNA interference screen identifies gene networks controlling *Drosophila melanogaster* blood cell homeostasis. *BMC Dev Biol* 10:65
38. Lesch C, Jo J, Wu Y, Fish GS, Galko MJ (2010) A targeted UAS-RNAi screen in *Drosophila* larvae identifies wound closure genes regulating distinct cellular processes. *Genetics* 186:943–957
39. Llamusi B, Bargiela A, Fernandez-Costa JM et al (2012) Muscleblind, BSF and TBPH are mislocalized in the muscle sarcomere of a *Drosophila* myotonic dystrophy model. *Dis Model Mech* 6:184–196
40. Ni J-Q, Markstein M, Binari R et al (2008) Vector and parameters for targeted transgenic RNA interference in *Drosophila melanogaster*. *Nat Methods* 5:49–51
41. Ni J-Q, Liu L-P, Binari R et al (2009) A *Drosophila* resource of transgenic RNAi lines for neurogenetics. *Genetics* 182:1089–1100
42. Yamamoto-Hino M, Goto S (2013) In vivo RNAi-based screens: studies in model organisms. *Genes (Basel)* 4:646–665
43. Reim G, Hruzova M, Goetze S, Basler K (2014) Protection of armadillo/β-catenin by armless, a novel positive regulator of wingless signaling. *PLoS Biol*. doi:10.1371/journal.pbio.1001988.s012
44. Yan D, Neumüller RA, Buckner M et al (2014) A regulatory network of *Drosophila* germline stem cell self-renewal. *Dev Cell* 28:459–473
45. Feng K, Palfreyman MT, HAsemeyer M, Talsma A, Dickson BJ (2014) Ascending SAG neurons control sexual receptivity of *Drosophila* females. *Neuron* 83:135–148
46. Kvon EZ, Kazmar T, Stampfel G, Yáñez-Cuna JO et al (2014) Genome-scale functional characterization of *Drosophila* developmental enhancers in vivo. *Nature* 512:91–95
47. Jenett A, Rubin GM, Ngo T-TB et al (2012) A GAL4-driver line resource for *Drosophila* neurobiology. *Cell Rep* 2:991–1001
48. Hayashi S, Ito K, Sado Y et al (2002) GETDB, a database compiling expression patterns and molecular locations of a collection of Gal4 enhancer traps. *Genesis* 34:58–61
49. McGuire SE, Mao Z, Davis RL (2004) Spatiotemporal gene expression targeting with the TARGET and gene-switch systems in *Drosophila*. *Sci STKE* 2004:l6
50. Anant S, Roy S, VijayRaghavan K (1998) Twist and Notch negatively regulate adult muscle differentiation in *Drosophila*. *Development* 125:1361
51. Bryantsev AL, Baker PW, Lovato TL, Jaramillo MS, Cripps RM (2012) Differential requirements for Myocyte Enhancer Factor-2 during adult myogenesis in *Drosophila*. *Dev Biol* 361:191–207
52. Lee YS, Nakahara K, Pham JW et al (2004) Distinct roles for *Drosophila* Dicer-1 and Dicer-2 in the siRNA/miRNA silencing pathways. *Cell* 117:69–81
53. Fortier E, Belote JM (2000) Temperature-dependent gene silencing by an expressed inverted repeat in *Drosophila*. *Genesis* 26:240–244
54. Staller MV, Yan D, Randklev S et al (2013) Depleting gene activities in early *Drosophila* embryos with the ‘maternal-Gal4-shRNA’ system. *Genetics* 193:51–61
55. McGuire SE, Le PT, Osborn AJ, Matsumoto K, Davis RL (2003) Spatiotemporal rescue of memory dysfunction in *Drosophila*. *Science* 302:1765–1768

56. Starz-Gaiano M, Cho NK, Forbes A, Lehmann R (2001) Spatially restricted activity of a *Drosophila* lipid phosphatase guides migrating germ cells. *Development* 128:983–991

57. Schönbauer C, Distler J, Jährling N et al (2011) Spalt mediates an evolutionarily conserved switch to fibrillar muscle fate in insects. *Nature* 479:406–409

58. Sigoillot FD, King RW (2011) Vigilance and validation: keys to success in RNAi screening. *ACS Chem Biol* 6:47–60

59. Mohr SE, Perrimon N (2011) RNAi screening: new approaches, understandings, and organisms. *Wiley Interdiscip Rev RNA* 3:145–158

60. Echeverri CJ, Beachy PA, Baum B et al (2006) Minimizing the risk of reporting false positives in large-scale RNAi screens. *Nat Methods* 3:777–779

61. Kulkarni MM, Booker M, Silver SJ et al (2006) Evidence of off-target effects associated with long dsRNAs in *Drosophila melanogaster* cell-based assays. *Nat Methods* 3:833–838

62. Ma Y, Creanga A, Lum L, Beachy PA (2006) Prevalence of off-target effects in *Drosophila* RNA interference screens. *Nature* 443:359–363

63. Bartel DP (2009) MicroRNAs: target recognition and regulatory functions. *Cell* 136:215–233

64. Surendranath V, Theis M, Habermann BH, Buchholz F (2013) Designing efficient and specific endoribonuclease-prepared siRNAs. *Methods Mol Biol* 942:193–204

65. Grimm D, Streetz KL, Jopling CL et al (2006) Fatality in mice due to oversaturation of cellular microRNA/short hairpin RNA pathways. *Nature* 441:537–541

66. Khan AA, Betel D, Miller ML et al (2009) Transfection of small RNAs globally perturbs gene regulation by endogenous microRNAs. *Nat Biotechnol* 27:549–555

67. Markstein M, Pitsouli C, Villalta C, Celniker S, Perrimon N (2008) Exploiting position effects and the gypsy retrovirus insulator to engineer precisely expressed transgenes. *Nat Genet* 40:476

68. Morin X, Daneman R, Zavortink M, Chia W (2001) A protein trap strategy to detect GFP-tagged proteins expressed from their endogenous loci in *Drosophila*. *Proc Natl Acad Sci U S A* 98:15050–15055

69. Clyne PJ, Brotman JS, Sweeney ST, Davis G (2003) Green fluorescent protein tagging *Drosophila* proteins at their native genomic loci with small P elements. *Genetics* 165:1433–1441

70. Busczak M, Paterno S, Lighthouse D et al (2007) The carnegie protein trap library: a versatile tool for *Drosophila* developmental studies. *Genetics* 175:1505–1531

71. Quiñones-Coello AT, Petrella LN, Ayers K et al (2007) Exploring strategies for protein trapping in *Drosophila*. *Genetics* 175:1089–1104

72. Lowe N, Rees JS, Roote J et al (2014) Analysis of the expression patterns, subcellular localisations and interaction partners of *Drosophila* proteins using a pigP protein trap library. *Development* 141:3994–4005

73. Venken KJT, Schulze KL, Haelterman NA et al (2011) MiMIC: a highly versatile transposon insertion resource for engineering *Drosophila melanogaster* genes. *Nat Methods* 8:737–743

74. Neumuller RA, Wirtz-Peitz F, Lee S et al (2012) Stringent analysis of gene function and protein-protein interactions using fluorescently tagged genes. *Genetics* 190:931–940

75. Pastor-Pareja JC, Xu T (2011) Shaping cells and organs in *Drosophila* by opposing roles of fat body-secreted collagen IV and perlecan. *Dev Cell* 21:245–256

76. Stavropoulos N, Young MW (2011) Insomniac and Cullin-3 regulate sleep and wakefulness in *Drosophila*. *Neuron* 72:964–976

77. Lim C, Chung BY, Pitman JL et al (2007) Clockwork orange encodes a transcriptional repressor important for circadian-clock amplitude in *Drosophila*. *Curr Biol* 17:1082–1089

78. Schulz JG, David G, Hassan BA (2009) A novel method for tissue-specific RNAi rescue in *Drosophila*. *Nucleic Acids Res* 37:e93

79. Kondo S, Booker M, Perrimon N (2009) Cross-species RNAi rescue platform in *Drosophila melanogaster*. *Genetics* 183:1165–1173

80. Langer CCH, Ejsmont RK, Schönauer C, Schnorrer F, Tomancak P (2010) In vivo RNAi rescue in *Drosophila melanogaster* with genomic transgenes from *Drosophila pseudoobscura*. *PLoS One* 5:e8928

81. Ejsmont RK, Sarov M, Winkler S, Lipinski KA, Tomancak P (2009) A toolkit for high-throughput, cross-species gene engineering in *Drosophila*. *Nat Methods* 6:435–437

82. Spletter ML, Barz C, Yeroslaviz A et al (2015) The RNA-binding protein Arrest (Bruno) regulates alternative splicing to enable myofibril maturation in *Drosophila* flight muscle. *EMBO Rep* 16:178–191

83. Parks A, Cook K, Belvin M et al (2004) Systematic generation of high-resolution deletion coverage of the *Drosophila melanogaster* genome. *Nat Genet* 36:288–292

84. Zhang X, Koolhaas WH, Schnorrer F (2014) A versatile two-step CRISPR-and RMCE-based strategy for efficient genome engineering in *Drosophila*. *G3 (Bethesda)* 4:2409–2418

85. Port F, Chen H-M, Lee T, Bullock SL (2014) Optimized CRISPR/Cas tools for efficient germline and somatic genome engineering in *Drosophila*. *Proc Natl Acad Sci* 111:E2967–E2976

86. Zambon AC, Gaj S, Ho I et al (2012) GO-Elite: a flexible solution for pathway and ontology over-representation. *Bioinformatics* 28:2209–2210

87. Eden E, Navon R, Steinfeld I, Lipson D, Yakhini Z (2009) GOrilla: a tool for discovery and visualization of enriched GO terms in ranked gene lists. *BMC Bioinformatics* 10:48

88. Supek F, Bošnjak M, Škunca N, Šmuc T (2011) REVIGO summarizes and visualizes long lists of gene ontology terms. *PLoS One* 6:e21800

89. Huang DW, Sherman BT, Tan Q et al (2007) DAVID Bioinformatics Resources: expanded annotation database and novel algorithms to better extract biology from large gene lists. *Nucleic Acids Res* 35:W169–W175

90. NCBI Resource Coordinators (2015) Database resources of the National Center for Biotechnology Information. *Nucleic Acids Res* 43:D6–D17

91. Vinayagam A, Hu Y, Kulkarni M et al (2013) Protein complex-based analysis framework for high-throughput data sets. *Sci Signal* 6:rs5

92. Schmidt EE, Pelz O, Buhlmann S, Kerr G, Horn T, Boutros M (2013) GenomeRNAi: a database for cell-based and in vivo RNAi phenotypes, 2013 update. *Nucleic Acids Res* 41:D1021–D1026

93. Shannon P, Markiel A, Ozier O et al (2003) Cytoscape: a software environment for integrated models of biomolecular interaction networks. *Genome Res* 13:2498–2504

94. Yu J, Pacifico S, Liu G, Finley RL (2008) DROID: the *Drosophila* Interactions Database, a comprehensive resource for annotated gene and protein interactions. *BMC Genomics* 9:461

95. Aranda B, Blankenburg H, Kerrien S et al (2011) PSICQUIC and PSISCORE: accessing and scoring molecular interactions. *Nat Methods* 8:528–529

96. Bader GD, Hogue CWV (2003) An automated method for finding molecular complexes in large protein interaction networks. *BMC Bioinformatics* 4:2

97. Wang J, Zhong J, Chen G et al (2015) ClusterViz: a Cytoscape APP for clustering analysis of biological network. *IEEE/ACM Trans Comput Biol Bioinform* 12(4):815–822

98. Maere S, Heymans K, Kuiper M (2005) BiNGO: a Cytoscape plugin to assess over-representation of gene ontology categories in biological networks. *Bioinformatics* 21:3448–3449

99. Bindea G, Mlecnik B, Hackl H et al (2009) ClueGO: a Cytoscape plug-in to decipher functionally grouped gene ontology and pathway annotation networks. *Bioinformatics* 25:1091–1093

100. Franceschini A, Szklarczyk D, Frankild S et al (2013) STRING v9.1: protein-protein interaction networks, with increased coverage and integration. *Nucleic Acids Res* 41:D808–D815

101. Green EW, Fedele G, Giorgini F, Kyriacou CP (2014) A *Drosophila* RNAi collection is subject to dominant phenotypic effects. *Nat Methods* 11:222–223

Chapter 7

Creating Heritable Mutations in *Drosophila* with CRISPR-Cas9

Fillip Port and Simon L. Bullock

Abstract

Reverse genetics—the creation of mutations in preselected target genes—has until recently been a bottleneck in many *Drosophila* projects. The advent of clustered, regularly interspaced, short palindromic repeat (CRISPR) genome engineering systems has transformed this situation. A short time after the *in vitro* demonstration of target site cleavage by the RNA-guided endonuclease CRISPR-associated nuclease 9 (Cas9) (Jinek et al., *Science* 337:816–821, 2012), hundreds of fly researchers are using CRISPR technology to generate loss-of-function mutant alleles in specific genes, as well as to create specific point mutations or tagged protein products. It appears that most target genes can be edited with remarkably high efficiency, with engineered strains often available a few weeks after conception of a project. Here, we provide a step-by-step protocol for creating loss-of-function mutations in *Drosophila* using transgenic Cas9 sources, which is based on optimized reagents and procedures that have been evaluated in our laboratory. We also provide guidance on extending this protocol to produce precise genomic alterations by homology-directed repair in the presence of a donor sequence. Additional information and updates are available from our website, www.crisprflydesign.org.

Key words CRISPR-Cas9, Genome engineering, *Drosophila*, gRNA design and cloning, Indel, Genotyping

1 Introduction

CRISPR genome editing systems take advantage of bacterial adaptive immune mechanisms that use RNA-guided endonucleases to recognize and cleave foreign DNA [1–3]. Although endonucleases with different properties have been used for CRISPR genome engineering, the prototypical Cas9 from *Streptococcus pyogenes* is still the most commonly used. The enzyme is directed to a specific site in the genome by a single chimeric guide RNA (gRNA) that typically includes a sequence match of 18–20 nucleotides (nts) to the target. The choice of a genomic target site is only constrained by the need for a flanking protospacer-adjacent motif (PAM), which for *S. pyogenes* Cas9 is NGG. The creation of a double-strand break (DSB) at the target site can result in imprecise repair by

non-homologous end joining (NHEJ), which often results in small insertions or deletions (indels) of between 1 and 15 bp that disrupt gene function. Alternatively, precise genome alterations can be created when homology-directed repair (HDR) occurs in the presence of experimentally provided donor DNA.

Several studies have described and evaluated strategies for editing the germline of *Drosophila melanogaster* with CRISPR-Cas9 (reviewed in refs. 4, 5). The efficiency with which mutagenesis occurs means that classical methods for inducing mutations at specific sites, such as P-element excision, have quickly fallen out of favor. The provision of Cas9 by a stably integrated transgene simplifies genome engineering protocols and consistently produces high rates of mutagenesis. Injection of an expression plasmid into embryos represents a rapid and convenient way of delivering the gRNA to the germline. Alternatively, the gRNA can be expressed from a stable transgene, with the two CRISPR components brought together by a genetic cross (see Subheadings 3.5.1 and 3.5.2 for a comparison of these methods).

Here, we focus on the use of transgenic Cas9 sources to generate loss-of-function indels in target genes. An overview of the procedure, including approximate timings for different stages, is presented in Fig. 1. Our protocols can be extended to produce precise genome alterations by HDR of Cas9-induced DSBs. Guidance on how to achieve these precise modifications is given in Subheading 4 to this chapter.

2 Materials

2.1 Cloning of gRNA Expression Plasmids

1. Empty gRNA expression plasmids: pCFD1 (Addgene 49408), pCFD2 (Addgene 49409), pCFD3 (Addgene 49410), or pCFD4 (Addgene 49411) (Fig. 2a).
2. Custom-designed oligonucleotides (desalted, dried).
3. T4 DNA ligase (400 U/μl) with 10× T4 DNA ligase buffer (New England Biolabs (NEB) cat. no. M0202S).
4. T4 Polynucleotide Kinase (10U/μl; NEB cat. no. M0201S).
5. BbsI restriction enzyme (10U/μl) with compatible reaction buffer (NEB cat. no. R0539S).
6. For cloning into pCFD4: Q5 hot start 2× master mix (NEB cat. no. M0494S) or similar.
7. Gel extraction kit (Qiagen cat. no. 28704 or similar).
8. For cloning into pCFD4: Gibson assembly master mix (NEB cat. no. M5510A).
9. Bacterial plates and liquid media containing Ampicillin.

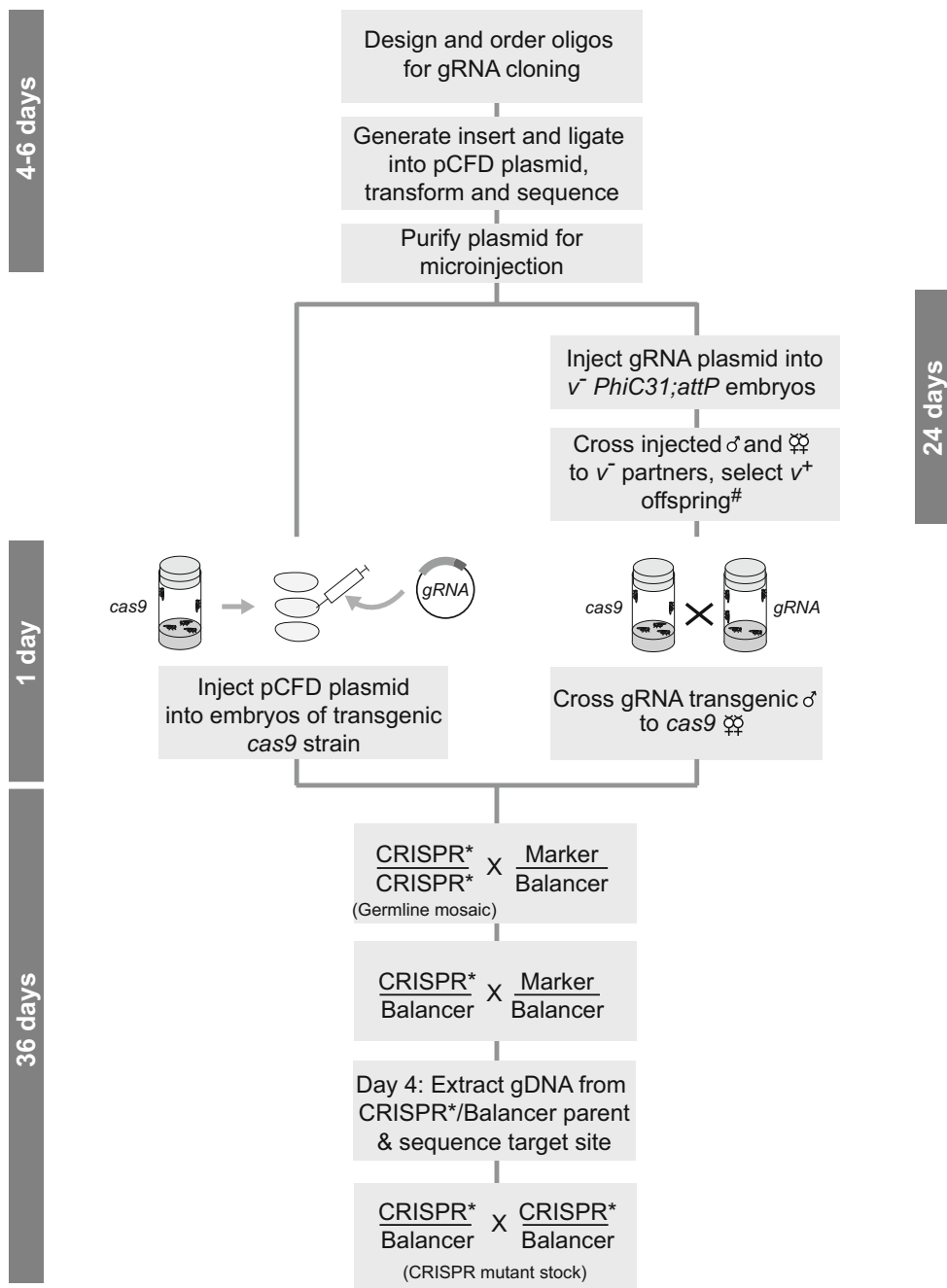


Fig. 1 Overview of workflow to produce loss-of-function mutations in the germline using CRISPR-Cas9. Approximate duration of the different phases of one experiment is indicated on the side. Generation of a transgenic gRNA line requires two addition generations. [#], in parallel to crossing transgenic gRNA flies to cas9 partners, a stable transgenic gRNA stock should be established for future use. gDNA genomic DNA. This workflow can be extended to produce precise mutations by HDR (see text for details)

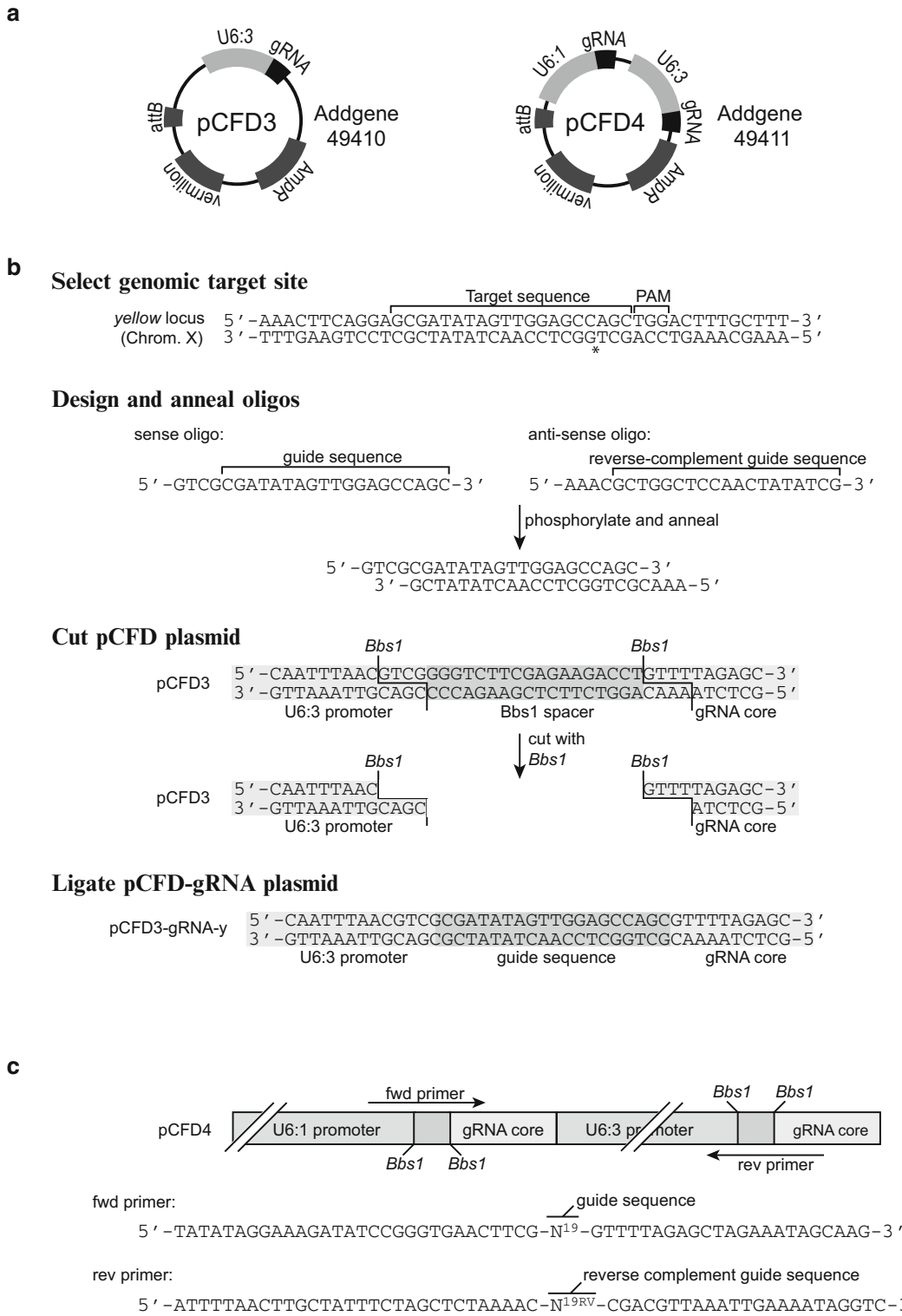


Fig. 2 Cloning of gRNA expression plasmids with pCFD plasmids. (a) Overview of most popular pCFD plasmids. Plasmid sequences are available at www.crisprflydesign.org. pCFD plasmids with promoters that result in less

2.2 gRNA Plasmid Purification

1. PCR purification kit (Qiagen cat. no. 28104 or similar).

2.3 Transgenic Fly Lines

1. Cas9 lines are available from the Bloomington *Drosophila* Stock Center, the fly stock center of the National Institute of Genetics (NIG) or by request from the lab that generated the line.
2. Balancer lines for the chromosomes of interest and (optional) PhiC31/attP lines for integrating gRNA transgenes (e.g. Bloomington stocks (BL)25709 and BL25710). A wide range of suitable stocks is available from the Bloomington *Drosophila* Stock Center.

2.4 Microinjection of gRNA Plasmids

1. Refer to [6] for a detailed description of the materials required for *Drosophila* microinjections. Alternatively, microinjections can be outsourced to commercial companies.

2.5 Detection of CRISPR-Induced Mutations by Direct Sequencing

1. Microlysis-Plus DNA extraction solution (Microzone cat. no. 2MLP-100) or similar.
2. Custom-designed oligonucleotides for use as PCR primers.
3. Q5 hot start 2× master mix or similar.
4. Qiagen PCR purification kit or similar.

3 Methods

3.1 Design of gRNAs

The gRNA consists of a variable sequence (termed the spacer or guide sequence), which is typically 20 nt long, that determines where in the genome the Cas9 nuclease will bind and cut. This sequence is followed by an invariant 80-nt “core” sequence (a fusion of *S. pyogenes* crRNA and tracrRNA), that interacts with the Cas9 enzyme. The target site in the genome must be directly followed by a PAM, although the sequence corresponding to the PAM is not included in the gRNA (Fig. 2b). gRNAs are typically transcribed from RNA polymerase III-dependent promoters of U6 snRNA genes, which require a 5' G nucleotide for optimal transcriptional efficiency. Since gRNAs usually tolerate truncations and

◀ **Fig. 2** (continued) efficient gene targeting (at least with transgenic gRNAs) are not shown. These plasmids (pCFD1, *U6:1* promoter; and pCFD2, *U6:2* promoter [11]) contain the same backbone as pCFD3 but require different oligonucleotide designs for cloning of the guide sequence. (b) Cloning of a single gRNA plasmid with pCFD3. An example is shown in which a gRNA plasmid targeting the *yellow* gene is constructed. The guide sequence is introduced via two annealed, phosphorylated oligos that are ligated into the plasmid backbone. *, Cas9 cut site. (c) Cloning of two gRNAs with pCFD4. Specific guide sequences are introduced through the fwd and rev primers, which are used for PCR with pCFD4 as the template. The PCR product is then cloned into a BbsI-digested pCFD4 backbone using Gibson assembly

mismatches at the 5' end [7, 8], the 5' G can be introduced even if the genomic target site does not start with a G. We therefore choose genomic target sites irrespective of their 5' nucleotide. If the first position of the genomic target site is not a G, we use 19 nt of complementary to the target site and a 5' mismatched G. One exception is when a target site has a G at position 2, in which case we use this G as the first nucleotide of a 19 nt guide sequence. Apart from these general design principles, the following issues should also be considered when choosing a target site.

3.1.1 Position

Choice of target site position depends on the genomic alteration one wishes to produce. If the goal is to create a null mutation in a protein-coding gene, generation of an indel that disrupts the reading frame is usually the most straightforward solution. To that end, the gRNA should target a common coding exon at the 5' end of the gene. We advise against removing the first translational initiation codon, as this can result in translation from a downstream AUG and a polypeptide that is merely truncated at the N-terminus. We favor generating out-of frame indels shortly after the initiation codon, which will result in a short in-frame peptide followed by nonsense protein sequence and a stop codon from another reading frame.

Null mutations can also be made using a combination of two gRNAs that target the 5' and 3' ends of the gene, thereby creating a large deletion (the pCFD4 dual gRNA plasmid facilitates this process) (Fig. 2a,c; Subheading 3.2.2). Such events often occur at a lower frequency than small indels induced by single gRNAs. This is presumably because large deletions require two efficient gRNAs and the formation of small indels at individual target sites competes with deletion of the intervening sequence. However, the reduced efficiency of this approach is often offset by the ease with which large deletions can be identified by diagnostic PCR. To create precise knock-ins using CRISPR-induced HDR, the gRNA should target a site at or close to the insertion site. While some offset is generally tolerated, the efficiency of the process decreases with increasing distance of the insertion site from the gRNA target site [9].

3.1.2 Efficiency

Several studies have attempted to define sequence features of guide sequences that determine gRNA activity, but there has been surprisingly little overlap in their conclusions. As a result the available online tools that predict gRNA efficiency (see Note 1) often produce a different ranking for the same sets of gRNAs. While it is expected that these algorithms will improve in the future, we currently place little emphasis on their output when designing gRNAs. One study reported that a high GC content in the 6 nt at the 3' end of the guide sequence substantially increases mutagenesis rates when gRNA plasmids are injected into transgenic Cas9

flies [8] (see Note 2). We did not observe the same trend when gRNAs were provided from transgenes [10], which may reflect the increased efficiency of DSB induction with this method. One factor that certainly has the potential to affect cleavage efficiency is polymorphic sequence between the strain being targeted and the genomic reference used for the gRNA design. In our experience, the frequency of synonymous single nucleotide differences to the Flybase reference genome makes pre-sequencing the target sequence in experimental strains worthwhile (see Note 3).

3.1.3 Specificity

Generating a mutation only at the intended genomic locus requires the choice of a unique gRNA target site. However, off-target prediction is non-trivial as Cas9/gRNA complexes can tolerate some RNA:DNA mismatches. Several groups have developed algorithms to predict potential gRNA off-target sites in the *Drosophila* genome and the associated online tools should be used to select gRNAs that are likely to have the highest specificity (see Note 1). Using two independent gRNAs to target the same gene is an effective way of controlling for the contribution of off-target mutations to a mutant phenotype, as is genetic backcrossing and rescue experiments using a transgene expressing a wild type copy of the gene.

3.2 Cloning of gRNA Expression Plasmids

3.2.1 Single gRNA Plasmids (pCFD1–3)

To produce gRNA expression plasmids, the sequence matching the genomic target site is cloned 5' to the gRNA core sequence. We have generated a series of vectors that simplify this process for mutagenesis in *Drosophila* [11].

1. Order desalted, dried sense and antisense oligonucleotides suitable for the plasmid of choice (Fig. 2b, c).
2. Resuspend the oligos in dH₂O to a concentration of 100 μM. Mix 1 μl of sense oligo, 1 μl of antisense oligo, 1 μl 10× T4 ligation buffer, 6.5 μl dH₂O, and 0.5 μl T4 polynucleotide kinase.
3. Phosphorylate and anneal the oligos in a thermocycler using the following conditions: 37 °C for 30 min, 95 °C for 5 min, then ramp temperature to 20 °C at a speed of 0.1 °C/s. Dilute the reaction 1:200 in dH₂O.
4. Digest pCFD plasmid with BbsI restriction enzyme and dephosphorylate with calf intestinal phosphatase according to the enzyme manufacturers' recommendations. Purify the digested vector from a 1% agarose gel and elute in dH₂O (see Note 4).
5. Set up the following ligation reaction: 50 ng digested pCFD plasmid, 1 μl diluted oligo mix, 1.5 μl 10× T4 ligation buffer, 1 μl T4 DNA ligase, dH₂O to a total reaction volume of 15 μl.
6. Ligate DNA for 30 min at room temperature (see Note 5).

7. Transform plasmids into competent bacteria and spread on bacterial plates containing Ampicillin.
8. Make mini-preps from clones and verify successful guide sequence cloning by Sanger sequencing using primer 5'-ACG TTTTATAACTTATGCCCTAAG-3' (pCFD3), 5'-TTATAG TCAATAATCGAACTG-3' (pCFD2), or 5'-TACAGACACA GCGCGTACGTCCCTT-3' (pCFD1) (see Note 6).

3.2.2 Double gRNA Plasmid (pCFD4)

1. Order desalted and dried forward and reverse primers to generate a PCR product containing the guide sequences of both gRNAs and complementarity to the plasmid backbone (Fig. 2c).
2. Perform a 50 μ l PCR reaction using pCFD4 plasmid as a template, forward oligo, reverse oligo, and a high-fidelity DNA polymerase (see Note 7). Extract the PCR product from a 1% agarose gel (expected size 600 bp) and resuspend in dH₂O.
3. Digest pCFD4 plasmid with BbsI restriction enzyme, dephosphorylate and gel purify the digested vector (see Subheading 3.2.1, step 4; see Note 5).
4. Assemble the PCR product and the digested vector using a Gibson assembly master mix according to the manufacturer's instructions (see Note 8).
5. Follow steps 7 and 8 of Subheading 3.2.1 above, with cloning verified by Sanger sequencing using fwd primer 5'-TACAGA CACAGCGCGTACGTCCCTT-3' and rev primer 5'-GCCGAG CACAATTGTCTAGAATGC-3'.

3.3 gRNA Plasmid Purification

gRNA plasmid DNA must be subjected to further purification before injection, otherwise the survival of embryos can be compromised. We use the Qiagen PCR purification kit for this purpose. We follow the manufacturer's instructions, except the spin to remove residual wash buffer is increased to 3 min to remove traces of ethanol from the column before elution. Following a 1 min incubation with 30 μ l of sterile dH₂O on the column, eluted DNA is collected by centrifugation and concentration measured with a spectrophotometer. A₂₆₀/A₂₈₀ should be between 1.8 and 1.9.

3.4 Choosing Transgenic *cas9* Lines

Several labs have created transgenic *cas9* lines. For a detailed experimental comparison of these lines, please refer to [10]. Transgenic strains useful for creating mutations in the germline can be broadly classified as having ubiquitous or germline-restricted *cas9* expression (Table 1) and high, intermediate, or low activity [10]. Germline-restricted *cas9* expression is desirable when biallelic gene disruption in somatic tissue is expected to interfere with viability of the fly. However, lines with ubiquitous expression can be used to create heritable mutations in non-essential genes. Lines with

Table 1
Summary of cas9 lines with intermediate to high activity

Name ^a	Chromosomal insertion site of cas9	Stock center number	Widespread activity	Germline-restricted activity
act-cas9	attP-ZH2a (X)	BL54590	+	-
vas-cas9	attP-VK00037 (2L)	BL56552	+	-
vas-cas9	attP-VK00027 (3R)	BL51324	+	-
vas-cas9	attP-ZH2a (X)	BL51323	+	-
vas-cas9	attP-ZH2a (X)	BL52669	+	-
nosG4VP16 UAS-cas9 ^b	attP2 (3L)	BL54593	+	-
nos-cas9	attP-ZH2a (X)	BL54591	-	+
nos-cas9	attP2 (3L)	N/A ^c	-	+
nos-cas9	attP40 (2L)	N/A ^c	-	+
nos-cas9	attP40 (2L)	NIG CAS-0001	-	+

Lines differ in codon usage, nuclear localization signals, regulatory sequences, and chromosomal insertion site. . See ref. 10 for information on relative activities of the lines, which differ significantly, as well as for original references and information on additional lines with lower activity

^aact-, vas- and nos- refer to regulatory sequences from the *actin5C*, *vasa*, and *nanos* genes, respectively; G4VP16 refers to sequences encoding Gal4VP16 transcriptional activation domain

^bThis line gives restricted germline targeting with a subset of gRNAs, presumably due to relatively little Cas9 activity in the soma compared to the germline

^cNot yet available in a stock center; contact corresponding authors of ref. 20 (attP2 and attP40 lines are referred to as TH00787.N and TH00788.N, respectively)

ubiquitous Cas9 activity have the added advantage of potentially revealing mutant phenotypes in the first generation, in particular in combination with transgenic gRNAs. While high mutagenic activity of cas9 lines is desirable for most applications, lines with lower activity can be useful in some cases, for example when biallelic mutations in the germline have a strong impact on fertility. Finally, the chromosome on which the cas9 transgene is inserted, as well as any fluorescent markers for landing sites, should be taken into account with regard to subsequent experiments planned (see Note 9).

3.5 gRNA Delivery

Injection of in vitro transcribed gRNA can induce DSBs in the presence of Cas9 [12]. However, we and many other groups favor DNA-based gRNA delivery, either by direct injection of pCFD1–4 into cas9 strains or the use of these plasmids to create stable gRNA transgenic strains that are then crossed to cas9 strains (we refer to this latter method as CRISPR with independent transgenes, or CRISPR-it [10]). DNA-based gRNA delivery methods are technically straightforward, result in efficient mutagenesis and allow part of the workflow to be outsourced to commercial *Drosophila* injection services if desired.

3.5.1 Microinjection of gRNA Plasmids

Injecting gRNA plasmids into transgenic *cas9* embryos often results in efficient induction of mutations at the gRNA target site. Ren et al. [8] reported that adults developing from injected *cas9* embryos transmitted loss-of-function indel mutations to between 10 and 100% of their offspring, and our results to date are consistent with these figures. The prime advantage of this method is speed, as it does not require the generation of transgenic lines expressing gRNA. However, relying on microinjection means that only a fraction of injected animals will give rise to mutant offspring, increasing the average number of flies that need to be screened to find the desired mutation.

Purified gRNA plasmids are microinjected at the posterior pole (i.e. in the vicinity of the germ plasm) using standard methods for DNA transformation [6].

1. Set up egg-laying cages with the transgenic *cas9* strain of choice.
2. Inject purified gRNA plasmid at a concentration of 100 ng/μl at the posterior pole of 100–200 dessicated, dechorionated embryos 15 min to 1 h after egg-laying. For convenience, perform injections at room temperature. Optional: Co-inject a donor template for HDR (see Note 10).
3. Incubate injected embryos at 18 °C until larvae hatch (approx. 48 h) and then transfer first instar larvae to a culture vial and rear injected animals to adulthood at 25 °C (see Note 11).
4. Set up individual crosses of males and virgin females (potential founders) with a balancer line appropriate for the chromosome of the targeted gene (see Note 12).
5. Collect offspring that potentially harbor a CRISPR-induced mutation over the balancer chromosome (CRISPR*/balancer), and cross individuals to the balancer line so that stocks can be established if necessary.
6. Allow crosses to lay eggs for a few days, then collect CRISPR*/balancer adults and screen for the presence of a desirable CRISPR-induced mutation (see Subheading 3.6).
7. Crosses that contain CRISPR mutations of interest should be established as balanced stocks, with other crosses discarded (see Note 13).

3.5.2 Use of Transgenic gRNA Lines

This approach requires the generation of a transgenic gRNA fly line, which takes approximately one month (although the amount of hands-on time is significantly less than this and much of the work can be outsourced to a commercial injection service if desired). However, this method has notable advantages, which make it worth considering if the time until a mutant is available is not the most important consideration. First, gRNAs from a transgenic source mediate the most efficient and robust gene targeting.

We have found that the majority of transgenic gRNAs are active [10] and that often all offspring of flies expressing *cas9* and gRNA transgenes inherit mutant alleles. Therefore, this method can reduce screening efforts for desired mutations to an absolute minimum. The increased efficiency of DSB induction can be particularly useful for more challenging applications such as the introduction of precise changes by HDR without the use of selectable markers [10] or targeting genes in heterochromatin, which might be less accessible to the Cas9-gRNA complex. Second, transgenic gRNA lines allow controlled gene disruption outside the germline [11, 13], an application that is not possible with microinjected gRNAs.

1. Set up egg-laying cages with the PhiC31/attP line of choice (see Note 14). This line must not contain the selectable marker present on the gRNA plasmid (see Note 15).
2. Inject purified gRNA plasmid at a concentration of 150 ng/μl at the posterior pole of 100 dessicated, dechorionated embryos 15 min to 1 h after egg-laying. Collect larvae and rear as described in Subheading 3.5.1, step 3.
3. Set up individual crosses of adults and an appropriate balancer line, select transgenic offspring using the selectable marker and establish balanced stocks.
4. Cross transgenic gRNA male flies to females of the *cas9* line of choice. Optional: cross transgenic gRNA males to *act-cas9* females to check for gRNA activity (see Note 16). Optional: collect embryos from *gRNA* × *cas9* cross in an egg-laying cage and inject at the posterior pole with a donor template for HDR (see Note 10).
5. Cross individual male *cas9/gRNA* double transgenic flies (potential founders) to a balancer line appropriate for the chromosome of the target gene.
6. Screen for the presence of the desired mutations and balance validated CRISPR alleles as described in Subheading 3.5.1, steps 6 and 7.

3.6 Identification of CRISPR Mutant Flies

The strategy used to identify flies with the desired mutation depends on the molecular nature of the lesion and the efficiency with which it is induced. The most direct way to detect small indel mutations and point mutations introduced by HDR is by direct Sanger sequencing of PCR products from genomic DNA that include the target site (Subheading 3.6.1). This is the method we favor for almost all of our experiments. For rarer events it may be cost- and time-effective to first screen for the presence of sequence changes using an alternative method that detects heteroduplex DNA, such as the T7 endonuclease 1 assay (see www.crisprfly-design.org for a protocol). Larger deletions, such as those caused

by the concerted action of two gRNAs, can be detected using standard genomic PCR with primers flanking the missing sequence. Sanger sequencing can then be used to define the breakpoints. Diagnostic genomic PCRs are also the method of choice to detect targeted integration of donor DNA. In this case PCR primers outside both homology arms should be included to test for integration at the target locus and the absence of unwanted sequences from the donor plasmid backbone. Sanger sequencing should then be used to verify precise integration. Here, we focus on the identification of indels and point mutations by direct sequencing.

3.6.1 Direct Sequencing

Flies heterozygous for a mutation will yield a sequencing trace that contains an overlay of the sequence of both alleles.

1. Extract genomic DNA from individual candidate flies by crushing with a pipette tip in 10 µl of Microlysis-Plus solution.
2. Perform the following steps in a thermocycler: 65 °C, 15 min; 96 °C, 2 min; 65 °C, 4 min; 96 °C, 1 min; 65 °C, 1 min; 96 °C, 30 s; 20 °C, hold.
3. Amplify the target sequence by PCR using 1 µl of the solution produced from **step 2** and primers flanking the target site. Use a high fidelity DNA polymerase (e.g. Q5 hot start) according to the manufacturer's instruction. The size of the PCR product should ideally be in the range of 300–800 bp. Check that the procedure gives a single band by agarose gel electrophoresis of 1/5th of the PCR reaction.
4. Perform PCR purification of the product.
5. Submit PCR product for Sanger sequencing using the forward PCR primer.
6. Inspect the sequencing trace manually. Mutations at the gRNA target site will result in double peaks appearing in the chromatogram [11]. Software such as TIDE (<http://tide.nki.nl>) [14] can also identify the nature of the indel, provided a sequencing file of the wild type allele (e.g. from the balancer chromosome) is available. However, the conclusions should be checked manually. Ambiguous mutant sequences can be confirmed using the reverse PCR primer in an additional sequencing reaction.

4 Notes

1. There are many online tools that can be used to design gRNAs, with new ones emerging at a rapid pace. Most tools select potential gRNAs from a submitted sequence or genome identifier, predict potential off-target sites in the genome or transcriptome, and estimate gRNA efficiency. In our view, it is too early to judge which tools perform particularly well for

gRNA design in *Drosophila*. Tools developed by groups with a *Drosophila* background include: <http://e-crisp.org>, <http://www.flyrnai.org/crispr2/> and <http://tools.flycrispr.molbio.wisc.edu/targetFinder/>.

2. A G nucleotide as the last nucleotide of the guide sequence (genomic target: N₁₉-G-NGG) is one of the few features of active gRNAs that have been identified in several studies [8, 15, 16], although this feature is not essential for efficient mutagenesis with gRNA transgenes [11].
3. Use the same protocol as in Subheading 3.6.1. Pre-sequencing the strain to be targeted also helps establish optimal PCR conditions for screening for CRISPR-induced mutations at a later stage.
4. The user has different options for single gRNA expression plasmids. We have shown that when the gRNA is provided from a transgene, the gene editing efficiency is strongly influenced by the choice of U6 promoter [11]. The *U6:3* promoter in pCFD3 gives the highest rates of mutagenesis, the *U6:2* promoter used in pCFD2 is least active, and the *U6:1* promoter on pCFD1 has intermediate activity. It is not known if the choice of U6 promoter is significant when gRNAs are produced from an injected plasmid.
5. Cut, dephosphorylated, and purified pCFD plasmid should be subjected to a control ligation without the addition of an insert. Preparations that result in no or few colonies can be stored at -20 °C and used for multiple rounds of cloning.
6. If the enrichment of colonies from an insert ligation over the no-insert control ligation is strong, it should be sufficient to process two colonies per insert. In the vast majority of cases, the sequence of the insert is correct.
7. We typically use 61 °C annealing temperature and 32 cycles with the NEB Q5 hot start 2x PCR master mix. If there is no product or nonspecific products with these reaction conditions, the annealing temperature can be decreased or increased by a few degrees.
8. For the successful transformation of plasmids prepared by Gibson assembly, it is important not to add too much Gibson assembly master mix to the competent cells. Different preparations of chemically competent cells can differ in their tolerance to the Gibson assembly mix, so users should determine the optimal amount that can be added to their cells. We add 2 µl of master mix to 70 µl of chemically competent cells (Alpha-Select Silver Efficiency (Bioline cat. no. BIO-85026)).
9. In addition to lines expressing wild type *cas9*, lines expressing mutant forms of *cas9* (Cas9 nickase, Fok1-dCas9), which require dimerization to generate double-strand breaks, are also

available from the Bloomington *Drosophila* Stock Center (BL58983, BL58984, BL58985, and BL58986). These alternative *cas9* systems have been shown in mammalian cells to have higher specificity than wild type *cas9* [17–19]. However, their overall lower activity ([11]; unpublished observations) and more restrictive target site requirements limits their appeal for *Drosophila* experiments.

10. While donor templates for introducing small tags and single nucleotide changes can be single-stranded oligonucleotides, knock-in of longer sequences requires the use of plasmid-based donors (*see* refs. 10, 11 for recommended donor DNA concentrations). We usually use 60 nt homology arms for oligo donors and 1–1.5 kb homology arms for plasmid donors, which are injected in a circular form. Homology arms for plasmid donors are amplified from the *cas9* strain to be targeted. All donors should be designed such that once integrated they are no longer recognized by the respective gRNA (e.g. by introducing a mutation(s) in the PAM sequence or 3' guide sequence). All sequence changes should be included in the same homology arm relative to the Cas9 cleavage site as it appears that only a single arm from the donor is included in the repaired allele.
11. Injection of gRNA plasmids into *cas9* transgenic embryos typically results in a relatively low hatch rate (typically 30–50 % of embryos).
12. Screening the offspring of approximately 10 potential founders is normally sufficient to recover multiple useful mutations (e.g. [8, 11]). Screening for mutations in the offspring can be scaled to a 96-well plate format if desirable. For genome edits which can be easily identified by diagnostic PCR (e.g. deletions, larger knock-ins), it can be worthwhile to screen the G₀ flies that develop from injected embryos for the presence of the desired modification. To that end, collect G₀ flies once an adequate number of their larval offspring is visible in the vial and prepare genomic DNA, followed by PCR (as described in Subheadings 3.6.1, steps 1–3). Offspring from flies that test positive for the desired sequence change can then be prioritized for downstream screening.
13. Crosses should be designed such that the *cas9* transgene and ideally other chromosomes that do not harbor the target locus are removed. Cas9 lines which have the transgene integrated on the X chromosome (Table 1) facilitate *cas9* removal. Where available, CRISPR mutant strains generated from different parents should be maintained. These independent CRISPR alleles will help validate the specificity of observed phenotypes (*see* also Subheading 3.1.3).
14. We have validated attP40 on the second chromosome and attP2 on the third chromosome as suitable landing sites for

gRNA transgenes. While transgenes inserted at both of these sites give rise to high levels of mutagenesis, gRNAs integrated at attP40 have the highest activity.

15. The original series of pCFD gRNA vectors uses the eye pigmentation gene *vermillion* as the transformation marker. For these plasmids, lines BL25709 and BL25710 from the Bloomington *Drosophila* Stock Center are suitable acceptor lines. We recently deposited pCFD3 and pCFD4 vectors containing the fluorescent eye marker 3xP3-RFP at the plasmid repository Addgene, which can be integrated using RFP-negative PhiC31/attP strains. The *white*⁺ minigene is not straightforward to use as a marker for pCFD plasmids due to the presence of multiple BbsI sites.
16. Generating *act-cas9/gRNA* double transgenic flies can be helpful to establish if a gRNA transgene is active. Active gRNAs are expected to give rise to phenotypes associated with loss-of-function mutations of the target gene. When phenotypes are unknown or not visible, *act-cas9/gRNA* flies can be used to establish effective mutagenesis by a T7 endonuclease 1 assay (see Subheading 3.6), diagnostic PCR or PCR followed by Sanger sequencing.

Acknowledgements

We are grateful to Nadine Muschalik and Mohammad Mofatteh for discussions and comments on the manuscript, David Stern for providing pCFD4-3xP3RFP, Hui-Min Chen, Tzumin Lee, Kelly Beumer and other members of the *Drosophila* CRISPR community for sharing results. The work was supported by MRC Project number MC_U105178790.

References

1. Jinek M et al (2012) A programmable dual-RNA-guided DNA endonuclease in adaptive bacterial immunity. *Science* 337:816–821
2. Doudna JA, Charpentier E (2014) The new frontier of genome engineering with CRISPR-Cas9. *Science*. doi:[10.1126/science.1258096](https://doi.org/10.1126/science.1258096)
3. Hsu PD, Lander ES, Zhang F (2014) Development and applications of CRISPR-Cas9 for genome engineering. *Cell* 157:1262–1278
4. Xu J et al (2015) A toolkit of CRISPR-based genome editing systems in *Drosophila*. *J Genet Genomics* 42:141–149
5. Bassett AR, Liu J-L (2014) CRISPR/Cas9 and genome editing in *Drosophila*. *J Genet Genomics* 41:7–19
6. Bachmann A, Knust E (2008) The use of P-element transposons to generate transgenic flies. *Methods Mol Biol* 420:61–77
7. Fu Y, Sander JD, Reyon D, Cascio VM, Joung JK (2014) Improving CRISPR-Cas nuclease specificity using truncated guide RNAs. *Nat Biotechnol*. doi:[10.1038/nbt.2808](https://doi.org/10.1038/nbt.2808)
8. Ren X et al (2014) Enhanced specificity and efficiency of the CRISPR/Cas9 system with optimized sgRNA parameters in *Drosophila*. *Cell Rep* 9:1151–1162
9. Beumer KJ, Trautman JK, Mukherjee K, Carroll D (2013) Donor DNA utilization during gene targeting with zinc-finger nucleases. *G3 (Bethesda)*. doi:[10.1534/g3.112.005439](https://doi.org/10.1534/g3.112.005439)

10. Port F, Muschalik N, Bullock SL (2015) Systematic evaluation of *Drosophila* CRISPR tools reveals safe and robust alternatives to autonomous gene drives in basic research. *G3* (Bethesda) 5:1493–1502
11. Port F, Chen H-M, Lee T, Bullock SL (2014) Optimized CRISPR/Cas tools for efficient germline and somatic genome engineering in *Drosophila*. *Proc Natl Acad Sci U S A* 111:E2967–E2976
12. Bassett AR, Tibbit C, Ponting CP, Liu J-L (2013) Highly efficient targeted mutagenesis of *Drosophila* with the CRISPR/Cas9 system. *Cell Rep* 4:220–228
13. Xue Z et al (2014) CRISPR/Cas9 mediates efficient conditional mutagenesis in *Drosophila*. *G3* (Bethesda) 4:2167–2173
14. Brinkman EK, Chen T, Amendola M, van Steensel B (2014) Easy quantitative assessment of genome editing by sequence trace decomposition. *Nucleic Acids Res* 42:e168
15. Farboud B, Meyer BJ (2015) Dramatic enhancement of genome editing by CRISPR/Cas9 through improved guide RNA design. *Genetics* 199:959–971
16. Doench JG et al (2014) Rational design of highly active sgRNAs for CRISPR-Cas9-mediated gene inactivation. *Nat Biotechnol* 32:1262–1267
17. Ran FA et al (2013) Double nicking by RNA-guided CRISPR Cas9 for enhanced genome editing specificity. *Cell* 154:1380–1389
18. Guilinger JP, Thompson DB, Liu DR (2014) Fusion of catalytically inactive Cas9 to FokI nuclease improves the specificity of genome modification. *Nat Biotechnol* 32:577–582
19. Tsai SQ et al (2014) Dimeric CRISPR RNA-guided FokI nucleases for highly specific genome editing. *Nat Biotechnol* 32:569–576
20. Ren X et al (2013) Optimized gene editing technology for *Drosophila melanogaster* using germ line-specific Cas9. *Proc Natl Acad Sci U S A* 110:19012–19017

Chapter 8

Performing Chromophore-Assisted Laser Inactivation in *Drosophila* Embryos Using GFP

Anne Pélissier-Monier, Bénédicte Sanson, and Bruno Monier

Abstract

Chromophore-assisted laser inactivation (CALI) is an optogenetic technique in which light-induced release of reactive oxygen species triggers acute inactivation of a protein of interest, with high spatial and temporal resolution. At its simplest, selective protein inactivation can be achieved via the genetic fusion of the protein to a photosensitizer such as EGFP, and using standard optical setups such as laser scanning confocal microscopes. Although use of CALI in *Drosophila* is relatively recent, this technique can be a powerful complement to developmental genetics, especially *in vivo* as it allows visualization of the immediate consequences of local protein inactivation when coupled to time-lapse microscopy analysis. In addition to providing examples of protocols, this chapter is intended as a conceptual framework to support the rational design of CALI experiments.

Key words Chromophore-assisted laser inactivation (CALI), Conditional protein inactivation, Genetic photosensitizer, Green fluorescent protein (GFP), Optogenetics, *Drosophila*, Live imaging

1 Introduction

Perturbation of key genes or gene products is a necessary step toward the mechanistic understanding of cellular and developmental processes. An increasing number of strategies have been developed, ranging from classical genetics to RNA interference, but inactivation may take hours and it may be difficult to precisely target the cells of interest. Moreover, such strategies do not allow one to untangle the relative contribution of distinct subcellular pools of a given protein within a cell of interest. This led in the late 1980s to the development of a new optogenetic technique called “chromophore-assisted laser inactivation”, or CALI, whose aim was to provide acute protein inactivation by light [1]. The effect of CALI is in principle reversible, and should be rescued when newly synthesized proteins or non-inactivated proteins elsewhere move in the targeted area. With spatial and temporal resolutions of respectively about 1 μm and hundreds of milliseconds, CALI is appropriate for the study of fast

cellular processes. Because of these properties, CALI can be used to uncouple the involvement of a protein of interest in sequential temporal events, as exemplified by the analysis of α -actinin [2]. Because α -actinin is necessary for focal adhesion formation in the first place, a role in later stages of focal adhesion could not be assessed using conventional loss-of-function methods. Rajfur and colleagues selectively destroyed α -actinin by CALI once focal adhesions had formed, proving that α -actinin bridges β -integrin to polymerized actin in those structures [2]. CALI can also be used to discriminate between contributions of distinct subcellular pools to a given cellular process. For instance, non-muscle myosin II plays a role both in cytokinesis during cell division and in a supracellular cable-like structure that inhibits cell mixing at the boundary between cell populations with distinct identities [3]. CALI targeting of the cable-like structure in dividing boundary cells did not affect division. The targeted daughter cells, however, could now cross the boundary and invade the adjacent compartment, a behavior not seen in wild type. This experiment demonstrated a role for the Myosin II supracellular cable in cell sorting [3].

The principle of CALI consists in bringing into close vicinity a photosensitizer (historically the Malachite Green non-organic dye) and a protein of interest. Upon intense illumination, the chromophore of the photosensitizer reacts with oxygen in the environment and emits reactive oxygen species (ROS), most commonly singlet oxygen (${}^1\text{O}_2$) [4]. This reaction is concomitant yet independent of photobleaching [5]. Protein inactivation is a consequence of ${}^1\text{O}_2$ (and, to some extent, of other ROS) toxicity which causes protein oxidization on specific residues (His, Tyr, Trp, Met, and Cys), leading to intra- and intermolecular crosslinks or aggregates and, in some cases, to fragmentation of the peptide backbone (Fig. 1a) [6]. Although highly noxious, ROS have a very short half-life and a range of action usually estimated around 5–6 nm, limiting the nonspecific inactivation of molecules that are not directly in contact with the source of ROS [4]. To illustrate this, western blot analysis has shown that selective inactivation of the Regulatory Light Chain (MRLC) subunit in the Myosin II macromolecular complex can be performed without affecting the Heavy Chain (MHC), its direct interactor [3]. The consequences of CALI are therefore distinct of that of femtosecond pulsed lasers that physically can cut structures (such as the actomyosin cytoskeleton), but cannot specifically inactivate a given protein (such as MRLC) within the structure [7].

In pioneer CALI experiments, the photosensitizer was coupled to a specific non-blocking antibody and delivered by microinjection to cells in culture (Fig. 1b) [1, 10]. Because of the difficulty in generating non-blocking antibodies, an alternative method was developed in which the protein of interest was tagged with a short motif. Samples were then incubated with the photosensitizer

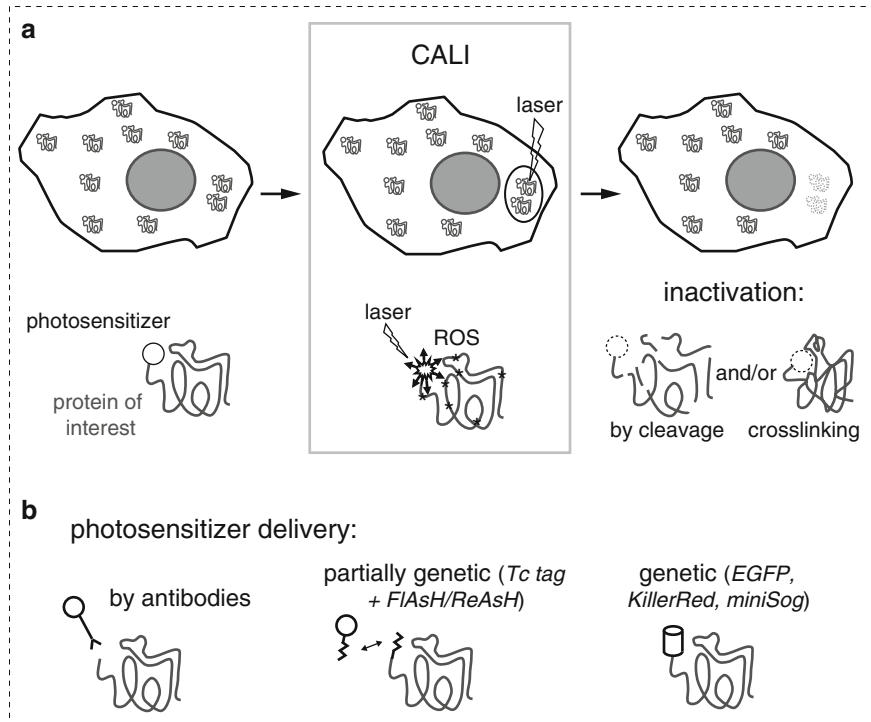


Fig. 1 Principle of CALI. **(a)** Illustration of CALI at the cellular and molecular levels (top and bottom respectively). **(b)** Illustration of the various methods used to target photosensitizers to proteins of interest

coupled to an external compound that binds the tag with strong affinity, such as the membrane-permeant biarsenical green and red fluorescent dyes, FlAsH and ReAsH, that interact specifically with tetracysteine motifs (Fig. 1b) [11, 12]. Unfortunately, antibody microinjection or incubation with external compounds makes CALI highly challenging in living model organisms, although a few attempts show that it is possible in *Drosophila* [11, 13–17]. Furthermore, as external molecules can bind nonspecifically, their use may lead to side-effects. In this context, several fluorescent proteins emerged as promising tools as they could behave like genetically encoded photosensitizers (Fig. 1b). The expected advantages were that off-target effects should be minimized because only the protein of interest is fused to the photosensitizer and the use of external compounds could be avoided, facilitating protein inactivation in living organisms. Enhanced GFP (EGFP) was the first fully genetic photosensitizer identified [2]. Subsequently, KillerRed, a red fluorescent protein derived from a hydrozoan chomoprotein and identified in a screen for phototoxicity in *E. coli*, was shown to be a strong CALI mediator [18]. A monomeric variant, SuperNova, has recently been introduced [19] and finally, miniSog (short name for “mini Singlet Oxygen Generator”), a small monomeric green fluorescent flavoprotein

initially developed as a tag for electron microscopy, has been reported to efficiently mediate CALI in worms and in hippocampal cultures from rat [20].

In developing embryos, several proteins fused to EGFP or miniSog have been successfully inactivated. For instance, CALI inactivation of the adhesion molecule E-cadherin and of the SNARE protein VAMP2 were reported in the live nervous system of *Drosophila* and *C. elegans*, respectively (see Note 1) [8, 20]. CALI of myosin II subunits (MRLC in *Drosophila* and the *nmy-2* encoded MHC in *C. elegans*) fused to GFP led to an immediate and local block of cytokinesis at the laser-targeted membranes of live dividing cells, in both organisms (Fig. 2) [3, 21]. As a whole, even if additional work is required to determine whether CALI based on fluorescent proteins can inactivate any type of protein, experiments over the last decade bring proof-of-principle that fluorescent proteins, including GFP, behave as genetic photosensitizers to mediate CALI in living organisms. Here, we present in Subheading 3 examples of protocols to inactivate a GFP fusion protein either intracellularly (in early embryos) or within a large

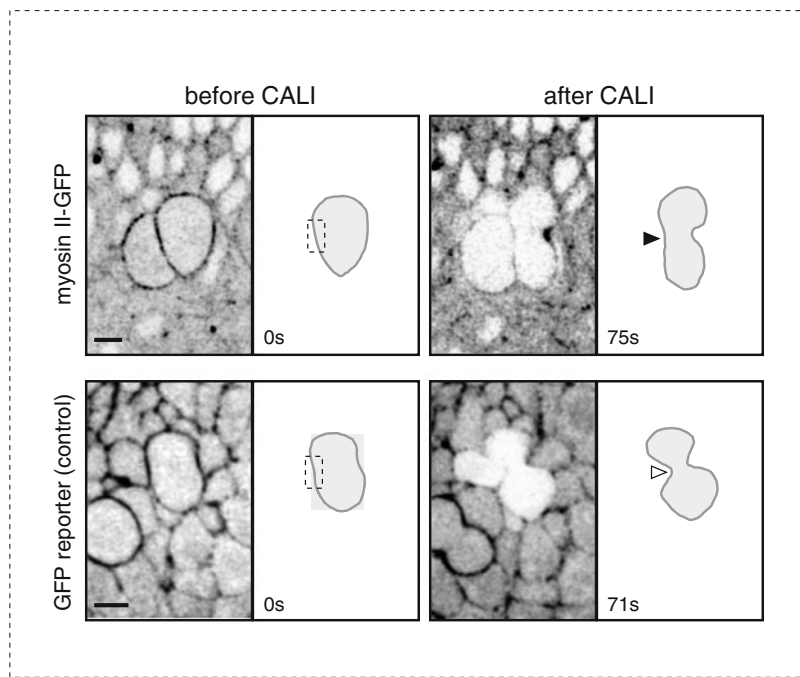


Fig. 2 Local protein inactivation by CALI in a living *Drosophila* embryo. (Top) CALI of myosin II-GFP on one side of the cytokinesis ring of a dividing cell (schematized in grey) blocks membrane ingression (black arrowhead). This shows that myosin II activity can be acutely abolished by light treatment. (Bottom) A similar experiment conducted on a control GFP line (Moesin-ABD-GFP, an actin reporter that does not play any physiological role) does not perturb cytokinesis (open arrowhead), showing that neither ROS nor intense laser illumination per se produces side-effects in this context. Images are taken from time-lapse movies. The targeted area is indicated by the dashed rectangle. Adapted from ref. 3 as permitted by Nature Publishing Group, 2010

tissue domain (later in embryogenesis, in the amnioserosa). The consequences of CALI can be determined, respectively for each example, by following cell behavior by time-lapse microscopy or stopping development and analyzing protein integrity by immunolabeling of whole mount tissue or western blot. We also provide in Subheading 4 some general principles regarding the design of CALI experiments using partially (FlAsH/ReAsH) or fully genetically encoded photosensitizers. Readers looking for advice on CALI using antibody-bound chromophores are referred to the discussion by Jay and colleagues [22].

2 Materials

1. *Sample preparation*: laying cages (allowing breathing), agar plates, yeast paste, brush, basket, bleach (commercial), distilled water in squirt bottle, needle, coverslips (22 × 40), glass slides, heptane glue [23], Voltalef oil 10S (VWR).
2. *Imaging equipment*: stereomicroscope (for handling embryos during mounting and post-fixation steps), inverted laser scanning confocal microscope fitted with a FRAP module, objectives (×10, ×40, and ×63). It should be noted that, although most reports in the literature mention that CALI is performed using a custom-made set up, CALI can be performed using laser scanning confocal or two-photon excitation microscopy, where laser illumination at maximum power can be targeted to a given ROI [3, 8, 9].
3. *Post-CALI fixation*: heptane, petri dish, glass pipet, glass vial, formaldehyde 37%, squirt bottle of Phosphate-buffered saline (PBS) 1× + Triton X-100 0.1%, basket.
4. *Manual devitellinization*: PBS 1×, agar plate, brush, double-sided tape, coverslip, syringe needle, petri dish lid.

3 Methods

The protocols described here were developed to study non-muscle myosin II function in *Drosophila* embryos [3]. Below provides a general strategy for performing CALI using GFP fusion proteins and, between brackets, examples of parameters that we used to locally inactivate MRLC-GFP at the cytokinesis ring during mitosis (Subheading 3.2) or within the dorsal region during dorsal closure (Subheading 3.3). Those protocols are intended as guidelines: modifications will be necessary to study other proteins, as each case is likely to be unique.

3.1 Sample Preparation

1. Place adult flies in a cage with an agar plate coated with yeast paste. Allow females to lay eggs on the agar for the required length of time depending on the embryonic stage of interest.
2. Collect the agar plate. Add distilled water and use a brush to resuspend the embryos. Transfer them into a basket and wash extensively with distilled water.
3. In order to dechorionate the embryos, incubate the basket in 50% bleach (diluted with water) during 2 min 30 s. Then, wash thoroughly the embryos using the squirt bottle filled with distilled water.
4. Dry the embryos by placing the basket on a paper towel. With a brush, transfer the embryos onto a piece of agar on a glass slide. Select embryos of stage of interest under a stereomicroscope. Use a needle to align them and orient the region to image upward. Discard unselected embryos.
5. Spread a drop of heptane glue on a coverslip and wait until complete heptane evaporation. Transfer the embryos by pressing the sticky coverslip upside down on the agar. Cover them immediately with Voltalef oil.
6. Place the coverslip on an inverted laser scanning microscope [we used a Zeiss LSM510 laser scanning microscope fitted with a FRAP module and a Lasos 50 mW Argon laser set at 50% of its power].
7. Use a low-resolution objective to place embryos on the centre of the stage. Switch to a high-resolution objective to identify embryos suited for the experiment (right stage, correct orientation) [we used Plan-Apochromat 63 \times /1.4 Oil DIC objective and Plan-Neofluar 40 \times /1.3 Oil DIC objective from Zeiss]. Use fast scanning with 488 nm laser line set at 1–4%.

3.2 CALI Inactivation of a Protein Subcellular Pool Coupled to Time-lapse Imaging

1. Select the cell to analyze based on fluorescent reporters or morphological markers [we used cell rounding to identify cells ready to divide]. A numerical zoom can be used to focus on the cell of interest [we used respectively 3 \times or 5 \times numerical zoom in conjunction with 63 \times or 40 \times objectives].
2. Select image size and depth [we acquired 512 \times 512 pixels, 8 bits images].
3. Set up the FRAP module. In typical FRAP experiments, only one blast is performed and recovery of fluorescence is followed (unbleached GFP proteins from the surrounding areas repopulate the targeted area). For CALI, GFP proteins repopulating the targeted area need to be blasted repetitively using cycles of intense illumination, in order to reveal a phenotype [for targeting the cytokinesis ring, the duration of a typical laser pulse was 3–6 s with a gap of 10 s]. Important parameters to consider for inactivation are:

- Size of the region of interest (ROI) to encompass the subcellular structure of interest [$5 \times 2 \mu\text{m}$].
- Scan speed and number of scans per frame [respectively 9 and 1; those combined parameters led to a pixel time of 1.6 μs].
- Number of iterations [10].
- Laser intensity at maximal power [477 nm laser line at 100% + 488 nm laser line at 100%].

Empirical determination of those parameters is required in order to inactivate efficiently the protein of interest. Different combinations of parameters may lead to the same effect. Note also that, in live samples, it may be necessary to slightly shift the ROI during the experiment in order to follow the structure of interest during cycles of intense illumination and imaging.

4. Set up the time-lapse parameters to follow cell behavior during CALI, by acquiring images (in the entire frame window, not just in the ROI) in between rounds of intense illumination. Record at least one image before the first intense illumination round to provide a reference. Parameters to set up for recording between intense illumination cycles are:
 - Number of images to acquire [10];
 - Frequency of capture [1 image/s];
 - Laser wavelength and laser intensity [488 nm laser line at 1–4%; we used residual GFP to follow the cell membranes]. The GFP-fusion protein can be combined with a red fluorescent reporter to mark the cell contours, for example or, alternatively, residual GFP fluorescence can be used for this purpose. We used this latter strategy by increasing the contrast for each image post-acquisition (for example using the softwares ImageJ or Photoshop) in order to visualize the weaken GFP signal in the area of interest. Although the GFP signal outside the targeted image becomes saturated, this does not interfere with the interpretation of the CALI experiment as long as the GFP signal does not need to be quantitatively analyzed. Note also that it may be possible to slightly open the pinhole during image acquisition in order to recover more GFP signal.

3.3 CALI Inactivation at the Tissue Level Coupled to Western Blot/Immunostaining Assessment of Protein Integrity

In this protocol, the ROI used is much larger than the one reported in Subheading 3.2. Inactivation was therefore less efficient. To compensate, instead of using the FRAP module, we continuously acquired images with high laser intensity during 5 min. Importantly, single embryos were mounted on each coverslip in order to be able to collect them immediately after CALI treatment.

1. Select image size and depth [512×512 pixels, 8 bits images].
2. Take a snapshot of the embryo to serve as a reference, using the 488 nm laser line set at 1–4 %.
3. Select a ROI encompassing a large region of the embryo [we focused on the amnioserosa, and used a ROI of up to 200×120 μm (x, y)].
4. Set up Z stack parameters, i.e. first and last slice of the stack as well as step size [for western blot analysis, we scanned 15 images every 1.5 μm , generating a 21 μm stack]. Illuminating the ROI through a series of Z planes enhanced the proportion of inactivated protein in the embryo.
5. Set up scanning parameters in order to scan slowly, and thus to maximize protein inactivation. Parameters to play with are scan speed and number of scans per frame [we used scan speed of 5–6 and frame average of 1–2, leading to a scan time per frame of 550–800 ms].
6. Set up time parameters to continuously scan the ROI (x, y, z) during the time window chosen.
7. Continuously scan the ROI with laser intensity set up at maximal power [477 nm laser line at 100% + 488 nm laser line at 100%].
8. Following CALI treatment, remove the excess of oil using a paper towel and transfer the coverslip into a heptane bath (within a petri dish) to unglue the embryo. Pre-coat a glass pipet with heptane and use it to transfer the embryo in a glass vial with a fixative solution (formaldehyde 37%: heptane (1:1)). Fix for 5 min (*see Note 2* should fixation be avoided). Transfer the embryo in a basket and thoroughly rinse it with PBS 1× Triton 0.1 % using a squirt bottle. Then proceed to western blot using standard protocols. Note that, for highly expressed proteins such as myosin II, a single embryo is sufficient for western blot analysis. Otherwise, several embryos can be pooled. Alternatively, proceed to immunostaining following a step of manual devitellinization. In practice, the post-fixation PBS 1× Triton 0.1 % rinse is followed by a PBS 1× only rinse. Next steps are performed under a stereomicroscope. The embryo is dried out, and transferred onto an agar plate with a paintbrush. It is then glued on a coverslip covered with double-sided tape and immediately transferred onto a small petri dish lid filled with PBS 1×. A syringe needle is then used to press gently on the sides of the embryo until tearing of the vitelline membrane releases the embryo. The embryo is next transferred into an eppendorf vial and processed for immunostaining using standard protocols.

3.4 Designing CALI Experiments: Practical Considerations

Although CALI can prove extremely useful to answer specific biological questions, it is important to carefully design experiments with a clearly defined hypothesis and with specific controls to assay CALI efficiency and check for off-target effects. For example prolonged illumination, especially with blue light when using GFP, may prove deleterious for cells or tissues. Importantly, two main aspects are critical for a successful CALI experiment: to achieve inactivation with both high efficiency (all or most of the protein of interest is inactivated in the targeted area) and high specificity (only the protein of interest is inactivated). Several parameters need to be considered, and may impinge on both aspects at the same time. Below provides some advice on parameters and considerations about possible pitfalls.

3.5 Influence of the Nature of the Protein of Interest

Various properties of the protein of interest that can impact on the outcome of a CALI experiment are described below:

1. *Subcellular mobility of the protein of interest.* When applying CALI at the subcellular scale, the outcome may depend upon the dynamics of the protein targeted. For instance, a highly dynamic, soluble protein may quickly repopulate the targeted region and rescue any phenotype resulting from inactivation of the initial pool of protein. This would prevent any clear conclusion being reached regarding the role of the molecule of interest. Performing FRAP analysis beforehand might prove important to predict whether fast recovery might be problematic. As demonstrated by Vitriol and colleagues [24], increasing the targeted area may be necessary in such cases to prevent compensation by intact, non-irradiated proteins from surrounding areas. Alternatively, as we have shown, repetitive cycles of illumination can be used to not only inactivate the local pool of a protein but also inactivate any new pool moving into the targeted area [3].
2. *Quantity of tagged protein of interest.* The proportion of proteins of interest tagged by the photosensitizer relative to non-tagged proteins in a cell or tissue may also influence the output of a CALI experiment. Abundance of the protein of interest relative to the quantity of dye introduced may be a problem when performing CALI using membrane-permeable photosensitizers such as FlAsH/ReAsH: non-labeled proteins will escape inactivation and may rescue any phenotype. This can be circumvented when using a genetic tag (EGFP, KillerRed, miniSog) by either inserting the tag at the endogenous gene locus or using a fusion construct rescuing a null mutation for the gene encoding the protein of interest. We followed the latter strategy in our work by using a *sqh-GFP* construct rescuing the null allele *sqh^{AX3}* (*sqh* codes for MRLC), ensuring that all the MRLC proteins were tagged with GFP [3, 25]. Working with only a fraction of tagged

proteins (for example via overexpression of a fusion protein) may or may not produce a phenotype depending on the nature of the protein: for those that dimerize, even if only half are tagged within a complex, this may be sufficient to abolish the function of the protein complex. For example, successful CALI inactivations of α -actinin or myosin II were reported in contexts where only a subset of molecules was tagged with GFP [2, 21].

3. *Modularity of the protein of interest.* The consequences of CALI on large proteins might rely on the modularity of the proteins involved. Experiments have been reported in which CALI targeting of a protein affects one domain out of two. For example, molecular analyses proved that in vitro illumination of α -actinin-GFP abolishes its binding to β -integrin but not to F-actin, while illumination of FAK-GFP abolishes its catalytic activity but not its binding to its substrate, paxillin [2]. As a further example, in cultured cells, KillerRed-mediated CALI of a GFP-PH domain-KillerRed fusion leads to a cytoplasmic relocalization of an initially membrane-bound molecule [18]. This relocalization was visualized by following the GFP fluorescence, showing that KillerRed damaged the PH domain, but not the GFP one.

3.6 Choice of the Photosensitizer

The choice of the photosensitizer can directly impinge on both efficiency and specificity of the CALI effect. GFP is a weaker ROS producer than molecules such as KillerRed, miniSog, or FlAsH/ReAsH. The ability of CFP and YFP to mediate CALI was also tested in vitro: they are less efficient than GFP and may not behave as workable photosensitizers [26]. KillerRed was therefore recently referred to as “the first choice for protein-based CALI because of its high efficiency in generating ROS” [27]. However, the dimeric state of KillerRed is a problem when generating fusion proteins [19]. Indeed, it was recently reported that the fusion of KillerRed to various types of protein leads to altered subcellular localization of the fusions. A monomeric variant of KillerRed, named SuperNova, has been introduced to circumvent this limitation [19], but its efficiency as a genetic photosensitizer for CALI needs to be thoroughly tested. FlAsH/ReAsH have the advantage to be more efficient than GFP in mediating CALI (in vitro, FlAsH has a relative CALI efficiency about 7 times higher than EGFP [26]), while ReAsH is markedly stronger than FlAsH [12] and transgenic platforms have been developed to tag proteins of interest with an optimized Tetracycline motif [28, 29], recently leading to the release of protein trap lines carrying both an EGFP and a Tc tag [30]. However, incubation or, more generally when working with living flies, injection, may be rather constraining. Moreover, those compounds may, to some extent, bind to and inactivate endogenous molecules, especially when they are present at high concentrations [12]. The Tc tag has however been optimized [31], which might limit nonspecific inactivation caused by CALI of FlAsH/ReAsH compounds. miniSog is a

small genetic tag (half the size of GFP) that has been recently used for CALI in *C. elegans* [20]. Concerns about possible side-effects have however been raised, since CALI of a miniSOG-SNT-1 fusion expressed in a wild-type background leads to a phenotype possibly stronger than the one observed for a *snt-1* null mutant [32]. Although the proposed explanation was that miniSog causes the nonspecific destruction of the entire machinery responsible for synaptic vesicle release, it is also possible that CALI turns the SNT-1 molecule into a dominant negative. Alternatively, genetic compensation may occur in *snt-1* mutants, which may not be seen following acute inactivation with CALI. Further investigations are required to clarify whether miniSog might be too potent a photosensitizer. To summarize, all photosensitizers possess advantages and drawbacks (summarized in Table 1) that need to be taken into consideration.

Table 1
Summary of photosensitizer properties

Photosensitizer	Advantages	Weaknesses
EGFP	Genetic photosensitizer Monomeric Many transgenic <i>Drosophila</i> lines already available	Weak photosensitizer (but might be advantageous as might minimize off-target effects) Excitation by blue light which may cause phototoxicity
KillerRed	Genetic photosensitizer Strong photosensitizer Excitation by green light: (1) might induce less phototoxicity than blue light, (2) can be combined with GFP reporters for two-channel imaging	Dimeric Reported to perturb localization of fusion proteins
Supernova	Monomeric variant of KillerRed	Only one report so far (not in <i>Drosophila</i>), so lack of perspective
miniSog	Genetic photosensitizer Strong photosensitizer	Only few reports of CALI (none in <i>Drosophila</i>) Some suspected off-target effects Excitation by blue light which may cause phototoxicity
FlAsH/ReAsH	Strong photosensitizers (ReAsH is stronger) ReAsH: Excitation by green light which might induce less phototoxicity than blue light	Not a genetic photosensitizer (genetic tetracysteine (Tc) tag, but needs incubation or injection of compound) May bind nonspecifically to endogenous proteins FlAsH: Excitation by blue light which may cause phototoxicity

Details and references are given in the main text

Importantly, we would like to point out that emphasis is rarely put on EGFP when it comes to choosing a photosensitizer. However, EGFP presents key advantages: it is a genetic photosensitizer but unlike KillerRed, it is in addition monomeric; many transgenic strains already exist where proteins are fused to GFP, including existing collections of protein traps, which have the advantage of tagging endogenous loci [30, 33–35]. ROS can be produced upon intense illumination during CALI, but also with routine light exposure during image acquisition or during development of the transgenic organism or growth of transfected cultured cells. The weaker activity of GFP as a photosensitizer can in fact be an advantage by limiting the exposure of the cells and tissues to ROS produced by the transgenic photosensitizers. To be successful, a CALI experiment needs to generate enough ROS to destroy the molecule of interest, but not too much to avoid off-target effects and impact on the viability of the organism.

3.7 Controls

Two types of control experiments are critical when performing CALI: controls to validate the efficiency of the inactivation and controls to rule out off-target effects. Because CALI is not a routine experiment and may be complex to run, we would advise testing whether more traditional knockdown strategies (mutants, RNAi, dominant negatives) produce similar phenotypes as CALI.

1. *CALI efficiency.* CALI efficiency can be tested by assessing the integrity of the targeted protein after treatment. For example, Rajfur and co-workers used a GST-pull-down assay to prove that EGFP- α -actinin binding to β -integrin was lost following CALI in vitro [2]. Western blot analysis can also be performed to ask if the levels of the protein targeted are decreased. For example, we found that upon CALI on MRLC-GFP, levels of GFP and MRLC were both reduced on western blots (Fig. 3a, b) [3]. Immunostaining can also reveal the impact on protein integrity following CALI (Fig. 3a). Another possible test is to check if CALI phenocopies a characterized phenotype for the protein of interest. For instance, as expected from the known role of Myosin II in cytokinesis, CALI on MRLC-GFP or MHC-GFP locally blocks membrane ingression in dividing cells (Fig. 2) [3, 21].
2. *CALI specificity.* Nonspecific photo-damage may occur because of strong laser illumination of live tissues. This may be especially true when using GFP, miniSog, or FlAsH as a photosensitizer, as cells are more sensitive to blue light. Moreover, local ROS generation by photosensitizers might not only inactivate the protein of interest but also proteins in the close vicinity. Experiments need therefore to be performed in order to control for potential CALI side-effects. This can be done by targeting the region of interest in control cells using parameters

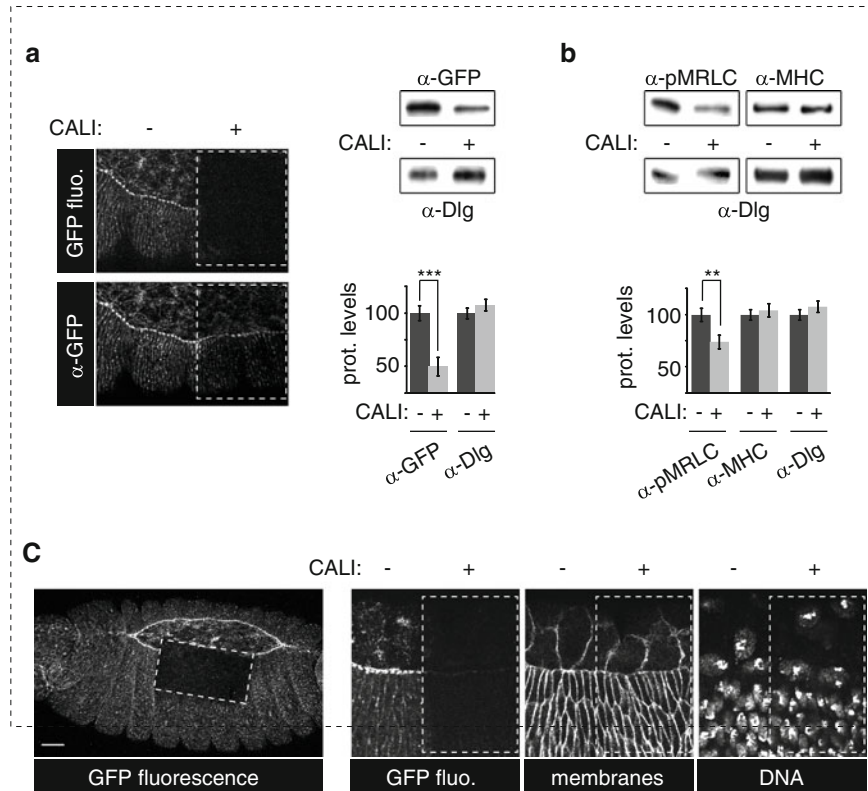


Fig. 3 Control experiments for CALI. **(a)** Controlling CALI efficiency by immunostaining (*left*) or western blot (*right*) after illumination of embryos carrying a fusion between GFP and the regulatory light chain of myosin II (MRLC-GFP). CALI of a small zone (+) of the dorsal side of an embryo during dorsal closure abolishes GFP endogenous fluorescence (*top*) and destroys the GFP protein, as revealed by immunostaining using an anti-GFP antibody (*bottom*). The non-illuminated region (−) serves as an internal control. The targeted region is similar to the one shown in **(c)**. On the *right*, the dorsal side of embryos was illuminated (+) or not (−) and analyzed by western blot. Dlg was taken as a loading control. Quantifications are shown on the *bottom*; protein levels are given in arbitrary units. **(b)** Controlling CALI specificity by western blot after illumination (+) of the dorsal side of MRLC-GFP expressing embryos during dorsal closure. Non-illuminated embryos (−) were taken as a control. Quantifications (in arbitrary units) are given on the *bottom*. While MRLC and MHC (respectively encoded by *spaghetti squash* and *zipper*) are direct binding partners, CALI of the MRLC-GFP fusion decreases only MRLC levels, highlighting CALI specificity in this context. Dlg is taken as a loading control. **(c)** Assessment of possible side-effects by CALI in a MRLC-GFP embryo. Illumination was performed during 5 min in the *boxed region* (*left image*). Close up images are shown on the *right*. Membranes and DNA, as revealed by Dlg and DAPI staining respectively, are unaffected by CALI treatment of MRLC-GFP (+) when compared to the internal control side (−). Adapted from ref. 3 as permitted by Nature Publishing Group, 2010

(such as laser intensity, blast duration, and frequency) similar to those used in the CALI experiments. Fusions between a photosensitizer and a reporter protein (for example a protein that localizes like the protein of interest but which has no function in the process studied, or no physiological function at all) are invaluable to establish that laser illumination *per se* has no deleterious effects during the timescale of the analysis, and that

generation of ROS in the targeted area does not affect the biological process studied nonspecifically. For example, illumination of dividing cells expressing a fusion protein between GFP and the actin binding domain of Moesin (Moesin-ABD-GFP, an actin-binding domain from Moesin which colocalizes with Myosin II at the cell cortex but has no cellular function) has no effect on cytokinesis in *Drosophila* embryos, while the same experiment with MRLC-GFP embryos immediately blocks cytokinesis (Fig. 2) [3]. When a reporter line is not available, it is possible to test for laser-induced photodamage by targeting the area of interest in control cells that are unlabeled or labeled with a fusion between the protein of interest and a fluorescent protein with similar spectral properties to the photosensitizer but unable to efficiently release ROS. For example, Bulina and co-workers used a GFP-PH-DsRed fusion to rule out noxious effect of the laser in their CALI experiment on GFP-PH-KillerRed [18]. When knowledge is available regarding the involvement of a protein in a macromolecular complex, western blot analysis can allow one to test whether inactivation of the molecule of interest also alters other components of the complex. As mentioned earlier, because MHC and MRLC are direct interactors in myosin II complexes, we checked by western blot that MHC levels were unaltered while the levels of MRLC and GFP dropped following CALI on MRLC-GFP (Fig. 3b) [3]. A final test is to check that cell or tissues are intact following CALI treatment. This can be done either on live or fixed embryos, using reporters of membranes, cytoskeleton or any other structure that has been targeted in a CALI experiment (Fig. 3c) [2, 3].

4 Notes

1. VAMP2 is a mammalian molecule that shares about 63 % overall homology with *C. elegans* synaptobrevin. When expressed in the *synaptobrevin[md247]* mutant line, miniSOG-VAMP2 is able to rescue locomotion defect, restoring the absence of function of synaptobrevin [20].
2. Depending on the antibody used for western blot, the embryo should be fixed or not. Should fixation be avoided, the unglued embryo is immediately transferred with a pipette into a basket and is thoroughly rinsed with PBS 1× Triton 0.1 %. The embryo is then transferred in 20 µl Laemli buffer: PBS 1× (1:1) and carefully crushed with a needle and boiled for 5 min. Samples can be pooled if required. Then proceed following standard western blot procedures.

Acknowledgements

We thank Andrew Davidson and Will Wood for critical reading of the manuscript. BS acknowledges funding from a Wellcome Trust Investigator Award [099234/Z/12/Z]. APM and BM are supported respectively by Université Toulouse III-Paul Sabatier and Centre National de la Recherche Scientifique (CNRS).

References

1. Jay DG (1988) Selective destruction of protein function by chromophore-assisted laser inactivation. *Proc Natl Acad Sci U S A* 85:5454–5458
2. Rajfur Z, Roy P, Otey C, Romer L, Jacobson K (2002) Dissecting the link between stress fibres and focal adhesions by CALI with EGFP fusion proteins. *Nat Cell Biol* 4:286–293
3. Monier B, Péliéssier-Monier A, Brand AH, Sanson B (2010) An actomyosin-based barrier inhibits cell mixing at compartmental boundaries in *Drosophila* embryos. *Nat Cell Biol* 12:60–65, sup pp 61–69
4. Jacobson K, Rajfur Z, Vitriol E, Hahn K (2008) Chromophore-assisted laser inactivation in cell biology. *Trends Cell Biol* 18:443–450
5. Horstkotte E, Schröder T, Niewöhner J, Thiel E, Jay DG, Henning SW (2005) Toward understanding the mechanism of chromophore-assisted laser inactivation—evidence for the primary photochemical steps. *Photochem Photobiol* 81:358–366
6. Davies MJ (2003) Singlet oxygen-mediated damage to proteins and its consequences. *Biochem Biophys Res Commun* 305:761–770
7. Rauzi M, Lenne PF (2015) Probing cell mechanics with subcellular laser dissection of actomyosin networks in the early developing *Drosophila* embryo. *Methods Mol Biol* 1189:209–218
8. Pollarolo G, Schulz JG, Munck S, Dotti CG (2011) Cytokinesis remnants define first neuronal asymmetry *in vivo*. *Nat Neurosci* 14:1525–1533
9. Tanabe T, Oyamada M, Fujita K, Dai P, Tanaka H, Takamatsu T (2005) Multiphoton excitation-evoked chromophore-assisted laser inactivation using green fluorescent protein. *Nat Methods* 2:503–505
10. Wang FS, Jay DG (1996) Chromophore-assisted laser inactivation (CALI): probing protein function *in situ* with a high degree of spatial and temporal resolution. *Trends Cell Biol* 6:442–445
11. Marek KW, Davis GW (2002) Transgenically encoded protein photoinactivation (FlAsH-FALI): acute inactivation of synaptotagmin I. *Neuron* 36:805–813
12. Tour O, Meijer RM, Zacharias DA, Adams SR, Tsien RY (2003) Genetically targeted chromophore-assisted light inactivation. *Nat Biotechnol* 21:1505–1508
13. Kasprowicz J, Kuenen S, Miskiewicz K, Habets RL, Smitz L, Verstreken P (2008) Inactivation of clathrin heavy chain inhibits synaptic recycling but allows bulk membrane uptake. *J Cell Biol* 182:1007–1016
14. Kasprowicz J, Kuenen S, Swerts J, Miskiewicz K, Verstreken P (2014) Dynamin photoactivation blocks Clathrin and α -adaptin recruitment and induces bulk membrane retrieval. *J Cell Biol* 204:1141–1156
15. Schröder R, Tautz D, Jay DG (1996) Chromophore-assisted laser inactivation of even skipped in *Drosophila* precisely phenocopies genetic loss of function. *Dev Genes Evol* 206:86–88
16. Heerssen H, Fetter RD, Davis GW (2008) Clathrin dependence of synaptic-vesicle formation at the *Drosophila* neuromuscular junction. *Curr Biol* 18:401–409
17. Poskanzer KE, Marek KW, Sweeney ST, Davis GW (2003) Synaptotagmin I is necessary for compensatory synaptic vesicle endocytosis *in vivo*. *Nature* 426:559–563
18. Bulina ME, Chudakov DM, Britanova OV, Yanushevich YG, Staroverov DB, Chepurnykh TV, Merzlyak EM, Shkrob MA, Lukyanov S, Lukyanov KA (2006) A genetically encoded photosensitizer. *Nat Biotechnol* 24:95–99
19. Takemoto K, Matsuda T, Sakai N, Fu D, Noda M, Uchiyama S, Kotera I, Arai Y, Horuchi M, Fukui K et al (2013) SuperNova, a monomeric photosensitizing fluorescent protein for chromophore-assisted light inactivation. *Sci Rep* 3:2629
20. Lin JY, Sann SB, Zhou K, Nabavi S, Proulx CD, Malinow R, Jin Y, Tsien RY (2013)

Optogenetic inhibition of synaptic release with chromophore-assisted light inactivation (CALI). *Neuron* 79:241–253

21. Ou G, Stuurman N, D'Ambrosio M, Vale RD (2010) Polarized myosin produces unequal-size daughters during asymmetric cell division. *Science* 330:677–680
22. Hoffman-Kim D, Diefenbach TJ, Eustace BK, Jay DG (2007) Chromophore-assisted laser inactivation. *Methods Cell Biol* 82:335–354
23. Cavey M, Lecuit T (2008) Imaging cellular and molecular dynamics in live embryos using fluorescent proteins. *Methods Mol Biol* 420:219–238
24. Vitriol EA, Utrecht AC, Shen F, Jacobson K, Bear JE (2007) Enhanced EGFP-chromophore-assisted laser inactivation using deficient cells rescued with functional EGFP-fusion proteins. *Proc Natl Acad Sci U S A* 104:6702–6707
25. Royou A, Sullivan W, Karess R (2002) Cortical recruitment of nonmuscle myosin II in early syncytial Drosophila embryos: its role in nuclear axial expansion and its regulation by Cdc2 activity. *J Cell Biol* 158:127–137
26. McLean MA, Rajfur Z, Chen Z, Humphrey D, Yang B, Sligar SG, Jacobson K (2009) Mechanism of chromophore assisted laser inactivation employing fluorescent proteins. *Anal Chem* 81:1755–1761
27. Sano Y, Watanabe W, Matsunaga S (2014) Chromophore-assisted laser inactivation--towards a spatiotemporal-functional analysis of proteins, and the ablation of chromatin, organelle and cell function. *J Cell Sci* 127:1621–1629
28. Venken KJ, Kasprowicz J, Kuenen S, Yan J, Hassan BA, Verstreken P (2008) Recombineering-mediated tagging of Drosophila genomic constructs for in vivo localization and acute protein inactivation. *Nucleic Acids Res* 36:e114
29. Venken KJ, Schulze KL, Haelterman NA, Pan H, He Y, Evans-Holm M, Carlson JW, Levis RW, Spradling AC, Hoskins RA et al (2011) MiMIC: a highly versatile transposon insertion resource for engineering Drosophila melanogaster genes. *Nat Methods* 8:737–743
30. Nagarkar-Jaiswal S, Lee PT, Campbell ME, Chen K, Anguiano-Zarate S, Gutierrez MC, Busby T, Lin WW, He Y, Schulze KL et al (2015) A library of MiMICS allows tagging of genes and reversible, spatial and temporal knockdown of proteins in Drosophila. *Elife* 4:e08469
31. Martin BR, Giepmans BN, Adams SR, Tsien RY (2005) Mammalian cell-based optimization of the biarsenical-binding tetracysteine motif for improved fluorescence and affinity. *Nat Biotechnol* 23:1308–1314
32. Hermann A, Liewald JF, Gottschalk A (2015) A photosensitive degron enables acute light-induced protein degradation in the nervous system. *Curr Biol* 25:R749–R750
33. Morin X, Daneman R, Zavortink M, Chia W (2001) A protein trap strategy to detect GFP-tagged proteins expressed from their endogenous loci in Drosophila. *Proc Natl Acad Sci U S A* 98:15050–15055
34. Buszczak M, Paterno S, Lighthouse D, Bachman J, Planck J, Owen S, Skora AD, Nystul TG, Ohlstein B, Allen A et al (2007) The carnegie protein trap library: a versatile tool for Drosophila developmental studies. *Genetics* 175:1505–1531
35. Quiñones-Coello AT, Petrella LN, Ayers K, Melillo A, Mazzalupo S, Hudson AM, Wang S, Castiblanco C, Buszczak M, Hoskins RA et al (2007) Exploring strategies for protein trapping in Drosophila. *Genetics* 175:1089–1104

Chapter 9

deGradFP: A System to Knockdown GFP-Tagged Proteins

Emmanuel Caussinus and Markus Affolter

Abstract

Protein depletion by genetic means, in a very general sense including the use of RNA interference [1, 2] or CRISPR/Cas9-based methods, represents a central paradigm of modern biology to study protein functions *in vivo*. However, acting upstream the proteic level is a limiting factor if the turnover of the target protein is slow or the existing pool of the target protein is important (for instance, in insect embryos, as a consequence of a strong maternal contribution). In order to circumvent these problems, we developed deGradFP [3, 4]. deGradFP harnesses the ubiquitin-proteasome pathway to achieve direct depletion of GFP-tagged proteins. deGradFP is in essence a universal method because it relies on an evolutionarily conserved machinery for protein catabolism in eukaryotic cells; *see* refs. 5, 6 for review. deGradFP is particularly convenient in *Drosophila melanogaster* where it is implemented by a genetically encoded effector expressed under the control of the Gal4 system. deGradFP is a ready-to-use solution to perform knockdowns at the protein level if a fly line carrying a functional GFP-tagged version of the gene of interest is available. Many such lines have already been generated by the *Drosophila* community through different technologies allowing to make genomic rescue constructs or direct GFP knockins: protein-trap stock collections [7, 8] (<http://cooley.medicine.yale.edu/flytrap/>, <http://www.flyprot.org/>), P[acman] system [9], MiMIC lines [10, 11], and CRISPR/Cas9-driven homologous recombination.

Two essential controls of a protein knockdown experiment are easily achieved using deGradFP. First, the removal of the target protein can be assessed by monitoring the disappearance of the GFP tag by fluorescence microscopy in parallel to the documentation of the phenotype of the protein knockdown (*see Note 1*). Second, the potential nonspecific effects of deGradFP can be assessed in control fly lacking a GFP-tagged target protein. So far, no nonspecific effects of the deGradFP effector have been reported [3].

Key words GFP, Nanobodies, F-Box, Proteasome, Gene expression

1 Introduction

In eukaryotes, ubiquitin-dependent protein degradation is carried out by a complex cascade of enzymes (E1, E2, and E3) which covalently attach multiple ubiquitin molecules to the target proteins [5], either on internal lysine residues or on the N-terminal residue [12]. Polyubiquitinated proteins are then forwarded to the proteasome to be degraded (Fig. 1a). E3 enzymes are key players in determining the specificity of the polyubiquitination step.

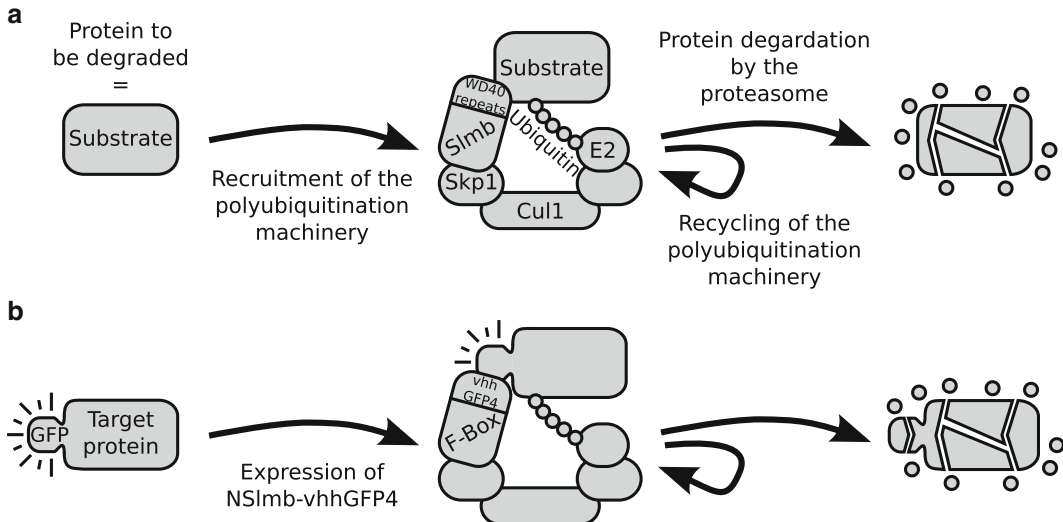


Fig. 1 Schematic illustration of deGradFP. **(a)** The normal ubiquitin-proteasome pathway. **(b)** Hijacking the ubiquitin-proteasome pathway. For details see text

SKP1-CUL1-F-Box protein ligase complexes (SCFs) are E3 enzymes that share common subunits (S-phase Kinase-associated Protein 1, Cullin 1, and RING proteins), but also contain distinct F-Box Proteins (FBP) that determine substrate specificity. Usually, FBPs bind to Skp1 via their F-box domain, and to their specific protein substrates via different protein–protein interaction motifs (such as WD40 repeats [13]).

The effector of deGradFP is a UAS transgene whose specific spatial and temporal expression is achieved using different Gal4 drivers. We fused the F-box domain contained in the N-terminal part of Slmb (a FBP found in *Drosophila melanogaster* [13]) to a nanobody (a single-domain antibody fragment hereafter called VhhGFP4 [14]) (Fig. 1b). VhhGFP4 strongly binds to GFP, Venus, Yellow Fluorescent Protein (YFP), or Enhanced YFP (EYFP), but does not cross react with Cerulean, dsRed, mCherry, and the other fluorescent proteins that are not derived from GFP [14, 15]. Nslmb-vhhGFP4 fusion proteins function in synthetic E3 enzyme complexes whose substrates are GFP-tagged proteins. Upon inducible expression of *Nslmb-vhhGFP4* via a Gal4 driver, target proteins fused to GFP (or one of its close derivatives, see above) are specifically polyubiquitinated and degraded by the proteasome in a couple of hours [3].

Drosophila melanogaster being one of the most convenient eukaryotic genetic systems to work with, the use of deGradFP often consists in setting up simple genetic crosses and observing the phenotype of their progeny by fluorescence microscopy [4]. However, besides imaging techniques, any suitable assay can be used to document and analyze the phenotypes generated with

deGradFP. In order not to overlap with other chapters in this book or in the first volume of *Drosophila Methods and Protocols*, imaging techniques will only be superficially referred to and we will focus on the genetical aspects of deGradFP.

2 Materials

Basic fly husbandry material will be required throughout the different sections of this protocol.

2.1 How to Know Whether a GFP-Tagged Protein of Interest Can Be Knocked Down by deGradFP?

1. Fly vials.
2. Fly food.
3. Stereomicroscope.
4. CO₂ fly station.
5. Baker's yeast powder or paste.
1. Apple juice agar plates. There are several recipes for preparing those plates. For instance, mix 3 l of water and 90 g of agar. In another container, mix 1 l of apple juice, 6 g of Sodium methyl-paraben (E219, a broad spectrum antimicrobial agent), and 100 g of sucrose. Bring to boil the two mixtures in a microwave, allow to cool to about 60 °C, and mix them. Pour into Petri dishes. Apple juice plates can be kept at 4 °C for several weeks.
2. Fluorescence microscope able to image GFP and mCherry on two distinct channels (either epifluorescence microscope, confocal microscope, spinning disk microscope, or selective plane illumination microscope) (see Chapter 10).
3. Fly line carrying a functional GFP-tagged gene denoted as *target::GFP*. Here, in contrast to the other sections of this protocol (see below, Protein knockdown in embryos and Protein knockdown in late developmental stages), the genetic background of this line is not important; that is to say that *target::GFP* can coexist with the wild-type untagged version of that gene simply referred to as *target*.
4. Fly line carrying an *engrailed-Gal4* (*enGal4*) driver, a *UAS_Nslmb-vhhGFP4* transgene, and a *UAS_mCherry-NLS* transgene. Such a fly line is readily available from the Bloomington *Drosophila* Stock Center (<http://flystocks.bio.indiana.edu/Browse/misc-browse/deGradFP.htm>).

2.2 Protein Knockdown in *Drosophila* Embryos

1. Basic fly husbandry material and apple juice agar plates (see above).
2. Fly line carrying *target::GFP*.
3. If *target::GFP* is a genomic rescue, fly line carrying a *target* null mutation referred to as *target**.

4. Fly line carrying a *UAS_Nslmb-vhhGFP4* transgene (see Note 2).
5. Fly line carrying a Gal4 driver, referred to as *promoter::Gal4*, whose expression domain corresponds to the spatio-temporal territory in which the knockdown of Target::GFP needs to be achieved.

2.3 Protein Knockdown in Late Developmental Stages

1. Basic fly husbandry material and apple juice agar plates (see above).
2. Fly line carrying *target::GFP*.
3. Fly line carrying a *UAS_Nslmb-vhhGFP4* transgene (see Note 2).
4. Fly line carrying *promoter::Gal4*, whose expression domain corresponds to the spatio-temporal territory in which the knockdown of Target::GFP needs to be achieved.
5. Fly line carrying a *tubP_Gal80ts* transgene (see Note 3).
6. 29 °C incubator.
7. If fluorescent balancers are used, fluorescence stereomicroscope.

3 Methods

Two requirements need to be met for a successful use of deGradFP in order to generate a loss-of-function effect. First, since the method is designed for knocking down GFP-tagged proteins, the only source of the target protein has to be a functional GFP-tagged gene. This can be a GFP-tagged genomic rescue in a null mutant background, or a GFP knockin (see Note 4). Second, the GFP-tagged target protein needs to be accessible to the ubiquitin-proteasome pathway. This excludes extracellular proteins and transmembrane proteins in which the GFP tag is not intracellular (see Note 5). Unfortunately, other reasons we do not understand prevent the ubiquitin-proteasome pathway to knockdown some GFP-tagged proteins with deGradFP (see Note 6) [3, 4]. It is likely that, for some targets, the action of deGradFP is outcompeted by some specific deubiquitinating enzymes which cleave ubiquitin-protein bonds [6]. From our own experience and the feedback we got from other laboratories, deGradFP works in approximately 60% of the cases (see Note 7).

How to fulfill the first requirement if a functional GFP-tagged version of the target protein has not been generated is out of the scope of this chapter; to that aim, the reader might refer to the chapters by Port and Bullock in this Volume. Coping with the second requirement is addressed in the next section.

3.1 How to Know Whether a GFP-Tagged Protein of Interest Can Be Knocked Down by deGradFP?

Some individual steps described in this chapter are not time-consuming as such, but are interspaced by longer intervals of time (typically a generation time). Moreover, more often than not, these steps involve the tedious creation and amplification of complex fly lines. Before undertaking a long series of experiments, quickly

testing whether a Target::GFP protein can be knocked down by deGradFP can be achieved as follows if two conditions are met. First, the signal generated by the expression of target::GFP must be strong enough to be detectable by the fluorescent microscope that will be used. Second, the expression domain of target::GFP must overlap with the expression domain of *engrailed* (*en*); otherwise, another driver line has to be used.

1. Amplify a fly line that carries *target::GFP*. Here, *target::GFP* is arbitrarily placed on the second chromosome (Fig. 2a).
2. Collect 20–30 virgins from this line and cross them to a few males (around 5) carrying *en::Gal4*, *UAS_Nslmb-vhhGFP4*, and *UAS_mCherry-NLS* (Fig. 2a). *en::Gal4* is used to express both *Nslmb-vhhGFP4* and *mCherry-NLS* in a simple pattern (the posterior compartment of each segment of the epidermis from stages 6 to 17 [16]).
3. Keep the cross in a fly tube supplemented with a bit of baker's yeast for 3 days.
4. Once the females lay abundantly, transfer the cross on an apple juice agar plate supplemented with a bit of baker's yeast; perform an overnight embryo collection (typically 16 h at room temperature).

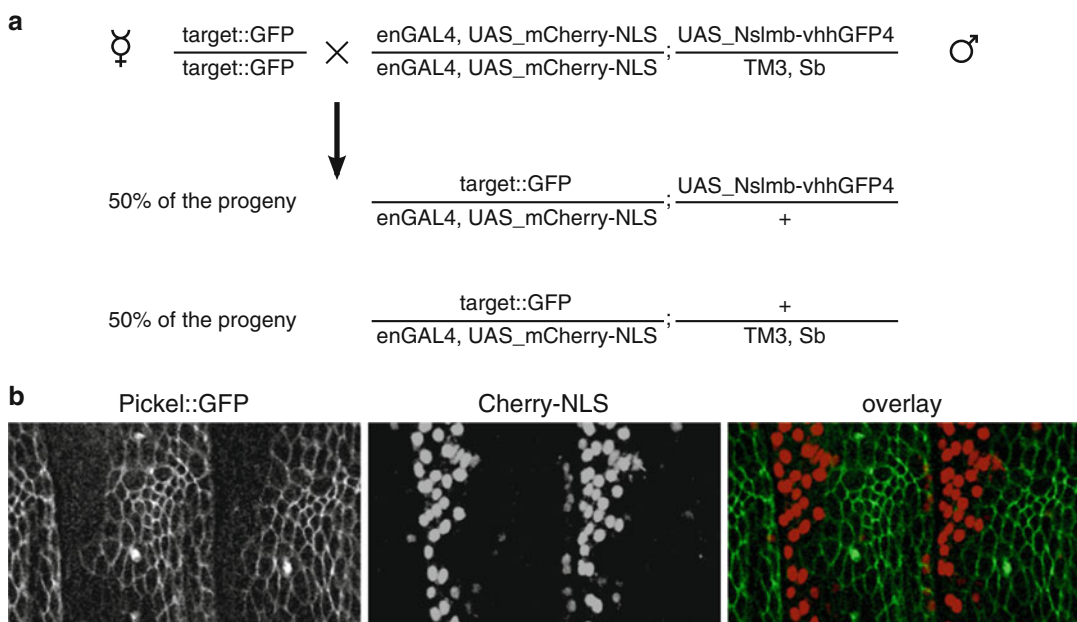


Fig. 2 Determining whether deGradFP can target a specific GFP-tagged protein. (a) Crossing scheme. (b) deGradFP degrades Pickel::GFP [27]. Confocal imaging of a stage 13 embryo of the following genotype, *w**, *enGal4, UAS_mCherry-NLS/pickel::GFP; UAS_Nslmb-vhhGFP4/+*. Two channels, corresponding to Pickel::GFP (green in overlay panel) and mCherry-NLS (red in overlay panel), were acquired

5. Mount 10 embryos (see Note 8) for live imaging as described in the chapter by Cavey and Lecuit of Volume I of this book (see Note 9).
6. Image the embryos on the fluorescence microscope. Compare the GFP signal in embryos in which mCherry-NLS, but not Nslmb-vhhGFP4, is expressed in the *en* expression domain to embryos in which both mCherry-NLS and Nslmb-vhhGFP4 are expressed (Fig. 2a). A disappearance of the GFP signal in the *en* expression domain of the later embryos confirms that Target::GFP is knocked down by deGradFP (see Note 10) (Fig. 2b).

3.2 Protein Knockdown in Embryos

1. Generate and amplify a fly line A that carries *target::GFP* and *promoter::Gal4*. Here, *target::GFP* is arbitrarily a rescue construct of *target** located on the second chromosome, and *promoter::Gal4* is on the third chromosome; both *target::GFP* and *promoter::Gal4* are homozygous viable transgenes (see Note 11) (Fig. 3).
2. Make two fly lines (B and C) that carry *target::GFP* in a *target** background. Line C does not have any further requirements, but line B needs to carry *UAS_NslmbVhhGFP4*, the effector of deGradFP (Fig. 3).
3. Collect approximately 20 virgins from lines A and cross them to a few males from line B. This cross corresponds to the actual protein knockdown experiment (Fig. 3).
4. Independently, collect approximately 20 virgins from lines A and cross them to a few males from line C. This cross corresponds to a negative control, in which the effector of deGradFP is not expressed (see Note 12) (Fig. 3).

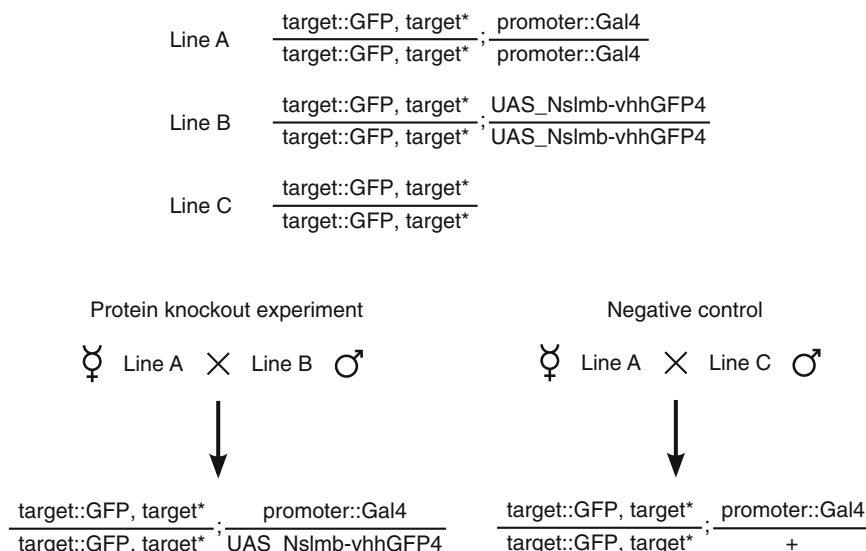


Fig. 3 Crossing scheme for performing a protein knockdown in embryos. This crossing scheme is just illustrative and would need to be adapted if, for instance, *target::GFP* was not located on the second chromosome

5. Keep the crosses in two fly tubes supplemented with a bit of baker's yeast for 3 days.
6. Once the females lay eggs, transfer the crosses on apple juice agar plates supplemented with a bit of baker's yeast to perform embryo collections.
7. The following steps are highly dependent on the assay one wants to perform upon the knockdown of Target::GFP. For biochemical assays, one might need to scale up the amount of flies involved in the crosses. Hence, the number of flies indicated in **steps 3** and **4** are purely indicative for further analysis of the phenotypes by live imaging techniques as described, for instance, in the chapter by Schmied and Tomancak in this Volume.

3.3 Protein Knockdown in Late Developmental Stages

Working on larvae, pupae, or adults instead of embryos allows the morphological determination of the sex of individuals in many cases (see Note 13). Moreover, one can select animals against genetic markers carried by balancer chromosomes, including fluorescent markers visible at the larval stages [17, 18]. All together, these features ease the implementation of deGradFP (see Note 14).

When development time increases, it may become necessary to further restrict *Nslmb-vhhGFP4* expression to a specific period of time. Expressing *Gal80^{ts}* can be used to this aim. Below 25 °C (permissive temperature), *Gal80^{ts}* binds to *Gal4* and blocks its transcription activity. At 29 °C (restrictive temperature), *Gal80^{ts}* cannot bind to *Gal4* anymore, due to a changes in conformation, and becomes inactive [10, 19, 20].

1. Make and amplify a fly line D that carries *target::GFP* and *UAS_Nslmb-vhhGFP4*, the effector of deGradFP (Fig. 4). Here, *target::GFP* is arbitrarily a GFP knockin located on the X chromosome, and *UAS_Nslmb-vhhGFP4* is on the second chromosome (Fig. 4).
2. Make a fly line E that carries *promoter::Gal4* and *tubP_Gal80ts*. Here, for the sake of exploring several possibilities, *promoter::Gal4* is arbitrarily on the second chromosome and homozygous lethal; *tubP_Gal80ts* is on the third chromosome (Fig. 4).
3. Collect approximately 20 virgins from lines D and cross them to a few males from line E (see Note 15). This cross will produce flies that correspond to the actual protein knockdown experiment and two negative controls (Fig. 4).
4. Keep the cross in a standard fly tube supplemented with a bit of baker's yeast for 3 days.
5. Once the females lay abundantly, transfer the cross into a fresh fly tube supplemented with a bit of baker's yeast.
6. Do an embryo collection to get flies whose development stages are synchronized (see Note 16).

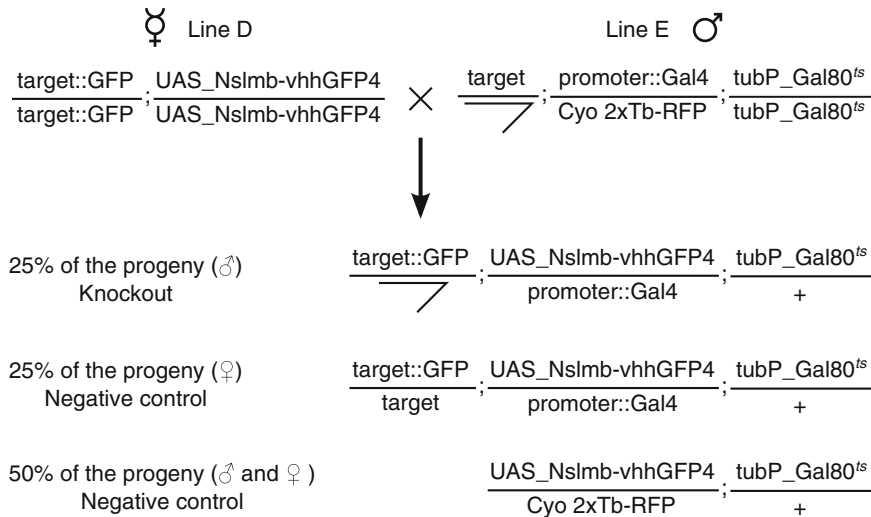


Fig. 4 Crossing scheme for performing a protein knockdown in late developmental stages. This crossing scheme is just illustrative and would need to be adapted if, for instance, *target::GFP* was not located on the X chromosome

7. At the required developmental stage, put the tube containing the progeny of the cross in a 29 °C incubator. Gal80^{ts} will become inactive by changing conformation and allow Gal4 to drive the expression of Nslmb-vhhGFP4 in the *promoter::Gal4* expression domain.
8. Leave the flies at 29 °C until you want to revert the knockdown [10] or to document the phenotype of the protein knockdown; sort them in three categories with the help of a fluorescence stereomicroscope.
 - (a) Male flies that do not carry the fluorescent balancer correspond to the actual Target::GFP knockdown.
 - (b) Female flies that do not carry the fluorescent balancer correspond to a Target::GFP knockdown, but in a background where Target is expressed. This is a negative control that does not give rise to a knockdown of the function of *target* (see Note 17).
 - (c) Flies that carry the fluorescent balancer do not express Nslmb-vhhGFP4 and represent another negative control.
9. The following steps are highly dependent on the assay one wants to perform after the knockdown of Target::GFP. For biochemical assays, one might need to scale up the amount of flies involved in the crosses. Hence, the number of flies indicated in steps 3 and 4 are purely indicative for further analysis of the phenotypes by live imaging techniques as described, for instance, in the chapters by Restrepo et al. and Cetera et al. in this volume (see Note 18).

4 Notes

1. This of course does not preclude performing western blots or immunostainings with polyclonal anti-GFP antibodies to double-check the efficiency of the knockdown.
2. Several lines carrying *UAS_Nslmb-vhhGFP4* either on the second or on the third chromosome are available from the Bloomington *Drosophila* Stock Center.
3. Several lines carrying *tubP_Gal80ts* either on the X, the second, or the third chromosome are available from the Bloomington *Drosophila* Stock Center.
4. If alternative splicing is involved in the generation of different transcripts of a GFP-tagged gene, the GFP tag must label all the splice isoforms, or at least the splice isoforms of interest.
5. deGradFP is able to knockdown GFP-tagged versions of transmembrane protein such as Crumbs, but deGradFP is only active on Crumbs::GFP-C whose GFP tag is intracytoplasmic, and is not active on Crumbs::GFP-A whose GFP tag is extracytoplasmic [3]. deGradFP has also been shown to knockdown Neurogian::GFP [21].
6. For instance, deGradFP is not effective on GFP on its own, or on any GFP-tagged version of E-cadherin we have tested.
7. In the case of Spaghetti_squash::GFP [22], we have observed that although the target protein is withdrawn from the cytoplasm, the GFP signal persists in some spotted structures (inclusion bodies?). This seems to be a minor inconvenience since a loss of function condition is still clearly created [3].
8. On average, five embryos of each possible genotype will be mounted (Fig. 2a).
9. In order to best appreciate the effect of deGraFP on Target::GFP, we advise to select stage 12–15 embryos and orient them laterally.
10. Monitoring the disappearance of the GFP signal as *Nslmb-vhhGFP4* starts to be expressed in the *en* expression domain allows to estimate how fast Target::GFP is knocked out by deGradFP.
11. If some transgenes are not homozygous viable, dfd-GMR yellow fluorescent balancers can be used to trace the different chromosomes from embryonic stage 13 on [17].
12. A second kind of negative control can be obtained by crossing a fly line carrying *UAS_Nslmb-vhhGFP4* to a fly line carrying *promoter::Gal4*. This simple cross tests the potential nonspecific effects of deGradFP in the absence of Target::GFP. So far, even with strong and ubiquitous drivers such as *tubulinGal4*, no nonspecific effect of the deGradFP effector has been reported.

13. Male wandering L3 larvae have “prominent” gonads seen as clear symmetrical structures embedded in the fat bodies that lie along the sides in the posterior part of the larvae; testes are much larger than ovaries and are easily recognizable. Male black pupae have sex combs on their anterior legs. In contrast to larvae and pupae, sexing embryos is far more challenging. One might take advantage of a fluorescent 5XQE-DsRed transgene located on the chromosome X [23]. Alternatively, one might use a monoclonal antibody raised against Sex-lethal [24] (available from The Developmental Studies Hybridoma Bank), but this precludes live imaging.
14. In an elegant series of experiments, deGradFP was used to knockdown proteins in the adult nervous system and asses their function in memory generation [10].
15. In contrast to the other crosses described in this chapter, it is important not to swap the stocks. That is to say virgins need to be collected from line E and males from line D.
16. Overnight embryo collection is usually a good compromise between the precision of the synchronization and the number of flies required for the cross.
17. In our experience, Target::GFP knockdowns in the presence of the untagged Target does not produce dominant negative effects. In different words, Target::GFP/Target oligomers do not induce the degradation of Target. However, this might be different for each tagged protein.
18. *UAS_Nslmb-vhhGFP4* was cloned in P{UAST} (available from Addgene; <https://www.addgene.org>), and the *UAS_Nslmb-vhhGFP4* fly lines available from the Bloomington *Drosophila* Stock Center cannot be used to drive the expression of *Nslmb-vhhGFP4* in the female germline. To that purpose, a *UAS_Nslmb-vhhGFP4* transgene cloned in P{UASp} has been generated [25].
deGradFP has been also used to knockdown GFP fusion proteins during spermatogenesis [26].

Acknowledgements

The authors thank the Bloomington *Drosophila* Stock Center (Indiana University, Bloomington) for providing fly stocks, and Addgene for providing plasmids.

References

- Dietzl G, Doris CD, Schnorrer F et al (2007) A genome-wide transgenic RNAi library for conditional gene inactivation in *Drosophila*. *Nature* 448:151–156
- Ni JQ, Zhou R, Czech B et al (2011) A genome-scale shRNA resource for transgenic RNAi in *Drosophila*. *Nat Methods* 8:405–407
- Caussinus E, Kanca O, Affolter M (2012) Fluorescent fusion protein knock-out mediated by anti-GFP nanobody. *Nat Struct Mol Biol* 19:117–121
- Caussinus E, Kanca O, Affolter M (2013) Protein knockouts in living eukaryotes using deGradFP and green fluorescent protein fusion targets. *Curr Protoc Protein Sci* 73:Unit 30.2
- Ciechanover A (1998) The ubiquitin-proteasome pathway: on protein death and cell life. *EMBO J* 17:7151–7160
- Varshavsky A (2012) The ubiquitin system, an immense realm. *Annu Rev Biochem* 81:167–176
- Morin X, Daneman R, Zavortink M et al (2001) A protein trap strategy to detect GFP-tagged proteins expressed from their endogenous loci in *Drosophila*. *Proc Natl Acad Sci U S A* 98:15050–15055
- Lowe N, Rees JS, Roote J et al (2014) Analysis of the expression patterns, subcellular localisations and interaction partners of drosophila proteins using a pigp protein trap library. *Development* 141:3994–4005
- Venken KJT, Carlson JW, Schulze KL et al (2009) Versatile P[acman] bac libraries for transgenesis studies in *Drosophila melanogaster*. *Nat Methods* 6:431–434
- Nagarkar-Jaiswal S, Lee PT, Campbell ME et al (2015) A library of Mimics allows tagging of genes and reversible, spatial and temporal knockdown of proteins in *Drosophila*. *Elife*. doi:[10.7554/eLife.05338](https://doi.org/10.7554/eLife.05338)
- Nagarkar-Jaiswal S, DeLuca SZ, Lee PT et al (2015) A genetic toolkit for tagging intronic mimic containing genes. *Elife*. doi:[10.7554/eLife.08469](https://doi.org/10.7554/eLife.08469)
- Ciechanover A, Ben-Saadon R (2004) N-terminal ubiquitination: more protein substrates join in. *Trends Cell Biol* 14:103–106
- Jiang J, Struhl G (1998) Regulation of the hedgehog and wingless signalling pathways by the F-box/WD40-repeat protein Slimb. *Nature* 391:493–496
- Saerens D, Pellis M, Loris R et al (2005) Identification of a universal VHH framework to graft non-canonical antigen-binding loops of camel single-domain antibodies. *J Mol Biol* 352:597–607
- Rothbauer U, Zolghadr K, Tillib S et al (2006) Targeting and tracing antigens in live cells with fluorescent nanobodies. *Nat Methods* 3:887–889
- Tabata T, Eaton S, Kornberg TB (1992) The *Drosophila* hedgehog gene is expressed specifically in posterior compartment cells and is a target of engrailed regulation. *Genes Dev* 6:2635–2645
- Le T, Liang Z, Patel H et al (2006) A new family of *Drosophila* balancer chromosomes with a w-Dfd-GMR yellow fluorescent protein marker. *Genetics* 174:2255–2257
- Pina C, Pignoni F (2012) Tubby-RFP balancers for developmental analysis: FM7c 2xTb-RFP, Cyo 2xTb-RFP, and TM3 2xTb-RFP. *Genesis* 50:119–123
- Matsumoto K, Toh-e A, Oshima Y (1978) Genetic control of galactokinase synthesis in *Saccharomyces cerevisiae*: evidence for constitutive expression of the positive regulatory gene gal4. *J Bacteriol* 134:446–457
- McGuire SE, Le PT, Osborn AJ et al (2003) Spatiotemporal rescue of memory dysfunction in *Drosophila*. *Science* 302:1765–1768
- Tilmann B, Dominique F, Stefan L (2014) The transmembrane protein Macroglobulin complement-related is essential for septate junction formation and epithelial barrier function in *Drosophila*. *Development* 141:899–908
- Rouyou A, Field C, Sisson JC et al (2004) Reassessing the role and dynamics of non-muscle myosin II during furrow formation in early *Drosophila* embryos. *Mol Biol Cell* 15:838–850
- Zecca M, Struhl G (2007) Recruitment of cells into the *Drosophila* wing primordium by a feed-forward circuit of vestigial autoregulation. *Development* 134:3001–3010
- Bopp D, Bell LR, Cline TW et al (1991) Developmental distribution of female-specific sex-lethal proteins in *Drosophila melanogaster*. *Genes Dev* 5:403–415
- Urban E, Nagarkar-Jaiswal S, Lehner CF et al (2014) The cohesin subunit Rad21 is required for synaptonemal complex maintenance, but not sister chromatid cohesion, during *Drosophila* female meiosis. *PLOS Genetics* 10:e1004540
- Rubliaychaudhuri N, Dubruille R, Orsi GA et al (2012) Transgenerational propagation and quantitative maintenance of paternal centromeres depends on Cid/Cenp-A presence in *Drosophila* sperm. *PLoS Biol* 10:e1001434
- Harder B, Schomburg A, Pflanz R et al (2008) Tev protease-mediated cleavage in *Drosophila* as a tool to analyze protein functions in living organisms. *Biotechniques* 44:765–772

Chapter 10

Sample Preparation and Mounting of *Drosophila* Embryos for Multiview Light Sheet Microscopy

Christopher Schmied and Pavel Tomancak

Abstract

Light sheet fluorescent microscopy (LSFM), and in particular its most widespread flavor Selective Plane Illumination Microscopy (SPIM), promises to provide unprecedented insights into developmental dynamics of entire living systems. By combining minimal photo-damage with high imaging speed and sample mounting tailored toward the needs of the specimen, it enables *in toto* imaging of embryogenesis with high spatial and temporal resolution. *Drosophila* embryos are particularly well suited for SPIM imaging because the volume of the embryo does not change from the single cell embryo to the hatching larva. SPIM microscopes can therefore image *Drosophila* embryos embedded in rigid media, such as agarose, from multiple angles every few minutes from the blastoderm stage until hatching. Here, we describe sample mounting strategies to achieve such a recording. We also provide detailed protocols to realize multiview, long-term, time-lapse recording of *Drosophila* embryos expressing fluorescent markers on the commercially available Zeiss Lightsheet Z.1 microscope and the OpenSPIM.

Key words *Drosophila melanogaster*, Embryogenesis, Live imaging, Light sheet microscopy, SPIM, Multiview

1 Introduction

Light sheet fluorescent microscopy (LSFM) is an emerging imaging technique ideally suited for imaging cellular dynamics in intact developing *Drosophila* embryos expressing fluorescent markers. With LSFM it is possible to record the developing embryos from early blastoderm stage until the fully hatched larva. LSFM is using a laser light sheet to illuminate the sample and an objective lens positioned at a 90° angle with respect to the light sheet to image the illuminated plane (Fig. 1a). This arrangement achieves optical sectioning and since only the current acquired section is illuminated leads to very low bleaching and phototoxicity. A digital camera captures the light, with high signal-to-noise ratio and allows very high speed of acquisition [1]. Although several flavors of light sheet microscopy are relevant to *Drosophila* imaging [2], the most commonly used modality is Selective Plane Illumination Microscopy

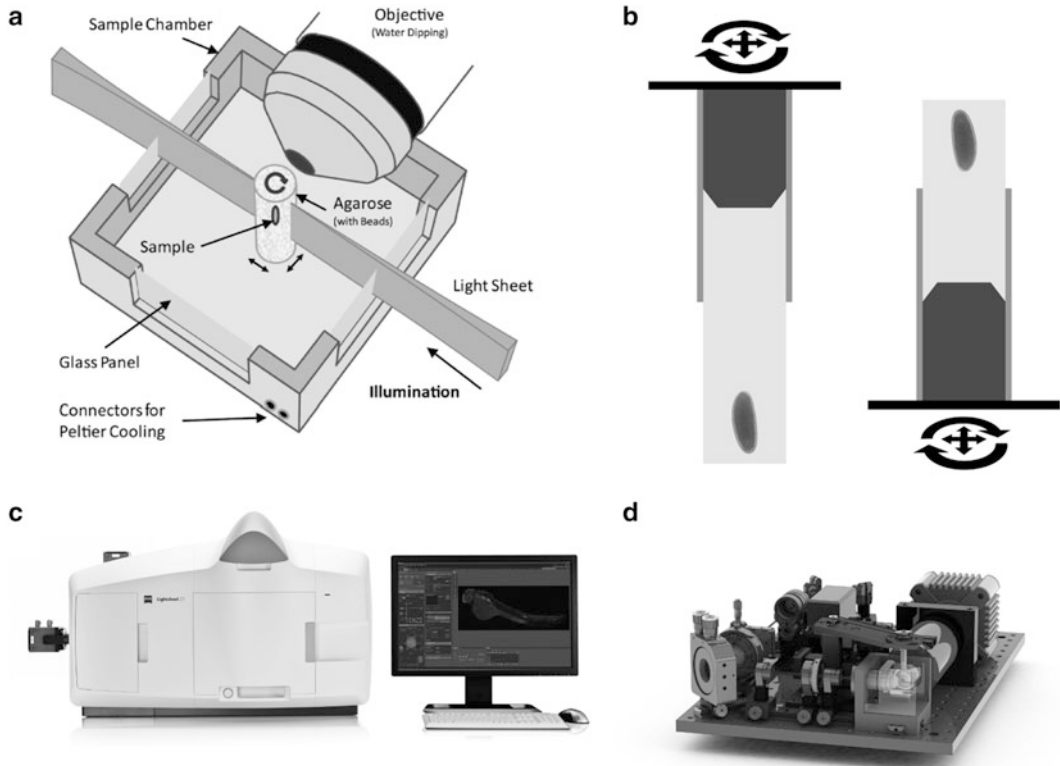


Fig. 1 SPIM principle, sample mounting, and readily available SPIM set-ups. The sample is illuminated with a thin laser light sheet. The lens is positioned orthogonally in respect to the light sheet. The sample can be moved in x, y, z and can be rotated around its axis (a). Mounting with sample suspended from above and below, a metal plunger (dark grey) pushes the agarose (light grey) with the embryo specimen out of a capillary (medium grey) into the sample chamber buffer (b). Commercially available SPIM from Carl Zeiss Microscopy—Lightsheet Z.1 (c) and DIY Open SPIM (d). Figure (a) adapted from ref. [13]. Figure (b) adapted from ref. [11]. Figure (c) © Copyright of Carl Zeiss Microscopy GmbH

(SPIM) that achieves complete coverage of the embryo specimen by imaging it from multiple angles over time [1].

The so-called multiview SPIM imaging of ubiquitously expressed nuclear markers has been used to demonstrate the ability of light sheet microscopy to record developmental anatomy *in toto* [3, 4]. In combination with the plethora of available gene expression reporters [5, 6], SPIM also provides the means to record the dynamics of the gene expression pattern formation during the entire process of *Drosophila* embryogenesis.

The major change SPIM imposes on established imaging protocols are the fundamentally different approaches to sample preparation. In SPIM, the sample is typically embedded in agarose inside a glass capillary. For imaging, the embryos immobilized in agarose are pushed outside of the capillary to enable penetration of the light sheet from the side while avoiding diffraction of the light sheet. The capillary with the agarose column is suspended in a

chamber filled with buffer [7]. This can be done either from above or from below, however most available SPIM set-ups implement the sample suspension from above (Fig. 1b). This sample-mounting paradigm allows moving the sample through the light sheet in the z-axis and thus the acquisition of 3D image stacks (series of 2D images produced by optical sectioning with the light sheet). Moreover, the sample can be rotated and multiple stacks (views) of the same specimen from different angles can be imaged. This allows imaging of even very thick or opaque samples in their entirety [1]. Coupled with image processing [8], these different views can be fused and the sample can be reconstructed *in toto* with isotropic resolution. Typically, fluorescent beads are embedded in the agarose together with the embryos to serve as fiduciary markers facilitating the multiview reconstruction and fusion of the views by multiview deconvolution [9, 10].

Principally, two hardware implementations are readily available to achieve multiview imaging: the commercially available Lightsheet Z.1 from Carl Zeiss Microscopy (Fig. 1c) and the “do-it-yourself” (DIY) open access OpenSPIM [11] (Fig. 1d). In both set-ups, a cylindrical lens forms the light sheet. Lightsheet Z.1 offers dual-sided illuminations and pivoting of the light sheet. This reduces the degradation of the light sheet across the field of view and the “stripe” artifacts caused by absorption of the light sheet within the sample [12].

Here, we present a detailed description of the mounting methods for SPIM and the imaging setup employed in our lab, for long-term time-lapse live imaging of *Drosophila* embryogenesis on Lightsheet Z.1. Both the mounting method and the imaging set-up can be easily adapted for imaging with OpenSPIM.

2 Materials

1. Embryo Collection Cages with Stainless steel mesh—97 μ m.
2. Phosphate-buffered saline—1× without Mg, Ca.
3. Sodium hypochlorite solution (6–14 % active chlorine)—2.5 l.
4. Sterile Cell Strainer—100 μ m mesh size.
5. Piston rod f.Transferpettlor Fix+Dig. 10 μ l.
6. n-Heptane.
7. Tape—natural rubber.
8. Fluorescent Microspheres—F-Y 050 and F-Z 050 (*see Note 1* for selection, *Note 2* for preparation).
9. Low melting point (LMP) agarose; Sea Plaque Agarose (*see Note 3* for preparation).
10. Eppendorf tubes—1.5 ml.

11. Petri dishes—60 × 15 mm.
12. Plastic Pasteur pipettes—3 ml.
13. Powder free gloves—Nitril gloves.
14. Thermomixer.
15. Vortex.
16. Centrifuge.
17. Microscope slides—76 × 26 mm.
18. Brushes
19. Blunt forceps.
20. Beaker.

3 Methods

3.1 Mounting of Embryos

3.1.1 Mounting in Agarose for Multiview Imaging

In order to perform multiview imaging the sample needs to be accessible to the illumination and detection optics from all sides. For this we embed the embryos in low melting point (LMP) agarose and mount them in a glass capillary. For imaging, the agarose is pushed out of the capillary and the sample is suspended freely in the sample chamber (see Fig. 1b). The agarose has a similar refractive index as the immersion medium in the sample chamber of the microscope, thus the light sheet can penetrate the agarose column with minimal refraction or scattering [1].

To computationally reconstruct the sample, the different views need to be registered onto each other. We use fluorescent beads in the surrounding agarose as fiduciary markers to achieve this (see Note 1). The beads are simply added at an appropriate concentration to the agarose before it polymerizes. After detection of the beads registration overlays the corresponding beads from the different angles. Then the views can be fused either by content-based multiview fusion or multiview deconvolution. This recovers the complete volume of the sample at isotropic resolution [8–10].

1. Prepare beforehand:

- (a) Liquid 2% LMP agarose in PBS cooled down to min. 37 °C (see Note 3).
- (b) 1:100 bead dilution of fluorescent beads matching the imaging experiment conditions (see Notes 1 and 2)
- (c) Prepare capillaries with plungers such that the plunger sticks out a few millimeters at the bottom of the capillary to avoid drawing in air.
- (d) 50 ml 20% bleach in PBS.
- (e) Timed *Drosophila* embryos.
- (f) Beaker filled with PBS.

2. Remove excess yeast paste from the apple juice plate.
3. Add water to the apple juice plates and loosen the embryos with a brush (see Fig. 2a).
4. Transfer the embryos into a sieve by pouring the water into the sieve.
5. Wash the embryos briefly with water (see Fig. 2c).
6. Transfer the sieve into a petri dish filled with 20% bleach.
7. During bleaching apply fresh bleach onto the side of the sieve with a plastic Pasteur pipette (see Fig. 2d).
8. Bleach embryos under a stereomicroscope for up to 2 min or until properly dechorionated (see Fig. 2e for dechorionated

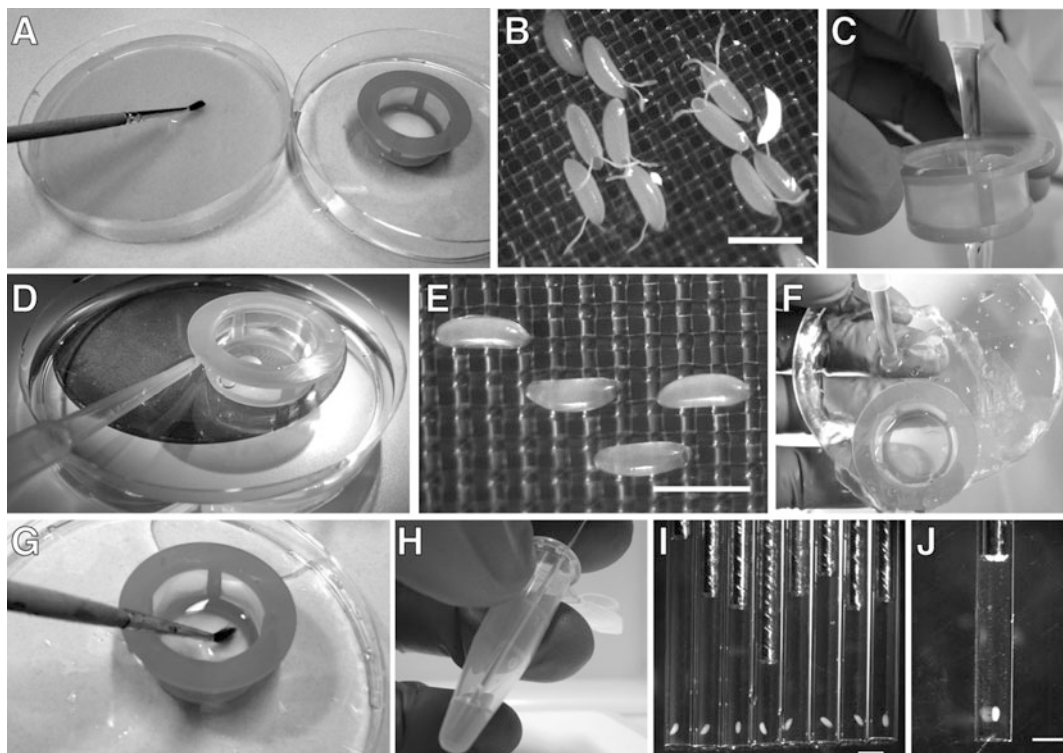


Fig. 2 Agarose mounting of embryos. The embryos are loosened with a brush from the apple juice plate (a). *Drosophila* embryos with intact chorion, note the dorsal appendages (b). After transfer into the sieve the embryos are washed briefly (c) and dechorionated under a stereomicroscope (d). Dechorionated *Drosophila* embryos with removed dorsal appendages, the surface is glossier and the embryos are more transparent (e) as compared to (b). After bleaching the embryos are washed briefly with ddH₂O, apply water onto the outside of the sieve (f). The embryos are transferred into an eppendorf tube with agarose using a brush (g). The agarose with an embryo is drawn into a capillary (h). Several embryos are mounted and a suitable sample is selected under the stereomicroscope (i). A suitable mounting with 1 embryo length of agarose below the sample and several millimeters above (note the end of the metal plunger). The embryo is upright with the AP axis roughly aligned with the axis of the glass capillary or in the desired orientation (j). Scale bars: 500 μ m (b and e) and 1 mm (i and j)

embryos and compare to Fig. 2b showing embryos with intact chorion).

9. Immediately wash the embryos with ddH₂O, by applying ddH₂O onto the side of the sieve, not directly on the embryos (see Fig. 2f).
10. Place the sieve into a petri dish filled with 1× PBS to avoid drying the embryos.
11. Mix 125 µl of 2% agarose with 112.5 µl of PBS.
12. Vortex the 1% agarose mixture briefly and put back on max. 37 °C.
13. Vortex 1:100 bead dilution for 1 min.
14. Add 12.5 µl of the bead dilution (final conc. of beads 1:2000) to the 1% agarose (see Note 4).
15. Vortex agarose bead mixture for 1 min.
16. Transfer 100 µl of agarose bead mixture into a fresh 1.5 ml eppendorf tube.
17. Place the remaining 1% agarose mixture back on max. 37 °C.
18. Transfer embryos with a brush into the 1% agarose bead mixture (see Fig. 2g).
19. Draw one embryo in each capillary and prepare 10 or more capillaries (see Note 5 and Fig. 2h).
20. Place the capillaries carefully into a beaker filled with PBS (see Note 6).
21. Check capillaries and select a sample that fulfills the following criteria (see Fig. 2i, j and Note 5):
 - (a) Embryo of the proper stage and morphology.
 - (b) Embryo properly aligned for imaging.
 - (c) No bubbles near the sample or close to the plunger.
 - (d) No debris of the chorion near the sample.
22. Repeat until one or more suitable samples for live imaging are found.
23. Store mounted embryos in PBS at room temperature until imaging.

3.1.2 Mounting on Capillaries for Multi-sample Imaging

Mounting the embryos in agarose does not lend itself easily toward imaging multiple samples at the same time. Mounting one *Drosophila* embryo in the desired orientation in agarose can be a challenge because of its shape. Mounting several of them after each other in the same orientation is therefore not practical. Additionally, extending the agarose too much will lead to an increase of swinging of the column during imaging and increases the risk of drift of the agarose column out of the capillary. Thus only a limited

number of embryos can be mounted robustly in one experiment using the agarose mounting. This limits the throughput of SPIM imaging significantly.

We addressed this problem by developing a mounting method for *Drosophila* embryos that allows imaging multiple embryos in the same recording. This method is based on gluing the embryos to the side of a glass capillary (see Note 7). Only the range of the stage in the *y*-axis and the time resolution limits the number of embryos one is able to image in a single experiment. This method thus is ideal for screening and testing of imaging conditions.

1. Prepare beforehand:

- (a) Capillaries coated with glue (see Note 8).
- (b) Mounting setup: A microscopy slide is fixed on the cover of a petri dish using double-sided tape. The capillary is fixed with plasticine next to the slide with the coated side on top. Adjacent to the capillary a piece of double-sided tape is placed on the microscopy slide (see Fig. 3a)
- (c) Staged *Drosophila* embryos.

2. Take up embryos with blunt forceps (see Fig. 3b)

3. Place the embryos on the double-sided tape next to the capillary (see Fig. 3c).

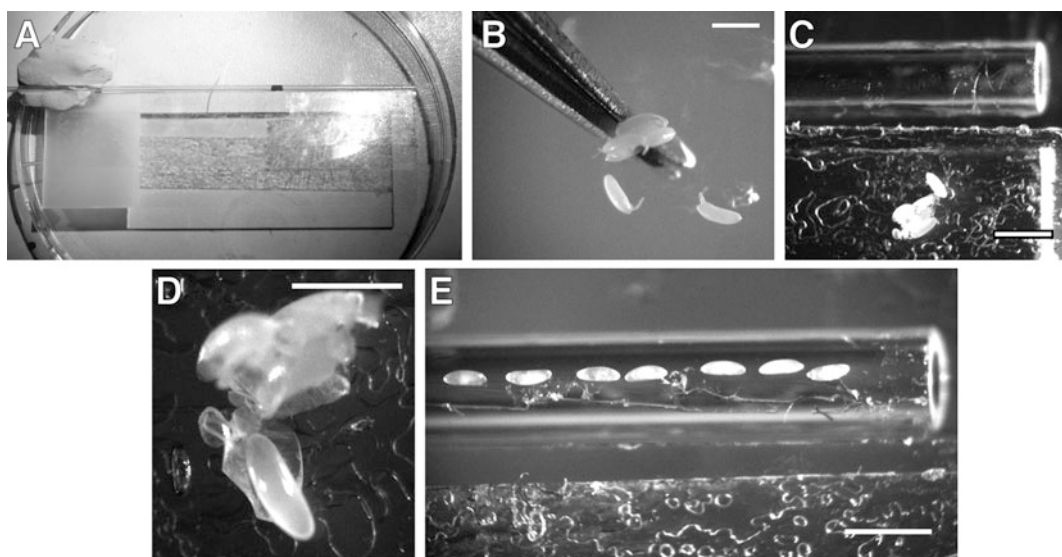


Fig. 3 Multi-sample mounting of embryos. A slide is fixed on the lid of a petri dish with double-sided tape. The capillary is fixed adjacent to the slide with plasticine. Double-sided tape is on the slide adjacent to the capillary (a). Embryos are transferred from the apple juice plate onto the double-sided tape with blunt forceps (b and c). The embryos are dechorionated by gently rolling them on the tape (d). The embryos are mounted on the coated glass capillary in the desired orientation (e). Scale bars: 500 μ m (b and d) 1 mm (c and e)

4. Roll each embryo carefully on the tape until the embryo pops out of the chorion (see Fig. 3d).
5. Transfer the embryo with its intended orientation onto the coated capillary (see Fig. 3e).
6. Submerge the capillary in PBS after enough embryos are mounted.

3.2 Live Imaging Experiment Using Lightsheet Z.1

3.2.1 Light Sheet alignment

First, we will describe the microscope setup for both multiview and multi-sample imaging (see Note 9). Specific conditions for each of the methods are found in their respective sections.

The key step for successful LSFIM imaging is the alignment of the center of the light sheet in the focus of detection objective (see Note 9). We are using the symmetry of point-spread functions (PSF) of fluorescent beads as readout for the correctness of the alignment. Alternatively, one can also use the intensity and sharpness of the sample for alignment [14, 15].

1. Prepare beforehand:
 - (a) Bead sample without biological sample (see Note 9)
 - (b) Prepare the sample chamber and the microscope according to the company protocol.
 - (c) Set the correction collar of the objective lens to 1.33 (refractive index of water).
2. Set up the basic parameters for your imaging experiment in the ZEN black software of the Lightsheet Z.1 microscope:
 - (a) Activate the necessary laser lines.
 - (b) Select the correct objective in the software (see Note 10).
 - (c) Choose the correct laser-blocking filter for your lasers.
 - (d) Choose suitable emission filters.
 - (e) Set the zoom: for the 20 \times /1.0 lens, a zoom of 0.8x is sufficient to cover the entire *Drosophila* embryo. Only for the alignment: Select single-sided illumination, untick *online dual side fusion* and *pivot scan*.
 - (f) Set the frame size to 1200 \times 1920 px (for an upright embryo).
 - (g) Laser setting for 488 nm laser: 8 mW 561 nm laser: 15 mW, exposure time: 30 ms (see Note 11).
3. For the first alignment use the automatic light sheet alignment of the software or move the manual setting such that the beads are in focus and appear in their highest intensity (see Fig. 4c for aligned light sheet and compare to Fig. 4a for misaligned light sheet).

4. Acquire a stack of the agarose column closest to the objective using the lowest possible interval size. A stack of 20 μm is sufficient.
5. Evaluate the axial symmetry of the PSF using the *ortho* tool in ZEN black (see Fig. 4b for aligned light sheet and compare to Fig. 4d for misaligned light sheet).
6. Move the light sheet and repeat the stack until an optimal symmetry is reached for one side of the light sheet (see Fig. 3d).
7. Repeat for the second light sheet.
8. Optional: reset the correction collar on the objective to reduce spherical aberrations and then readjust the light sheet to achieve again a symmetrical PSF.
9. After the light sheets are adjusted, switch to dual-sided illumination, tick *online dual side fusion* and *pivot scan*.

3.2.2 Setup for Multiview Imaging

1. Insert the capillary into the sample holder from the top.
2. The red mark of the capillary should be at the bottom of the sample holder (see Fig. 4e arrowhead).
3. Place the sample holder into the stage of the microscope.
4. Move the capillary into the field of view of the objective.
5. Push out the agarose until the embryo is visible.

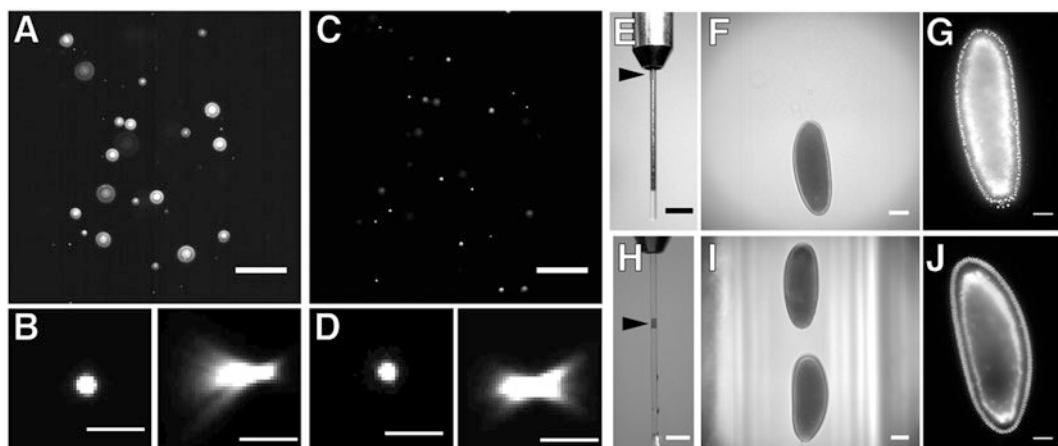


Fig. 4 Light sheet alignment. Diffraction rings of out of focus beads in a *xy*-slice through a stack acquired with a misaligned light sheet (a). *xy*- and *yz*-slices of a PSF of a bead acquired with a misaligned light sheet (b). Beads appear sharp in a *xy*-slice through a stack acquired with an aligned light sheet (c). *xy*- and *yz*-slices of the PSF of a bead acquired with an aligned light sheet. The PSF appears symmetrical in *yz* (d). Sample holder for multiview mounting, the red marker on the capillary (arrowhead) is positioned below the bottom of the sample holder (e). The agarose is pushed 2–3 embryo lengths out of the capillary, such that the capillary is out of the field of view of the microscope (f). Expression of His-YFP imaged with multiview agarose mounting (g). Sample holder for multi-sample mounting, the red marker (arrowhead) is positioned 1 cm below the sample holder (h). *Drosophila* embryos imaged using multi-sample mounting (i and j). Scale bars: 50 μm (a, c, g, and j), 5 μm (b and d), 5 mm (e and h) and 100 μm (f and i)

6. Further push out the agarose, until the embryo is 2–3 embryo lengths away from the bottom of the glass capillary (see Fig. 4f).
7. Wait until the agarose is stable (see Note 12).
8. Move the sample to the position were the first view should be. Read out the angle of the first position from the *specimen navigator* of the software and calculate the angles for the rest of the positions (see Note 13).
9. For each stack move the sample into the centre of the field of view. Set the first slice 10–15 μm on top of the embryo and the last one well past the waist of the embryo and set the step size to 1.5 μm (see Note 14).
10. When the first and the last slice of the stack are determined add the positions in the *multiview setup*.
11. Type in the next angle into the angle field of the *specimen navigator*.
12. Move the embryo again into the centre of the field of view and set the stack for this view and add it to the *multiview setup*.
13. After all views are added, set the number of cycles and the interval of the time-lapse in the *time series* tab and start the recording (see Note 15).
14. Observe the first couple of time points.
15. If there is dramatic movement of the agarose adjust the *multiview setup* and restart the time-lapse or replace the sample.

3.2.3 Setup for Multi-sample Imaging

1. Insert the capillary from below into the sample holder.
2. Between the bottom of the sample holder and the red mark should be about 1 cm, since there will be no agarose (see Fig. 4h arrowhead).
3. Carefully mount the sample holder in the stage. Do not touch the stage with the capillary.
4. Move the capillary into the field of view.
5. Locate the embryos and rotate them such that they are now facing the objective (see Fig. 4i).
6. Since there is no agarose that can move, directly start to prepare the recording.
7. Rotate the sample until the first embryo is in the correct position and such that the capillary does not reflect the light sheet (see Note 7).
8. Set the first stack 10–15 μm above the embryo and the last stack until the image quality is too degraded or the capillary starts to reflect the light sheet (see Note 16).
9. Set the interval, we recommend using the optimal setting suggested by the software.

10. After the first and the last slice are set, add the position to the *multiview setup*.
11. Move to the next embryo, adjust the stack and add it to the *multiview setup*
12. Choose *new* in the group tab, this assigns a new group to this embryo.
13. After each group has been set up, select the number of cycles in the time series tab and start the recording.
14. Observe the first few time points and determine if the entire embryo is acquired for each group.

4 Notes

1. Choose and test the fluorescent beads based on the laser lines, laser power, and filter settings used in the imaging experiment. For example for single channel imaging, using a 488 nm laser and a longpass filter we use the Estapor fluorescent microspheres F-Y 050. For single channel imaging, using a 561 nm laser and a longpass filter we use the Estapor fluorescent microspheres F-Z 050 beads. For dual channel experiments it is recommended to use beads that are visible in both imaged channels since different wavelengths have different effects on the registration. Sometimes this is not practical, either no beads can be found that are visible in all imaged channels or the beads would dominate the image too much in certain channels. To address this problem, suitable beads in one channel can be imaged and the registration of this channel is then applied to the others.
2. Prepare a 1:100 dilution from the stock solution: Vortex the bead stock for 1 min. Add 10 μ l of the bead stock to 990 μ l of sterile ddH₂O and store at 4 °C until use. The bead dilution should be sterile and in ddH₂O, contamination or use of buffers leads to the formation of bead clumps. In general vortexing before use is enough to dissociate the beads but sonication can also be helpful. Never heat up the Estapor fluorescent latex microspheres since they will lose their dye. Always vortex the bead dilution before use!
3. Preparation of 2% LMP agarose: Weigh in 30 mg of LMP agarose in 1.5 ml of 1× PBS. Heat up to 70 °C at 900 rpm on a thermomixer until the agarose is fully dissolved. Spin in a centrifuge for 5 min at max speed at 37 °C and transfer supernatant into a new tube to get rid of any undissolved agarose. Keep on 37 °C 900 rpm on a thermomixer until use or store at RT and heat up before use. The buffer in the agarose should

match the buffer used for the experiment to avoid shrinking or swelling of the agarose.

4. We found that a dilution of 1:2000 in the final sample works best with our imaging setup and gives a robust registration. Depending on your multiview setup, the size of the stacks, and the overlap between the different views, you may want to vary this concentration.
5. We found that it is best to have only a small column of agarose. One or two embryo lengths below the sample and about 2–3 mm above is best. At most there should be a half a cm of agarose column in total. This prevents that the agarose column falls out of the capillary during imaging, reduces swinging of the agarose column during imaging and reduces the initial swelling and shrinking of the agarose.
6. Avoid dropping the capillaries into the beaker. If the room temperature exceeds 25 °C the capillaries need to be placed briefly at 25 °C before putting them into the buffer in order for the agarose to solidify, otherwise the embryos fall out of the capillary.
7. Please note that the glass capillary is restricting the angle of imaging by blocking or scattering the light sheet, thus true multiview is not possible with this method and only a limited number of views can be acquired reliably. This drawback is offset by the increased throughput allowing imaging of multiple embryos with high speed. Also the software allows using different imaging conditions (i.e. laser power) and thus multiple different setups can be explored efficiently.
8. Cut pieces of double-sided tape and transfer them into a bottle with n-Heptane. Incubate at room temperature overnight before use, to allow the glue to dissolve from the tape and store at room temperature. Prepare glass capillaries by dispensing and distributing n-heptane glue with a tip onto the capillaries.
9. We generally recommend setting up the microscope before starting the mounting procedure, since the embryos are already developing. We use an agarose bead sample without biological specimen for the alignment and we recommend using beads that are visible in all imaged channels. This not only allows judging proper alignment of the light sheet in all channels but also ensures that the channels are aligned to each other. The alignment is then based on beads in the centre of the field of view and in the top section of the agarose close to the objective. The PSFs of beads in this part are the least influenced by optical aberrations introduced by the agarose or the objective.

10. The calibration contains the voxel size in xy and z . These parameters are stored in the metadata of the .czi format. The xy size depends on the magnification of the lens and the selected zoom. Whereas the z size is determined by the step size of the motors in the z direction. It is very important to select the correct lens in the program otherwise the xy to z ratio is incorrectly stored in the metadata of the dataset and the processing will fail.
11. We in general use the smallest exposure time available and rather adjust the laser intensity settings, very fast and dynamic processes would otherwise get distorted or blurred. The embryos are most sensitive to 488 nm irradiation and are more tolerant against 561 nm.
12. In the beginning, the agarose will expand or shrink in the capillary. Wait until the agarose is equilibrated or alternatively readjust the stacks during imaging. We usually observe that the agarose is shrinking and thus moving up into the capillary, but it is also possible that the agarose is expanding out further. Equilibration usually takes 15–45 min, in rare cases this can take even longer. Thus plan your experiment around this and start the mounting accordingly and prepare multiple samples or adjust the multiview setup during the recording.
13. We recommend designing the principle multiview setup before starting the experiment to avoid exposing the sample unnecessarily. Decide on the number of views and the angles between the views. Then calculate the angles for each view once you determined the first view.
14. For us 130.5 μm work best, we also recommend setting each stack to the same size. We use a step size of 1.5 μm , this allows faster acquisition of each time point.
15. Before beginning the recording, we recommend to save the multiview setup and make a screenshot of the window. We also recommend splitting the .czi files by time points and views in the *separate files* tab.
16. Usually a stack of 140 μm is possible, we recommend setting each stack to the same size. Test the time it takes to acquire one stack. This will determine the time resolution one can achieve by multiplying this number by the number of groups. For example if one stack takes 30 s, 5 groups will take about 2 min and 30 s to acquire. Set this number with a bit extra time to account for the movement of the stage in the time-lapse interval.

References

- Huisken J, Swoger J, Del Bene F, Wittbrodt J, Stelzer EH (2004) Optical sectioning deep inside live embryos by selective plane illumination microscopy. *Science*, 305(5686): 1007–1009.
- Keller PJ (2013) Imaging morphogenesis: technological advances and biological insights. *Science*, 340(6137):1234168. doi:[10.1126/science.1234168](https://doi.org/10.1126/science.1234168)
- Kržić U, Gunther S, Saunders TE, Streichan SJ, Hufnagel L (2012) Multiview light-sheet microscope for rapid *in toto* imaging. *Nat Methods*, 9(7):730–3. doi:[10.1038/nmeth.2064](https://doi.org/10.1038/nmeth.2064)
- Tomer R, Khairy K, Amat F, Keller PJ (2012) Quantitative high-speed imaging of entire developing embryos with simultaneous multiview light-sheet microscopy. *Nat Methods*, 9(7):755–63. doi:[10.1038/nmeth.2062](https://doi.org/10.1038/nmeth.2062)
- Ejsmont RK, Sarov M, Winkler S, Lipinski KA, Tomancak P (2009) A toolkit for high-throughput, cross-species gene engineering in *Drosophila*. *Nat Methods*, 6(6):435–7. doi:[10.1038/nmeth.1334](https://doi.org/10.1038/nmeth.1334)
- Nagarkar-Jaiswal S, DeLuca SZ, Lee P-T, Lin W-W, Pan H, Zuo Z, Lv J, Spradling AC, Bellen HJ (2015) A genetic toolkit for tagging intronic MiMIC containing genes. *eLife*, 4. doi:[10.7554/eLife.08469](https://doi.org/10.7554/eLife.08469)
- Reynaud EG, Kržić U, Greger K, Stelzer EHK (2008) Light sheet-based fluorescence microscopy: more dimensions, more photons, and less photodamage. *HFSP J*, 2(5):266–75. doi:[10.2976/1.2974980](https://doi.org/10.2976/1.2974980).
- Schmied C, Stamataki E, Tomancak P (2014) Open-source solutions for SPIMage process-
ing. *Methods Cell Biol*, 123:505–29. doi:[10.1016/B978-0-12-420138-5.00027-6](https://doi.org/10.1016/B978-0-12-420138-5.00027-6)
- Preibisch S, Saalfeld S, Schindelin J, Tomancak P (2010) Software for bead-based registration of selective plane illumination microscopy data. *Nat Methods*, 7(6):418–9. doi:[10.1038/nmeth0610-418](https://doi.org/10.1038/nmeth0610-418).
- Preibisch S, Amat F, Stamataki E, Sarov M, Singer RH, Myers E, Tomancak P (2014) Efficient Bayesian-based multiview deconvolution. *Nat Methods*, 11(6):645–8. doi:[10.1038/nmeth.2929](https://doi.org/10.1038/nmeth.2929)
- Pitrone PG, Schindelin J, Stuyvenberg L, Preibisch S, Weber M, Eliceiri KW, Huisken J, Tomancak P (2013) OpenSPIM: an open-access light-sheet microscopy platform. *Nat Methods*, 10(7):598–9. doi:[10.1038/nmeth.2507](https://doi.org/10.1038/nmeth.2507)
- Huisken J, Stainier DYR (2007) Even fluorescence excitation by multidirectional selective plane illumination microscopy (mSPIM). *Opt Lett*, 1;32(17):2608–10.
- Preibisch S, Saalfeld S (2009) Bead-based mosaicing of single plane illumination microscopy images using geometric local descriptor matching. *SPIE Medical Imaging*, 7259, 72592S–725102S. doi:[10.1117/12.812612](https://doi.org/10.1117/12.812612)
- Weber M, Mickoleit M, Huisken J (2014) Light sheet microscopy. *Methods Cell Biol*, 123:193–215. doi:[10.1016/B978-0-12-420138-5.00011-2](https://doi.org/10.1016/B978-0-12-420138-5.00011-2)
- Gao L, Shao L, Chen B-C, Betzig E (2014) 3D live fluorescence imaging of cellular dynamics using Bessel beam plane illumination microscopy. *Nat Protoc*, 9(5):1083–101. doi:[10.1038/nprot.2014.087](https://doi.org/10.1038/nprot.2014.087)

Chapter 11

Cultivation and Live Imaging of *Drosophila* Imaginal Discs

Simon Restrepo, Jeremiah J. Zartman, and Konrad Basler

Abstract

The ex vivo cultivation and live imaging of wing discs open exciting new research avenues by overcoming the limitations of end-point analysis of fixed tissues. Here we describe how to prepare an optimized wing disc culture medium (WM1) and how to dissect and arrange wing discs for cultivation and live imaging. This protocol enables the study of dynamic phenomena such as cell division and delamination as well as the use of pharmacological compounds and biosensors. Wing discs cultured and imaged as described here, maintain constant levels of proliferation during the first ten hours of culture.

Key words Wing disc, *Drosophila*, Live imaging, Ex vivo, In vitro, Culture medium

1 Introduction

The *Drosophila* imaginal wing disc has proven to be an exquisite model organ for investigating cell signaling, signal transduction, growth control, and morphogenesis. Nonetheless, wing disc studies have been mainly limited to end-point analysis of fixed discs. To fully comprehend wing disc development we must be able to observe, characterize, and quantify dynamic phenomena ranging, for example, from morphogen transport and endo/exocytosis to cell rearrangements, proliferation, and apoptosis.

The interest in cultivating wing discs ex vivo stimulated some pioneering studies during the 1960–1980s. In particular, Robb [1], Wyss [2], Miyake [3], Milner [4], and Shearn [5] achieved transient maintenance of wing disc explants, ex vivo. Recently, a second wave of investigations has led to further advances in ex vivo culture methods and live imaging solutions for wing discs [6–9]. The work is still in its infancy and consequently the field has not settled on common practices and almost each study has been performed in unique conditions. Progress is needed, since in the absence of standardized conditions and medium formulas, reproducibility issues can arise.

Aldaz et al. reported the culture and live imaging of imaginal wing discs in Shields and Sang M3 medium supplemented with insulin—and to prevent disc movement, Methylcellulose [6]. The authors reported that this formula could be used to study proliferation, apoptosis, and wing disc eversion. However, no rationale was provided as to why M3 was chosen as a basal medium, nor was any information given on whether this formula resulted from optimization efforts.

We undertook a careful exploration of both medium formulation and live imaging setup composition [7]. To systematically cover the large parameter space of culture conditions, we implemented a high-throughput medium optimization screen on wing imaginal disc derived cells (Clone8 [4]) based on multifactorial design-of-experiments and response surface methods. Our results indicated that the choice of the basal medium formula was critical and that Schneider's insect medium was a superior choice to M3 medium as measured by the number of proliferation events that occur during *ex vivo* cultivation. Further, we showed that Schneider's medium synergized better with Insulin in comparison to other commercially available basal medium formulas. We also showed that Fly Extract was an important supplement that preferentially should not be omitted. Based on these findings we designed an optimized wing disc cultivation formula, WM1.

In parallel, we explored many different *ex vivo* culture and live imaging setups including hanging and standing drops, hyperoxic chambers, sealed and permeable culture chambers, alginate hydrogels, and extracellular matrix gels (based on Matrigel). We settled for a simple imaging setup, based on a filter membrane that can be easily assembled from commercial components: an imaging dish and a modified “Millicell” insert. Since our initial report we have realized that the Millicell insert suffices to reduce movement such that no further thickening agent such as methylcellulose (or as in our original report, an alginate gel) is required. Omitting the alginate gel greatly simplifies the procedure and increases reproducibility among samples.

Recently, Handke and collaborators decided to characterize the current limitations of wing disc *ex vivo* culture methods [9]. Their report focused mainly on Clone8 medium (a formula already shown to be suboptimal for wing disc culture in Zartman et al. [7]). They confirmed that cell proliferation slows down and eventually halts in cultured discs. In addition, they showed that extremely high levels of insulin (6.2 μ g/mL in WM1 [7] versus 200 μ g/mL in Handke et al. [9]) are able to enhance the performance of Clone8 medium to levels similar to WM1. Handke and collaborators also report that a partial dissection protocol whereby the discs are left attached to a bisected body further enhances cultivation results [9]. We have not tried this procedure, but it could potentially further enhance the results obtained with this protocol.

We consider that WM1 [7] remains a better choice than Clone8 with very high levels of Insulin (200 μ g/mL). Because it leverages

on the synergy between Schneider's medium, Fly Extract, and insulin, WM1 [7] requires an insulin concentration that is 30 times lower than what is proposed in Handke et al. [9]. Further, partial dissections tend to increase disc movement during live imaging. For these reasons, we will present a protocol based on the results published in Zartman et al. [7].

With this protocol, live imaging can be performed for upwards of ten hours during which up to 20% of cells divide—a good indication of disc health. The method presented here was originally developed for wing discs but could potentially be applied to other organs. For example, we have successfully imaged eye discs and we are confident that leg discs should be amenable too. As for our culture chamber, it would be interesting to see if it can be employed for egg chamber live imaging [10] where the employment of halocarbon oil and at times excessive compression could be negatively affecting performance.

The live imaging analysis of cultured wing discs has already started to transform our understanding of wing disc development; in particular—the study of wing disc biomechanics, such as the role of mechanical tension in cell sorting [11, 12], and orienting tissue growth [8, 13].

Future improvements to this method would include the development of a culture medium that would enable the full recapitulation of wing disc development *ex vivo*. We hope that our field will progressively reach this goal in the future.

2 Materials

2.1 WM1

1. *Schneider's Drosophila Medium* (see Note 1): Insulin (see Note 2), Penicillin/Streptomycin, 10,000 U/mL (=200× concentrated stock solution), Fly Extract.
2. *Schneider's medium stock*: Add 2.5 mL Pen/Strep solution to a 500 mL bottle of Schneider's medium.

2.2 Fly Extract

Fresh adult flies (preferentially of the y,w, genotype), Shields and Sang M3, Thermosealable plastic, 45 µm filter cup EMD, 22 µm filter cup EMD, 50 mL tubes.

2.3 Equipment for Fly Extract Preparation

1. Thermometer.
2. Waterbath.
3. Large Centrifuge.
4. Large glass pipette *or* Large glass bottle.

2.4 Material for Sterile Dissections

1. Horizontal flow hood.
2. Dissection microscope.
3. A siliconized glass dish (see Note 17).

4. To siliconize the glass dish:
5. Sigmacote.
6. Sterilin 90 mm cell culture dish (*see Note 14*).
7. Two pairs of Dissection forceps.
8. Dissection probe.
9. 200 μ l Micropipette with disposable filter tips.
10. 20 μ l Micropipette with disposable filter tips.
11. Optional, 6-well plate—*We use a 6-well plate to wash and sterilize larvae prior to dissection.*
12. Sterile Agar petri dish—*We use sterile Agar petri dishes to keep the larvae healthy but sterile after the washing step.*

2.5 Material for Imaging Chamber

1. Zell-kontakt Imaging dish 1.0 *or*
2. Mattek glass bottom dishes.
3. Millicell standing inserts, EMD.
4. Surgical scalpel.
5. Whatman filter paper.
6. Oil for Embryo Culture.

2.6 Material for Wing Disc Culture in Multi-well Plates

1. Hydrocell, low-adhesion 24-well cell culture plates.
2. Nunclon Delta Surface, 24-well cell culture plates.

2.7 Solutions

1. Ringer's (1 L): NaCl, 6.5 g, KCl, 0.42 g, CaCl₂, 0.25 g, NaHCO₃, 0.2 g
2. PBS (1 L): NaCl 8 g, KCl 0.2 g, Na₂HPO₄ 1.44 g, KH₂PO₄ 0.24 g.

3 Methods

3.1 Large-Scale Fly Extract Preparation (Fig. 1)

We developed a quick and easily scalable fly extract preparation protocol. The fly extract can be aliquoted and stored at -20 °C for at least 2 years.

1. *Fly collection:* Collect large amounts of 2–3 days old *yw* adult flies (*see Notes 3 and 4*). Anesthetize the flies with CO₂ and pour them into 50 mL Falcons kept on ice. Store at -80 °C for 2 h at least, but frozen flies can be kept up to a month (Fig. 1, 1 and 2).
2. *Fly homogenization (see Note 5)*
Prepare a long bag with thermosealable plastic (*see Note 6*) (Fig. 1, 3).
3. Gather and weigh the previously frozen flies (Fig. 1, 3). Determine the appropriate amount of M3 medium (*see Note 7*) to add:

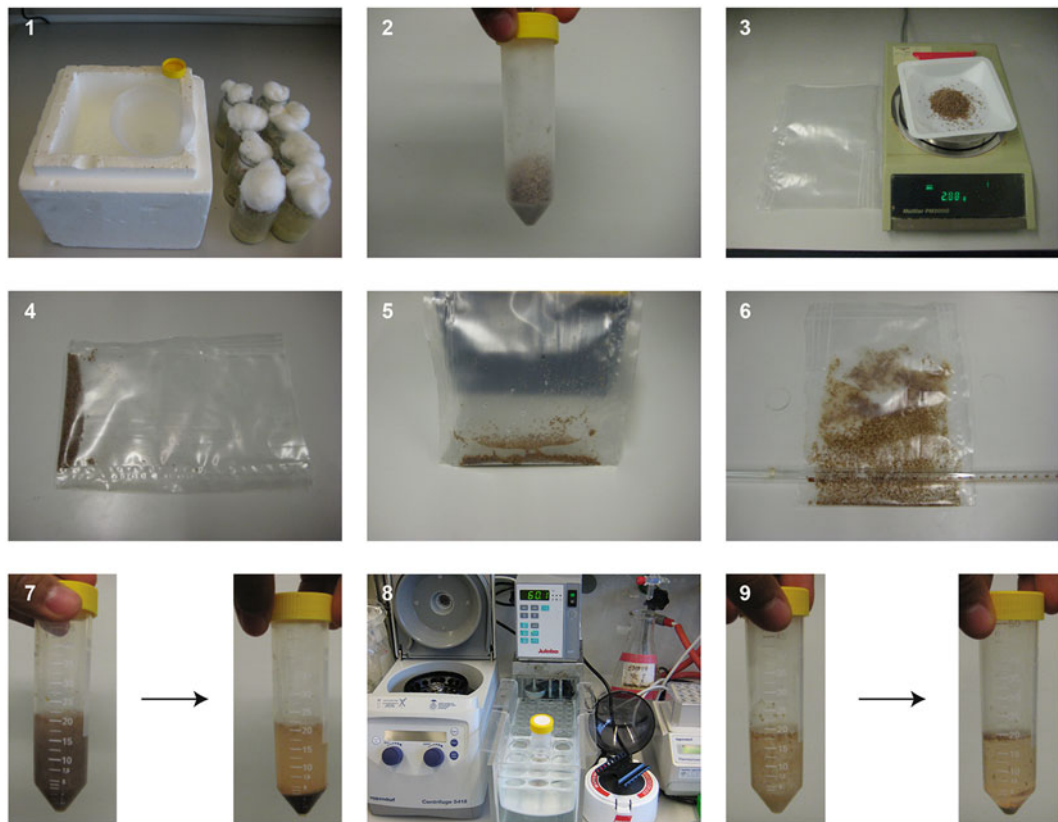


Fig. 1 Fly extract preparation 1: Anesthetize flies with CO_2 and collect them in 50 mL falcon tubes. 2: Freeze the flies at -80°C . 3: Weigh the flies. 4: Place the flies in plastic bag made of thermosealable plastic. 5: Add enough M3 medium to cover the flies. 6: Homogenize the flies with repeated rolling motions of a large glass pipette. 7: Spin down to get rid of the fly carcasses. Collect the supernatant in a new falcon tube. 8: Heat-inactivate at 60°C for 20 min. 9: The solution should have turned cloudy. Spin down to precipitate the denatured proteins. Collect the cleared supernatant. Filter sterilize and aliquot

$$\text{Required volume of M3 (mL)} = (\text{Fly weight (g})/0.22) \times 1.5$$

4. Add just enough cold M3 to cover the flies inside the bag (Fig. 1, 4)—Do not exceed the amount calculated above (see Note 8).
5. Expel any air left and seal the bag.
Ideally the following steps should be carried in a cold room at 4°C (see Note 5).
6. Squash flies with a large glass pipette or bottle with a rolling motion. Repeat until thoroughly homogenized (see Note 9) (Fig. 1, 6).
7. Carefully open bag and bring M3 volume up to required amount with fresh cold M3. Pour everything into 50 mL falcon(s) tubes (Fig. 1, 7).
8. Centrifuge at $1500 \times g$ at 4°C for 15 min (Fig. 1, 7).
9. Prepare a waterbath at 60°C (see Note 10)

10. After centrifugation, collect supernatant including surface fat/oil. Discard rest (Fig. 1, 7).
11. Heat-inactivate at 60 °C in a waterbath for 5 min (see Note 11). The solution should have turned cloudy (Fig. 1, 8 and 9).
12. Centrifuge at 1500 $\times g$ at 4 °C for 90 min to pellet denatured proteins (Fig. 1, 9).
13. Collect the solution (the Fly Extract!) and pool it in one bottle.
14. If the Fly Extract is still cloudy, filter it through a 0.45 µm filter.
15. If the Fly Extract looks clear (or after step 14), filter-sterilize it through 0.22 µm filters. The Fly Extract can be aliquoted (see Note 12) and stored at -20 °C.

3.2 WM1 Preparation

Add adequate amount of freshly thawed Fly Extract and Insulin to a chosen volume of Schneider's medium in order to reach the final concentrations:

6.2 µg/mL Insulin
5 % v/v Fly Extract.

WM1 can be kept at 4 °C for up to a month but should be discarded as soon as a precipitate or filamentous crystals can be observed.

3.3 Sterile Dissection of Wing Discs (Fig. 2)

This procedure allows the dissection of wing imaginal discs in sterile conditions (see Note 13). Our protocol was optimized to require as little medium as possible. It has the added advantage of minimizing the surface of the medium that could potentially be exposed to contaminants. This is mediated by dissecting inside stable medium drops generated by hydrophobic interactions.

1. Collect the larvae to dissect (see Note 14).
2. Sterilize larvae. Prepare a 6-well plate with 4 wells containing a sterile saline (such as Ringer's or PBS) (see Note 15) and two wells with 70 % ethanol (Fig. 2, 1). Wash the larvae twice in the saline solutions and transfer into the 70 % ethanol well. Wait 3 min and wash away the ethanol in the final saline well.
3. Place larvae on a sterile agar petri dish until dissecting (see Note 16).
4. Prepare a clean siliconized glass platform (see Note 17) for dissecting.
5. Make a 30 µl drop for dissection with WM1 (Fig. 2, 2).
6. Place a larva inside the dissection drop (Fig. 2, 3).
7. Seize larva by cuticle at mid-body with two pairs of forceps (Fig. 2, 4).
8. Tear larva open and pull the posterior side of larva outside of the medium drop, while holding the anterior side (which contains the discs). Pay attention to not rupture gut (Fig. 2, 5 and 6).

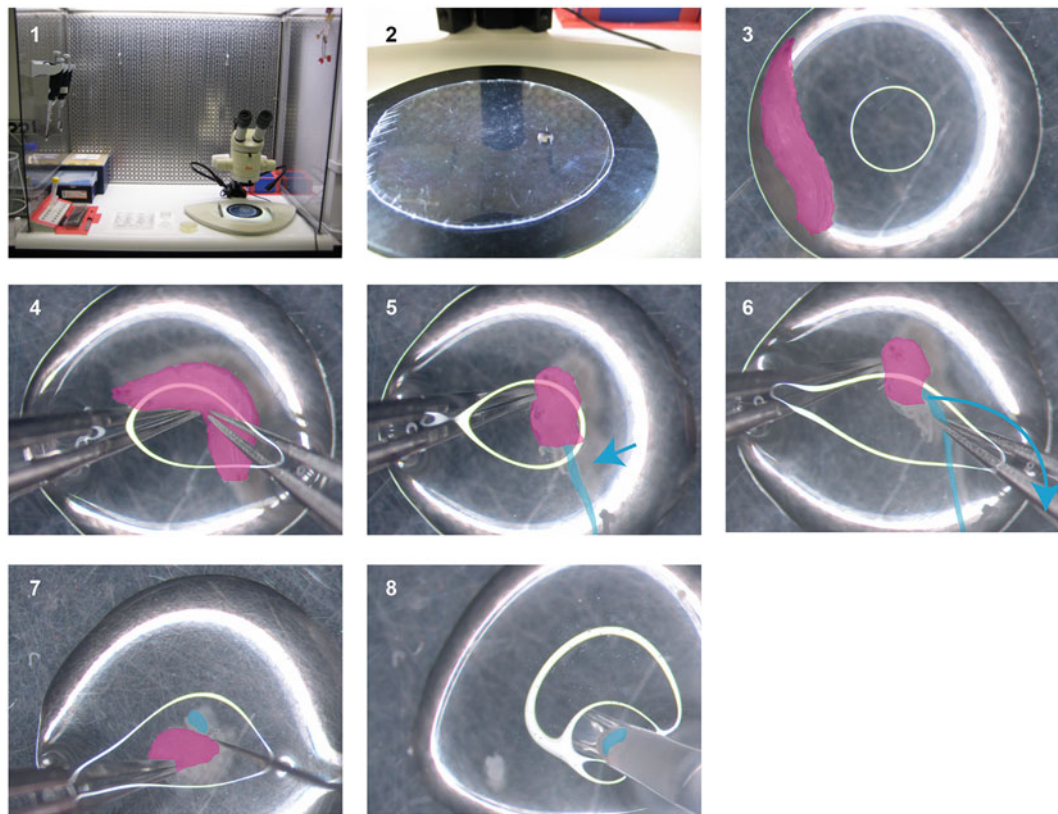


Fig. 2 Sterile dissection protocol. 1: Example of a sterile dissection station consisting of a horizontal flow hood, a dissection microscope, pipette holders, and micropipettes. Note the 6-well plate for washing and surface-sterilizing larva and a sterile petri dish to store the sterilized larvae before dissecting. Finally, note the hydrophobic dissection platform—here, the bottom of a cell culture dish. 2: Example of a dissection drop (30 μ l). 3: The surface tension of the drop is strong enough to keep the larva trapped. 4: Seize the larva by the cuticle only. Do not pinch the gut. Remove the posterior half of the larva from the drop. 5: Note that the gut is still intact (cyan). 6: Grab the anterior-most part of the gut and remove it from the dissection drop. Invert the larva. 7: Use a dissection probe to gently remove the wing discs. Be careful not to harm the discs. 8: Use a p20 micropipette to transfer the discs. Wash the discs by transferring them sequentially through three drops and proceed with the live imaging chamber assembly

9. Remove the gut gently by pulling it out of the medium drop from the anterior-most point. Pay attention not to rupture gut (Fig. 2, 6).
10. Invert the larva.
11. Cut the discs free with the dissection probe while paying attention not to stretch, scratch, or cut the discs (Fig. 2, 7).
12. Wash the discs by transferring them sequentially three times through fresh 30 μ l drops with a p20 micropipette. We use 2 μ l as a carrier volume (Fig. 2, 8). This step is used to dilute any contaminants that might have leaked during the dissection.

13. The dissected discs can be stored in a 30 μ l drop until you have sufficient specimens. About ten discs are required to be sure to find a good disc to image later.
14. Prepare an imaging chamber as described in the next section.

3.4 Preparation of the Wing Disc Live Imaging Chamber (Fig. 3)

1. Place a strip Whatman paper (10×0.5 cm) upon the walls of the live imaging dish (Fig. 3, 1). Use a p1000 to humidify the paper with PBS (400 μ l is usually enough).
2. Prepare the Millicell filter chamber by cutting off the bottom legs with a scalpel (Fig. 3, 2) (see Note 18).
3. Place a 20 μ l drop of WM1 in the middle of the live imaging dish.
4. Transfer the discs from their current “holding” drop with a p20 micropipette in 2 μ l of medium (Fig. 3, 3).
5. Ensure that the peripodial membrane facing down (you can use the dissection probe to orient the discs) (Fig. 3, 4).
6. Place the chamber on top of the disc gently but rapidly, avoiding lateral movements (Fig. 3, 5) (see Notes 19 and 20).
7. Add 200 μ l of WM1 into the imaging chamber (see Note 21).
8. Close the live imaging chamber (see Note 22).
9. Go to the microscope (see Notes 23 and 24)

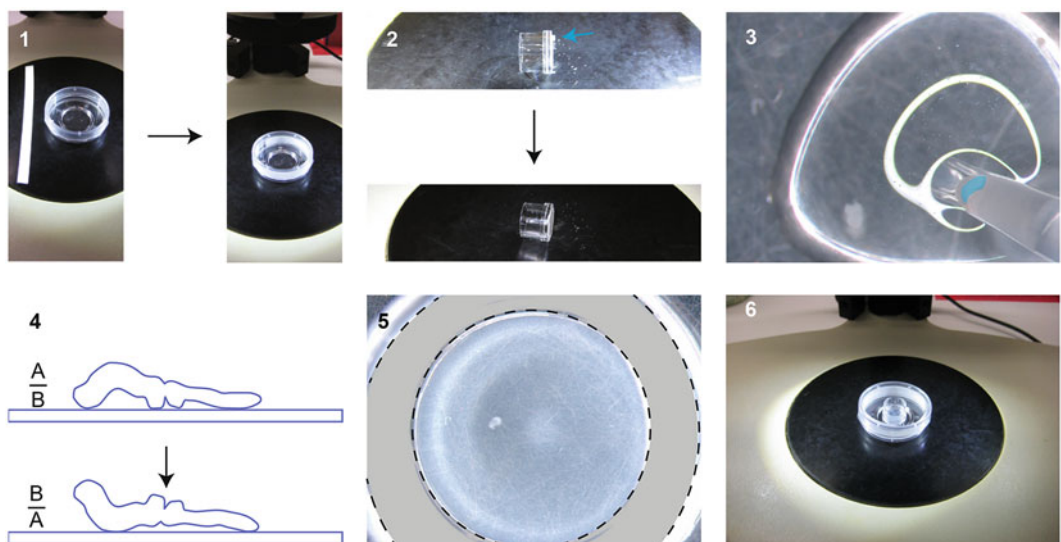


Fig. 3 Live imaging chamber setup. 1: Prepare a strip of filter paper, place it along the imaging dish wall, and humidify with PBS using a micropipette (400 μ l). 2: Prepare the inner imaging chamber by cutting off the legs of the Millicell insert with a sharp knife or scalpel. 3: Place a 20 μ l drop of WM1 inside the imaging chamber, at the center of the cover slip, and transfer the discs with a micropipette. 4: Use the dissection probe to gently orient the discs such that the apical side of the disc proper cells faces downwards to the coverslip. 5: Place the inner imaging chamber on top of the WM1 drop. Fill the inner chamber with 200 μ l of WM1. 6: Fully assembled live imaging chamber

3.5 Live Imaging of Cultured Wing Discs

We recommend employing a spinning disc confocal microscope. We were able to approximately double the amount of time during which divisions could be recorded simply by switching from a scanning point to a spinning disc confocal. It is likely that short-term live imaging might still be done on a scanning point confocal, in addition there are other considerations, such as the precision of the stage, that are usually better on live imaging dedicated microscopes.

The time intervals between imaging also matter. For long-term imaging (up to 12 h) we usually only scan every 6 min. We have also performed 10–30 s intervals but this will usually start to affect disc health negatively after about 2 h. Finally, try to keep the laser intensity as low as the detection capacity allows (see **Notes 25** and **26**). In addition, note that the *z*-axis of wing discs is significantly larger than the working distance that can be achieved with confocal microscopy. For this reason one cannot easily study phenomena that take place along the entire apico-basal axis of columnar wing disc cells. Hence, the wing disc morphology lends itself much better for the analysis of apical structures and phenomena. For the study of basal structures it is possible to resort to younger discs (100 AEL) since they are flatter and mount them basal side down.

3.6 Wing Disc Culture in Multi-well Plates

Sometimes an experiment might require cultivating several discs in parallel, in order to evaluate the effect of a pharmacological agent, for example. In this case, it is preferable to cultivate the explants in multi-well cell culture plates. Proceed with the sterile dissections as described above and collect the discs in multi-well plates. We normally use 24-well plates for cell culture (see **Note 27**) and cultivate the discs in 1 mL of WM1 (with up to 20 discs per well).

4 Notes

1. Schneider's medium is not very stable and starts degrading after approximately 2 months at 4 °C. Look for precipitates. Small filamentous-like crystals can be observed during dissection if the medium has turned bad.
2. We solubilize insulin in slightly acidified water (with 1/1000 glacial acetic acid) at 2 mg/mL. Keep aliquots at -20 °C and avoid repeated freeze-thaw cycles.
3. We only use *yw* flies. The use of Oregon-R flies to prepare fly extract resulted in suboptimal results.
4. Optional, rear the flies for 1 day on fresh food. This increases yield by making the females fatter.
5. Hemolymph melanizes quickly at room temperature. Hence, proceed fast and work under cold conditions when preparing Fly Extract. If the Fly Extract turns black at any point during the procedure, discard it.

6. A different type of plastic bag can be used if it is durable enough.
7. Before you begin, make sure to have a large icebox ready, a centrifuge at 4 °C and ice-cold M3 medium.
8. You want to have enough medium inside the bag to dilute the hemolymph, but not too much or it becomes difficult to homogenize the flies.
9. Make sure to have properly homogenized flies to minimize batch variability.
10. Make sure to have the waterbath ready in time.
11. Place a thermometer inside the solution to make sure that it stays 5 min at 60 °C.
12. We prefer small aliquots of 1 mL in order to avoid freeze-thaw cycles or long storage periods at 4 °C.
13. We dissect inside a horizontal flow hood. However, this is likely not required for short culture sessions.
14. We have noticed that “stressed” larva usually yield poorly performing discs. Take good care of your flies and avoid crowding or old crosses. Use “healthy” larva as donors for wing disc explants.
15. Use RT° PBS, do not use cold PBS. Always try to minimize stress.
16. Larvae that have been kept too long in PBS prior to being dissected become hypoxic.
17. Alternatively, you can also cut out the bottom of a cell culture petri dish.
18. Ensure that the bottom of the Millicell chamber is flat and that the filter membrane is not broken.
19. This step is difficult. You need to repeat and practice in order to gain a steady hand.
20. Some discs will flip over when you place the Millicell chamber. Always prepare more discs than required to guarantee that enough end up in the correct orientation.
21. To prevent changes in osmolality caused by evaporation during long-term imaging, you can add 50 µl of Embryo Culture Oil on top of the culture medium.
22. You can seal the imaging chamber with parafilm, for example. However, this is generally not necessary.
23. Walk carefully when going to the microscope. Strong movements might displace the Millicell chamber and the discs. Preferentially, work close to the microscope room.
24. Care should be taken to keep temperatures below RT° during imaging. For example, our live imaging room is maintained at 21°C.
25. Image quality can be improved after acquisition with deconvolution (we use Huygens). This is especially true if the images are acquired with a spinning disc microscope.

26. Alternatively, a Gaussian filter or CLAHE can be employed in Fiji (Image-J).
27. For sensitive processes such as proliferation assays we use low-adhesion cell culture plates (Hydrocell). For more robust assay such as wing eversion normal cell culture plates work well enough.

References

1. Robb JA (1969) Maintenance of imaginal discs of *Drosophila melanogaster* in chemically defined media. *J Cell Biol* 41:876–885
2. Wyss C (1982) Ecdysterone, insulin and fly extract needed for the proliferation of normal *Drosophila* cells in defined medium. *Exp Cell Res* 139:297–307
3. Ui K, Ueda R, Miyake T (1987) Cell lines from imaginal discs of *Drosophila melanogaster*. In *Vi^{tro} Cell Dev Biol* 23:707–711
4. Currie D, Milner M (1988) The growth and differentiation in vitro of leg and wing imaginal disc cells from *Drosophila melanogaster*. *Development* 102:805–814
5. Davis KT, Shearn A (1977) In vitro growth of imaginal disks from *Drosophila melanogaster*. *Science* 196:438–440
6. Aldaz S, Escudero LM, Freeman M (2010) Live imaging of *Drosophila* imaginal disc development. *Proc Natl Acad Sci* 107:14217–14222
7. Zartman J, Restrepo S, Basler K (2013) A high-throughput template for optimizing *Drosophila* organ culture with response-surface methods. *Development* 140:667–674
8. Mao Y, Tournier AL, Hoppe A, Kester L, Thompson BJ, Tapon N (2013) Differential proliferation rates generate patterns of mechanical tension that orient tissue growth. *EMBO J* 32(21):2790–2803
9. Handke B, Szabad J, Lidsky PV, Hafen E, Lehner CF (2014) Towards long term cultivation of *Drosophila* wing imaginal discs in vitro. *PLoS One* 9:e107333
10. Prasad M, Jang A, Starz-Gaiano M, Melani M (2007) A protocol for culturing *Drosophila melanogaster* stage 9 egg chambers for live imaging. *Nat Protoc* 2(10):2467–2473
11. Landsberg KP, Farhadifar R, Ranft J, Umetsu D, Widmann TJ, Bittig T, Said A, Jülicher F, Dahmann C (2009) Increased cell bond tension governs cell sorting at the *Drosophila* anteroposterior compartment boundary. *Curr Biol* 19:1950–1955
12. Umetsu D, Aigouy B, Aliee M, Sui L, Eaton S, Jülicher F, Dahmann C (2014) Local increases in mechanical tension shape compartment boundaries by biasing cell intercalations. *Curr Biol* 24:1798–1805
13. LeGoff L, Rouault H, Lecuit T (2013) A global pattern of mechanical stress polarizes cell divisions and cell shape in the growing *Drosophila* wing disc. *Development* 140:4051–4059

Chapter 12

Cultivation and Live Imaging of *Drosophila* Ovaries

Maureen Cetera, Lindsay Lewellyn, and Sally Horne-Badovinac

Abstract

Drosophila egg chamber development depends on a number of dynamic cellular processes that contribute to the final shape and function of the egg. We can gain insight into the mechanisms underlying these events by combining the power of *Drosophila* genetics and ex vivo live imaging. During developmental stages 1–8, egg chambers rotate around their anterior-posterior axes due to collective migration of the follicular epithelium. This motion is required for the proper elongation of the egg chamber. Here, we describe how to prepare stage 1–8 egg chambers for live imaging. We provide alternate protocols for the use of inverted or upright microscopes and describe ways to stabilize egg chambers to reduce drift during imaging. We discuss the advantages and limitations of these methods to assist the researcher in choosing an appropriate method based on experimental need and available resources.

Key words *Drosophila*, Egg chamber, Follicle, Live imaging, Collective cell migration, Morphogenesis

1 Introduction

The *Drosophila* egg chamber has emerged as an important model system for the study of cellular mechanisms controlling morphogenesis. The egg chamber is an ovarian structure that serves as the precursor to the fly egg. It has a core of germ cells, composed of 15 nurse cells and one oocyte, that is surrounded by a somatic epithelium of follicle cells. When an egg chamber forms it is 20 μm in diameter and spherical. As it matures, it progresses through 14 developmental stages, increases in volume almost 1000-fold, and undergoes a dramatic series of morphological changes that transform it into a highly structured, elliptical egg [1, 2].

Studies of egg chamber morphogenesis have been greatly enhanced by ex vivo live imaging [3]. Processes that occur during stages 10b–14, such as nurse cell dumping and dorsal appendage formation, have long been amenable to this approach [4–9]. There is an excellent video

Electronic supplementary material: The online version of this chapter (doi:[10.1007/978-1-4939-6371-3_12](https://doi.org/10.1007/978-1-4939-6371-3_12)) contains supplementary material, which is available to authorized users. Videos can also be accessed at http://link.springer.com/book/10.1007/978-1-4939-6371-3_12.

protocol currently available for working with these stages [10]. The breakthrough that allowed the live imaging of younger egg chambers came with the recent discovery that insulin needs to be added to the culture media [11]. This protocol was first used to study border cell migration at stage 9 [12, 13], but subsequently led to the discovery of two novel biological processes: oscillating contractions of the basal follicle cell surfaces, which occur during stages 9–10 [14], and egg chamber rotation, which occurs during stages 1–8 [15, 16]. The preparation of stage 1–8 egg chambers for live imaging requires particular care, as these egg chambers are small and easily damaged. This protocol will focus on these stages. Although the procedures that we present have been optimized for the study of egg chamber rotation (discussed below), they could easily be adapted for investigations of other events that occur during these stages [17, 18].

Egg chamber rotation is the result of a fascinating collective migration of the follicle cells. The follicle cell epithelium is oriented with its apical surface contacting the germ cells and its basal surface contacting the basement membrane matrix that ensheathes the egg chamber. During stages 1–8, the basal follicle cell surfaces crawl along the inside of the basement membrane, perpendicular to the egg chamber’s anterior-posterior axis. This collective motion causes the entire egg chamber to rotate within its surrounding matrix, which remains largely stationary [16]. Through mechanisms that are still not well understood, rotation causes the egg chamber to elongate from a spherical to an ellipsoidal shape [19–21]. Because the important events in this system all occur near the egg chamber’s outer surface, they are highly accessible for live imaging. When the basement membrane is pressed against the coverslip, the interactions between the basal follicle cell surfaces and the matrix, or between the follicle cells themselves, can be imaged at high resolution with both confocal and near-total internal reflection fluorescence (TIRF) microscopy [22, 23]. Studies of this migration are also facilitated by the powerful genetic tools of *Drosophila* and a wealth of new fluorescent markers that can be visualized in live tissue [24]. Together, these features allow for mechanistic studies of collective cell migration within the context of a living, organ-like structure [15, 16, 25, 26].

In this chapter, we describe multiple techniques that can be used to isolate and prepare stage 1–8 egg chambers for live imaging on either an inverted or upright microscope. We also describe strategies to reduce drift of the samples in the XY plane, as well as a method to correct for drift after the images have been acquired.

2 Materials

2.1 Aging Female Flies

1. Vial with fly food.
2. Yeast powder, dry active yeast ground to a fine powder in a coffee grinder.

2.2 Egg Chamber Dissection

1. Pen/Strep: penicillin G-sodium 10,000 U/ml, streptomycin sulfate 10,000 μ g/ml in 0.85 % saline.
2. Acidified water: 1 μ l concentrated HCl in 1 ml water.
3. Insulin: 1 mg dissolved in 100 μ l acidified water.
4. Live imaging media (LI media) [11]: Schneider's S2 media, 0.6 \times Pen/Strep, 15% vol/vol fetal bovine serum (FBS), 0.2 mg/ml insulin (see Note 1).
5. FM4-64 dye.
6. Pyrex 9-Cavity Spot Plate.
7. Dumont forceps: #5, 0.1 \times 0.06 mm tip, and #55, 0.05 \times 0.02 mm tip (see Note 2).
8. Wire tool: sharpened and curved tungsten wire, original diameter 0.125 mm, inserted into a 27G $\frac{1}{2}$ ' needle attached to a 3 ml syringe (see Fig. 1a, Note 3).
9. Eyelash tool: insert an eyelash into a slightly melted p1000 pipet tip (see Fig. 1a) or attach to a toothpick with nail polish.
10. Glass Pasteur pipets, 5 $\frac{3}{4}$ in.
11. 5 ml pipet pump.
12. Stereomicroscope with magnification of at least 10 \times .

2.3 Live Imaging Setup for an Inverted Microscope

1. Aluminum slide, 76 mm \times 26 mm \times ~1 mm with a 12 mm diameter hole in the center surrounded by an 18 mm hole with ~0.5 mm depth on the top of the slide (see Fig. 1b, Note 4).
2. Coverslip, 50 mm \times 22 mm, cleaned with ammonia-free glass cleaner and lens paper.
3. Parafilm.
4. Razor blade or needle.
5. Lumox gas permeable membrane slide, 76 mm \times 26 mm, removed from a tissue culture chamber (see Note 5).

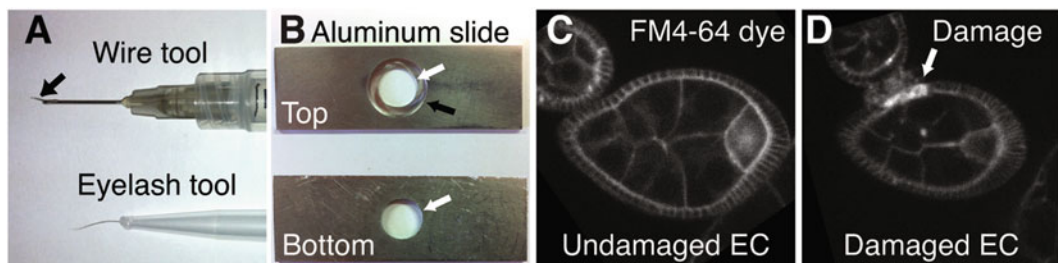


Fig. 1 Specialized tools. (a) The wire tool consists of a curved tungsten wire (black arrow) inserted into a needle attached to a syringe. The eyelash tool consists of an eyelash inserted into a pipet tip that has been partially melted. (b) The aluminum slide has a center hole (12 mm in diameter) that goes through the entire slide (white arrow). On the top of the slide, a concentric 18 mm diameter hole is cut out to a depth of ~0.5 mm (black arrow). (c and d) FM4-64 dye marks cell membranes and is taken up at higher levels by damaged tissue (white arrow).

6. Low melt agarose (LMA), 2.5 % dissolved in hot water, store 1 ml aliquots at room temperature (optional).
7. Coverslip cut to approximately 4 mm×4 mm with a diamond tip pen (optional).
8. Polystyrene beads, 20–50 μm (optional).

2.4 Live Imaging Setup for an Upright or Inverted Microscope

1. Lumox gas permeable membrane slide, 76 mm×26 mm, removed from a tissue culture chamber (*see Note 5*).
2. Coverslip, 30 mm×22 mm, cleaned with ammonia-free glass cleaner and lens paper.
3. Low melt agarose (LMA), 2.5 % dissolved in hot water, store 1 ml aliquots at room temperature.
4. Vacuum grease.
5. Halocarbon oil 27.

3 Methods

3.1 Preparing Female Flies for Dissection

1. Females must be well fed with yeast for healthy egg chamber production. Incomplete nutrition will slow egg chamber production by inducing cell death in the germarium and in stage 8 egg chambers [27–29]. Sprinkle yeast powder on fly food in a vial, covering about one half of the surface. Add up to 10, 1–2 day old females and an equal number of young males to the vial.
2. Age females for 1–3 days (*see Note 6*). Move animals to a new vial with fresh yeast the day before dissecting.

3.2 Ovary/Ovariole Dissection

For ex vivo live imaging, it is first necessary to dissect the ovaries from the abdomen of well-fed females and then isolate the individual egg chambers from the ovary. Because this process invariably induces some tissue damage, we provide alternate techniques to avoid damaging egg chambers of particular stages (*see steps 5 and 6*). The entire process is documented in Video 1.

These procedures require a basic understanding of ovary structure. Here we define some key terms. Within each ovary there are 15–18 developmental arrays of egg chambers, called ovarioles. The germarium is a structure at the anterior end of each ovariole; this is the site of egg chamber production. Within the ovariole, each egg chamber is connected to its neighbors like beads on a string by thin multicellular structures called stalks. Each ovariole is then surrounded by a tubular sheath of muscle that pushes the maturing egg chambers toward the oviduct.

1. Prepare LI media and allow it to come to room temperature. Add 1 μl FM4-64 membrane dye/100 μl LI media. The dye can be used to image cell membranes, but more importantly it highlights tissue damage [12] (*see Fig. 1c, d, Note 7*).

2. Using a glass pipet, place 500–800 μ l of LI media into a well in the spot plate. Using a black background on the stage, place the well under the stereomicroscope. At 10 \times magnification, focus the microscope toward the bottom of the well.
3. Anesthetize the flies using CO₂. With the #5 forceps in your non-dominant hand, grab a single female from the dorsal side at the thorax. Without letting go, submerge the fly in the LI media and use the #55 forceps to grab the abdomen between the two posterior-most pigmented segments. Pull the forceps posteriorly to tear the abdomen; the ovaries should pop out of the abdomen (see Fig. 2a, Note 8). Detach the ovaries from the posterior cuticle and remove all nonovarian tissue from the well (see Fig. 2b). Dissect 1–3 females and collect all ovaries within the same well of the spot plate.
4. Place the tip of closed #5 forceps over the mature egg chambers at the posterior end of the ovary with your nondominant hand and gently stab through the ovary to pin it against the bottom of the well.

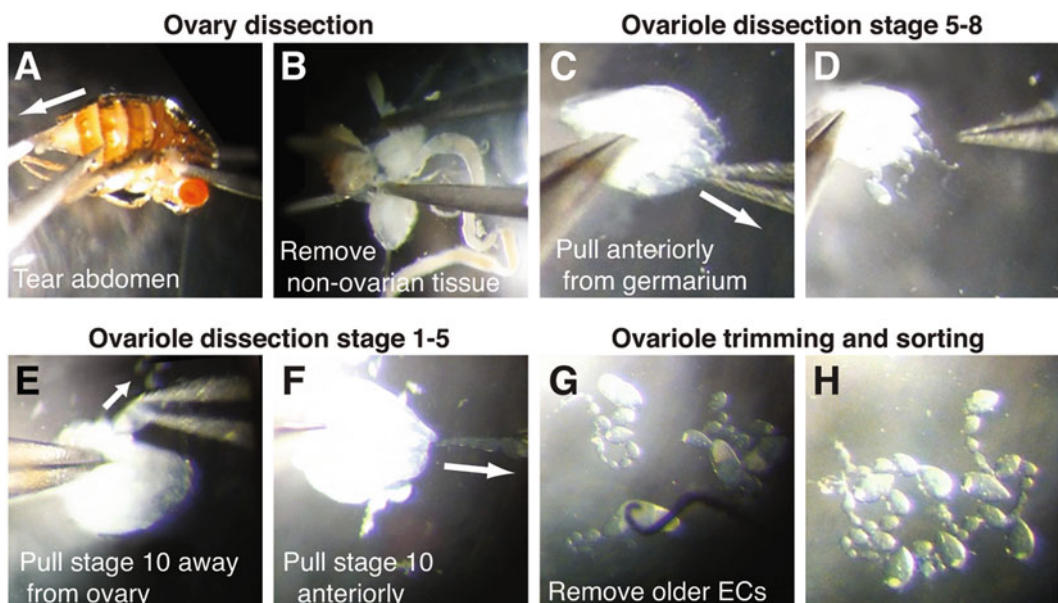


Fig. 2 Ovary/ovariole dissection. (a) Hold on to the dorsal side of the fly's thorax with #5 forceps (right). With #55 forceps (left), grab between the two posterior-most pigmented segments and pull posteriorly to tear the abdomen (white arrow). (b) Separate the ovaries from the posterior cuticle and remove other tissue using forceps. (c and e) Pin the ovary against the glass well by gently stabbing with the #5 forceps in the posterior region of the ovary. (c and d) When isolating stages 5–8, grab ovarioles with #55 forceps from the anterior of the ovary near the germarium and pull anteriorly to remove them from the ovary and muscle (white arrow). (e) When imaging stages 1–5, grab near the stage 10 egg chambers with #55 forceps and pull out and away from the ovary (white arrow). (f) Then, pull the ovariole anteriorly to remove it from the muscle (white arrow). (g) Use the wire tool to remove older egg chambers by severing the stalk between two egg chambers. (h) Check for damage and move the ovarioles to a new well

5. To obtain stage 5–8 egg chambers, with the #55 forceps in your dominant hand, gently grab the anterior tip of the pinned ovary at or just posterior to the germaria and quickly pull anteriorly to remove single ovarioles from the ovary and their muscle sheath (*see Fig. 2c, d*). Perform this pulling motion on the same ovary until previtellogenetic egg chambers are no longer visible. Continuing to pull beyond this point can induce damage, so you may only end up with a few. Repeat this process with the remaining ovaries in the well.
6. To obtain stage 1–5 egg chambers, with the #55 forceps in your dominant hand, grab single ovarioles from the region of the pinned ovary (*see step 4*) that contains stage 10 egg chambers. This will be approximately halfway between the anterior and posterior tips of the ovary. Pull the ovariole orthogonally away from the ovary’s anterior-posterior axis, then pull anteriorly to remove the ovariole from the muscle sheath (*see Fig. 2e, f*).
7. Separate the ovarioles from the debris using an eyelash tool. Avoid ovarioles that are still in the muscle even if it does not cover the egg chamber of interest as muscle contraction will cause the ovariole to move during imaging. Remove older egg chambers with the wire tool. Place the curved wire between two egg chambers and press down to sever their connecting stalks (*see Fig. 2g, Note 9*). Use a sawing motion if necessary. Do not break the stalk directly adjacent to an egg chamber of interest as this process can cause damage.
8. Gather ovarioles with the eyelash tool (*see Fig. 2h*) and perform an initial check for tissue damage at 25–40 \times magnification. Transfer 10–15 ovarioles with a glass pipet to a new well in the spot plate with LI media.

3.3 Live Imaging Setup

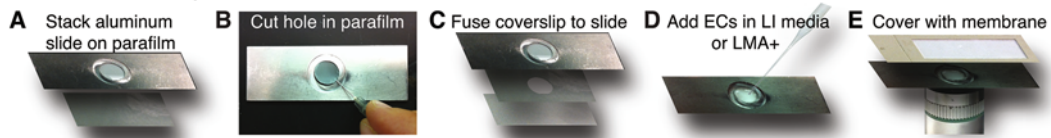
In this section, we describe four options for mounting ovarioles for live imaging that are specialized for different styles of microscopy. Initially, we describe the simplest method, imaging in LI media alone using an inverted microscope. This method allows the exchange of media and the addition of pharmacological reagents. However, drift of the samples in the XY plane is common. To limit drift, a smaller coverslip can be placed on top of the ovarioles to compress them against the main coverslip. This compression is ideal for near-TIRF microscopy as it increases the surface area of the egg chamber available for imaging. Alternatively, low melt agarose (LMA) can be added to the LI media to cause it to partially solidify (LMA+). When using an upright microscope, the ovarioles can be placed between a LMA+ pad and the coverslip. The use of LMA does not allow for the exchange of media or the ability to recover the egg chambers after imaging for fixation. Although these methods do reduce XY drift, they may not eliminate it. In the final section, we describe an image-processing

method to correct for this problem. Image acquisition settings are not discussed, as they are highly specific to the microscope being used and experiment being performed.

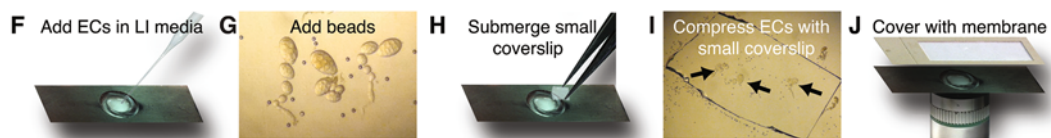
3.3.1 Inverted Microscope Using LI Media Alone

1. Cut a piece of parafilm approximately the size of the 50 mm × 22 mm coverslip. On a flat surface, place the aluminum slide on the parafilm with the smaller hole facing down (see Fig. 3a). While pressing the aluminum slide down, use a razor blade or a needle to trace the hole in the aluminum slide on the parafilm (see Fig. 3b). Remove the parafilm circle and sandwich the parafilm between the aluminum slide and a clean coverslip (see Fig. 3c).

Inverted microscope



Inverted TIRF



Upright/ Inverted microscope

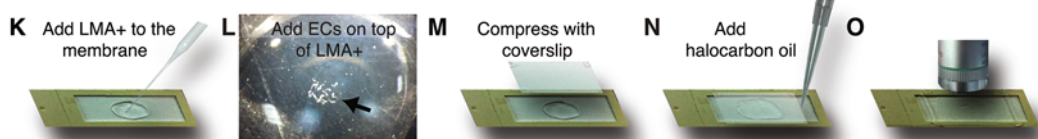


Fig. 3 Sample mounting strategies for live imaging. Preparations for an inverted microscope (a–j), and an upright or inverted microscope (k–o). (a–c) Preparing the aluminum slide. (a) Place the aluminum slide onto a piece of parafilm with the top side up. (b) Use a needle to trace the circumference of the inner hole on the parafilm, and remove the circular cutout. (c) Stack the parafilm on top of a coverslip and place the aluminum slide on top of the parafilm. Use a heat block (metal slide part down) to melt the parafilm and fuse the aluminum slide to the coverslip. (d) Add dissected ovarioles in LI media or LMA+ to the hole in the center of the aluminum slide. (e) Cover the aluminum slide with a gas permeable membrane slide to prevent evaporation. (f) Add ovarioles in LI media to the metal slide (prepared as described above). (g) Add beads to the ovarioles and LI media. (h) Use #5 forceps to submerge a ~4 mm × 4 mm coverslip in the LI media and gently place it on top of the beads and ovarioles. (i) The coverslip will compress the ovarioles (black arrows). (j) Cover the aluminum slide with a gas permeable membrane slide to prevent evaporation. (k) Add ~100 μ l LMA+ to the center of the gas permeable membrane slide and spread it out evenly before it solidifies to form the LMA+ pad. (l) Add dissected ovarioles to the top of the LMA+ pad; use an eyelash tool to bring the ovarioles to the center (black arrow). (m) Add vacuum grease to the corners of a coverslip, and gently lower it onto the LMA+ pad, vacuum grease side down. (n) Add halocarbon oil around the LMA+ pad to prevent evaporation. (o) Image from above (as shown) or invert the slide to image on an inverted microscope

2. Set a heat block to 70–100 °C. Place the sandwich on the heat block with the aluminum slide facing down until the coverslip is adhered to the aluminum slide (1–2 min). Gently clean coverslip with ammonia-free glass cleaner and lens paper (optional).
3. Using a glass pipet, transfer newly dissected ovarioles from Subheading 3.2 along with ~100 μ l LI media into the center of the hole in the aluminum slide so that they rest on the coverslip (*see* Fig. 3d, Note 10).
4. Cover the slide with the gas permeable membrane slide to prevent evaporation (*see* Fig. 3e). The membrane should not touch the media.

3.3.2 Inverted Microscope Using Compression

1. Prepare an aluminum slide and transfer ovarioles to the slide as described in Subheading 3.3.1, steps 1–3 (*see* Fig. 3a–d, f).
2. Wash polystyrene beads in LI media. Add enough beads to the ovarioles and LI media on the slide so the coverslip added in the following step will lay flat against the beads, preventing the egg chambers of interest from being overcompressed (*see* Fig. 3g).
3. Under the stereomicroscope, use forceps to submerge a ~4 mm \times 4 mm coverslip in the LI media and gently place it on top of the ovarioles and beads (*see* Fig. 3h). The egg chambers will be compressed between the two coverslips [30] (*see* Fig. 3i, Note 11).
4. Cover the aluminum slide with the gas permeable membrane slide to prevent evaporation (*see* Fig. 3j).

3.3.3 Preparing LI Media with LMA (LMA+)

1. Melt 2.5% LMA at 65 °C.
2. Prepare LI media with FM4-64 (*see* Subheading 3.2, step 1) and warm to 37 °C. Add LMA to the media at a final concentration of 0.4–0.8% to make LMA+. Place the mixture at 37 °C so it remains liquid until use.

3.3.4 Inverted Microscope Using LMA+

1. Prepare an aluminum slide as described in Subheading 3.3.1, steps 1 and 2.
2. Immediately following the dissection procedures in Subheading 3.2, remove as much liquid as possible from the ovarioles in the spot plate well. Using a glass pipet, add ~100 μ l of liquid LMA+ to the ovarioles, and then quickly transfer the ovarioles and LMA+ to the aluminum slide (*see* Fig. 3d).
3. Before the LMA+ solidifies, use the eyelash tool to drag the ovarioles down to the coverslip if they do not sink on their own. Allow 10 min for the LMA+ to fully solidify before imaging.
4. Cover the aluminum slide with the gas permeable membrane slide to prevent evaporation (*see* Fig. 3e).

3.3.5 Upright or Inverted Microscope Using LMA+ Pad

1. Using a glass pipet, transfer ~100 μ l of liquid LMA+ to the center of the gas permeable membrane at room temperature (see Fig. 3k). Try to spread the mixture evenly before it solidifies. This will form a soft pad on which to place the ovarioles.
2. After the LMA+ solidifies, transfer the ovarioles in a minimal volume of LI media to the LMA+ pad (see Fig. 3l). Remove as much liquid LI media from the pad as possible.
3. Use the eyelash tool to bring the ovarioles to the center of the LMA+ pad.
4. Place vacuum grease on the four corners of a clean 30 mm \times 22 mm coverslip and gently drop it onto the LMA+ pad, vacuum grease side down (see Fig. 3m). Push lightly on each corner with a pipet tip moving from corner to corner until the coverslip lays flat against the plastic frame surrounding the membrane. This will slightly compress the egg chambers (see Note 12).
5. Pipet Halocarbon oil between the coverslip and the membrane on all four sides to prevent evaporation while imaging (see Fig. 3n, o).

3.4 Image Processing to Correct for Drift (See Note 13)

1. Open the image sequence as a stack in ImageJ. Duplicate the stack.
2. Apply a Gaussian blur filter to the duplicated stack so individual cells are no longer visible, Sigma (radius) of ~15–20.
3. Convert the blurred stack to a mask. Each egg chamber should be converted to a single ellipsoid shape with no holes (see Note 14).
4. Using the MultiStackReg v1.45 plugin (B.L. Busse: <http://bradbisse.net/downloads.html>), align the mask using translational transformation and save the transformation file.
5. On the original stack, use the same plugin but load the transformation file from the mask to align the original image sequence.

4 Notes

1. S2 media, Pen/Strep, and FBS can be combined and stored at 4 °C. We make 10 ml at a time and have used it up to 1 month later. Insulin in acidified water can be stored at 4 °C for up to a week. Insulin should be added to the S2 media/antibiotics/FBS just before use. Although the pH of the media is critical when culturing stage 9 egg chambers [11], it is less important for culturing younger egg chambers. We no longer adjust it.
2. For precise dissection with limited tissue damage, maintain the #55 forceps with great care.
3. To make the wire tool, start with a 1.5" piece of tungsten wire. Insert the end of the wire into the needle attached to the

syringe. *Use caution while performing the following steps.* A 10 V power supply and a 1 M NaOH solution in a small beaker is required to electrolytically erode the wire. Attach a metal rod to the negative electrode of the power supply. Submerge the end of the rod in the NaOH solution. Using another alligator clip, attach the needle to the positive electrode of the power supply. Holding the syringe vertically, dip the end of the wire into the beaker for 1–2 s. Repeat this action until the wire is thinned to the desired diameter. Under a stereomicroscope, bend the thinned wire with forceps to create a curved edge or a loop. Stabilize the connection between the wire and the needle with super glue or nail polish.

4. The slide can be custom made at a machine shop. If you are unable to acquire an aluminum slide, use the setup described in Subheading 3.3.5.
5. The lumox slides have been discontinued by Grenier Bio-One but will be available from Sarstedt (94.6150.101). The slides are reusable. LI media, LMA, and halocarbon oil can be washed off. Use ethanol to remove the oil [11]. If the membrane becomes detached from the plastic slide, use nail polish to readhere it.
6. The time it takes for healthy ovaries to develop is dependent on the age and genotype of the female, and temperature. If females are too young, the ovarioles will not be fully mature, whereas females that are too old will accumulate mature egg chambers at the expense of younger egg chambers. Low temperatures will slow development and high temperatures will speed the process. If the female is of a genotype that produces round eggs, the oviduct can become blocked. Dissecting these females at earlier time points could decrease secondary defects induced in younger egg chambers from the blockage.
7. Damaged cells will take up more dye than their neighbors and will stain intensely (*see* Fig. 1d). Briefly scan through the egg chambers before and after imaging to check for damage. Even a small amount of tissue damage can block egg chamber rotation.
8. If the ovaries do not come out of the abdomen when the posterior cuticle is removed, they can be coerced by gently squeezing the sides of the abdomen or by pulling on the ovaries directly with the forceps if they are visible. We recommend practicing dissections prior to performing live imaging experiments, as these alternate procedures can induce excessive damage.
9. When imaging, the presence of older egg chambers in the ovariole will increase the distance between the egg chambers of interest and the coverslip. Additionally, older egg chambers will deplete the media of nutrients [11], limiting the amount of time you can image.

10. When transferring the ovarioles to the aluminum slide, ensure the media either does not touch the aluminum slide or does so evenly around the circumference of the hole. If the media touches the aluminum slide unevenly, the egg chambers will drift as the media spreads along the coverslip by capillary action.
11. The size of the beads should be adjusted depending on the stage of the egg chamber you are imaging. Egg chambers that are much larger than the beads will be damaged by compression.
12. Increasing the LMA concentration of the LMA+ pad will increase egg chamber compression between the pad and the coverslip. If the concentration is too low, the ovarioles will sink into it. If it is too high, the LMA+ pad will crack when you press the coverslip against it.
13. Correcting for drift only works if the egg chambers are drifting within the XY plane. This will not correct for Z drift or egg chamber rolling.
14. If you have holes in your mask, increase the radius of the blur. If holes are present, the stack may be aligned based on the hole, not the overall shape of the egg chamber.

Acknowledgements

We thank members of the Horne-Badovinac lab for input, Guillermina Ramirez-San Juan for the dissection video, and Claire Stevenson for the images in Fig. 1c. M.C. was supported by NIH T32 GM007183 and work in the Horne-Badovinac lab is supported by NIH R01 GM094276.

Video 1 *Drosophila* ovary dissection. Video showing dissection of *Drosophila* ovaries using a stereomicroscope. Alternate dissection methods are shown for acquiring stage 6-8 or stage 1-5 egg chambers. After dissection, healthy ovarioles are sorted and older egg chambers are trimmed away. Please see Fig. 2 for stills of this video and a detailed procedural description.

References

1. Horne-Badovinac S, Bilder D (2005) Mass transit: epithelial morphogenesis in the *Drosophila* egg chamber. *Dev Dyn* 232(3):559–574
2. Wu X, Tanwar PS, Raftery LA (2008) *Drosophila* follicle cells: morphogenesis in an eggshell. *Semin Cell Dev Biol* 19(3):271–282
3. He L, Wang X, Montell DJ (2011) Shining light on *Drosophila* oogenesis: live imaging of egg development. *Curr Opin Genet Dev* 21(5):612–619
4. Dorman JB, James KE, Fraser SE et al (2004) bullwinkle is required for epithelial morphogenesis during *Drosophila* oogenesis. *Dev Biol* 267(2):320–341
5. Gutzeit H, Koppa R (1982) Time-lapse film analysis of cytoplasmic streaming during late oogenesis of *Drosophila*. *J Embryol Exp Morph* 67:101–111

6. Huelsmann S, Ylanne J, Brown NH (2013) Filopodia-like actin cables position nuclei in association with perinuclear actin in *Drosophila* nurse cells. *Dev Cell* 26(6):604–615
7. Osterfield M, Du X, Schupbach T et al (2013) Three-dimensional epithelial morphogenesis in the developing *Drosophila* egg. *Dev Cell* 24(4):400–410
8. Petri WH, Mindrinos MN, Lombard MF et al (1979) In vitro development of the *Drosophila* chorion in a chemically defined organ culture medium. *Dev Genes Evol* 186:351–362
9. Spracklen AJ, Fagan TN, Lovander KE et al (2014) The pros and cons of common actin labeling tools for visualizing actin dynamics during *Drosophila* oogenesis. *Dev Biol* 393(2):209–226
10. Spracklen AJ, Tootle TL (2013) The utility of stage-specific mid-to-late *Drosophila* follicle isolation. *J Vis Exp* 82:50493
11. Prasad M, Jang AC, Starz-Gaiano M et al (2007) A protocol for culturing *Drosophila melanogaster* stage 9 egg chambers for live imaging. *Nat Protoc* 2(10):2467–2473
12. Bianco A, Poukkula M, Cliffe A et al (2007) Two distinct modes of guidance signalling during collective migration of border cells. *Nature* 448(7151):362–365
13. Prasad M, Montell DJ (2007) Cellular and molecular mechanisms of border cell migration analyzed using time-lapse live-cell imaging. *Dev Cell* 12(6):997–1005
14. He L, Wang X, Tang HL et al (2010) Tissue elongation requires oscillating contractions of a basal actomyosin network. *Nat Cell Biol* 12(12):1133–1142
15. Cetera M, Ramirez-San Juan GR, Oakes PW et al (2014) Epithelial rotation promotes the global alignment of contractile actin bundles during *Drosophila* egg chamber elongation. *Nat Commun* 5:5511
16. Haigo SL, Bilder D (2011) Global tissue revolutions in a morphogenetic movement controlling elongation. *Science* 331(6020):1071–1074
17. Aioldi SJ, McLean PF, Shimada Y et al (2011) Intercellular protein movement in syncytial *Drosophila* follicle cells. *J Cell Sci* 124(Pt 23):4077–4086
18. Lerner DW, McCoy D, Isabella AJ et al (2013) A Rab10-dependent mechanism for polarized basement membrane secretion during organ morphogenesis. *Dev Cell* 24(2):159–168
19. Bilder D, Haigo SL (2012) Expanding the morphogenetic repertoire: perspectives from the *Drosophila* egg. *Dev Cell* 22(1):12–23
20. Gates J (2012) *Drosophila* egg chamber elongation: insights into how tissues and organs are shaped. *Fly (Austin)* 6(4):213–227
21. Horne-Badovinac S (2014) The *Drosophila* egg chamber—a new spin on how tissues elongate. *Integr Comp Biol* 54(4):667–676
22. Konopka CA, Bednarek SY (2008) Variable-angle epifluorescence microscopy: a new way to look at protein dynamics in the plant cell cortex. *Plant J* 53(1):186–196
23. Tokunaga M, Imamoto N, Sakata-Sogawa K (2008) Highly inclined thin illumination enables clear single-molecule imaging in cells. *Nat Methods* 5(2):159–161
24. Hudson AM, Cooley L (2014) Methods for studying oogenesis. *Methods* 68(1):207–217
25. Lewellyn L, Cetera M, Horne-Badovinac S (2013) Misshapen decreases integrin levels to promote epithelial motility and planar polarity in *Drosophila*. *J Cell Biol* 200(6):721–729
26. Viktorinova I, Dahmann C (2013) Microtubule polarity predicts direction of egg chamber rotation in *Drosophila*. *Curr Biol* 23(15):1472–1477
27. Drummond-Barbosa D, Spradling AC (2001) Stem cells and their progeny respond to nutritional changes during *Drosophila* oogenesis. *Dev Biol* 231(1):265–278
28. Mazzalupo S, Cooley L (2006) Illuminating the role of caspases during *Drosophila* oogenesis. *Cell Death Differ* 13(11):1950–1959
29. Pritchett TL, Tanner EA, McCall K (2009) Cracking open cell death in the *Drosophila* ovary. *Apoptosis* 14(8):969–979
30. Robin FB, McFadden WM, Yao B et al (2014) Single-molecule analysis of cell surface dynamics in *Caenorhabditis elegans* embryos. *Nat Methods* 11(6):677–682

Chapter 13

Segmentation and Quantitative Analysis of Epithelial Tissues

Benoit Aigouy, Daiki Umetsu, and Suzanne Eaton

Abstract

Epithelia are tissues that regulate exchanges with the environment. They are very dynamic and can acquire virtually any shape; at the cellular level, they are composed of cells tightly connected by junctions. Most often epithelia are amenable to live imaging; however, the large number of cells composing an epithelium and the absence of informatics tools dedicated to epithelial analysis largely prevented tissue scale studies. Here we present Tissue Analyzer, a free tool that can be used to segment and analyze epithelial cells and monitor tissue dynamics.

Key words Tissue Analyzer, Epithelia, Cells, Junctions, Segmentation, Live imaging, Cell tracking, Junctional remodeling, Quantitative biology

1 Introduction

Epithelia cover body structures, organs, and cavities. They act as barriers and regulate the passage of molecules between the internal milieu and the environment. Epithelia often consist of a single layer of cells tightly connected by junctions. They are very dynamic and can acquire almost any shape. Their plasticity of shape is driven by a series of cellular events, including cell death, proliferation, shape changes, and neighbor exchanges. Fully understanding epithelial development therefore requires the quantitative description of cellular events as well as collective behaviors. This is made possible thanks to the advent of affordable powerful computers that allowed biology to become quantitative. Computers are nowadays capable of executing various computer science algorithms to extract pixel information from images and convert it into biological knowledge. While biologists used to focus on local and potentially non-representative phenomena, now quantitative biology makes large-scale analysis possible. Besides being unbiased and more accurate, quantitative biology allowed for the development and in-depth validation of theoretical modeling of biological processes. Epithelia, because of their very

large number of cells, are typical examples of tissues that strongly benefited from the development of quantitative biology [1–6].

Here we introduce Tissue Analyzer (TA, formerly known as Packing Analyzer), a free software, capable of segmenting and analyzing single-layered epithelia. TA conveniently integrates, in a single package, all the tools necessary to study epithelial development, from basic cell segmentation up to quantitative analysis of cell properties such as area and shape, as well as neighbor and lineage relationships. In this chapter we describe software installation (Subheading 2.1) and introduce epithelial segmentation (Subheading 3.2). Later we discuss cell tracking (Subheading 3.4) and highlight how the software can be used to follow cell rearrangements. We finally give a brief overview of the data collected by TA (Subheading 3.7) and demonstrate the plotting capabilities of the software (Subheading 3.8).

2 Materials

2.1 Software Installation

1. The software can be installed on any recent computer capable of running JAVA 1.6 (or superior) (*see Notes 1 and 2*).
2. Download/install Tissue Analyzer
 - (a) To install TA update site in FIJI [7], please follow the FIJI guidelines (http://imagej.net/How_to_follow_a_3rd_party_update_site) (*see Note 3*).
 - (b) To install TA as an ImageJ [8] plugin, download the file from <https://grr.gred-clermont.fr/labmirouse/software/WebPA/index.html>, unzip it and place the entire folder in your ImageJ plugins directory. Restart ImageJ and search for the “Tissue Analyzer” entry in the “Plugins” menu of ImageJ (*see Fig. 1a, b*).
 - (c) To use TA as a standalone, download the appropriate version from <https://grr.gred-clermont.fr/labmirouse/software/WebPA/index.html>, unzip it and double click on the “launcher.jar” file (*see Note 4*).

2.2 Input Data

1. TA supports monochrome or RGB images.
2. TA supports pixel intensities up to 16 bits.
3. TA reads TIF, JPEG, PNG, BMP, and TGA images (*see Note 5*).
4. TA is intended to segment two dimensional Z projections of epithelial tissues (*see Note 6*).
5. TA handles single images only not stacks (*see Note 7*).

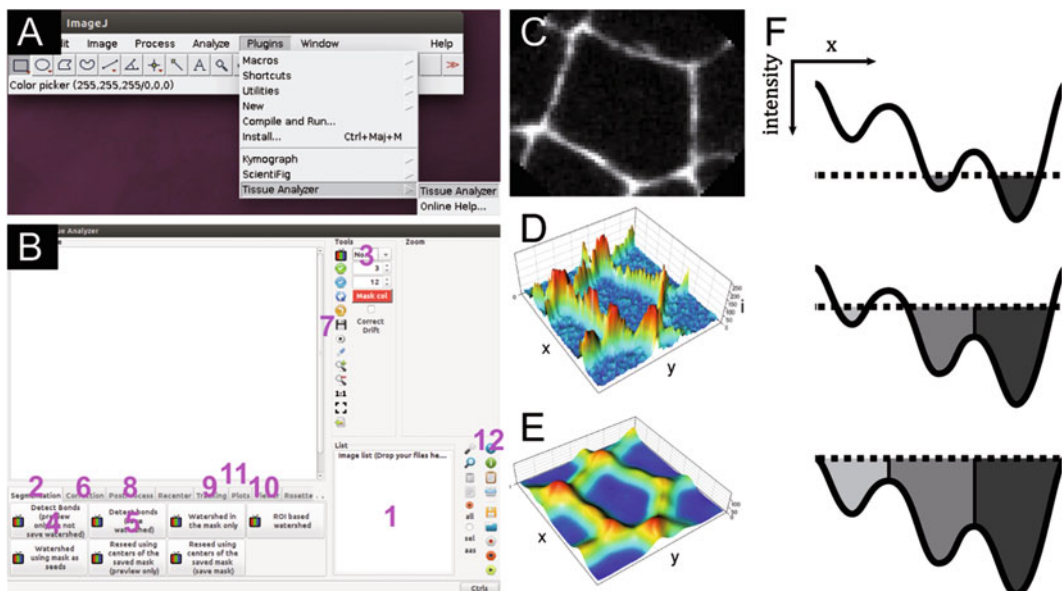


Fig. 1 Interacting with Tissue Analyzer (a) Tissue Analyzer can be found in the « Plugins » menu of ImageJ/Fiji. (b) Graphical user interface of Tissue Analyzer. (1) Image list, (2) Segmentation tab, (3) Channel selection tool, (4) “Detect Bonds (preview)” button, (5) “Detect Bonds and Save Mask” button, (6) Correction tab, (7) “save” button, (8) PostProcess tab, (9) Tracking tab, (10) Viewer tab, (11) Plots tab, (12) “help” button. (c) Confocal microscopy image of an epithelial cell. (d) 3D representation of the cell shown in (c), bright pixels form hills (membranes) and low intensity pixels form basins (cytoplasm). (e) 3D representation of the image shown in (c) after blurring, note the disappearance of small “hills” in the cell cytoplasm. (f) Scheme explaining the watershed algorithm. There are three basins in this image. The water level is indicated by a dotted line. *Top panel*, two basins contain water, but the water from these two basins did not contact. *Central panel*, the water from the two right most basins contacted and is separated by a watershed line. *Bottom panel*, the flooding is now complete and the three cells are separated by watershed lines

3 Methods

TA can be used to segment still images of immunostained epithelia and image sequences of living samples expressing fluorescently tagged proteins.

3.1 Image Acquisition Guidelines

Optimizing image acquisition is a tedious task that largely extends beyond the scope of this chapter. Nevertheless we would like to mention that even if image segmentation requires a good signal to noise ratio, overexposing samples can lead to photobleaching and tissue damage (see Note 8) which will inevitably alter the quality of the measurements and impact data analysis and should therefore be avoided.

1. TA is implemented to detect cell outlines in single layered epithelia—cells need to be labeled with a continuous membrane marker (e.g., E-cadherin in *Drosophila* or ZO-1 in *Zebrafish*).

2. If pixel intensity measurements are important for the study, make sure to avoid both bleaching and pixel saturation.
3. Post-acquisition, ensure epithelial integrity by verifying that the epithelium continues to develop.

3.2 Automated Segmentation

TA relies on the watershed algorithm (*see Note 9*) to segment epithelial cells. Since watershed segmentation is not error free, TA ships with tools to rapidly edit segmentation masks. We will now guide you through the segmentation procedure.

1. Drag and Drop images containing epithelial cells anywhere over the TA interface (*see Note 10*).
2. Select a representative image in the list (*see Fig. 1b1*). This image will be used to find appropriate settings for segmentation.
3. Click on the “Segmentation” tab (*see Fig. 1b2*).
4. Select the channel (*see Fig. 1b3* and **Note 11**) that needs to be segmented (typically any channel showing a cell outline labeling).
5. Press the “Detect Bonds (preview only)” button (*see Fig. 1b4*).
6. A dialog window opens. Please ensure that all its checkboxes are unticked.
7. Set the sigma value for the blur so that you obtain a good segmentation of cell centroids even if junctions are not properly outlined (*see Fig. 2b* and **Note 12**)—typically the bigger the cells the higher the sigma must be.
8. Press “Ok” and wait until the segmentation mask is overlaid over the image.
9. Write down the blur value, we refer to it as “strong blur” throughout this chapter.
10. Repeat **step 5**.
11. Tick the checkbox labeled “Use two blurs (better cell outlines)”. Use the strong blur value obtained at **step 9** and try several values for the “weak blur” (*see Notes 13 and 14*) until the cells are correctly outlined (*see Fig. 2d*).
12. Once the values for strong and weak blurs are determined, try ticking the “merge basins” and the “remove small cells” checkboxes to further reduce over-segmentation (*see Note 15*).
13. Once parameters are optimized for the representative image, press the “Detect bonds (save watershed)” (*see Fig. 1b5*) button to segment all the images present in the list.

3.3 Correction of Segmentation Masks

1. Select the “Correction” tab (*see Fig. 1b6*).
2. Select an image from the list and scroll over it to detect missing (*see step 3*) or erroneous cell junctions (*see step 4*).

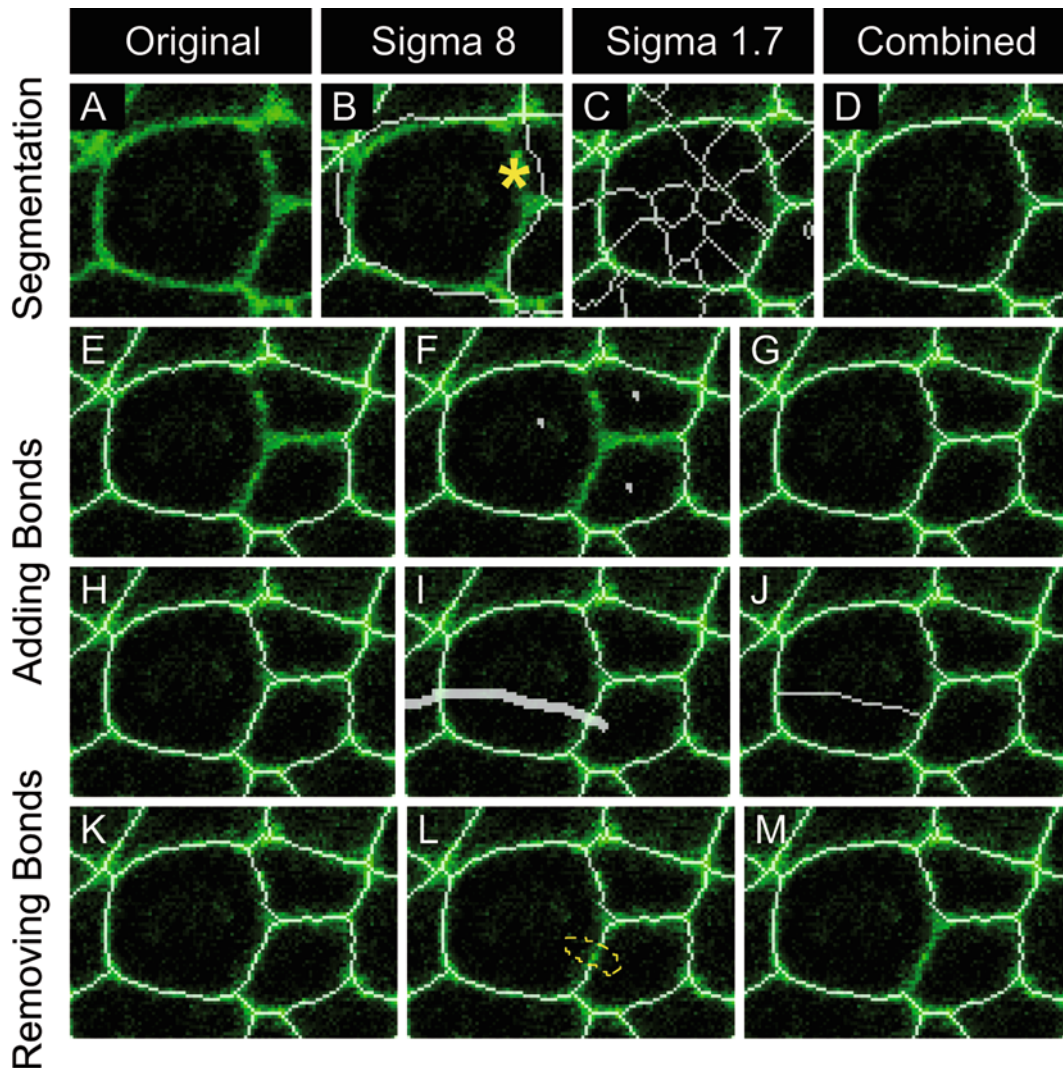


Fig. 2 Epithelial segmentation and mask edition (a) Original image. (b) Watershed mask (white) obtained with a strong blur value ($\sigma=8$), note that junctions are not properly outlined (asterisk). (c) Watershed mask (white) obtained for a blur $\sigma=1.7$, note that cell junctions are nicely outlined but there is a lot of over-segmentation (i.e., erroneous contacts in the cell cytoplasm). (d) Mask (white) obtained using cell centroids detected in (b) as seeds for the watershed segmentation (same σ as in c). (e) Image with missing junctions. (f) Same as (e) where cell centroids have been marked (these marks will be used as seeds in g). (g) Locally running the watershed algorithm using seeds/marks drawn in (f) restores junction outline. (h) Segmented image. (i) Same as in (h) but a new junction bisecting a cell was drawn manually (note the new junction is intersecting two existing junctions). (j) The software removes extra mask pixels when pressing Shift+Enter. (k) Segmented image. (l) Same image as in (k) where a small piece of cell contact mask was removed using the mouse right click (dashed outline). (m) The entire junction has been removed after pressing Shift+Enter

3. Adding missing cell contacts—Left click on the centroid of all the cells surrounding the missing junctions and press **Ctrl/Cmd+D** (compare Fig. 2e, f, see Note 16) to run the watershed algorithm locally and have the missing junctions appear (see Fig. 2g).

4. Removing false cell contacts—Right click on any pixel of the junction (compare Fig. 2k, l) and press Shift+Enter. All the pixels contained between the two vertices of the selected junction will disappear (see Fig. 2m).
5. Once done editing the mask of an image, press the “save” button (see Fig. 1b7) to store the corrected mask.
6. Finalize segmentation:
 - (a) Repeat steps 2–5 for all the images in the list until there are no segmentation errors left (see Notes 17)
 - (b) Select the “PostProcess” (see Fig. 1b8) tab and press the “Finish all” button (see Note 18).

3.4 Cell Tracking

Identifying the same cells in time and space is essential to understand tissue morphogenesis. Cell tracking is achieved in TA by pairing cells from consecutive frames and attributing them a unique identity throughout the movie.

1. Please complete “Epithelial cell segmentation” before tracking cells (see Notes 19 and 20).
2. Select the “Tracking” tab (see Fig. 1b9).
3. Press “Track cells (static tissue)” if cells don’t move much between two consecutive frames or “Track cells (dynamic tissue)” otherwise (see Note 21).

3.5 Correction of Cell Tracks

The tracking algorithm in TA is very robust, especially when the segmentation is good and the time between consecutive frames is chosen appropriately (see Note 22). However, two types of tracking errors may occur: (1) cell swapping errors where two adjacent cells exchange their identities (compare Fig. 3a, b and c, d) and (2) cell pairing errors where tracks are interrupted (compare Fig. 3a, b and e, f).

1. Identify tracking errors:
 - (a) Select the “Tracking” tab (see Fig. 1b9).
 - (b) Click on the “Correct/edit cell tracks” button to access to the “Track editor” window.
 - (c) Visually identify swapped cells (see step 2) or an interrupted track (see step 3).
2. Correction of a cell swapping error:
 - (a) Select the time point where swapping is first detected.
 - (b) Left click on the centroid of the two swapped cells (their colors should appear in the “track editor” window).
 - (c) Upon success, the button previously labeled “Nothing to do” should be renamed as “Swap cells”.
 - (d) When pressed, the “Swap cells” button will fix the swapping error on the current frame and all consecutive frames.

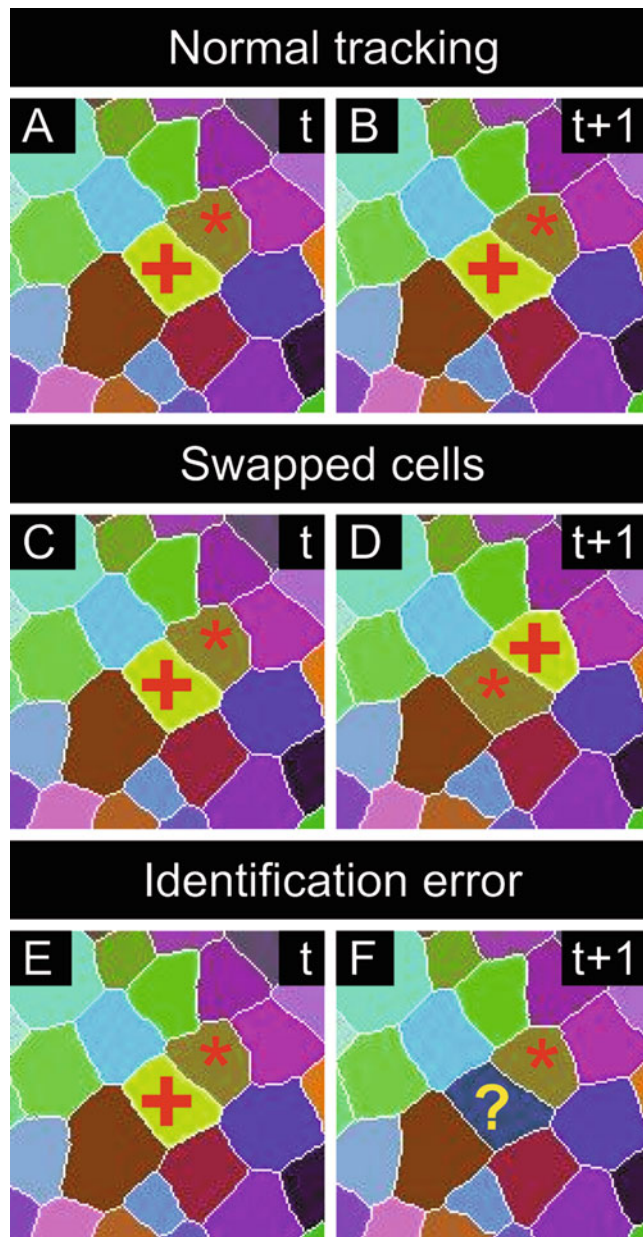


Fig. 3 Cell tracking errors (a) Cell tracks at time t (each color corresponds to a unique cell identity). (b) Same cells as in (a) at time $t+1$ (there are no tracking errors in this image). (c) Same image as in (a). (d) same image as in (c) at time $t+1$, note that the two cells in the center have swapped their identities. (e) Same image as in (a). (f) same image as in (e) at time $t+1$, note that one cells in the center has been assigned a new identity (i.e., the cell was lost)

3. Correction of an interrupted track error:

- Select the last image where the cell is still tracked properly (i.e., show the right color/identity).

- (b) In this frame, left click on the cell of interest (the color of the clicked cell should appear in the “track editor” window).
- (c) Move to the next frame and click on the cell that exhibits the wrong identity/color.
- (d) Upon success, the button previously labeled “Nothing to do” should be renamed to “Connect track”
- (e) When pressed, the “Connect track” button will fix the tracking error on all frames of the movie (*see Note 23*).

3.6 Automated Detection of T1 Transitions

Epithelia are dynamic tissues where cells often change neighbors. In particular, groups of four adjacent cells can be involved in a process called a T1 transition [9] where two cells that were in contact lose their contact while the two other cells that were not contacting suddenly gain contact. TA has a function that can detect those events; this function can be used as follows:

1. Click on the “Tracking” tab (*see Fig. 1b9*).
2. Press the “Detect T1s” button (*see Note 24*).
3. To view the result, click on the “Viewer” tab (*see Fig. 1b10*) and select the “T1s.tif” file in the “Preview” combobox.

3.7 Data Analysis and Quantifications

TA provides the user with a thorough description of cells including cell area, perimeter, elongation, division orientation, planar distribution of proteins, cell neighborhood (number and identity of neighbors) [10]. TA additionally provides information on junction length, orientation, and intensity. Any data described above is stored in a SQLite database (*see Note 25*). For the purposes of plotting using third party software, Tissue Analyzer can export tables as tab separated files that can be further opened using classical spreadsheet editors as follows:

1. Click on the “Plots” tab (*see Fig. 1b11*).
2. To export cell data, press the “Export cell data” button and select the desired columns (*see Note 26*).
3. To export junction data, press the “Export bond data” button and select the desired columns.

3.8 Data Presentation

Because visual presentation of quantitative data is often key to our understanding of tissue dynamics, TA offers the possibility to overlay/blend virtually any data over epithelial images.

1. Select the “Misc” tab.
2. Press the “Image compositer” button.
3. Select a background image and a foreground image (*see Note 27*).
4. Select the foreground opacity value (0 totally transparent; 100 totally opaque).

5. Press “Ok” to create the composite/blended image.
6. Click the “Viewer” tab (*see* Fig. 1b10) and select the newly generated image to preview it.

3.9 Going Further with Tissue Analyzer

So far, we have covered basic TA functionalities from segmentation to data presentation. However, due to space limitations and for the sake of simplicity we have left aside several useful TA functionalities. We leave it to you try advanced functions that haven't been documented here. To assist you in that respect, we have associated most buttons, spinners and tabs of Tissue Analyzer with short video demos. To open a video tutorial, press on the question mark button (*see* Fig. 1b12), then press on the button, spinner or tab of interest. Alternatively, place your mouse cursor over the desired TA component for a few seconds and wait for a small tooltip text to appear.

4 Notes

1. If JAVA is not installed on your system or if the installed version is <1.6 (*see* Note 2), please download and install the most recent JAVA runtime environment available for your system from <http://www.oracle.com/technetwork/java/javase/downloads/index.html>.
2. To determine the version of JAVA running on a computer
 - (a) Open a terminal:
 1. On a Mac: open the command line terminal by pressing together the Command and Space keys, then type in the new window “terminal” without the quotes.
 2. On Windows: press the Windows key and the “R” letter, then type “cmd” without the quotes.
 3. On Linux (Ubuntu): press Alt + F2 then type “gnome-terminal”.
 - (b) Type in the terminal “java -version” without the quotes.
3. Update sites always keep TA up to date.
4. The launcher allocates computer RAM to TA. Please never allocate more than 75 % of the total computer RAM.
5. The JPEG compression deeply modifies pixel data and should not be used for quantifications. Instead we recommend using TIF images with non-lossy or no compression. The TIF format is convenient because it preserves metadata (pixel size ...).
6. If the acquired image is a Z stack, please create a projection (e.g., maximum/average projection) using ImageJ/FIJI before using TA.

7. To split a time series to single images, open it with ImageJ/FIJI, then press File > Save As > Image Sequence... and select “TIFF” as output format.
8. If your analysis allows it, you can increase the amount of light collected without increasing laser power simply by opening the pinhole of a confocal microscope.
9. TA uses the watershed algorithm [11] to segment epithelial cells. Briefly, the watershed algorithm simulates flooding. To understand it, you should visualize your image as a landscape with pixels of low intensities (cell cytoplasm) being valleys/basins and pixels of high intensities (boundaries) being hills (compare Fig. 1c, d). Imagine now there is underground water in the soil, if the water level raises it is first going to accumulate in the lowest valleys (catchment basins) (see Fig. 1f). At early steps of immersion the water of one valley is not in contact with water of another valley (see Fig. 1f top panel). However, when the water level is further raised, water from valleys will climb uphill and ultimately meet uphill (see Fig. 1f). At the meeting point between water originating from different valleys a watershed line will be drawn (see Fig. 1f)—this watershed line can be considered as a mask outlining the membrane of an epithelial cell.
10. If an image cannot be opened/read, it will not appear in the list.
11. TA output might be either channel dependent or independent, buttons having a channel dependent output are labeled with a small RGB icon.
12. The watershed algorithm is a very sensitive algorithm affected by noise (consider hot pixel noise as extra hills giving rise to additional watershed lines). Blurring an image attenuates or removes noise (extra hills) (compare Fig. 1d, e). Importantly a strong blur gives very good detection of cell bodies but the outlining of junctions is poor (see Fig. 2b). In contrast weak blur nicely outlines junctions but cells are over-segmented (see Fig. 2c).
13. Usually weak blur value is about half that of the strong blur or less.
14. The strong blur is used to identify cell bodies, the centroids of those cells are then used as watershed seeds (basins) for the weakly blurred image—Limiting the number of seeds prevents over-segmentation and preserves the quality of boundary outlines.
15. We noted that erroneous watershed lines usually appear early during immersion, i.e., when the catchment basins are still small, the “basin fusion” parameter can be used to merge basins, thereby reducing over-segmentation. Some noise dependent erroneous basins do not grow well and give rise to very small cells (having an area less than 10px). Those cells can be removed automatically by ticking the “remove small cell” checkbox.

16. If junctions are not properly detected, manually draw the missing contacts (*see Fig. 2h–j*)—make sure that the drawn line intersects two existing junctions in the image—then press Shift + Enter to remove all unconnected pixels.
17. Identifying segmentation errors can be difficult. We found that using cell tracks can help.
18. Tissue Analyzer stores the segmentation mask and various output files for a given image in one folder. To open this folder double-click on an image in the list (*see Fig. 1b1*).
19. When tracked, each cell is given a unique random color corresponding to its identity. Cells keep this identity as long as they are tracked and are attributed a new identity when lost.
20. The tracking algorithm in TA works as follows. TA opens an image at time t , sorts all the cells contained in this image by area. TA then opens the next time point ($t+1$) in the list and tries to pair cells identified at time t with cells identified at time $t+1$. Big cells are likely to be easier to pair, less prone to pairing errors than small cells, and are therefore paired first. Cells from image at time $t+1$ that could not be paired with cells at time t are being assigned to the closest unidentified cell. Finally, cells that could not be paired (lost cells) as well as new cells that appeared at time $t+1$ are given a new unique identity. The tracking algorithm is applied recursively to all images.
21. When “Track cells (dynamic tissue)” is used, the image at time t is cut into small pieces (the size of which is specified by the “Box Size” parameter) and cross correlations are computed after sliding each image piece over the image at time $t+1$ in order to identify local cell/tissue displacement (the size of the x/y sliding box can be set using the “+/- displacement Y” and “+/- displacement X” parameters). Those local translations are used to improve the matching of cells between consecutive frames, thereby allowing for a better reidentification of cells. In order to work properly this algorithm requires that consecutive frames are relatively alike (i.e., that the time separating two consecutive frames is short).
22. Tracking errors are often associated with segmentation errors; fixing those segmentation errors and rerunning the tracking algorithm is often sufficient to solve problems.
23. Sometimes you may think you are facing an interrupted track error but you rather have encountered a swapping error that wasn’t identified. Forcing a track connection in this situation will duplicate a cell identity and affect measurements, to prevent this, the software warns you before you duplicate a track.
24. T1s involving very tiny contacts are often incorrect. They occur because of small segmentation errors. Often those “false” T1s are detected as T1s that go back and forth but always involve

the same group of four cells. TA offers the possibility to filter out those erroneous T1s by pressing the “Remove all oscillating T1s” button. The result is saved in the “stable_T1s.tif” file.

25. Those databases can be accessed directly by users having experience with manipulating SQL databases. Since SQL databases are heavily used by TA, it is important that all TA generated tables remain unmodified. Experienced users can nevertheless create extra tables or duplicate existing tables and modify them at will. We recommend closing TA before accessing databases using an external software to avoid database locking problems and similarly we recommend closing external database browsers before launching TA.
26. When cells have been tracked and tracks have been added to the TA database, it is possible to append tracking identity to the exported cell data (by selecting the column labeled “track_id_cells”, i.e., the last column).
27. Optionally the negative of the foreground and/or the background image can be used. Also mathematical morphology procedures (erosion or dilatation) can be applied the foreground image, each unique color/identity in the foreground image being treated as a separate object.

Acknowledgement

We are grateful to all Tissue Analyzer users for reporting bugs and suggesting new features. In particular we are grateful to R. Etournay, A. Sagner, J.C. Roepel, C. Collinet, Q. Mao, J. Sedzinski, and the Dahmann team. This work was supported by CNRS (BA), RIKEN (DU) and the Max-Planck-Gesellschaft (SE).

References

1. Levayer R, Lecuit T (2013) Oscillation and polarity of E-cadherin asymmetries control actomyosin flow patterns during morphogenesis. *Dev Cell* 26:162–175. doi:[10.1016/j.devcel.2013.06.020](https://doi.org/10.1016/j.devcel.2013.06.020)
2. Bosveld F, Bonnet I, Guirao B, Tlili S, Wang Z, Petitalot A, Marchand R, Bardet P-L, Marcq P, Graner F, Bellaïche Y (2012) Mechanical control of morphogenesis by Fat/Dachsous/Four-Jointed Planar Cell Polarity Pathway. *Science* 336:724–727. doi:[10.1126/science.1221071](https://doi.org/10.1126/science.1221071)
3. Blankenship JT, Backovic ST, Sanny Justina SP, Weitz O, Zallen JA (2006) Multicellular Rosette formation links planar cell polarity to tissue morphogenesis. *Dev Cell* 11:459–470. doi:[10.1016/j.devcel.2006.09.007](https://doi.org/10.1016/j.devcel.2006.09.007)
4. Marinari E, Mehonic A, Curran S, Gale J, Duke T, Baum B (2012) Live-cell delamination counterbalances epithelial growth to limit tissue overcrowding. *Nature* 484:542–545. doi:[10.1038/nature10984](https://doi.org/10.1038/nature10984)
5. Gelbart MA, He B, Martin AC, Thibierge SY, Wieschaus EF, Kaschube M (2012) Volume conservation principle involved in cell lengthening and nucleus movement during tissue morphogenesis. *Proc Natl Acad Sci U S A* 109:19298–19303. doi:[10.1073/pnas.1205258109](https://doi.org/10.1073/pnas.1205258109)
6. Monier B, Pelissier-Monier A, Brand AH, Sanson B (2010) An actomyosin-based barrier inhibits cell mixing at compartmental boundaries in *Drosophila* embryos. *Nat Cell Biol* 12 (1):60–65; sup pp 61–69. doi:[10.1038/ncb2005](https://doi.org/10.1038/ncb2005)

7. Schindelin J, Arganda-Carreras I, Frise E, Kaynig V, Longair M, Pietzsch T, Preibisch S, Rueden C, Saalfeld S, Schmid B, Tinevez JY, White DJ, Hartenstein V, Eliceiri K, Tomancak P, Cardona A (2012) Fiji: an open-source platform for biological-image analysis. *Nat Methods* 9(7):676–682. doi:[10.1038/nmeth.2019](https://doi.org/10.1038/nmeth.2019)
8. Schneider CA, Rasband WS, Eliceiri KW (2012) NIH Image to ImageJ: 25 years of image analysis. *Nat Methods* 9(7):671–675
9. Umetsu D, Aigouy B, Aliee M, Sui L, Eaton S, Jülicher F, Dahmann C (2014) Local increases in mechanical tension shape compartment boundaries by biasing cell intercalations. *Curr Biol*. doi:[10.1016/j.cub.2014.06.052](https://doi.org/10.1016/j.cub.2014.06.052)
10. Aigouy B, Farhadifar R, Staple DB, Sagner A, Röper J-C, Jülicher F, Eaton S (2010) Cell flow reorients the axis of planar polarity in the wing epithelium of *Drosophila*. *Cell* 142:773–786. doi:[10.1016/j.cell.2010.07.042](https://doi.org/10.1016/j.cell.2010.07.042)
11. Vincent L, Soille P (1991) Watersheds in digital spaces: an efficient algorithm based on immersion simulations. *IEEE Trans Pattern Anal Mach Intell* 13(6):583–598. doi:[10.1109/34.87344](https://doi.org/10.1109/34.87344)

Chapter 14

Laser Ablation to Probe the Epithelial Mechanics in *Drosophila*

Pruthvi C. Shivakumar and Pierre-François Lenne

Abstract

Laser ablation is nowadays a widespread technique to probe tissue mechanics during development. Here we describe the setup of one such ablation system and ablation experiments performed on the embryo and pupa of *Drosophila*. We describe in detail the process of sample preparation, how to disrupt single-cell junctions and perform linear or circular cuts at the tissue scale, and how to analyze the data to determine relevant mechanical parameters.

Key words Tissue mechanics, Force measurements, Epithelia, Morphogenesis

1 Introduction

During the development of an animal, cells change their shape and position to give rise to a large variety of tissue morphologies [1]. To understand how mechanical forces shape tissues in *Drosophila*, laser ablation has proven a versatile approach from the subcellular scale to the tissue scale [2–4]. Pulsed laser, in particular the near-infrared (NIR) femtosecond (fs) lasers, can ablate multiple cells or subcellular structures such as cytoskeletal filaments, thereby revealing the forces they convey [5]. In subcellular ablation and cell junction ablation, a tightly focused laser is targeted on the cellular structure of interest; the cut produces a force imbalance. By this sudden imbalance between severed and non-severed structures, ablation creates a change in cellular geometry. For instance, severing of actin-myosin networks at epithelial junctions in *Drosophila* results in the movement of cell vertices (tricellular junctions). The initial velocity of vertices after ablation is a proxy to tension of the severed actin-myosin network or cell-cell junction. Comparison between tensions along different junctions can reveal anisotropy of stresses. At the tissue scale, laser ablation can sever several cells. The initial velocity of wound margin after

ablation measures the stress-to-viscosity ratio in the direction of the velocity within the tissue [6, 7]. Here we present a laser ablation setup and its application to cellular and tissue level ablation in the *Drosophila* embryo and pupa.

2 Materials

2.1 Safety Measures

1. Use adapted light-protecting goggles (typically with optical density 7 at 1030 nm wavelength).
2. Build the setup in a dedicated room with controlled access.
3. Wear a lab coat to protect the skin and do not wear any jewels to avoid light reflection.

2.2 Laser Specification

1. Yb::YAG solid-state laser (T-Pulse, Amplitude systems, Pessac, FRANCE) with 1 W average power, 1030 nm wavelength with spectral width 7 nm, 50 MHz, 160 fs. Femtosecond lasers at different near-infrared wavelengths can also be used.

2.3 Optical Path

1. A mechanical shutter with opening/closing time scale of 1 ms.
2. A polarizer to vary the power of the laser, one $\lambda/2$ waveplate for 1030 nm wavelength.
3. IR-coated mirrors to change the direction of the path of the laser.
4. A dual-axis galvanometer optical scanners.
5. A telescope containing two lenses with IR coating.
6. Periscope to change the path of the laser perpendicular to the current one.
7. A dichroic mirror for IR light reflection and visible light transmission.
8. An inverted microscope with high numerical aperture and a high-magnification IR-corrected objective lens.
9. A commercial spinning disc coupled to microscope with fast imaging.
10. An optical bench with mirror holders and screws.

2.4 Imaging and Ablation Software

1. A spinning disc microscope (PerkinElmer) with objective 100 \times (NA 1.40, oil immersion, PlanApoVC, Nikon) for imaging.
2. Homemade Qt software to control opto-mechanical components, such as shutter and voltage control of galvanometer mirrors (via National Instruments card). This will produce different cuts, such as a point, line, or a circle.
3. Image processing software, such as Fiji/ImageJ, to analyze data.

2.5 Samples for the Experiment

1. To locate the laser point: 0.17 mm cover slip, fluorescent marker pen.
2. For the biological sample: 0.17 mm cover slip, bleach, heptane glue, halocarbon oil and embryos (of preferable stage), glass slide, Blu-tack/Patafix (a reusable pressure-sensitive adhesive), two-sided gum tape, 0.17 mm cover slip, paper pieces (approximately 0.2 mm), and the Pupae (of preferable time point, after puparium formation (APF)).

3 Methods

All the experiments are carried out at room temperature (22 °C).

3.1 Safety Methods

1. Wear IR protective goggles to avoid eye damage.
2. Wear a lab coat to protect the skin and avoid wearing any jewellery.
3. Make sure that the optical bench is not at eye level.
4. Use the IR visor and IR fluorescent paper to visualize the laser beam.

3.2 Setting Up the Laser Dissection Optical Path (See Note 1)

1. Place the laser and microscope on the optical bench in such a way that the laser beam is deflected 90° twice along its path to reach the microscope (see Fig. 1).
2. Place the shutter just in front of the laser (see Note 2).

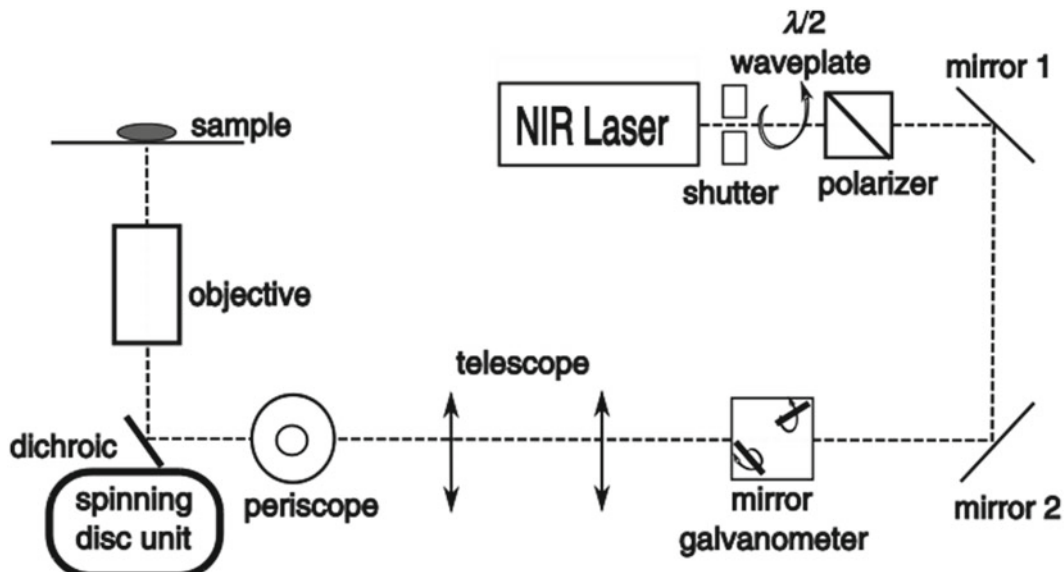


Fig. 1 Schematic of the laser ablation setup. This view combines both a top view (from NIR laser to telescope) and a side view (from periscope to sample)

3. After the shutter, place $\lambda/2$ waveplate before the polarization prism; they have to be as close as possible to the laser. While setting up, first place the prism on a manual rotator, with maximum transmission, and then position the $\lambda/2$ waveplate in front of it (see Note 3). Both of these act as a variable laser beam attenuator (see Note 4).
4. Use two mirrors to change the path of the laser by 90° (see mirrors 1 and 2 in Fig. 1). These two mirrors should be mounted on holders with two degrees of freedom and aligned in such a way that the laser path is directed towards the mirror galvanometer.
5. Place the dual-axis mirror galvanometer on the laser path (see Note 5). And the galvanometer mirrors have to be optically conjugated with the back aperture of the objective (see Note 6).
6. Place the telescope after the mirror galvanometer to expand the laser beam to match the diameter of the back aperture of the objective (see Note 7). The telescope has to be perfectly aligned with the laser beam (see Note 8).
7. Put two irises in front of the telescope to help align the laser beam by tilting the two mirrors. Use the two mirrors to align the beam to the center of two lenses (see Note 9).
8. Use a periscope with two mirrors to lift the laser beam towards the microscope entry port (see Note 10).
9. Mount the dichroic mirror under the back aperture of the objective at $\sim 45^\circ$ angle so that the laser beam is directed from the periscope to the objective (see Note 11).

3.3 Laser Point Alignment on the Screen and Calibration of the Laser Cut

1. Place the cover slip coated with fluorescent ink in the sample holder of the microscope. Proper alignment with the shutter open and no input to the galvanometer mirrors will show a laser point on the imaging software screen (see Note 12).
2. This laser spot is used for the point cut. Get the correspondence between the voltages fed to the galvanometer mirrors and the laser spot position on the imaging software screen (see Note 13).
3. The input parameters must be calibrated in the program for other cuts (i.e., circle or line) to specify the preferred length of the line or diameter of the circle in the image. In our program, the signals sent to the galvanometer mirrors are sinusoidal, and variation in the amplitude and phase difference of these two sinusoidal signals gives different cuts. For example, two signals with equal amplitude but with a 90° phase difference gives a circle cut (see Note 14).
4. The calibration will vary depending on the magnification of the objective lens used in the setup (see Note 15).

3.4 Sample Preparation

3.4.1 Biological Sample Preparation: Embryo

1. To perform ablation experiments during embryo gastrulation, collect *Drosophila* embryos after 4 h of egg-laying, then bleach, and wash with water. Depending on the stage of interest, collect the eggs after the appropriate amount of time at the preferred temperature.
2. Place the embryos on a plate of agar gel, and using a brush align them.
3. Spread some heptane glue on the cover slip. Gently press the cover slip on the embryos so they stick to the glue.
4. Put a few drops of halocarbon oil over the embryos so they stay hydrated and survive over long time periods [8].

3.4.2 Biological Sample Preparation: Pupa

1. Collect zero-hour pupae and keep them at 25 °C until preferred ablation stage (i.e., 28 h after puparium formation (APF) for retina ablations described here) (see Note 16).
2. Place two-sided gum tape (approx. 30× mm) on the glass side. Attach a small piece of paper (approx. 30× mm) on the tape as a headrest for the pupa and to raise the eye slightly.
3. Place the pupa sideways on the gum tape so the head is on the paper (see Note 17).
4. For imaging and ablation experiments, gently remove the puparium from the pupa head with forceps without damaging the pupa (see Note 18).
5. Once the puparium is removed, apply adhesive (e.g., blu-tack/patafix) to the four corners of the gum tape to mount the cover slip over the pupa.
6. Place a tiny drop of oil (e.g., Voltalef oil) on the cover slip, and gently place the cover slip on the adhesive in such a way that the oil drop is on the pupa eye (see Note 19).
7. Gently press the cover slip on the adhesive carefully without damaging the pupa. This process slightly flattens the curved eye structure, which enables a large portion of the tissue to be in focus under the microscope.

3.5 Laser Dissection

3.5.1 Embryo Ablation

1. Use *Drosophila* embryos expressing either fluorescently tagged myosin-II (sqh::GFP) to mark the myosin network or E-cadherin::GFP to mark the adherens junctions.
2. Set the average power of the ablation laser to be 250 mW at the back aperture of the objective, and the duration of the exposure to be 50–100 ms (see Note 20).
3. Use a spinning disc confocal microscope set to the following parameters: exposure time of 250 ms, laser power at 10% (maximum 20% for GFP), and a recording rate of 1 frame per second or higher (see Note 21).

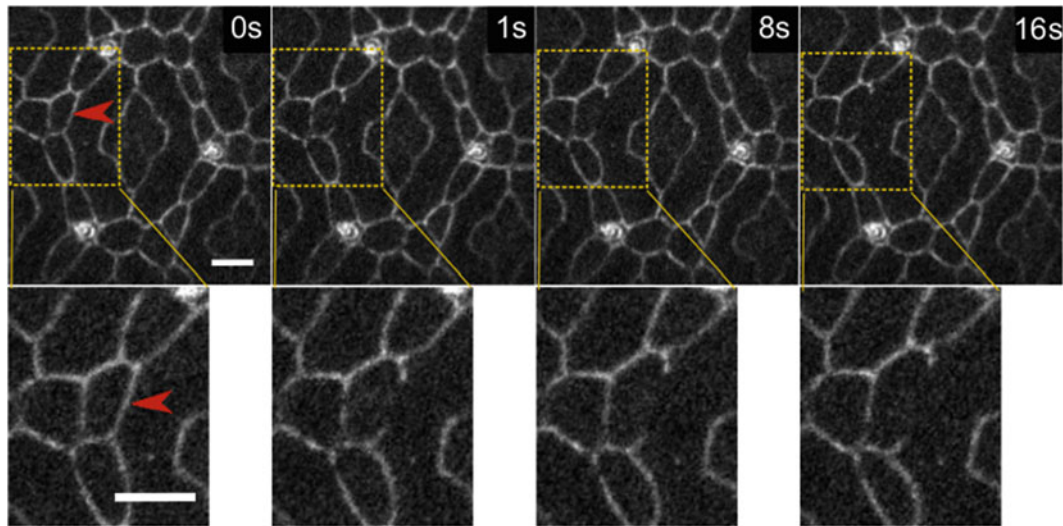


Fig. 2 A cell junction cut ablation experiment in a 28-h APF *Drosophila* pupal eye. The pupae express E-cadherin tagged with GFP (E-cad::GFP) to visualize cell junctions, and the site of the ablation is identified by the red arrowhead. The bottom panels are zoomed insets of the areas within the yellow rectangles for each time point. Scale bar: 4 μ m

4. Apply the same procedure for a cell junction cut in the embryo, although the ablation laser power may vary slightly.

3.5.2 Pupal Eye Ablation (Fig. 2)

1. Use the *Drosophila* pupae with the α -catenin tagged with GFP to label the membranes (adherens junction plane) (see Note 22).
2. Place the targeted cell junction within the focal plane and align the laser point on the junction.
3. For 28-h APF pupae, the average laser power must be 380 mW at the back aperture of the objective and the duration of the exposure within 50–200 ms.
4. Use a spinning disc confocal microscope set to the following parameters: exposure time of 250 ms, power at 10%, and a recording rate of 1 frame per second (see Note 23).
5. Apply the same procedure for tissue-level ablation in the eye, varying the duration of exposure depending on the radius of the circular ablation.

3.6 Analysis

1. Open the recorded ablation images in Fiji/ImageJ and measure the opening distance between vertices of the ablated junction as they move apart over the time (Fig. 3). Plot the vertex-to-vertex distance over time. The initial velocity of the vertices just after the ablation is determined by the ratio of the remaining force in the non-severed structure over the friction coefficient; this ratio is proportional to the tension of the severed junction just prior to the ablation (see Note 24).

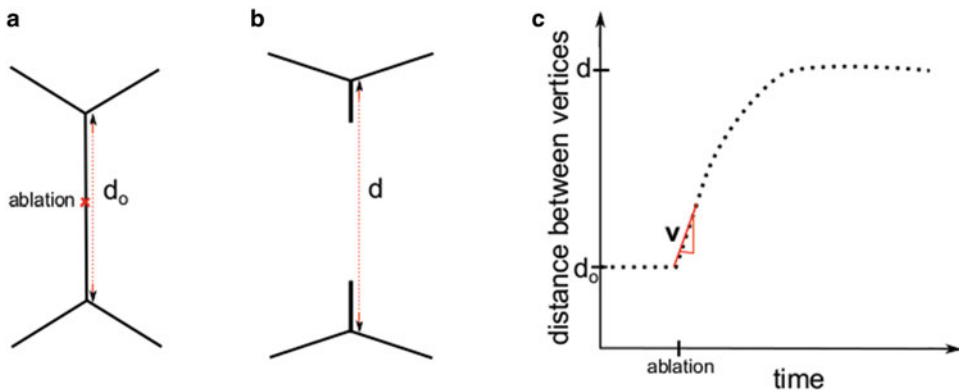


Fig. 3 Schematic of junctional cut. Schematic of a cell junction (a) before ablation with junction length d_0 and (b) after ablation with the two vertices opening length d . (c) A graph of the distance between two vertices over time with a linear fit (in red), slope of this linear fit measures the initial velocity

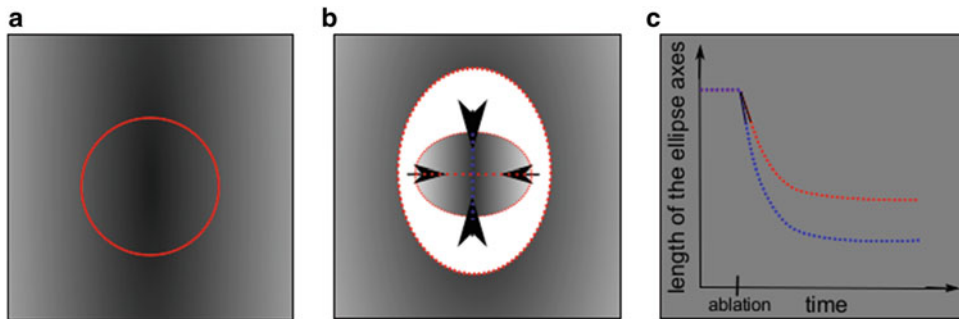


Fig. 4 Schematic of a circular cut. Schematics of circular cut in a tissue (a) before ablation with the circle to be cut in red and (b) after ablation with a fitted ellipse to measure the minor and major axes (blue and red perpendicular line). (c) A graph of minor (blue) and major (red) axis lengths versus time with a linear fit for both curves, with slope measuring the initial velocity

2. Circular ablation of a tensed tissue results in the contraction of the tissue inside the circle. The tissue retracts with an elliptic shape if stresses are anisotropic (see Note 25). Fit the shape outline over time and measure the minor and major axes (Fig. 4). The initial velocity of retraction in one axis is equal to the stress-to-viscosity ratio along that axis. The ratio of velocities of the two axes gives the anisotropy of stress (see Note 26).

4 Notes

1. Here we describe the design of a home-built setup. Alternatively two-photon microscopes, which use NIR-fs lasers, are also suitable for these types of experiments. UV pulsed lasers have also been used successfully [9].

2. Most mechanical shutters function like an iris, so when it is fully closed there is still a small aperture. Therefore, place the shutter in such a way that when the shutter is closed it should completely block the laser beam, and when it is open it fully transmits the laser beam.
3. The efficiency of a $\lambda/2$ waveplate is normally $<100\%$, so if the polarization prism is not oriented along the laser beam polarization, the maximum transmission of the attenuator will be reduced. Therefore place the power meter after the prism and adjust it to get the maximum power for optimal orientation.
4. Light reflected by the attenuator should be sent to a beam trap (a black metal chamber for light absorption).
5. The galvanometer mirrors are used to obtain different cuts (point, line, or circle). In our setup the ablating laser spot moves to produce cuts of different shapes; alternatively, one can move the stage of the sample holder (with a software to control the movement in order to obtain different cuts) instead of the laser.
6. The galvanometer mirrors must be conjugated with the back aperture of the objective; otherwise when the mirrors move, laser beam goes out of the aperture and laser beam will be lost.
7. The focal length of two lenses should be such that $|f_1/f_2|$ gives the preferred beam expanding factor. If the back aperture of the objective is 8 mm and the beam diameter is 1 mm, then the expanding factor is 8. So one can use $f_1 = 240$ mm, and $f_2 = -30$ mm. The distances between two lenses should be $|f_1| - |f_2|$. The focal lengths below 20–30 mm degrade the integrity of the laser beam, so it is better not to use lenses below this value. The lens with the smallest focal length must be placed first. Use a plano-convex lens and position the convex part of the lens facing outwards.
8. To focus the laser beam in the same plane as the imaging laser beam and to compensate the chromatic aberration of the microscope objective, the telescope lenses must be adjusted to produce a small divergence of the beam. An easy way is to observe the laser spot on the imaging software screen as one adjusts the telescope lenses in order to obtain a bright and focused spot.
9. For the laser beam alignment on telescope lenses, use the mirror which reflects the laser beam first to align the laser beam on first lens of the telescope and second mirror to align the beam on the second lens. Continue doing this till the laser beam is properly aligned.
10. Accurately select the size of the two mirrors that are placed after the telescope and mounted on the periscope and the size of the dichroic mirror. The minor axis should be at least as long as the diameter of the back aperture of the objective used and the major axis should be at least twice as long.

11. Inverted microscopes are suitable for laser ablation setups because they can have accessible space below the back aperture of the objective lens.
12. If the laser beam is aligned properly, then the high-intensity laser spot is observed on the imaging software screen. If not, slightly adjust the periscope mirrors to get the correct spot position, which corresponds to maximum intensity. Moving one periscope mirror forms a line on the screen, while moving the other periscope mirror forms a line perpendicular to the previous one. The point of intersection of these two is the correct laser spot.
13. Extract the coordinates of the resulting ablation shape using the imaging software. This is then used to center/position the sample for the ablation experiments or use the corresponding voltage values (previously calibrated) to move the laser spot on the preferred ablation position.
14. The resultant parameters obtained can later be used to get the cuts of desired units (normally in μm) for length or diameter.
15. Calibration varies for different objectives. For example, in our ablation system with a 100 \times objective, the two sinusoidal signals of 0.3 V amplitudes and a 90° phase difference sent to the galvanometer mirrors correspond to a circle with a 14 μm diameter.
16. An easy way to recognize a zero-hour pupa is that it looks like a pupa in shape but still has the light-whitish color of a larva.
17. Placing the pupa sideways is crucial because we need to have access to one of the eyes. To avoid confusion always use the same eye, consistently analyzing either the right or the left eye only.
18. A trick to remove the puparium: There is a cap-like structure near the head, and it is easier to remove this cap first so the puparium can be peeled off easily.
19. Using an oil drop helps to locate the eye under the microscope.
20. The ablation laser parameter sometimes varies from sample to sample, so if this happens, slightly change the laser power (20–30 mW). This applies to all samples, pupae, or embryos.
21. When imaging over long periods of time, sometimes it might be necessary to correct Z-drift while recording; otherwise analyzing the cuts will be a problem. This applies to all samples, pupae, or embryos.
22. Markers other than α -catenin: GFP can be used to label cell junctions, such as E-cadherin::GFP. However, since the E-cadherin signal is low in some junctions, α -catenin is preferable.

23. The recording time can be lowered below 250 ms but imaging laser exposure time must be changed accordingly. Quality of imaging is essential as the first few time points after ablation are used to extract recoil velocities by linear fitting. It is important to keep the number of points and the recording time interval the same to be able to compare tension at different junctions.
24. Ablation of a cell-cell junction leads to force imbalance as the tension of the targeted junction is abolished. The recoil velocity ν just after ablation is determined by the ratio of the tension T of the targeted junction just prior to ablation and the friction forces, which resist the movement of vertices:

$$\nu = T(t=0+)/\mu$$
, where ν is the initial velocity, T is the junction tension, and μ denotes the friction coefficient. The relaxation time, τ , is obtained by fitting an exponential to the curve and is determined by the ratio of friction over elastic modulus.
25. In a tissue-level cut, many cell-cell contacts are ablated at once; for a single-cell junction cut, the tension of the ablated junction is given by the initial velocity of vertices and the friction coefficient.

$$T = \nu \mu$$

Applying the same argument over many cell-cell contacts leads to

$$\sigma \sim \eta \nu / L$$

$$\nu \sim L \sigma / \eta$$

where L is the diameter of the ablation circle (used before cutting). The σ/η value for each axis gives stress-to-viscosity ratio in that direction and the ratio of σ/η values for the both the axes provides the anisotropy of stress in the tissue.

The relaxation time, τ , for both the axes can be calculated by fitting an exponential curve.

26. One can measure the σ/η by doing line cuts; however the advantage of a circular cut is that it is possible to get the stress-to-viscosity ratio and stress anisotropy from a single experiment. This also makes the comparison easy.

Acknowledgments

We thank all members of the Lenne and Lecuit groups for discussions and comments on the manuscript, in particular Claire Chardès and Crystal Love. This work has been supported by the Fondation de la Recherche Médicale (DEQ20130326509) and the Labex INFORM (ANR-11-LABX-0054) and of the A*MIDEX project (ANR-11-IDEX-0001-02), funded by the « Investissements d’Avenir » French Government program. PS is supported by a PhD fellowship from the Labex INFORM.

References

1. Heisenberg C-P, Bellaïche Y (2013) Forces in tissue morphogenesis and patterning. *Cell* 153:948–962
2. Hutson MS, Tokutake Y et al (2003) Forces for morphogenesis investigated with laser microsurgery and quantitative modeling. *Science* 300:145–149
3. Farhadifar F, Roper J-C, Aigouy B et al (2007) The influence of cell mechanics, cell-cell interactions, and proliferation on epithelial packing. *Curr Biol* 17:2095–2104
4. Rauzi M, Verant P, Lecuit T et al (2008) Nature and anisotropy of cortical forces orienting *Drosophila* tissue morphogenesis. *Nat Cell Biol* 10:1401–1410
5. Rauzi M, Lenne P-F (2011) Cortical forces in cell shape changes and tissue morphogenesis. *Curr Top Dev Biol*. doi:[10.1016/B978-0-12-385065-2.00004-9](https://doi.org/10.1016/B978-0-12-385065-2.00004-9)
6. Bosveld F, Bonnet I, Guirao B et al (2012) Mechanical control of morphogenesis by Fat/Dachsous/Four-Jointed Planar Cell Polarity Pathway. *Science*. doi:[10.1126/science.1221071](https://doi.org/10.1126/science.1221071)
7. Bonnet I, Marcq P (2012) Mechanical state, material properties and continuous description of an epithelial tissue. *J R Soc Interface*. doi:[10.1098/rsif.2012.0263](https://doi.org/10.1098/rsif.2012.0263)
8. Cavey M, Lecuit T (2008) Imaging cellular and molecular dynamics in live embryos using fluorescent proteins. *Methods Mol Biol*. doi:[10.1007/978-1-59745-542-8_8](https://doi.org/10.1007/978-1-59745-542-8_8)
9. Kiehart DP, Galbraith CG, Edwards KA et al (2000) Multiple forces contribute to cell sheet morphogenesis for dorsal closure in *Drosophila*. *J Cell Biol* 149:471–490

Chapter 15

Rapid Ovary Mass-Isolation (ROMi) to Obtain Large Quantities of *Drosophila* Egg Chambers for Fluorescent In Situ Hybridization

Helena Jambor, Pavel Mejstrik, and Pavel Tomancak

Abstract

Isolation of large quantities of tissue from organisms is essential for many techniques such as genome-wide screens and biochemistry. However, obtaining large quantities of tissues or cells is often the rate-limiting step when working *in vivo*. Here, we present a rapid method that allows the isolation of intact, single egg chambers at various developmental stages from ovaries of adult female *Drosophila* flies. The isolated egg chambers are amenable for a variety of procedures such as fluorescent *in situ* hybridization, RNA isolation, extract preparation, or immunostaining. Isolation of egg chambers from adult flies can be completed in 5 min and results, depending on the input amount of flies, in several milliliters of material. The isolated egg chambers are then further processed depending on the exact requirements of the subsequent application. We describe high-throughput *in situ* hybridization in 96-well plates as example application for the mass-isolated egg chambers.

Key words Ovary, Egg chamber, Mass isolation, FISH, *Drosophila*, Rapid ovary mass-isolation, ROMi

1 Introduction

Biological research aims towards understanding proteins, cells, tissues, and animals by observing, recording, or manipulating them ideally in their native *in vivo* state to test hypotheses. Isolation of high-quality material that can serve as an *in vivo* model for many cell biological, biochemical, and developmental questions is therefore key for many applications and often presents a bottleneck for analytical or high-throughput analyses. The isolation of material without the need for laborious micro-dissection has therefore many applications in biological research.

The *Drosophila* ovary is a key model to study cell biological, developmental, and cell cycle questions but also allows insights into mechanisms of post-transcriptional gene regulation [1–5]. Adult female *Drosophila* flies have paired ovaries that each is organized into chain-like ovarioles that harbor egg chambers of all develop-

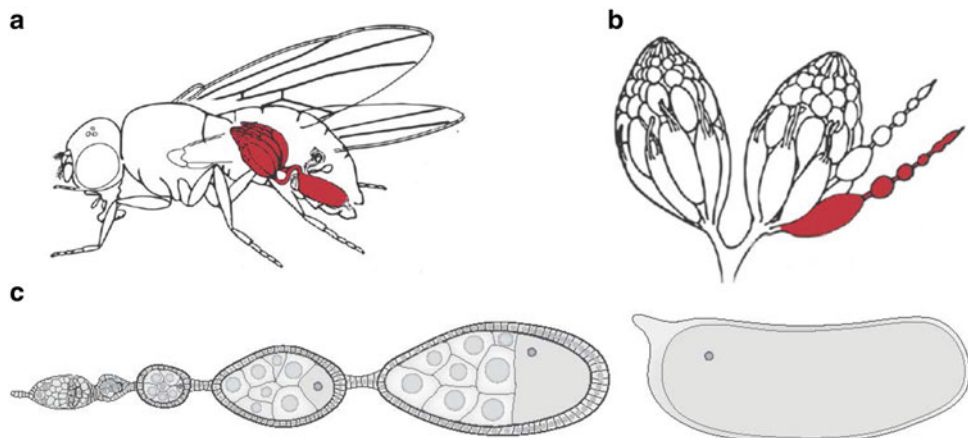


Fig. 1 Schematic representation of an ovary in a female *Drosophila* fly (a), of an isolated ovary with one ovariole highlighted in red (b), and organization of egg chambers in an ovariole (c)

mental stages (Fig. 1a, b). Each egg chamber is composed of somatic epithelial cells that overlay the germline cells, the oocyte, and the accompanying nurse cells (Fig. 1c). To obtain ovary material, the abdomen must be opened with dissection forceps, the ovaries pulled out, and remaining abdominal cuticle removed. For the analysis of single egg chambers or for whole-mount staining procedures it is essential that the muscle sheet covering the ovary is removed, ovaries are separated into single ovarioles, and individual egg chambers are isolated from the chain-like ovarioles. All these steps, opening of the abdomen and the ovary and obtaining single egg chambers, are typically done manually while inspecting the material under the microscope.

The goal was therefore to develop a protocol that would allow us to rapidly obtain large quantities of intact but individualized egg chambers that are amenable to total RNA isolation and genome-wide fluorescent *in situ* hybridization that typically required egg chambers from ~100,000 adult female flies. In particular the separation of the ovary into ovarioles and separate egg chambers is essential for whole-mount staining, mounting of the samples on a microscopic slide, and rapid inspection and imaging. Previous protocols have focused on isolation of stage-specific egg chambers primarily for biochemical analyses [6, 7]. Here we introduce an alternative method that is based on a kitchen-type grinding mill instead of a blender to isolate ovaries from the adult *Drosophila* abdomen that we call **rapid ovary mass isolation (ROMi)**. The advantage of the grinding mill is that it produces homogeneous and intact samples. It reduces the tissue loss due to damaged egg chambers and circumvents lengthy steps involving separation of egg chambers by gravity. We also describe in detail how we used the ROMi egg chambers for subsequent isolation of total RNA

and for genome-wide fluorescent *in situ* hybridization (FISH) screen to identify localized mRNAs [8]. For *in situ* hybridization we adapted a previous method for *Drosophila* embryos [9, 10] and performed the experiments in a 96-well plate format. Our protocol can be easily adapted to other types of *Drosophila* tissue such as embryo imaginal discs, testis, and even other specimen. Taken together, we have developed ROMi, a rapid ovary mass isolation, that produces (1) intact but singularized egg chambers in large quantities, (2) permits the egg chambers to be used for multiple purposes such as whole-mount staining, and (3) can be completed rapidly in five minutes.

2 Materials

2.1 Rapid Ovary Mass Isolation

1. Beaker to collect flies in, e.g., embryo collection cage (see Note 1).
2. Fixative solution: 4% Formaldehyde in PBS or PBST buffer. PBS buffer composition: 2.2.3. PBST buffer composition: 2.2.4.
3. Grinding mill (e.g., Kitchen Aid Classic Series Tilt-Head Stand Mixer with All Metal Grain Mill (Kitchen Aid, St. Joseph, MI, USA))
4. Metal Sieves (8" Ø × 2" height) 850, 425, 212 µm mesh size.
5. Embryo collection cages with stainless steel mesh—97 µm.

2.2 96-Well Fluorescent *In Situ* Hybridization

1. 96-Well MultiScreen_{HTS} DV Filter Plates, 0.65 µm.
2. Aspirator for solutions: Eppendorf Perfect Vac Manifold Quad.
3. PBS: NaCl—8 g, KCl—0.2 g, KH₂PO₄—0.24 g, Na₂HPO₄·7H₂O—2.72 g.
Dissolve in 0.8 l H₂O, adjust pH to 7.4 with HCl, and volume to 1 l.
PBT: Add 1 ml Tween-20 to 1 l of PBS.
4. 20×SSC: NaCl 87.7 g, sodium citrate 44.1 g. Dissolve in 0.4 l H₂O, adjust pH to 7.0 with 10 N NaOH, and adjust volume to 0.5 l.
5. Hybridization buffer (Hyb buffer): H₂O 150 ml, formamide 250 ml, 20× SSC 100 ml, Tween 20 0.5 ml. Total 500 ml.
6. Hybridization buffer with dextran sulfate (Hyb-Dextran): DEPC-treated H₂O 100 ml, formamide 250 ml, 20× SSC 100 ml, Tween 20 0.5 ml, 50% dextran sulfate 50 ml. Total 500 ml. For dextran sulfate: prepare 100 g of dextran sulfate in DEPC H₂O and adjust volume to 200 ml. Store at 4 °C.
7. Wash buffer: H₂O 200 ml, formamide 250 ml, 20× SSC 50 ml, Tween 20 0.5 ml. Total 500 ml.

8. Mounting solution: 20 mM Tris–HCl pH 8.0, 0.5% *N*-propyl gallate, 90% glycerol.
9. Anti-digoxigenin-POD Fab fragments.
10. Cy3-reagent.
11. 4',6-Diamidine-2-phenylindol (DAPI) was used at 1:1000 dilution.
12. Mounting medium—100% glycerol with 2% *N*-propyl-gallate.

3 Methods

3.1 Rapid Ovary Mass Isolation

1. Flies were raised on standard laboratory conditions (see Note 2). Prior to egg-chamber isolation, mixed-sex flies were fed with a fresh suspension of active, dry baker's yeast (see Note 3). To obtain a mixture of egg chambers of all developmental stages, we mixed batches of flies fed with fresh yeast for 2 days at 21 °C and for 1 day at 25 °C (see Note 4).
2. Flies were narcotized with CO₂, collected in a beaker, and kept narcotized for a maximum of 5 min before proceeding (Fig. 2a and see Note 5).
3. To prepare flies for whole-mount fluorescent *in situ* hybridization, narcotized flies were immediately immersed in 4% formaldehyde in PBS (see Note 6). Alternatively, for the preparation of ovarian extract, for biochemical analyses, or isolation of total RNA from egg chambers, flies were immersed in ice-cold PBS instead.
4. Collected flies were rapidly processed twice through a metal grain mill adaptor for a standard food processor and the entire flow-through collected (Fig. 2b) (see Note 7). The grinding settings can vary from fine to coarse; we used a fine setting (grade step “3”) (see Note 8).
5. The ground flies were size-separated using 850, 425, and 212 µm sieves successively (see Note 9) and collected in an embryo collection cage (mesh size 97 µm) that was placed in a large glass beaker (Fig. 2c, d) (see Note 10). The flow-through was highly enriched for individual egg chambers of all developmental stages (Figs. 2f and 3a). To ensure that all egg chambers passed the mesh, the sieves were briefly rinsed with a little amount of PBS (e.g., from a squeeze bottle, see Note 9).
6. Collection of mass-isolated material (Fig. 2) varied depending on the subsequent application:
 - (a) For *whole-mount fluorescent in situ hybridization experiments* the co-isolation of testis and gut materials did not disturb the subsequent analysis (see Note 11). The filtrated material was kept in the embryo collection cage and

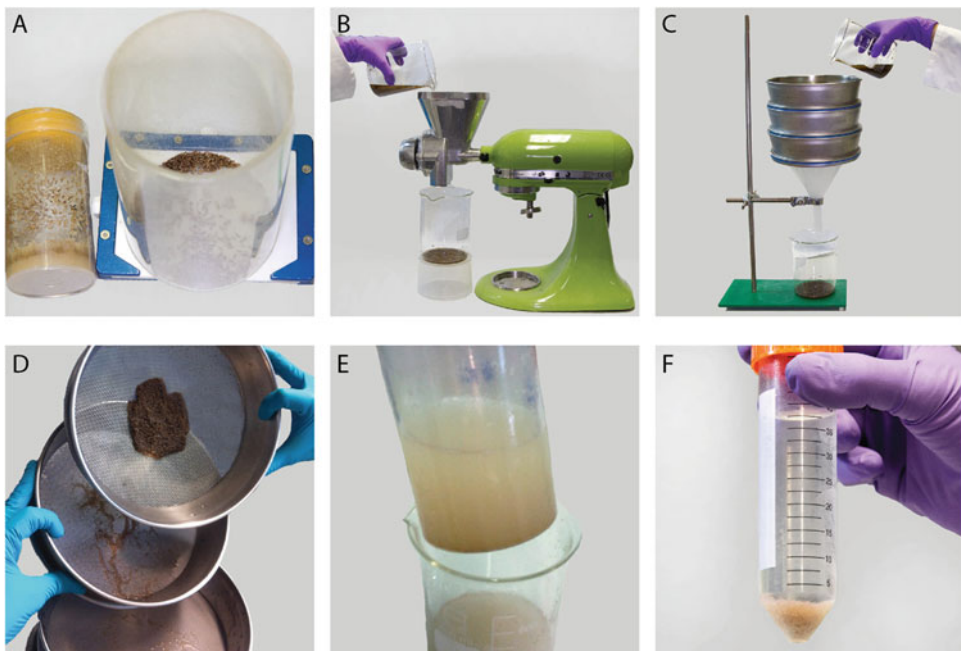


Fig. 2 Steps of rapid ovary mass isolation from whole flies to isolated egg chambers in a reaction tube. **(a)** Anesthetized flies in the collection cage on a fly pad. **(b)** Grinding of flies in a kitchen-type grinding mill. **(c)** Separation of the ovary material by sieving the ground flies. **(d)** Close-up view of the fractions retained in each level of the sieve pyramid. **(e)** Repurposed inverted embryo collection cage used to wash the ovary material after isolation. **(f)** Isolated ovary material in a Falcon tube

remained in fixative solution for an additional 15 min, resulting in an overall fixation time of 20 min interrupted by occasional stirring of the material. The cage with egg chambers was then transferred to a new beaker containing PBS and washed twice for 5 min, replacing the PBS solution after the first round. The egg chambers in the embryo collection cage were then transferred stepwise into 100% methanol in the following sequence: 25% methanol in PBS, 50% methanol in PBS, and 75% methanol in PBS. At each step egg-chambers were equilibrated for 5–10 min with occasional swirling of the beaker. Finally, egg chambers were removed from the cage/sieve by gently tipping them into a 50 ml reaction tube and releasing egg chambers from the bottom of the sieve using a methanol-filled squeeze bottle (*see Note 12*). The washing methanol was replaced with fresh methanol after allowing the egg chambers to settle by gravity (~5 min). The egg chambers were then used for whole-mount *in situ* hybridization (*see Subheading 3.2*) or stored at -20 °C (*see Note 13*).

(b) For *isolation of total RNA* we kept the mass-isolated egg chambers on ice in cold PBS and manually selected

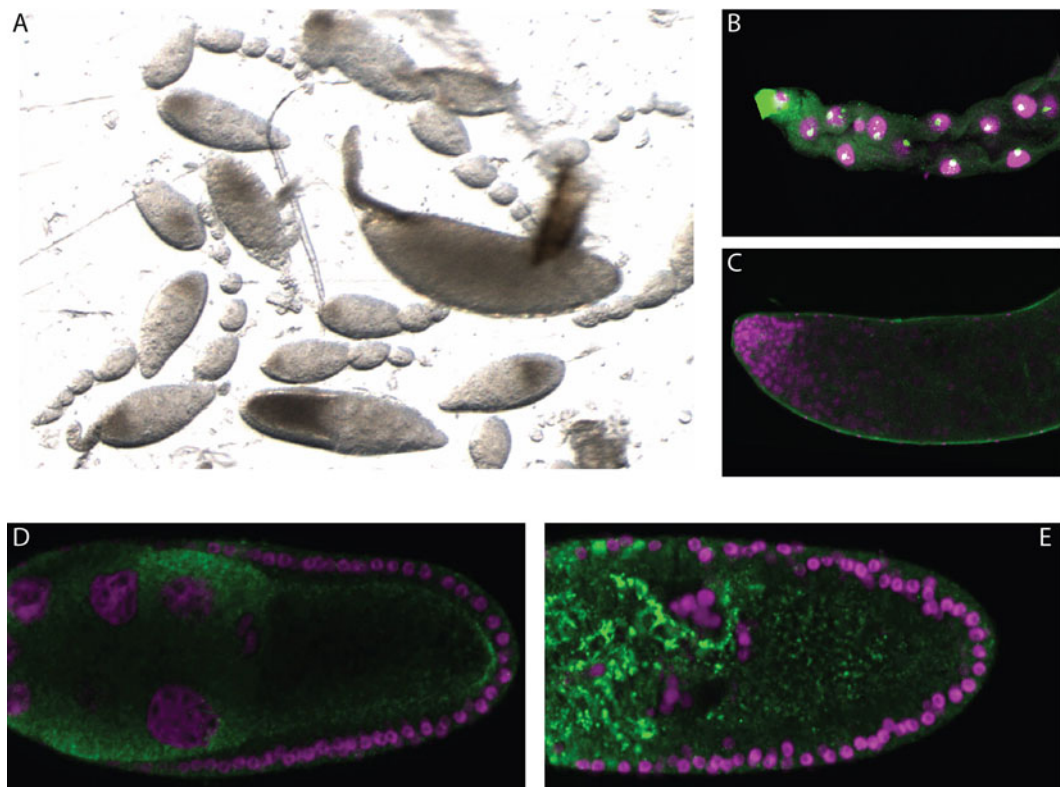


Fig. 3 Image of egg chambers isolated by mass isolation (a). Fluorescent signal in gut (b) and testis (c) tissue “contaminations” after *in situ* hybridization. Properly fixed mass-isolated egg chambers after fluorescent *in situ* hybridization against *mapmodulin* mRNA (d) compared with material fixed only after isolation (e)

egg chambers at early stages (germanium to stage 7, previtellogenesis), late stages (stage 9–10, postvitellogenesis), and full ovaries highly enriched for stage 11+ egg chambers using a stereomicroscope. For each stage we collected at least 10 μ l of total material that was snap-frozen immediately.

- (c) For preparation of *ovarian extract*, mass-isolated egg chambers were collected in a 50 ml reaction tube and briefly spun down (e.g., at 1000 rpm in a table-top megafuge) and any excess PBS supernatant removed. This yielded a highly concentrated egg-chamber extract useful for example for *in vitro* translation reactions [11].

3.2 96-Well Fluorescent *In Situ* Hybridization

1. Mass-isolated egg chambers were transferred stepwise into PBT in a suitable reaction tube (see Note 14). Each step was allowed 5-min washing time on a rotating table and ~5 min

to settle by gravity. The following solutions were used sequentially: 75 % methanol in PBT, 50 % methanol in PBT, and 25 % methanol in PBT.

2. Egg chambers were then washed six times in PBT to remove any methanol, each wash step again taking 5 min on a rotating table and another 5 min to allow egg chambers to settle by gravity.
3. Egg chambers were then briefly washed in a solution of PBT and Hyb (1:1) before being pre-hybridized in 100% Hyb for 1 h at 55 °C.
4. Egg chambers in Hyb solution were then transferred to a 96-well plate by using a pipette tip with a wide opening that prevents material from getting stuck. Hyb solution was then removed by vacuum and replaced with 200 µl of Hyb-dextran buffer containing the antisense RNA probes (see Note 15). Hybridization of RNA probes was allowed overnight at 55 °C on a rocking platform (see Note 16).
5. The next day 100 µl of pre-warmed (55 °C) wash buffer was added to each well and immediately removed together with probe solution by vacuum.
6. Egg chambers were once more rinsed with 150 µl of wash buffer and then washed four times for 1 h each in 150 µl of wash buffer at 55 °C.
7. We next washed egg chambers five times for 1 h each at 55 °C in 150 µl PBT; the last wash was left overnight at 55 °C (see Note 17).
8. The next day, egg chambers were washed twice for 1 h in 150 µl PBT at room temperature.
9. After the last wash, 200 µl antibody solution was added per well and incubated overnight at room temperature. The antibody solution contained anti-DIG antibodies diluted 1:200 in PBT.
10. On the last day, egg chambers were rinsed with 150 µl of PBT and then washed ten times in 150 µl of PBT for 30 min at room temperature (see Note 18).
11. For detection egg chambers were incubated with Cy3-tyramides 1:70 diluted in 50 µl of amplification buffer for 30 min.
12. Egg chambers were then washed ten times for 30 min at room temperature in 150 µl of PBT. DAPI, diluted 1:1000, was included in one of the wash steps (see Note 19).
13. Finally, all PBT was removed and ~100 µl mounting medium was added (see Note 20).

4 Notes

1. To collect adult flies we used an embryo collection cage that has a perforated bottom (stainless steel mesh) that we placed on a fly pad. This way, the flies were kept narcotized until enough were collected.
2. For standard laboratory conditions of raising flies please refer to the webpage of the Bloomington Stock Center (http://flystocks.bio.indiana.edu/Fly_Work/culturing.htm) or standard literature on *Drosophila* as model system for example [12].
3. For the purpose of whole-mount staining or hand-selection of egg chambers for RNA isolation, the presence of gut and testis from male adult flies in the preparation is unproblematic (Fig. 3b, c). If necessary, adult males could be removed prior to mass isolation either manually or genetically using the hs-hid system that prevents eclosion of male flies [13].
4. The time and temperature at which flies were fed with fresh yeast prior to mass isolation are not critical; instead, the incubation time (1–2 days) and temperature (18–29 °C) can be experimentally determined and adjusted depending on required material. Prolonged incubation time and higher temperature simply increase developmental speed and result in enrichment of older egg chambers.
5. The beaker had a diameter of 10 cm and we collected between ~400 and up to ~4000 flies per round of mass isolation. These were between 0.3 and 3 g of fly material, but the exact weight can vary with feeding conditions and strains used. Too many flies per round of mass isolation can decrease the purity of the sample.
Keeping flies narcotized for prolonged time periods strongly impaired the egg-chamber constitution and resulted in necrotic egg chambers.
6. Grinding the flies in the presence of fixative greatly improved the condition of the egg chambers: flies that were subjected to grinding in PBS and fixed subsequently experienced deformation of the egg chamber due to physical stress; such deformations were clearly visible in the staining procedure and can greatly influence the mRNA distribution (Fig. 3d, e). The volume of the fixative is not relevant; however we typically used 100 ml fixative for 400–4000 flies (0.3–3 g).
7. Using a grinding mill instead of a blender as described in previous protocols is critical—by using a kitchen-type grinding mill each fly will experience a similar pressure and pass the grinder only once. In a blender flies are often cut repeatedly and the site where the blade cuts is variable. Consequently, using a blender the tissue is inhomogeneous and many ovaries are damaged.

8. The grinding step size will have to be determined for the specific equipment used for the grinding. The standard Kitchen Aid grinding mill has 10 step-sizes. Counting from the finest setting, we used the third-grade step. In our hands, a finer setting destroyed the egg chambers; a coarser grinding step size left flies mostly intact.
9. Smaller mesh sizes can be used depending on the requirements. For instance to obtain only young egg chambers of stages 2–8 it is possible to remove older egg chambers using a 90 μm or even a 75 μm wide sieve. In instances, for example to prevent dehydration, it might be advantageous to perform the washing while the sieve is partially immersed in solution, e.g., for isolating material for biochemistry.
10. We repurposed embryo collection cages into a container with a mesh bottom (Fig. 2e). The mesh size was small enough to prevent egg chambers from leaking but allowed them to be immersed in solution. Using the sieve, egg chambers could be easily transferred from one solution to the next.
11. In the whole-mount staining procedure experiments are inspected by eye and non-egg chamber materials are therefore easily spotted. In some cases, the small amount of gut or testis material even provided useful information.
12. Be careful not to loose material. It is also possible to collect the egg chambers into a beaker first and then gently tip them into a 50 ml reaction tube. In case you are also using the plastic embryo collection cage, be careful to immediately wash the methanol off after removing the material; otherwise the plastic easily cracks when methanol is evaporating.
13. We have stored our egg chambers in methanol at $-20\text{ }^{\circ}\text{C}$ for up to 2 years without visible damage.
14. We used approximately 1.5 ml of mass-isolated egg-chamber material for one 96-well plate. For this, a suitable container is a 15 ml reaction tube and for each washing step 12 ml of buffer was used. Whenever mass-isolated tissue immersed in methanol is being transferred by a pipette be sure to pre-wet the tips and use tips with wide opening.
15. The hybridization buffer differed from the pre-hybridization buffer solely by the presence of dextran. Of the in vitro-transcribed probes 0.5–5 ng labeled RNA per reaction was typically sufficient.
16. All washes and incubation in 96-well plates were done on rocking platform to gently mix the solution. To avoid evaporation of buffer overnight at high temperatures, seal the lid of the plate.
17. Again, to avoid evaporation of buffer overnight, seal the lid of the plate.

18. The total volume of the washes is more critical than the incubation time; if necessary shorten the washes to 10 min, but do not use less than ten washes.
19. Again, the total volume of the washes is more critical than the incubation time; if necessary shorten the washes to 10 min, but do not use less than ten washes.
20. A little bit of PBT left does not do any harm. Make sure to let the egg chamber equilibrate in mounting solution at least overnight before mounting them on a microscope slide. When transferring egg chambers from 96-well plates to microscopic slides wet the pipet tips in mounting solution, use tips with wide opening, and pipet carefully due to high viscosity of the mounting solution.

Acknowledgements

We would like to thank Daniel Lakatos and Franziska Friedrich for drawings of fly ovaries, Michaela Rupprecht for photos of ROMi procedure and help with processing the photos, and Daniel Lakatos for critical reading of the manuscript.

References

1. Zhao T et al (2012) Growing microtubules push the oocyte nucleus to polarize the *Drosophila* dorsal-ventral axis. *Science* 336(6084):999–1003
2. Cai D et al (2014) Mechanical feedback through E-cadherin promotes direction sensing during collective cell migration. *Cell* 157(5):1146–1159
3. Tadros W et al (2007) SMAUG is a major regulator of maternal mRNA destabilization in *Drosophila* and its translation is activated by the PAN GU kinase. *Dev Cell* 12(1):143–155
4. Martin KC, Ephrussi A (2009) mRNA localization: gene expression in the spatial dimension. *Cell* 136(4):719–730
5. Ashburner M, Bergman CM (2005) *Drosophila melanogaster*: a case study of a model genomic sequence and its consequences. *Genome Res* 15(12):1661–1667
6. Petri WH, Wyman AR, Kafatos FC (1976) Specific protein synthesis in cellular differentiation. III. The eggshell proteins of *Drosophila melanogaster* and their program of synthesis. *Dev Biol* 49(1):185–199
7. Theurkauf WE, Hawley RS (1992) Meiotic spindle assembly in *Drosophila* females: behavior of nonexchange chromosomes and the effects of mutations in the nod kinesin-like protein. *J Cell Biol* 116(5):1167–1180
8. Jambor H et al (2015) Systematic imaging reveals features and changing localization of mRNAs in *Drosophila* development. *Elife*. doi:[10.7554/elife.05003](https://doi.org/10.7554/elife.05003)
9. Lecuyer E et al (2007) Global analysis of mRNA localization reveals a prominent role in organizing cellular architecture and function. *Cell* 131(1):174–187
10. Lecuyer E et al (2008) High-resolution fluorescent *in situ* hybridization of *Drosophila* embryos and tissues. *CSH Protoc.* 2008:pdb prot5019
11. Castagnetti S et al (2000) Control of oskar mRNA translation by Bruno in a novel cell-free system from *Drosophila* ovaries. *Development* 127(5):1063–1068
12. Ashburner M, Golic KG, Hawley RS (2005) *Drosophila*: a laboratory handbook, vol 1, 2nd edn. Cold Spring Harbor Laboratory Press, Cold Spring Harbor, New York
13. Starz-Gaiano M, Lehmann R (2001) Moving towards the next generation. *Mech Dev* 105(1-2):5–18

Chapter 16

Chromatin Immunoprecipitation for Analyzing Transcription Factor Binding and Histone Modifications in *Drosophila*

Yad Ghavi-Helm, Bingqing Zhao, and Eileen E.M. Furlong

Abstract

Chromatin immunoprecipitation followed by next-generation sequencing (ChIP-seq) is an invaluable technique to assess transcription factor binding and histone modifications in a genome-wide manner, an essential step towards understanding the mechanisms that govern embryonic development. Here, we provide a detailed protocol for all steps involved in generating a ChIP-seq library, starting from embryo collection, fixation, chromatin preparation, immunoprecipitation, and finally library preparation. The protocol is optimized for *Drosophila* embryos, but can be easily adapted for any model organism. The resulting library is suitable for sequencing on an Illumina HiSeq or MiSeq platform.

Key words *Drosophila*, Transcription, Development, Chromatin immunoprecipitation, ChIP-seq, Next-generation sequencing

1 Introduction

Chromatin immunoprecipitation (ChIP) is a powerful method to analyze transcription factor occupancy or histone modifications in vivo and has been successfully used to identify the binding sites of a wide range of proteins in *Drosophila* embryos [1–4]. The method is based on the immunoprecipitation, using specific antibodies, of the protein of interest bound to chromatin [5]. ChIP experiments generally involve the cross-linking of proteins to chromatin using formaldehyde, especially for DNA-binding factors. For histone modifications, ChIP can be performed on either formaldehyde-cross-linked or native samples [6, 7]. In both cases, the chromatin is extracted and sheared by sonication or using micrococcal nuclease into short fragments of approximately 200 bp. The DNA fragments specifically bound by the protein of

These authors contributed equally.

interest are isolated by immunoprecipitation using an antibody directed against the protein of interest, or against a tag attached to the protein. After the immunoprecipitation step, the cross-links are reversed, and the DNA purified. The subsequent identification of the genomic regions bound by the immunoprecipitated protein can be performed either by quantitative real-time PCR for a small number of regions or by sequencing (ChIP-seq) to obtain a genome-wide view.

We routinely prepare chromatin from a minimum of 0.2 g of *Drosophila* embryos, which corresponds to ~200 million nuclei for a staged collection at 6–8 h after egg lay (or about 10,000 embryos from stages 10 to 11). This provides enough material (about 100 µg of chromatin) to perform 3–20 ChIP experiments, depending on the immunoprecipitated protein. Typically for transcription factors more input chromatin is required for a good ChIP compared to histone modifications, which generally have a much higher percentage recovery. Alternatively, to perform ChIP in a specific cell type, we prepare chromatin from FACS-sorted fixed nuclei using our BiTS method (batch tissue-specific ChIP [1, 8]), which is an optimized easy protocol to dissociate intact nuclei from fixed embryos and use FACS to sort cell-type-specific nuclei based on a transgenic tag or a good antibody directed against a nuclear tissue-specific protein. When working with very rare cell populations, fixed embryos can be stored at –80 °C until enough embryos are obtained to sort. For the analysis of histone modifications, an alternative protocol that requires less input material can be used [9].

This chapter provides a detailed description of the different steps needed to prepare a ChIP-seq library, including many important quality controls. The initial steps of the protocol are tailored for preparing chromatin from *Drosophila* embryos, but could be adapted to any organism with minor modifications. The obtained library is suited for high-throughput sequencing using the Illumina platform.

2 Materials

2.1 Embryo Collection and Cross-Linking

1. Staged *Drosophila* embryos collected on apple-juice-agar plates as described in ref. 10 (see Note 1).
2. Collection sieves (112 µm/355 µm/710 µm bottom to top).
3. Nitex membranes (approximately 5 × 5 cm each), 125 µm.
4. 37% Formaldehyde solution (w/w).
5. Cross-linking solution: 1 mM EDTA, 0.5 mM EGTA, 100 mM NaCl, 50 mM HEPES, pH 8.0. Filter (0.22 µm) each batch after preparation. Store at room temperature.
6. Glycine solution: 125 mM Glycine, 0.1% Triton X-100 (v/v) in PBS. Store at room temperature.
7. Heptane.

8. Methanol.
9. Dechorionating solution: 3% Sodium hypochlorite (v/v) (or 50% commercial bleach). Prepare fresh.
10. PBT solution: 0.1% Triton X-100 (v/v) in PBS. Store at room temperature.
11. 50 mL Greiner centrifuge tubes.
12. 1.5 mL Tubes with safe lock (*see Note 2*).

2.2 Evaluation of Embryo Developmental Stage Distribution Within a Collection

1. PBT solution: 0.1% Triton X-100 (v/v) in PBS. Store at room temperature.
2. Methanol.
3. DAPI 1 μ g/mL (100 \times stock), store at 4 °C.
4. Glycerol.
5. Microscope slides and cover slips.
6. Colorless nail polish.

2.3 Chromatin Preparation

1. Protease inhibitor stock solutions (1000 \times stock): 10 mg/mL Aprotinin (in water), 10 mg/mL leupeptin, and pepstatin (in DMSO). Store in small aliquots at -20 °C.
2. Phenylmethylsulfonyl fluoride (PMSF): 100 mM Stock (100 \times) in 2-propanol. Store at room temperature.
3. PBT solution: 0.1% Triton X-100 (v/v) in PBS. Store at room temperature.
4. 7 mL Dounce homogenizer (Kontes glass co.).
5. Cell lysis buffer: 85 mM KCl, 0.5% IGEPAL CA-630 (v/v) (Sigma), 5 mM HEPES, pH 8.0. Autoclave without IGEPAL and then add appropriate amount of IGEPAL from 10% stock. Store at 4 °C. Add protease inhibitors and PMSF just prior to use.
6. Nuclear lysis buffer: 10 mM EDTA, 0.5% *N*-lauroylsarcosine (w/v), 50 mM HEPES, pH 8.0. Store at 4 °C. Add protease inhibitors and PMSF just prior to use.
7. Bioruptor® Pico sonication device.
8. 15 mL Greiner centrifuge tubes.
9. 15 mL Bioruptor® tubes and sonication beads.
10. 1.5 mL Eppendorf® RNA/DNA LoBind microcentrifuge tubes.
11. TE buffer: 1 mM EDTA, 10 mM Tris-HCl, pH 8.0. Filter (0.22 μ m) before storage at 4 °C.
12. RNase A: Prepare 1 mg/mL aliquot and store at -20 °C.
13. Proteinase K: Prepare 10 mg/mL aliquots and store at -80 °C.
14. 10% SDS solution (w/v): Store at room temperature.
15. Phenol:chloroform:IAA, 25:24:1, pH 7.9.

16. Chloroform.
17. Glycogen: Prepare 5 mg/mL aliquots and store at -20 °C.
18. Qubit® fluorometer.
19. Qubit® dsDNA HS Assay Kit.

2.4 Chromatin Immunoprecipitation

1. 1.6 mL Low-binding reaction tubes.
2. Dynabeads® Protein A and Protein G.
3. DynaMag™-2 Magnet.
4. RIPA buffer: 140 mM NaCl, 1 mM EDTA, 1% Triton X-100 (v/v), 0.1% SDS (w/v), 0.1% sodium deoxycholate (w/v), 10 mM Tris-HCl, pH 8.0. Filter (0.22 µm) before storage at 4 °C.
5. IP dilution buffer: 0.35 M NaCl, 2.5% Triton X-100 (v/v), 0.25% SDS (w/v), 0.25% sodium deoxycholate (w/v). Store at 4 °C. Add protease inhibitors and PMSF just prior to use.
6. RIPA500 buffer: RIPA buffer adjusted to 500 mM NaCl. Filter (0.22 µm) before storage at 4 °C. Add protease inhibitors and PMSF just prior to use for the immunoprecipitation but not to the wash buffers.
7. LiCl buffer: 250 mM LiCl, 1 mM EDTA, 0.5% IGEPAL CA-630 (v/v), 0.5% sodium deoxycholate (w/v), 10 mM Tris-HCl, pH 8.0. Filter (0.22 µm) before storage at 4 °C.
8. TE buffer: 1 mM EDTA, 10 mM Tris-HCl, pH 8.0. Filter (0.22 µm) before storage at 4 °C.
9. RNase A: Prepare 1 mg/mL aliquot and store at -20 °C.
10. Proteinase K: Prepare 10 mg/mL aliquots and store at -80 °C.
11. 10% SDS solution (w/v): Store at room temperature.
12. 2 mL Phase-lock gel heavy tubes.
13. Phenol:chloroform:IAA, 25:24:1, pH 7.9.
14. Chloroform.
15. Glycogen: Prepare 5 mg/mL aliquots and store at -20 °C.
16. Qubit® fluorometer.
17. Qubit® dsDNA HS Assay Kit.

2.5 Library Preparation

1. NEBNext® ChIP-Seq Library Prep Master Mix Set for Illumina®.
2. 0.5 mL Eppendorf® RNA/DNA LoBind microcentrifuge tubes.
3. SPRIselect Reagent.
4. 0.1× TE buffer.
5. Qubit™ fluorometer.
6. Qubit® dsDNA HS Assay Kit.
7. Agilent 2100 Bioanalyzer.

8. Agilent High Sensitivity DNA kit.
9. NEBNext Singleplex Oligos for Illumina (*see Notes 3 and 4*).
10. Paired-end PCR primers (*see Note 5*).

3 Methods

3.1 Preparation of Cross-Linked Embryos

1. After four pre-lays, allow flies to lay embryos for the appropriate time window (e.g., we regularly do 2 h) and then age to the appropriate time point.
2. To collect embryos, wash the embryos from the apple-agar plates with tap water and a paintbrush into the collection sieve (*see Notes 1 and 6*).
3. Transfer embryos to 150 mL fresh dechorionating solution and incubate for 2.5 min at room temperature with stirring to dechorionate.
4. Pour the embryos into the 112 μ m size sieve and wash extensively with tap water (*see Note 7*).
5. Transfer embryos with PBT through a funnel into a 50 mL tube, and let the embryos sink.
6. Place a Nitex membrane onto a pile of tissue paper and pipette 2 mL of embryo suspension (corresponding to approximately 0.2 g of embryos) onto the membrane. Fold the membrane over to cover the embryos and gently blot the embryos dry through the membrane with a paper towel (*see Note 2*).
7. Transfer the membrane into a separate 50 mL tube containing 9.5 mL of cross-linking solution and 30 mL of heptane. Shake off the embryos, recover the membrane, and add 485 μ L of 37% formaldehyde solution. Shake the tube vigorously at room temperature (20–25 °C) for 15 min (*see Note 8*).
8. Pellet the embryos in each tube by gentle centrifugation at 500 $\times g$ for 1 min. Replace the supernatant with 30 mL of glycine solution and shake vigorously at room temperature for at least 1 min to stop the cross-linking reaction.
9. Pellet the embryos by gentle centrifugation at 500 $\times g$ for 1 min. Carefully decant the supernatant and wash the pellet with 50 mL of ice-cold PBT solution.
10. Pellet the embryos by gentle centrifugation at 500 $\times g$ for 1 min, decant the supernatant, and resuspend the embryos in approximately 10 mL of PBT solution per tube. Transfer the embryos onto separate Nitex membrane as in **step 5**, fold the membrane over to cover the embryos, and blot them dry with a paper towel.
11. Transfer a small aliquot of embryos (100–200 embryos) from the membranes into a microfuge tube containing 0.5 mL of heptane and 0.5 mL of methanol. Shake vigorously to devitellinize

the embryos, let them settle, and then remove as much liquid as possible. Wash the embryos with methanol twice and store them at -20°C in methanol. This sample from each collection, and therefore chromatin preparation, is set aside to evaluate the developmental stage of the collection (Subheading 3.2).

12. Transfer the bulk of the dry cross-linked embryos from the Nitex membrane into a 1.5 mL tube and freeze in liquid nitrogen. Cross-linked embryos can be stored at -80°C for at least 1 year.

3.2 Evaluation of Embryo Developmental Stage Distribution Within a Collection

1. To confirm the stage of each chromatin preparation, rehydrate the small sample set aside in step 11 (Subheading 3.1) by rinsing the embryos once in 1 mL of 50% of methanol/50% of PBT for 5 min.
2. Incubate the embryos with PBT containing 1 \times DAPI for 5 min. Wash the embryos twice for 5 min with PBT.
3. Replace the supernatant with 80% of glycerol, wait for the embryos to sink (clear), and mount the embryos on a microscope slide. Cover with cover slip of appropriate size and seal the sides with colorless nail polish.
4. The developmental stages present in the collection can now be examined microscopically using the morphological features defined by Campos-Ortega and Hartenstein [11]. Compare the distribution of developmental stages between repeated collections and exclude those containing inappropriate stages, or wide distribution of stages, from further analysis.

3.3 Chromatin Preparation

1. Quickly thaw embryos at room temperature and resuspend in 1 mL of ice-cold PBT solution containing protease inhibitors and PMSF. Transfer the suspension to a 7 mL Dounce homogenizer (see Note 2), add 6 mL PBT containing protease inhibitors and PMSF.
2. Homogenize 0.2 g of embryos in a 7 mL Dounce homogenizer on ice by applying 20 strokes with the loose-fitting pestle A.
3. Transfer the lysate into a 15 mL centrifuge tube and centrifuge at $400 \times g$ at 4°C for 1 min to precipitate the vitelline membranes and large debris (see Note 9).
4. Decant the supernatant into a fresh 15 mL centrifuge tube and centrifuge at $1100 \times g$ at 4°C for 10 min. Decant the supernatant and discard it.
5. Resuspend the cell pellet in 7 mL ice-cold cell lysis buffer containing protease inhibitors and PMSF.
6. Homogenize the cells in a 7 mL Dounce homogenizer on ice by applying 20 strokes with the tight-fitting pestle B. Transfer the sample into a fresh 15 mL centrifuge tubes.
7. Centrifuge the samples at $2000 \times g$ at 4°C for 4 min to pellet the nuclei. Discard the supernatant (see Note 10).

8. Resuspend the nuclear pellet in 1 mL of ice-cold nuclear lysis buffer containing protease inhibitors and PMSF, transfer into fresh 15 mL Bioruptor tube, and incubate at room temperature for 20 min.
9. Add 1 mL of ice-cold nuclear lysis buffer containing protease inhibitors and PMSF to the sample, add 300 μ L sonication beads rinsed with PBS, and sonicate using a Bioruptor Pico sonication device (15 cycles, 30 s on/30 s off) (see Notes 11 and 12).
10. Transfer the chromatin into two 1.5 mL Eppendorf low-binding tubes and centrifuge at 20,000 $\times g$ at 4 °C for 10 min.
11. Pool the supernatants to ensure a homogenous sample, keep 30 μ L for quality assessment, and freeze the remaining chromatin in 200 μ L aliquots (typically 8–10 per chromatin preparation) in liquid nitrogen. Chromatin can be stored at –80 °C for at least 1 year.
12. To determine the yield and average fragment length of the chromatin preparation, dilute the 30 μ L of chromatin set aside in step 11 with 70 μ L of TE buffer. Add 50 μ g/mL of RNase A, and incubate at 37 °C for 30 min. Treat the sample as described in steps 9–13 in Subheading 3.4 and resuspend the purified DNA in 30 μ L of TE buffer. Determine the concentration of sheared DNA using a Qubit™ fluorometer and verify its size distribution by gel electrophoresis using a 1.2% agarose gel (see Note 13). The Bioruptor settings used in this protocol give rise to an average fragment length of approximately 100–250 bp. An example is shown in Fig. 1.

3.4 Chromatin Immunoprecipitation

1. Thaw an aliquot of chromatin on ice. Based on the chromatin concentration, estimated in step 12 above, transfer the appropriate volume of chromatin to a 1.6 mL low-binding reaction tube to reach the desired amount of chromatin. For example, for chromatin modifications, 10 μ g of chromatin is sufficient, while for some transcription factors 30 μ g of chromatin may be required (see Note 14). Adjust the final volume to 500 μ L with ice-cold TE buffer and add 400 μ L of ice-cold IP dilution buffer containing protease inhibitors and PMSF. Retain 10 μ L of the sample (1% input) in a separate tube and store at 4 °C until step 8.
2. Add 1–20 μ L of serum or a suitable amount of purified antibody to each tube. Incubate at 4 °C overnight on a rotating wheel (see Notes 15 and 16).
3. For each immunoprecipitation, wash 25 μ L Dynabeads coated with protein A/protein G (1:1 mix) with 1 mL of RIPA buffer twice for 10 min each on a rotating wheel at 4 °C. Put the tube on the magnet stand, and remove the supernatant when it becomes clear (see Note 17).
4. Resuspend the beads in 100 μ L of RIPA buffer per reaction.

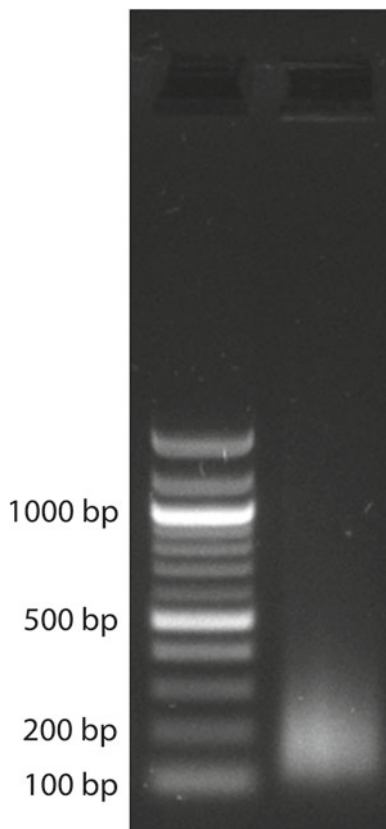


Fig. 1 Verification of sonicated fragment length. A 30 μ L aliquot of chromatin is treated with RNase A and proteinase K, reverse cross-linked, purified by phenol-chloroform extraction, and ethanol precipitated. The average length of sonicated chromatin is assessed by electrophoresis on a 1.2% TAE agarose gel. The sonication settings should produce fragments with an average size of 150–250 bp

5. Add 100 μ L of bead suspension to each chromatin sample from **step 2** and incubate at 4 °C on a rotating wheel for 3 h (*see Note 18*).
6. To purify the antigen–antibody complexes, pellet the beads by putting the tubes on the magnet stand, discard the supernatant, and rinse the beads once with 1 mL of ice-cold RIPA buffer.
7. Pellet the antigen–antibody complexes again by putting the tubes on the magnet stand and wash with 1 mL of each of the following buffers at 4 °C on a rotating wheel for 10 min: 1 \times with RIPA buffer, 4 \times with RIPA500 buffer, 1 \times with LiCl buffer, and 2 \times with TE buffer.
8. Resuspend the beads in 100 μ L of TE buffer supplemented with 50 mg/mL of RNase A and incubate at 37 °C for 30 min. From this point on, include a tube containing the 1% input sample retained in **step 1**. Add 90 μ L of TE buffer to yield a final volume of 100 μ L before RNase A addition.

9. Add SDS to a final concentration of 0.5% (w/v) from a 10% stock and incubate with 0.5 mg/mL of proteinase K at 37 °C overnight.
10. Transfer the samples to 65 °C for at least 6 h to reverse the cross-links.
11. Adjust the samples to 200 µL with TE buffer. Extract the immunoprecipitated DNA by combining the sample with 300 µL of phenol:chloroform:isoamyl alcohol in a pre-spun phase-lock tube. Mix briefly and centrifuge at 15,000×*g* at room temperature for 5 min. Add 300 µL of chloroform, mix briefly, and centrifuge again at 15,000×*g* at room temperature for 5 min. Transfer the aqueous sample to a fresh 1.6 mL low-binding reaction tube.
12. Supplement the samples with 0.25 mg/mL of glycogen, add 20 µL of 3 M sodium acetate solution, pH 5.2, and 550 µL of 100% ethanol, vortex briefly, and incubate the sample at -80 °C for at least 1 h.
13. Centrifuge the sample at 4 °C at 15,000×*g* for 30 min to precipitate the DNA, wash the pellet once with 1 mL of 70% ethanol, and centrifuge again at 15,000×*g* at 4 °C for 10 min.
14. Resuspend the purified DNA in 30 µL of TE buffer.
15. If sequence-specific binding sites for the protein of interest are known, evaluate the efficiency of enrichment by quantitative real-time PCR (see Note 19). An example of result obtained from immunoprecipitation of the Mef2 transcription factor and histone modification H3K27ac is shown in Fig. 2.
16. Determine the concentration of ChIP DNA using a Qubit fluorometer and a Qubit dsDNA HS Assay Kit following the manufacturer's instructions.

3.5 Library Preparation

1. Combine and mix the following components in a 0.5 mL PCR tube: 1–10 ng of ChIP (or input) DNA to be end-repaired (see Notes 20 and 21), 5 µL of 10× NEBNext End Repair Reaction Buffer, and 1 µL of NEBNext End Repair Enzyme Mix. Adjust final volume to 50 µL with water.
2. Incubate the reaction for 30 min at 20 °C in a thermal cycler.
3. Purify the reaction using 1.8× SPRIselect Beads. Elute the end-repaired DNA in 50 µL of 0.1× TE buffer.
4. Add and mix the following components to 44 µL of the end-repaired DNA: 5 µL of 10× NEBNext dA-Tailing Reaction Buffer and 1 µL of Klenow Fragment (exo-).
5. Incubate the reaction for 30 min at 37 °C.
6. Purify the reaction using 1.8× SPRIselect Beads. Elute the A-tailed DNA in 25 µL of 0.1× TE buffer.

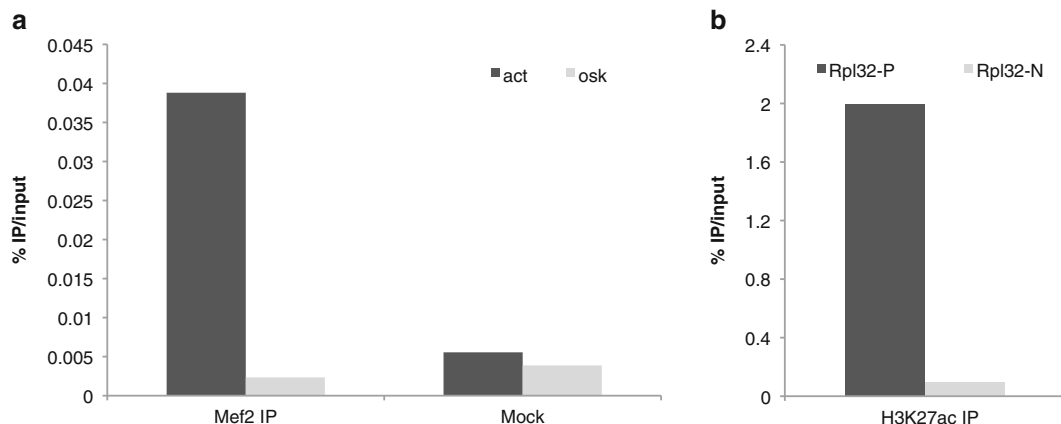


Fig. 2 Examples of qPCR results for successful ChIP experiments. (a) Enrichment of a known Mef2-binding site within the *Act57B* locus compared to a mock control. A chromatin immunoprecipitation experiment was realized using 3 μ L of anti-Mef2 antiserum (IP) or 3 μ L of pre-immune serum (mock), and assayed by quantitative real-time PCR. A specific enrichment can be observed within the *Act57B* enhancer (*actin*), a known binding site of Mef2, compared to a negative control region (*oskar*). (b) Enrichment of H3K27ac in the promoter region of *Rpl32*, compared to a negative control in the upstream of *Rpl32*

7. Add and mix the following components to 19 μ L of the A-tailed DNA: 6 μ L of Quick Ligation Reaction Buffer, 1 μ L of diluted NEBNext Adaptors (or 1 μ L of 1.5 μ M multiplexing oligonucleotide adaptors), and 4 μ L of Quick T4 DNA Ligase (see Note 22).
8. Incubate the reaction for 15 min at 20 $^{\circ}$ C (see Note 23).
9. If using NEBNext Adaptors, add 3 μ L of USERTM Enzyme Mix, and incubate the reaction for 15 min at 37 $^{\circ}$ C.
10. Purify the reaction using 1.8 \times SPRIselect Beads. Elute the adaptor-ligated DNA in 105 μ L of 0.1 \times TE buffer. Transfer 100 μ L to a new tube.
11. Perform size selection: For an insert size of 150 bp, perform dual-SPRIselect bead size selection using a ratio of 0.9 \times for the first bead selection and 0.2 \times for the second bead selection. Elute the DNA in 22 μ L of 0.1 \times TE buffer.
12. Combine and mix the following components in a 0.5 mL PCR tube: 20 μ L of size-selected DNA, 2.5 μ L of Universal PCR Primer, 2.5 μ L of Index Primer, and 25 μ L of NEBNext Q5 Hot Start HiFi PCR Master Mix.
13. Amplify using the following PCR protocol:
 - Step 1: 30 s at 98 $^{\circ}$ C
 - Step 2: 10 s at 98 $^{\circ}$ C
 - Step 3: 75 s at 65 $^{\circ}$ C
 - Step 4: GO TO step 2 for 10–15 times (see Note 24)
 - Step 5: 5 min at 65 $^{\circ}$ C
 - Step 6: Hold at 4 $^{\circ}$ C

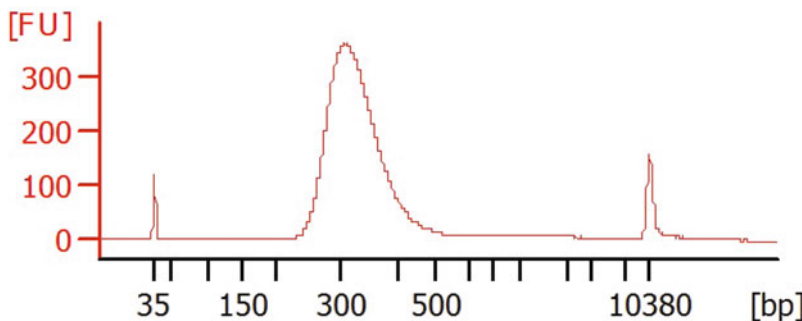


Fig. 3 Agilent 2100 Bioanalyzer analysis of a successful library before Illumina sequencing. A successful library is characterized by a single intense peak with an expected size between 300 and 400 bp

14. Purify the reaction using 0.9× SPRIselect Beads. Elute the DNA in 20 μ L of 0.1× TE buffer.
15. Determine the concentration of the library using a Qubit fluorometer and a Qubit dsDNA HS Assay Kit following the manufacturer's instructions.
16. Verify the size, purity, and concentration of the library using an Agilent 2100 Bioanalyzer with the Agilent High Sensitivity DNA kit (5–500 pg/ μ L) following the manufacturer's instructions (Fig. 3).
17. If sequence-specific binding sites for the protein of interest are known, verify that the library has maintained a specific enrichment by quantitative real-time PCR (i.e., repeat **step 15** in Subheading 3.4).
18. If using multiplexing oligonucleotide adaptors, prepare an equimolar mix of the different multiplexed libraries and repeat **step 15** again (see Note 25).
19. The library is now ready for sequencing on the Illumina platform (HiSeq or MiSeq). Follow instructions from your sequencing facility for sample submission.
20. Approximately 20 million uniquely mapped reads should be sufficient to identify all the binding sites of a given transcription factor. For organisms with a smaller genome, this is likely to be a huge excess; therefore multiplexing of different transcription factor libraries will significantly reduce costs.

4 Notes

1. For staged embryo collections, it is advisable to perform four embryo “pre-lays” of 1 h each before taking any embryos for experiments.

2. All conditions listed here are optimized for processing about 0.2 g of embryos. Larger quantities of embryos can be processed with minor modifications, as reported in [5].
3. Multiplexing oligonucleotide adaptors can be purchased from Illumina or NEB; however we routinely use our own adaptors. We purchase single-stranded HPLC-purified oligonucleotides from Sigma. The 3' thymine overhang is protected from digestion with a phosphorothioate and the 5' extremity of the non-overhanging oligonucleotide is phosphorylated. The oligonucleotides are annealed as described in [12]. Briefly, the oligonucleotides are resuspended and mixed to a final concentration of 50 μ M in annealing buffer (10 mM Tris-HCl pH 8.0, 50 mM NaCl, 0.1 mM EDTA), and then incubated in a thermal cycler using the following protocol:

2 min at 95 °C

Ramp from 95 to 75 °C at 0.1 °C/s, hold for 2 min at 75 °C

Ramp from 75 to 65 °C at 0.1 °C/s, hold for 2 min at 65 °C

Ramp from 65 to 50 °C at 0.1 °C/s, hold for 2 min at 50 °C

Ramp from 50 to 37 °C at 0.1 °C/s, hold for 2 min at 37 °C

Ramp from 37 to 20 °C at 0.1 °C/s, hold for 2 min at 20 °C

Ramp from 20 to 4 °C at 0.1 °C/s, hold at 4 °C

The multiplexing oligonucleotide adaptors are further diluted to 0.2 μ M in EB buffer and stored at -20 °C.

4. The multiplexing adaptors we use: set-of-4: ATTCCG, GCCTAA, CAAGTT, TGGAGC; set-of-10: GATGCT, CCGTAT, TTGCGG, CGTACG, TACAAG, TCCGTC, CCACTC, AAGTGC, ATTATA, GGAGAA.
5. Paired-end PCR primers can be purchased from Illumina or NEB; however we routinely use our own primers. HPLC-purified primers are purchased from MWG, diluted to 10 μ M in EB buffer, and stored at -20 °C.
6. Depending on the amount of embryos to process, we start collecting the embryos from 15 to 20 min before they reach the desired time point, which is approximately the required time to reach the fixation step (step 7, Subheading 3.1).
7. Wash embryos until bleach smell is gone. Removal of the chorion will cause the embryos to float and clump together.
8. This step cross-links proteins to chromatin as well as to other proteins. The time required for this step should be kept constant between repeated collections. Importantly, as some proteins are more easily cross-linked to chromatin than others, the formaldehyde concentration/length of cross-linking reaction might require optimization for different proteins of interest. It is important not to over-cross-link as this will result in what looks like spreading of the ChIP signal from the actual site of binding.

9. Use only tubes that are designed for centrifugation. Some tubes (e.g., polystyrene conical tubes) might break during centrifugation and cause sample loss.
10. **Steps 5 to 7** allow nuclei isolation, which increases the final signal-to-noise ratio.
11. We sonicate in 15 mL Bioruptor tubes. However 1.5, 0.5, and 0.1 mL tubes may also be used by adjusting the sample volume and the number of cycles. Sonication conditions should be optimized for each sonicator and may vary depending on the extent of cross-linking and sample type. Ensure that the water bath remains cold by using a cooling system.
12. One can also sonicate the nuclei in RIPA buffer with protease inhibitors and PMSF. In Subheading 3.4, **step 1**, bring the chromatin to a total volume of 900 μ L with RIPA buffer with protease inhibitors and PMSF.
13. Load different amounts of reverse-cross-linked DNA (we routinely run between 200 and 600 ng of DNA) to assess the size range accurately. Migration of too large quantities of DNA on agarose gel might not reflect the real DNA fragmentation distribution.
14. The optimal concentration of chromatin for a given factor should be empirically tested by ChIP-qPCR by increasing the concentration of chromatin used in the IP with a fixed amount of antibody.
15. The optimal amount of serum/antibody is difficult to predict, as it depends on the abundance of the protein of interest, the concentration of specific IgGs in the serum, etc. We recommend to test a range of different serum/antibody amounts (e.g., 3, 5, and 10 μ L), while keeping the amount of chromatin and beads constant, and monitor the enrichment of a known binding site, compared to a negative control, using quantitative real-time PCR.
16. Where possible, always include a mock control. The mock control is done by performing all steps of the chromatin immunoprecipitation protocol but using the equivalent amount of pre-immune serum (or IgG) instead of antibody, when available.
17. Depending on the species in which the antibodies have been raised, protein A or protein G-Dynabeads can be used. Sepharose beads coated with protein A or protein G can also be used. We recommend testing different options to find the optimal condition.
18. ChIP can be done in two different ways: (1) Incubate the chromatin with antibody first, and then add beads (often referred to as “indirect” method). (2) Incubate the beads with antibody first, and then add the chromatin (direct method). We found that the two methods work with different efficiencies depending on the antibody.
19. If high background is observed, additional washes may be needed. Alternatively, a preclearing step may be added by incubating the

chromatin with protein A/G-Sepharose beads for 1 h prior to **step 1**. Any nonspecific binding of chromatin to protein A/G-Sepharose beads will be removed during this additional step. For ChIPs using Dynabeads, preclearing is not necessary. Transfer the supernatant to a new 1.6 mL low-binding tube, retain 10 μ L of the sample as 1% input control, and add the appropriate amount of antibody as described in **step 1**. The quality of the immunoprecipitation should be assessed before next-generation sequencing by calculating the percentage recovery of a positive (located over a region known to be bound by the protein) and a negative (located over a region not bound by the protein) region, if available, using real-time PCR calculating the percentage of immunoprecipitated DNA compared to the input (%IP/input—*see* Fig. 2). The percentage recovery for transcription factors is generally at least one order of magnitude lower than for histone modifications (*see* Fig. 2), although the enrichment of positive/negative primers could be roughly the same—as a consequence significantly more chromatin is required for a good ChIP for transcription factors.

20. Although the library preparation could be performed with as low as 100 pg of immunoprecipitated DNA, we recommend using as much as possible to avoid the requirement of too many amplification cycles during **step 13**. For transcription factors we typically use 1–2 ng, while for chromatin modification up to 8 ng, if available. If the amount of ChIP DNA obtained from one immunoprecipitation is too low, up to three replicates can be pooled together. If using less than 1 ng of starting material, we recommend the NEB Ultra DNA Library Prep Kit for Illumina. We routinely use the NEB kits for library preparation, but other providers can be used, although we have not directly compared the results.
21. We routinely sequence at least two immunoprecipitation replicates (independent chromatin preparation, independent immunoprecipitations with different antibodies if available, and independent library preparation) as well as one input library for each condition to be analyzed.
22. The amount of adaptors to be used may have to be titrated relative to starting material. If starting from less than 2 ng of ChIP DNA, consider further diluting the adaptors, as the presence of non-ligated adaptors will promote the formation of adaptor dimers during the amplification step. Adaptor dimers will migrate at approximately 120 bp and, if present in the final library, yield useless reads.
23. When starting with less material, the incubation time for adaptor ligation can be extended to 30–45 min.
24. We recommend keeping the number of amplification cycles as low as possible to avoid amplification artifacts. Too many amplification cycles will result in a low-complexity library. The complexity of a library can be defined as the number of independent

DNA molecules that compose it. This complexity should be significantly higher than the total number of sequenced reads, as a low-complexity library will increase the likelihood of generating duplicated reads.

25. Depending on the desired sequencing coverage, up to ten libraries can be multiplexed for chromatin modifications, and even more for most transcription factor ChIPs. The coverage required to identify all the binding sites of a given transcription factor depends on the transcription factor itself and on the size of the genome to be analyzed. It can thus not be predicted in advance. A saturation analysis should be performed, *a posteriori*, to verify whether the sequencing depth was sufficient enough to identify all the binding sites of the transcription factor of interest. Briefly, a saturation analysis consists in sampling the data and analyzing how the number of predicted binding sites changes when only a subset of the data is used for prediction. By sampling increasing fractions of the data, the number of identified binding sites should reach a plateau corresponding to the number of binding sites identified from the complete data set. See also ref. 13 for more information about sequencing depth.

References

1. Bonn S, Zinzen RP, Girardot C, Gustafson EH, Perez-Gonzalez A, Delhomme N et al (2012) Tissue-specific analysis of chromatin state identifies temporal signatures of enhancer activity during embryonic development. *Nat Genet* 44(2):148–156
2. Zinzen RP, Girardot C, Gagneur J, Braun M, Furlong EEM (2009) Combinatorial binding predicts spatio-temporal cis-regulatory activity. *Nature* 462(7269):65–70
3. Junion G, Spivakov M, Girardot C, Braun M, Gustafson EH, Birney E et al (2012) A transcription factor collective defines cardiac cell fate and reflects lineage history. *Cell* 148(3):473–486
4. Roy S, Ernst J, Kharchenko PV, Kheradpour P, Negre N, Eaton ML et al (2010) Identification of functional elements and regulatory circuits by *Drosophila* modENCODE. *Science* 330(6012):1787–1797
5. Ghavi-Helm Y, Furlong EEM (2012) Analyzing transcription factor occupancy during embryo development using ChIP-seq. In: Gheldof N, Deplancke B (eds) *Gene regulatory networks*. Humana Press, Totowa, NJ, pp 229–245
6. Teves SS, Henikoff S (2011) Heat shock reduces stalled RNA polymerase II and nucleosome turnover genome-wide. *Genes Dev* 25(22):2387–2397
7. Kasinathan S, Orsi GA, Zentner GE, Ahmad K, Henikoff S (2014) High-resolution mapping of transcription factor binding sites on native chromatin. *Nat Methods* 11(2):203–209
8. Bonn S, Zinzen RP, Perez-Gonzalez A, Riddell A, Gavin A-C, Furlong EEM (2012) Cell type-specific chromatin immunoprecipitation from multicellular complex samples using BiTS-ChIP. *Nat Protoc* 7(5):978–994
9. Lara-Astiaso D, Weiner A, Lorenzo-Vivas E, Zaretsky I, Jaitin DA, David E et al (2014) Chromatin state dynamics during blood formation. *Science* 345(6199):943–949
10. Sisson JC (2007) Culturing large populations of *Drosophila* for protein biochemistry. *Cold Spring Harb Protoc* (3):pdb.top4
11. Campos-Ortega JA, Hartenstein V (1997) *The embryonic development of Drosophila melanogaster*. Springer, New York, 432 p
12. Ng P, Wei C-L, Ruan Y (2001) Paired-end diTagging for transcriptome and genome analysis. In: *Current protocols in molecular biology*. Wiley, New York
13. Park PJ (2009) ChIP-seq: advantages and challenges of a maturing technology. *Nat Rev Genet* 10(10):669–680

Chapter 17

Protocols to Study Growth and Metabolism in *Drosophila*

Katrin Strassburger and Aurelio A. Teleman

Abstract

Signaling pathways such as the insulin/insulin-like growth factor pathway concurrently regulate organismal growth and metabolism. *Drosophila* has become a popular model system for studying both organismal growth and metabolic regulation. Care must be taken, however, when assessing such phenotypes because they are quantitative in nature, and influenced by environment. This chapter first describes how to control animal age and nutrient availability, since growth and metabolism are sensitive to these parameters. It then provides protocols for measuring tissue growth, cell size, and metabolic parameters such as stored lipids and glycogen, and circulating sugars.

Key words Wing size, Protein, Weight, Hemolymph, Glucose, Trehalose, Glycogen, Triglycerides

1 Introduction

1.1 Controlled Conditions

Animal growth and metabolism are highly dependent on nutrient availability, age, genetic background, and gender [1]. Therefore, it is extremely important to control for these parameters. The first protocols (Subheadings 3.1 and 3.2) describe how to do this. Briefly, animals of the same genetic background are grown at a defined density, and then aged in parallel. This handling precedes any metabolic or growth-related measurement.

1.2 Quantifying Growth

Subheadings 3.3–3.5 describe methods for quantifying tissue and cell growth. The adult wing is an ideal system to measure animal growth. Wing size usually correlates with total body size, and its “two-dimensional” structure allows an easy way to sensitively and robustly quantify size. One option is to compare total wing size of test wings versus control wings. Using this method, however, small differences in size will only be revealed upon quantification. A second option is to manipulate a part of the wing, leaving the rest of the wing as a control. In this setup, size changes lead to changes in wing proportions, causing growth defects to be more visually apparent. For instance, if one drives expression of a transgene or an RNAi construct using apterous-GAL4,

it will express only on the dorsal surface of the wing. Over- or under-growth of this dorsal layer will cause the wing to bend downwards or upwards, respectively (Fig. 1a). This is useful for screening, yet tricky to image and quantify. Another example is engrailed-GAL4, which drives expression only in the posterior compartment (Fig. 1b). Looking at the bending and relative distance of the wing veins will make even small size differences visible [2].

Changes in size can either result from changes in cell number, or in cell size, or both. To measure cell size, Subheading 3.3 can be followed to count the number of cells in an area of predefined size. Cell number can be determined by counting wing trichomes, as every cell secretes one trichome. Cell size (area per cell) is the inverse of this number. If the percent change in cell area is smaller in magnitude than

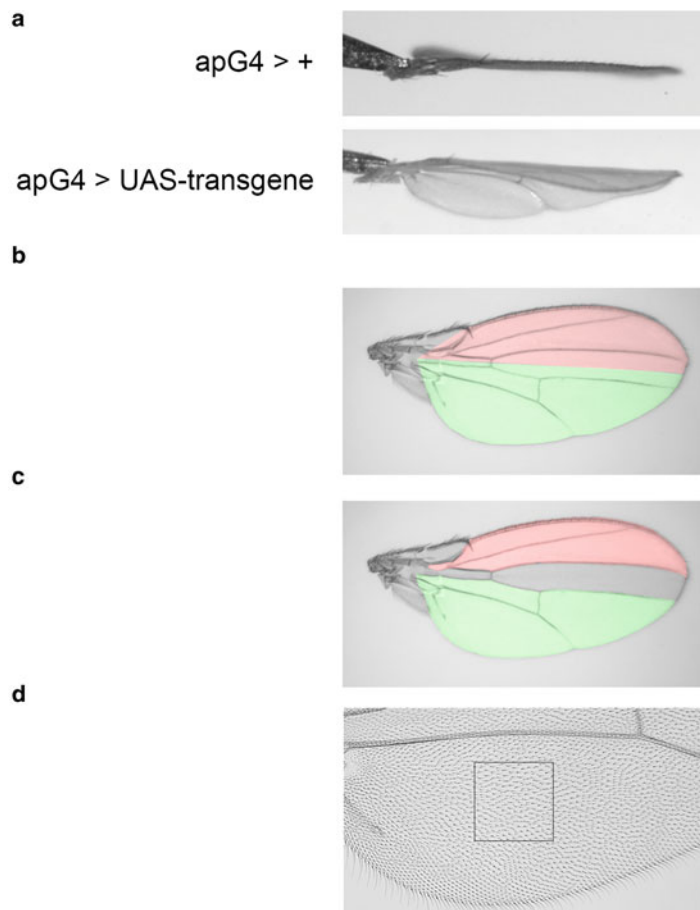


Fig. 1 Compartment-specific alterations of growth. (a) Apterous-driven transgene expression causes wing bending. (b) Wild-type wing at 2.5 \times magnification with posterior (green) and anterior (red) compartment margins highlighted. (c) For simplicity the area between veins L1/L3 and L4/posterior wing margin can be measured as readouts for anterior (red) and posterior (green) compartment size, respectively. (d) Posterior part of a wing at 10 \times magnification with a defined area highlighted (square) in which the number of trichomes can be determined

the percent change in wing area, then changes in cell number must also be contributing to the effect.

If adult wings are not available, growth can also be assessed in larvae by generating clones in imaginal wing discs with either gain of function or loss of function for the gene of interest, and clone area can be measured. Larval clone size, however, is very variable. This setup is not very sensitive and will work only for large size differences; hence it is not described in detail here but the reader is referred to the literature. Cell size and cell cycle parameters of larval clones can be quantified accurately by FACS [3]. A detailed description of this can be found in the previous edition of this book.

As indirect estimates of growth, Subheadings 3.4 and 3.5 describe how to measure weight and protein content of flies.

1.3 Metabolic Parameters

Subheadings 3.6 and 3.12 explain how to measure circulating glucose and trehalose, and stored triglycerides and glycogen. Depending on the parameter, the starting material varies. Glucose and trehalose are measured from hemolymph (Subheadings 3.8 and 3.9, adapted from ref. 4). Hence protocols for extraction of hemolymph from larvae (Subheading 3.6) and adults (Subheading 3.7) without contamination of other tissues are described. Glycogen and triglyceride measurements are described from whole animals (Subheadings 3.10 and 3.11). Glycogen and triglyceride levels can be measured in a combined assay from the same sample (see below).

2 Materials

2.1 Genetic Background

1. One fly strain containing a traceable genetic modification (e.g., a white + transposon insertion).
2. One isogenic fly strain that will serve as a control.

2.2 Controlled Density and Age

1. Fly cages
2. Coarse dissection needle
3. Apple plates: In a 2 l beaker heat up 330 ml apple juice to 180 °C, constantly stirring. Dissolve 24 g agar in 750 ml water by warming up in a microwave and mixing with a spoon. Combine hot apple juice with agar solution. Boil mixture, stirring until it becomes clear. Add 9–10 spoons of sugar beet syrup or molasses, and mix. Under the fume hood pour mixture into petri dishes of 6 cm diameter. Let plates solidify and cool down, and store at 4 °C. Before use add live yeast to the middle of the plate (see Note 1).

2.3 Cell Size and Cell Number

1. Per genotype ten flies obtained as described in Subheadings 3.1 and 3.2.
2. Glass slides.

3. Cover slips 24×40 mm.
4. Weights (200 g), one for each glass slide..
5. 2 ml Eppendorf tubes.
6. SH medium: 70 % EtOH, 30% glycerol.
7. Hoyer's medium: Prepare under the fume hood. Add 15 g of gum arabic to 25 mL of H₂O in a glass beaker. Heat to 60 °C, and stir overnight on a magnetic stirrer. Successively add 100 g of chloral hydrate. After the chloral hydrate has dissolved, add 10 g of glycerol. Centrifuge the solution for 30 min at 10,000×*g* and filter the solution through glass wool. Store the solution at room temperature in a tightly sealed flask. Shortly before use, centrifuge Hoyer's medium in a table-top centrifuge for at least 15 min to pellet undissolved particles.

2.4 Weight

1. Per genotype 3×10 flies obtained as described in Subheadings 3.1 and 3.2.
2. 1.5 ml Eppendorf tubes (three tubes per genotype).
3. Precision balance (0.1 mg precision).

2.5 Protein

1. Per genotype 3×6–10 flies obtained as described in Subheadings 3.1 and 3.2.
2. 1.5 ml Eppendorf tubes (three tubes per genotype).
3. Homogenization buffer: 1% Triton X-100 in PBS (*see Note 2*).
4. Bradford protein assay dye reagent concentrate: Dilute 1:5 in H₂O.
5. Plastic pestle for microtubes.
6. Plastic cuvette.

2.6 Hemolymph Extraction: Larvae

1. Per genotype 3×8 larvae obtained as described in Subheadings 3.1 and 3.2.
2. Glass slides.
3. No. 5 forceps.
4. Per genotype three 200 µl clear-walled PCR tubes.

2.7 Hemolymph Extraction: Adults

1. Per genotype 3×80 flies obtained as described in Subheadings 3.1 and 3.2.
2. Per genotype 3×0.5 ml Eppendorf tubes
3. Per genotype 3×1.5 ml Eppendorf tubes.
4. 25-gauge needle.
5. Fine tungsten needle.
6. Refrigerated centrifuge.

2.8 Glucose Measurement from Hemolymph

1. Per genotype $3 \times 1 \mu\text{l}$ hemolymph as described in Subheading 3.6 or 3.7.
2. Per genotype three $200 \mu\text{l}$ PCR tubes containing $19 \mu\text{L}$ of TBS pH 6.6 (137 mM NaCl, 2.7 mM KCl, 5 mM Tris pH 6.6), on ice.
3. Per genotype three marked, $10 \mu\text{L}$ pipette tips (see Note 3).
4. Glucose reagent (Sigma G3293, alternatively Sigma GAGO-20).
5. 96-Well plate with UV transparent flat bottom.
6. Plate reader that can measure absorbance at 340 nm (for GAGO-20 measure at 540 nm).

2.9 Trehalose Measurement from Hemolymph

1. Per genotype $3 \times 1 \mu\text{l}$ hemolymph as described in Subheading 3.6 or 3.7.
2. Per genotype three $200 \mu\text{l}$ PCR tubes containing $19 \mu\text{L}$ of TBS pH 6.6 (137 mM NaCl, 2.7 mM KCl, 5 mM Tris pH 6.6), on ice.
3. Per genotype three marked, $10 \mu\text{L}$ pipette tips (see Note 3).
4. Porcine trehalase.
5. Glucose reagent (Sigma G3293, alternatively Sigma GAGO-20).
6. 96-Well plate with UV transparent flat bottom.
7. Plate reader that can measure absorbance at 340 nm (for GAGO-20 measure at 540 nm).

2.10 Glycogen

1. Per genotype $3 \times 6\text{--}8$ flies/larvae (see Note 4).
2. PBST: 0.05% Tween in PBS.
3. Amyloglucosidase: Amyloglucosidase has ~ 70 U/mg. Prepare a stock solution of $14 \text{ U}/\mu\text{l}$ in $d_2\text{H}_2\text{O}$.
4. Glucose reagent.
5. Plastic pestle.
6. 96-Well plate with UV transparent flat bottom.
7. Plate reader that can measure absorbance at 340 nm (for GAGO-20 measure at 540 nm).

2.11 Triglycerides

1. Per genotype $3 \times 6\text{--}8$ flies/larvae (see Note 4).
2. PBST: 0.05% Tween in PBS.
3. 96-Well plate with standard plastic bottom.
4. Plastic pestle.
5. Free glycerol reagent.
6. Lipoprotein lipase: LPL has 2500 U/mg. Prepare a stock solution of $10 \text{ mg}/\text{ml}$ in $d_2\text{H}_2\text{O}$.
7. Plate reader that can measure absorbance at 540 nm.

3 Methods

3.1 Genetic Background (Fig. 2)

1. Cross males carrying your traceable mutation or transgene to females of an isogenic control stock (e.g., w¹¹¹⁸).
2. Backcross heterozygous female progeny to males from the isogenic control stock for five generations.
3. In parallel also backcross your balancer chromosome to the isogenic control stock.
4. After five generations of backcrossing, cross heterozygous females carrying your mutation or transgene of interest to backcrossed males carrying the balancer chromosome, respectively. Make sure to backcross the balancer chromosome one more time to the isogenic control stock in order to obtain female virgins for the next cross.
5. Set up several independent stocks by crossing single males carrying your mutation or transgene of interest balanced over the balancer chromosome to females from the backcrossed balancer stock.

3.2 Controlled Density and Age

1. Put circa 100 well-nourished females together with circa 50 males into the collection cage and close the cage with an apple plate.

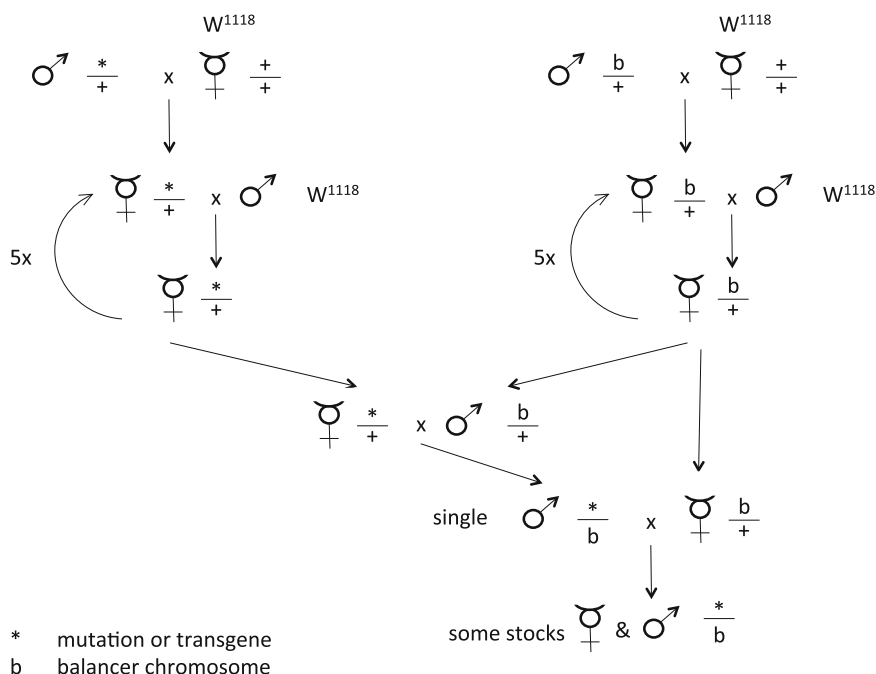


Fig. 2 Crossing scheme to isogenize mutant- or transgene-carrying stocks. *mutant chromosome, b balancer chromosome

2. Change apple plate in the mornings and evenings until females lay enough eggs (see Note 5).
3. To stage progeny according to age: Change the apple plate after a short collection time period (6 h). After 22 h, when L1 start hatching, clear the plate of all hatched L1 larvae, and collect newly hatched larvae after a short time period (1–6 h).
4. Keep the plate upside down at 25 °C until L1 hatch (see Note 6).
5. With a needle pick 60 L1 under the stereoscope and transfer them to vials containing fly food but with no extra yeast added (see Note 7).

3.3 Cell Size and Cell Number

1. Collect males or females separately in Eppendorf tubes filled with SH medium.
2. Equilibrate at RT overnight.
3. With a cut P1000 tip transfer animals to a dissection dish.
4. Remove mounting medium and rinse twice with distilled water.
5. Put a drop of Hoyer's medium in the middle of a glass slide and spread it evenly to cover a square of roughly 1 cm².
6. In water, rip off wings, one at a time, dry them by touching a piece of tissue paper, and transfer them to a glass slide with Hoyer's medium.
7. Arrange wings so that ample space is between them, and push them down into the Hoyer's medium. This will minimize wing movement when the cover slip is placed on top. Up to ten wings should fit per slide (see Note 8).
8. Carefully put a cover slip and a weight on top (see Note 8).
9. Let dry at RT overnight.
10. Image wings using a 2.5× objective for whole wing area measurements or a 10× objective to determine hair density (Fig. 1d).
11. Measure wing area, or various wing compartments, using the ImageJ polygon selection tool and area measurement features (Fig. 1b–d) [5].

3.4 Weight

1. Weigh empty tubes to 0.1 mg precision and write down weight for each tube.
2. Put ten animals per tube and weigh again (see Note 4).
3. Calculate weight per fly by dividing the difference between full and empty tubes by 10.

3.5 Protein

1. Anesthetize flies and transfer 3×6–10 animals per genotype into 1.5 ml Eppendorf tubes, kept on ice (see Note 4).
2. Add 100 µl homogenization buffer and thoroughly homogenize the animals using a plastic pestle.
3. Add 400 µl homogenization buffer to the tube by pipetting it over the plastic pestle to rinse off any remaining tissue.

4. Spin $2500 \times g$ for 1 min.
5. Transfer 5 μ l lysate into a new tube and add 500 μ l 1 \times Bradford reagent (see Note 9).
6. Mix and incubate for 5 min at RT.
7. Transfer to cuvettes and measure the optical density at 595 nm.

3.6 Hemolymph Extraction: Larvae

1. Take eight larvae, rinse briefly in PBS, and transfer onto a piece of tissue paper to dry them off (see Note 10).
2. Place the eight larvae on a glass slide under a dissecting microscope.
3. Quickly but gently break them open by tearing at the middle, and press lightly on them, so that the hemolymph comes out but not tissue (see Note 11).
4. Take >2 μ l of hemolymph with a pipette tip and transfer to the empty, clear-walled 200 μ l PCR tube (see Note 12).

3.7 Hemolymph Extraction: Adults [6]

1. Push the 25-gauge needle into the 0.5 ml Eppendorf tube to make a hole in the bottom.
2. Place each punctured 0.5 ml tube into a 1.5 ml Eppendorf tube.
3. Anesthetize the flies on a CO₂ pad.
4. Pierce 40 flies in the thorax using a tungsten needle (see Note 13).
5. Transfer pierced flies to the punctured 0.5 ml Eppendorf tube.
6. Close the 0.5 ml tube and leave the 1.5 ml tube open.
7. Spin for 5 min at $2500 \times g$ at 4 °C.
8. Keep on ice to prevent melanization.

3.8 Glucose Measurement from Hemolymph

1. Under the dissecting microscope, take 1 μ l of hemolymph (obtained as described in Subheading 3.6 or 3.7) using the marked pipette and transfer it to the tube containing 19 μ l TBS pH 6.6 on ice.
2. When you have collected all your samples, put the tubes in a PCR machine with heated lid for 5 min at 70 °C (see Note 14). After this, samples can be stored at -20 °C.
3. Transfer to a 1.7 mL Eppendorf tube and spin for 1 min at 20,000 $\times g$ (see Note 15).
4. Transfer supernatant into a new tube.
5. Measure the amount of glucose in all of your samples using the glucose reagent and follow the manufacturer's instructions.
6. In a 96-well plate (with UV transparent glass bottom) mix 200 μ l glucose reagent or 200 μ l water with 4 μ l sample each.
7. Incubate for 15 min at room temperature.

8. Measure absorbance at 340 nm.
9. Subtract values of “water” sample from values of “glucose reagent” sample.

3.9 Trehalose Measurement from Hemolymph

A certain volume of hemolymph will be collected and heat inactivated. Half of the sample will be digested with porcine trehalase to convert the trehalose into glucose, whereas the other half of the sample will not be treated with trehalase, to measure circulating glucose. The amount of glucose in each sample will be measured using a standard assay kit with colorimetric readout.

1. Under the dissecting microscope, take 1 μ l of hemolymph (obtained as described in Subheading 3.6 or 3.7) using the marked pipette and transfer it to the tube containing 19 μ L TBS pH 6.6 on ice.
2. When you have collected all your samples, put the tubes in a PCR machine with heated lid for 5 min at 70 °C (see Note 14). After this, samples can be stored at –20 °C.
3. Transfer to a 1.7 mL Eppendorf tube and spin for 1 min at 20,000 $\times g$ (see Note 15).
4. Split supernatant into two tubes containing 9 μ l sample each and add 1 μ l porcine trehalase into one of them (see Note 16).
5. Freeze sample without trehalase and incubate the one with trehalase overnight at 37 °C.
6. Measure the amount of glucose in all of your samples using the Sigma Glucose Reagent and follow the manufacturer’s instructions.
7. In a 96-well plate (with UV transparent glass bottom) mix 200 μ l glucose reagent or 200 μ l water with 4 μ l sample each.
8. Incubate for 15 min at room temperature.
9. Measure absorbance at 340 nm.
10. Subtract values of “-trehalase” (“glucose reagent–water”) sample from “+trehalase” sample (“glucose reagent–water”).

3.10 Glycogen

The principle of the method is to digest the glycogen to glucose with amyloglucosidase and then measure the amount of glucose using a standard assay kit with colorimetric readout.

1. Put 6–8 animals into a 1.5 ml Eppendorf tube and homogenize them in 250 μ l PBST using a plastic pestle (see Note 17).
2. Add another 250 μ l PBST, thereby rinsing the pestle.
3. Take an aliquot of 100 μ l for protein measurement (see chapter 3.5).
4. Immediately heat inactivate the remaining sample at 70 °C for 5 min.
5. Cool down on ice.

6. Take 200 μ l into a new tube and spin at 20,000 $\times g$ for 3 min (*see Note 18*).
7. Pipet 30 μ l of the supernatant into each of the two tubes.
8. Add 1 μ l amyloglucosidase solution (14 U/ μ l) to one of the tubes (*see Note 19*).
9. Incubate at 50 °C for 1 h.
10. Transfer 15 μ l of each sample into a UV-transparent 96-well plate (use PBST as blank).
11. Add 150 μ l glucose reagent.
12. Cover the plate and incubate at 37 °C for 30 min.
13. Measure absorbance at 340 nm.
14. Subtract values of “-amyloglucosidase” sample from “+amyloglucosidase.”
15. Calculate from triplicates average glycogen levels relative to protein content.

3.11 Triglycerides

1. Put 6–8 animals into a 1.5 ml Eppendorf tube and homogenize them in 250 μ l PBST using a plastic pestle (*see Note 17*).
2. Add another 250 μ l PBST to rinse the pestle.
3. Take an aliquot of 100 μ l for protein measurement (*see chapter 3.5*).
4. Immediately heat inactivate the remaining sample at 70 °C for 5 min.
5. Cool down on ice.
6. Transfer 200 μ l to a new tube and add 3 μ l lipoprotein lipase (LPL).
7. Incubate at 37 °C overnight.
8. Spin down at 20,000 $\times g$ for 3 min.
9. Transfer 15 μ l supernatant to 96-well plate.
10. Add 150 μ l free glycerol reagent.
11. Incubate at 37 °C for 6 min.
12. Measure absorbance at 540 nm.
13. Calculate from triplicates average glycogen levels relative to protein content.

4 Notes

1. Yeast is the protein source for the females, required to produce large amounts of eggs. Some people use yeast paste (yeast dissolved in a small amount of water) as flies can eat it easily. We simply sprinkle dried yeast pellets onto one spot on the plate,

which quickly turn into paste upon contacting the humidity of the apple plate. If the yeast is finished before you change the plate, put more yeast next time. Remove excessive yeast after removing the plate from the cage, since L1 will otherwise dive into it and it will be more challenging to pick them.

2. Detergents can interfere with the reaction. To not use too much; follow the instructions of your protein assay kit.
3. Most of the error in this method comes from imprecisely pipetting the volume of hemolymph. To exactly pipet 1 μ l, pipet 1 μ l of water into a clean 10 μ L tip, and mark the height of the liquid by making a scratch with a razor blade under a dissection microscope. Use this marked tip as a “template” to mark all the 10 μ l tips you will need in this experiment, by placing clean tips next to the “template tip” under a dissection microscope and marking the 1 μ l mark on all of them. Since hemolymph is quite viscous, 1 μ l of hemolymph needs to be pipetted by visual inspection under a dissection microscope by pulling up hemolymph until it reaches the 1 μ l mark.
4. If you use larvae, first rinse them in PBS and dry them off to clean them from food.
5. It can take a couple of days until the flies start laying eggs well. If after 3 days you still do not get enough eggs, increase the number of flies.
6. Individual plates should be placed singly on tissue paper, separated from neighboring plates, and not stacked on top of each other, to prevent contaminating larvae from leaving one apple plate and entering another.
7. It might be tricky to get the first larva to stick to the needle. Further larvae, however, will easily stick to previous ones. We typically pick up 30 larvae in one go before transferring them to a tube of food. Sixty larvae per 10 ml food ensures that the food becomes neither limiting, nor too dry.
8. Putting several wings per glass slide speeds up the procedure; yet the wings risk folding and floating on top of each other. Using little gluing medium and pushing down the wings helps avoid this. A stellar arrangement of the wings will make them migrate away from each other when putting the cover slip. By pushing the cover slip gently with forceps at different spots, it is possible to control the movement of the wings while the medium is spreading. It is necessary to flatten the wings with a weight for imaging all cells of the wing in the same focal plane.
9. If you have large sample numbers you can also scale down the volumes and use 96-well plates. 3 μ l Lysate with 200 μ l Bradford reagent can be read out in a plate reader.

10. This is to remove any sugars from the food.
11. Be careful not to mash up the larvae too badly, because otherwise it will be difficult to pipette hemolymph without also getting adipose tissue and other organs.
12. This step does not need to be measured precisely. Subsequent to this, 1 μ l of hemolymph will be taken with precision (see for instance Subheading 3.8).
13. For 1 μ l of hemolymph you will need circa 40 flies. Per tube you can put maximally 40 flies. You should be fast to not get a wounding response, which makes the hemolymph useless. A practiced person can process up to 200 flies before the wounding response starts.
14. This is necessary to kill most of the enzymes.
15. This step will precipitate all denatured proteins.
16. Porcine trehalase turns trehalose to glucose. This will allow you to measure the amount of (trehalose + glucose) that was in your sample. In the other tube, where you do not add trehalase, you will measure the glucose in your sample. Larval hemolymph has very little glucose, and roughly 70 mM trehalose.
17. You can also attach the plastic pestle to a table-top drill that can revolve at 4000 rpm. This setup is more effective and faster in particular for a large number of samples.
18. You can keep the remaining lysate to use 200 μ l of it for triglyceride measurement.
19. The tube containing amyloglucosidase will measure the glucose coming from glycogen + glucose. The tube without amyloglucosidase will measure endogenous glucose, which will be subtracted to obtain glycogen content.

References

1. Edgar B (2006) How flies get their size: genetics meets physiology. *Nature Reviews Genetics* 7:907–916
2. Hahn I, Fuss B, Peters A, Werner T, Sieberg A, Gosejacob D, Hoch M (2013) The Drosophila Arf GEF Steppke controls MAPK activation in EGFR signaling. *Journal of Cell Science* 126:2470–2479
3. Neufeld TP, de la Cruz AFA, Johnston LA, Edgar BA (1998) Coordination of growth and cell division in the Drosophila wing. *Cell* 93:1183–1193
4. Zhang W, Thompson BJ, Hietakangas V, Cohen SM (2011) MAPK/ERK signaling regulates insulin sensitivity to control glucose metabolism in *Drosophila*. *Plos Genetics* 7(12):e1002429
5. Dobens AC, Dobens LL (2013) FijiWings: an open source toolkit for semiautomated morphometric analysis of insect wings. *G3 (Bethesda)* 3(8):1443–1449
6. A video that shows how to extract hemolymph from adults can be found here. <https://www.youtube.com/watch?v=im78OIBKIPA>

Chapter 18

Protocols to Study Aging in *Drosophila*

Matthew D.W. Piper and Linda Partridge

Abstract

The fruit fly *Drosophila melanogaster* offers a host of advantages for studying the biology of aging: a well-understood biology, a wide range of genetic reagents, well-defined dietary requirements, and a relatively short life span, with a median of ~80 days and maximum ~100 days. Several phenotypes can be used to assess the aging process, but the simplest and most widely used metric is length of life. Here we describe a standard life span assay for *Drosophila* housed on a simple sugar/yeast diet.

Key words *Drosophila melanogaster*, Life span, Aging, Method, Diet, Genetic interventions, Pharmacological interventions, Backcross

1 Introduction

As populations around the world age, increasing effort is being devoted to the development of new approaches to improve the health of older people. Remarkably, experimental work on worms, flies and mice over the last 20 years has provided a positive outlook on this prospect [1, 2]. For these model organisms, genetic, environmental, and pharmacological interventions have been described that extend healthy life span [3]. Even more remarkably given the very different life spans of these model organisms, these interventions often act on common mechanisms to extend life span, implying some degree of evolutionary conservation of mechanisms of aging. Thus there is great promise that studies of aging in laboratory model organisms will yield insights into aging that will ultimately benefit humans.

The challenges of experimental gerontology are enormous. Experiments require long time-scales, genetic manipulations, large populations, and well-controlled animal stocks and conditions. These factors make the work perfectly suited to the small, short-lived, and well-characterized model organisms such as the fruit fly *Drosophila melanogaster*.

Life span experiments have been conducted on *Drosophila* for the last 100 years [4] and over time the conditions have been refined [5]. In general, the protocol can be simple, but small and seemingly insignificant modifications to experimental protocols can have large effects on outcomes. For example, by not controlling for diet quality, genetic background or the interactions between mating frequency and diet, the experiment may report the effects on life span of an uncontrolled, trivial experimental procedure, rather than the focal intervention of the study [6].

Here we outline the basic procedure for rearing, isolating, and maintaining flies for life span experiments, highlighting a number of the known pitfalls that have misled researchers in the past. We provide a basic protocol for wild type flies housed under our standard laboratory conditions and then we provide modified protocols for studying the effects on life span of diet, drugs, or genetic interventions.

2 Materials

2.1 Media

All media are prepared using reverse osmosis water. Cooking can be done on a gas hob using a standard saucepan and stirring with a heavy-duty whisk (see Note 1).

1. Egg collection medium (volume sufficient for ~10 × 15 cm petri dishes): to 250 ml cold water add 12.5 g agar and stir to mix. Bring to boil while stirring and maintain boiling for ~2 min to ensure agar is completely melted. Add 150 ml red grape juice (see Note 2) and stir until the mixture returns to the boil. Remove from heat. Add 25 ml cold water and stir until temperature drops to ~65 °C. Make 10.5 ml 10% Nipagin (methyl 4-hydroxybenzoate in 95% ethanol) and pour solution into petri dishes. Allow to cool at room temperature, allowing steam to escape. Ensure to protect the plates from any flies at this stage to avoid contamination. Cover and store at 4 °C.
2. Fly food for rearing and maintenance (makes 1 L of 1SY [7], see Note 3): add 15 g agar to 700 ml cold water and stir. Heat until boiling. While continuing to stir, add 50 g table sugar (sucrose) and 100 g yeast (whole yeast autolysate and not water soluble yeast extract). After returned to boil, remove from heat and add cold water to make up to final volume of 1 L. Stir and allow to cool to ~65 °C. Mix in 30 ml 10% nipagin and 3 ml propionic acid to act as preservatives. This is also the point at which to mix in any small volume additions of drugs/transgene inducers/vehicle control. For larger volume additions, reduce the cold water addition after cooking to ensure final total volume remains at 1 L. Using a peristaltic pump with clean, sterilized tubing, dispense into clean vials or

bottles. Allow to cool at room temperature for several hours (*see Note 4*). To avoid contamination, ensure to protect cooling food from flies (*see Note 5*). Plug individual vials with cotton balls (*see Notes 6* and *7*). Store at 4 °C.

3. Live yeast paste for stimulating egg laying: Mix dried baker's yeast granules with cold water at a ratio of approx. 1:1 by weight to make a stiff paste (ice cream consistency). Best when used immediately, but can be stored covered at 4 °C for 2 weeks.

2.2 Plastic/ Glassware for Housing and Handling Eggs and Flies (See Note 8)

1. 15 cm diameter plastic petri dishes (*see Note 9*).
2. Fly "cage" for housing parental flies: an ~15 cm long plastic cylinder that fits a petri dish snugly at one end, and is covered with mesh at the other.
3. Bottles: ~250 ml (polypropylene or glass; ~60 mm OD × 130 mm H).
4. Vials/tubes: ~15 ml (polystyrene, polypropylene or glass; ~25 mm O.D. × 95 mm H).
5. Cotton wool balls or high density synthetic bungs to close tubes.
6. Squeeze bottle.
7. Pipette (20–100 µl).
8. Wide bore pipette tips (**Note 10**).
9. CO₂ stream—supplied via a water bubbler and low-static porous diffusion pad.
10. Fine paint brush (size 000–0000).
11. Handle-mounted metal pick.

2.3 Solutions for Handling Eggs and Flies

1. Phosphate buffered saline. Mix pre-formulated tablets with water according to instructions on container. This yields 0.01 M phosphate buffer, 0.0027 M potassium chloride, 0.137 M sodium chloride, pH 7.4.

3 Methods

3.1 Parental Generation

3.1.1 Preparing Stocks for Egg Collection

Most laboratory stocks are kept in small numbers and under crowded conditions, both of which alter adult life span [*6, 8*].

It is important to implement procedures to control these factors so that they do not confound interpretations of alterations in fly life span.

1. "wild types": to escape the transgenerational effects of stock crowding on life span, we passage stock-derived flies through two generations of our standard density procedure before use in life span experiments.

2. Genetic crosses: it is extremely important to standardize the genetic background of all mutant lines to be compared in a life span experiment. Failure to do so is common and leads to incorrect conclusions about the effects of genetic interventions to extend life. Most experimental transgenic flies are generated by crossing two inbred lines, with one containing the transgene to be activated and the other containing a genetic construct that drives the expression of the first. This cross also produces a hybrid genetic background, and this will generally increase life span when compared with that of the inbred controls, as a consequence of heterosis and irrespective of any effect of the transgenes [9]. To avoid this problem, all transgenes and mutants should first be backcrossed into a standardized genetic background for at least six generations. To maintain the lines an additional 2–3 backcrosses should be repeated every 6–12 months (see Note 11). Furthermore, each of the transgenic lines used to construct the experimental line should be included as a control in the life span experiment, because transgenes can cause insertional mutagenesis, which can in turn modify longevity.

3.1.2 To Collect Staged Embryos

1. House parental flies in “cages.” Provide a generous smear of live yeast paste (~1 tsp) at the center of the egg laying plate.
2. After 48 h, replace egg laying surface (see Note 12) with a fresh plate harboring a fresh aliquot of live yeast paste (egg laying peaks ~72 h after introduction to rich food) (see Note 13).
3. Leave overnight (see Note 14).
4. Collect embryos for development at standard density. To achieve this, we either use a pipette to allocate a fixed volume of a dense embryo suspension into new media for development, or use a mounted metal pick to collect and transfer individual larvae to development media (see Note 15):

Pipetting method (ideal for robust genotypes, to yield large numbers of experimental flies):

1. Anesthetize flies in cage, remove egg laying plate on which fertilized eggs lie and discard any yeast paste not consumed (see Note 16).
2. Using a squeeze bottle containing PBS, cover the plate with a thin layer of buffer.
3. Dislodge eggs by “brushing” the egg laying surface with a fine paint brush.
4. Pour egg/PBS suspension into a 15 ml falcon tube and allow eggs to settle.
5. Pour off most of the PBS and add more fresh PBS to wash the eggs.

6. Allow eggs to settle and pour off most of the PBS, leaving only sufficient to cover the settled egg mass.
7. Allow eggs to settle.
8. Using 100 μ l pipette with wide bore tip (*see Note 10*), set volume to 18–20 μ l and insert tip into the solution so the tip is level with the top of settled egg mass; quickly release plunger while dropping tip into the mass of eggs.
9. Inspect tip for a dense, even, mass of eggs (*see Note 17*).
10. Dispense egg mass on to surface of ~70 ml SY medium in a 250 ml bottle.

Picking method (more labor-intensive than pipetting, but more fragile genotypes tend to fare better using this method):

1. Incubate egg laying plate with staged embryos for 24 h at 25 °C (*see Note 18*)
2. Using a dissecting microscope, locate first instar larvae (*see Note 19*) on plate and touch with the metal pick. They will stick.
3. With practice, up to ~20 larvae can be collected on one pick.
4. Gently transfer picked larvae into a fresh vial with food for development by wiping larvae off the needle on to the surface of the food (*see Notes 20 and 21*)
5. Plug vial/bottle tightly with cotton wool ball(s) (*see Note 22*)
6. Incubate at 25 °C with 65% humidity and 12:12 h light–dark

3.2 Experimental Generation

3.2.1 Measuring Life Span of One Batch of Mated Wild Type Flies on One Food Type

1. After 10 days, transfer freshly emerged flies to fresh bottles or vials containing SY medium (*see Notes 23 and 24*)
2. Return bottles of flies to controlled environment (25 °C, 65% humidity and 12:12 h light–dark) for 48 h to allow all flies to mate
3. Anesthetize flies with CO₂ and manipulate carefully using a soft brush (*see Note 25*)
4. Separate males from females and allocate target individuals to experimental containers (refer to **Notes 26–30**). Various aspects of courtship and mating modify life span of the different sexes to different extents [10–14]. Also, genotype and food quality interact with courtship and mating frequency [15, 16]. Housing experimental flies as a single sex population avoids the confounding effects of sex X treatment interactions that modify life span.
5. Store vials at 25 °C, 65% humidity, 12:12 h light–dark (refer to **Note 31**)
6. Transfer flies to fresh food every 2–3 days (refer to **Notes 32–35**)

(a) If recording female egg laying of experimental flies, a good and simple summary can be generated by counting all eggs in all vials once or twice a week for the first 4–5 weeks

- Count the number of eggs on the surface of the food ~18 h after transferring in flies (see Notes 36–38)
- Data for a vial are expressed as the number of eggs per fly per day. For each vial, sum the egg lay for the average female across all count days to generate an index of lifetime egg laying.

7. For each transfer, score deaths and censors until all flies are dead (see Fig. 1 for survival data examples).

3.2.2 Protocol Modifications for Measuring the Effects of Dietary Interventions

1. Repeat steps 1–3 from Subheading 3.2.

2. Separate males from females and allocate target individuals to experimental containers (refer to Note 39).

3. Store vials at 25 °C, 65 % humidity, 12:12 h light–dark.

4. Transfer to fresh food every 2–3 days. Conduct egg counts as described in Subheading 3.2.

5. At each transfer score deaths and censors until all flies are dead.

3.2.3 Protocol Modifications for Measuring Effects of Genetic Interventions to Modify Life Span

1. Repeat steps 1–3 from Subheading 3.2 (see Note 40).

2. Separate males from females and allocate target individuals to experimental containers (refer to Note 41).

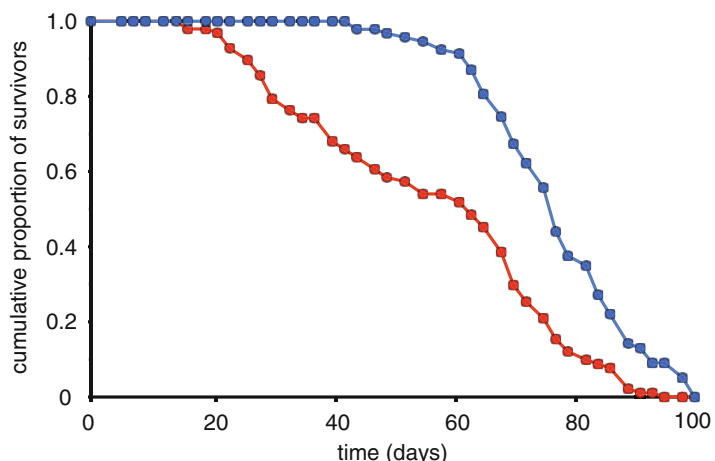


Fig. 1 Examples of good and poor quality survival data. The survival characteristics of a healthy population of flies are demonstrated in blue. There are relatively few deaths up until day 60, from which point there is rapid loss of life. By contrast, the population illustrated by the red line suffers substantial numbers of deaths beginning at day 20. Thus many flies are dying at young and middle ages, rather than predominantly at old age. This is a sign of poor housing conditions or a genetically fragile stock

3. Store vials at 25 °C, 65% humidity, 12:12 h light–dark.
4. Transfer to fresh food every other day. Conduct egg counts as described in Subheading 3.2.
5. For each transfer, score deaths and censors until all flies are dead.

3.2.4 Modifications for Measuring the Effects of Pharmacological Interventions to Alter Life Span

1. Repeat steps 1–3 from Subheading 3.2
2. Separate males from females and allocate target individuals to experimental containers (refer to Note 42).
3. Store vials at 25 °C, 65% humidity, 12:12 h light–dark.
4. Transfer to fresh food every other day. Conduct egg counts as described in Subheading 3.2.
5. For each transfer, score deaths and censors until all flies are dead

3.3 Data Handling

1. For each life span, record the date on which the experiment started, the genotype, and conditions used in the experimental setup as well as any notes about the experimental setup that will modify or help interpretation of the outcomes. For consensus guidelines on what constitutes the minimal information to be recorded for life span experiments, see ref. 17.
2. Throughout the experiment, record deaths and censors for each vial for each day on which they were observed (see Note 43).
3. These data can be used to generate life span curves for comparison using standard life table analyses [18].
4. An important recent advance has been the publication of an openly available database for storing life span data, called SurvCurv [17, 19, 20]. Users can upload data for secure storage as well as use an array of statistical tools to analyze the experimental outcomes. Additional tools available on the site allow the life spans to be compared to others in the database and so can be used to aid further biological discoveries.

4 Notes

1. Automatic cookers with built-in stirrers like the Joni Multimix (Joni Foodline) are useful for standardizing large volume cooks.
2. We use red grape juice that is designed for use in home wine production. Many laboratories use apple juice.
3. Our simple recipe of sugar and whole yeast lysate provides nutrition for optimal development and life span. Many alternatives exist, but not all are optimal (see supplement to [5]). Most recently, we have described a standardized holidic diet

that contains all necessary nutrients to support long life [21]. It is important to note that our recipes contain the nutritional complement of whole yeast preparations, which cannot simply be replaced by water soluble yeast extract that does not support long life [7].

4. In a relatively cool climate where room temperatures do not exceed 22 °C, this can be overnight. If medium shrinks in vials and pulls away from the edges, this is a sign of over-drying.
5. Housing trays of vials/bottles in pillowslips as they cool is a useful way to protect them from stray flies.
6. Alternatives to cotton wool balls exist: for example polyurethane foam plugs (available from www.drosophilacenter.com) are mite resistant, retain their structure and are reusable after washing.
7. To avoid the need to plug hundreds of vials before storage, it is possible to seal trays with Glad® Press'n Seal. If doing so, it is extremely important to ensure the seal is sound, there are no holes in the plastic film and all vials are covered to avoid both contamination and food from excessive drying when cooled.
8. A useful resource for equipment suitable for use in *Drosophila* research is the supplier: www.flystuff.com (a division of Genesee Scientific).
9. In situations where small numbers of parental flies are used for egg lays, it is more space and resource efficient to use small (~5 cm diameter) petri dishes and cages.
10. We use tips from StarLab (Cat Number: E1011-5100), but it is also possible to cut back a standard pipette tip a few mm to make a wide opening.
11. Backcrossing for six generations is, in almost all cases, sufficient to eliminate the confounding effects of genetic background. It should be noted that this should be performed to each laboratory's own genetic stocks since even inbred lines with the same name will differ between laboratories [22].
12. If not experienced with fly handling, replacing the egg laying plate may require flies to be lightly anesthetized with CO₂.
13. It is important not to use too much live yeast for the egg collection plate as it interferes with egg collection. Nor do you want to use too little such that the yeast supply is exhausted. Aiming to have a small amount left at the egg lay is ideal. A cage of ~300 flies will consume ~1 tsp of live yeast overnight.
14. While overnight egg lays produce adequate synchronization for most life span experiments, this egg collection window can be reduced.
15. To time the emergence of adults so that it falls on a weekday, transfer embryos to fresh food for development on a Friday. Emerging flies will be available on Monday, 9.5 days later.

16. If egg yield is a problem, the same parents can be used for an additional lay on a fresh plate containing live yeast.
17. A dense mass of eggs yields ~300 adult flies.
18. Before incubating, it is best to remove any leftover yeast paste from the egg laying plate as emerging larvae will burrow into it, making them hard to collect.
19. This is the smallest of three larval stages.
20. Before transferring larvae into fresh media, make a dent in the food to make it easier to wipe off the larvae against a slope of food.
21. For practical reasons, collecting larvae by picking is more manageable using 30 ml vials containing ~7 ml of SY food. Overcrowding can be avoided with 30–50 larvae.
22. At the larval densities recommended in this protocol, larvae will migrate to the cotton wool to pupate. If the container is not tightly plugged, the larvae will escape from the bottle.
23. In order to collect virgin flies, check bottles at 9 days after egg transfer and clear any flies that have emerged. Check the bottle every ~4 h for newly emerged flies—these will all be virgins. Transfer virgin flies to a cold, clean bottle on ice and sort males from females while they remain in a chill coma. CO₂ should be avoided as the fly's cuticle is immature, and exposure to the gas can lead to adverse effects on life span. Genders can only be distinguished with the use of a dissecting microscope to examine the genitalia.
24. It is best to transfer newly emerged flies without using CO₂.
25. In order to anesthetize a whole bottle of flies rapidly, fill a fresh empty (without food), dry bottle with CO₂ and transfer all flies into it. When sorting anesthetized flies, work on a perforated plate through which a stream of CO₂ is passing. To avoid desiccating the flies, it is ideal to bubble the CO₂ through water before it reaches the flies.
26. When allocating experimental flies to treatment, ensure the representation of individuals from each rearing container is balanced between experimental treatments.
27. For standard experiments, 100–150 flies per treatment housed as groups of 10–15 flies per vial are a manageable size. The lifetime outcome for all flies per vial should be recorded. Although the population across all vials for a treatment is treated as one during analysis, this approach allows the performance of individual vials to be revisited if outliers are suspected.
28. Experimental conditions can be blinded to the experimenter at this stage.

29. Fly life span varies with the size of their housing. Experiments comparing the life spans of flies kept in 25 ml versus 500 ml flasks, but at a standard density per container volume, found that life span was significantly shorter in the larger volume flasks. Shorter life span was associated with higher levels of flying activity [23].
30. There is a range of densities of flies per container that is optimum for life span. In a series of 30 ml vials [24] found the life span optimum to be for 2–15 flies per container and above this density saw a decrease in life span for each increase in population density.
31. As flies age and become frail, they have an increased risk of falling and becoming stuck in their food. They will also spend more time at the base of the vial. Storing the vials on their sides during life spans, so the food is a vertical surface at one end of the vial rather than the floor, reduces the risk of these accidental causes of death.
32. Depending on experience with handling *Drosophila*, during the first 2 weeks of a life span experiment the flies may be too fast to transfer between vials without light anesthesia. Males are more active and move more quickly than females and so are more likely to escape without anesthesia. With practice and good technique, it should be possible to transfer flies without CO₂.
33. When transferring flies, record deaths and censors (accidental deaths or escapees). Remember to note any dead flies transferred to new vials so that they can be deducted from the number of deaths recorded during the next transfer.
34. Some flies are bang sensitive, and appear to become mores so with age. These can appear dead during the disturbance of transfer. To avoid counting these as dead, first scan vials for deaths, then transfer all vials to new food and after that, check vials for dead flies transferred to fresh media.
35. To reduce labor and use of resources, it is possible to reuse the cotton ball that stoppers a vial by transferring it to the fresh vial to which flies are transferred. However, over time the cotton balls will deteriorate and so it is best to replace them at least once a month.
36. A sample timetable for transferring flies and counting eggs can be: transfer flies to fresh food on Mon, Wed and Fri afternoons, count eggs on Tuesady and Thursday mornings.
37. Record the time the flies go on the food and the time at which eggs in the vial were counted.
38. For young flies, there may be a lot of eggs. If there are too many to count with 10–15 flies in a vial, consider setting up a parallel cohort of flies with fewer females per vial. These flies will not contribute information to the life span experiment (as their den-

sity of housing is different from those in the experiment) and they can be discarded when egg counting is complete.

39. To control for rearing conditions in larger experiments, it is good practice to use one rearing bottle per experimental replicate vial. For example: for an experiment with 15 vials of flies per food type, generate 15 rearing bottles; when allocating flies to treatment, anesthetize rearing bottle 1 and allocate 10 flies to experimental vial number 1 for treatment A, then B, C, D and so on until all treatments have one vial populated from the same rearing bottle. Repeat this system with a new rearing bottle for the second replicate vial for each treatment.
40. Some genetically modified lines will have altered (usually longer) development time. In order to synchronize the start of the life span experiment, initiate the parental crosses for the retarded lines so that egg collection is performed before that of the non-delayed lines. To buffer against slight variations in the delay, it is best to rear multiple batches of the experimental generation, derived from consecutive days of egg laying. This way it will be possible to collect flies from all lines that have emerged within 24 h of each other.
41. It may not be possible to control for rearing conditions when using different genotypes in the same way as for single genotypes between multiple experimental foods. However, if the genetic scheme allows, it may be possible to use sibling flies as controls for experimental flies. Alternatively, it may be possible to rear multiple genotypes in a single rearing container. However, it is important to determine first that these larval conditions do not interact with life span outcomes.
42. To control for rearing conditions, use the protocol employed for testing the effects of multiple food types on one genotype (Note 40).
43. Each laboratory has its own method of recording and plotting these data. An Excel sheet used in our laboratories can be found at: <http://piperlab.org/resources/>. More sophisticated and automated packages can be found through the Pletcher laboratory (see ref. 25 and associated URLs).

Acknowledgements

We would like to thank members of the Partridge and Piper laboratories who contributed helpful suggestions and tips. In particular: S. Grönke, T. Niccoli, A. Tillmann, and N. Woodling. We acknowledge the following sources of funding: the Royal Society (UF100158 & RG110303), Australian

Research Council (FT150100237) (MDWP); the Wellcome Trust UK (098565/Z/12/Z), Max Planck Society, and the European Research Council under the European Unions Seventh Framework Programme (FP7/2007-2013), European Research Council grant agreement 268739 (L.P.)

References

- Kenyon CJ (2010) The genetics of ageing. *Nature* 464(7288):504–12
- Partridge, L., Alic, N., Bjedov, I., and Piper, M.D. (2011). Ageing in *Drosophila*: the role of the insulin/Igf and TOR signalling network. *Exp. Gerontol.* 46, 376–381.
- Niccoli T, Partridge L (2012) Ageing as a risk factor for disease. *Curr Biol* 22(17):R741–52
- Loeb J, Northrop JH (1916) Is there a temperature coefficient for the duration of life? *Proc Natl Acad Sci U S A* 2(8):456–7
- Piper MD, Partridge L (2007) Dietary restriction in *Drosophila*: delayed aging or experimental artefact? *PLoS Genet* 3(4):e57
- Partridge L, Gems D (2007) Benchmarks for ageing studies. *Nature* 450(7167):165–7
- Bass TM, Grandison RS, Wong R, Martinez P, Partridge L, Piper MD (2007) Optimization of dietary restriction protocols in *Drosophila*. *J Gerontol A Biol Sci Med Sci* 62(10):1071–1081
- Zwaan BJ, Bijlsma R, Hoekstra RF (1991) On the developmental theory of ageing. I. Starvation resistance and longevity in *Drosophila melanogaster* in relation to pre-adult breeding conditions. *Heredity* 66(Pt 1):29–39
- Pearl R (1921) The biology of death–VI. Experimental studies on the duration of life. *Sci Mon* 13:144–164
- Partridge L, Andrews R (1985) The effect of reproductive activity on the longevity of male *Drosophila melanogaster* is not caused by an acceleration of ageing. *J Insect Physiol* 31:393–395
- Partridge L, Farquhar M (1981) Sexual activity reduces lifespan of male fruitflies. *Nature* 294:580–582
- Partridge L, Fowler K, Trevitt S, Sharp W (1986) An examination of the effects of males on the survival and egg-production rates of female *Drosophila melanogaster*. *J Insect Physiol* 32:925–929
- Partridge L, Green A, Fowler K (1987) Effects of egg-production and of exposure to males on female survival in *Drosophila melanogaster*. *J Insect Physiol* 33:745–749
- Sgro CM, Partridge L (1999) A delayed wave of death from reproduction in *Drosophila*. *Science* 286(5449):2521–4
- Chapman T, Partridge L (1996) Female fitness in *Drosophila melanogaster*: an interaction between the effect of nutrition and of encounter rate with males. *Proc Biol Sci* 263(1371):755–9
- Wigby S., Slack, C., Grönke, S., Martinez, P., Calboli, F., Chapman, T., and Partridge, L. (2011). Insulin signalling regulates remating in female *Drosophila*. *Proc Roy Soc B* 278, 424–431.
- Ziehm, M., Ivanov, D.K., Bhat, A., Partridge, L., and Thornton, J.M. (2015) SurvCurv database and online survival analysis platform update. *Bioinformatics* 31(23):3878–80
- Lee E, Wang J (2003) Statistical methods for survival data analysis. Wiley, Hoboken, NJ
- Ziehm M, Thornton JM (2013) Unlocking the potential of survival data for model organisms through a new database and online analysis platform: SurvCurv. *Aging Cell* 12(5):910–6
- Ziehm M, Piper MD, Thornton JM (2013) Analysing variation in *Drosophila* aging across independent experimental studies: a meta-analysis of survival data. *Aging Cell* 12(5):917–22
- Piper MDW, Blanc E, Leitão-Gonçalves R, Yang M, He X, Linford NJ, Hoddinott MP, Hopfen C, Souloukis GA, Niemeyer C, Kerr F, Pletcher SD, Ribeiro C, Partridge L (2014) A holidic medium for *Drosophila melanogaster*. *Nat Methods* 11(1):100–5
- Berger J, Suzuki T, Senti K-A, Stubbs J, Schaffner G, Dickson BJ (2001) Genetic mapping with SNP markers in *Drosophila*. *Nat Genet* 29(4):475–81
- 70Magwere, T., Pamplona, R., Miwa, S., Martinez-Diaz, P., Portero-Otin, M., Brand, M., and Partridge, L. (2006). Flight activity, mortality rates, and lipoxidative damage in *Drosophila*. *Journals Gerontology* 61(2): 136–145
- Pearl, R (1928). Experiments on longevity. *The Quarterly Review of Biology* 3(3):391–407
- Linford, N., Bilgir, C., Ro, J., and Pletcher, S. (2013). Measurement of lifespan in *Drosophila melanogaster*. *J Vis Exp* (71), e50068, doi:10.3791/50068

Chapter 19

Protocols to Study Behavior in *Drosophila*

Wendi S. Neckameyer and Parag Bhatt

Abstract

Drosophila melanogaster is an incredibly versatile organism capable of both innate and higher-order behaviors. These behaviors offer not only a way to assay whether or not the animal is physiologically compromised (e.g., feeding, locomotion), but also serve to assess changes in centrally mediated functions. Here we describe several high throughput, reproducible, yet inexpensive and facile behavioral assays for both larval and adult *Drosophila*. The larval assays all employ an agar substrate in a petri dish; the adult assays are grouped into “vial-based” and “arena-based” paradigms. While these protocols are largely designed to assess individual animals, they are sufficiently rapid that ample numbers can be tested to determine behavioral significance. Importantly, this also allows for one to control for reproductive status, age, and sex, since these factors all have a significant impact on adult behaviors. In general, it is best to designate a dedicated area for any assay, so that lighting conditions are consistent, and all animals should be tested at roughly the same time each day to minimize circadian fluctuations. Temperature and humidity should also be maintained at a constant level to minimize variability in the assays.

Key words Locomotion, Feeding, Geotaxis, Exploratory behavior, Odor discrimination, Righting reflex, Phototaxis, Chemotaxis, Ethanol sedation, Escape behavior, Courtship

1 Introduction

Behavior is inherently variable, and therefore, steps must be taken to minimize environmental or other effects that could influence a given behavior. Not only should *Drosophila* populations be reared under a constant temperature and humidity, but they should be density controlled to encourage consistent and healthy development. This can be achieved by allowing flies to lay eggs on a collection plate, allowing the larvae to hatch, and aging them on collection plates with ample yeast paste until second instar (or the first day of third instar). If assaying adult behavior, larvae should be harvested as second instars (first instars are too fragile), and a standard number of larvae should be added to bottles containing standard fly food medium. It is critical to control for reproductive status, age, and sex, since these factors all have a significant impact on adult behaviors [1, 2]. In addition, adult flies should never be

anesthetized by either ether or carbon dioxide immediately before analyzing behavior, but should be gently aspirated into a vial or arena (“poofting”). These anesthetics have been shown to alter behaviors (e.g., [3]).

The larval assays include locomotion, feeding, chemotaxis and phototaxis. The adult “vial-based” assays include loss of righting reflex, geotaxis, odor sensitivity, and response to the sedative effects of ethanol. The adult “arena-based” assays include geotaxis, loss of righting reflex, odor discrimination, ethanol sedation, locomotion, light–dark box, forced swim test, and courtship behavior.

2 Materials

Husbandry: The relevant materials are depicted in Fig. 1.

1. Embryo collection cages. These can be purchased or made (using a 500 ml plastic beaker). A circle the size of a 60 mm petri dish should be cut out of the bottom of the beaker, and the top should be covered in Nitex nylon mesh, ~100 μ m. The mesh can be stably attached to the beaker with electrical tape, and is required for breathability and to minimize condensation under the humid conditions preferred by *Drosophila*.
2. Egg laying plates—60 mm petri dishes (or appropriate size for collection chamber) filled with an agar solution containing grape juice or apple juice and a mold inhibitor (Nipagin). The recipe (makes about twenty 60-mm plates) is as follows: 3.03-g Agar-agar, 0.2-g *p*-Hydroxybenzoic acid methyl ester [Nipagin] (Sigma), 3.33-g granulated sugar (store brand works fine), 100-ml distilled water, 33.3-ml apple juice (store brand works fine) (see Note 1).

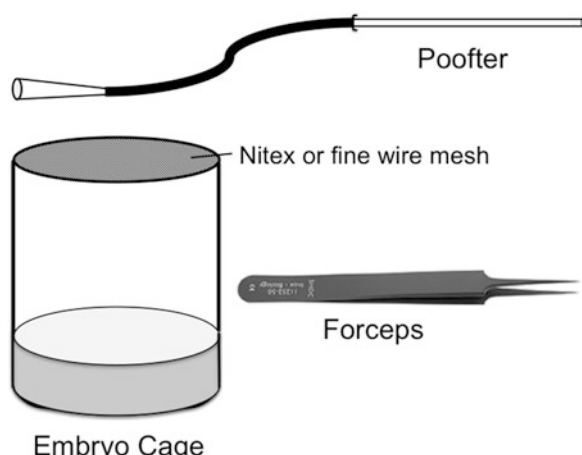


Fig. 1 Items required for *Drosophila* husbandry to establish proper density controls for behavioral experiments

3. Yeast paste—combine inexpensive wine (red or white, they like them both! or beer) with baker's yeast (Red Star Active Dry Yeast, store bought) to make a soft paste. This encourages females to lay eggs and provides a food source for hatching larvae (see **Notes 2** and **3**).
4. Stainless steel spatula to apply yeast paste, remove used agar from dishes and transfer hatched larvae that have migrated into the yeast to a new agar plate.
5. Jewelers forceps, Dumont No. 5. Student quality is acceptable, and far less expensive; used for carefully moving larvae either into bottles for density-controlled adults, or for assaying larval locomotion or feeding.
6. “Poofters”—these are constructed from thin walled black rubber tubing (inner diameter 1/8" and wall thickness 1/32") into which has been inserted a glass microcapillary pipette (200 μ l volume) covered at one end with a small square of Nitex mesh. The capillary is taped to the tubing to prevent separation; the Nitex prevents accidental inhalation of any flies. The small bore end of a blue (100–1000 μ l) plastic pipette tip is inserted at the other end and serves as the disposable mouthpiece. Aspiration should only be done in acceptable laboratory settings (e.g., no radioactivity or biohazardous materials present).

2.1 Larval Locomotion

1. Locomotor behavior plate—100 mm petri dish filled with 15 ml of 2% agar-agar solution at room temperature.
2. Tally counter—used to measure the number of body wall contractions as the larvae traverse the agar substrate.
3. Count-down timer.
4. Early third instar larvae (first day of the third instar, approximately 72+h after hatching).

2.2 Larval Feeding

1. Feeding behavior plate—100 mm petri dish filled with 15 ml of 2% agar-agar solution. Agar substrate is overlaid with 2% yeast solution (made with 0.1 g active-dry yeast in 5 ml deionized water). Solution is made fresh daily (Fig. 2).
2. Tally counter—used to count number of larval mouth hook contractions in a given time period.
3. Count-down timer.
4. Dumont forceps for transferring individual larvae.
5. Early third instar larvae.

2.3 Larval Chemotaxis

1. Chemotaxis behavior plate—100 mm petri dish filled with 15 ml of 2% agar-agar solution. Using PowerPoint or similar program, draw a circle the size of the petri dish and three smaller circles on a horizontal line through the middle of the plate (~1.5 cm in

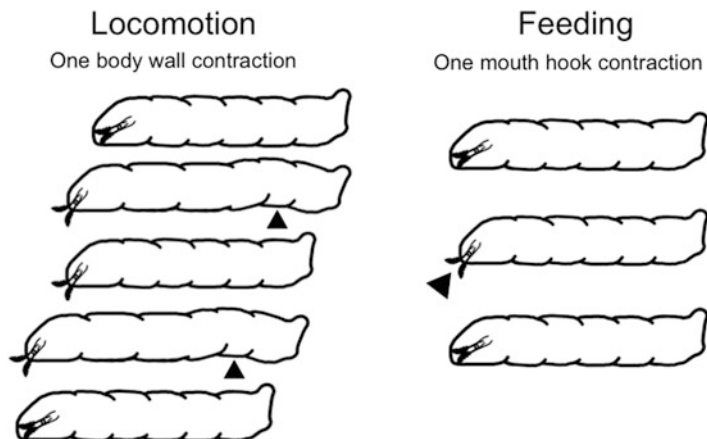


Fig. 2 Larvae use their mouth hooks for locomotor and feeding behaviors. For locomotor behaviors, larvae dig their mouth hooks into the agar substrate, then lengthen and contract their body to propel themselves along the surface. For feeding, larvae extend and retract their mouth hooks in the yeast solution overlaid on the agar plate to shovel food into the esophagus

diameter)—a circle at either end, and one in the middle. Bisect the large circle to establish two “arenas” (see Fig. 3a). Print out the figure and place the agar dish directly on top.

2. Attractive odorant—Heptanol.
3. Aversive odorant—Benzaldehyde.
4. Countdown timer.
5. “spoonula” type spatula for handling larvae.
6. Filter paper disks (1.5 cm).

2.4 Larval Phototaxis

1. Phototaxis behavior plate—100 mm petri dish filled with 15 ml of 2% agar-agar solution. Divide plate into four quadrants and diametrically color quadrants black and white. This can be done by drawing a 100 mm circle on paper, and drawing a cross to bisect top and bottom and left and right, to create the four quadrants. Color two opposing quadrants black, and draw an ~1.5 cm sized circle in the center (See Fig. 3b).
2. Light box (can be purchased at the hardware section of a department store, or online).
3. Countdown timer.
4. “spoonula” type spatula for handling larvae.

2.5 Geotaxis

1. 23×75 mm polystyrene vial marked with a line drawn horizontally 5 cm below the top.
2. Count up timer.
3. Poofter.

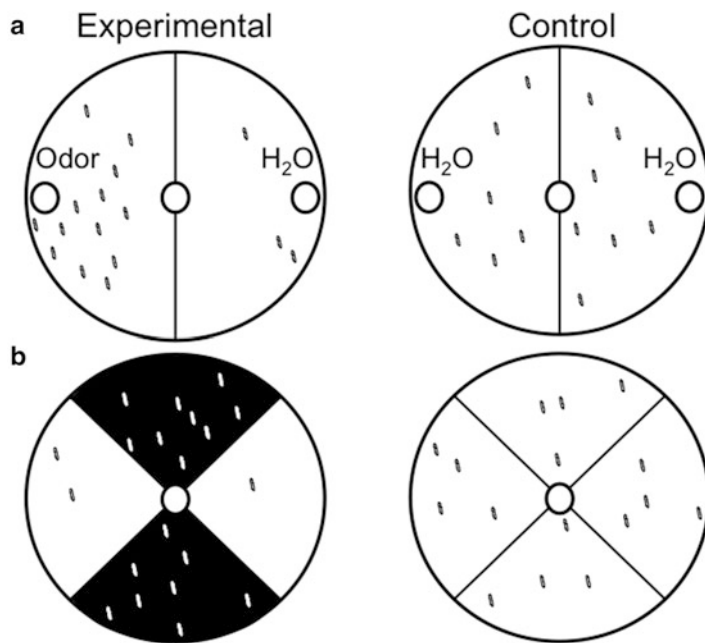


Fig. 3 Representative example of outcomes for larval chemotaxis using an attractive odorant (a) and for negative phototaxis (b). The control plates display an equitable distribution of larvae across the agar substrate. If this is not observed, it is likely there is an environmental condition that affects the outcome of the assay, which must be corrected

2.6 Loss of Righting Reflex

1. 23×75 mm polystyrene vial.
2. Vortexer.
3. Count up timer.
4. Poofter.

2.7 Odor Response

1. Several 2.5×9.5 cm polystyrene vials marked at 3 cm from the bottom and 3 cm from the top. This can be accomplished by measuring the distance, and placing a mark with a Sharpie pen to generate a dashed line encircling the vial for each demarcation.
2. Foam plugs for vials.
3. Cotton tipped applicators (long stems).
4. Odorants (a strong aversive odor is benzaldehyde).
5. Count-up timer.

2.8 Response to the Sedative Effects of Ethanol

1. 2.5×7.5 cm polystyrene vials..
2. Hard cotton plugs for vials
3. Wand for ethanol saturation. This is created from a length of chenille stem stably inserted into a cotton plug. It should clear the bottom of the vial.

4. Poofter.
5. Count up timer.
6. 200 proof absolute ethanol.

2.9 Locomotion

1. 60×15 mm petri dishes, each marked with a grid of 1 cm squares.
2. Count-up timer.
3. Handheld clicker counter.
4. Poofter.

2.10 Light–Dark Box

1. Arenas—constructed from 5 cm L \times 2 cm W \times 1.5 cm H transparent Lucite box with cover, with one half of the lower and upper chambers painted black with nail polish.
2. Light box (generally 16 W).
3. Timer.
4. Poofter.

2.11 Forced Swim Test

1. Arenas—Lab-Tek II 4 well Chamber slides or similar slides that contain polystyrene media chambers for growing cells.
2. Sodium Dodecyl Sulfate, 0.08%.
3. Video camera mounted to stereozoom microscope (this assay can also be scored manually in “real time”).
4. poofter.
5. flat-ended spatula.

2.12 Courtship

1. plastic or plexiglass arena measuring 1 cm \times 0.3 cm diameter. The latency until first courtship behavior will be increased if the arena is too large. These are usually designed as a 10 chamber wheel. A small hole (approximately the size of a 22 g needle) should be bored through the wall of the arena to allow for entry of air. While the wheel can be designed with a movable lid, it is also possible to use a clear glass microscope slide to cover the arena as soon as the flies have been poofted inside.
2. Stereozoom microscope (this assay can be accomplished without a video camera if scored in “real time”).
3. Poofter.
4. Count up timer.

3 Methods

3.1 Fly Husbandry

3.1.1 Egg Laying Plates

Add distilled water and agar-agar together in an Erlenmeyer flask and place on hot/stir plate and let reagents combine (solution will become transparent). Once solution boils turn off the heat but

keep stir setting on. Add Nipagin and granulated sugar to agar-agar solution and wait a few seconds to dissolve. Once combined, add apple juice and turn off stir setting. Pour to cover the bottom of petri dish. Allow to cool. Adjust the recipe as needed for different size batches.

3.1.2 Population Cages for Larval Behaviors

1. Using an egg-laying plate (see above) add a small square (~1 mm diameter) of Whatman 3MM (or similar grade) paper and add a small dollop of yeast paste to the paper and place in the center of the plate. The yeast paste entices egg-laying, and it is placed on the paper to allow easy removal of the yeast.
2. Add adult males and females to a population cage and place the egg-laying plate (Day 0) on the bottom to create the population cage (make sure to label with appropriate genotype and current date).
3. Allow adult flies to lay eggs for 24 h.
4. The next day, change out the plates on the cage to create a new “Day 0” plate. Remove the Whatman/yeast paste from first “Day 0” egg-laying plate and replace with a fresh dollop of yeast paste (no Whatman paper). This is now “Day 1.”
5. Allow this plate to age for another 24-h so that the hatched larvae can mature to first instar larvae and migrate into the yeast paste.
6. The following day, harvest the yeast paste containing the first instar larvae that have hatched, and remove them from the plate with unhatched eggs by transferring the yeast paste dollop to a fresh egg-laying plate. Add fresh yeast paste to ensure there is sufficient food for the larvae and to minimize drying out of the food. This plate is now “Day 2.”
7. Allow the larvae to mature for another 24 h (“Day 3,” second instar).
8. On Day 3, collect ~100 second instar larvae and place them on a new egg-laying plate with fresh yeast so that the larvae may mature to third instar under ideal density conditions.

3.1.3 For Adult Behaviors

Second instar larvae are counted and placed into a plastic or glass bottle containing fly food (approximately 100 larvae for the standard plastic bottles and 150 for glass milk bottles)

1. Gently squirt a few drops of water from a squeeze bottle onto the yeast paste with feeding larvae on the agar plate; the water will encourage the larvae to leave the yeast paste for the perimeter and facilitate picking them up with the forceps.
2. Larvae are gently removed from the forceps by dipping them into a small amount of water collected in the edge of the cover of the agar dish that is stably tilted.

3. The group of larvae is then transferred into the bottle by tapping them into the bottle and using a small amount of water to rinse the remaining larvae. Be careful not to use too much water since this will encourage mold growth (even if you use a mold inhibitor in your food).
4. Keep the bottles at ~25 °C with at least 60% relative humidity on a 12 h light–dark cycle until the adults eclose.

3.2 Larval Locomotion

A single larva is gently placed onto the 2% agar-agar petri dish using a blunt Inox forceps (*see Note 4*) and allowed to acclimate to the environment for 30 s. Larval body wall contractions are counted for 1 min using a tally counter. This can be viewed through a stereozoom microscope and counted in real time. A minimum of 20 larvae per genotype should be assayed (*see Notes 5–7* and Fig. 2).

3.3 Larval Feeding

Early third instar larvae are used to assay feeding behavior. During this period of development, larval mouth hook contractions are more consistent [4]. A single larva is placed on the agar substrate of the feeding behavior plate overlaid with yeast solution and allowed to acclimate for 30 s. Each extension and retraction (counted as one contraction) of the larval mouth hooks are counted for 1 min using a tally counter. A minimum of 20 larvae per genotype should be assayed (*see Notes 8* and *9* and Fig. 2).

3.4 Larval Chemotaxis

The larval chemotaxis assay is designed to identify a response towards an attractive or aversive odorant by measuring the number of larvae in each hemisphere (*see Notes 10* and *11*)

1. Place two 1.5 cm filter disks on opposite sides of the petri dish (using your diagram, placed underneath the dish, as a guide). You will need two plates per experiment: a control plate on which the two filter disks are saturated (generally 7 μ l volume) with H₂O, and an experimental plate containing 7 μ l H₂O on one disk (control) and 7 μ l of odorant on the other (experimental). The orientation of the filter disk with the odorant should be randomly changed to control for environmental factors during the assay.
2. Add ~75 larvae to the middle of the plate, using the diagram as a placement guide and set countdown timer for 5 min. The larvae are collected and placed on a spoonula, and gently pushed off the spoonula with spatula onto the center circle. Replace the lid (to minimize loss of odorant into the atmosphere).
3. After 5 min, remove the lid, and score the number of larvae on each side; do not count larvae that are dead or who have not migrated outside of the center circle. Calculate the response index by subtracting the number of larvae from the control

side (C) from the number of larvae on the side with the stimulus (S) and divide by the total [$RI = (S - C)/(S + C)$] [5, 6]. A minimum of ten independent trials should be run. A cartoon of this assay is depicted in Fig. 3a.

3.5 Larval Phototaxis

1. Place an assay plate on the paper diagram on an illuminated surface (e.g., portable light box), and reduce ambient light by performing the assay in a dark room. You will need two plates per experiment: a control plate (no black quadrants), and an experimental plate with two black and two white opposing quadrants. The orientation of the black quadrants should be randomly changed to control for environmental factors during the assay (see Notes 12 and 13).
2. Place larvae onto the center of the plate (as described for larval chemotaxis, above), and allow larvae to migrate for 5 min.
3. Record the number of larvae in positive (white quadrants) and negative (black quadrants) areas of the dish. Do not include dead animals or animals that have not migrated out of the center circle. The response index (RI) of a larva displaying negative phototactic behavior can be calculated by dividing the total number of larvae in the black quadrants by the total number of larvae used in the assay. An RI value of 0.5 is indicative of an equal distribution. A minimum of ten independent trials should be run. A cartoon of this assay is depicted in Fig. 3b.

3.6 Geotaxis

Geotaxis can be measured for individuals, or as a group assay with five flies per vial [7] (see Notes 14 and 15).

1. Flies are puffed into a polystyrene vial marked with a line drawn horizontally 5 cm below the top of the vial. The flies are tapped to the surface and given 10 s to demonstrate startle-induced negative geotaxis by migrating to the top of the vial (see Fig. 4).
2. If calculating statistics for groups of flies, the data are represented by percentages where the number of flies above the 5 cm mark is divided by the total number of flies tested within each group. The walking speed for an individual to reach the 5 cm mark can also be assessed (e.g., [8]).

3.7 Loss of Righting Reflex

1. A single fly is aspirated into a polystyrene vial, the vial is capped, and the fly is then allowed to recover for 30 s. The vial is then briefly (5 s) vortexed to deliver a mechanical shock, and the fly is tapped into a supine position at the bottom of the vial.
2. The fly is then given 10 s to right itself; if the fly succeeds in righting within 10 s, the response is scored as positive (Fig. 4). If the fly does not right itself within this time period, the response is scored as negative. This is a quantal response (the

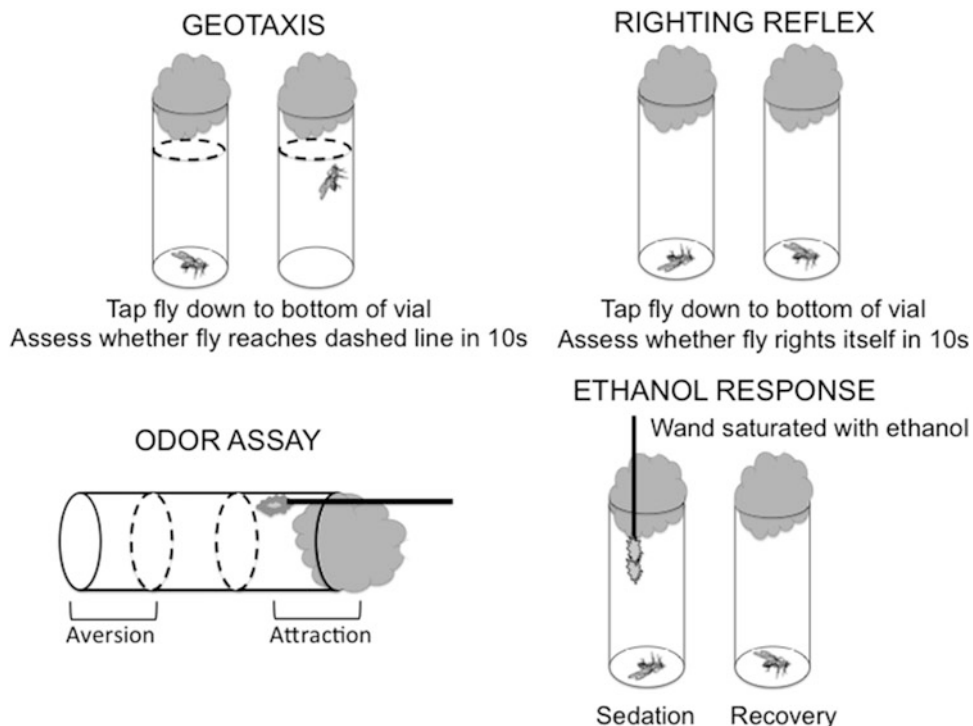


Fig. 4 Vial based assays. This figure demonstrates the basic setup for each of these paradigms

fly either rights itself or it does not), and therefore the percentage of positive responders is used to assess this behavior [7] (see Notes 16–18).

3.8 Odor Response

This assay is used to determine response to an attractive or repulsive odor by determining the number of flies at the near end (attraction, close to the odor) or far end of the vial (avoidance), and was first developed by Robert Anholt [9, 10]. This is a strong innate behavior, since aversion to repellent odorants is necessary for survival and for reproduction; when flies are exposed to a repulsive odor, they will rapidly fly or walk away (see Notes 19–23).

1. Five flies are “poofted” into a vial, gently tapped to the bottom, and a cotton-tipped applicator saturated (but not dripping) with odorant is inserted into the vial so the tip is lined up at the 3 cm mark from the top of the vial. The flies must be of the same sex since this behavior is sexually dimorphic [11] (see Fig. 4).
2. Place the vial on its side on a sheet of white paper to enhance visualization and allow 15 s for flies to recover from the tap down. Determine the number of flies in the bottom compartment every 5 s for the next 45 s (so that each assay runs for 1 min).
3. The “avoidance” score is calculated as the number of flies in the bottom sector of the vial, averaged over the ten measure-

ments. The range of avoidance scores is between 0 (maximal attraction to the odor source) and 5 (all flies are in the compartment away from the odor source for the entire assay period, i.e., a maximal repellent response). A minimum of ten individual trials of five flies/group should be used; distilled water is used in place of odorant as a (neutral) control.

4. Use separate vials for each odor and allow them to air out in between use.

3.9 Response to the Sedative Effects of Ethanol

1. Submerge the plug with the chenille stem into a 50 ml conical filled with 200 proof ethanol, and flick off the excess liquid. Gently aspirate a single fly into a vial, cap with the plug with the ethanol-saturated stem, immediately start the count-up timer, and determine the time, in sec, until the fly is sedated.
2. After 2 min of continuous sedation, gently “flip” the fly into a new vial, cap with a normal cotton plug, and determine the time, in sec for recovery (which is determined by the ability of the fly to right itself and walk away, or initiate grooming) (Fig. 4).
3. 30 animals are generally assayed per genotype/experimental condition [2] (see Notes 24–26).

3.10 Locomotion

This simple locomotor paradigm can be used to assay general activity for adult flies. Rodents explore all parts of an open field arena; similar behavior is observed in *Drosophila* [2]. The covered petri dish provides an arena that limits flying behavior and promotes walking. Since there is a trend for locomotor activity to diminish over time with habituation to the novel environment of the arena, both exploratory (first 2 min) and basal (last 2 min of the 15 min observation period) can be assayed in the same chamber [12] (Fig. 5) (see Notes 27–29).

1. A single fly is aspirated into an empty chamber, and the dish is then covered with the lid. Allow 30 s for the fly to recover, and count the number of lines crossed in the first 2 and last 2 min of a 15 min observation period. These numbers can be recorded using a handheld clicker counter.
2. After each day of use, the chambers are wiped clean and exposed to air to minimize any pheromonal or waste products.
3. Generally, a minimum of 30 individual trials per population will provide sufficient numbers for statistical analyses.

3.11 Light–Dark Box

This paradigm was originally developed to assess the anxiolytic effects of benzodiazepines in rats [13]. In this assay, the animal must choose between the natural preference of rodents for a dark environment with the innate desire for exploratory activity in a well-lit open arena. These paradigms induce both fear/avoidance as well as exploratory/approach behaviors [14]. While *Drosophila*

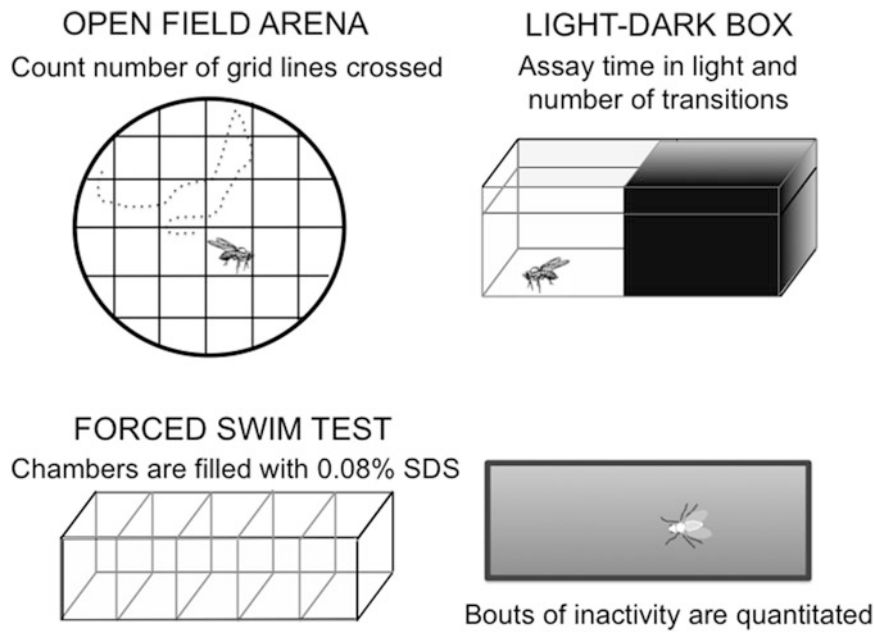


Fig. 5 Arena based assays. This figure demonstrates the basic setup for each of these paradigms

are normally positively phototactic, in this assay, their preference is for the dark side of the arena, and it can be used to assess exploratory behavior [2] (Fig. 5) (*see Notes 30 and 31*).

1. Place the chamber on the light box and gently aspirate a fly into the light side of the box and cover the container. This assay is performed in an otherwise dark room.
2. Immediately start the timer. Time spent in light and the number of transitions are recorded for the last 5 min of a 15 min observation period [2].
3. The fly is considered in the light when the head and at least half of the body is in the light side of the chamber.
4. Alternate the orientation of the light box with every assay.
5. Assay 30 animals per genotype or condition.

3.12 Forced Swim Test

This is a modification (Fig. 5, *see ref. 2*) of the original assay developed by Porsolt [15] to assess the effects of antidepressants on rats, which was then modified for use by mice [16]. The assay in flies is used to assess motivation for escape behavior (*see Notes 32 and 33*).

1. Fill each chamber with 0.08 % SDS. Rinse chambers after use.
2. Aspirate a single fly into the chamber until it settles into an individual well.
3. Viedotape (or observe) for 5 min.

4. Parameters to be scored include the latency until first immobility, and the duration and number of immobility bouts for each minute min of the 5 min assay period.
5. 30 animals are assayed for each population or condition.
6. To establish that the fly is not in any way compromised by exposure to the SDS, at the end of the assay, remove the animal with the flat end of a spatula. Gently flick onto a Kimwipes, and assess for the ability to immediately walk off. Compromised animals should be excluded from the final analyses.

3.13 Courtship

Both female and male behavior can be assayed; while the male runs through an elegant repertoire of behaviors designed to entice the female to allow him to mate, the female actually makes the decision as to whether or not the male is acceptable. Immature females (<3 days old) will be uninterested but not combative; females who have mated will aggressively spurn the male's courtship attempts (until there is no longer any sperm in her spermatheca) (see Notes 34 and 35).

1. Animals must be collected as newly eclosed virgins and aged until sexually mature (>3 days but preferably 5–6 days of age). They may be maintained singly in vials or in small groups (over-crowding is a stressor and will affect the outcome of the assay).
2. Gently poof an individual male and an individual female into the arena, cover, and observe or record. There are numerous descriptions of the courtship repertoire, which include: (1) orientation, when the male recognizes the female as an “object of interest” and orients towards her abdomen, generally at a 45° or 90° angle; (2) wing extension, when a male extends the wing closest to the female's field of vision and vibrates it at a specific intensity, creating the courtship song; (3) tapping, when the male extends a foreleg and taps the females abdomen; (4) licking, when the male extends his proboscis and licks the female's genitalia; (5) curling, when the male curls his abdomen in preparation for mating; and mounting, when the male actually attempts to copulate with the female. Temporally, the first two (orientation and wing extension) tend to occur together, often followed by a small gap in time, before the first appearance of licking and curling. However, as with all behaviors, there is tremendous variability and a male may repeat components of the courtship repertoire, or simply attempt to copulate. The courtship repertoire is depicted in Fig. 6.
3. The assays can be run for 20–30 min or until copulation ensues. Generally, if a male makes no advances after 10 min, or the female has refused to copulate after 30 min, the assay may be then stopped.

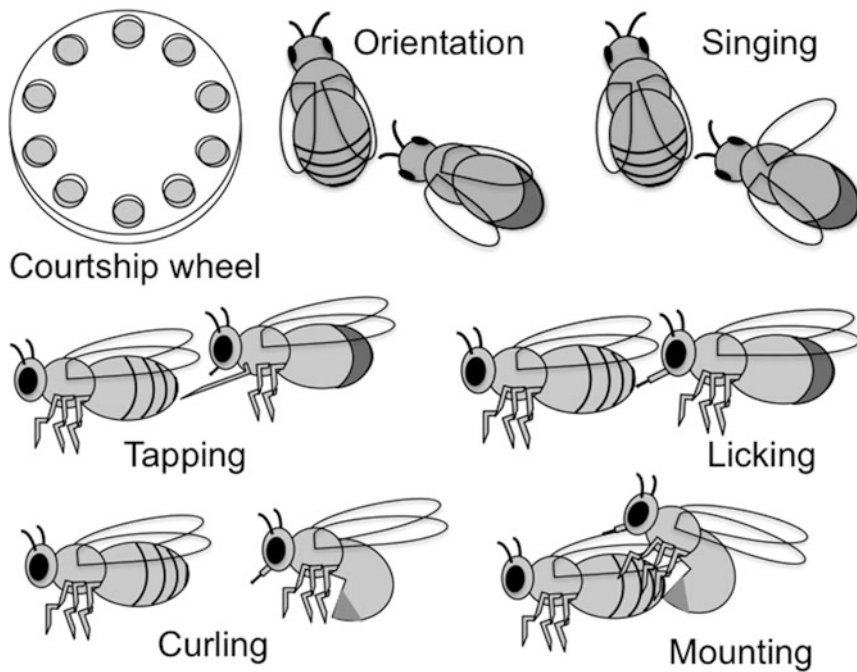


Fig. 6 Courtship. A traditional 10-chambered courtship wheel is shown, along with cartoons representing the major displays of courtship behavior by the male

4. Time (in seconds) to latency of the first appearance of any of the courtship elements may be quantitated. The Courtship Index (CI) reflects the total amount of time in which a male engaged in any courtship behavior divided by the total time of the assay (30 min or until copulation ensues). Descriptions of courtship behaviors have been detailed in several reviews [17, 18].

4 Notes

1. When making apple juice (or grape juice) plates, be certain that the agar mixture is fully dissolved in water (rolling boil)—but be careful the solution does not boil over on the hot plate. Use a 1 l Erlenmeyer flask for a 300 ml recipe to allow for room for the solution to expand as it boils. It is also critical to pour the solution as soon as the apple juice, sugar, and Nipagin are mixed in, since the juice contains an agarase and the agar will otherwise not harden sufficiently.
2. The consistency of the yeast paste for the population cages is important. If too thin and runny, parental flies will be trapped in it and die; if too thick, it will be too dry and females will be less encouraged to lay their eggs.

3. On the larval collection/aging plates, make sure there is sufficient yeast paste of the appropriate consistency. Too few larvae, and the food will not remain sufficiently soft and moist to promote feeding. Too many larvae, and the animals will suffer from poor nutrition. These conditions are detrimental and will affect developmental times and behavioral outcome.
4. It requires some manual dexterity to gently lift a single larva with blunt forceps. Be careful to avoid injuring the animals in any way.
5. Laboratory conditions for this assay are recommended to be between 24 and 28 °C, as this is their preferred temperature [19, 20]. Cooler conditions in the testing room pull moisture from the agar plates, thus drying them out and must be re-wetted as to maintain a moist (not wet) agar surface.
6. This assay is also used as a physiological control to assess whether the animal to be is in any way physiologically compromised, since larvae use their mouth hooks to traverse the agar substrate. Larvae with 40 body wall contractions or less should be excluded from analyses as those ranges are indicative of ill or injured animals [4].
7. It is important to maintain the moisture of the agar. If the agar is too dry, then the larvae cannot traverse the surface easily and will eventually stop. Conversely, if the agar is too wet then the larvae are not able to dig into the agar and will spend the assayed time “swimming.”
8. During the assay, the yeast solution has a tendency to settle, making it difficult to visualize the larvae, and thus accurately measure the feeding response. Swirl the plate by gently rotating the plate in between assays so that the yeast will remain suspended in solution.
9. The conditions of the testing room must be maintained between 24 and 28 °C. If the testing room is too cold, moisture will be pulled from the yeast solution causing the yeast to concentrate and settle more often. It is recommended to add water to the dish if this is observed; however, if too much water is added it will occlude visibility of the larval mouthhooks [4].
10. Before the assay, gently rinse a group of ~100 s instar larvae with distilled water to remove any residual yeast paste before collection onto the spoonula. The larvae will migrate towards food, which will skew the assay if not removed.
11. The timing is critical for this assay, because after 5 min the odorant will be sensed even on the “control” side of the agar assay plate, and the larvae will randomly disperse across the agar. Depending upon the age and genotype, larvae will migrate slower or faster and the time for response may need to be adjusted.

12. Animals should also be gently rinsed to remove any yeast residue before this assay.
13. As for larval chemotaxis, the time for response may need to be adjusted depending upon the experimental population.
14. This assay is very simple and quick, and can be used to test for physiological competence before a more complicated paradigm.
15. Air out the vials after each use; occasionally wipe the insides with a Kimwipes.
16. This assay can also serve as an easy test for physiological competence before a more complicated paradigm.
17. Air out the vials after each use; occasionally wipe the insides with a Kimwipes.
18. Limit the intensity and extent of vortexing; just use a short pulse to flip the fly on its back. This can also be done by flicking the vial with your fingertips. Continued vortexing will serve as a stressor and is not recommended.
19. It is easier to manipulate foam rather than hard or soft cotton plugs, and simpler to insert the cotton-tipped applicator.
20. If the cotton tip is too heavily saturated with odorant, flies may become stuck on the tip, so flick excess odorant off the tip before you begin the assay.
21. Be careful not to allow the cotton tip saturated with benzaldehyde to touch the side of the plastic vial as this will damage the plastic and obscure viewing the flies.
22. If the flies are not all tapped down to the bottom of the vial, flies in the immediate vicinity of the odorant may become immediately habituated and therefore unresponsive to the odor.
23. Oxidation of benzaldehyde occurs rapidly and forms a precipitate of benzoic acid, so it is best to remove small aliquots from the source bottle to use for each assay.
24. Be careful not to poof the fly directly onto the saturated wand, or its wings will get wet and it will be unable to complete the assay.
25. Additional assays may be run concurrently.
26. It is helpful to place the vials upright on a white sheet of paper to enhance visualization of the fly.
27. The simplest way to create the arenas is to use Microsoft PowerPoint (or a similar program) to draw a 60 mm circle, then add vertical and horizontal lines 1 cm apart to create the grid. The circles are printed, cut out, and applied to the bottom of the petri dish using a glue stick.
28. For ease of observation, place the arenas on a plain white sheet of paper, which increases contrast and minimizes glare using typical laboratory lighting.

29. Up to five arenas can be monitored at one time, by starting the next fly after the initial observation period has been completed for the previous fly.
30. Two assays can be run concurrently.
31. A guide can be made by tracing the outline of the chamber with a felt-tipped marker on a clear acetate sheet. This can be tape to the light box so that the chamber is always in the same position on the light box (except that the dark and light sides are alternated for each assay).
32. The SDS solution cannot be reused for more than 1 day. Even when the chamber is covered, there is some evaporation, and higher concentrations of SDS are toxic.
33. Eliminate any animals that fall into the arena on their back or side, or any animals that were accidentally submerged into the SDS solution as a consequence of overenthusiastic poofing.
34. It is absolutely critical to wipe clean and air out the courtship chambers after every use since pheromones can be deposited by the previous couple that can confuse the next pair of flies.
35. Since courtship requires sensory processing of auditory, gustatory, and visual cues, fly strains carrying mutations that result in deficits in any of these processes will take considerably longer to mate, and aspects of their courtship repertoire will obviously be lacking.

References

1. Neckameyer W, Weinstein J (2005) Stress affects dopaminergic signaling pathways in *Drosophila melanogaster*. *Stress* 8:117–131
2. Neckameyer W, Nieto-Romero A (2015) Response to stress in *Drosophila* is mediated by gender, age and stress paradigm. *Stress* 18:254–66
3. Barron AB (2000) Anaesthetising *Drosophila* for behavioural studies. *J Insect Physiol* 46(4):439–442
4. Bhatt PK, Neckameyer WS (2013) Functional analysis of the larval feeding circuit in *Drosophila*. *J Vis Exp* 81:e51062
5. Leal SM, Kumar N, Neckameyer WS (2004) GABAergic modulation of motor-driven behaviors in juvenile *Drosophila* and evidence for a nonbehavioral role for GABA transport. *J Neurobiol* 61(2):189–208
6. Rodrigues V, Siddiqi O (1978) Genetic analysis of chemosensory pathway. *Proc Indian Acad Sci B Anim Sci* 87B:147–160
7. Leal SM, Neckameyer WS (2002) Pharmacological evidence for GABAergic regulation of specific behaviors in *Drosophila melanogaster*. *J Neurobiol* 50(3):245–61
8. Strauss R, Heisenberg M (1993) A higher control center of locomotor behavior in the *Drosophila* brain. *J Neurosci* 13(5):1852–61
9. Anholt RR, Lyman RF, Mackay TF (1996) Effects of single P-element insertions on olfactory behavior in *Drosophila melanogaster*. *Genetics* 143(1):293–301
10. Anholt RR, Mackay TF (2001) The genetic architecture of odor-guided behavior in *Drosophila melanogaster*. *Behav Genet* 31(1):17–27
11. Mackay TF et al (1996) Quantitative genetic variation of odor-guided behavior in a natural population of *Drosophila melanogaster*. *Genetics* 144(2):727–35
12. Neckameyer W (1998) Dopamine modulates female receptivity in *Drosophila melanogaster*. *J Neurogenet* 12:101–114
13. Crawley J, Goodwin F (1980) Preliminary report of a simple animal behavior model for

the anxiolytic effects of benzodiazepines. *Pharmacol Biochem Behav* 13:167–70

- 14. Montgomery KC (1955) The relation between fear induced by novel stimulation and exploratory behavior. *J Comp Physiol Psychol* 48(4):254–60
- 15. Porsolt RD, Le Pichon M, Jalfre M (1977) Depression: a new animal model sensitive to anti-depressant treatments. *Nature* 266(5604):730–2
- 16. Castagne V et al (2011) Rodent models of depression: forced swim and tail suspension behavioral despair tests in rats and mice. *Current protocols in neuroscience/editorial* board, Jacqueline N. Crawley ... [et al.] Chapter 8:Unit 8 10A
- 17. Greenspan R, Ferveur J (2000) Courtship in *Drosophila*. *Annu Rev Genet* 34:205–232
- 18. Spieth HT (1974) Courtship behavior in *Drosophila*. *Annu Rev Entomol* 19:385–405
- 19. Garrity PA et al (2010) Running hot and cold: behavioral strategies, neural circuits, and the molecular machinery for thermotaxis in *C. elegans* and *Drosophila*. *Genes Dev* 24(21):2365–82
- 20. McKemy DD (2007) Temperature sensing across species. *Pflugers Arch* 454:777–791

Chapter 20

Electrophysiological Recordings from Lobula Plate Tangential Cells in *Drosophila*

Alex S. Mauss and Alexander Borst

Abstract

Drosophila has emerged as an important model organism for the study of the neural basis of behavior. Its main asset is the experimental accessibility of identified neurons by genetic manipulation and physiological recordings. *Drosophila* therefore offers the opportunity to reach an integrative understanding of the development and neural underpinnings of behavior at all processing stages, from sensing to motor control, in a single species. Here, we will provide an account of the procedures involved in recording the electrical potential of individual neurons in the visual system of adult *Drosophila* using the whole-cell patch-clamp method. To this end, animals are fixed to a holder and mounted below a recording chamber. The head capsule is cut open and the glial sheath covering the brain is ruptured by a combination of shearing and enzymatic digest. Neuronal somata are thus exposed and targeted by low-resistance patch electrodes. After formation of a high resistance seal, electrical access to the cell is gained by small current pulses and suction. Stable recordings of large neurons are feasible for >1 h and can be combined with controlled visual stimulation as well as genetic and pharmacological manipulation of upstream circuit elements to infer circuit function in great detail.

Key words *Drosophila*, Electrophysiology, Patch-clamp, Visual processing, Lobula plate tangential cell, Motion vision

1 Introduction

Drosophila has emerged as a powerful model organism for a comprehensive study of the neural basis of behavior at all processing levels. A key asset is its genetic tool box. For most neurons and brain regions of interest, increasingly selective driver line collections are being generated [1]. This is paralleled by the development of many effector transgenes, which can be expressed in a cell-specific manner using these driver lines for sophisticated and highly selective functional manipulations of various kinds [2, 3]. Resulting phenotypes in behaviors under investigation provide a means to deduce the neural mechanisms. Complementary to behavioral analysis, the application of electrophysiological methods to record from individual neurons has long been restricted to other

animals with larger neurons for practical reasons. However, spurred by its advancing genetics, intracellular recordings by way of whole-cell patch-clamp have been established for *Drosophila* during the past two decades at various developmental stages and are now being routinely used [4–6]. Patch-clamp recordings have been successfully utilized for instance to dissect the mechanisms underlying olfactory or visual processing. The patch-clamp technique requires micropipettes with rather large low-resistance openings that are directed at a cell membrane to establish a high resistance seal. By suction or current pulses the membrane is locally ruptured to gain electrical access to the intracellular compartment. Membrane potential and current flow, for instance during sensory stimulation, can now be read out in single neurons at high temporal resolution. In flies, recordings can be obtained *in vivo* from neuronal somata of preferably large size and superficial location after removal of the glial sheath. Here, we provide an account of the materials and steps involved in obtaining electrical access to identified motion-sensitive wide-field neurons via whole-cell patch-clamp in the adult *Drosophila* visual system. Furthermore, we briefly outline the combination of this method with pharmacological and optogenetic intervention. *Drosophila* tangential cell patch-clamp recordings in the visual system as described below have been pioneered by Joesch et al. [6], based upon Wilson et al. [5], and have been further modified by Maimon et al. [7] and Mauss et al. [8].

2 Materials

2.1 Equipment

1. General lab equipment: Dissection scope, pH-meter, osmometer, peristaltic pump, electrode puller.
2. Specific electrophysiology equipment: air-suspended table, amplifier (preferably true voltage follower), digital-analog-converter, computer with data acquisition card and suitable software, cables, oscilloscope, micromanipulators, audio monitor, electrode holders, upright microscope (space below microscope required for visual stimulation arena) with 5× air and 40× long distance water-immersion lens (0.8 NA) equipped with two polarization filters for polarized reflected light microscopy, current source connected to holder with wire for melting beeswax.
3. Recording and enzyme dissection pipettes: Borosilicate glass capillaries with filament (thin-wall, 100 mm, 1.5 mm OD, 1.12 mm ID).
4. Custom-made holder for flies and attachable recording chamber with in- and out-flow.
5. Tubing, syringes (1 ml) with filters (0.45 µm membrane, e.g., Minisart RC4), forceps, hypodermic needles (0.4×20 mm), Microfil needles or equivalent for backfilling, beeswax, silver wire.

2.2 Reagents

1. Extracellular normal solution (Table 1), in mM: 103 NaCl, 3 KCl, 5 TES, 10 trehalose, 10 glucose, 7 sucrose, 26 NaHCO₃, 1 NaH₂PO₄, 1.5 CaCl₂, and 4 MgCl₂, ~pH 7.3, ~280 mOsmol/kg. Carboxogenate with 95 % O₂/5 % CO₂ and perfuse over the preparation at 2 ml/min. Long-term storage of extracellular solution, which usually lasts for a few days at 4 °C, is not recommended. However, a 10× stock omitting sugar, NaHCO₃, and CaCl₂ can be maintained at 4 °C for several weeks.
2. Extracellular Ca²⁺-free/ high Mg²⁺ solution (Table 2), in mM: 66 NaCl, 3 KCl, 5 TES, 10 trehalose, 5 glucose, 26 NaHCO₃, 1 NaH₂PO₄, 22 Na gluconate, and 20 MgCl₂, ~pH 7.3, ~280 mOsmol/kg.
3. Collagenase solution for enzymatic digestion: Extracellular solution containing 0.5 mg collagenase type IV/ml.
4. Intracellular solution (Table 3), in mM: 140 K-aspartate, 10 HEPES, 4 Mg-ATP, 0.5 Na-GTP, 1 EGTA, 1 KCl, and ~0.1 Alexa Fluor hydrazide salt. Adjust to pH 7.26 with 1 M KOH. Osmolality should be at ~265 mOsmol/kg. Intracellular solution can be stored in small aliquots at -20 °C.

Table 1*Drosophila* normal patch-clamp external solution

Compound	MW	Conc. [mM]	1 l 10× stock solution	1 l external solution
NaCl	58.44	103	60.19 g	100 ml
KCl	74.55	3	2.24 g	10× sugar-free fridge stock
TES	229.20	5	11.46 g	
NaH ₂ PO ₄	120.00	1	1.20 g	
MgCl ₂	95.22	4	3.81 g	
Trehalose	378.30	10		3.78 g
Glucose	198.17	10		1.98 g
Sucrose	342.30	7		2.40 g
NaHCO ₃	84.01	26		2.18 g
CaCl ₂ ·2H ₂ O	147.02	1.5		0.22 g
<i>pH ~7.3. ~280 mOsmol/kg</i>				

Table 2
Drosophila zero Ca^{2+} /high Mg^{2+} patch-clamp external solution

Compound	MW	Conc. [mM]	1 l external solution
NaCl	58.4	66	3.87 g
KCl	74.6	3	0.22 g
TES	229.3	5	1.15 g
NaH_2PO_4	120.0	1	0.12 g
MgCl_2	95.2	20	1.90 g
Na gluconate	218.1	22	4.80 g
Trehalose	378.3	10	3.78 g
Glucose	198.2	5	1.98 g
NaHCO_3	84.0	26	2.18 g
<i>pH ~7.3. ~280 mOsmol/kg</i>			

Table 3
Drosophila patch-clamp internal solution

Compound	MW	Conc. [mM]	Stock solutions	20 ml internal solution
K-aspartate	171.2	140	1 M	2.8 ml
HEPES	238.3	10	1 M	0.2 ml
EGTA	380.4	1	100 mM (pH 8.6 with 5 M KOH)	0.2 ml
KCl	74.55	1	1 M	0.02 ml
Example: Alexa Fluor 488 Hydrazide	570.5	0.05	10 mM	0.1 ml
Mg-ATP	507.2	4		40.6 mg
Na-GTP	523.2	0.5		5.2 mg
<i>Adjust pH to 7.26 with 1 M KOH. Osmolality should be at ~265 mOsmol/kg</i>				

3 Methods

3.1 Mounting and Surgery

- Flies selected for recordings should be between about 0.5 and 3 days of age, since young flies have a soft cuticle and old flies accumulate fat tissue and have a thicker glial sheath, which hamper dissection and recording. We routinely use female flies, since they are larger than male flies. Transfer fly to small glass vial and

immobilize on ice for ~1 min. Pick up fly at legs with forceps. At the same time melt beeswax within a loop of a rigid wire through which current is passed (adjust current beforehand to the lowest value so that wax is just melting). Apply small droplet of melted wax onto holder (Fig. 1), remove hot wire and swiftly lower fly into wax droplet so that it will become attached to holder by hardening wax. The head and about half of the thorax, depending on the holder, should protrude the holder edge (Fig. 2). Immobilize legs by attaching them with wax to holder.

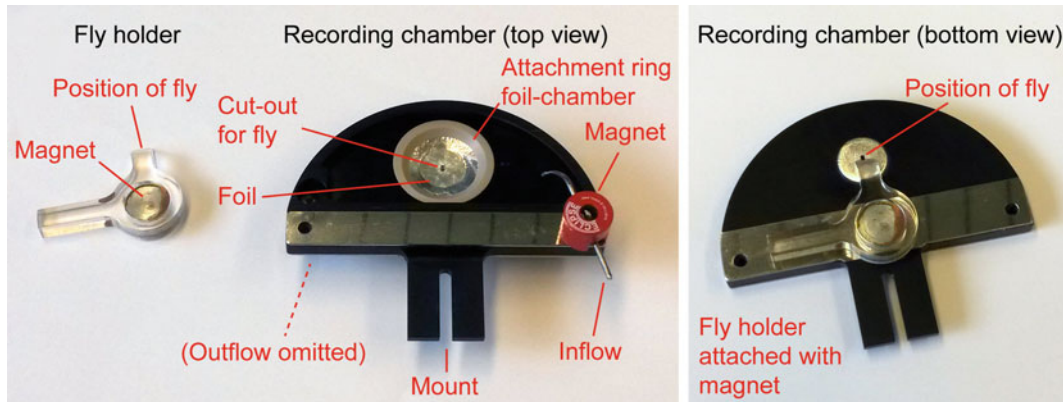


Fig. 1 Custom-made fly holder and recording chamber

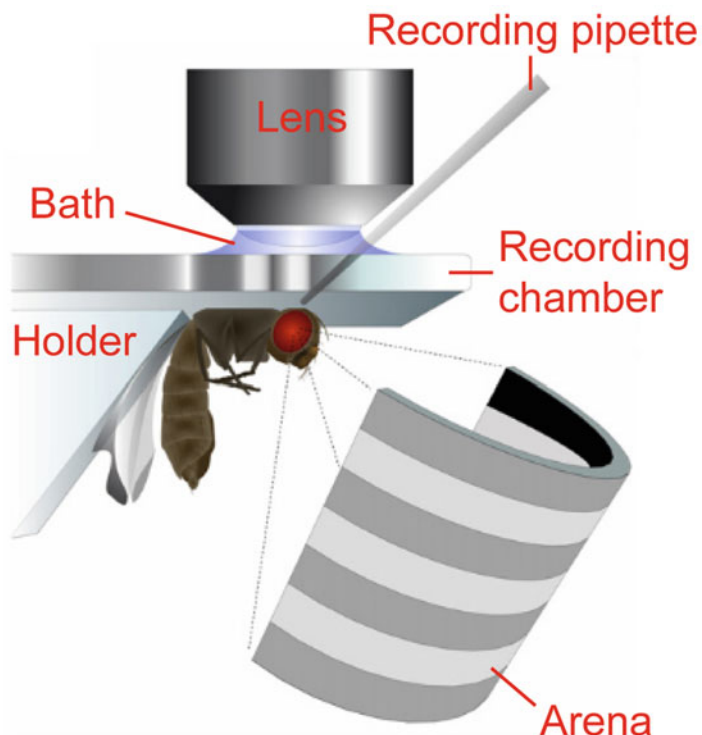


Fig. 2 Schematic fly preparation within recording setup (adapted from ref. 6)

2. Under the dissection scope, bend down head (to later obtain access to the back of the head) by attaching proboscis to thorax using a tiny droplet of beeswax. Attach holder with fly beneath a recording chamber with small cut-out in bottom ($\sim 1 \times 2$ mm; Fig. 1), so that the head is plane with edges and accessible through the hole (Fig. 2). Gently attach thorax and head to edges of cut-out with wax on side opposite of intended recording.
3. Fill chamber (Fig. 1) with external solution. Use hypodermic needle attached to a syringe as a holder to cut hole in cuticle at the back of the head. To this end, insert hypodermic needle fronto-medially, and enlarge cut in both directions by sawing movements until cuticle remains attached to the head only at the back. Detach cuticle lid from rest of head capsule by lifting it using forceps in one hand and cutting below using hypodermic needle in the other hand. Remove fat body and muscle lying on top of brain using forceps (see Note 1). The muscle is advised to be removed because it partly occludes the tangential cells and it can also cause tissue movements due to contractions. We do not recommend to pull out trachea.
4. Transfer preparation to microscope and switch on perfusion with carboxygenated extracellular solution (Tables 1 and 2; ~ 2 ml/min; perfusion does not seem vital for the condition of the preparation initially, but it is expected to increase lifetime and it allows washing in and out pharmacological substances). Check orientation and condition of preparation. Slight regular pulsation indicates a healthy preparation and is usually not a problem for whole-cell recordings (see Note 2).

3.2 Exposing Neuronal Cell Bodies for Recording

1. Fill a ~ 5 μ m opening pipette with filtered external solution containing 0.5 mg collagenase/ml [7]. Connect pipette to a mouth piece via a holder, tube and valve, and use micromanipulator to maneuver it to the preparation. To practise, tangential cell bodies can be identified by expression of GFP or other fluorescent markers using genetic driver lines such as DB331-Gal4 [6]. However, the large size and stereotypic superficial position of their cell bodies with respect to tracheal branching (Fig. 3) allows the identification also without genetic marker.
2. Under polarization contrast visual control (see Note 3), apply positive pressure to eject a gentle constant stream of collagenase solution to the subsequent recording site in order to digest the glial sheath. Rupturing of glia may also be promoted mechanically by cutting and sucking in small portions into the pipette. Typically, rupturing of glia occurs in two steps. Thereafter, somata boundaries emerge clearly and their dense packing should loosen up visibly.
3. Use positive pressure pulses to expose and separate cell bodies as well as clear them from glia and other cellular fragments.

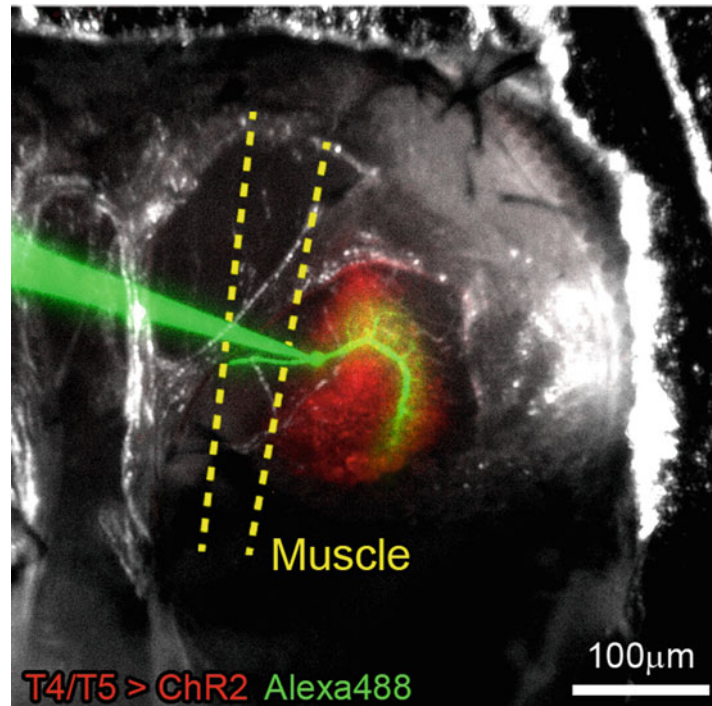


Fig. 3 Image of preparation with recording pipette and dye-filled lobula plate tangential cell (adapted from ref. 8). T4/T5 neurons, which are presynaptic to tangential cells, are genetically labeled with fluorescent Channelrhodopsin-H134R-mCherry

Once somata of cells of interest are exposed, well discernible and appear round-shaped with a smooth surface, they are ready for recording (*see Note 4*).

3.3 Establishing Whole Cell Configuration

1. Immerse chlorided silver indifferent electrode in bath. Pull thin-walled patch pipettes of borosilicate glass filament capillaries. Back-fill the tip with filtered intracellular solution (Table 3; from small frozen aliquots) and insert pipette into holder such that the tip of the different chlorided silver wire is immersed in the solution. Apply and lock slight positive pressure, insert pipette into bath and swiftly maneuver electrode to the preparation. Check electrode resistance (~5–8 MΩ).
2. Constantly apply current pulses of ~50 pA at ~1–2 Hz to monitor resistance. Resistance R is linearly related to the measured voltage deflection V upon current injection I according to Ohm's law ($R=V/I$). Approach exposed cell body with slight positive pressure held via mouthpiece. Ideally, though not always, a small dip in the cell membrane from jet of ejecting solution becomes visible or somata are gently moved away by ejected stream. Release pressure and observe formation of contact and seal, as indicated by an increase in the amplitude of the measured voltage deflections (*see Note 5*).

During this step, it is useful to make the voltage deflections audible by an auditory monitor. If necessary, very gently apply negative pressure to aid seal formation. Aim for resistance of $>1\text{ G}\Omega$. If high resistance seal does not form, discard recording pipette. The same cell may be repeatedly targeted with fresh pipettes.

- Upon seal formation, apply few brief ($\sim 0.5\text{ s}$) current pulses of $-200\text{--}300\text{ pA}$ which often leads to drop in potential and input resistance, indicating increased intracellular access. Apply further gentle or sharp suction via mouthpiece if necessary (see Note 6). A stable potential of $\sim -40\text{ mV}$ (not taking into account liquid junction potential of $\sim 12\text{ mV}$ for normal extracellular and intracellular solution) and lively neuronal activity (e.g., noticed by auditory monitoring) indicates whole-cell configuration. Dye contained in the intracellular solution usually perfuses into the cell within $\sim 10\text{--}20\text{ min}$ without applying current pulses, allowing anatomical identification (Fig. 3).

3.4 Assessing Recording Quality

Stable recordings can usually be obtained for $>1\text{ h}$ (see Note 7) but recording quality and condition of the preparation (see Note 8) needs to be monitored over time, for instance by injecting small negative current pulses at regular intervals. The measured total resistance R_{input} reflects the sum of R_{membrane} , R_{pipette} and R_{access} , with the latter two ideally being much smaller than the cell's membrane resistance, which is in the range of $200\text{ M}\Omega$ [7, 9]. Note that R_{input} typically gradually increases over time (e.g., from 176 ± 46 to $205 \pm 45\text{ M}\Omega$ (mean \pm s.d.) during the first 10 min) [9], perhaps by increasing seal quality or slight clogging of the pipette tip. A sudden and substantial increase in R_{input} however may indicate deteriorating access to the recorded cell by re-formation of a seal across the pipette tip. This is reflected in the recorded voltage signals in that especially higher frequency components become reduced in amplitude, which can be noticed on the oscilloscope or via the audio-monitor. In this case, access to the cell may be reestablished by suction (check pipette tip position on recorded cell via the microscope beforehand). Conversely, an input resistance drop may indicate decreasing membrane resistance indicative of membrane disintegration and poor cell condition, though we have observed this rarely. A complementary way to assess recording quality is to measure the resting membrane potential V_{rest} and to probe visual response properties in regular intervals, for instance by presenting wide-field motion. Generally, R_{input} , V_{rest} and visual responses should remain stable throughout the recording session (see Note 9).

3.5 Pharmacology and Optogenetics to Probe Synaptic Connectivity

- Intrinsic electrical properties of neurons as well as their responses to visual stimulation and/ or to current injection can be probed [6]. Particularly if combined with genetic silencing in the upstream circuit, neural mechanisms underlying visual processing can be studied in great detail [10, 11]. Alternatively,

presynaptic neurons can be stimulated optogenetically [8, 12], and the resulting synaptic potential change measured, for instance to probe connectivity and synaptic transmission on a fast time scale. To this end optogenetic tools such as Channelrhodopsin2-H134R [13] may be expressed genetically in presynaptic neurons of interest (Fig. 3) while adult flies are being fed with *all-trans*-retinal (~1 mM, e.g., mixed in yeast paste, ~1 day). Light delivery is straight-forward via the epifluorescent light path of the microscope coupled to a light source such as an arc lamp, allowing the use of arbitrary excitation wavelengths and band widths by way of optical filtering. Temporal control at millisecond precision can be achieved with a mechanical shutter or a galvanometer mirror system as implemented in the Sutter Lambda DG-4 wavelength switcher. Alternatively, LEDs or lasers might be used as light sources, conveying potential advantages by allowing fast triggering with electric pulses. While spatial control over illumination is low without further modification, cell-type specific stimulation can be achieved by use of selective genetic driver lines [1]. A problem poses the activation of photoreceptors by optogenetic light stimuli, evoking flicker responses in tangential cells. This can be eliminated by using blind *norpA*-mutant flies lacking phospholipase C, an essential enzyme of the visual transduction cascade [8, 12]. Alternatively, flies can be reversibly blinded with a prolonged depolarizing afterpotential (PDA), evoked by intense blue light directed at their eyes [14]. Visual artifacts are also expected to be less of a problem by using long wavelength light (>600 nm) to activate red-shifted Channelrhodopsins such as CsChrimson [15], since fly photoreceptors respond mostly to light of shorter wavelength. Thus, optogenetic manipulation within the circuit can potentially be combined with visual probing of the system.

2. In combination with optogenetic stimulation, solutions with pharmacological substances or altered salt concentrations may be washed in and out to interfere with synaptic transmission in a selective way. For instance, Mecamylamine, α -Bungarotoxin and Methyllycaconitine antagonize cholinergic receptors to different degrees of efficacy, selectivity and reversibility while Picrotoxinin reversibly but less selectively blocks GABA- and glutamate-gated chloride channels [8, 12]. This approach allows to infer the underlying transmitter systems between the stimulated and the recorded neurons. Extracellular solution lacking Ca^{2+} but with elevated Mg^{2+} (20 mM) may be used to silence all chemical synaptic transmission (Table 2). This has been used to probe direct effects of neurotransmitters on tangential cells [8] but could also be suitable to test for electric coupling between presynaptic candidate neurons and postsynaptic tangential cells.

4 Notes

1. The translucent muscle in the back of the head lying on top of the brain with tangential cells can be difficult to discern. Use fine sharp forceps to gently pick at the expected dorsal attachment site above the main lateral trachea branch (Fig. 3). Once the muscle has been grabbed by the forceps, it is much easier to detect. We suggest to carefully remove it from dorsal attachment site step-by-step first and then pull the entire muscle so that it becomes detached from ventral site. Often, the muscle cannot be removed in one single piece.
2. Reduced viability of preparation is indicated by ceasing pulsation. Potential reasons might be damages occurring during dissection (dissect more gently), temperature for melting wax too high (reduce temperature until wax just melts; if applicable consider using wax melting at lower temperature), trachea openings—spiracles located in thorax laterally below wings—are waxed (avoid covering thorax excessively) or problems with external solution (check compounds, pH and osmolality).
3. A good image with sufficient tissue contrast is a critical success factor. To enhance tissue contrast two polarization filters can be used in the microscope filter slider/cube (one as a polarizer to produce linearly polarized light and the other one as an analyzer) in conjunction with a beam-splitting mirror in between [10]. Vary the polarization plane offset between the two filters until maximal contrast is achieved. Ideally, the aperture and field diaphragm in the light path should be centered and adjusted to produce homogenous illumination and optimal contrast. Note that light-scattering objects in the preparation, such as gas bubbles, fat tissue, or partly severed trachea above the recording site, decrease contrast.
4. Soma exposure is an important and difficult step and it is hard to convey how to apply the right level of vigor in order to expose clean cell bodies yet leave the neural tissue undamaged. To complicate matters, we observe a certain variability in the efficacy of collagenase-aided soma exposure. This step therefore requires some practice and experience to develop the necessary skills and routine. If problems persist in rupturing the glial sheath try collagenase dissection pipettes with different tip sizes (~3–10 μm), increase enzyme concentration or temporarily elevate bath temperature to ~30 °C to accelerate enzyme function [7]. Desheathing tends to be easier in younger flies (we routinely use 1 day old flies).
5. Establishing a high resistance seal between pipette and a well-exposed target cell is usually rather reliable. If a high resistance seal fails to form repeatedly cells might not be sufficiently

exposed. Problems could also arise if positive pressure in recording pipette is not maintained constantly. Check whether tube or holder are leaky, for instance by assessing pressure drop over time by closing the pipette holder opening and pulling out the plunger of the syringe connected to the tubing at the other end. Negative pressure locked in the tubing/holder system should keep pulling syringe plunger back in. Alternately, lock positive pressure with recording pipette in bath and monitor fluorescence dye ejection under microscope. Fire polishing recording pipettes could also aid seal formation. Try contacting cell either from above or from the side.

6. If break-in to achieve whole-cell configuration is difficult and/ or a putative seal is often lost during that step, clogging of the pipette tip might in fact have increased the input resistance, also a potential consequence of insufficiently exposed cell bodies. Try to expose cells more thoroughly. Breaking proper seals can be achieved by brief current pulses (~200 pA), gentle slow suction, more vigorous sharp suction or a combination thereof.
7. In case cells in whole-cell configuration are lost frequently at early stages check potential micromanipulator drifts and air table suspension. Movements can also arise from preparation, e.g., if the head is not properly fixated or if pulsation is too prominent.
8. We noticed that recorded visual tangential cell responses considerably depend on the quality of the fly culture from which experimental animals are drawn, in that some unusual properties or weak responses to certain features being tested may arise under unhealthy conditions. This notion is supported by the finding that nutritional state influences visual motion processing in *Calliphora* [16]. We suggest to routinely use fresh high-quality fly food with some added yeast, keep fly cultures at low densities and perform experiments only on the flies that eclose during the first ~3 days in each culture.
9. If potential drifts occur check the chloridation state of different and indifferent silver electrodes. Shiny silver wires indicate loss of the necessary AgCl. Chloridation can be achieved for example by immersing the clean wire for few minutes in Clorox, until a dull light gray color is observed.

Acknowledgement

This work was supported by the Max Planck Society and the German Science Foundation (CRC 870). We thank Alexander Arenz for help on designing the recording chamber and Georg Ammer for valuable feedback on the manuscript.

References

1. Jenett A, Rubin GM, Ngo TT, Shepherd D, Murphy C, Dionne H, Pfeiffer BD, Cavallaro A, Hall D, Jeter J, Iyer N, Fetter D, Hausenfluck JH, Peng H, Trautman ET, Svirskas RR, Myers EW, Iwinski ZR, Aso Y, DePasquale GM, Enos A, Hulamm P, Lam SC, Li HH, Laverty TR, Long F, Qu L, Murphy SD, Rokicki K, Safford T, Shaw K, Simpson JH, Sowell A, Tae S, Yu Y, Zugates CT (2012) A GAL4-driver line resource for *Drosophila* neurobiology. *Cell Rep* 2:991–1001
2. Borst A (2009) *Drosophila*'s view on insect vision. *Curr Biol* 19:R36–R47
3. Venken K, Simpson J, Bellen H (2011) Genetic manipulation of genes and cells in the nervous system of the fruit fly. *Neuron* 72:202–230
4. Baines RA, Bate M (1998) Electrophysiological development of central neurons in the *Drosophila* embryo. *J Neurosci* 18:4673–4683
5. Wilson R, Turner G, Laurent G (2004) Transformation of olfactory representations in the *Drosophila* antennal lobe. *Science* 303:366–370
6. Joesch M, Plett J, Borst A, Reiff D (2008) Response properties of motion-sensitive visual interneurons in the lobula plate of *Drosophila melanogaster*. *Curr Biol* 18:368–374
7. Maimon G, Straw A, Dickinson M (2010) Active flight increases the gain of visual motion processing in *Drosophila*. *Nat Neurosci* 13:393–399
8. Mauss AS, Meier M, Serbe E, Borst A (2014) Optogenetic and pharmacologic dissection of feedforward inhibition in *Drosophila* motion vision. *J Neurosci* 34:2254–2263
9. Cuntz H, Forstner F, Schnell B, Ammer G, Raghu SV, Borst A (2013) Preserving neural function under extreme scaling. *PLoS One* 8:e71540
10. Joesch M, Schnell B, Raghu S, Reiff D, Borst A (2010) ON and OFF pathways in *Drosophila* motion vision. *Nature* 468:300–304
11. Maisak MS, Haag J, Ammer G, Serbe E, Meier M, Leonhardt A, Schilling T, Bahl A, Rubin GM, Nern A, Dickson BJ, Reiff DF, Hopp E, Borst A (2013) A directional tuning map of *Drosophila* elementary motion detectors. *Nature* 500:212–216
12. Mauss AS, Pankova K, Arenz A, Nern A, Rubin GM, Borst A (2015) Neural circuit to integrate opposing motions in the visual field. *Cell* 162:351–362
13. Pulver SR, Pashkovski SL, Hornstein NJ, Garrity PA, Griffith LC (2009) Temporal dynamics of neuronal activation by Channelrhodopsin-2 and TRPA1 determine behavioral output in *Drosophila* larvae. *J Neurophysiol* 101:3075–3088
14. Kim AJ, Fitzgerald JK, Maimon G (2015) Cellular evidence for efference copy in *Drosophila* visuomotor processing. *Nat Neurosci* 18:1247–1255
15. Klapoetke NC, Murata Y, Kim SS, Pulver SR, Birdsey-Benson A, Cho YK, Morimoto TK, Chuong AS, Carpenter EJ, Tian Z, Wang J, Xie Y, Yan Z, Zhang Y, Chow BY, Surek B, Melkonian M, Jayaraman V, Constantine-Paton M, Wong GK, Boyden ES (2014) Independent optical excitation of distinct neural populations. *Nat Methods* 11:338–346
16. Longden KD, Muzzu T, Cook DJ, Schultz SR, Krapp HG (2014) Nutritional state modulates the neural processing of visual motion. *Curr Biol* 24:890–895

Chapter 21

Methods to Establish *Drosophila* Cell Lines

Alain Debec, Timothy L. Megraw, and Antoine Guichet

Abstract

Hundreds of *Drosophila* cell lines have been established in the labs of many researchers over the last decades and have been important tools for research. Although these cells often deviate from normal cell physiology and genetic composition, such systems nonetheless are powerful models for biochemical, cell biological, and genetics studies that are experimentally difficult *in vivo*. While published descriptions of cell line generation are available in the literature, how to generate new *Drosophila* cell lines can be challenging for beginners. Here, we describe a detailed, simple protocol to establish new *Drosophila* cell lines.

Key words *Drosophila*, Cell lines, Cell culture, Embryonic cells

1 Introduction

1.1 The Benefits and Drawbacks of *Drosophila* Cell Lines as a Model System

Drosophila cell lines represent a widely used biological system by many laboratories. Examples of some recent breakthroughs using *Drosophila* cell lines include: systematic screening by genome-wide ribonucleic acid interference (RNAi), which revealed new factors in mitotic spindle assembly [1, 2] and the mechanisms for centrosomes clustering [3]. Similar high-throughput screens lead to the identification of new drugs against *Wolbachia* [4]. Cell lines derived from mutants have also been a powerful tool for investigators (for instance [5]), and numerous other studies. The purpose of this chapter is to provide a detailed protocol for researchers to generate *Drosophila* cell lines in their labs.

In conversations with colleagues, we became aware that despite several good method descriptions in the literature [6–8] attempts by various labs ultimately failed to generate cell lines. Realizing this need for the research community, we have written this chapter with the goal of providing a detailed method for deriving new cell lines of *Drosophila* (and related dipteran species). We also refer the reader to useful protocols and tips on *Drosophila* cell culture at the *Drosophila* Genomic Resource Center (DGRC): <https://dgrc.bio.indiana.edu/Protocols?tab=cells>.

Despite their clear utility to researchers for many purposes, *Drosophila* cell culture is not a “perfect” model (there is no such thing as the ideal model). Therefore, before you proceed, first consider whether the cell line you plan to derive will provide you with key advantages (e.g. *see* Subheading 1.1.1), over approaches to study the process or function *in vivo*. We list the following pros and cons of this biological model for the investigator to consider before deciding to launch into a project that involves the development of new cell lines.

1.1.1 Benefits (Pros)

1. Amenable to biochemistry; can grow cultures on a large scale.
2. RNAi is simple to apply and efficient (works without transfection, simply pipet dsRNA into culture) [9, 10].
3. Can grow at ambient temperature, and no need for CO₂ or special incubators.
4. Convenient for protein mass spectrometry techniques (has been used for proteome mass spectrometry analysis).
5. Cell lines are usually transfection competent.
6. Stably transfected cell lines can be generated and expression from transgenes can be controlled.
7. Many mutant cell lines are available
8. Easy to image either live or fixed samples [10]
9. Excellent system for screens on a large scale, including genome-wide analysis (RNAi) or high-throughput screening for new drugs.
10. Cell lines can be generated from complex mutant plus transgenic stocks.
11. New genome editing tools like TALENs and CRISPR-Cas9 can be used to generate mutant cell lines [11].

1.1.2 Drawbacks (Cons)

1. Derived cell lines will always represent a departure from the physiology of cells *in vivo*. First of all the very essence of a cell line involves an immortalization process and therefore these cells should bear genomic alterations. The changes that make a cell immortalized are not well documented, but we can suspect mutations in various oncogenes, plus more subtle epigenetic changes. There is a constant selective pressure for rapid cell cycles and loss of differentiated state and a cell line will tend to lose many of its original characteristics. In addition, cell lines often deviate from normal chromosome ploidy. Karyotypes of cultured cells frequently reveal polyploidy and aneuploidies. Various families of transposons are also strongly mobilized during the process of cell line immortalization [12]. These changes notwithstanding, derived cell lines have been extremely useful to understand many cellular pathways and processes; the literature is replete with thousands of examples.

2. There is a common presence of numerous types of viruses (some being introduced by the fetal calf serum (FCS)).
3. Often, especially when embryos are the source, the tissue of origin is unknown (although most of the time they probably derive from the ectoderm).
4. If the immortalization properties of derived cell lines are problematic for your research purposes, consider working with primary cultures instead, as these are much closer to normal cells [13]. A useful protocol for Primary cultures (PCs) generation was published recently [14].
5. Finally, there is the possibility to stably transfect already existing cell lines. The difficulty with such strategy concerns the high heterogeneity between individual cells and often a strong overexpression of the transgene even with inducible expression systems like the metallothionein promoter.

Before you begin, check the available cell lines at the DGRC site (<https://dgrc.bio.indiana.edu/cells/Catalog>) where more than 150 cell lines are available, if any line of interest for you already exists. In addition a variety of labs have created many other interesting cell lines not deposited to DGRC, although such information is not readily available (see Note 1).

Considering all the pros and cons, if you decide that a new cell line with a defined genetic makeup is suitable to your research goals, we present here a protocol that should yield some lines of your favorite genotype in about 2–3 months.

2 Materials

1. Culture medium for Primary Cultures (PCs) and very young lines: Shields and Sang's M3 medium + 20% FBS, for 500 ml: 400 ml Shields and Sang M3 medium (see Note 2), 100 ml fetal bovine serum (heat inactivated for 45 min at 56 °C), 5 ml of 100X Penicillin-Streptomycin (60 and 100 µg/ml final concentration), 2.5 ml of 10 mg/ml Gentamycin (50 µg/ml final concentration). Stock the medium in small quantities (about 50 ml), at 4 °C. Pre-warm at 23 °C before use, but do not leave the medium at room temperature (RT) for long time.
2. Culture medium for established cell lines: Use the same medium, but with 10% of FCS (see Note 3). Antibiotics are then optional.
3. Freezing medium (10% DMSO): for 20 ml: 18 ml M3 medium with 20% FCS 2 ml DMSO, Molecular Biology Grade. Use a recent batch of DMSO as toxic compounds can form after prolonged storage. Store at room temperature in the dark, no more than 1 year.

4. Cryotubes: Choose a brand with a silicone gasket seal (for example Greiner Bio-One Cryo.s). Run trials to test the resilience of the label under -80 °C or liquid nitrogen storage.
5. Egg-lay plates: For 1 l (we usually make 500 ml lots): 800 ml water, 200 ml apple or grape juice (use a brand without any pulp), 24 g agar, 26 g sucrose, Autoclave, cool to about 60 °C and pour on 55 mm Petri plates. Avoid bubbles on plates, as this will result in agar fragments appearing in the embryo preps. Passing a flame over a newly poured plate will pop any bubbles that result from pouring. Store in plastic bags at 4 °C with plates oriented upside-down.
6. 10% Triton X-100: Prepare 10 ml. Use a cut-off pipet tip to dispense the Triton X-100 as it is very viscous. Place on rocker for several hours to mix. Do not autoclave.
7. Sterile water: Prepare about ten 100–200 ml bottles of autoclaved diH_2O . Avoid re-use of a bottle after one round of embryo dissociation.
8. Muslin cloth or Cell strainers for embryo collection: We usually use squares of dark-colored muslin cloth (about 30×30 cm), purchased from a local fabric store, draped over a 1000 ml glass beaker to collect embryos (see Fig. 2 step 4a). Alternatively, embryos can be collected in commercial, sterile disposable Nylon mesh strainers (Falcon; Cell Strainer, 100 μm Nylon, cat # 2360).
9. Embryo homogenizers: This is a critical instrument for this protocol. We use 2 ml Tenbroeck type tissue grinder from Wheaton (VWR company, reference 432-1276). An example is shown in Fig. 1a. Wrap each homogenizer in aluminum foil and autoclave. Unwrap in the hood when ready to use. You can also use other kinds of glass homogenizers successfully; the important thing being the tightness of the spacing between the plunger and vessel, which should be sufficient to crush embryos but permit the preservation of cell clusters.
10. Autoclaved yeast: Prepare yeast paste. Mix active dry yeast with water in a small glass bottle. Stir and adjust water: yeast mixture until you achieve a thick paste, suitable for spreading onto egg-lay plates. If too much water, the flies will become stuck and die; if not enough water, the yeast will form a dry crust. You want to avoid the yeast crust, as it will be difficult to dissolve and difficult to separate from the embryos when you are preparing them for lysis. *Autoclave the yeast paste*. We recommend autoclaving the yeast paste *twice*, in order to thoroughly kill it. If the yeast paste is not completely inactivated, then contamination by yeast will take over the PCs. Test a sample of the autoclaved yeast by inoculating some M3 medium to assure it is inactive.
11. Cell Scrapers: Any kind; for example TPP Cell Scraper, 24 cm long.

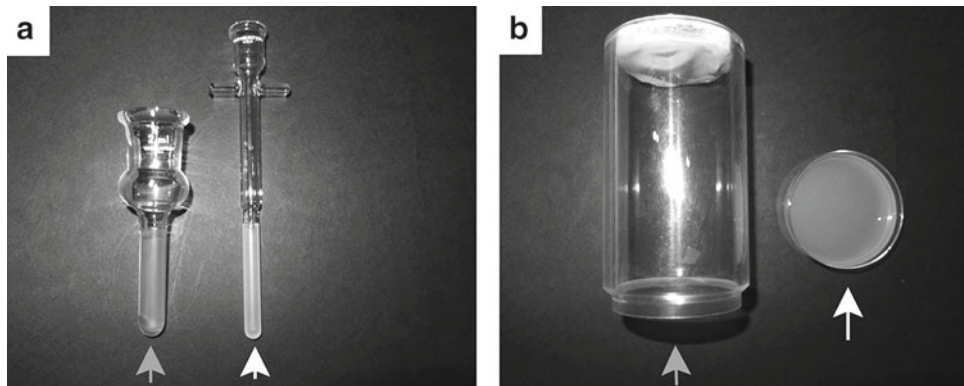
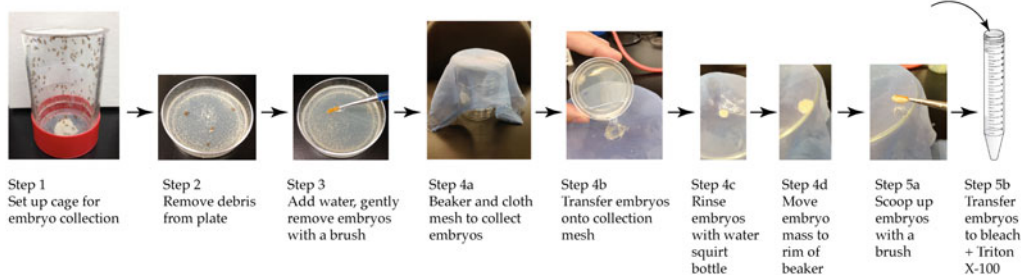


Fig. 1 (a) Tenbroeck tissue grinder, 2 ml. (b) Example of homemade fly cage used for embryo collection. We use 11 cm polystyrene cylinders with filter cloth on one end (grey arrow), with a fitting to attach 55 mm plastic Petri dishes (egg-lay plate, white arrow)

On the bench:



Inside the sterile hood:

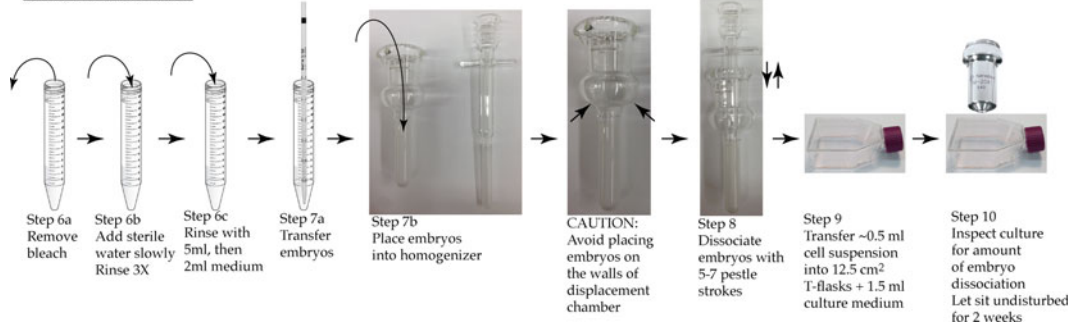


Fig. 2 The procedure at a glance. Shown is an abbreviated protocol where the steps correspond to those listed in the text

12. Tissue Culture flasks.

Use the small flasks (12.5 cm²) for PCs. The only available brand in this size is Falcon. You can use larger flasks (25 cm²) for routine transfer of established cell lines. Any brand should be suitable. Purchase the tight seal cap, not the vented seal cap, as there is no need for CO₂ in the incubator.

3 Methods

3.1 Preparing Cell Lines from Embryos

As already mentioned, we saw a need for a detailed protocol for researchers needing to make *Drosophila* cell lines in their labs. Our goal here is to explain this technique in sufficient detail, hopefully appealing to the novice at the risk of appearing obvious to those already experienced at cell culture methods.

Before you start: We strongly recommend, if you have little or no experience in *Drosophila* cell culture, to start with previously established *Drosophila* cell lines and become familiar with the basic care of cell cultures. Choose 2–3 lines, which grow in M3 medium. We advise you to choose well-attached cell lines (often more challenging to culture; check on the DGRC site and with colleagues), and one “easy” to maintain (e.g. Kc167 or S2). You will then be able to test your culture facility, employ assays for choosing a good batch of serum, to check if you are successful with the freezing procedure, etc. This will be time and effort well spent! We believe it is essential to gain experience with maintaining cell lines and become familiar with visually tracking their progress as they grow. When you generate your own cell lines, one of the major criteria for monitoring the progress of developing cell lines relies on your ability to visually assess their health in culture.

3.1.1 Choosing Your *Drosophila* Mutant Genotype to Make a Line from

The following technique is devised to initiate cultures from post-cellularized embryos (aged about 6–12 h, roughly). Mutants that are homozygous viable will be the simplest to generate cell lines from. You can also generate cell lines from lethal mutations, as long as they are not lethal at the cellular level. If the mutant flies must be balanced, you need to select against heterozygous embryos. One approach is to use a conditional dominant cell lethal balancer chromosome, for example one bearing a Hs-hid transgene. Hid will induce apoptosis if overexpressed from the transgene upon induction by heat shock (2 h at 37 °C). Be sure to test your stocks to assure that no flies bearing the balancer survive the heat shock treatment. In our hands, a construct with Hs-hid on TM3 (Bloomington stock #1558, from R. Lehmann) works very well with no individuals surviving after two 2 h heat shock on second and third instar larvae. This approach was used successfully to generate *Sas-4* mutant cell lines [5]. However, we found that the Hs-hid CyO stock (Bloomington stock #1557, from R. Lehmann), while effective at eliminating all CyO-containing adult progeny from HS-treated larvae, resulted in cell lines that were heterozygous. So we caution against this chromosome to eliminate heterozygous cells from PCs. Because embryos (even wild type) are very fragile under heat shock treatment (and PCs as well) this selective step should be done only in young, nearly established cell lines (see later where this step should be employed).

Expand the fly stocks in bottles so that you have several thousand flies.

3.1.2 Set Up Cages

Place about 200 young females and about the same number of males together in each cage. You can purchase or build your own cages to house the flies; we used either the one described in Fig. 1b, or cages from Genesee Scientific (Cat # 59–100; *see image in Fig. 2 step 1*). Set up a minimum of three or four cages for a run. Prepare the cages 2 days before you plan to start collecting embryos for primary culture preparation; this gives the flies time to acclimate and egg production to increase. Feed flies in cages on apple or grape juice agar plates with a thin layer of autoclaved yeast paste spread on top of it. Yeast is absolutely necessary for females to produce robust egg-laying. Make sure yeast paste is sterile (critical): place some in culture medium to assure none will grow, as it often happens that some yeast cells may survive autoclave treatment. This is absolutely essential; otherwise you will always have contamination by living yeast, with no hope to cure the culture of the infection. Change the fly cages twice daily. Place the cages at 18 °C overnight and 25 °C during the daytime. Plan to collect and process embryos twice daily: once in the morning and once in the late afternoon. This will help avoid the development of first instar larvae in the embryo collection. Larvae are more difficult to sterilize at the bleach step and their lysis at the homogenization step could release microbes into the culture. As you will need to repeat this procedure during 3–4 weeks, plan the fly cultures accordingly to provide a steady supply in order to set up fresh cages each week.

3.1.3 Preparing Embryos and Homogenizing Them for PCs

Prepare these items so they will be ready

A: on the bench:

A clean and soft paintbrush devoted to this purpose (one for each genotype).

Fresh 40% bleach + 0.025% triton X-100.

Muslin filter cloth and 1000 ml glass beaker (see Reagents).

15 ml screw-capped sterile Falcon tubes.

B: in the hood or in the vicinity of it:

Pre-warmed Shields & Sang M3 culture medium + 20% FCS (see Reagents).

Autoclaved bottles of water.

Autoclaved 2 ml Wheaton Tenbroeck homogenizers (need one per cage) (see Reagents).

Several 12.5 cm² culture flasks (four per each cage, if egg-laying is robust). Label these with respect to the homogenate layer (bottom, middle1, middle2, top).

Several 10 ml, 5 ml, and 2 ml sterile plastic pipets.

A clean plastic 1 l beaker for waste.

A clean, preferably sterile, 15 ml tube rack.

1. To collect embryos, first inspect the egg-lay plate under a dissecting microscope and remove all debris (dead flies, body parts, cotton fibers, etc.) and first instar larvae, if any. Try not to scrape or disrupt the agar surface of the egg lay plate.
2. Using a squirt bottle, add enough water to the egg-lay plate to cover the embryos. Collect embryos by gently brushing the plate under a small amount of water.
3. Pour embryos onto the center of a pre-wetted muslin filter cloth draped over a 1 l-size beaker, and rinse well to remove the yeast paste (you can use a squirt bottle with water for this purpose). Take care that brush, filter cloth, and all instruments are not contaminated by embryos of a different genotype (from other samples). Also, do not brush too hard and avoid transferring agar fragments from the egg-lay plates along with the embryos.
4. Pull the edges of the muslin filter tight over the top of the beaker, and scoop up the embryos with the brush. Place embryos into a nearly full 15 ml screw-capped Falcon tube containing the bleach-Triton solution. Keep in this solution for 15 min. Mix by gentle inversion 10–20 times every once in a while (or place on a rocker). Do not let the embryos settle in pellet too long to avoid anoxia. The high concentration and long exposure of bleach will not only dissolve the chorion of embryos but it will also sterilize the surface of the embryos (protected by their vitelline membrane) and also any first instar larvae or other debris which may be present in the embryo collection. Take the 15 ml tube with embryos to a laminar flow hood and use sterile techniques for all following procedures.
5. Remove the top of the 15 ml tube and discard. Using a 10 ml pipette, remove most of the bleach solution without disturbing the embryo pellet. Carefully, and slowly, add sterile water to rinse the embryos (fill a 10 ml pipet to the 13 ml mark). The water should be dispensed from the 10 ml pipet sufficiently slowly to prevent disturbing the embryo pellet. If the embryo pellet gets disturbed/suspended, the embryos will stick to the wall of the tube. Remove the water using the same 10 ml pipet. Repeat the water rinse two more times with fresh 10 ml pipets. The goal of these washes is to remove most of the bleach not only from the embryos, but also from the walls of the 15 ml tube. Add 5 ml of M3 + 20% FCS culture medium, again adding it slowly in order to rinse the embryos.
6. Unwrap one of the sterile Tenbroek homogenizers (in the hood), remove the plunger allowing it to rest on the sterile surface of the aluminum foil wrapper, and place the homogenizer vessel into the tube rack. Using a 5 ml pipet, remove the culture medium. Slowly add 2 ml of fresh culture medium to the embryo pellet.

Quickly draw the embryo pellet into the 5 ml pipet. This is a crucial step as the embryos have a tendency to stick to the pipet. Absolutely avoid drawing air bubbles into the pipet. The pipetting should be relatively prompt in order that embryos are efficiently transferred from the Falcon tube into the pipet but not so quickly that air bubbles are drawn up.

Dispense the embryos into the homogenizer vessel similarly as above but reversed, to force the embryos out of the pipet. Again, avoid air bubbles. Try to dispense the embryos near the bottom of the vessel.

Remove some of the M3 medium so that the tube portion of the vessel is half full (about 1 ml usually).

7. Place the plunger into the vessel and push all the way to the bottom while turning/rotating the plunger as you push it down. A few short strokes may be necessary to suspend the embryo pellet at the bottom of the vessel. Homogenize the embryos with 5–7 strokes. The goal is to disrupt all the embryos, while maintaining the tissues in “chunks” to foster their growth in culture. You will have to test to see what works optimally in your hands, according to the number and manner of strokes and quality of the homogenizer. Any embryo that fails to be ground in the homogenizer may hatch and the resulting larva will disrupt the culture significantly. This happens especially when some embryos are left on the rim of the homogenizer displacement chamber (*see* “Caution” in Fig. 2). On the other hand, you do not want to homogenize too much, as the embryo fragments promote the growth and expansion of PC colonies.

Let the suspension sit for about 2–3 min to separate the vitellus supernatant from embryo fragments (which sink). The vitellus is not by itself toxic but it will stick to the flask bottom and will impair the attachment of cell clusters. However, it is good practice to keep the vitellus fraction, which may also yield acceptable PCs.

8. Using a 2 ml pipet draw up the embryo homogenate, and dispense into three to four 12.5 cm² tissue culture flasks that each contain 1.5 ml of M3 culture medium. Place the layers into separate flasks (bottom, middle, supernatant). If the egg collection is low, place all the homogenate into one flask. Tightly close the flasks, the cells do not need so much oxygen. Place the flasks in an incubator at 23 °C (*see* Note 4). Place flasks into a container or onto a tray to avoid disturbing the flasks too much during transport between the incubator and the microscope to visualize their progress.
9. Inspect the flask on the microscope. Ideally, you will see large chunks of cells (roughly 50–200 cells) and no intact embryos.

If the homogenization is too intense, there will be few or small cell aggregates; individual cells will not proliferate.

With the cages active, repeat this procedure each morning and every afternoon to accumulate many primary cultures and improve your chances of successfully generating some cell lines. The PCs are fragile. In particular, cell clusters are only loosely attached to the bottom of flasks. Therefore, handle the flasks very gently and move them the minimum amount possible. Treat them like Ming porcelain! Check however for possible bacterial or fungal contamination in the following days. Immediately discard any flask infected by yeast/mold. No need to inspect PCs every day, it is preferable to leave them undisturbed (see Note 5). Remove any larvae that appear in the PCs with a sterile Pasteur glass pipette and bulb.

Usually, leave PCs for 2 weeks. However, this period can be shorter if the culture is very dense. Remove 1 ml of medium and replace with 1 ml of fresh medium. If you suspect that the 1 ml of the removed medium contains interesting cells, you can place it in another flask + another 1 ml of fresh medium.

Aim to establish approximately 50 PCs of the same genotype to have a good chance to generate a few cell lines. Keep a careful record of all PCs and their multiple subsequent transfers.

Here again, this is a matter of judgment; usually change half the medium every week. Sometime there is a lot of material floating but still living (in particular the spheres, see later); in this case it is a good idea to transfer this material to a new flask to “liberate” the cells growing underneath it. Gently dissociate the transferred structures with 4–5 pipet strokes (no bubbles!) and place it in a new flask with approximately the same amount of fresh medium. Replenish the amount you have withdrawn from the original flask with fresh medium.

3.1.4 Progression of the PCs and Assessment of Their State

During the first few days, for a good primary culture, many cells of all types will emerge from the clusters, attach and expand on the flask bottom. If there is too much vitellus, it will stick to the flask bottom and limit the expansion of new cells. Normally you should see many cell types which will differentiate (nerve cells, muscle cells, etc.). The appearance of muscle contractions from colonies of myoblasts (see movie 1, Note 6) is a sign of a healthy culture. Frequently, some cells will form empty spheres that resemble blastocysts in their appearance. These structures (presumably coming from imaginal disks) are a positive sign for a future cell line and should not be discarded. If they are transferred to a new flask, they can attach and give nice colonies.

Do not be disappointed if, even for seemingly healthy PCs, that many of them die off after about 5–6 weeks. This is probably the normal senescent behavior of wild type cells. That is why you need to initiate many PCs to recover some that immortalize. In some cases however, some colonies of undifferentiated, usually roundish

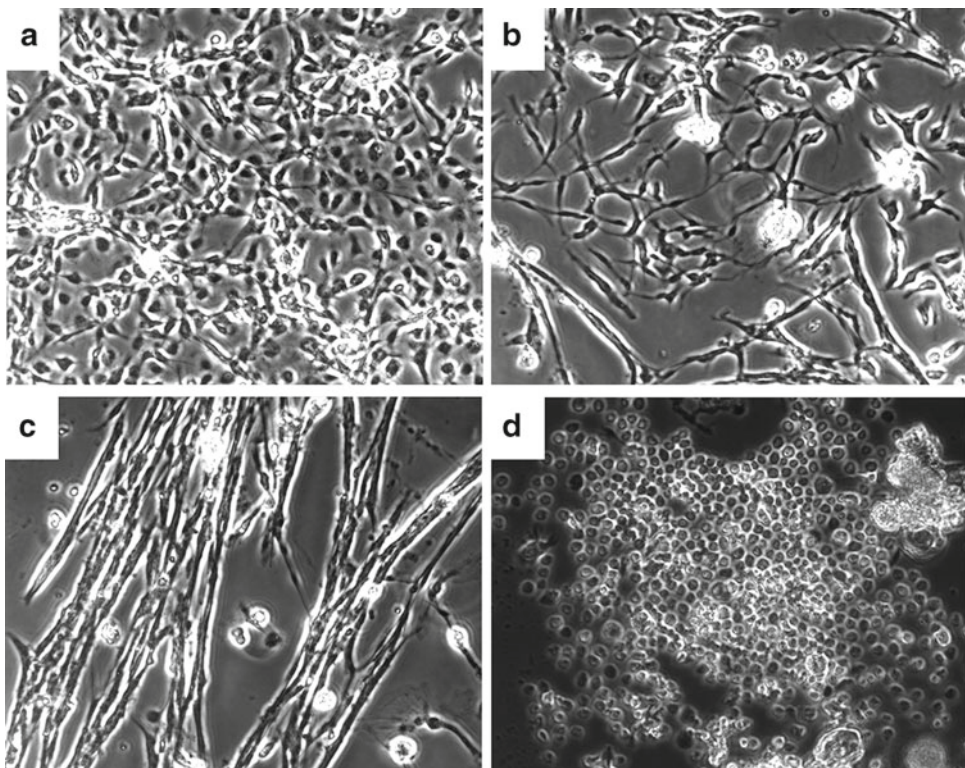


Fig. 3 Examples showing the diversity of morphologies of primary cultures. These pictures represent favorable cases of primary cultures on the verge to becoming a cell line. However in about half of the cases these cultures will degenerate and die. Note the variety of cell morphologies

or fibroblastic-like cells start to proliferate, and this represents an excellent diagnostic for the start of a cell line. Some examples of such “starting” cultures are shown in Fig. 3. It is not exactly known what happens, but we can reasonably presume that some oncogene mutations occur coincident with mobilization of transposons. In any event, there is selective pressure for the fastest dividing cells.

In these cases, after such “undifferentiated” cells occupy most of the flask bottom, very gently detach them using a cell scraper, and transfer all the cell suspension into a new culture flask, while keeping the original flask (which usually still contain many cells not detached with this soft treatment). Supplement the transferred cells in the new flask with an equal volume of fresh culture medium and add 2 ml of fresh medium to the original flask and continue to culture it. Never use trypsin (commonly used with vertebrate cell lines) for cell transfers (see Subheading 3.2).

Monitor the behavior of this first transfer. This step is usually crucial, if the cells re-establish, this is a very good sign. Sometimes, however, everything dies after the first attempt of transfer. Wait for a reasonable growth of this first transfer. This can take from 1 to 2 weeks.

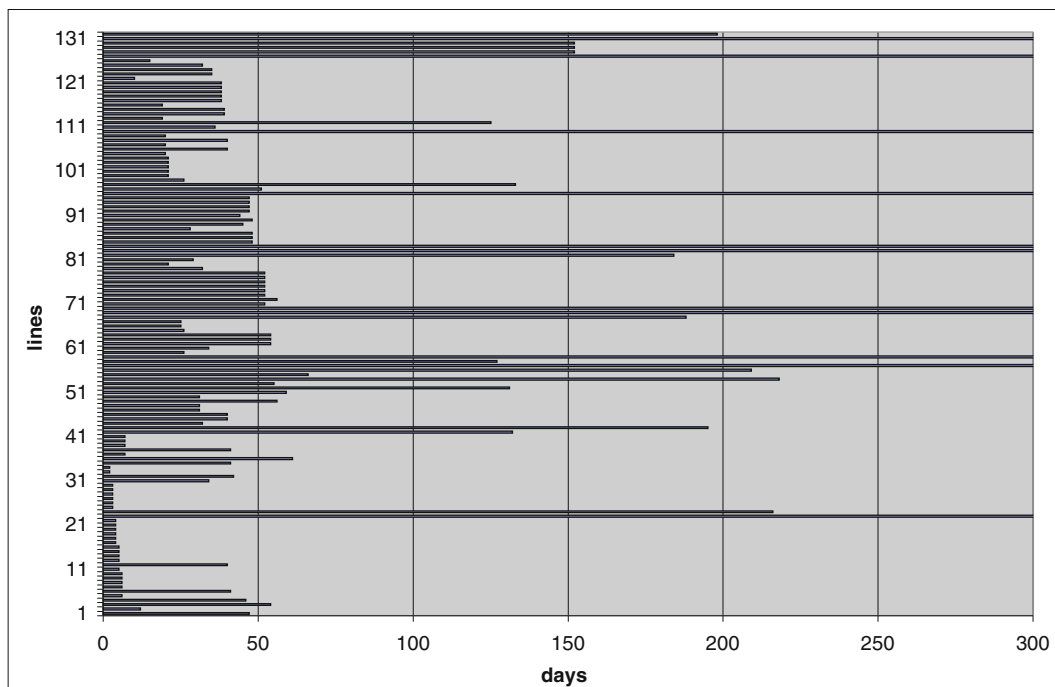
Continue to transfer the PCs as they grow in each new flask. In the first 2–3 transfers, do not split the cultures, unless the cells are growing rapidly (are becoming confluent a few days after these transfers). The cultures will consume the medium quicker as they progress, so also take care to not let them exhaust the medium. During this intermediate phase, cells are less fragile than PCs so you can check them frequently. An important point regarding the culture medium (see “Reagents section”) is to keep exactly the same medium and particularly the same batch of FCS for all transfers.

Eventually expand the culture into 25 cm² flasks. If necessary, this is when you can select against heterozygous cells with heat shock treatment, permitting only homozygous mutant cells to survive, provided the parental fly stock had a conditional lethal balancer chromosome (see Subheading 3.1.1). The cultures will grow progressively better during the subsequent transfers, when you can gradually try higher dilutions, on the order of 1/2, 1/3, 1/4, etc. There is no precise rule for these dilutions, but, in general, the quicker the cells divide, the higher the dilution that is permissible.

Table 1

Progress chart of PCs for a project to establish acentriolar *Drosophila* cell lines

Representation of the survival of primary cultures generated from DSas-4 mutant embryos (from Lecland et al., 2013, *Biology Open*, 2(3) 314–323 [5]). In this experiment, 131 PCs were initiated. Most of these differentiated, arrested growth, and finally died after 10–50 days. But some of them spontaneously immortalized. 11 permanent cell lines were ultimately created (about 8 % of PCs)



Once established, a good cell line can be transferred with as low as 1/20 dilution each week. Once these cultures are growing well and can be considered a new cell line, freeze away some aliquots.

The whole process usually takes 2 months, but may take as long as 3 months. The established cell lines are usually cultivated with only 10% of FCS. Altogether, you can expect a success rate of 5–10% of PCs becoming a cell line (see also the possible facilitation effect of Wolbachia presence in Subheading 3.3). See Table 1 as an example of the progress of a set of mutant PCs toward immortalized lines. Freezing the cells: Freeze away aliquots of new cell lines once the flasks show strong growth and healthy appearance. Freeze the cells away when the culture is high density, a little before confluence. Prepare cryovials and carefully label them with date and cell line name. Remove the culture medium from a 25 cm² flask and replace with 1.8 ml of freezing medium (see Reagents) (see Note 7). Scrape the cells and place the suspension in one cryovial, then tightly close it. Place each cryovial on ice as you proceed. Two common procedures are used to freeze away cell lines (we recommend either). In both cases the cooling rate should be slow, close to -1 °C/min.

1. Deep freezer (-80 °C): often easier to find the stored samples, but prone to power failures. Place the tubes in a small polystyrene (foam) container in order to slow the cooling rate of the samples. Keep in the Styrofoam box for at least 48 h. You will need to test whether cells survive your freezing protocol by thawing one of the samples and plating them to see if they will grow. We have had excellent results with a freezing chamber filled with isopropyl alcohol.
2. Liquid nitrogen: certainly the best solution for long-term storage, but it requires a continuous supply of liquid N₂. Place the cryovials in N₂ vapors just behind the cap of the storage tank, then transfer vials into the liquid N₂ after 48 h. For storage, you can place frozen cryovials from the -80 °C directly into a liquid nitrogen storage container. Take careful records of frozen stocks. This should be easily understandable by other persons even after many years!

3.2 General Information on the Organization of the Cell Culture Facility

The necessity to have a close relationship between the cell culture equipment and the fly lab introduces a strong hazard of contamination of the cultures by yeast, especially during the first steps of making numerous PCs. Even if the cell culture room is physically separated from the main lab, keep in mind that nearly everything is contaminated by living yeast in a fly lab, including the workers. In addition, close proximity of cell culture equipment (cell incubator, inverted microscope, and sterile hood) will facilitate the process and save time. Try therefore to avoid the use of powdered active yeast close to the area where cells are cultivated, passaged, and examined as much as possible.

3.2.1 Cell Incubator

Thanks to the composition of the media devised for *Drosophila* cell culture, there is no need for a controlled atmosphere involving the infusion of CO₂ as is common for vertebrate cell culture. Choose an incubator that maintains a stable temperature in the range of 10–30 °C. The usual culture temperature is 23 °C, although of course this can be adjusted according to your cell line genotype if necessary (e.g. for a temperature-sensitive mutant). Be aware that you will need to manage many flasks during the first weeks of PCs establishment (on the order of 100–200 flasks), so an incubator with 400 l capacity is a minimum space requirement. We advise placing cell culture flasks on plastic trays. Place flasks of the same “genealogy” on the same tray, to easily compare flasks. Clean the trays with ethanol regularly, but be cautioned that *Drosophila* culture cells are extremely sensitive to ethanol (1% ethanol in the medium will kill most cell lines). Again, when moving the flasks take care to avoid jostling and other rough handling.

If there is a glass door on the incubator it should not be placed in front of the sterile hood, as exposure to UV, even attenuated through the glass, can cause genome damage to the cells.

3.2.2 Inverted Microscope

You will need too an inverted phase contrast microscope of good quality, to regularly check the health of your cultures. This is even more important to assess the behavior of PCs. This is an important investment for this project and is not very expensive. To give an idea we use an Olympus CK 30 microscope with four objectives (4×, 10×, 20×, 40×). Other brands are equally suitable (e.g. Nikon TS100), and 10× + 20× objectives are sufficient for this project. Once again this microscope should be placed close to the cell culture incubator, to avoid stressing the cells when transporting them between the incubator and the microscope.

3.2.3 Keep Detailed Records

As with any experimental procedure it is best to keep your data well-organized in your notebook. You will need to know the “genealogy” of each line, and to keep track of the relationships between all flasks. This will help you both to know the origin and independency of each culture, and also to keep track of procedures (change of medium, cell transfer, etc.) on your flasks (you will have many of them to keep track of). Carefully note on each flask the date of culture and a special number to identify it, and report it in your laboratory notebook.

3.2.4 Low Temperature (14 °C)

For various reasons (breakdown in medium availability, etc.) you may need to suspend the care of your cell cultures. In our hands, for most cell lines it is possible to maintain them with minimal loss of viability at 14 °C for 1 month without any cell transfer. The low temperature slows them down considerably and extends the time needed between medium changes. Such procedure is not recommended for PCs or very young cell lines.

3.2.5 Trypsin

Unlike vertebrate cells, *Drosophila* cells are very sensitive to trypsin and it should generally not be used for cell transfer. It may be necessary however that for few lines that are extremely well attached and spread to the bottom flask, such as S2R+ cells, that a moderate trypsin treatment is better than a simple detachment by scraping. We recommend a dilute trypsin solution (on the order of 0.05%) and a very short incubation time (3 min maximum; stop by addition of medium + FCS immediately when you see cells detaching). A detailed protocol is available on DGRC site (see Note 8).

3.2.6 Avoid Cell Line

Cross-Contamination

Blending

Beyond microorganism's contamination, the worse error that could happen is to mix your new cell line with another *Drosophila* line. This error will not be apparent and could go undetected. Take all cautions, and instill best practices with new trainees. For example, work with only one line at a time under the hood, keep track of which caps belong to which flasks, always use a new pipet when dispensing medium, etc.

3.2.7 Microorganism

Contamination Problems

We can distinguish two kinds of possible microorganism contaminations; either exogenous (accidental, from the environment) or endogenous (from infected flies used for cell line generation).

3.2.8 Exogenous

Contaminations

1. *Bacteria*. The high concentrations of antibiotics we recommend (Penicillin, Streptomycin, and Gentamycin, see Reagents section) usually prevent bacterial growth. This is helpful during the first steps of PCs establishment, but not as necessary later with established lines.
2. *Yeast and various molds* (*Penicillium*, *Aspergillus*, etc.). Such contamination will be “game over” for your culture. All anti-fungal drugs are very toxic to *Drosophila* cells. Discard contaminated flasks immediately to avoid spreading of the fungi or molds in the lab.

3.2.9 Endogenous

Contaminations

1. *Endosymbionts*

There are only two known heritable endosymbionts in *Drosophila*: *Wolbachia* and *Spiroplasma* bacteria. *Wolbachia* are strictly intracellular while *Spiroplasma* are mainly extracellular [15, 16].

It would not be unusual to find the presence of *Wolbachia* in your new cell lines. This actually will not represent an accidental contamination of your cell culture but simply the recovery of intracellular symbionts already present in the fly stock you started with, as many laboratory fly stocks bear these bacteria. For example about 30% of stocks in the Bloomington *Drosophila* Stock Center are infected [17]. You can check for their presence as cytoplasmic spots either with Syto 11 DNA staining [4] (see Note 9) or by PCR of *Wolbachia* sequences (see Note 10). Eradication of these bacteria is possible after extended Doxycyclin or Tetracycline treatment (see Note 11).

To our knowledge, no *Drosophila* cell line has been reported to be infected by *Spiroplasma* and you have few risks to have such problem.

2. Viruses

This is probably the most challenging issue with *Drosophila* cell lines. Various DNA or RNA viruses contaminate nearly all lines. Some viruses originate directly from the fly tissues. Other may come from the FCS as some vertebrate viruses can multiply in *Drosophila* cells. Virus contamination is difficult to assess and this state is often discovered only after electron microscopy analysis of the cells.

To conclude, for all these reasons try to keep frozen many aliquots of your cell lines, and freeze it away as early in its establishment as possible.

3.3 Alternative Methods and Potential Improvements

3.3.1 Media

Drosophila cell culture is by far less efficient than vertebrate cell cultures. For example any human skin biopsy will readily grow in a culture flask in standard medium. It is therefore clear that *Drosophila* primary cell culture methodology is underdeveloped.

3.3.2 Fly Extract and Supplemented Media

Other *Drosophila* media might be tried for raising cell lines: the more common alternatives being D-22 and Schneider's media. Many companies commercialize Schneider's medium. The D-22 medium is very rich in peptides and could possibly sustain cell types that M3 medium may not support.

3.3.3 Wolbachia as "Facilitators"?

Success for establishing *Drosophila* cell lines from more differentiated tissues such as imaginal disks and ovary stem cells have been accomplished through the use of supplemented media, mainly with low amounts of 20-hydroxyecdysone, insulin, and Fly Extract [18–20]. Fly Extract has been used for many years [21] but is not typically used to culture PCs. It could offer an improvement to cell line generation. We tested the effect of Fly Extract on 10 of our established cell lines, and only one responded very positively, with a net acceleration of growth. Be aware however that Fly Extract is a possible source of virus contamination. Fly Extract is sold by DGRC, which also provides the protocol to make it on your own.

As already mentioned, *Wolbachia* can be a source of contamination for cell lines as many fly stocks are infected. However, when purposely raising cell lines infected by these bacteria we noticed a very high percentage of PCs giving rise to cell lines (on the order of 70% whereas the usual rate of success is in the range of 5–10%). The number of PCs we generated is still too low (about 50) to be statistically robust, but it is an interesting possibility that *Wolbachia* could promote cell line establishment (A. Debec, L. Serbus and W. Sullivan, unpublished data).

3.3.4 Other *Drosophila* or Dipteran species

It is extremely likely that the methods described here can be applied to establish cell lines from other *Drosophila* species. Cell lines have already been established from other *Drosophila* species, for example *D. hydei*, *D. simulans*, *D. teissieri*, *D. erecta*, *D. pseudoobscura*, *D. auraria*, *D. yakuba*, *D. sechellia*, *D. immigrans*, and *D. virilis*. All are available at the DGRC.

It is well probable that this method is valid for other dipteran species as well. For example, cell lines of the Mediterranean fruit fly *Ceratitis capitata* have been obtained through a similar protocol [22]. Some species of special interest as disease vectors like *Glossina* (Tsetse fly) would however be more difficult to manage due to their adenotrophic viviparity. Scale-down techniques that permit the generation of cell lines from only a few embryos or larvae should be devised for such species.

Methods to obtain cell lines from more evolutionary distant insects species like, for example, ants and bees, could also reasonably be attempted with slight modifications to this protocol, although the culture medium composition will probably need to be adapted.

4 Notes

1. An open forum for the exchange of information on *Drosophila* cell lines among investigators worldwide will soon be open on the DGRC website.
2. M3 medium is also sold by Sigma as a powder (cheaper) but this does not support growth of primary cell lines in our hands. We also found that the quality of the medium S3652 can vary according to the batch. It is always a good idea to first test your medium on a previously established *Drosophila* line.
3. Choice of the serum batch: This is critical. There is a high variability of FCS quality among manufacturers and also between batches from the same company. Some serum batches simply are not very efficient to promote cell growth, others are even toxic to *Drosophila* cells. In addition, the fragile PCs are very sensitive to any FCS change. We strongly recommend that you first try different FCS on permanent *Drosophila* cell lines. When you establish one that works efficiently, try to acquire many bottles of the same batch (at least 20 × 100 ml) so you will have enough to take care of all your PCs and subsequent lines. Be aware that most batches of FCS contain low amounts of Tetracycline.
4. We found this temperature optimum for most of *Drosophila* cell lines. Cells can be grown in a range of 18–27 °C.
5. In a classical story in his seminars, Professor Guy Echalier told that his first *Drosophila* cell lines he obtained after many trials (the Kc and Ca lines) correspond to flasks which were left

unattended for one month in the lab where he had no access due to the strikes of May 1968 in Paris and therefore he described these lines as “the daughters of revolution”!

6. See movie 1 on the website: <http://med.fsu.edu/index.cfm?page=megrawLab.gallery>.
7. Some people prefer using glycerol (10%) instead of DMSO as a cryoprotective agent; it is possible that the best choice will depend of the cell lines. In our hands, DMSO has always been always efficient.
8. <https://dgrc.bio.indiana.edu/include/file/Transferring%20CellsUsingTrypsinization.pdf>.
9. Stain *Wolbachia* by incubating live cells for only 1 min with SYTO 11 dye (Molecular Probes, Cat # S 7573) diluted 1: 50,000.
10. One of the most widely used general primer pairs for overall detection of *Wolbachia* is the WspF81 and WspR691 set from Zhou et al. Proc. R. Soc. Lond. B (1998) 265, 509–515.
11. For eradication of *Wolbachia*, the tissue culture cells were treated with either Tetracycline or Doxycycline for 4–5 weeks. In each weekly passage of the cells, the antibiotic was added to the new media to a final concentration of 50 µM. (Same procedure regardless of which antibiotic used.) Laura Serbus personal communication.

References

1. Goshima G, Wollman R, Goodwin SS, Zhang N, Scholey JM, Vale RD, Stuurman N (2007) Genes required for spindle assembly in *Drosophila* S2 cells. *Science* 316:417–421
2. Moutinho-Pereira S, Stuurman N, Afonso O, Hornsveld M, Aguiar P, Goshima G, Vale RD, Maiato H (2013) Genes involved in centrosome-independent mitotic spindle assembly in *Drosophila* S2 cells. *Proc Natl Acad Sci U S A* 110(49):19808–19813
3. Kwon M, Godinho SA, Chandhok NS, Ganem NJ, Azioune A, Thery M, Pellman D (2008) Mechanisms to suppress multipolar divisions in cancer cells with extra centrosomes. *Genes Dev* 22(16):2189–2203
4. Serbus LR, Landmann F, Bray WM, White PM, Ruybal J, Lokey RS, Debèc A, Sullivan W (2012) A cell-based screen reveals that the Albendazole metabolite, Albendazole sulfone, targets *Wolbachia*. *PLoS Pathog* 8(9):e1002922
5. Lecland N, Debèc A, Delmas A, Moutinho-Pereira S, Malmanche N, Bouissou A, Dupré C, Jourdan A, Raynaud-Messina B, Maiato H, Guichet A (2013) Establishment and mitotic characterization of new *Drosophila* acentriolar cell lines from DSas-4 mutant. *Biol Open* 2(3):314–323
6. Echalier G (1997) *Drosophila* cells in culture. Academic, San Diego
7. Karpova N, Bobiniec Y, Fouix S, Huitorel P, Debèc A (2006) Jupiter, a new *Drosophila* protein associated with microtubules. *Cell Motil Cytoskeleton* 63(5):301–312
8. Ueda R, Ui-Tei K, Roberts J, Cherbas L (2007) Standard protocol for establishing cell lines from *Drosophila* embryos. CGB Technical report 2007-4. <https://dgrc.bio.indiana.edu/include/file/CGB-TR-200704.pdf>
9. Zhou R, Mohr S, Hannon G, Perrimon N (2014) Inducing RNAi in *Drosophila* cells by soaking with ds RNA. Cold Spring Harbor Protocols. Cold Spring Harbor Laboratory Press, Cold Spring Harbor, NY
10. Kao LR, Megraw TL (2004) RNAi in cultured *Drosophila* cells. *Methods Cell Biol* 247:443–457

11. Morh S, Smith J, Shamu C, Neumüller R, Perrimon N (2014) RNAi screening comes of age: improved techniques and complementary approaches. *Nat Rev Mol Cell Biol* 15(9):591–600
12. Di Franco C, Pisano C, Fourcade-Peronnet F, Echalier G, Junakovic N (1992) Evidence for de novo rearrangements of *Drosophila melanogaster* transposable elements induced by the passage to the cell culture. *Genetica* 87:65–73
13. Bai J, Sepp K, Perrimon N (2009) Culture of *Drosophila* primary cells dissociated from gastrula embryos and their use in RNAi screening. *Nat Protoc* 4:1502–1512
14. Perrimon N, Zirin J, Bai J (2011) Primary cell cultures from *Drosophila* gastrula embryos. *J Vis Exp* (48):2215
15. Mateos M, Castrezana SJ, Nankivell BJ, Estes AM, Markow TA et al (2006) Heritable endosymbionts of *Drosophila*. *Genetics* 174:363–376
16. Hamilton P, Perman S (2013) Host defense via symbiosis in *Drosophila*. *PLoS Pathog* 9(12):e1003808
17. Clark M, Anderson C, Cande J, Karr T (2005) Widespread prevalence of *Wolbachia* in laboratory stocks and the implications for *Drosophila* research. *Genetics* 17(4):1667–1675
18. Ui K, Ueda R, Miyake T (1987) Cell lines from imaginal discs of *Drosophila melanogaster*. In *Vitro Cell Dev Biol* 23:707–711
19. Currie D, Milner M, Evans C (1988) The growth and differentiation in vitro of leg and wing imaginal disc cells from *Drosophila melanogaster*. *Development* 102:805–814
20. Niki Y, Yamaguchi T, Mahowald A (2006) Establishment of stable cell lines of *Drosophila* germ-line stem cells. *Proc Natl Acad Sci U S A* 103(44):16325–16330
21. Wyss C (1982) Ecdysterone, insulin and fly extract needed for the proliferation of normal *Drosophila* cells in defined medium. *Exp Cell Res* 139:297–307
22. Cavalloro R (1981) Establishment of continuously in vitro growing cell lines of med-fly (*Ceratitis capitata* wied.). *Rev Can Biol* 40(2):181–186

INDEX

A

Aging.....291–301

B

Behavior 105, 303–319, 321, 342, 343, 346
Binary expression system 47, 53, 54, 60, 74
Bipartite system 36

C

Cell
culture 13, 22, 87, 88, 97, 105–107,
113, 118, 206, 211–213, 333, 334, 338, 345–348
line 3, 21, 34, 39, 80, 83, 87, 88,
105–108, 113, 333–351
tracking 228, 232
Cell-based assays 96
Chemotaxis 304–307, 310–311, 318
Chimeric transactivators 54, 57, 60
Chromatin immunoprecipitation (ChIP) 263–277
Chromatin immunoprecipitation followed by next-
generation sequencing (ChIP-seq) 264, 266
Chromophore-assisted laser inactivation
(CALI) 161–174
Clonal analysis 39–42, 46
Collective cell migration 216
Conditional protein inactivation 161, 163,
164, 168, 170
Courtship 295, 304, 308, 315–316, 319
CRISPR-Cas9 145–159
Cultivation of imaginal discs 203–213
Cultivation of ovaries 215–225
Culture medium 106, 212, 335, 339–341,
343–345, 349

D

Data analysis 24–28, 97, 110, 111, 136, 229, 234
Database 1–30, 99, 129–131, 137, 138, 234, 238, 297
deGradFP 177–186
Dicer-2 125, 126
Diet 292, 297
Double-stranded RNA 43, 118, 125, 126, 132

E

Egg chamber 205, 215–220, 222–225, 253–262
Electrophysiology 322

Embryogenesis 36, 84, 165, 190, 191
Embryonic cells 336, 338–339, 341
Epithelia 227–229, 234
Epithelial mechanics 241–250
Escape behavior 314
Ethanol sedation 304
Exploratory behavior 314
Ex vivo 203–205, 215, 218

F

False-discovery 87, 118, 124, 125
F-Box 178
Feeding 56, 59, 118, 260, 304–306, 309, 310, 317
Fluorescent in situ hybridization (FISH) 255
FlyBase 1–30, 119, 124, 136, 151
Follicle 215, 216
Force measurements 246

G

GAL4 10, 11, 33–47, 53–60, 67, 69–71,
73, 74, 88, 90, 118, 120, 124–128, 131, 132, 135, 138,
139, 178–180, 183, 184
GAL4QF 54, 58–60, 62, 63, 66–67, 74
GAL4-UAS 118, 135
GAL80 37–41, 47, 54, 57, 59, 60,
71, 73, 74, 121, 132, 183–185
Gene expression 12, 26, 33–47, 80,
95, 135, 190, 253
Gene expression profiling 44
Genetics 21, 33, 47, 55, 120, 149, 161, 322
interventions 292, 294, 296–297
photosensitizer 163, 164, 170–172
screens 82, 117
Genome engineering 136, 145, 146
Genomics 21, 29
Genotyping 21
Geotaxis 304, 306, 311
Glucose 55, 281, 283, 286–288, 290, 323
Glycogen 266, 271, 281, 283, 287–288, 290
Green fluorescent protein (GFP) 10, 53, 67,
69, 71–74, 82, 103–105, 135, 139, 161–174, 177–186,
245, 246, 249, 326
gRNA design and cloning 151, 157
Growth 98, 105–107, 109, 110, 113–115,
121, 133, 172, 203, 205, 279–290, 310, 341, 343, 345,
347–349

H

Hemolymph 60, 211, 212, 281–283, 286–287, 289, 290

High-throughput screening 105, 114

High-throughput screens 333

Histone modification analysis 263–277

I

Imaginal disc cultivation 203–213

Indel 146, 150, 154–156

Intersectional expression 60, 74

J

Junctional remodelling 227, 232, 234

Junctions 16–17, 80, 227, 230–232, 236, 237, 241, 245, 249, 250

L

Laser ablation 241–250

LexAQF 54, 58–60, 63, 71, 74

Life span 291–301

Light sheet microscopy 189–201

Live imaging 65, 132, 182–184, 186, 191, 194, 196–199, 203–213, 215–225

Lobula plate tangential cell 327

Locomotion 174, 304, 305, 308, 310, 313

M

Mass isolation 260

Mechanics 216, 326

Metabolism 34, 55, 124, 133, 279–290

MicroRNA (miRNA) 7, 36, 42, 43, 79–91, 122, 133

Mitotic recombination 41, 42, 71–73, 118

Morphogenesis 87, 123, 124, 203, 215, 232

Mosaic analysis 41, 42, 70, 90

Mosaic Analysis with a Repressible Cell Marker (MARCM) 40–42, 55, 59, 60, 70, 71, 73, 74

Motion vision 322, 328, 331

Multiview light sheet microscopy 189–201

N

Nanobodies 178

Neurospora crassa 55

Next-generation sequencing 84, 276

NIG-FLY 119–122, 125, 127, 138, 139

O

Odor discrimination 304

Off-target effects 42, 44, 91, 96, 99, 118, 120, 132, 133, 163, 169, 171, 172

Optogenetics 328–329

Ovary 218–220, 253–262, 348

cultivation 215–225

P

Patch-clamp 322–324

Pharmacological interventions 291, 297

Phenotypic readouts 107–110

Phototaxis 304, 306, 307, 311

Proteasome 23, 177, 178, 180

Q

QF2 57–60, 62, 67, 74

QF2^w 57–60, 62, 74

QS 54, 56–60, 65–67, 70–74

Q-system 53–74

Quantitative biology 227

QUAS 54, 57–59, 63, 74

Quinic acid 55–57, 59–60

R

Rapid ovary mass-isolation (ROMi) 253–262

Righting reflex 304, 307, 311–312

RNA interference (RNAi) 10, 15–17, 19–22, 42, 53, 74, 87, 95–115, 117–139, 172, 279

S

Segmentation 109, 228–232, 235, 237

Selective plane illumination microscopy (SPIM) 189–191, 195

Split GAL4 38, 39, 47

T

Tissue analyzer 228, 234, 235, 237

Transcription 15–17, 19, 20, 22, 33, 34, 37, 39–41, 44, 54–59, 64, 67, 69, 70, 80, 82–85, 97, 99–103, 105, 137, 149, 153, 183, 263, 264, 269, 271, 273, 276, 277

Transcription factor binding analysis 263–277

Transgenic RNAi project (TRIP) 42, 119–122, 125, 133, 138, 139

Translational research 15, 16, 28

Trehalose 281, 283, 287, 290, 323

Triglycerides 281, 283, 288

U

Upstream activation sequence (UAS) 34–37, 40–42,

53–55, 57, 59, 60, 65–67, 70, 71, 88–90, 118, 120, 122,

133, 178, 179

V

Vienna *Drosophila* Resource Centre (VDRC)..... 21, 36,
42, 119–122, 125–127, 132, 138, 139
Visual processing 322

W

Weight 59, 260, 281, 282, 285, 289, 293
Wing disc 203–206, 208, 210–212, 281
Wing size 279